Program and Abstracts for

CPIMS 16

Sixteenth Condensed Phase and Interfacial Molecular Science (CPIMS) Research Meeting

Hilton Washington DC/Rockville Hotel
& Executive Meeting Center
Rockville, MD
November 15-17, 2023

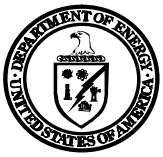

U.S. DEPARTMENT OF ENERGY | Office of Science

Office of Basic Energy Sciences
Chemical Sciences, Geosciences & Biosciences Division

The research grants and contracts described in this document are supported by the U.S. DOE Office of Science, Office of Basic Energy Sciences, Chemical Sciences, Geosciences and Biosciences Division.

FOREWORD

We are excited to begin again in-person research meetings for the Condensed Phase and Interfacial Molecular Science (CPIMS) Program, sponsored by the U.S. Department of Energy (DOE), Office of Basic Energy Sciences (BES). These meetings are not merit reviews, nor conferences, but an opportunity to bring together a unique set of BES-supported investigators in a forum to share the latest news about their projects, fulfilling a foundational goal of the CPIMS Program (starting at the 1st CPIMS PI Research Meeting on October 24, 2004): the cross-fertilization of ideas. Many of the circumstances that block advances can result from our assumptions, limiting us should we choose to work in isolation. Other scientists can bring a different perspective, revealing new paths for our work. Finding connections allows us to face our inner world outward, participate together in the next scientific advances, and push collectively the boundary of knowledge in exciting new directions.

Special thanks are reserved for the staff of the Oak Ridge Institute for Science and Education, who, along with the staff of the Hilton Washington DC/Rockville Hotel & Executive Meeting Center, worked to ensure the success of the meeting. We also thank Teresa Crocket of the DOE Office of Basic Energy Sciences for overseeing the meeting operation.

This year's participants are gratefully acknowledged for their investment of time and for their willingness to attend CPIMS 16, either in-person or virtually, no matter how they participated, through chairing sessions, giving formal presentations, asking questions during presentations, submitting abstracts (listed in the Table of Contents, which begins on the next page), being present at the poster session, or through informal conversations with participants. All these things are gifts to the CPIMS community. Thank you for trusting us with your ideas.

Gregory Fiechtner, Marat Valiev, and Thomas Settersten
Chemical Sciences, Geosciences and Biosciences Division
Office of Basic Energy Sciences

CPIMS 16

U.S. DEPARTMENT OF ENERGY | Office of Science

Office of Basic Energy Sciences
Chemical Sciences, Geosciences & Biosciences Division

Sixteenth Condensed Phase and Interfacial Molecular Science (CPIMS) Research Meeting
Hilton Washington DC/Rockville Hotel & Executive Meeting Center, Rockville, MD
November 15-17, 2023

All presentations will be held in the Plaza Ballroom

Wednesday, Nov. 15

7:30 – 8:30 am *** Breakfast ***

OPENING SESSION

8:30 – 8:45 am BES Update,
Gail McLean, Acting Division Director, DOE BES/CSGB

8:45 – 9:00 am CPIMS Program Update
Gregory Fiechtner, DOE BES/CSGB

SESSION I

Chair: **Adam Willard**, Massachusetts Institute of Technology

9:00 – 9:30 am "Solution Structure and Nucleation: Beyond Debye Screening and Bragg Peaks"
Shawn Kathmann, Pacific Northwest National Laboratory

9:30 – 10:00 am "Understanding and Predicting Phase Transitions in Solvated Confined Systems"
Pratyush Tiwary, University of Maryland

10:00 – 10:30 am ***Break***

SESSION II

Chair: **Munira Khalil**, University of Washington

10:30 – 11:00 am "Tracking excited state proton transfer and the coupled solvent reorganization with femtosecond X-rays"
Elisa Biasin, Pacific Northwest National Laboratory

11:00 - 11:30 am "Understanding Aqueous Solutions and their Liquid-Vapor Interface by X-ray Photoelectron Spectroscopy"
Monika Blum, Lawrence Berkeley National Laboratory

11:30 – 12:00 am "Imaging Electrolyte Behaviors using 2D IR Imaging--A Snapshot of a New Project"

Amber Krummel, Colorado State University

12:00 pm – 1:30 pm ***Lunch (Regency Room)***

SESSION III

Chair: **Carlos Baiz**, University of Texas at Austin

1:30 – 2:00 pm "Chemical Kinetics in Microdroplets"
Kevin Wilson, Lawrence Berkeley National Laboratory

2:00 - 2:30 pm "Programmable Cascade Reactions Enabled by Plasma-Microdroplet Fusion"
Abraham Badu-Tawiah, The Ohio State University

2:30 – 2:45 pm "*The DROPLETS Earthshot project: identifying key factors driving reactivity in aqueous microdroplet systems"*
Joaquín Rodríguez-López, University of Illinois Urbana-Champaign

2:45 – 3:00 pm "*Stern Water Flipping over Hematite Photoanodes from Nonlinear Optics*"
Franz Geiger, Northwestern University

3:00 – 3:30 pm ***Break***

SESSION IV

Chair: **Susan Sinnott**, Pennsylvania State University

3:30 - 3:45 pm "*The Nature, Dynamics, and Reactivity of Electrons in Ionic Liquids"*
David Blank, University of Minnesota

3:45 - 4:00 pm "*Testing a quadrupolar solvation hypothesis of CO2 in doubly polymerizable ionic liquids"*
Sean Garrett-Roe, University of Pittsburgh

4:00 - 4:15 pm "*Towards Soft X-ray Second Harmonic Generation of Solar Materials"*
Craig Schwartz, University of Nevada, Las Vegas

4:15 – 4:30 pm "*Probing the ultrafast electron and phonon dynamics of 2D materials on the nanoscale"*
Sarah King, University of Chicago

4:30 - 4:45 pm ***Break***

SESSION: V

Chair: **Patrick El-Khoury**, Pacific Northwest National Laboratory

4:45 – 5:00 pm "*What is the matter within polaritons: Energy transport and disorder effects"*
Andrew Musser, Cornell University

5:00 – 5:15 pm "*New Experimental Platforms for Polariton Reaction Dynamics"*
Marissa Weichman, Princeton University

5:15 – 5:30 pm "*Advancing Atomistic Understanding of Electronic Energy Transfer"*
Christine Isborn, University of California, Merced

5:30 – 5:45 pm "*Disentangling nonlinear spectroscopy to control nonequilibrium energy transport"*
Andres Montoya-Castillo, University of Colorado

6:00 pm **** Reception (No Host, Lobby Lounge) ****
**** Dinner (on your own) ****

Thursday, November 16

7:30 – 8:30 am *** Breakfast ***

SESSION VI

Chair: **Walter Drisdell**, Lawrence Berkeley National Laboratory

8:30 – 9:00 am "High energy X-rays as a probe of buried functional interfaces"
Tod Pascal, University of California, San Diego

9:00 – 9:30 am "Resolving Catalytic Mechanism at an Electrode Surface: Thermodynamics & Kinetics of Reaction Steps"
Tanja Cuk, University of Colorado

9:30 – 10:00 am "Ion Transport and Interplay in Angstrom Solid Ionic Channels"
Chong Liu, University of Chicago

10:00 – 10:30 am ***Break***

SESSION VII

Chair: **Sotiris Xantheas**, Pacific Northwest National Laboratory

10:30 – 11:00 am "The Impact of the Electric Field in Microsolvated Metal Ion-Peptide Complexes"
Etienne Garand, University of Wisconsin-Madison

11:00 – 11:30 am "Molecular-level aspects of functionalized ionic liquids and water-assisted proton transport with cryogenic ion chemistry and spectroscopy"
Mark Johnson, Yale University

11:30 – 12:00 am "Liquid-Liquid Phase Separation in Submicron Aerosol Particles"
Miriam Freedman, Pennsylvania State University

12:00 pm – 1:30 pm ***Lunch (Regency Room)***

SESSION VIII

Chair: **Christopher Fecko,** DOE BES/CSGB

1:30 – 2:00 pm "Understanding Rate Constants of Hydrated Electron Reactions"
Ward Thompson, University of Kansas

2:00 – 2:30 pm "Ultrafast Hole Capture and Impact on Complexants for UNF Separation"
Andrew Cook, Brookhaven National Laboratory

2:30 – 3:00 pm "Understanding Ionizing Radiation-Induced Speciation, Chemistry, and Transport in Nuclear Materials"
Greg Holmbeck, Idaho National Laboratory

3:00 – 3:30 pm "Oxidation rates of hyper-reduced metal ions in high-temperature water"
Aliaksandra Lisouskaya, Notre Dame Radiation Laboratory

3:30 pm – 4:00 pm ***Break***

SESSION IX

Chair: **Ismaila Dabo**, Pennsylvania State University

4:00 – 4:15 pm "*Controlling water availability and reactivity in electrochemical transformations"*
Chibueze Amanchukwu, University of Chicago

4:15 – 4:30 pm "*Towards Understanding the Effect of Interfacial Ions on the Atomistic Structure and Chemical Reactivity at Solid/Liquid Interfaces Using Machine Learning Interatomic Potential Simulations"*
Tibor Szilvási , University of Alabama

4:30 – 4:45 pm "*Rational Design of Concentrated Electrolytes for Beyond-Li-ion Batteries with Machine Learning and Quantum Calculations"*
Mirza Galib, Howard University

4:45 – 5:00 pm "*The Molecular Building Block Sampling Approach for Polymorphic Free Energy Calculations"*
Omar Valsson, University of North Texas

5:00 pm – 7:00 pm ***Dinner (on your own)***

POSTER SESSION

7:00 pm – 9:00 pm

Friday, November 17

7:30 – 8:30 am *** Breakfast ***

SESSION X

Chair*:* **Ian Carmichael**, Notre Dame Radiation Laboratory

8:30 – 9:00 am "The Role of the Solvent in Chemical Identity, Chemical Reactivity and Quantum Decoherence"
Benjamin Schwartz, University of California, Los Angeles

9:00 – 9:30 am "Participation of Electrochemically Inserted Protons in the Hydrogen Evolution Reaction on Tungsten Oxides"
Veronica Augustyn, North Carolina State University

9:30 – 10:00 am "Solvated Ionic Liquid Electrolytes: Experiments, Modeling and Applications in Energy Storage"
Daniel Kuroda, Louisiana State University

10:00 – 10:30 am ***Break***

SESSION XI

Chair: Scott Anderson, University of Utah

10:30 – 11:00 am "Computational insights for light-driven excitation and interfacial molecular transformation"
Bin Wang, University of Oklahoma

11:00 – 11:30 am "Angle-dependent electrochemistry of moiré superlattice flat bands"
Kwabena Bediako, University of California, Berkeley

11:30 am Adjourn

TABLE OF CONTENTS

DOE Office of Science Early Career Research Program Abstracts

Fluxional Nature of Heterogeneous Catalysts

Patricia Poths,[1] Santiago Vargas,[1] Simran Kumari,[2]
Philippe Sautet,[1,2] Anastassia N. Alexandrova[1,3]
[1]Department of Chemistry and Biochemistry, [2]Department of Chemical and Biomolecular Engineering, [3]Department of Materials Science and Engineering, UCLA

Abstract

Our program develops a paradigm for heterogeneous catalysis stating that catalysts are not static, but dynamic, fluxional, metastable, and strongly evolving under reaction conditions, creating new active sites, not present in as-prepared catalysts. The approach combines Density Functional Theory, grand canonical global optimization under relevant partial pressures and temperatures, high-dimensional Neural Networks, as well as kinetic Monte Carlo. The work features strong collaboration with the experiment. Several catalytic systems, from supported cluster catalysts to amorphous bulk interfaces, are considered. First, we consider oxidative dehydrogenation of propane on h-BN. We show that a flexible amorphous, off-stoichiometric BO(OH) layer forms on the edge of the h-BN stack, presenting a wide variety of coordinations for the B under reaction conditions, as proven by the agreement of the ensemble NMR and XPS spectra with the experiment. The reactivity is driven by specific B atoms, which initiate the radical gas phase chemistry. Next, we study the nature of the zirconia on copper inverse catalyst under the conditions of CO_2 hydrogenation to methanol. We consider a model three atom Zr cluster on a Cu(111) surface decorated with various O, OH and formate ligands, noted $Zr_3O_x(OH)_y(HCOO)_z$/Cu(111), revealing major changes in the active site induced by various reaction parameters such as the gas pressure, temperature, conversion levels, and CO_2:H_2 feed ratios. Calculations provide insights into the dynamic behavior of the catalyst, and indicate a large number of compositions and structures with changing the type, number, and binding sites of the ligands, are present under reaction conditions. Lastly, we challenge the Boltzmann statistics for the catalyst the ensemble representation, by explicitly equilibrating the ensembles of supported PtH clusters using kinetic Monte Carlo. We show that depending on the support and H-coverage, some cluster may exhibit kinetic trapping on the time-scales of the catalyzed reaction, and operate off-equilibrium.

DE-SC0019152: Ensemble Representation for the Realistic Modeling of Cluster Catalytic Reactivity at Heterogeneous Interfaces

PI: Anastassia Alexandrova, **co-PI:** Philippe Sautet
Postdoc(s): Harry Morgan, Geng Sun, Han Guo
Student(s): Simran Kumari, Vaidish Sumaria, Patricia Poths, Edison Cummings, Santiago Vargas, Robert Lavroff, Zisheng Zhang

RECENT PROGRESS

i) boride catalysts for oxidative dehydrogenation of propane

Using GCGA, we have searched for the global minimum and low-energy local minima structures of hBN armchair and zigzag edges under relevant conditions of oxidative dehydrogenation of propane (ODHP). Surface phase diagrams are constructed from the grand canonical ensemble of surface states, and the evolution of surface structure as a

function of chemical potential (Fig. 1a, corresponding to temperature and partial pressure) can be used to simulate condition-dependent ^{11}B chemical shift spectra, which is in good agreement with previous experimental reports (Fig. 1b) and offers detailed atomistic insights. The effects of sliding dynamics of hBN sheets on the reactivity of restructured edges are studied by AIMD simulations. Multiple sliding configurations are found to be accessible at timescale of a few ps, and each has differently strained B-O linkages at the edges. The metastable sliding configurations are found to be more active towards propane and water activation as compared to the global minimum sliding configuration (Fig. 1c). Such phenomenon is likely the origin of hBN's higher ODHP activity than those of the metal borides.

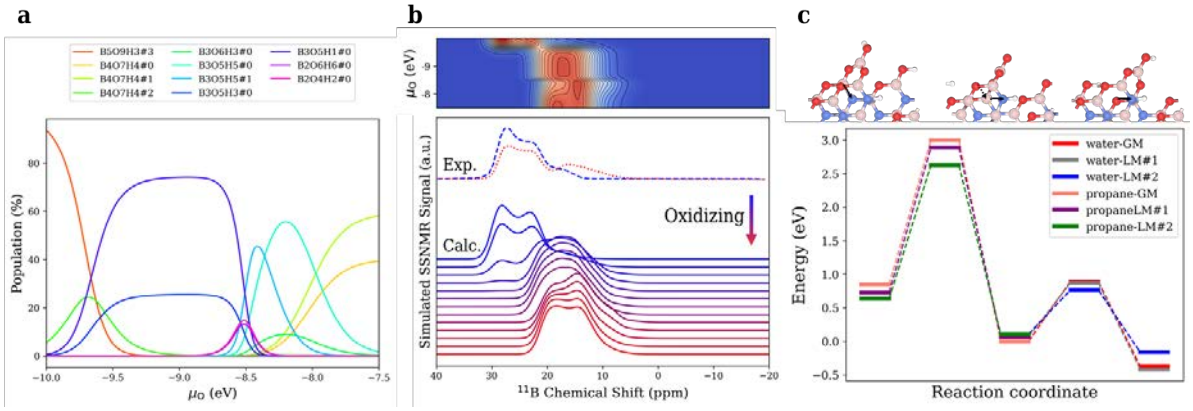

Figure 1. Off-stoichiometric restructuring and sliding dynamics of hBN edges. (a) The evolution of population of accessible surface phases as a function of oxygen chemical potential μ_O. $B_xO_yH_x$#n denotes the n-th local minima (zeroth is the global minimum) of the surface stoichiometry of $B_xO_yH_z$. (b) Evolution of the ^{11}B SSNMR spectra as a function of μ_O. The experimental data are also shown in the lower panel for comparison. (c) The energy diagram of a restructured h-BN armchair edge interconverting among the three sliding configurations of the lowest energy.

ii) hydrogenation of CO_2 to methanol on zirconia-modified Cu.

The hydrogenation of CO_2 to value added products such as methanol has numerous benefits such as mitigating the greenhouse gas emissions by capturing CO_2 and re-using it to make alternative liquid fuels. Zirconia-modified copper catalysts have been shown to be effective in CO_2/H_2 conversion to methanol with a good water tolerance, high thermal stability, and high ability to reduce CO_2 and other reaction intermediates.

We use our Grand Canonical Basin Hopping (GCBH) code to find the energetically relevant structures in reaction conditions. Under the conditions of CO_2 hydrogenation ($CO_2 + 3H_2 \rightarrow CH_3OH + H_2O$), it is very important to determine the right H and O coverage of the Zirconia clusters deposited on Cu(111), to correctly identify the catalytic environment of the reaction. Using the GCBH code, we have identified the potential energy surface of these clusters under varying O and H chemical potential. In order to accurately replicate the reaction conditions for the CO_2

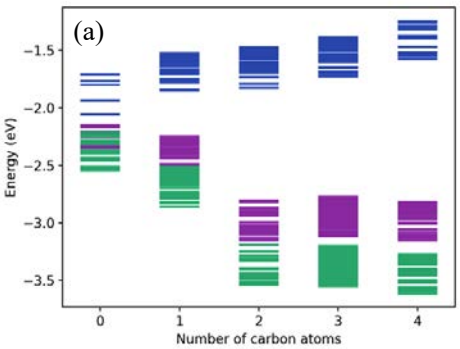

Figure 2. Adsorption energies of the $Zr_3O_xOH_yHCOO_z$ cluster at three different reaction conditions corresponding to experimental works. Blue: P = 0.013 atm, conv = 2%, CO2/H2 ratio = 9, and T = 500K, Purple: P = 4.93 atm, conv = 0.8%, CO_2/H_2 ratio = 1:3, and T = 493.15K and Green: pressure = 30 atm, conv = 19.7%, CO_2/H_2 ratio = 3, and T = 493.15 K. The x axis represents the number of formates on the cluster.

hydrogenation reaction, it is essential to calculate the chemical potentials of all species involved as a function of (a) Initial feed pressure of CO_2 and H_2, (b) the ratio of CO_2: H_2 in the initial feed, (c) the temperature at which the reaction is conducted, and (d) the total conversion to methanol.

The Cu(111) surface was selected, along with a Zr cluster consisting of three Zr atoms, as the model for studying the catalytic properties of the highly dispersed Zirconia-Copper inverse catalyst under CO_2 hydrogenation conditions. Using this model, the optimum coverage of oxygen, hydroxyl, and formate species on the Zirconia-Copper inverse catalyst under CO_2 hydrogenation conditions was investigated. Under reaction conditions, we observe a large number of composition and structures with similar free energy for the catalyst (Fig. 2), with respect to changing the type, number, and binding sites of adsorbates, suggesting that the active site should be regarded as a statistical ensemble of diverse structures that easily interconvert.

iii) kinetics of isomerization of catalytic clusters

We constructed exhaustive isomerization networks for Pt_4 in the gas phase (Fig. 3) and on alumina support, under varying amount of H-coverage, with two goals: 1) to see if the presence of ligands affects fluxionality (we found that it does, and in particular both the H and the support tends to increase the isomerization barriers and also make the potential energy surface more complicated and richer in minima); 2) to determine the extent to which the Boltzmann statistics holds up, and the time required to equilibrate the ensemble. For the latter, we have been using the Boltzmann statistics, and we found that in a large number of studies we cannot agree with, nor predict the experiment without ensemble averaging. However, the accuracy of Boltzmann statistics can be questioned. Indeed, we found that kinetic trapping of some isomers is not uncommon, and for some systems the exit from the trapped state requires more than 450K and more than 100 µs. Our current goal is to develop descriptors that would permit identifying such off-Boltzmann cases quickly, in order to formalize the approach to their modeling beyond Boltzmann.

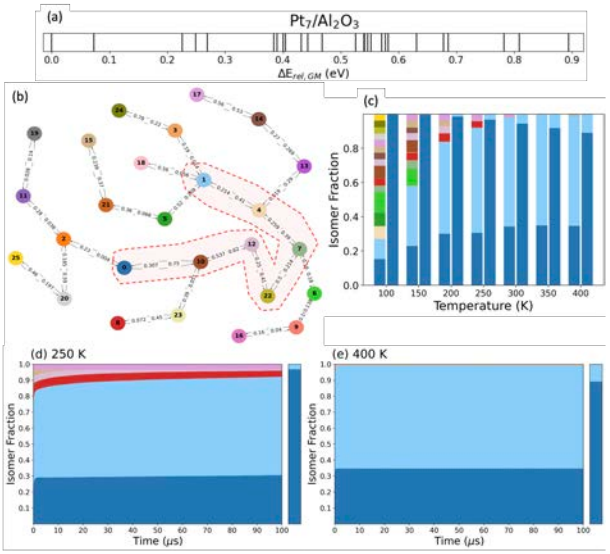

Figure 3. Pt_7/Al_2O_3 isomer energy distribution (a) and isomerization network (b) slightly coarsened to run with kMC. (c) Comparison of the full network kMC simulations with time (left bars) with the Boltzmann populations at the corresponding temperatures (right). (d) and (e) show stacked plots of isomer populations for 250 K and 400 K respectively, highlighting a kinetically-trapped system, and one that is thermalizing, but on timescales longer than 100 µs

Publications Acknowledging this Grant in 2021-2023

(I) Intellectually led by this grant

1. Cendejas, M. C.; Mellone, O. A. P.; Kurumbail, U.; Zhang, Z.; Jansen, J. H.; Ibrahim, F.; Dong, S.; Vinson, J.; Alexandrova, A. N.; Sokaras, D.; Bare, S. R.; Hermans,

I. Tracking Active Phase Behavior on Boron Nitride during the Oxidative Dehydrogenation of Propane Using Operando X-Ray Raman Spectroscopy. *J. Am. Chem. Soc.* **2023**, accepted.
2. Kumari, S.; Alexandrova, A. N.; Sautet, P. Nature of Zirconia on Copper Inverse Catalyst under CO_2 Hydrogenation Conditions. *J. Am. Chem. Soc.* **2023**, accepted.
3. Zhang, Z.; Hermans, I.; Alexandrova, A. N. Off-stoichiometric Restructuring and Sliding Dynamics of Hexagonal Boron Nitride Edges in Conditions of Oxidative Dehydrogenation of Propane. *J. Am. Chem. Soc.* **2023**, 145, 17265.
4. Morgan, H. W. T.; Alexandrova, A. N., Structures of LaH_{10}, EuH_9, and UH_8 superhydrides rationalized by electron counting and Jahn–Teller distortions in a covalent cluster model. *Chem. Sci.* **2023**,14, 6679
5. Lavroff, R. H.; Wang, J.; White, M.G.; Sautet, P.; Alexandrova, A. N. Mechanism of Stoichiometrically Governed Titanium Oxide Brownian Tree Formation on Stepped Au(111). *J. Phys. Chem. C* **2023**, 127, 8030.
6. Lavroff, R. H.; Morgan, H. W. T.; Zhang, Z.; Poths, P.; Alexandrova, A. N. Ensemble representation of catalytic interfaces: soloists, orchestras, and everything in-between. *Chem. Sci.* **2022**, 2022,13, 8003.
7. Poths, P.; Sun, G.; Sautet, P.; Alexandrova, A. N. Interpreting operando XANES of supported Cu and CuPd clusters in conditions of oxidative dehydrogenation of propane: dynamic changes in composition and size. *J. Phys. Chem. C* **2022**, 126, 1972.
8. Morgan, H. W. T.; Alexandrova, A. N. Electron Counting and High Pressure Phase Transformations in Metal Hexaborides. *Inorg. Chem*. **2022**, 61, 18701.
9. Guo, H.; Poths, P; Sautet, P; Alexandrova, A. N. Oxidation Dynamics of Supported Catalytic Cu Clusters: Coupling to Fluxionality. *ACS Catalysis* **2022**, 12, 818.
10. Sun, G; Sautet, P. Active Site Fluxional Restructuring as a New Paradigm in Triggering Reaction Activity for Nanocluster Catalysis. *Acc. Chem. Res.* **2021**, 54, 3841.
11. Hülsey, M.J.; Sun, G.; Sautet, P.; Yan, N. Observing Single-Atom Catalytic Sites During Reactions with Electrospray Ionization Mass Spectrometry, *Angew. Chem. Int. Ed.* **2021**, 60, 4764.
12. Sun, G.; Fuller, J. T.; Alexandrova, A. N.; Sautet, P. Global Activity Search Uncovers Reaction Induced Concomitant Catalyst Restructuring for Alkane Dissociation on Model Pt Catalysts. *ACS Catalysis* **2021** 11, 1877.

(II) Jointly funded by this grant and other grants with intellectual leadership by other funding sources

13. Wan, C.; Zhang, Z.; Dong, J.; Xu, M.; Pu, H.; Baumann, D.; Lin, Z.; Wang, S.; Huang, J.; Shah, A. H.; Pan, X.; Hu, T.; Alexandrova, A. N.; Huang, Y.; Duan, X. Amorphous nickel hydroxide proton sieve tailors local chemical environment on Pt surface for high-performance hydrogen evolution reaction in alkaline medium. *Nat. Mater.* **2023**, 22, 1022.
14. Shah, A. H.; Zhang, Z.; Huang, Z.; Wang, S.; Zhong, G.; Wan, G.; Alexandrova, A. N.; Huang, Y.; Duan, X. Unriddling the role of alkali metal cations and Pt-surface hydroxide in alkaline hydrogen evolution reaction. *Nature Catal.* **2022**, 5, 923.

Controlling Aqueous Interfacial Phenomena of Redox-Active Ions with External Electric Fields

DE-SC0016381

Heather C. Allen
The Ohio State University, Department of Chemistry and Biochemistry
100 W. 18th Ave, Columbus, OH 43210
allen.697@osu.edu

Project Scope

This project embarks on a comprehensive exploration of inherent and externally applied electric fields on the interfacial organization and hydration of ions at aqueous-air interfaces with focus on iron, thus providing significance across various domains including but not limited to geochemistry and energy infrastructure. We posit that inherent and external electric fields exert notable effects on several critical aspects at aqueous interfaces, including ion hydration properties, ion pairing, ion speciation and complexation, and the organization of interfacial water. Controlling interfacial organization of ions and their solvation environment has far reaching consequences for a myriad of applications. Redox ions, characterized by their multivalent states, wield a profound influence on interfacial chemistry. Here we aim to unravel the surface speciation of ferric and ferrous salts at aqueous surfaces, to examine surface hydration, to elucidate the acid/base behavior at aqueous surfaces, to explore the effect of external electric fields, and to develop methods and instrumentation toward these aims. To carry out this research, advanced techniques are employed and developed: vibrational sum frequency generation spectroscopy, second harmonic generation, surface potential methods, polarized Raman spectroscopy, and surface tension measurement. The anticipated outcomes of this research encompass advancements in instrumentation essential for elucidating ion behavior at aqueous interfaces. Overall, this project seeks to deepen our understanding of the intricate interplay between electric fields and ions at aqueous-air interfaces including avenues to control interfacial phenomena.

Recent Progress

Progress from 2021-2023 includes a series of firsts with respect to developing a thorough understanding of $FeCl_3$ at the air/aqueous interface under inherently acidic conditions, advancing our understanding of ions at interfaces, and applying an electric field across the air-water interface to drive ion behavior.

We proposed a circuit model for an ionizing surface potential method based on the alpha decay of a radioactive americium-241 electrode. We evaluated the robustness of the circuit model for quantifying the surface potential at the air-aqueous interface and then showed successful validation of our circuit model through determination of the surface tension of the air-electrolyte interface with comparison to respective surface tension literature values. This validation reveals the reliability of surface potential measurements using the americium-241 ionizing method. We then measured surface potentials using the Am^{241} ionizing method with

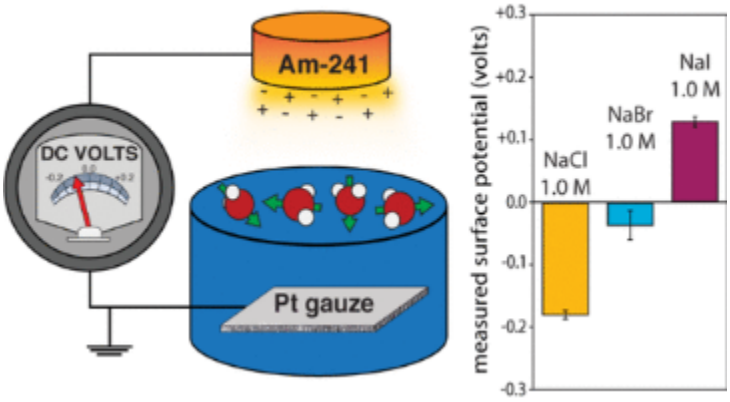

Figure 1. Ionizing method surface potential measurement of sodium halides.

varying reference electrode and ionizing gas environment. With potential measurements of sodium halide solutions, we show that iodide has a dominant effect on the air–aqueous electric field. Compared to chloride and bromide, iodide is observed with a net negatively charged surface potential at all salt concentrations measured. Free energies of adsorption were measured and reported. Moreover, we have established a framework for evaluating measured surface potential data, including the absolute measurement of neat water at -0.4V. We developed methodology using calibrants of sodium dodecyl sulfate (SDS) and cetyltrimethyl ammonium bromide (CTAB) for negative and positive surface potential data points respectively. Interestingly NaCl exhibits a negative surface potential and sodium iodide a positive surface potential (Figure 1). With rigorous fits to concentration data, free energies of adsorption provide important insight to the adsorption process albeit not an absolute scale of adsorption quantity. We have further compared the vibrating plate method to the ionizing method.

In our prior work, we speculated on $FeCl_3$ speciation at the air/aqueous interface using vibrational sum frequency generation (VSFG) and X-ray methods. In 2023, we expanded our understanding using an array of different tools. Particularly useful was the relationship between the UV-Visible spectroscopic signature and resonant and nonresonant second harmonic generation (SHG) to evaluate the electric dipole moment of additional iron(III)-chloro species. Through a highly methodical approach, we observed two different interfacial concentration regimes marked by two distinctly different SHG E-field trends. Nonresonant SHG behavior was observed below 2 mol/kg H_2O, similar to the E-field generated from an aqueous sodium iodide surface, but much larger in magnitude than aqueous NaCl and NaBr solution surfaces. Above 2.0 mol/kg H_2O, an increase in the SHG slope was observed, significantly larger than that of the aqueous sodium halide electrolyte surfaces. Through further evaluation of symmetry and resonant SHG behavior, data pointed to the existence of the neutral $[FeCl_3(H_2O)_3]$ complex at the air-aqueous interface. In our prior work, we had determined a 1:2 Fe:Cl ratio at the surface, and moreover, VSFG suggested the existence of the centrosymmetric monovalent

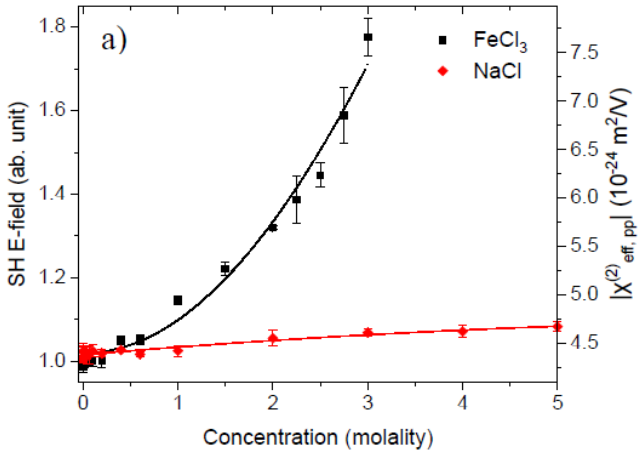

Figure 2. SHG E-field showing the air/aqueous surface of $FeCl_3$ solutions with uniquely exponential behavior.

$FeCl_2$:$(H_2O)_4$ species. Thus, the identified neutral species is a new and interesting finding that points to the possibility of compound neutrality being a defining characteristic for surface activity.

We further explored ion pairing signatures using polarized Raman spectroscopy to evaluate the nuanced behavior of the OH stretching bands of the solvating water molecules. This work revealed that contrary to prior molecular dynamics simulation showing larger water perturbation of solvating water of isolated and solvent shared ion pairs, contact ion pairs showed the largest hydration perturbation. Aqueous NaCl and KCl were rigorously evaluated. Our results have implications for both theoretical analysis and experimental polarized Raman methods of solution phase ion pairing analysis.

Over the past several years we have developed robust methods to apply large electric fields across the air-water gap and to measure the effect on the air-water interface. Given the complexity of the experiment and interpretation, our work is ongoing in this area. However, through theoretical collaboration with the A. Willard (MIT), we now more thoroughly understand the shortcomings of interfacial models. Our work revealed that there is a minimum SHG value at large and positive applied fields. Through theory we learned that most of the potential drop is across the air gap. Yet, the small potential felt by the interface, the topmost layer and the underlying water layers, reveals that the topmost layer is relatively robustly stable when interrogated by VSFG, yet the net electric dipole, as reported by the SHG, is highly perturbed. Applying our knowledge with respect to the third order susceptibility and an understanding of the autoionization of water into submicromolar solution concentrations of hydroxyl and hydronium ions, it was borne out of the result that these ions, OH^- and H_3O^+, are driven by the applied E-field. This then controls and drives water alignment from the internal field set up by the seemingly miniscule concentrations of OH^- and H_3O^+, albeit enhanced concentrations under the applied field conditions in our experiments.

We have further made strides toward understanding Fe(II) salts and Fe(III) salts of sulfate and nitrate (unpublished). Additionally evaluating Al(III) salts has allowed us to establish comparative metrics for iron. Moreover, our surface potential data, without applied electric fields, has been immensely interesting in particular through evaluation relative to surfactant calibrants of SDS and CTAB.

Future Plans

Given our recent progress in surface potential measurement development and in advancing the area of surface electric field impact on aqueous interfaces, we will continue to investigate ions and hydration with and without applied electric fields. We have yet to establish the connection robustly between water alignment using VSFG, net electric dipole alignment via SHG, and surface potential measurement using vibrating plate and ionizing probe methods, and plan to further explore the molecular details and meaning of the measurements. Further understanding iron redox pairs is of utmost importance and through perfecting our calibrant surface potential methods and comparison against a series of ions with various properties, we plan to methodically evaluate and report on the surface hydration and speciation of additionally complex systems. Our current and future work on Fe(II), Fe(III), and Al(III), in addition to surfactant and alkali and alkali earth metal salts is yielding unanticipated results of great interest to energy

infrastructure, corrosion, and geochemical systems. Preliminary data has recently shown hugely negative surface potentials of trivalent salts, of various systems. This is particularly intriguing and challenging to further our calibrant framework for molecular interpretation.

Peer-Reviewed Publications Resulting from this Project (2021-2023)

1. Circuit Analysis of Ionizing Surface Potential Measurements of Electrolyte Solutions; Tehseen Adel, Juan Velez-Alvarez, Anne C. Co, Heather C. Allen*; OPEN ACCESS: https://doi.org/10.1149/1945-7111/abd649, **2021** J. Electrochem. Soc.168 016507.
2. Insight into the Ionizing Surface Potential Method and Aqueous Sodium Halide Surfaces; Tehseen Adel, Ka Chon Ng, Maria G. Vazquez de Vasquez, Juan Velez-Alvarez, and Heather C. Allen*; DOI 10.1021/acs.langmuir.1c00465, Langmuir, **2021**, 37, 26, 7863–7874.
3. Iron(III) Chloro Complexation at the Air–Aqueous $FeCl_3$ Interface via Second Harmonic Generation Spectroscopy, Ka Chon Ng, Tehseen Adel, KU Lao, Meredith G. Varmecky, Z Liu, M Arrad, Heather C. Allen*, J. Phys. Chem. C **2022** 126 (36), 15386-15396.
4. Identification of Ion Pairs in Aqueous NaCl and KCl Solutions in Combination of Raman Spectroscopy, Molecular Dynamics and Quantum Chemical Calculations; Lin Wang, (Tohoku Univ), Akihiro Morita (Tohoku Univ), Nicole North, Elliot Springfield, Stephen Baumler, Heather C. Allen, DOI: 10.1021/acs.jpcb.2c07923 J. Phys. Chem. B **2023** 127 (7), 1618-1627.
5. Array Based Machine Learning for Functional Group Detection in Electron Ionization Mass Spectrometry; Nicole M. North, Abigail A. Enders, Morgan L. Cable, Heather C. Allen, (funded by NASA (NMN), JPL (MLC), NSF-CHE (AAE), and DOE-BES CPIMS DE-SC0016381 (HCA)), ACS Omega **2023**, 8, 27, 24341–24350.
6. Second-harmonic generation provides insight into the screening response of the liquid water interface; Kamal K. Ray §, Aditya Limaye §, Ka Chon Ng, Ankur Saha, Sucheol Shin, Marie-Pierre Gaigeot, Simone Pezzotti, Adam P. Willard*, and Heather C. Allen* J. Phys. Chem. C **2023**, 127, 30, 14949–14961.

Tuning bulk and interfacial electrolyte solvation to control electrochemical transformations
Award Number: DE-SC0024103

Chibueze Amanchukwu (chibueze@uchicago.edu)
Pritzker School of Molecular Engineering
University of Chicago
5640 South Ellis Avenue, ACC 201, Chicago, IL 60637

Program Scope

The goal of this research project is to understand how controlling water solvation in aprotic media in the bulk and at a solid-liquid interface can modulate electrochemical transformations such as electrocatalytic carbon monoxide conversion. Electrochemical transformations are required to accelerate decarbonization. In all these transformations, water often serves a dual purpose. It can be a reactant (proton source, reagent) and a bulk solvent. However, for transformations such as carbon dioxide reduction (CO2RR) and carbon monoxide reduction (COR), that duality poses a dilemma: how does one enable high selectivity of hydrogenated products such as ethylene, while suppressing undesired hydrogen evolution reaction (HER) from water breakdown? We hypothesize that controlling water's hydrogen bonding environment through confinement in an aprotic solvent provides a handle to suppressing HER while enabling valuable hydrogenated products. The objectives are to (1) quantify bulk ionic solvation and water hydrogen bonding behavior in relevant aprotic-water mixtures using experiments and computation (2) design and synthesize novel catalysts that support C-C coupling in these electrolyte media, and (3) probe the electrochemical solid-liquid interfacial changes *in situ*. Fundamental insights garnered from both the electrolyte and catalyst design as well as the interfacial changes will be transformative for a wide range of electrochemical transformations (COR, CO2RR, HER, nitrogen reduction reaction) relevant for clean energy and manufacturing.

Recent Progress

Our recent progress has focused on experiments and computation to understand water hydrogen bonding behavior in a variety of electrolytes. The influence of these systems on carbon monoxide reduction is also progressing. In addition, we have submitted a beamline request at Oak Ridge to pursue neutron-based scattering experiments.

Future Plans

Our future work will focus on in depth understanding of water solvation behavior, and synthesis of novel catalysts for carbon monoxide electrochemical reduction. We will also begin work on *in situ* characterization of the electrode/electrolyte interfaces using Raman and infrared techniques.

Peer-Reviewed Publications Resulting from this Project (2021-2023)

There are currently no publications to report for this new award. The project began September 1, 2023

Size-Selected Sub-Nano Electrocatalysis - DE-SC0020125

PI: Scott L. Anderson, Chemistry Dept., Univ. of Utah, Salt Lake City, UT 84112, anderson@chem.utah.edu
Co-PIs Anastassia Alexandrova, Chemistry and Biochemistry, UCLA, Los Angeles, CA 90095, ana@chem.ucla.edu and Philippe Sautet, Chemical. and Biochemical. Engineering, UCLA, Los Angeles, CA 90095, sautet@ucla.edu

Project Scope:

A combined experimental and theoretical approach is being used to examine the effects on electrocatalytic activity of sub-nano catalytic site size and composition, as well as effects of different electrode supports. The focus is on simple reactions of fundamental interest that are also important in energy conversion, including the hydrogen evolution reaction (HER), the oxygen reduction reaction (ORR), CO redox and CO_2 reduction, and alcohol oxidation.

The experiments exploit capability to prepare electrodes by depositing atomically size-selected clusters on planar supports such as highly oriented pyrolytic graphite (HOPG), or conductive oxide films such as indium-tin oxide (ITO) and fluorine-tin oxide (FTO). These are characterized by a variety of surface spectroscopic methods, electron microscopy, and scanning tunneling microscopy. Electrocatalysis can be studied using a unique *in situ* cell that allows electrochemistry to be studied without exposing the electrodes to air, which can lead to poisoning by adventitious species. In addition, a conventional benchtop electrochemical cell can be used, and as needed we can collaborate to use techniques such as scanning electrochemical cell microscopy (SECCM) and differential electrochemical mass spectrometry (DEMS). XPS, He^+ ion scattering (ISS), STM and STEM can be done at Utah, and we plan to collaborate with Sooyeon Hwang at Brookhaven National Lab for probe-corrected STEM.

The theoretical approach consists of a combination of grand canonical global optimization of supported clusters using a Genetic Algorithm or Basin Hopping approach, and grant canonical density functional theory (DFT). The cluster structures, landing sites on the supports, and stoichiometries are sampled simultaneously, allowing for adsorbate exchange with the solution phase, subject to the change of their chemical potential (e.g., pH, for hydrogen). The grand canonical DFT scheme explicitly charges the electrode surface and uses the capacitor model to estimate the free energy as a quadratic function of the applied voltage. The solvent and electrolyte are treated implicitly, with the linearized Poisson-Boltzmann non-uniform distribution of the background charge, to mimic the electric double layer in a computationally affordable manner. We note that the combination of grand canonical global optimization and DFT at constant potential is unique to our team and results from the joining the expertise of Alexandrova and Sautet. The approach accesses electrode restructuring and stoichiometric changes that would not be seen in the widely-used computational hydrogen electrode model. Other researchers use an improved approach, but without global optimization. This is crucial, since we see a dramatic change in the nature of the available active sites on the fluxional clusters, as the potential changes. Furthermore, we have found it necessary to include all accessible isomers of the adsorbate-covered clusters, and all reaction channels connecting them, to model the cluster size effects on electrocatalytic reactions.

Recent Progress

HER catalyzed by Pt_n/ITO and Pt_n/FTO

We started this project with a pair of studies examining hydrogen underpotential deposition (H_{upd}) and hydrogen evolution catalyzed by small Pt clusters deposited on ITO (J.

Am. Chem. Soc. 145 (2023) 5834-5845) and on FTO (Angew. Chem., Int. Ed. 135 (20), e202218210). In these studies, mass-selected Pt_n were deposited in ultra-high vacuum at 3% ML coverage on clean ITO and FTO electrodes, which where then transferred to an electrochemical cell where the HER was studied. The main results were:

1. Single Pt atoms do not catalyze HER, which DFT indicated was due to a high barrier to adsorption of a second H atom. Small Pt_n do catalyze HER, with activity that increases with increasing cluster size.

2. The clusters are reasonably stable under electrochemical cycling, probably due to the strong binding of Pt to the oxide supports, particularly ITO.

3. In the potential range between 0.45 and the HER threshold at ~0 V vs. RHE, there was substantial current attributed to underpotential deposition, i.e., adsorption of H^+_{aq} on the clusters to generate H_{ads}. For bulk Pt surfaces, this H_{upd} process saturates at one H atom *per* surface Pt atom, but the clusters were able to absorb ~2 H/Pt atom. DFT showed that this effect results from the fluxional nature of the clusters, which elongate on the oxide support as the potential is scanned toward the HER threshold, creating additional H atom binding sites.

4. In order to reproduce the observed cluster size effects by DFT, it was necessary to include all accessible isomers of the H-loaded clusters and all reaction pathways connecting them. If only the global minimum isomers were considered, the predicted size dependence was qualitative wrong, i.e., the size dependence proved to be a stringent test of the DFT modeling approach.

5. The mass activity of the Pt_n/ITO and Pt_n/FTO samples was found to increase from ~0 for Pt_1 to ~1 A/mg_{Pt} for Pt_8/ITO and to ~1.2 A/mg_{Pt} for Pt_7 and Pt_8 on FTO, both measured at -0.027 V vs. RHE. For comparison, the mass activity of the *surface monolayer* of polycrystalline Pt (Pt_{poly}) was measured to be ~0.5 A/mg_{Pt} under the same conditions. Note that any catalyst containing Pt nanoparticles of more than a few nm size (and therefore with bulk-like chemistry), would have mass activity lower than the surface layer of Pt_{poly}, i.e., small Pt_n/FTO or ITO have *very attractive mass activities*, probably because of their ability to distort to adsorb more H atoms than is possible for bulk Pt.

Activity and Stability of Pt_n on HOPG

Carbon-based electrodes are far more commonly used than ITO and FTO, and our current work focuses on electrodes prepared by depositing size-selected Pt_n clusters on HOPG, which was chosen because its structure is well characterized, unlike vitreous or typical high surface area carbon supports, allowing accurate DFT modeling. In preliminary experiments, we found that the Pt_n/HOPG catalysts were highly active for HER, ORR, and alcohol oxidation. Indeed, for HER, the mass activity was ~five times greater than for Pt_n/FTO, which as noted above, already had very attractive activity. For all these reasons, we are focusing on HOPG as an electocatalyst support.

The difficulty with HOPG is that the basal planes interact weakly with adsorbed metal clusters, such that the clusters tend to sinter rapidly even at room temperature in vacuum. It has been found that clusters can be stabilized on HOPG by deposition at high-enough energies to create defects, pinning the clusters. Some authors have also reported success with stabilizing clusters by first sputtering the HOPG surface, then soft landing clusters.

We are currently exploring two approaches to depositing and stabilizing small Pt clusters, exploiting our ability to independently control cluster size, deposition energy, and cluster coverage. We are exploring the effects of deposition energy on electrochemical activity, cluster stability, and sticking probability, to optimize deposition conditions. Sticking probability must

be measured because there are results by Murakami for Ag clusters showing that clusters, or fragments thereof, can backscatter from HOPG at intermediate energies, while energies above a cluster-size-dependent threshold lead to partial implantation. Pt_n are heavier than Ag_n, reducing the tendency to backscatter, and their higher cohesive energy should reduce fragmentation. We have used XPS on a series of Pt_n/HOPG samples to show that backscattering, if it occurs at all for Pt, is a minor effect, and to observe the onset of implantation.

As we work to determine the optimal deposition conditions, we are using XPS to probe sticking, He^+ ion scattering (ISS) to probe the fraction of Pt on the surface, vs. implanted, and electrochemistry to probe cluster size and stability. Once interesting conditions have been identified, we will use STM in a colleague's lab, and STEM (on multilayer graphene grids) both at Utah and Brookhaven National Lab to image the catalysts, revealing the structure and properties of the catalytic sites, so that DFT can be used to model the catalysts quantitatively.

Initially, we are using electrochemistry as a quick *in situ* probe of whether the clusters are exposed on the surface and whether they sinter or remain small. We are using HER and ORR as test reactions – HER because we want to measure H_{upd}, relating to the fraction of Pt atoms exposed on the surface, and because the reaction is fast. ORR is used because there is an interesting feature that we can exploit to qualitatively assess the cluster size and stability. We showed with previous CPIMS support that ORR on small clusters tends to produce substantial amounts of H_2O_2 in addition to the normal product, H_2O, and that the branching to H_2O_2 increases monotonically with decreasing cluster size. We observed this both for Pt_n/ITO and Pt_n/glassy carbon, and since then, several groups exploited this behavior to make selective H_2O_2 electrosynthesis catalysts by stabilizing Pt atoms and small clusters on other supports. While the quantitative relationship between cluster size and peroxide branching for Pt_n/HOPG still needs to be measured, we exploit the ease of electrochemical peroxide measurement, via the hydrogen peroxide oxidation reaction (HPOR) to probe how the size of the catalytic sites varies with the cluster size and deposition energy.

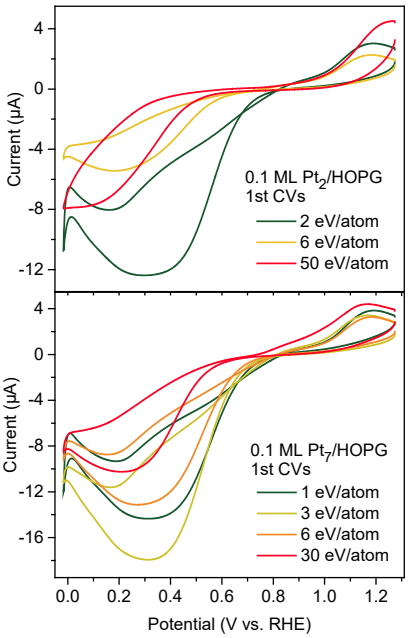

The results so far show that clusters soft landed result in catalysts that are highly active for HER and ORR, however, the cluster size effects are relatively weak, and the hydrogen peroxide branching in ORR is small – both factors suggesting some degree of cluster sintering. At cluster-size-dependent deposition energies in the 50 to 100 eV range, activities for the smallest clusters decrease, but the peroxide branching increases substantially, suggesting that cluster size is better preserved. The electrocatalytic currents are also quite stable over potential cycling, again suggesting that the clusters are pinned to the support.

A second approach to stabilizing clusters on HOPG was suggested by experiments of Yasumatsu, who used a W^+ ion beam to implant tungsten atoms in HOPG, and then soft-landed W_n clusters on the surface, which were found to be stably pinned. Furthermore, they found by STEM that W_6 landed on W-implanted HOPG formed clusters with 7 W atoms, presumed to represent W_6 clusters on the surface complexed to a single implanted W atom. We have just started to examine the analogous approach for Pt. We have shown that 0.05

ML of Pt atoms implanted in the surface at 100 eV have no electrochemical activity, and further, Pt implantation does not destabilize HOPG with respect to electrooxidation or other reactions. At 0.2 or 0.35 ML coverages, in contrast, the implanted Pt atoms are initially inactive, but activity grows rapidly during potential cycling, suggesting that Pt atoms implanted at such high loadings migrate to the surface and form clusters. The plan in these experiments is, therefore, to work only with implanted atom coverages low enough to avoid this problem, and then soft land Pt_n on top. Again, electrocatalysis will be used for initial assessment of cluster size and stability, but we then will use XPS, ISS, STM, and STEM to study the nature of the catalytic sites. Should Pt atoms not bind to carbon strongly enough to act as anchors, we can implant other atomic ions (e.g. W^+), prior to Pt_n soft-landing.

Future Plans:

Once suitable hard-landing or atomic anchoring conditions are identified, we will proceed with detailed experimental and theoretical studies of HER, ORR, CO redox, CO_2 reduction, and alcohol oxidation, starting with HER and ORR. Depending on how well the above methods produce active, stable clusters, we may also explore other approaches such as using O reactions or N reactions with sputtered HOPG to create larger, O- or N-functionalized defects to serve as binding sites.

Publications from this project (2021-2023):

1. Zhang, Z.; Masubuchi, T.; Sautet, P.; Anderson, S. L.; Alexandrova, A. N., "Hydrogen Evolution on FTO-Supported Ptn Clusters: Ensemble of Hydride States Governs the Size Dependent Reactivity", Ang. Chemie Int. Ed. e20221821, 2023, DOI: 10.1002/anie.202218210. Freely available version plus data files: chemrxiv.org/engage/chemrxiv/article-details/6393826acfb5ff2a84647dea
2. Kumari, S.; Masubuchi, T.; White, H.; Alexandrova, A. N.; Anderson, S. L.; Sautet, P., "Electrocatalytic hydrogen evolution at full atomic utilization over ITO-supported sub-nano Ptn clusters: High, size-dependent activity controlled by fluxional Pt hydride species.", J. Am. Chem. Soc., 145, 2023, 5834-5845, DOI: 10.1021/jacs.2c13063. Freely available version plus data files: chemrxiv.org/engage/chemrxiv/article-details/63d2f10c66069483f83f8722
3. Simran Kumari and Philippe Sautet, "Elucidation of the Active Site for the Oxygen Evolution Reaction on a Single Pt Atom Supported on Indium Tin Oxide", J. Phys. Chem. Lett., 14, 2635, 2023, DOI: 10.1021/acs.jpclett.3c00160. Freely available with data: escholarship.org/uc/item/8pg1p8f1
4. Zhang, Z.; Zandkarimi, B.; Munarriz, J.; Dickerson, C. E.; Alexandrova, A. N., "Fluxionality of Subnano Clusters Reshapes the Activity Volcano of Electrocatalysis", ChemCatChem, 14, e202200345, 2022, DOI: 10.1002/cctc.202200345. Freely available with data: chemrxiv.org/engage/chemrxiv/article-details/61b92cf6d1f6625b0338aec6
5. Munarriz, J.; Zhang, Z.; Sautet, P.; Alexandrova, A. N., "Graphite-supported Pt_n Cluster Electrocatalysts: Major Change of Active Sites as a Function of the Applied Potential", ACS Catal., 12, 14517, 2022, DOI: 10.1021/acscatal.2c04643. Freely available with data: chemrxiv.org/engage/chemrxiv/article-details/62f1c4efe78f7008a3348b24
6. Simran Kumari, Philippe Sautet, "Highly dispersed Pt atoms and clusters on hydroxylated indium tin oxide: a view from first- principles calculations", J. Mater. Chem. A, 9, 2021, 15724, DOI: 10.1039/D1TA03177E. Freely available with data: escholarship.org/uc/item/7rp8p99h

Probing Electrochemical Reactivity Under Nanoconfinement Using Molecularly Pillared Two Dimensional Materials

Award Number: DE-SC0020234

Veronica Augustyn (vaugust@ncsu.edu), Dept. of Materials Science and Engineering
North Carolina State University, Raleigh, NC 27695

Project Scope

The goal of this research is to understand how the confinement of liquid phase reactants within a layered material influences their electrochemical reaction kinetics. The hypothesis driving this research is that there will be an optimum interlayer spacing of layered materials to enable electrochemical reactivity in the interlayer. Layered and 2D materials have broad applications in catalysis and electrocatalysis, where it is hypothesized that the catalytically active sites reside at edges and surface defects. This research will investigate how the interlayer of these materials can be made accessible for electrocatalytic activity. Nanoconfinement has been shown to affect the physical properties of molecules and solvents and may be utilized to further tune electrochemical activity. This research utilizes a materials chemistry approach to define the nanoconfinement environment via molecular pillars – molecules of defined length anchored within the interlayer. To test this hypothesis, the research investigates how molecular pillaring of a layered material influences the electrocatalysis of the hydrogen evolution reaction (HER), which is of technological interest for the electrochemical synthesis of hydrogen fuel. The objectives of this research include: (1) The synthesis of layered materials with molecular pillars and controlled interlayer spacing; (2) Characterization of the structure, chemical composition, and dynamics of the interlayer confined molecules; and (3) Characterization and mechanistic understanding of a liquid-phase electrochemical reaction under nanoconfinement by these hybridized layered materials. The understanding in materials synthesis and electrochemistry developed over the course of this research will be applicable to both fundamental and applied electrochemical energy research.

Recent Progress

1. Synthesis and characterization of layered materials with molecular pillars that control the interlayer spacing. This project requires the synthesis of molecularly pillared layered materials. Our recent synthesis efforts focused on the pillaring of two redox-active transition metal oxide hosts, tungsten and titanium oxides.

Partial pillaring of $WO_3 \cdot nH_2O$: During the previous reporting period, we reported the synthesis and physical characterization of tungsten oxides fully-pillared by alkylamines (AA) and their electrochemical characterization.[1] We showed that fully pillared tungsten oxides restrict proton and ion insertion and this decreased the activity for the HER. Based on these results, we hypothesized that decreasing the pillar density will activate the interlayer for electrochemical reactivity, leading to phenomena such as the insertion of otherwise size-restricted cations and interlayer activity for the HER. To study the effects of pillar density, research efforts during this reporting period focused on (1) synthesizing low-pillar density WO_3, and (2) electrochemical characterization of these materials in Li^+ and TBA^+ non-aqueous electrolytes. The following strategies were employed to achieve partial pillaring of monodentate propylamine pillared WO_3: (2) synthetic control by adjusting the propylamine concentration in the precursor solution (AA : W molar ratio), (2) post-synthesis vacuum heating of the fully pillared structure, (3a) mixed

pillaring with two different chain lengths, and (3b) selective removal of one type of pillar through thermal treatment. We used scanning electron microscopy (SEM), XRD, and thermogravimetric analysis (TGA) to investigate the structure and chemical composition of molecularly pillared metal oxides. Using these methods, we conclude that the synthesis of molecularly pillared $WO_3 \cdot nH_2O$ proceeds through three sequential steps: (1) a rapid soft chemistry transformation leading to an expanded structure, (2) a subsequent dissolution reorganization step with two interlayer peaks, and finally (3) formation of a uniform crystalline pillared phase. We further investigated the electrochemical behavior of molecularly pillared tungsten oxides using cyclic voltammetry in non-aqueous electrolytes containing either a small cation (Li^+) or a "bulky" cation (TBA^+). Our results indicate that partial pillaring leads to higher degree of TBA^+ adsorption than in fully pillared or hydrated metal oxides, suggesting an increased accessibility of the interlayer upon partial pillaring.

Molecularly pillared $Na_2Ti_3O_7$: Our prior work on proton insertion into hydrogen titanates showed that electrochemical proton insertion is modulated by the degree of interlayer protonation, with a more "open" interlayer (most interlayer protonation) enabling the highest proton insertion capacity.[2] Recent work in our group showed that acidic electrolyte pK_a can modulate the proton-coupled electron transfer (PCET) reactions occurring at $H_2Ti_3O_7$ (HTO), including the hydrogen evolution reaction (HER).[3] HTO shows activity for the HER, with PCET involving both the bulk and surface. This project period, we synthesized molecularly pillared HTO to understand the relationship between the HER and bulk PCET processes. We developed a synthesis route towards molecularly pillared layered titanate using sodium titanate and an organohalide precursor, butylammonium chloride. We determined the acid-base ion exchange mechanism that leads to molecular pillaring of $Na_2Ti_3O_7$ and performed electrochemical characterization to distinguish surface vs. bulk PCET activity related to the HER.

Layered oxides with confined redox active molecules: In addition to studying the reactivity of liquid phase reactants within layered materials, we further studied the confinement of redox-active molecules in layered materials to understand how nanoconfinement alters electrochemical reactivity of the confined redox species. To do this, we reacted a redox-active molecule, aminoferrocene ($FcNH_2$), with a layered transition metal oxide, MoO_3. This synthesis yielded a blue solid, denoted as $FcNH_2$-MoO_3, which indicates the reduction of the initially white MoO_3. The reduction was not sufficient to lead to a structural transformation of layered MoO_3 via XRD. Electrochemical cycling of $FcNH_2$-MoO_3 showed two sets of redox peaks, ascribed to the redox of $Fe^{4+/3+}$ and $Fe^{2+/3+}$ in $FcNH_2$. Cycling over both redox peaks led to current fade within 25 cycles, likely due to the instability of the Fe^{4+}-containing $FcNH_2$. We analyzed the kinetics of the peak current associated with the $Fe^{2+/3+}$ redox couple between 10 to 100 mV/s and found that the peak current varies with $v^{1/3}$. The kinetics of this redox couple cannot be explained by liquid-phase processes, such as surface redox or semi-infinite diffusion, suggesting that aminoferrocene was not dissolved in the electrolyte. Instead, we propose that confinement leads to decreased kinetics for $Fe^{2+/3+}$ redox in $FcNH_2$-MoO_3 owing to mass transport of counter-ions within the solid. If $FcNH_2$ were confined in the interlayer of MoO_3, the solid-state mass transport of a counter-ion (PF_6^-) would be necessary to compensate for the positive charge of $FcNH_2$ upon oxidation. From kinetic models of finite diffusion in a cyclic voltammetry experiment, b-values < 0.5 arise from sluggish mass transport kinetics in the solid state coupled with the turnover potential of the cyclic voltammetry measurement.

2. Electrochemical hydrogen evolution reaction under confinement: In the last project period, we determined that electrochemical proton insertion was necessary to activate tungsten oxide

towards the HER.[1] This leads to an interesting scenario whereby the reactant species (H^+) can undergo electron transfer and either insert into the bulk or combine and evolve from the surface as H_2. Many redox-active transition metal oxides can undergo proton insertion and will exhibit changes in their bulk properties as a function of the inserted proton content including solid state phase transitions. This project period, we investigated the mechanism by which electrochemical proton insertion leads to increased HER activity of tungsten oxide hydrogen bronzes. We studied the influence of the structural water content and degree of proton insertion of tungsten oxides on their HER activity using electrochemistry coupled with operando XRD. From this study, we found that $WO_3 \cdot H_2O$ is the most active for the HER. We hypothesize that this is due to its favorable combination of fast solid state proton insertion kinetics and high degree of proton insertion. In addition to the benefit of increased electronic conductivity from the formation of a hydrogen bronze, the dependence of the HER on the structural water content suggests that inserted protons themselves participate in the HER. In effect, hydrogen tungsten oxide bronzes could provide a reservoir of protons and electrons at high overpotentials. This presents an intriguing and unexpected benefit of the solid state confinement/storage of protons and electrons in layered materials for improving the kinetics of the HER.

Future Plans

Using molecularly pillared materials synthesized this project period, we will perform characterization of the dynamics of the confined molecular pillars to better understand the available volume for electrochemical reactivity. We will also perform transmission electron microscopy (TEM) characterization of these materials to image the interlayer under confinement. We will further continue to characterize the electrochemical reactivity of the molecularly pillared materials using aqueous and non-aqueous electrochemical techniques coupled to in situ and operando techniques. We seek to understand the relationship between the molecular pillar density in pillared tungsten oxides and their electrochemical capacitance in non-aqueous electrolytes. We will also characterize the mechanism of the hydrogen evolution reaction on pillared titanium oxide to understand the relationship between the HER and bulk PCET processes, as we did for tungsten oxides. Finally, we will continue to synthesize layered oxides with redox-active molecules.

References

1. M.A. Spencer, J. Fortunato, & V. Augustyn. “Electrochemical Proton Insertion Modulates the Hydrogen Evolution Reaction on Tungsten Oxides.” *J. Chem. Phys.* 156 (2022) 064704.
2. S. Fleischmann, Y. Sun, N.C. Osti, R. Wang, E. Mamontov, D.E. Jiang, & V. Augustyn. “Interlayer Separation in Hydrogen Titanates Enables Electrochemical Proton Intercalation.” *J. Mater. Chem. A* 8 (2020) 412.
3. J. Fortunato, Y.K. Shin, M.A. Spencer, A.C.T. van Duin, & V. Augustyn. “Choice of Electrolyte Impacts the Selectivity of Proton-coupled Electrochemical Reactions on Hydrogen Titanate.” *J. Phys. Chem. C* 127 (2023) 11810.

Peer-Reviewed Publications Resulting from this Project (2021 – 2023)

1. M.A. Spencer, J. Fortunato, & V. Augustyn. “Electrochemical Proton Insertion Modulates the Hydrogen Evolution Reaction on Tungsten Oxides.” *J. Chem. Phys.* 156 (2022) 064704.

2. J. Fortunato, J.W. Jordan, G.N. Newton, D.A. Walsh, & V. Augustyn. “Electrochemical reactivity of atomic and molecular species under solid-state confinement.” *Curr. Opin. Electrochem.* 34 (2022) 101014.

Super-Reactive Charged Microdroplets for Non-Equilibrium Interfacial Reactions

DE-SC0022097

Abraham Badu-Tawiah

Department of Chemistry and Biochemistry, The Ohio State University, Columbus, OH 43210

badu-tawiah.1@osu.edu

Program Scope

This research program seeks to develop highly reactive microdroplet systems for direct activation of less reactive polyatomic molecules without the use of catalysts. We proposed to use plasma-microdroplet fusion experiments where energetic electrons and reactive oxygen species (**ROS**) generated in the non-thermal plasma are instantaneously captured into charged microdroplets during electrospray. We use plasma discharge that can be generated by intermittent electrical energy at atmospheric pressure. The combination of non-thermal plasma with charged microdroplets from electrospray will provide solution to two long-standing challenges in gas-phase plasma chemistry, which are (1) selectivity to exclude unwanted reactions and (2) product collection and scale-up. Our experiment provides a means to evaluate reaction yield as a function of various plasma parameters by coupling the plasma-microdroplet fusion system as an ion source to a mass spectrometer, allowing online reaction studies and product characterization.

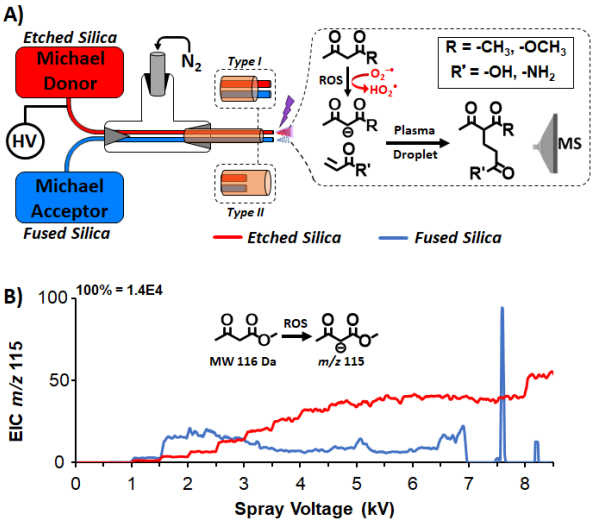

Figure 1. (**A**) Contained-electrospray ionization platform for fusing non-thermal plasma from etched silica capillary with microdroplets from fused silica capillary. ROS in the nonthermal plasma enables the activation of Michael donor reagents, which subsequently reaction with Michael acceptors during the fusion experiment to enable uncatalyzed C-C bond formation. (**B**) Extracted ion chronogram (EIC) for the formation of the Michael donor species from methylacetylacetate via etched capillary (red line) versus traditional electrospray (blue line).

Recent Progress

In our initial experiments, we have observed that chemically etched silica capillaries can produce non-thermal plasma discharge at low (3 kV) electrospray voltages and maintain stable spray during plasma discharge up to 7 kV of direct current (DC) high voltage (**Figure 1B**). This phenomenon is interesting because traditionally, electrospray and non-thermal plasma discharge are separate and incompatible physical processes. The mechanism of maintain plasma discharge in the wake of electrospray microdroplet generation is a topic of an ongoing fundamental study in our research group. However, we suggest the etched silica capillaries

facilitate plasma formation due to their physical properties including surface roughness, wettability, conductivity, and sharpness of the emitter tip produced via etching. We hypothesize that super reactive and analytically useful charged microdroplets can be created at low (3 kV) onset voltages by fusing the **ROS** from etched silica capillaries with microdroplets generated from conventional electrospray in a contained setup (**Figure 1A**). That is, the non-thermal discharge (plasma) from the etched capillary is allowed to mix (fuse) with charged microdroplets generated from deactivated fused silica capillary in real-time by spraying the two separate capillaries co-axially. The resultant plasma-microdroplet system is coupled with mass spectrometry (**MS**) to study the reaction cascade. The presence of ROS (e.g., $O_2^{\bullet-}$) in the plasma-microdroplet fusion experiment has been confirmed through (i) the use of radical scavenging reagent, (ii) characterization of internal energy distribution, and (iii) controls experiments performed without plasma, which lacked reaction acceleration. The fusion of ROS from the etched capillary with charged droplets from the fused silica can be brief (Type I operation mode, microseconds) or extended (Type II operation mode, seconds). The two operational modes are illustrated as inserts at the outlet of the emitter shown in **Figure 1A.**

Our method for producing etched silica capillaries is based on the use diluted hydrofluoric acid (HF; 10 % v/v), which is desirable to maximize user safety. We have optimized the HF chemical etching process so that up to five (5) emitters can be created at the same time, in a high throughput manner. Importantly, the process is reproducible, generating emitter tips that have comparable surface morphology and tip size, as well as their reproducible generation of reactive species when included in our novel contained-electrospray source. **HF Acid Safety Statement**: HF acid is very corrosive and hazardous due to production of fluoride anion. Extreme care should be taken to prevent bodily exposure to HF vapor and liquid. HF solutions should be handled only in a well-ventilated hood with chemically resistant PTFE containers and butyl rubber gloves.

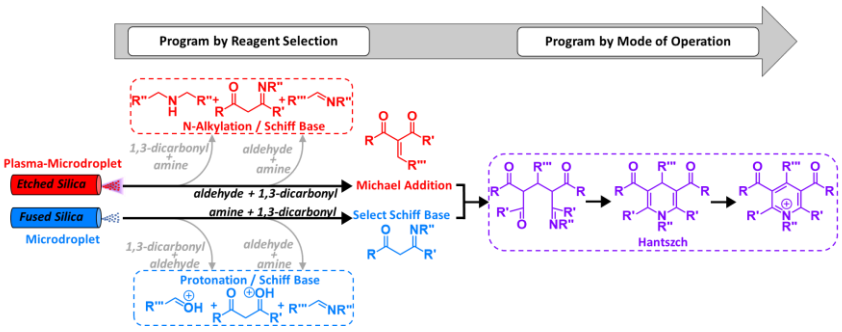

Figure 2. Programmable Hantszch cascade reaction sequence highlighting reaction programmability via reagent selection in co-axial etched and fused silica spray capillaries for Michael addition and Schiff base product selection, respectively, and programmability via platform operational mode to produce select Hantszch cascade reaction products.

We have used the plasma-microdroplet fusion phenomenon to study epoxidation reactions, uncatalyzed N-alkylation reactions, Michael addition, and Hantszch reaction. In this abstract, our ability to program cascade reactions in charged microdroplets is highlighted using Michael addition, Schiff's base, and Hantszch reactions. The Hantzsch synthesis is a classic multi-component reaction for the synthesis of 1,4-dihydropyridines. The reaction can be thought of as proceeding in several discrete steps; several byproducts can be formed if the reaction is not careful

controlled. In particular, the symmetric Hantzsch product often dominates, as opposed to the desired asymmetric product, when conducted through a one-pot system. As illustrated in **Figure 2**, we can program such multi-component cascade reactions through a selective spray system to independently generate the required intermediate, followed by the fusion of the intermediates in real-time. By controlling microdroplet lifetime (i.e., distance droplets traveled), we can select the type of Hantzsch product, symmetric versus asymmetric.

Our ability to program multi-component reactions using the plasma-microdroplet fusion system was demonstrated through (1) a novel reagent selection strategy in which nucleophiles (e.g., amines and alcohols) were turned into Michael acceptors for the first time and (2) the synthesis of symmetric and asymmetric 1,4-dihydropyridines. For example, the synthesis of symmetric 1,4-dihydropyridine derivative is illustrated in **Figure 3** where Michael addition and Schiff's base reactions were performed in parallel via the etched and fused silica electrosprays, respectively (**Figure 3A-C**), which fused to give the intermediate detected at *m/z* 376 (**Figure 3D**). By controlling microdroplet mixing time, which is in turn controlled by distance droplets travel (**Figure 3E**), we were able detect three specific species in the corresponding Hantzsch reaction (*m/z* 376, 358, and 356), with the abundance of final symmetric Hantzsch product reaching maximum at 10 mm (**Figure 3E,iii**).

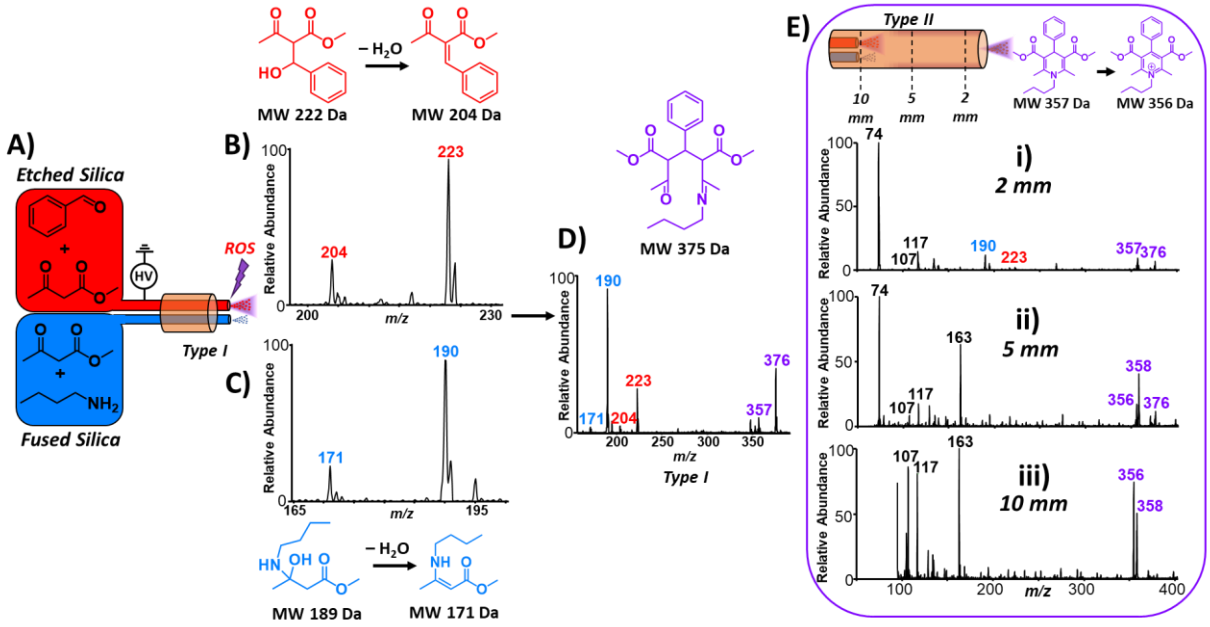

Figure 3. Methyl acetoacetate symmetric Hantzsch cascade reaction via plasma-water microdroplet fusing platform with **A**) reaction platform configuration showing spray of methyl acetoacetate and benzaldehyde from the etched silica capillary for Michael addition via plasma-water microdroplet fusion and methyl acetoacetate and butylamine from the fused silica capillary for enamine product formation via microdroplet. **B**) Mass spectrum for intermediate production of Michael addition products from the etched silica capillary at *m/z* 223 and 204. **C**) Mass spectra for intermediate production of enamine products from the fused silica capillary at *m/z* 190 and 171. **D**) Mass spectrum of initial coupling product at *m/z* 376 via Type I plasma-water microdroplet fusion. Type II plasma-water microdroplet operation is shown in **E**) with a 2 mm reaction cavity in i), a 5 mm reaction cavity in ii), and a 10 mm reaction cavity in iii) demonstrating the effect of cavity size on Hantzsch cascade product formation.

Future Plans

The focus of our work will remain (i) the development and refinement of methodologies to activate polyatomic ions in charged microdroplets, (ii) the development of suitable spray systems for large-scale product collection, and (iii) application to more inert compounds such as CO_2.

Recent Publications

1. Grooms, A.J.; Nordmann, A.; Badu-Tawiah, A.K. "Dual Tunability for Uncatalyzed N−Alkylation of Primary Amines Enabled by Plasma−Microdroplet Fusion" *Angew. Chem. Int. Ed.* **2023.** DOI:10.1002/ange.202311100
2. Grooms, A.J.; Nordmann, A.N.; Badu-Tawiah, A.K. "Plasma-Droplet Reaction Systems: A Direct Mass Spectrometry Approach for Enhanced Characterization of Lipids at Multiple Isomer Levels" *ACS Meas. Sci. Au* **2023**, 3, 1, 32–44.
3. Sahraeian, T.; Amoah, E.; Kulyk, D.S.; Badu-Tawiah, A.K. "High-Throughput Nanoliter Sampling and Direct Analysis of Biological Fluids Using Droplet Imbibition Mass Spectrometry" *Anal. Chem.* **2023**, 95 (18), 7093 -7099.
4. Amoah, E.; Kulyk, D.S.; Callam, C.S.; Hadad, C.M.; Badu-Tawiah, A.K. "Mass Spectrometry Approach for Differentiation of Positional Isomers of Saccharides: Toward Direct Analysis of Rare Sugars" *Anal. Chem.* **2023**, 95, 13, 5635–5642.
5. Burris, B.J.; Walsh, L.C.; Badu-Tawiah, A.K. "Online Cross-Linking of Peptides and Proteins during Contained-Electrospray Ionization Mass Spectrometry" *Anal. Chem.* **2023**, 95, 2, 1085–1094.
6. Sahraeian, T.; Kulyk, D.S.; Fernandez, J.P.; Hadad, C.M.; Badu-Tawiah, A.K. "Capturing Fleeting Intermediates in a Claisen Rearrangement Using Nonequilibrium Droplet Imbibition Reaction Conditions" *Anal. Chem.* **2022**, 94, 43, 15093–15099.
7. Sahraeian, T.; Zheng, J.; Lalisse, R.; Hadad, C.; Wu, Y.; Badu-Tawiah, A.K. "Resolving Graphite-Electrolyte Interphase in Li-Ion Batteries Using Air-Tight Ambient Mass Spectrometry" *Batteries & Supercaps* **2022**, e202200280.
8. Kulyk, D.; Wan, Q.; Sahraeian, T.; Badu-Tawiah, A.K. "Dehydration of gas-phase benzyl amine alcohols studied at atmospheric pressure" *International Journal of Mass Spectrometry* **2022**, 476, 16836.

Ultrafast Chemistry in Confined Environments: Understanding the role of H-bond dynamics

Award Number: DE-SC0023221
PI: Carlos R. Baiz, Associate Professor
Department of Chemistry, University of Texas at Austin,
105 E 24th St. A5300, Austin, TX 78712, USA
cbaiz@cm.utexas.edu

Project Scope

Characterizing molecular ensembles in confined or interfacial environments is the first step to obtaining fundamental models of chemical reactions in heterogeneous environments, particularly in multicomponent solutions. This DOE-funded project seeks to study ultrafast chemical dynamics in highly heterogeneous liquid-liquid and solid-liquid interfaces under confinement. We seek to investigate polymer dynamics at heterogeneous oil-water interfaces, and electron transfer processes in cosolvent mixtures using a suite of surface-sensitive methods including surface-enhanced infrared spectroscopy (SEIRAS), ultrafast methods, including two-dimensional infrared (2D IR) spectroscopy, and molecular dynamics (MD) simulations to interpret experimental results. Specifically, we study surfactant-water interfaces in reverse micelles and quantify the role of electrostatics and hydrogen bonding interactions in driving preferential localization of monomers and polymers towards surfactant interfaces. In addition, we investigate the role of microscopic liquid-liquid phase separation on electrocatalytic processes. Given the importance of interfacial and electrocatalytic processes in converting renewable electricity into sustainable materials, this project addresses the immediate need to develop a complete understanding of the molecular interactions that drive these processes in heterogeneous systems.

Recent Progress

Our progress on this project is on three separate fronts: 1. Characterizing surfactant interfaces, and chemical reactivity under confinement, focusing on interactions of polymers with surfactants. 2. Understanding electrochemical processes under confinement. 3. Development of transient and surface-sensitive ultrafast spectroscopy methods.

We have made significant progress along three goals with two peer-reviewed publications (see Publications below) and several seminar presentations on the first goal, along with a submitted manuscript on the second goal. We have begun developing surface-sensitive 2D IR methods to investigate dynamics at solution-electrode interfaces. Here we provide a summary of the main results from both goals:

Characterizing surfactant interfaces

Reverse micelles provide a unique platform to investigate the localization of polymers to the oil/water interface. Characterizing the environment around which chemical reactions take place is essential for controlling chemistry, and in a confined environment, molecular localization and interfacial effects play a significant role. For example, reactants and products can partition to

different regions of the interface. In the initial part of this project, we sought to investigate the interactions of charged polymers around charged interfaces (**Figure 1**). To control the interfacial charge, we used a neutral surfactant, sorbitan monostearate, the cationic DTAB, and anionic SDS surfactant, which were used as co-surfactants. The cationic polymer PEI was used to observe the role of attractive and repulsive electrostatic interactions in driving partitioning at the interface. We probed the ester carbonyl vibrations of the sorbitan monostearate, which are precisely located at the hydrophobic/hydrophilic interface and serve as localized reporters of hydrogen-bond structure and dynamics at the interface. Specifically, we used 2D IR spectroscopy to measure the frequency fluctuations of the carbonyls, whereby the changes in the frequency fluctuation correlation function are sensitive to changes in the dynamics of the environment that result from polymer-surfactant interactions as well as the disruption of the H-bond network. In brief, the measurements revealed a strong drive for polymers to localize to the interface and that electrostatic charge alone is not sufficient to predict polymer-surfactant interactions.

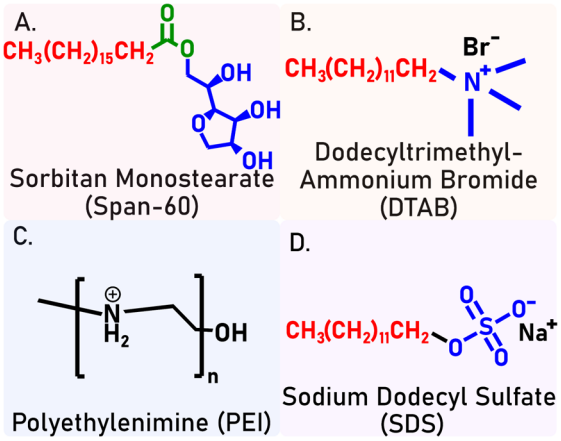

Figure 1: A. Structure of Span-60, the nonionic surfactant used in this study. The ester carbonyl, which serves as the vibrational probe in the experiments is shown in green. B. Structure of the cationic co-surfactant DTAB. C. Structure of the cationic polymer PEI. The secondary amine group becomes protonated at low pH. D. Structure of the anionic co-surfactant SDS. Reproduced from *J. Phys. Chem. B 2023, 127, 12, 2829–2836*

In the second part of this project, we investigated the relationship between the size of the reverse micelle and the interfacial dynamics using the well-studied surfactant AOT. The goal of this project was to extend current theories on how solvation dynamics change in reverse. Multiple studies have supported the "core/shell" model; a description of how the relative population of interfacial and bulk water varies as the size of the reverse micelle. In essence, the model is built on the co-existence of two environments: free "core" water and bound "shell" water.[1] Free water is defined as water that is separated from the interface and has essentially bulk-like characteristics. However, it is important to obtain chemical insight into how the interface itself changes with respect to the size variation and how these changes affect the interfacial solvation dynamics. To address this challenge, we measured the H-bond dynamics of reverse micelle interfaces as a function of size. We employed a combination of ultrafast two-dimensional infrared (2D IR) spectroscopy of the AOT ester carbonyl groups alongside newly developed analysis techniques to extract dynamics from overlapping vibrational transitions.[2] Our investigation focused on two AOT surfactant rotamers (**Figure 2**), one probing the confined water pool exclusively (with both carbonyls oriented towards the aqueous phase), while the other rotamer probing the interfacial water and the oil-phase dynamics simultaneously (one carbonyl towards the aqueous and other carbonyls towards the nonpolar phase). Our findings suggest that as reverse micelle size increases, the solvation dynamics of the two different surfactant rotamers increased. Moreover, the relative populations of these two

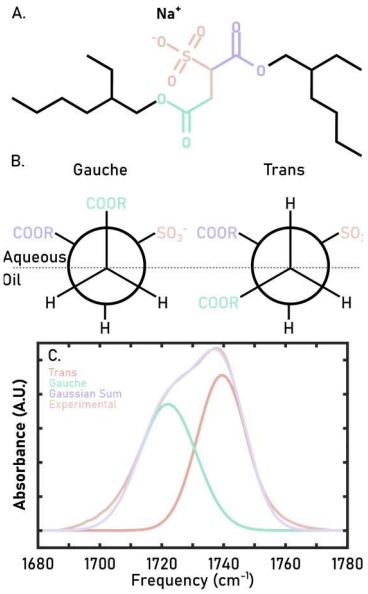

Figure 2: A. Structure of AOT. The headgroup is shown in pink and the two ester carbonyl moieties are colored in purple and teal, and the nonpolar chains are represented in black. **B.** Newman projection of the two different AOT conformation. **C.** Measured FTIR spectrum from 1680-1780 cm^{-1} shown in pink. Two-Gaussian showing the trans and gauche conformations in orange and teal, respectively. The sum of the two Gaussians is shown in purple. Reproduced from Garrett and Baiz, Journal of Physical Chemistry B, In press (2023).

rotamers also displayed size-dependent changes due to the water penetration into the interface. The measurements demonstrate that the interface undergoes substantial chemical changes and is not static as a function of reverse micelle size.

Electrochemical Processes Under Confinement

The hydrogen evolution reaction (HER), producing H_2 from water, is perhaps one of the most important electrochemical reactions, both from a fundamental, mechanistic, perspective as well as from its potential impacts as society transitions to renewable energy sources in the coming decades. Mechanistically, HER is a complicated reaction since water acts both as a reactant and a solvent, and despite decades of studies with a suite of techniques, the process is sufficiently complex that its mechanistic underpinnings are still debated.[3] In part this debate stems from the lack of knowledge about the interfacial properties how bulk solution conditions translate to interfacial environments at the electrode and how those environments drive reaction kinetics.

As part of this project, we investigate local hydrogen-bond networks at the electrode interface using surface-enhanced IR absorption spectroscopy (SEIRAS) which provides ~100 nm surface sensitivity and can measure changes in the local hydrogen-bonding environment as a function of potential (**Figure 3**).[4] We have chosen to use DMSO as a cosolvent due to its chemical properties including 1. The local heterogeneity that arises from DMSO's amphiphilic nature as well as 2. The ability of DMSO to disrupt the donor-acceptor balance at the interface. The measurements are then interpreted using MD simulations.

Spectra in the S=O stretching region, as well as the O–D stretching region, show that DMSO is dehydrated at the interface compared to the bulk, and that water only experiences minor changes in H-bond environments compared to the bulk. These measurements, together with the simulations, support the interpretation that DMSO forms clusters at the interface, leading to partially-dehydrated environments, as a result of the donor-acceptor imbalance. On the other hand, water remains relatively unchanged. Furthermore, simulations show that water molecules at the gold electrode interface assume a "buckled" configuration that further constrains its hydrogen-bonding geometries. These configurations persist for two solvation shells. Simulations also predict the size of water clusters to be between ~40 and 5 molecules as DMSO concentrations increase from 10 to 70 mol%. Altogether these results have important implications for the hydrogen evolution reaction. Namely the small water cluster sizes might inhibit hydrogen bonding of interfacial water molecules with the bulk inhibiting proton diffusion as required for efficient HER processes. In conclusion,

cosolvents can be used to control interfacial properties, and our initial studies have begun to elucidate the relationship between bulk concentrations and interfacial environments.

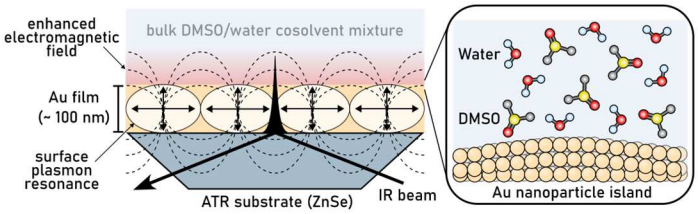

Figure 3: Figure 2. Illustration of an experimental SEIRAS setup with a water-DMSO cosolvent mixture (red gradient) on a gold surface (yellow) deposited on an attenuated total reflectance (ATR) prism (blue trapezoid). The dashed black lines represent the enhanced electromagnetic field from the generated surface plasmon resonances. A zoomed-in view of the interface is shown in the box on the right. Adapted from 10.26434/chemrxiv-2023-2fc3w.

Future Plans

We have recently finished our "open circuit" studies of cosolvents at bulk interfaces using SEIRAS. The immediate goals are to 1. Expand the set of organic cosolvents to obtain a more general view of how the donor-acceptor ratio is affected at the interface and how these properties change with concentration. 2. Explore the effect of electrochemical potential on the local H-bond environment using the same mixture of cosolvents characterized above. In particular, we seek to understand the effects of clustering and preferential solvation of gold at different voltages. 3. The future goal of this project is to link dynamics to electrochemical properties. We are currently working on implementing surface-enhanced 2D IR spectroscopy to measure not only the H-bond populations but also the interfacial dynamics to obtain a complete picture of the relation between interfacial environments and electrochemical properties.

References

1. Piletic, I. R.; Moilanen, D. E.; Spry, D.; Levinger, N. E.; Fayer, M., Testing the core/shell model of nanoconfined water in reverse micelles using linear and nonlinear IR spectroscopy. *The Journal of Physical Chemistry A* **2006,** *110* (15), 4985-4999.
2. Gurung, A.; Kuroda, D. G., A new method based on pseudo-Zernike polynomials to analyze and extract dynamical and spectral information from the 2DIR spectra. *The Journal of Chemical Physics* **2023,** *159* (3).
3. Kahyarian, A.; Brown, B.; Nesic, S., Mechanism of the hydrogen evolution reaction in mildly acidic environments on gold. *Journal of The Electrochemical Society* **2017,** *164* (6), H365.
4. Ataka, K.; Stripp, S. T.; Heberle, J., Surface-enhanced infrared absorption spectroscopy (SEIRAS) to probe monolayers of membrane proteins. *Biochimica et Biophysica Acta (BBA)-Biomembranes* **2013,** *1828* (10), 2283-2293.

Peer-Reviewed Publications Resulting from this Project (2022/06-2023/10)

1. Paul Garrett, and Carlos R. Baiz*, "*Hidden Beneath the Layers: Extending the Core/shell model of Reverse Micelles*", Journal of Physical Chemistry B, (2023) In press.
2. Paul Garrett, Joseph C. Shirley, and Carlos R. Baiz*, "Forced Interactions: Ionic Polymers at Charged Surfactant Interfaces", Journal of Physical Chemistry B 127.12 (2023): 2829-2836.

Chemical and Optical Control of Spin Crossover: Ultrafast XUV Spectroscopy of Molecular Magnets in Native Solvation Environments, DESC0020977

L. Robert Baker
100 W. 18th Ave.
Newman-Wolfrom Laboratory
The Ohio State University
Columbus, OH 43210
Email: baker.2364@osu.edu

Project Scope

In this work we utilize extreme ultraviolet (XUV) spectroscopy and sum frequency generation vibrational spectroscopy as probes of charge, spin, and solvation structure and dynamics in molecules and at interfaces. Progress in this project has been made in three areas: First, we have utilized ultrafast XUV reflection spectroscopy to measure electron and hole relaxation and trapping at TiO_2 surfaces.[1] These measurements provide assignments of the photoexcited states in TiO_2 during above band gap illumination (UV light) and below band gap illumination (visible light) where photoexcitation occurs through mid-gap states. We also resolve ultrafast electron and hole thermalization processes and show the effect of O vacancy defects on ultrafast hole trapping.

Second, we have made progress in extending these studies to molecular systems for understanding spin crossover dynamics in molecular magnets. The pentanuclear cluster, $Co_3Fe_2(tmphen)_6(\mu\text{-}CN)_6(t\text{-}CN)_6$ (tmphen = 3,4,7,8-tetramethyl-1,10-phenanthroline, abbreviated: Co_3Fe_2) is known to undergo a light-induced metal-to-metal charge transfer transition that leads to an ultrafast spin crossover. Understanding the mechanism of this charge transfer-induced spin transition requires the ability to resolve short lived intermediates with element, oxidation, and spin-state specific resolution, which can be achieved using ultrafast XUV spectroscopy at the Co and Fe M-edges. However, dynamics in this molecule are complicated by the fact that the ground state spin configuration is extremely sensitive to solvation environment, where H-bonding solvents induce a change from a high spin (S=7/2) to a low spin (S=3/2) state. In this project, we use a combination of near-ambient pressure X-ray photoelectron spectroscopy (NAP-XPS) and vibrational sum frequency generation spectroscopy (VSFG) to study the effect of chemical environment on the charge and spin states of the Co_3Fe_2 complex.[2]

Third, we have recently extended VSFG studies to understand cation hydration and interfacial solvation structures at metal electrode / aqueous electrolyte interfaces. This work seeks to address long-standing questions related to specific ion effects in CO_2 electrocatalysis. Considering the alkali cations, the rate of CO_2 reduction scales with the composition of the electrolyte in the order $Li^+ < Na^+ < K^+ < Rb^+ \approx Cs^+$. In this project, we have demonstrated the ability to measure cation-dependent hydration radii and interfacial water spectra, which both show strong correlations with CO_2 reduction activity.[3-5] This work has led to a collaboration with Prof. David Limmer (UC Berkeley) to understand ion pairing interactions and associated solvation structures at electrochemically active interfaces.[6]

Recent Progress

Visible Light Absorption and Hot Carrier Trapping in Anatase TiO_2

Anatase TiO_2 is a widely studied semiconductor photocatalyst, with applications in water splitting for clean H_2 production, pollutant degradation, hydrophilic protective coatings, dye-sensitized solar cells, and transparent electronics. However, developing these applications depends on understanding the properties, which govern the optical absorption and charge carrier transport. In photocatalytic applications, the high band gap of TiO_2 (3.2 eV) prevents visible light absorption,

and many attempts have been made to decrease the TiO_2 band gap for solar-driven photocatalysis. An attractive option is doping with O vacancy defects. The unoccupied oxygen site reduces neighboring Ti sites, which introduces two electronic mid-gap states. The first is a deep trap (small polaron, "SP") ~1 eV below the conduction band, which is a direct result of the O vacancy electrons creating local Ti^{3+} centers representing a small electron polaron. The second is a shallow trap near the conduction band edge (large polaron, "LP"). Despite the increased visible light absorption, which is promoted by exciting through the mid-gap states, the photophysics of O vacancy doped TiO_2 has remained an important open question.

In this project, we have employed XUV reflection spectroscopy at the Ti M-edge to study the electron and hole dynamics in TiO_2. Specifically, we compare the excited state dynamics following absorption of visible light (400 nm) by mid-gap defect states with the dynamics induced by direct band gap excitation using UV light (267 nm). Results show that visible light absorption occurs via promotion of an electron from the small polaron state to the TiO_2 conduction band as shown by pathway 2 in Figure 1A. In contrast, absorption of UV light results in direct band gap excitation followed by carrier relaxation during which hot holes trap as small polarons in 45 ± 42 fs, and hot electrons couple to polar optical phonons leading to vibrational coherence and large polaron formation in 945 ± 92 fs. These relaxation dynamics are schematically depicted in Figure 1B. This work has been published in *Journal of Physical Chemistry C*.[1]

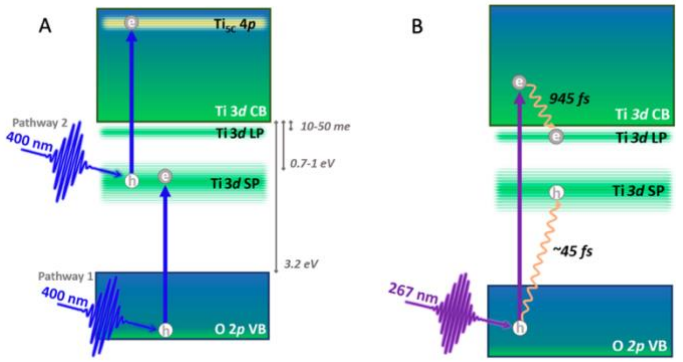

Figure 1. Two possible pathways for visible light absorption in O vacancy doped TiO_2 (A). Ultrafast XUV measurements at the Ti M-edge show that pathway 2 is primarily responsible for absorption of below band gap light. Depiction of ultrafast electron and hole thermalization and trapping rates in TiO_2 (B). Adapted from Ref. 1.

Water-Mediated Charge Transfer and Electron Localization in a Co_3Fe_2 Complex

In this project, we have also investigated the effects of temperature and chemical environment on a pentanuclear cyanide bridged, Co_3Fe_2 trigonal bipyramidal complex. Using element and oxidation state specific NAP-XPS to probe charge transfer and second order, nonlinear vibrational spectroscopy to probe symmetry changes based on charge (de)localization, a detailed picture of environmental effects on charge-transfer induced spin transitions was obtained. The Co_3Fe_2 molecular cluster shows significant changes in electronic behavior depending on chemical environment. NAP-XPS confirms that temperature changes induce a metal-to-metal charge transfer between a Co and Fe center, while cycling between ultrahigh vacuum and 2 mbar water at constant temperature, causes oxidation state changes not fully captured in a simple MMCT picture. VSFG measurements provide insight into the role of the cyanide ligand, which controls the electron (de)localization via the superexchange coupling. Spectral shifts and intensity changes in the VSFG spectra in the presence and absence of water vapor indicate a change from a charge delocalized, Robin-Day Class II/III high spin state in the absence of water to a charge localized, Class I low spin state in the presence of water. This change in Robin-Day classification of the complex as a function of chemical environment results in reversible switching of the dipole moment, analogous to molecular multiferroics. This chemically induced switch is schematically depicted in Figure 2. DFT calculations performed in collaboration with Prof. John Herbert (Ohio

State) and Prof. Christine Morales (University of Mount Union) confirm that in the charge delocalized, high spin state of the system, spin density is delocalized over multiple metal centers as well as the bridging CN ligands, consistent with a Class II/III electronic structure. These results illustrate the important role of chemical environment and solvation on underlying charge and spin transitions in this and related complexes and lay the foundation for future time-resolved studies of charge transfer induced spin transitions as a function of solvation environment. This work have been submitted for publication and is currently under review.[2]

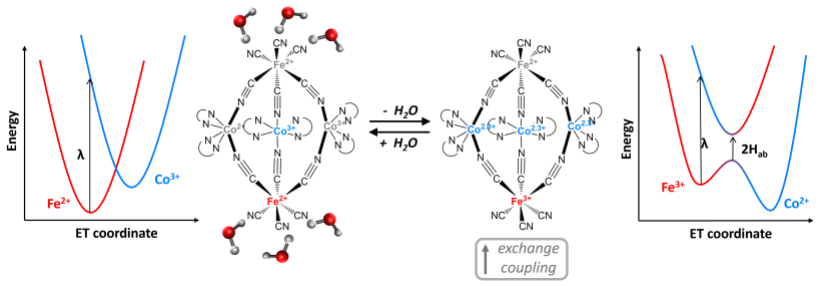

Figure 2. Change in the electronic structure of Co_3Fe_2 in the presence (left) and absence (right) of water vapor. On the left, the molecule has H-bonding water molecules at the terminal cyanide ligands, reducing the coupling and resulting in a Class I system. On the right, exchange coupling increases upon dehydration and the system behaves as a Class II/III molecule with indistinguishable Co oxidation states and the absence of an equatorial dipole.

Effects of Cation Hydration and Interfacial Solvation on Electrochemical CO_2 Reduction

In this project we have also applied VSFG spectroscopy to study the effects of cation hydration, interfacial electric fields, and interfacial solvation structure on the kinetics of electrochemical CO_2 reduction and the competing H_2 evolution reaction. Many reports indicate that the identity of the hydrated cation at the charged interface determines its catalytic activity, although the mechanism behind specific ion effects on CO_2 reduction remains an open question. Motivated by these observations, we have used VSFG to study cation hydration and interfacial electric fields on Au electrodes during active CO_2 reduction using CO as a vibrational Stark reporter.

Plasmon-enhanced VSFG signal enables detection limits of less than 1% of a surface monolayer during conditions of active CO_2 reduction.[7] Using this method, we can differentiate between CO adsorbed indiscriminately to the Au electrode due to CO purging of the electrolyte solution compared to intermediate CO formed selectively at active surface sites via in situ CO_2 reduction. Analysis of the potential dependent frequency shifts provides an estimate of the cation hydration radius within the Stern layer, which differs significantly between these two types of surface sites. Results show that at planar terraces, which are not active for CO_2 reduction, cations in the Stern layer retain their entire bulk hydration shell, while at undercoordinated active sites, cations adsorb to the Au with only a single layer of water in hydration shell. Measurements also show that the total interfacial electric field can be separated into two contributions: one from the electrochemical double layer (Stern field) and another from the polar solvation environment (Onsager field). Surprisingly, correlating VSFG spectra with reaction kinetics reveals that it is the solvation-mediated Onsager field that governs the chemical reactivity at the electrode/electrolyte interface. This work has been published in *Chemical Science and JACS Au*.[3-4]

More recently, we have begun to measure the spectra of interfacial water at the electrode/electrolyte interface. From these spectra, we can detect the presence of OH^- and CO_3^{2-} in the electrochemical double layer, which form from water reduction and bicarbonate reduction, respectively. Measuring the relative concentrations of these species provides information about the potential dependent proton source for H_2 evolution, and this work has been published in *Chemical Science*.[5] Finally, this work has led to an active collaboration with Prof. David Limmer to understand the effects of ion pairing and associated interfacial solvation structures on the

measured spectra of interfacial water. This collaboration has led to one submitted manuscript that is currently under review.[6]

Future Plans

Building from this work, we are actively pursuing two future directions: First, we will seek to correlate the VSFG spectra of interfacial water at active electrochemical interfaces with the presence of ion pairs and the influence of these ion pairs on the net alignment of interfacial water. Already, we have observed a strong correlation between the spectra of interfacial water as a function of electrolyte composition with the activity for electrochemical CO_2 reduction. This suggests that electrolyte composition influences H-bonding structure at metal surfaces in a way that significantly influences the kinetics of CO_2 activation. Correlating these interfacial water spectra with the formation of specific ion pairing interactions promises to provide molecular understanding of the mechanism for specific ion effects in electrocatalytic CO_2 reduction. Second, we plan to build on the work showing solvation-dependent electronic structure in photo-switchable molecular complexes such as Co_3Fe_2 to investigate the mechanism of light-induced spin state switching of these complexes in their native solvation environments using ultrafast XUV spectroscopy.

Peer Review Publications Resulting from this Project (2021–2023)

(Publications between 2021–2023 acknowledging CPIMS support are highlighted below)

References

1. Hruska, E.; Husek, J.; Bandaranayake, S.; Baker, L. R., Visible Light Absorption and Hot Carrier Trapping in Anatase TiO_2: The Role of Surface Oxygen Vacancies. *The Journal of Physical Chemistry C* **2022,** *126* (26), 10752-10761.
2. Hruska, E.; Zhu, Q.; Biswas, S.; Fortunato, M.; Broderick, D.; Mareles, C.; Herbert, J.; Turro, C.; Baker, L. R., Water-Mediated Charge Transfer and Electron Localization in a Co_3Fe_2 Cyanide-Bridged Trigonal Bipyramidal Complex. *ChemRxiv* **2023**.
3. Zhu, Q.; Wallentine, S. K.; Deng, G.-H.; Rebstock, J. A.; Baker, L. R., The Solvation-Induced Onsager Reaction Field Rather than the Double-Layer Field Controls CO_2 Reduction on Gold. *JACS Au* **2022,** *2* (2), 472-482.
4. Rebstock, J. A.; Zhu, Q.; Baker, L. R., Comparing interfacial cation hydration at catalytic active sites and spectator sites on gold electrodes: understanding structure sensitive CO_2 reduction kinetics. *Chemical Science* **2022,** *13* (25), 7634-7643.
5. Deng, G.-H.; Zhu, Q.; Rebstock, J.; Neves-Garcia, T.; Baker, L. R., Direct observation of bicarbonate and water reduction on gold: understanding the potential dependent proton source during hydrogen evolution. *Chemical Science* **2023,** *14* (17), 4523-4531.
6. Dodin, A.; Deng, G.-H.; Rebstock, J.; Zhu, Q.; Limmer, D. T.; Baker, L. R., Sodium Carbonate ion complexes modify water structure at electrode interfaces. *ChemRxiv* **2023**.
7. Wallentine, S.; Bandaranayake, S.; Biswas, S.; Baker, L. R., Plasmon-Resonant Vibrational Sum Frequency Generation of Electrochemical Interfaces: Direct Observation of Carbon Dioxide Electroreduction on Gold. *The Journal of Physical Chemistry A* **2020,** *124* (39), 8057-8064.

Manipulating interfacial reactivity with atomically layered heterostructures

DE-SC0021049
PI: D. Kwabena Bediako
University of California, Berkeley, CA 94720

Project Scope

Controlling electron transfer and chemical transformations mediated by surfaces and interfaces with a level of precision approaching that of molecular chemistry is a preeminent challenge for the sustainable conversion of energy resources. At the heart of this grand challenge is the difficulty in creating chemically interrogable surfaces that are both well-defined and tunable at the quantum level. To this end we are designing atomically precise, modular, and highly tunable multi-component materials based on atomically thin two-dimensional (2D) van der Waals (vdW) heterostructures. We place an emphasis on fine tuning the electronic genome—band structure, density of states, quantum capacitance—of our precisely configured heterostructures, leveraging this exquisite control over a surface's physical properties to control the interfacial chemistry. To understand the chemistry at our materials with molecular detail, we are also developing one-of-a-kind tools for the study of spatially resolved mechanistic behavior. Insights from complimentary mechanistic and structural probes will be used to identify the fundamental chemical principles that underlie interfacial charge transfer, allowing us to make systematic hypothesis-driven modifications and uncovering new design elements and approaches for efficient energy conversion and storage chemistry. As testbeds for our hypotheses we shall study a range of electrochemical reactions at our tailored materials, spanning reversible 1-electron redox couples and proton-coupled reactions to multi-electron electrocatalytic hydrogen evolution/oxidation reactions.

Recent Progress

Twisted bilayer graphene electrochemistry

Stacking atomically thin layers with a very small azimuthal misorientation to produce moiré superlattices enables the controlled engineering of electronic band structures and the formation of extremely flat electronic bands. By fabricating van der Waals (vdW) heterostructures of twisted bilayer graphene (TBG) on hexagonal boron nitride (hBN) and using scanning electrochemical cell microscopy (SECCM) to probe interfacial electron transfer (Figure 1),[1,2] we discovered a

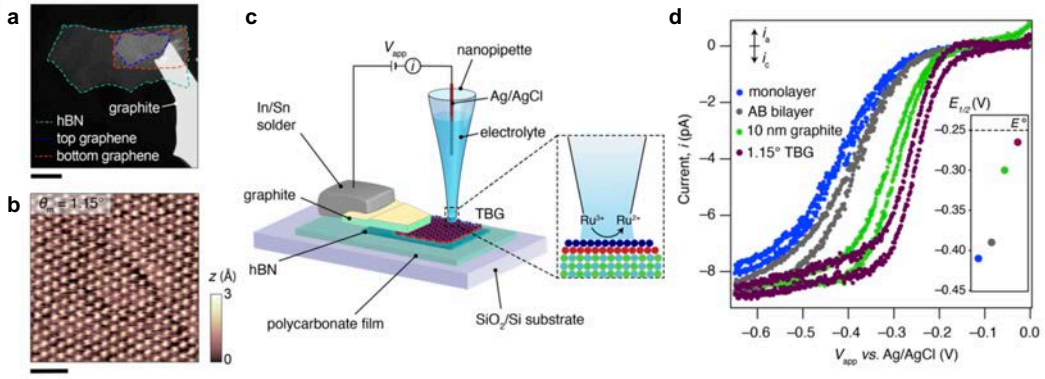

Figure 1. (a) Optical image of a TBG/hBN heterostructure connected to a graphite contact. (b) Constant-current STM image of 1.15° TBG. Scale bars: 50 nm. (c) Schematic of local voltammetric measurement at a TBG surface in an SECCM setup. (d) Representative steady-state voltammograms of 2 mM $Ru(NH_3)_6^{3+}$ in 0.1 M KCl solution obtained at graphene monolayer (blue), AB stacked bilayer (grey), 10-nm thick graphite (green), and 1.15° TBG (purple). The inset shows the half-wave potentials of each CV compared to E^0.

strong twist angle dependence of heterogeneous charge transfer kinetics at TBG electrodes with 'magic angle' (~1.1º) TBG showing nearly reversible electrode kinetics (Figure 1d).

A detailed kinetic analysis over a range of twist angles (Figure 2) showed that this effect is driven by the angle-dependent tuning of moiré-derived flat bands that modulate electron transfer processes with the solution-phase redox couple. Combined experimental and computational analysis reveals that the variation in electrochemical activity with moiré angle is controlled by atomic reconstruction of the moiré superlattice at twist angles <2º, and topological defects localized at AA stacking regions produce a large anomalous local electrochemical enhancement that cannot be accounted for by the elevated local density of states alone. This discrepancy between the experimental rate constant values and those calculated using the Gerischer–Marcus model alone may be explained by modifications to the electronic coupling strength or reorgnanization energy with θ_m. The highly localized flat bands in small angle TBG would result in significantly larger real-space overlap of the electronic wave functions of the TBG and solution-phase redox complexes as well as changes to electrode polarizability, inducing an additional augmentation of the measured rate.

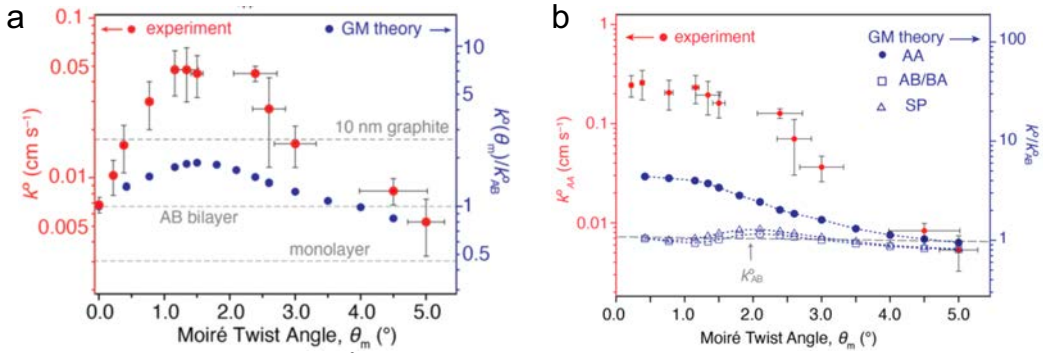

Figure 2. (a) Standard rate constants (k^0) extracted from the experimental voltammograms (red) as a function of twist angle compared to the theoretical values (blue). The horizontal and vertical error bars represent the standard deviations of θ_m and k^0, respectively. (b) Experimental local k^0 at AA sites as a function of θ_m extracted from panel (a) compared to the theoretically predicted values of k^0 at AA, AB/BA, and SP stacking regions.

Twisted trilayer graphene electrochemistry

Given the additional degrees of freedom available for stacking trilayers of graphene, we interrogated electrochemical devices of non-twisted and twisted trilayer graphene and measured the interfacial ET kinetics using cyclic voltammetry.[3] These measurements showed a strong stacking dependence of the electrochemical ET rate constant between Bernal and rhombohedral trilayer graphene, as well as very facile interfacial ET kinetics of twisted trilayer graphenes near their respective magic-angles. Notably, measurements of TTG electrochemistry as a function of twist angle, revealed that the M-t-B polytypes (Figure 3b) possessed faster interfacial ET kinetics than the A-t-A polytypes (Figure 3d) . This was unexpected, as the A-t-A polytype would have a higher overall DOS. Measurements of stacking area fraction, using scanning tunneling microscopy, and dark-field TEM, were used to resolve the standard ET rate constants at disparate atomic stacking types in TTG (Figure 3a). Together with theoretical calculations, the anomalous ET kinetics of A-t-A and M-t-B were understood to arise from the exact layer-wise localization of the DOS (Figure 3c,e), and not the overall DOS, as previously thought.

These results provide a powerful demonstration of the sensitivity of interfacial ET kinetics to the three-dimensional localization of electronic states at electrochemical surfaces and raise the question of whether traditional measurements of ET rates at macroscopic electrodes might severely

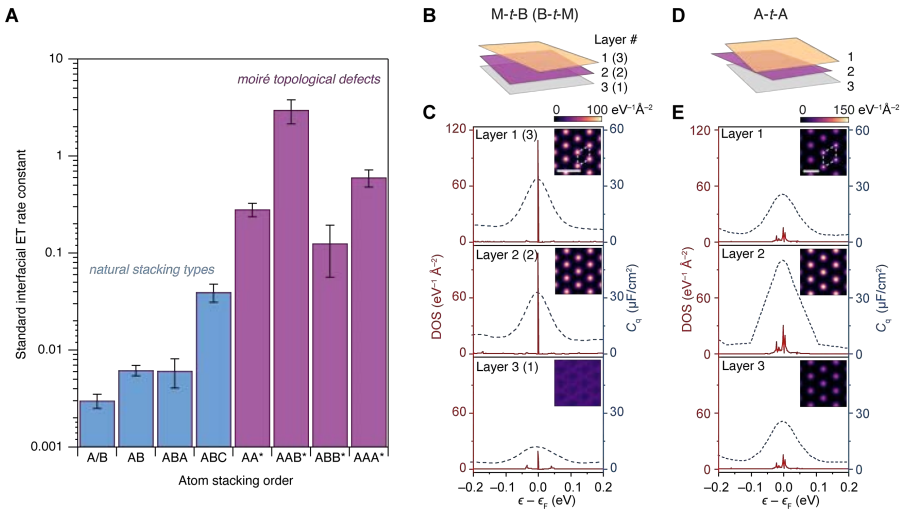

Figure 3. ET rates of few-layer graphene and layer-dependent DOS localization (a) Local standard $Ru(NH_3)_6^{3+/2+}$ ET rate constants at few-layer graphene in different stacking configurations. 'Artificial' moiré-derived stacking domains are labeled with an asterisk. Each bar is the mean local rate either measured (for natural stacking) or calculated (for aritifical stacking) for small twist angle samples. The error bars represent the standard errors for the rates. (b) Schematic of M-t-B/B-t-M graphene layers. (c) Layer-dependent DOS profile for AAB stacking domains in M-t-B and B-t-M graphene at θ_m = 1.2°. Insets show real space DOS maps of each layer at ε = –3 meV. (d) Schematic of the A-t-A layers. (e) Layer-dependent DOS profile for AAA stacking domains in A-t-A graphene at θ_m = 1.2°. The insets show real space DOS maps of each layer at ε = –1 meV for θ_m = 1.2°.

underestimate the true local rate constant, which may be mediated by atomic defects that strongly localize electronic DOS, at these interfaces. In turn, SECCM measurements are shown to be powerful tools for probing layer-dependent electronic localization in atomic heterostructure electrodes.

Field-effect tuning of interfacial ET

The twist angle dependence of heterogeneous charge transfer kinetics at twisted bilayer and trilayer graphene electrodes produces the greatest effects near the magic-angles. These effects are driven by the angle-dependent tuning of moiré-derived flat bands that modulate electron transfer processes with the solution-phase redox couple. For redox couples with E^0 poorly aligned with the charge neutrality point of graphene (e.g. $Co(Phen)_3^{2+/3+}$), the enhancement is significantly quenched due to the shift of Fermi level away from the flatbands at the electrochemical bias to drive this reaction. We have exploited the field effect as an orthogonal approach to tune the electronic

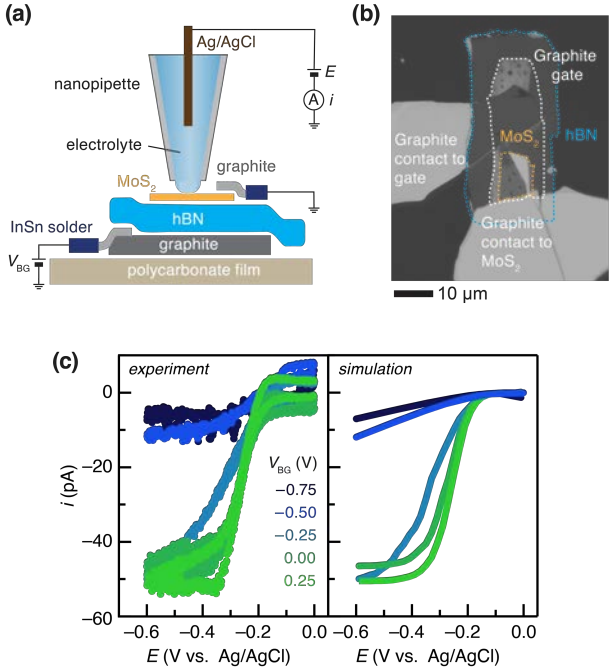

Figure 4. (a) Schematic of local voltammetric measurement in a SECCM setup (b) Optical micrograph of a bottom-gated monolayer MoS_2 electrode (hBN thickness: 20 nm) (c) Left: Experimental cyclic voltammograms of 1 mM $Ru(NH_3)_6^{3+}$ in 0.1 M KCl solution as a function of V_{BG}. Scan rate = 200 mV/s. Right: Simulated voltammograms using parameters in Table 1.

band alignment and tailor the interfacial electrochemical activities for a broader range of redox molecules.[4] Mesoscopic heterostructures of MoS_2, hBN, and graphene were fabricated to enable an electrostatic bias to be applied to the bottom gate of an MoS_2 flake while SECCM measurements are performed on the top surface (Figure 4a,b). Comparison of experimental CVs to those simulated using finite-element methods (Figure 4c), permitted the extraction of interfacial ET rate constants as well as conductance, G, values associated with intralayer charge transport (Table 1). This study showed how electrostatic gating of semiconducting electrodes results in the modulation of intrinsic electrochemical kinetics as well as electronic transport properties. The FET scheme provides an orthogonal knob to control interfacial charge transfer, distinct from the applied electrochemical bias, but the effects of in-plane transport must be considered.

Table 1. Values of conductance, G, and ET rate constant, k^0, of $Ru(NH_3)_6^{3+/2+}$ from simulation of CVs at monolayer MoS_2.

V_{BG} (V)	$\mathcal{E}$ (mV/nm)	k^0 (cm/s)	G (nS)
0.25	12.5	0.6	$\geq$2.5
0.0	0	0.4	$\geq$2.0
–0.25	–12.5	0.2	0.43
–0.50	–25.0	0.02	0.09
–0.75	–37.5	0.004	0.05

Future plans

Future experimental and theoretical work is needed to shed more light on the microscopic origin of the electron-transfer modulations in the context of reorganization energy, electronic coupling, and even electric double-layer structure. This work also heralds the use of moiré materials as a versatile and systematically tunable experimental platform for theoretical adaptations of the MHC framework applied to interfaces with localized electronic states, which are representative of defective surfaces that are ubiquitous to nearly all real electrochemical systems. We are also now exploring how twistronics may be a powerful pathway for engineering pristine 2D material surfaces to execute complex multi-step charge transfer processes with facile kinetics, holding implications for electrocatalysis and other energy conversion device schemes that could benefit from ultrathin, flexible, and/or transparent electrodes that retain high electron-transfer kinetics. Another direction is the exploration of solid-state electron donors/acceptors in lieu of electrostatic gates as means of manipulating band alignments in interfacial electron transfer reactions.

Peer-Reviewed Publications Resulting from this Project (2021–2023)

(1) "Tunable angle-dependent electrochemistry at twisted bilayer graphene with moiré flat bands" Yu, Y.; Zhang, K.; Parks, H.; Babar, M.; Carr, S.; Craig, I.; Van Winkle, M.; Lyssenko, A; Taniguchi. T.; Watanabe, K.; Viswanathan, V.; Bediako, D. K. *Nature Chemistry* **2022**, *14*, 267–273.

(2) "Tuning interfacial chemistry with twistronics" Yu, Y.; Van Winkle, M.; Bediako, D. K. *Trends in Chemistry* **2022**, *4*, 857–859.

(3) "Anomalous interfacial electron transfer kinetics in twisted trilayer graphene caused by layer-specific localization" Zhang, K.; Yu, Y.; Carr, S.; Babar, M.; Zhu, Z.; Kim, B.; Groschner, K.; Khaloo, N.; Taniguchi, T.; Watanabe, K.; Viswanathan, V.; Bediako, D. K. *ACS Central Science* **2023**, *9*, 1119–1128.

(4) "Decoupling effects of electrostatic gating on electronic transport and interfacial charge transfer kinetics at few-layer molybdenum disulfide" Maroo, S.; Yu, Y.; Taniguchi, T.; Watanabe, K.; Bediako, D. K. *ACS Nanoscience Au* **2023**, *3*, 204–210.

The Nature, Dynamics, and Reactivity of Electrons in Ionic Liquids

David A. Blank (blank@umn.edu), Department of Chemistry
University of Minnesota, 207 Pleasant St. SE, Minneapolis, MN 55455

Claudio J. Margulis (claudio-margulis@uiowa.edu), Department of Chemistry
University of Iowa, E331 Chemistry Building, Iowa City, Iowa 52242

Program Scope

This program, which started on September 1, 2023, uses a combination of time resolved optical and Raman spectroscopy, time resolved pulse radiolysis (in collaboration with Dr. James F. Wishart at Brookhaven National Laboratory), and computer simulations to investigate the nature, dynamics and reactivity of electrons in ionic liquids. The liquids are selected based on potential applications in radiolytic environments and they have constituent ions that have limited or no reactivity with excess electrons. The focus is on the competing mechanisms of reaction of the excess electrons with solutes and how these depend on the state of electron solvation and the electronic structure of the solutes. The specific questions that the program aims to address are:

- Why are there multiple products observed in the presence of excess charge? Is this the result of a single, common mechanism involving a series of basic events, or competing reaction pathways with branching determined in the earliest (sub-picosecond) moments following injection of charge?
- How does reactivity depend on the initial energy and state of the electron?
- How does the origin of the electron, detachment from the liquid or from a solute, change the reactivity of excess charge?
- How does the molecular structure of the ions and transient local structure within the liquid influence the reactivity of excess charge?

Recent Progress

We are assembling the research team by bringing on board a graduate student at the University of Minnesota and searching for a postdoctoral researcher at the University of Iowa. Building on our prior transient absorption work[1], we have done some initial time-resolved resonance Raman experiments in pyrrolidinium dicyanamide ionic liquids demonstrating our ability to probe structural details of transient photo-detached electrons. Working from our previous studies[2] we have also begun setting up the simulations and investigating methods to project out spectroscopic observables for direct comparison with experiments.

Future Plans

Computational studies will begin to benchmark predictions of electron localization against experimental observations. Spectroscopic measurements will focus on resonance Raman spectroscopy and pump-probe measurements of relaxed cavity electrons (6+ nanoseconds after

photodetachment) to probe the local molecular and electronic structure. Initial work will focus on pyrrolidinium based liquids and will include mixtures of anions. A graduate student from the University of Minnesota will be moving to Brookhaven National Laboratory in January 2024 as part of the SCGSR program to spend a year working with collaborator Wishart using pulse radiolysis techniques[3] that will directly complement the photolysis experiments and computational studies of excess charge in these ionic liquids.

References

[1] M. N. Knudtzon and D. A. Blank, J. Phys. Chem. B, **124** (2020) 9144-9153.
[2] C. Xu and C. J. Margulis, J. Phys. Chem. B, **119** (2015) 532-542.
[3] J. F. Wishart *et. al*, Faraday Discussions, **154** (2012) 353-363.

Peer-reviewed Publications Resulting from this Project (Project Start Date: 09/2023)

No publications to report.

RADIATION CHEMISTRY AND PHOTOCHEMISTRY IN THE CONDENSED PHASE AND AT INTERFACES

DE-FC02-04ER15533

Ian Carmichael, David M. Bartels, Ireneusz Janik,
Jay A. LaVerne, Aliaksandra Lisouskaya and Sylwia Ptasińska
Radiation Laboratory, University of Notre Dame, Notre Dame, IN 46556
carmichael.1@nd.edu

Project Scope

Radiation chemistry-related, BES-supported work at the Notre Dame Radiation Laboratory is organized around three subtasks. The first two focus on fundamental advances in radiation chemistry, the third on aspects particularly relevant to nuclear power generation. Accomplishments in these directions over the period, December 01, 2021 - November 30, 2023 are described below and future plans are also indicated.

Ionizing radiation, in the form of γ-rays or high-energy electrons, when impinging on a condensed phase, deposits energy (on the order of tens of eVs) in a series of widely separated (on the order of tens of nanometers) clusters of ionization and excitation events (spurs) along a twisting and potentially branching track. Along the length of this track, the overall energy dissipation - the linear energy transfer (LET), is less than one eV per nanometer. In contrast, heavy ions such as α-particles forge a dense columnar path of ionizations and excitations as spurs overlap, with much larger values of LET. These disparate energy-deposition environments result in different chemical outcomes. The first subtask advances the fundamental science underpinning the observed chemical outcomes and the continued development of models pertinent to many irradiated situations, including the wide range of extreme environments present across the DOE complex.

The action of ionizing radiation almost universally produces charge and spin separation, and a major focus of our proposed work, subtask 2 below, is devoted to the structure and reactivity of the resulting free radicals at a fundamental level, developing and deploying theoretical techniques to elucidate the observed behaviors. Issues addressed in this part will find strong overlap with other scientific disciplines.

Nuclear power is a vital resource in meeting our future sustainable energy needs and an important part of the portfolio of the Department of Energy's efforts to provide safe and reliable sources of electricity. Subtask 3 will provide essential knowledge on basic radiation chemical processes that are inherent in that industry for the management and further development of this key energy resource. The work is divided into three main topics: reactor water chemistry, radiolytic processes in separations, and radiation chemistry in waste storage.

This abstract describes progress made at the NDRL over the last three years supported by our overall award DE-FC02-04ER15533, but does not include similarly-supported work reported at recent Solar Photochemistry PI meetings. It also does not mention contributions by the NDRL team members through other awards. The publications listed at the end are similarly restricted.

1 Fundamental advances in radiation chemistry
From energy deposition to medium decomposition

We first consider the optical response of the medium starting with photons in the vacuum ultraviolet, then probe primary events, searching for a comprehensive understanding of the mechanisms behind low-energy-electron-induced fragmentations of simple (bio)molecules and the observed sharp differences between radiolytic yields in aromatics and aliphatic hydrocarbons. How this radiation chemistry impacts key modern structural characterization techniques, transmission electron microscopy and macromolecular X-ray crystallography, for example, is interrogated next. Track structure models are extended to account for extreme environments of temperature, pressure, and radiation dose and dose rate now likely to be encountered. This subtask concludes with a deep exploration of novel phenomena observed in non-traditional radiation sources; atmospheric pressure plasma jets and plasma/liquid surface electrodes.

2 Fundamental advances in radiation chemistry
Probing radical structure and kinetics

Experimental and theoretical investigations of solvated electron structure and reaction rates are proposed along with a resonance Raman study of radical ion hydration shells; Detailed measurements of redox reactions of reduced transition metal ions will be made at elevated temperatures. A quantitative assessment and modeling of chemically induced dynamic electron polarization of the hydrogen atom in water will be undertaken and a definitive treatment of radiolytic oxidation of aqueous halide ions will be obtained.

3 Basic radiation chemistry impacting nuclear power generation

We propose to examine the complex radiation chemistry of bulk water at the high temperatures of pressurized water reactors. Radiation accelerated corrosion will be probed at the interface of water with reactor cladding materials. The radiation chemistry of aqueous solutions high in chloride concentration will be investigated to mimic the effects of seawater on reactor components. We aim to provide a thorough knowledge of the radiation-induced changes in separation systems for spent nuclear fuels. Product formation in acidic nitrate solutions, used to dissolve waste materials, will be examined, especially at high LET, along with radiolytic decomposition of the organic phase and organic/aqueous mixtures. Resonance Raman techniques will identify radiation-induced species at interfaces. Safe long-term storage of radioactive materials requires extensive information on the radiation stability of storage components and the dissolution of elements that may occur following system failures. Gas production will be determined to aid in long-term stewardship. Metal oxides interface with aqueous solution and with organics will be examined for their radiation stability.

Recent Progress

1 Fundamental advances in radiation chemistry
From energy deposition to medium decomposition

Primary processes

Vacuum ultraviolet (VUV) response in sub- and supercritical fluids

Halides (Cl^-, Br^-, I^-), pseudohalides (SCN^-, $SeCN^-$, OH^-, *etc.*) and other simple inorganic anions (NO_3^-, SO_4^{2-}, *etc.*) do not have bound excited electronic states in the gas phase. Therefore, upon deep/vacuum ultraviolet light absorption they detach an electron that manifests with a broad structureless spectrum. Upon dissolution in high-polarity solvents, distinct strong absorption bands, characteristic for each anion, can be easily detected as representative of the presence of bound electronic states. Such excited states are collectively supported by many solvent molecules solvating the anion and are labeled charge-transfer-to solvent (CTTS) states. These states are of particular interest since they allow for probing the local solvent environment and because their partial delocalization onto neighboring water molecules promotes dynamical electron detachment to ultimately form solvated electrons such as are ubiquitous in aqueous radiation chemistry.

We have employed a simple diffuse polarizable continuum model to successfully describe the observed linear dependence of the CTTS absorption peak position versus temperature, in the range of 25 - 350 °C, for aqueous halides and hydroxide solutions but observed no ion-pairing effects, even up to 0.25 M. Extensive classical molecular dynamic simulations and time-dependent density functional theory calculations, supported by accurate ab initio treatments of the excitation spectra of some small structures. The resulting computed spectra are in excellent agreement with our experiment for the peak position, but in qualitative disagreement on the width, being only about half as wide. Presumably the classical molecular dynamics simulation fails to provide an adequate variety of structures to explain the experimental width.

We have also demonstrated that electronic perturbation of a water monomer under supercritical conditions is evidenced upon increase of pressure/density by gradual disappearance of the diffuse spectral vibrational structure and a blue shift of the first absorption band. Disappearance of such band undulations upon pressurization is suggested to arise from perturbation of the symmetric stretch mode in the upper valence electronic state. Rydbergization of the first absorption band was not needed to explain the blue shift of the first absorption band as it could rather be traced to hydrogen-bond acceptance by the molecules undergoing excitation, hence ground state stabilization, as shown by our computational studies on water dimers. However, he lowest "first continuum" absorption band of water observed at 7.4 eV in the gas phase was blue shifted by about 0.8 eV in ambient liquid water.

The nature of the lowest-lying electronic transitions in simple alcohols has been debated for decades, especially in the context of the assignment of excited states' character. Combining analysis of our results of VUV absorption in sub- and supercritical MeOH with TD-DFT computations, we found that the gas phase lowest-lying broad absorption band, demonstrating

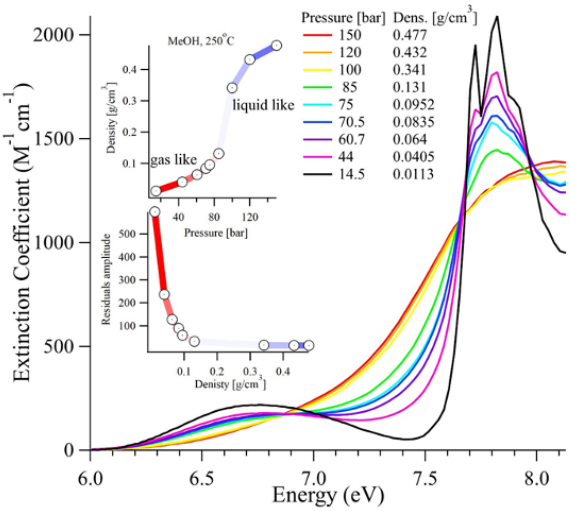

Figure A *Pressure/density effects on VUV absorption spectrum of MeOH under supercritical conditions.*

mixed valence/Rydberg character, loses Rydberg character as the avoided crossing of excited state potential energy surfaces vanishes upon upshift of the Rydberg state caused by condensation (Fig. A).

Dissociative electron attachment in complex environments

Dissociative electron attachment (DEA) is an important process involved in the damage of biomolecules by low-energy electrons produced from high-energy radiation. DEA to biomolecules such as DNA and protein constituents have been studied previously. Because of the complex structure of proteins and peptides, it is challenging to fully understand and characterize the fragmentation patterns observed following DEA. Simpler molecules that contain the amide bond, (O=C)-N, can be used to model the behavior of these larger biomolecules. Therefore, DEA to a systematic sequence of gas phase amides has been investigated as a first step towards better understanding this process.

We have expanded our recent studies of DEA to gas phase amides by investigating propionamide, N-methylacetamide, N-methylpropanamide, and N-ethylpropanamide. We measured the ion yield curves of all anionic fragments produced by DEA to these molecules, paying particular attention to amide bond dissociation because of its signal importance as the linkage between amino acids in peptides and proteins. We are also working towards measuring amide-containing molecules in water clusters to develop our understanding of low energy electron interactions with embedded biomolecules.

In the meantime, we have also performed a mass spectrometric study on cationic clusters of formamide and its hydrated form in collaboration with the Denifl group in Innsbruck. We obtained cationic mass spectra of bare and microhydrated amide clusters at the electron impact ionization energy of 70 eV. A comparison of a gas-phase spectra with the mass spectra for bare clusters indicated that the majority of species formed are protonated amide clusters derived from larger clusters upon electron ionization. Moreover, proton transfer from the carbonyl to the amino group was also observed for formamide in the gas phase and in its clusters. This process occurred during amide bond cleavage and led to the formation of a stable ion, NH_3^+. We have also observed other stable ionic products and provided possible fragmentation channels. In the case of the microhydrated clusters, the mass spectra are more complex, suggesting a larger number of reaction channels involved due to the presence of water.

Dissociative electron attachment (DEA) is one of the processes that involve low-energy electrons formed upon high-energy irradiation. Typical DEA studies focus on detection and yield measurements of negative ions produced as a function of the incident electron energy using mass spectroscopic techniques. Such studies are useful in determining the reaction pathways and the

resonant states, which are responsible for molecular decay. However, to gain more insight into the details of this process it is necessary to employ other techniques. Therefore, we have been developing a new experimental set-up, a velocity map imaging (VMI) spectrometer, which is capable of measuring the kinetic energy and angular distributions of the negative ions formed in the DEA process. This type of study will provide information about the DEA energy threshold and will reveal the symmetry of the resonant states, which are created prior to the dissociation. The construction of the experimental setup has now been completed and recently we have made significant progress on the spectrometer calibration, development of analysis codes, and obtained some preliminary data.

Using our VMI spectrometer, we have investigated dissociation dynamics of low-energy electron attachment to several simple molecules. We focus on dissociation of specific chemical bonds (*e.g.,* peptide bonds) and functional groups (*e.g.,* hydroxyl group). Differential laboratory-frame momentum distribution of fragmented ions has been measured for different incident electron energies over the energy range of resonances. These results allowed us to obtain the kinetic energy and angular distributions of the negative ions formed in the DEA process and to identify the molecular symmetry of resonance states.

Track structure

Hydroxyl radical yields in heavy-ion water radiolysis.

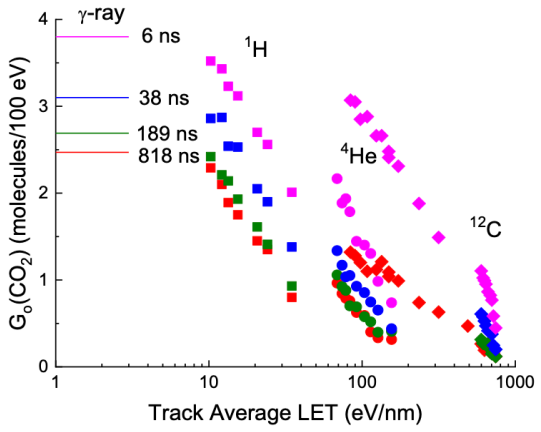

Figure B *Track average yields ($G_0(CO_2)$, molecules/100 eV) as a function of track average LET (eV/nm) for (■) protons, (●) helium ions, and (◆) carbon ions at four formic concentrations corresponding to 6 ns, 38 ns, 189 ns and 818 ns. The limiting yield for each formic acid concentration observed with γ rays is also shown.*

Hydroxyl radicals are one of the most oxidizing radical species produced in the radiolysis of water. Radiation effects in cells are almost exclusively driven by hydroxyl radical reactions so knowledge on their yields is extremely important in radiation protection. They are also the main precursors to hydrogen peroxide, a radiolytic product of concern for corrosion in nuclear power reactors. The yield of hydroxyl radicals has been known for several years for low linear energy transfer (LET) radiation like fast electrons and gamma rays, but very little is known for heavy ions. Using scavenger techniques, we have determined the yields of hydroxyl radicals in the radiolysis of water with protons, helium ions, and carbon ions of up to a few tens of MeV energy (Fig. B). These experimental values coupled with Monte Carlo track simulations have led to a good understanding of the variation of hydroxyl radicals as a function of LET.

Temperature dependence of spur kinetics.

We have continued to investigate, by Monte Carlo simulation, the temperature dependence of low energy electron scattering cross-sections in water up to 350 °C. These investigations have led

us to recognize a “disconnect” in understanding of low-energy cross-sections even at room temperature. Experimental data for “thermalization distance” and radiolysis spur recombination requires 2x larger cross-sections than are used to describe electron scattering in amorphous ice or in liquid microjet experiments. Indications are that a “transient negative ion” scattering mechanism (similar but distinct from dissociative electron attachment) must be invoked to reconcile the several data sets.

High-temperature, high-LET radiolysis by neutron capture

Boron-10 is injected into nuclear reactor cooling systems as a neutron “shim” for fine control of the neutron flux over the course of a fuel cycle. At the beginning of a cycle the boric acid is at concentration on the order of 0.15 M, and the $^{10}B(n,\alpha)^{7}Li$ fission reaction can account for roughly 30% of the radiation energy deposited into the water. We have just published the first measurements of H_2 yield from this fission event up to 300 °C, which will give much greater confidence in modeling of the water chemistry in the reactor core.

Impact on modern structural characterization techniques

Radiation damage in structural biology

Cyanine fluorophores are widely used in applications ranging from super-resolution microscopy to clinical imaging because of their intense fluorescence and narrow spectral bandwidth. Cyanine dyes tend to aggregate at micromolar concentration in aqueous solutions, a process that leads to changes in the absorption spectrum and, usually, to a significant loss of fluorescence. The irreversible photobleaching of the chromophore and reversible light-induced blinking of the fluorescent species are relevant for stochastic super-resolution microscopy. It has been demonstrated that the excited triplet state formed in non-halogenated cyanine dyes can participate in the photobleaching mechanism. There is, however, little experimental information available on the light-induced mechanisms for the blinking process and the role of redox species formed from cyanine dyes. Our research has demonstrated that self-association is also characteristic for the one-electron reduced and oxidized radicals derived from cyanine dyes in aqueous solution. Association between the neutral radical and a ground-state molecule results in the formation of dimers having an absorption spectrum quite different from either of its isolated precursors. Thus, this association could play a key role in optimizing the system for super-resolution microscopy.

We have performed research into a lipid model system reacting with OH radicals created by pulse radiolysis and/or using stopped-flow electron paramagnetic resonance spectroscopy. This approach, combined with well-integrated computational chemistry, allowed us to successfully demonstrate a combination of methods to make it possible to obtain information about not only the structure but also the kinetics of the radical intermediates formed.

In the context of oxidative stress-inducing protein damage, tyrosine is known as one of the most sensitive residues. Tyrosine dimerization, with the formation of di-tyrosine bridges, has been evidenced in many neuropathological diseases. Recently, five di-tyrosine bridges were found in a protein and peptide after radiolytic oxidation with $^{\bullet}OH$ and $^{\bullet}N_3$ radicals, and four tyrosine dimers were formed after radiolytic oxidation of amino acid. Pulse radiolysis experiments have also shown different pathways of radical reactions for the formation of tyrosine dimers in the presence of oxidizing radicals.

Radiation chemistry in Electron Energy Loss Spectroscopy (EELS)

Electron Energy Loss Spectroscopy (EELS) has been used to probe the radiolysis of thin water ice by electrons in a transmission electron microscopy. Conventional liquid water radiolysis would predict enhanced formation of hydrogen peroxide under these conditions whereas molecular oxygen is found to be the main oxygen containing species. The O atom seems to have a major role in the radiolysis of water under these circumstances. Extensive quantum-chemical calculations of X-ray absorption edges for various oxygen-containing species have been performed to allow unambiguous identification of such species.

X-ray-induced radiosensitization of gold nanoparticles

Nanoparticles (NPs) are considered a prospective material in a wide range of areas from catalysis and electronics to biosensors and medicine. The radiosensitization effect of AuNPs is well known

and can be described in the terms of 'physical' and 'chemical' enhancement of radiolysis product yields. We probed the influence of AuNPs on the yields of major water radiolysis products using the electron paramagnetic resonance (EPR) spin-trap method coupled with *in situ* X-ray irradiation and oxidized coumarin luminescence tracking after γ-irradiation. Using both methods, we found an enhanced production of hydroxyl radicals with the addition of AuNPs. These studies bring refined knowledge on the effect of both irradiation energy and dose rate on radio-enhancement and radioprotection properties of nanoparticles.

Non-traditional sources

Plasma irradiation

Low-temperature plasma (LTP) radiation generated at atmospheric pressure and room temperature produces an extent of reactive species, particularly reactive oxygen and nitrogen species that drive chemistry in an irradiated target. We have been able to alter the plasma-target interactions by varying the plasma process parameters of LTP, such as applied voltage, pulse frequency, irradiation time, and gas flow rate. Therefore, the knowledge of reactive species generation and how it evolves with plasma process parameters is essential to optimize these parameters for better control and deliberate application of this type of radiation.

Currently, our research focus is on developing novel plasma diagnostics tools using machine learning (ML) to extract crucial information on plasma interactions under varying process parameter combinations. For our investigations, we used plasmid DNA as an irradiation target. We performed extensive and systematic studies on plasma-induced DNA strand breaks for qualitative and quantitative diagnostics on reactive species generation and plasma-induced thermal denaturation of DNA for diagnostics of gas temperature of helium LTP. After our experimental effort, the large base of the data was used for creating several predictive ML models for plasma-induced DNA damage and for gas temperature estimation by coupling heat transfer simulations with ML models.

In addition, we have also been developing an ML model to estimate the dose rate for LTP. In this approach, we use a first-of-kind ML framework that blends the predictive modeling of plasma-induced DNA damage measured in our laboratory with the known dose-DNA damage correlations reported for other types of radiation. Our results revealed a dose rate dependence on plasma process parameters such as applied voltage and pulse frequency. Also, the dose rate of LTP will be compared with those for other radiation sources to assess the plasma yield and efficacy.

Recently we observed previously undetected DNA denaturation in addition to the DNA strand breaks present upon plasma irradiation. Moreover, we observed denaturation at the combination of plasma parameters with a temperature much below the thermal decomposition of DNA. To understand this effect, we implemented a physics-guided neural network model to predict the formation of strand breaks and denaturation and their yields for a given combination of plasma parameters. Based on our findings we suggested that denaturation of DNA can be attributed to transient local heating of the aqueous DNA, ("hotspots"), while bulk heating was not observed.

One-electron inorganic redox reactions

Oxidation rates of hyper-reduced metal ions

Understanding radiation effects on materials and the consequent enhanced corrosion is crucial for the success of both current and next-generation nuclear reactors. The corrosive environment generated due to water radiolysis continues to be a major challenge facing the nuclear industry. It can result in serious plant problems, such as primary water stress corrosion cracking of alloys, the deposition of corrosion products on fuel assemblies and high out-of-core radiation fields. Zinc addition into a reactor coolant system was first applied in 1987 at the Hope Creek Unit, New Jersey for a boiling water reactor. The original purpose of the zinc addition was to control the buildup of radiation fields from cobalt-60 on out-of-core piping, and since then, plant experience has demonstrated that it can also suppress the corrosion of materials in reactors. It was demonstrated that Zn^{2+} ions can replace other metal ions like Ni^{2+}, Fe^{2+}, and Co^{2+} in spinel-type oxides forming zinc-incorporated oxides, which are thermodynamically more stable. In the presence of divalent metal ions dissolved in water, the hydrated electrons will generate short-lived monovalent metal M^{+}_{aq} transients. These monovalent ions will subsequently react with the oxidizing species formed in the system during water radiolysis. However, the various roles of metal ions in complex reactor chemistry at high temperatures remain unclear.

Our work reports new experimental data on the redox reactions of hydrated metal ions under critical conditions of temperature and pressure, simulating the conditions of water radiolysis in the coolant loop of nuclear reactors.

We found that the kinetic model for Zn^{+} decay in the pure water system essentially consists of the reactions with OH radicals at a short time after electron pulse and with H_2O_2 and H atom on a long timescale. We demonstrated that at temperatures up to 300 °C, the spectrum of Zn^{+}_{aq} is well-preserved in terms of both shape and λ_{max}. The spectral characteristics at the longest wavelengths are well described by metal-centered s-p-like transitions. It is clear that the absorption of monovalent zinc is very sensitive to the pH of the medium. This can be explained by the number of protons in the system, which compete in the reaction with electrons, as well as the formation of Zn^{+}_{aq} hydroxo-forms in an alkaline medium. We performed pulse radiolysis experiments on zinc solutions with 0.1 M methanol, *tert*-butanol and formate to scavenge $^{\bullet}OH$ and $^{\bullet}H$. From the data obtained it follows that the disproportionation reaction does not contribute measurably to the decay kinetics. The kinetics data have demonstrated that Zn^{+} ions are reactive toward the radiolytically produced oxidizing species from water, particularly the $^{\bullet}OH$ radical. The reactions investigated follow an empirical Arrhenius relationship at temperatures up to 200 °C and then tend to reach a plateau value. These findings will be of particular importance in not only understanding the effect of zinc ions in water coolant radiolysis but also for deriving proper kinetics modeling to better handle corrosion.

Reaction kinetics of $Ni^{2+/+}$ and $Co^{2+/+}$ ions dissolved in water upon irradiation at high temperatures and pressure are revealed by pulse radiolysis. We found that the absorption spectrum of short-lived monovalent nickel ions shifts to ever shorter wavelengths with increasing temperature.

This phenomenon can be explained by a decrease in the average number of water molecules coordinated to the metal ion in the first solvation shell. To obtain the reaction constants, we performed extensive experiments and further fitting of the Ni^{+} kinetics in various salt concentrations, pH ranges and temperatures (Fig. C). All measured rate constants followed approximate Arrhenius behavior. The greatest contribution to the kinetics of Ni^{+} decay is its oxidation by the OH radical, but H atoms are just as important in acidic solutions. We discovered that the reaction of Ni^{+} with H_2O_2 gives an intermediate that absorbs in the UV region and has a lifetime of 30 microseconds. We found that the absorption spectra of monovalent cobalt ions at a wavelength of 320 and 380 nm at temperatures above 25 °C decrease and shift towards lower energies. Upon reaching 150 °C, the peak at 380 nm becomes completely indistinguishable. We noticed that at concentrations of the $CoSO_4$ higher than 0.5mM the absorption spectrum of the monovalent metal ions Co^{+} changes. This can be explained by the formation of clusters of cobalt ions. We found that at temperatures starting from 100 °C, the formation of stable cobalt clusters becomes noticeable in the kinetic curves at long timescale.

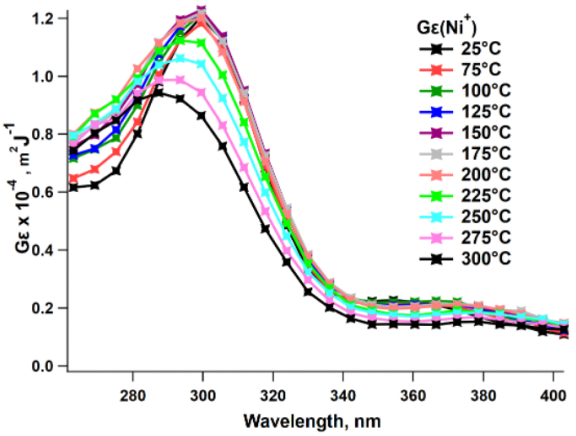

Figure C *Transient spectra of Ni^{+} formed in 0.3 mM $NiSO_4$ solutions saturated with Ar, observed at 2 μs after 15 ns (20.8 Gy) radiolysis pulse at 25 to 300 °C.*

The rate coefficients and Arrhenius parameters for the reactions of Fe^{2+} ions with e_{aq}^{-} and the $HO_2^{\bullet}$ radical to high temperatures were established using pulse radiolysis. The reaction between Fe^{2+} ions and the e_{aq}^{-} was studied from 25 to 250°C at natural pH in an Ar-saturated solution. It was found that the iron(II) reaction with the perhydroxyl radical forms a short-lived adduct species, Fe^{2+}-$HO_2^{\bullet}$. At 22 °C, the adduct extinction coefficient was found to be $\varepsilon(Fe^{2+}\text{-}HO_2^{\bullet}) = 780 \pm 10\ M^{-1}\,cm^{-1}$ at 419 nm. The extinction coefficient of the Fe^{2+}-$HO_2^{\bullet}$ adduct was assumed to be independent of temperature over the temperature range studied. In this work we report the corrected first-order decay rate of the Fe^{2+}-$HO_2^{\bullet}$ adduct to 70 °C.

The new kinetic data was measured for major reactions essential for understanding and modeling the behavior of aqueous Cr(VI) under irradiation using pulse radiolysis up to 325 °C. We find that the reduction reactions of Cr(VI) to Cr(V) by the e_{aq}^{-} or $H^{\bullet}$ atom are significantly reversed by the back reaction of the product Cr(V) with the $^{\bullet}OH$ radical and the extent of this oxidation reaction has a strong dependence on pH.

The obtained kinetic parameters can be used to predict the behavior of hydrated metal ions in models of aqueous systems for applications in nuclear technology, and industrial wastewater treatment.

Aqueous (pseudo)halide radiation chemistry

Halide ions are widely dispersed in nature, in isolated hydrated form in sea water and as ionic and/or covalently bonded species occurring on the earth's crust and its atmosphere. They play a vital role in innumerable chemical, biological, environmental and industrial processes. The excess electronic charge on anions (X^-, where X=Cl, Br, I) empowers them with reducing properties. The loss of electron produces highly reactive neutral halogen atoms ($X^\bullet$) which can combine with the parent anion to form short-lived dihalide radical anions ($X_2^{\bullet-}$). In waters with low halide concentrations, halogen radicals have also been implicated in contaminant degradation during treatment by chlorine photolysis.

Water remediation using aqueous chlorine-based advanced oxidation processes, oxidation/corrosion in containers in prospective disposition of nuclear waste sites, formation of carcinogenic bromate during oxidative treatment of bromide-containing drinking water, and potential release of volatile iodine species from the contaminants in a severe nuclear accident are just a few of many practical applications requiring a detailed and complete understanding of oxidative transformations in halides. There has been continuous research interest on this topic for decades, but the nature of the early chemical events, their pH dependence, and the identification of the transients formed have not yet been unquestionably established. One of the main reasons has been the lack of structure-sensitive techniques in most laboratories to fully characterize the transients in kinetic studies carried out mostly by means of transient absorption detection under ambient conditions. It has been proposed that upon $^\bullet$OH radical addition to (pseudo)halides, OH adducts, XOH^- (X=Cl, Br, I, SCN, SeCN, *etc*.), are formed and quickly undergo reaction of either pH dependent dissociation with electron transfer or reaction with a parent halide resulting in a second intermediate, the di(pseudo)halide radical anion, $X_2^{\bullet-}$.

With the ClO^- anion in an alkaline medium, we found the formation of transients that have three absorption peaks, one of which has a λ_{max} at 420 nm, which may be associated with an oxygen impurity. We did not find any visible formation of $ClO^\bullet$ at pH values less than 6. These data help demonstrate how reactive chlorine species induced by radiolysis may affect the overall salt repository conditions

Comparative time-resolved resonance Raman (TRRR) studies of the aqueous hemibonded $(NCS\text{-}SCN)^{\bullet-}$ symmetric dimer radical anion with its asymmetric aqueous hemibonded precursor $(NCS\text{-}OH)^{\bullet-}$ were previously performed in order to understand how the nature of the hemibonded OH counterpart, affects the overall structure of the asymmetric hemibonded radical anion in water. We have now further explored the effect of the nature of the counterpart in aqueous hemi-bonded $(X\text{-}SCN)^{\bullet-}$ asymmetric radical anions on their polarization by monitoring frequencies of CS and CN stretches by means of transient resonance Raman. For asymmetric analog moieties we have chosen simple halides (X = Cl, Br, and I) which show gradual change in both electron affinities and hydration energies and hence should exhibit different polarizations across X-S hemibonds.

Structure and reactivity of organic radicals

Radical chemistry of thioureas and thiopyrimidines

Sulfur-containing compounds exhibit a complex free-radical chemistry, which is distinctly different from that of their oxygen analogs, or indeed of carbon centered free radicals. The most characteristic feature is the ability of sulfur-centered radicals to form two-centered three-electron (2c-3e) bonded intermediates such as $RS\therefore SR^{-}_{aq}$, $R_2S\therefore SR^{+}_{2aq}$, or $R_2S\therefore OH$.

Surprisingly the Raman spectrum of the dimeric thiouracil intermediate recorded in resonance with its absorption at 425 nm appeared more complex to interpret than other known hemibonded intermediates recorded to date. A typical 2c-3*e* intermediate resonance Raman spectrum has a pseudo-diatomic character *i.e.*, is dominated by the fundamental band of the hemibond stretch vibration accompanied by its much weaker overtones and occasionally additional weak bands related to other Raman-allowed vibrations coupled to the hemibond stretching coordinate. We systematically studied dimer radical cations of thiourea and its methylated derivatives to gain an understanding of how consecutive methyl substitutions affect their apparent Raman spectra as a model of thiopyrimidine dimeric intermediates to help interpretation of the more complex hemibonded intermediates of 2-thiouracils.

Systematic observations allowed us to conclude that in polyatomic asymmetric hemibonded intermediates we can no longer expect a pseudodiatomic nature of the spectrum of the intermediate because, in larger molecules with many displaced modes, overtones are less likely to be observed as vibrational progressions merely redistribute the total absorption intensity, which is in itself constant. When a large number of normal modes are displaced, the intensity invested in any one mode is less, hence overtone progressions are less readily observed.

OH radical-induced oxidation of the simplest thiopyrimidine (2-mercaptopyrimidine, 2MP) in aqueous solutions was examined by means of transient absorption, conductivity, Raman spectroscopy, and DFT calculations. We found that some of the initially produced OH-adducts to 2MP transform to thiyl radicals, which then dimerize with parent 2MP, creating a mixture of S-S hemi-bonded neutral and anionic dimer radicals with proton-sensitive multi-peak broad absorption spectra across the 300-600 nm range.

Acetate anion in high temperature water

Acetate ion is added to nuclear reactors as the counterion to Zn^{2+} for corrosion inhibition. We have investigated the kinetics and optical spectroscopy of acetate radicals up to 350 °C using pulse radiolysis of N_2O-saturated water, expecting the result to be routine first-order production from OH radical, and second order decay. However, progress in data analysis has been greatly slowed by the recognition that acetate is also a buffer. At high temperature, yields of the acetate radical are significantly perturbed, and intra-spur chemistry from proton scavenging must be specifically addressed. The same problem will be found in similar studies of any buffer.

Vibrational characterization of prototype (hydroxy)cyclohexadienyl radicals in water

Both the simplest cyclohexadienyl and hydroxycyclohexadienyl radicals produced upon $^{\bullet}H$ and $^{\bullet}OH$ addition to benzene (or d6-benzene), respectively, were generated pulse radiolytically and

characterized vibrationally using Raman scattering in resonance with their optical absorption bands located near 312 nm. The most enhanced bands in resonance Raman spectra of both types of intermediates were assigned to CCC bending, CH bending, and C=C stretching ring modes, or 6a, 9a, and 8a in Wilson notation, respectively. Due to the lower symmetry of the intermediate, 18a and 19a Wilson modes were also evident in the hydroxycyclohexadienyl radical.

Hydrated electron reactions

Whenever water is subjected to ionizing radiation electrons are liberated and, in general, hydrated electrons are created by rearrangement of the solvent around the electrons. This is the most powerfully reducing species which can exist in liquid water. Thanks to the large absorbance of e^-_{aq} in the red, thousands of reaction rate constants with various molecules have been measured.

The Marcus Theory of such an electron transfer reaction suggests that the free energy should be related to its activation energy. For the hydrated electron this is not experimentally observed. Mixed quantum/classical MD simulations were performed to demonstrate that hydrated electrons MUST satisfy Gaussian statistics as required by the theory. Additional calculations have been carried out to demonstrate that a pseudopotential approach can be used to calculate the e^-_{aq} partial molar volume. Also, parameters of a pseudopotential have been optimized in bulk water for the first time (not just a monomer) to better reproduce the optical absorption and vertical detachment energies. Finally, we have begun to carry out ab initio simulations of e^-_{aq} reacting with CO_2 in a 64-water box of DFT water, and further calculations with acetone scavenger are planned. These calculations may finally uncover how and why the Marcus theory does not seem to apply.

Electron paramagnetic resonance spectra of solvated electrons

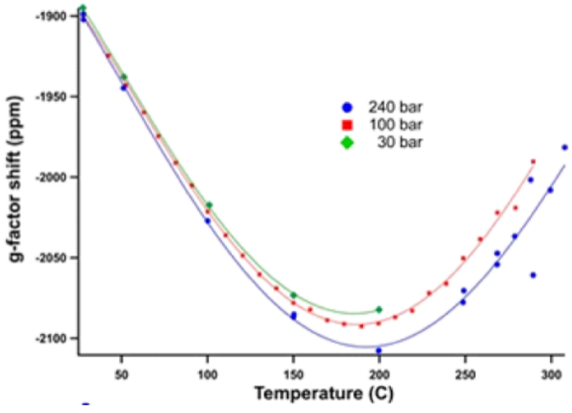

Figure D *EPR g-shift from free electron value with temperature at three different pressures.*

With the assistance of *ab initio* dielectric continuum and MD simulations, we have now been able to sensibly interpret previous results on the temperature and pressure dependence of the *g*-factor for the aqueous electron. At fixed pressures, changes in the g-factor are shown in Figure D. Normalizing to the water density reveals a simple linear increase in the g-factor with temperature, for fixed density. The g-shift is from spin-orbit coupling, proportional to spin density on water oxygen. This naturally increases with water density, but surprisingly also with temperature. Greater disorder at elevated temperature leads to less spin density in the central cavity, and more spin density on the water oxygens in the solvation shell.

At the reactor

Borate radical in high temperature water

We previously reported our discovery that OH radicals do react with the borate ion, $B(OH)_4^-$. This came as quite a surprise because, ever since a 1987 paper of Buxton and Sellers, a dogma of radiation chemistry has been that boric acid buffers are inert toward the primary radicals of water radiolysis, •OH, H and e_{aq}^-. It was in fact asserted that borax is the ideal buffer to use in radiation chemical studies and nuclear engineers have since used concentrated boric acid as a "neutron shim" in pressurized water reactor (PWR) cooling loops to fine control the neutron flux using the neutron capture by ^{10}B. An Arrhenius plot of the reaction rate revealed a 26 kJ mol^{-1} activation energy up to 200 °C, but it was not immediately obvious whether the product radical is neutral $•B(OH)_4$ or the anion $•BO(OH)_3^-$. Detailed quantum chemical calculations have now indicated, on the basis of reaction exothermicity, that only the route to the anion is thermochemically feasible.

An obvious question is whether this reaction is important to the overall mechanism of water radiolysis in PWRs? According to data from the Electric Power Research Institute, the concentration of boric acid buffer may be 0.14 M at the start of a new fuel cycle. Assuming the pH_T at 300 °C is 7.4, measured acid-base equilibrium constants suggest the borate ion concentration ought to be 1.1 mM. The reaction rate with the OH radical is then predicted to be 6.9×10^5 s^{-1}. Assuming 1.6 mM H_2 is used to suppress radiolysis (hydrogen water chemistry), we calculate that 35% of the OH radicals will react with borate rather than H_2. This is a significant perturbation of the chemistry that needs to be included in the water radiolysis model of PWRs. In the coming year we intend to investigate the second-order recombination mechanism of the borate radicals.

Extensive pulse radiolysis data have now been collected to characterize the kinetics of this hitherto unknown radical formed from OH radical reaction with borate ion, $B(OH)_4^-$ in boric acid buffer. There is no reaction with the boric acid molecule, $B(OH)_3$, itself. Three primary optical bands are observed in the deep UV, near UV and visible. The kinetics, which initially seem to be fairly straightforward first order growth and second order decay, are actually very complicated. The second order recombination rate depends on inverse of the boric acid concentration. This means that virtually all of the borate radicals, once created, form a dimer complex, but the second order decay is dominated by the cross-recombination of dimer with residual monomer. This behavior persists to quite high concentrations of borax, which means we only detect absorption of the dimer even at early times; dimerization rate is faster than the formation from OH radicals. At longer times one can see an additional process in the visible, whose rate is proportional to the boric acid concentration, which we interpret as an equilibration of radical dimer and trimer. A full mechanism with rate constants and optical spectra is under construction. In reactors, this radical species could be quite important in understanding the "axial offset anomaly" of neutron flux due to boron precipitation from subcooled boiling.

Radiolysis of new cladding materials

A variety of ceramic materials has been proposed as future nuclear fuel cladding to replace the zircaloy compounds currently in use. Ceramics display several desirable characteristics for nuclear energy applications, and thus understanding how they behave in a radiation field, particularly in accident scenarios, is necessary for their successful implementation. The work in this subtask focuses on the radiation chemical processes at the surface of nanoparticles of silicon and zirconium carbides and nitrides. Experiments were also performed with ZrO_2 and SiO_2 nanoparticles for comparison purposes. Radiation induced processes occurring at surfaces are dependent on the chemical structure of the surface itself, but the bulk also has an important role in determining the structure and stability of the surface.

Hydrogen generation from adsorbed water is used as a probe of radiation induced surface chemistry of ceramics. Most of our previous studies have focused on the radiolysis of nanoparticle oxides. Oxide surfaces produce H_2 radiolytically because they are prone to have chemisorbed water and/or hydroxyl groups that undergo radiolysis at the surface due to direct energy absorption or energy transported from the bulk medium. In non-oxide ceramics, such as carbides and nitrides, radiolytic activity of the surface to produce H_2 is expected to be minimal because of the lack of chemisorbed water species. Yields of H_2 for ZrC and ZrN are much lower than that observed with ZrO_2, where the latter is observed to have much more water on the surface.

Surface analysis techniques such as X-ray photoelectron spectroscopy and desorption studies with thermal gravimetric analysis reveal oxide layers at the particle surface of these carbides and nitrides, probably due to simple oxidation from the atmosphere. Fourier transform infrared spectroscopy also reveals oxide layers present at the surface. The thickness of the oxide layer is only few nanometers, but it seems to be enough to affect radiolysis at the surface and varies for each compound. Compounds that produce the most H_2 tend to have the greatest amount of adsorbed water and/or OH species. The energy of interactions of chemisorbed water with surface oxides and hydroxides might be an important factor that distinguishes activity of the particular surface.

All studied materials were found to have a layer of oxidation on the surface, and this layer is responsible for H_2 production. Radiation up to doses of 200 MGy were not found to affect the bulk material and very few changes to the surface. The amount of H_2 produced during irradiation correlated with the amount of water adsorbed by the ceramics, and the importance of the ceramic surface decreased as the water fraction increased. The exact nature of the surface of these ceramics is therefore incredibly important when assessing the effects of radiation.

Water radiolysis at the surface of zirconium and silicon nitrides and carbides has been examined to determine if these ceramic materials are suitable replacements nuclear fuel cladding to replace the zircaloy compounds currently in use. Focus has been on the production of H_2 as it is a readily observable product in water radiolysis. There is little adsorption of water on nitrides and carbides and the production of H_2 on the zirconium compounds is lower than has been previously observed on a variety of metal oxides including ZrO_2. Except for SiC, silicon compounds

seem to produce a reasonable amount of H_2. A substantial amount of H_2 is observed for SiN and SiO_2. A variety of surface analysis techniques have shown that those compounds producing a significant amount of H_2 have oxide surfaces that adsorb water. The effect of the surface can be readily shown by forming an oxide layer on the surface of the zirconium and silicon carbides. This oxidative layer can be formed by high heat in an oxygen atmosphere or by exposure to acid. Radiolysis of these modified carbides leads to a significant increase in H_2 production. A reexamination of materials that gave an unexpected high yield of H_2 were subsequently found to have an oxide surface layer. Atmospheric aging can have a large effect on surface chemistry and surface interactions are an important component of heterogeneous radiolysis.

In the waste stream

Persistent radicals in irradiated imidazolium ionic liquids probed by EPR spectroscopy

Room-temperature ionic liquids (RTILs) have gained popularity in extractions by virtue of their unique physical and chemical properties. Aromatic cations are often paired with the bis(trifluoromethylsulfonyl)amide anion, having beneficial properties for a variety of energy-related applications, such as high thermal stability, and variable viscosity (5.3–6410 mPa s). The radiolytic stability of aromatic RTILs has been widely studied to position them as possible extractants in nuclear fuel reprocessing technologies.

The EPR spectra of long-lived free radicals were identified in irradiated RTILs containing 1-butyl-3-methylimidazolium ($bmim^+$) and 1-hexyl-3-methylimidazolium ($hmim^+$) cations with the bis(trifluoromethylsulfonyl)imide (Tf_2N^-) anion at room temperature without a spin trap. The long-lived radical spectra presented easily recorded EPR spectra and within a 2-hour period after the irradiation the signal intensity increased almost 3 times. We did not find radical signals in the EPR spectra of irradiated RTILs, which contain various anions ($bmim^+PF_6^-$, $bmim^+Br^-$) and cations ($hmpy^+Tf_2N^-$, $hmmpy^+Tf_2N^-$). We assume that the Tf_2N^- anion stabilizes the long-lived radical species definitely formed from imidazolium cations. We also demonstrated that oxygen does not react rapidly with the persistent radical species. In an attempt to identify the long-lived radicals, the imidazolium ring was selectively deuterated at various positions. Substitution of the protons in the radicals with deuterium should dramatically reduce the hyperfine coupling constants (hfcs) and can help to explain the splitting of the remaining protons. Based on the spectral data obtained for irradiated deuterated $bmim+Tf_2N^-$ it can be assumed that the presence of methyl groups (with 8 Gauss splitting) at nitrogen atoms and of hydrogens at the C3 and C4 positions (with 2.8 Gauss) dominate the spectra.

Detailed quantum chemical calculations were conducted to identify the structure of these persistent radicals. Unfortunately, we have been unable to identify the final structures. However, based on the calculated data, it can be noted that the most suitable candidates for stable radicals are monomer or dimer radical cations. The spectrum consists of EPR lines that have splittings of 8 Gauss from 8 hydrogens that can come from methyl groups at nitrogen centers and another splitting of 2.8 Gauss from 2 hydrogens at C4, C5 positions of the imidazolium ring. The structure also has substituents (alkyls or another imidazole ring) at the second position of the imidazole

ring. The second radical is probably formed by deprotonation of this first radical and has 7 hydrogens with 8 Gauss isotropic hyperfine splitting.

These results should be considered when assessing the radiation stability of imidazole ILs, which were proposed as potential solvents for the extraction of spent nuclear fuel and other energy-related applications.

Identifying organic radicals in the nuclear waste stream

One of the most widely used solvent extraction processes is the PUREX (Plutonium - URanium EXtraction) process. The organic phase typically contains 30% tributyl phosphate (TBP) in kerosene or n-dodecane. There are some papers available on the quantitative kinetic and mechanistic investigations involving the reactions of these ligands with radical transient using pulse radiolysis. However, the structural and kinetic information about short-lived organic radical intermediates formed in such separating solutions remains questionable.

We applied EPR spectroscopic techniques to detect radical transients of organic ligands used in the solvent extraction processes. The efficiency of radiation-induced radical formation from tributyl phosphate (TBP) at room temperature was first evaluated by the PBN spin-trapping approach. The corresponding *G*-value for TBP$^{\bullet}$ is 0.22 μmol/J, which is in agreement with literature data for alkanes under the same conditions. A continuous-flow EPR method was used to study the reactions of tributyl phosphate (TBP) with the OH radical in aqueous solutions at room temperature. The half-life of the resulting TBP radicals is about 2 ms and follows an exponential decay. After careful spectral analysis, we were able to find that at least three carbon-centered alkyl radicals are formed during the reaction of TBP with $^{\bullet}$OH. Based on the calculated data, we predicted the formation of alkyl radicals formed after hydrogen abstraction from the 3rd and 4th carbon (R3 and R4 radicals), with a small contribution from the C1 radical.

Further experiments were continued with other ligands such as di-*n*-octylphthalate, di-2-ethylhexylbutyramide, and *N,N*-Diisobutyl-2-(octyl(phenyl)phosphoryl)acetamide, using low-temperature EPR spectroscopy. The proposed combined technique makes it possible to elucidate various aspects of the radiation stability of ligands, including primary and secondary processes occurring in a variety of media.

We have also explored the possibility of applying photochemical methods to generate radicals *in situ* and have carried out the first experiments to generate specific, individual carbon-centered radicals for direct measurement of their kinetics. In-house synthesized standards of dialkylazo species (C_xH_y-N=N-C_xH_y), provided by a collaborator, were used for direct detection of carbon-centered radicals ($C_xH_y^{\bullet}$) generated through photolysis. Symmetrically substituted dialkyl-azo compounds are known to be thermolabile and are useful sources for radicals. The favored mechanism for the photochemical degradation of azo compounds involves reductive cleavage of the azo group. We performed experiments with 1,2-dihexyldiazene (C_6H_{13}-N=N-C_6H_{13}) in n-dodecane or benzene saturated with Ar. We used an in-house made EPR flat flow cell to generate radicals in the EPR cavity. The samples were then irradiated in the cavity of the EPR spectrometer

with the focused light of a 1kW high-pressure mercury-xenon lamp at room temperature. Complementary to these experimental approaches, detailed quantum chemical calculations are conducted on a variety of potential radicals derived from such molecular species to help secure their identity.

Upon long-term storage

New model for the spent nuclear fuel-water interaction in deep geologic disposal conditions

One of the challenges for the future use of nuclear power to meet our energy needs while maintaining a low carbon footprint is the safe storage of the spent fuel elements. While the US has no current long-term plan, other countries such as Finland and Sweden are actively pursuing geological disposal. This task has developed a long-term radiological model that is more realistic in predicting radiation chemical effects in geological sites. A better estimate of the long-term stability of spent fuel will ultimately aid the US to develop strategic plans for spent nuclear fuel that are realistic and publicly acceptable.

Deep geological disposal is currently the leading strategy for the disposal of spent nuclear fuel. Unprocessed fuel will be stored as UO_2 encapsulated in canisters engineered to ensure long-term containment suitable for the environment of the geological site. The critical parameter is the predicted release of UO2 from its matrix to ground water followed by migration of radioactive materials to populated areas. The solubility if U(IV) is negligible but the oxidized U(VI) is very soluble. Most models for predicting oxidation of the UO_2 assume standard water radiolysis with the •OH radical and H_2O_2 molecule being the main oxidizing species. Corrosion by H_2O_2 is well known in nuclear reactors and much effort is given to mitigate its effects. However, many studies have shown that the environment in geological repositories is reducing. Deep groundwater is generally anoxic due to bacteria. The reaction of the hydrated electron with oxygen to produce superoxide anion does not occur so a source of H_2O_2 is significantly reduced.

Radiolysis of metal oxides with organic interfaces

Waste storage scenarios generally consider that surfaces will be covered by organic compounds remaining from reprocessing. Decorating surfaces with organics also leads to more fundamental scientific questions like how these molecules are adsorbed on the surface, how are they modified by direct energy absorption or by energy transfer from the bulk, how do organic compounds affect the chemistry of reactive species. The main medium for these studies was ZrO_2 because of the considerable amount of information on its radiolysis, especially the production of H_2 from adsorbed water. Nanoparticles of ZrO_2 were modified with small molecules (catechol, phenol, hydroquinone, phthalic acid, oxalic acid, and succinic acid) by simply mixing zirconium oxide with an aqueous solution of small molecules at pH ~3. Diffuse reflectance infrared Fourier transform spectroscopy, DRIFTS, spectra clearly demonstrated the presence of catechol, phthalic acid, as well as oxalic and succinic acid on the surface, while spectra of hydroquinone and phenol were not as persuasive. UV-vis also can be used for the detection of catechol, phthalic acid, phenol, and hydroquinone on the surface. Further experiments will attempt to prove surface binding as

opposed to simple adsorption. TGA of ZrO_2-catechol might prove to be a complex formation, as the degradation temperature detected was higher than the boiling point of pure catechol. Raman spectra do not reveal any small molecules. Changes in the recorded XPS were not pronounced enough use this method for detection of the changes after irradiation.

Adsorption of organic molecules on ZrO_2 nanoparticles is not completely understood so considerable effort was made to characterize the adsorbed species. Small organic molecules were dissolved in water and the pH was adjusted to 3 with HCl or NaOH (for catechol and acids). Concentrations of the solutions varied in 0.1-1 M range. 2.5 g of ZrO_2 were added to ~30 mL of the small molecule solution, shaken, and left for couple of hours to react. The next day, the precipitate was separated from the solution, thoroughly washed with water (in some variations dialyzed), and dried over Drierite at room temperature. Oxalic acid noticeably dissolved ZrO_2, so it was excluded from the study.

Radiolysis of nanoparticles containing adsorbed organic molecules clearly shows that aliphatic systems produce much more H_2 than aromatic compounds. This trend is somewhat expected as neat aliphatic compounds normally produce an order of magnitude more H_2 than aromatic compounds. The low coverage of adsorbed organic compounds to date complicate understanding the radiolysis mechanism because the surface still contains a substantial amount of adsorbed water. The organic compound may be just blocking active water sites or it could be absorbing H atoms that are expected to be the precursor to H_2. Direct production of H_2 from the organic must also be considered. Surface spectroscopic studies have not observed any noticeable changes due to radiolysis, but these techniques are known to be relatively insensitive. New studies are underway using EPR spectroscopy. This technique is extremely sensitive and is expected to provide more mechanistic information.

Aromatic dicarboxylic acids are also found to strongly attach to zirconia nanoparticles with a bidentate bond. Radiolysis of these systems leads to a reduced yield of molecular hydrogen than observed with only adsorbed water. There are several reasons why this outcome is possible and the observation of a stable radical species by electron paramagnetic resonance spectroscopy may lead to more mechanistic information of the radiolytic processes occurring at organic/solid oxide interfaces.

Future Plans

1 Fundamental advances in radiation chemistry
From energy deposition to medium decomposition

Vacuum ultraviolet (VUV) response in sub- and supercritical fluids

We will perform a series of studies in the lower-density range of supercritical water (up to 130 bar), where previously, we observed a gradual disappearance of the vibrational coherence in the first absorption band. This time we will use a high-pressure inert gas as a perturber to distinguish whether a long-range dipole effect or collisional interactions are responsible for extinguishing the vibrational coherence. After that, we will examine the impact of ion pair formation on the charge transfer to solvent (CTTS) spectra of halide anions. With our initial experiences in handling high-temperature hydroxide solutions, we will attempt to measure CTTS transitions for hydroxide anions up to supercritical conditions, also carefully examining the effects of ion pairing.

High-temperature, high-LET radiolysis by neutron capture

The detection of H_2 from neutron capture by ^{10}B represents a unique opportunity to study the source of H_2 in high-LET radiolysis at high temperature. Following on our previous experiments, we will try including a high concentration of NO_3^- to scavenge the formation of H_2 on a subpicosecond timescale, to probe the actual mechanism of radiolysis.

Temperature dependence of spur kinetics.

We have continued to investigate by Monte Carlo simulation the temperature dependence of low energy electron scattering cross-sections in water up to 350 °C. These investigations have led us to recognize a "disconnect" in understanding of low-energy cross-sections even at room temperature. Experimental data for "thermalization distance" and radiolysis spur recombination requires 2x larger cross-sections than are used to describe electron scattering in amorphous ice or in liquid microjet experiments. Indications are that a "transient negative ion" scattering mechanism (similar but distinct from dissociative electron attachment) must be invoked to reconcile the several data sets. We will continue to carry out simulations to find a mechanism that can explain all data sets.

X-ray-induced radiosensitization of gold nanoparticles

Going forward we will test these methods to characterize the sensitizing ability of other nanoparticles such as hafnium and scandium oxides. The pulse radiolysis method combined with optical absorption detection will be used to evaluate the effect of metal oxide nanoparticles on the kinetics of water radiolysis transients. A new EPR approach will be developed for the quantitative determination of the effect of nanoparticles on water radiolysis products upon exposure to ionizing radiation. This development should have broad applications.

Radiation chemistry in Electron Energy Loss Spectroscopy (EELS)

Electron Energy Loss Spectroscopy (EELS) of thin water ice has shown that molecular oxygen is the major stable product and that the O atom seems to have a major role in the radiolysis of water ice. The advantage of in-situ radiolysis studies with electron microscopy is in the

examination of water decomposition in contact with various substrates. Initial studies on the radiolysis of condensed water on silicon nitride shows different yields and trends compared to water alone. Further studies will determine the dependence of the radiolytic response of water ice at surfaces on various parameters such as exposure (dose) and ice thickness. High-level quantum chemistry calculation will offer secure identification, via X-ray absorption edges, of the proposed oxygen-containing transients.

Dissociative electron attachment (DEA) in complex environments

Our previous result, both experimental and computational, of the gas-phase DEA to three prototypical peptide molecules, formamide, *N*-methylformamide (NMF), and *N,N*-dimethylformamide (DMF) showed the common characteristics in resonance formation in the case of N-C bond cleavage. However, preliminary studies on kinetic energy and angular distribution of the fragment ions indicate strong differences in molecular symmetries of corresponding transient states for formamide and NMF. It is thus crucial to perform detailed VMI studies of resonances formed for NMF to obtain a better understanding of resonance formation.

Recently, we studied dynamics of dissociative electron attachment to ethanol with a particular focus on the Feshbach resonance formed around the incident electron energy of 9.5 eV. However, due to poor mass resolution of the current experimental setup the ion yield for this Feshbach resonance might contain contributions from both OH and O ions. Therefore, to identify the precise fragmentation pathways due to electron attachment to ethanol, isotopic studies in which deuterium or oxygen 18 are incorporated are planned.

Plasma irradiation

Our previous focus was on understanding any thermal effects of plasma irradiation and whether DNA denaturation, known to occur during heating, may be a reliable indicator of the plasma's elevated gas temperature. However, non-thermal effects, such as a pH-mediated process, can also cause denaturation. Therefore, we plan to perform systematic studies on pH measurements of plasma-treated liquids. Outcomes of these studies will contribute to better understanding of plasma radiation, which is a distinct type of radiation whose effects significantly differ from those observed for ionizing radiation.

In parallel to measurements of plasma acidities under different experimental conditions, we will use different fluorometric probes indirectly to detect electrons generated by a helium fed low-temperature plasma source. Our results on electron production as well as dose rate will be compared to those from γ and X-ray irradiation.

2 Fundamental advances in radiation chemistry
Probing radical structure and kinetics

Oxidation rates of hyper-reduced metal ions

In the next proposal period, we will investigate the clustering behavior of $Co^{2+/+}$ during radiolysis in aqueous solutions at high temperatures. This information will help to understand how cobalt ions behave in coolant water in nuclear reactors as a function of temperature.

The reactivity of chromium(III) species with the primary oxidizing and reducing radiolysis products of water will be probed up to high temperatures. The reaction between the Cr(III) species with both hydrated electrons and OH radicals will be the focus of new measurements.

In related work, we will probe the reactions of metal ions with the products of water radiolysis in oxygen-saturated solutions to more closely approximate real conditions in nuclear reactors.

Radical chemistry of thioureas and thiopyrimidines

Studies of the mechanism of radiation-induced transformations of thiourea and model thiopyrimidines, which we carried to date in anoxic conditions, will be expanded to dioxygen present conditions to understand what happens in real-world aerated solutions.

Acetate anion in high temperature water

Acetate ion is added to nuclear reactors as the counterion to Zn^{2+} for corrosion inhibition. We have investigated the kinetics and optical spectroscopy of acetate radicals up to 350 °C using pulse radiolysis of N_2O-saturated water, expecting the result to be routine first-order production from OH radical, and second order decay. However, progress in data analysis has been greatly slowed by the recognition that acetate is also a buffer. At high temperature, yields of the acetate radical are significantly perturbed, and intra-spur chemistry from proton scavenging must be specifically addressed. We will continue working on the quantitative description, which is needed to address similar experiments for any buffer.

Hydrated electron reactions

The Marcus Theory of an electron transfer reaction suggests that the free energy should be related to its activation energy. For the hydrated electron this is not experimentally observed. We have begun to carry out ab initio simulations of e_{aq}^- reacting with CO_2 in a 64-water box of DFT water, and further calculations with acetone scavenger are planned. These calculations may finally address how and why the Marcus theory does not seem to apply.

Reaction of e_{aq}^- and O_2^-

An important reaction in high temperature water radiolysis is recombination of e_{aq}^- with the O_2^- radical ion. It is very difficult to isolate this reaction for study, because the O_2^- must first be "prepared" from reaction of e_{aq}^- with O_2. We will attempt to study this reaction up to high temperature with a "long pulse" radiolysis experiment, where we first convert a large fraction of O_2 to O_2^-, then turn off the electron pulse, and measure the decay rate of residual e_{aq}^-.

Resonance Raman study of radical ion solvation shells

Resonance Raman studies of the solvated electrons generated radiolytically and photolytically in water and alcohols will be carried out in the function of temperature. The most definitive structural information on transient solvated electrons has come to date from resonance Raman measurement of the vibrational frequencies of the solvent molecules but only at room temperature.

Borate radical in high temperature water

Extensive pulse radiolysis data has been collected to characterize the kinetics of the hitherto unknown radical formed from OH radical reaction with borate ion, $B(OH)_4^-$ in boric acid buffer. The kinetics of this radical in boric acid buffer are actually very complicated. A full mechanism with rate constants and optical spectra is under construction. Further transient absorption experiments will be carried out as needed to complete the mechanistic description up to 350 °C.

Radiolysis of metal oxides with organic interfaces

The attachment of catechol to zirconia nanoparticles results in a decrease in the radiolytic production of molecular hydrogen compared to that observed with zirconia alone. Research will explore if this decrease could be due to the reaction of H atom precursors with the aromatic ring or other processes such as simple water displacement. Synthesis and radiolysis of nonaromatic di-alcohols will be used for comparison. In addition, catechol with several different side chains will be used to add additional sources or scavengers of H atom precursors.

Dependence of nanoparticle bandgap on H_2 production

The literature suggests that nanoparticles with a bandgap energy of 5 eV enhance the production of H_2 due to a coupling of adsorbed water with the surface. Such a coupling is not consistent with known adsorption spectra and preliminary experimental data using nanoparticles with significantly different bandgap energies. Bandgap measurements of nanoparticles are subject to a wide variety of factors and literature values vary widely. A series of nanoparticles will be specifically measured for their bandgap energies in conjunction with the radiolytic measurement of H_2. These data will greatly aid in the prediction of H_2 production from nanoparticles of various composition.

Identifying organic radicals in the nuclear waste stream

We plan to quantify the radiation resistance of other ligands used for the separation of nuclear waste by the EPR method. We will evaluate the effect of the medium and solvents, such as n-dodecane, on the resulting radical intermediates from ligands upon their irradiation.

Publications

2023

Abellan, P., E. Gautron, and J.A. LaVerne *The radiolysis of thin water ice in electron microscopy*. J. Phys. Chem. C **127** 15336−45. 10.1021/acs.jpcc.3c02936

Chakraborty, D. and A. Paul *Dissociation dynamics of ion-pair states accessed by low-energy electron collision: a review.* J. Phys. B: **56** 142001. 10.1088/1361-6455/ace40d

Conrad, J.K., A. Lisouskaya, L. Barr, C.R. Stuart, and D.M. Bartels *High temperature reaction kinetics of e_{aq}^- and $HO_2^\bullet$ radicals with aqueous iron (II) ions.* J. Phys. Chem. A **127** 5683–5688. 10.1021/acs.jpca.3c02436

Guerin, S., M. Al-Sheikhly, A. Thompson, C. Goodwin, S. Nam, and D. Bartels *H_2 generation by the $^{10}B(n,\alpha)^7Li$ reaction in high temperature water.* Radiat. Phys. Chem. **212** 111141. 10.1016/j.radphyschem.2023.111141

Hlushko, H., P.L. Huestis, and J.A. LaVerne *Silicon and zirconium ceramics radiolysis in the presence of water.* J. Phys. Chem. C **127** 3194–203. 10.1021/acs.jpcc.2c06787

Lisouskaya, A., O. Schiemann, and I. Carmichael *Unveiling the photodamage mechanism of sphingolipid molecules via laser flash photolysis and EPR.* Photochem. Photobiol. 10.1111/php.13804

Lisouskaya, A., P. Tarábek, D.M. Bartels, and I. Carmichael *Persistent radicals in irradiated imidazolium ionic liquids probed by EPR spectroscopy.* Radiat. Phys. Chem. **202** 110513. 10.1016/j.radphyschem.2022.110513

Markad, U., A. Lisouskaya, and D.M. Bartels *Reactions of nickel ions in water radiolysis up to 300°C.* J. Phys. Chem. B **127** 2784-91. 10.1021/acs.jpcb.3c00046

Neupane, P., D.M. Bartels, and W.H. Thompson *Relation between the hydrated electron solvation structure and its partial molar volume.* J. Phys. Chem. B **127** 5941-47. 10.1021/acs.jpcb.3c03158

Sebastian, A., D. Lipa, and S. Ptasińska *DNA strand breaks and denaturation as probes of chemical reactivity versus thermal effects of atmospheric pressure plasma jets.* ACS Omega **8** 1663-70. 10.1021/acsomega.2c07262.

2022

Alizadeh, E., D. Chakraborty, and S. Ptasińska *Low-energy electron generation for biomolecular damage inquiry: instrumentation and methods.* Biophysica **2** 475-97. 10.3390/biophysica2040041

Chatgilialoglu, C., M. Grzelak, K. Skotnicki, P. Filipiak, F. Kazmierczak, G.L. Hug, K. Bobrowski, and B. Marciniak *Evaluation of hydroxyl radical reactivity by thioether group 2 proximity in model peptide backbone: methionine versus S- 3 methyl-cysteine.* Int. J. Mol. Sci. **23** 6550. 10.3390/ijms23126550

Conrad, J.K., A. Lisouskaya, and D.M. Bartels *Pulse radiolysis and transient absorption of aqueous Cr(VI) solutions up to 325 °C.* ACS Omega **7** 39071–7. 10.1021/acsomega.2c04807

Danilović, D., A.R. Milosavljević, P. Sapkota, R. Dojčilović, D. Tošić, N. Vukmirović, M. Jocić, V. Djoković, S. Ptasińska, and D.K. Božanić *Electronic properties of silver-bismuth iodide Rudorffite nanoplatelets.* J. Phys. Chem C **126** 13739-47. 10.1021/acs.jpcc.2c03208

Hitachi, A., A. Mozumder, and K.D. Nakamura *Energy deposition on nuclear emulsion by slow recoil ions for directional dark matter searches.* Phys. Rev. D **105** 063014. 10.1103/PhysRevD.105.063014

Krancewicz, K., J. Koput, G.L. Hug, B. Marciniak, and K. Taras-Goślińska *Unusual photophysical properties of a new tricyclic derivative of thiopurines in terms of potential applications.* Spectrochim. Acta **281** 121620. 10.1016/j.saa.2022.121620

Lisouskaya, A., U. Markad, I. Carmichael, and D. M. Bartels *Reactivity of Zn^{+}_{aq} in high-temperature water radiolysis.* Phys. Chem. Chem. Phys. **24** 19882. 10.1039/D2CP02434A

Neupane, P., A. Katiyar, D.M. Bartels, and W.H. Thompson *Investigation of the Failure of Marcus Theory for Hydrated Electron Reactions.* J. Phys. Chem. Lett. 8971-7. 10.1021/acs.jpclett.2c02168

Ptasińska, S., M.T.N. Varella, M.A. Khakoo, D.S. Slaughter, and S. Denifl *Electron scattering processes: fundamentals, challenges, advances, and opportunities.* Eur. Phys. J. D **76** 1-34. 10.1140/epjd/s10053-022-00482-8

Sebastian, A., D. Spulber, A. Lisouskaya, and S. Ptasińska *Revealing low-temperature plasma efficacy through a dose-rate assessment by DNA damage detection combined with machine learning models.* Sci. Rep. **12** 1-10. 10.1038/s41598-022-21783-3

Skotnicki, K., I. Janik, K. Sadowska, G. Leszczynska, and K. Bobrowski *Radiation-induced oxidation reactions of 2-selenouracil in aqueous solutions: comparison with sulfur analog of uracil.* Molecules **27** 133. 10.3390/molecules27010133

2021

Bayda-Smykaj, M., K. Rachuta, G.L. Hug, M. Majchrzak, and B. Marciniak *White light from dual intramolecular charge-transfer emission in a silylene-bridged styrylcarbazole and pyrene dyad.* J. Phys. Chem. C **125** 12488-95. 10.1021/acs.jpcc.1c00990

Dietz, T.C., A. Thompson, M. Al-Sheikhly, M. Sterniczuk, and D.M. Bartels *H_2 production in the $^{10}B(n,\alpha)^{7}Li$ reaction in water.* Radiat. Phys. Chem. **180** 109319. 10.1016/j.radphyschem.2020.109319

Kazmierczak, L., I. Janik, M. Wolszczak, and D. Swiatla-Wojcik *Dynamics of ion pairing in dilute aqueous HCl solutions by spectroscopic measurements of hydroxyl radical conversion into dichloride radical anion.* J. Phys. Chem. B **125** 9564–71. 10.1021/acs.jpcb.1c05642

Lisouskaya, A., O. Shadyro, O. Schiemann, and I. Carmichael *OH radical reactions with the hydrophilic component of sphingolipids.* Phys. Chem. Chem. Phys. **23** 1639-48. 10.1039/d0cp05972b

Lisovskaya, A., I. Carmichael, and A. Harriman *Pulse radiolysis investigation of radicals derived from water-soluble cyanine dyes: implications for super-resolution microscopy.* J. Phys. Chem. A **125** 5779-93. 10.1021/acs.jpca.1c03776

Marin, T. and I. Janik *Ultraviolet spectroscopy of pressurized and supercritical carbon dioxide.* Commun. Chem. **4** 77. 10.1038/s42004-021-00516-z

Marin, T., I. Janik, D.M. Bartels, and D. Chipman *Failure of molecular dynamics to provide appropriate structures for quantum mechanical description of the aqueous chloride ion charge-transfer-to-solvent ultraviolet spectrum.* Phys. Chem. Chem. Phys. **23** 9109-20. 10.1039/d1cp00930c

Pastina, B. and J.A. LaVerne *An alternative conceptual model for the spent nuclear fuel/water interaction in deep geologic disposal conditions.* Appl. Sci. **11** 8566. 10.3390/app11188566

Ptasińska, S. *A missing puzzle in dissociative electron attachment to biomolecules: the detection of radicals.* Atoms **9** 77. 10.3390/atoms9040077

Smith, M., S.M. Pimblott, and J.A. LaVerne *Hydroxyl radical yields in the heavy ion radiolysis of water.* Radiat. Phys. Chem. **188** 109629. 10.1016/j.radphyschem.2021.109629

Suarez-Moreno, H.-A., L. Eckermann, F. Zappa, E. Arthur-Baidoo, S. Ptasińska, and S. Denifl *Electron ionization of clusters containing the formamide molecule.* Eur. Phys. J. D **75** 274. 10.1140/epjd/s10053-021-00281-7

Discovering the Mechanisms and Properties of Electrochemical Reactions at Solid/Liquid Interfaces

FWP Number: LAB 17-1761
Ethan J. Crumlin (ejcrumlin@lbl.gov)
Chemical Sciences Division, Lawrence Berkeley National Laboratory
1 Cyclotron Road, Berkeley, CA 94720

Project Scope:

This project will probe the molecular interactions at electrochemical interfaces through a unique multi-modal approach that combines novel spectroscopy with advanced theoretical modeling and computational science techniques. Our overarching hypothesis is that discovering the mechanisms governing interfacial electrochemical properties, in particular, the chemistry and electric potentials, will inform the development of more selective, stable, and efficient interfaces for reactions such as water splitting, CO_2 reduction, and N_2 reduction. Combining experimental approaches with theory, we will iteratively explore the complex molecular interactions of electrochemical interfaces. This strategy will expedite the discovery of new knowledge, enabling future material and device innovations.

Recent Progress:

Revealing the solid/liquid chemistry and potentials at interfaces. Probed a portfolio of metal/liquid interfaces and the influence of halide ions on interfacial chemistry as a function of applied potentials. We captured that for metallic nickel, despite being electrochemically cycled within the same pH electrolyte, changing the salt concentration and ion from KOH to KOH + KBr to KOH + KI drastically changed the interfacial chemistry as a function of applied potentials. First off, as expected, nickel hydroxide formed as we increased to more positive potentials. What we are able to explore is the thickness dependence of these surface layers, which, when compared to a standard Pourbaix diagram, only considers the bulk thermodynamic state. In all cases, we are able to observe electrochemical nickel dissolution products and the corresponding surface chemistry, which captured $NiBr_x$ surface (unexpected from computed Pourbaix diagrams). In contrast, in the presence of I^-, electrochemical dissolution was so fast that oxidized surface species would be removed faster than could be experimentally observed, generating a metallic nickel surface exposed for sustained reactivity.

We successfully directly probed the spontaneous pH-dependent polarization of metal nanoparticles on a nonconductive support. These experiments were performed on Pt and Au nanoparticles deposited on an insulating ZrO_2 support and immersed in aqueous solutions of varying pH's equilibrated in the presence of hydrogen. We were able to observe the quasi-Nernstian shifts of the electrochemical potential indicative of the spontaneous proton transfer of equilibrated H^+/H_2 interconversion that spontaneously polarizes metal nanoparticles. In addition to this finding, we were able to understand the reason for the deviation that took place. In the case of the Pt nanoparticles at pH 13, it started to shift from the expected trend. However, we were able to observe that the Pt nanoparticles no longer had a metallic surface but a hydroxide surface layer, which we attribute to changing the interfacial environment and, thus, its expected polarization.

Unraveling the polymer/liquid interface. An essential aspect of electrochemical interfaces is the complexity of the interface and what constitutes a solid/liquid interface. One of our goals was to develop the technical foundation for exploring polymer/liquid interfaces. Inspired by our initial

work to understand how water adsorbs at an atomic level on various polymers ranging from hydrophobic to hydrophilic interactions, we studied how amphiphilic polypeptoid side chains restructure and influence water adsorption depending on the host polymer. The polypeptoids under vacuum and to hydrated conditions in PEO were uniformly dispersed across the interface, while with PDMS the polypeptoids were buried beneath the surface under vacuum and restructured, segregating to the surface upon water exposure. Driving the restructuring was the polypeptoids water sorption of 2-3 waters per monomer compared to PDMS which did not sorb any water. In contrast, PDMS natively would sorb approximately 2 waters per monomer, resulting in similar sorption to the polypeptoid.

Beyond chemistry, charged membranes used for energy storage and conversion, water treatment, and many biological systems are the potential distribution induced by the difference in ion concentrations between the solid and liquid phase, generating the so-called Donnan electrical potential at a solution/membrane interface. For the first time since postulated over 100 years ago, we successfully measured an ion exchange membrane's solid/liquid Donnan Potential. Through this work, we leveraged ambient pressure XPS's (APXPS) potential sensitivity to directly measure the potential shift induced in the membrane as a function of external salt concentration. We clearly demonstrated how changing the cation charge from Na (+1) to Mg (+2) halved the expected Donnan potential. Our findings corroborated current established models for nominal membrane/liquid interface but will open the door for new advanced models and understanding of these relationships that could improve how membranes are designed and modeled in the future. One of the critical aspects of this study, beyond the experimental efforts, was the analytical model we developed to analyze the results. This is due to the complexity of the potential profile distributions generated across the membrane/liquid junction requiring an advanced spectral simulation of the electrochemical double layer in the liquid to facilitate alignment of the data.

Technique Development. We have made a lot of progress on electrochemical cell development for probing the interfacial chemistry of low-temperature fuel cells, electrolysis cells, and membrane (capacitive) desalination cells. In addition, we have successfully implemented our first electrochemical pump-x-ray probe measurements. This involved developing a data collection hardware-software interface to run the measurements and a robust data pipeline and data analysis framework to handle the significant quantity of data that is generated. We are nearing the completion of our first technical development that will demonstrate how we perform electrical pump-x-ray probe characterization up to 10 Hz.

Expanding beyond electrocatalysis and into energy storage, we successfully studied the solid/liquid surface chemistry evolution of a composite battery cathode electrode under *operando* conditions. A $Li_{1+x}[NiCoMn]_{1-x}O_2$ particles in a carbon and ionomer composite electrode was probed using APXPS to reveal the first cycle irreversible formation of an oxygen-depleted phase that correlated directly with the observation of oxygen release captured by off-line mass spectroscopy measurements. Thus, confirming and detailing the interfacial chemistry during the battery electrochemical cycling to understand what is forming and at what applied potentials.

Lastly, we have made significant progress in the development of our "Digital Twin" for simulating and processing time-resolved solid/gas surface interactions to accelerate the ability to compare experimentally collected spectra to theory and extract scientific understanding, such as the

chemical reaction microkinetic model, reaction rate constants, and interfacial chemistry from both. We are finalizing this initiative and plan to publish this work and release the code within the following year.

Future Directions:
As we move forward, I aim to continue our group's pursuit of understanding solid/gas and solid/liquid interfacial chemistry through innovation, experimentation, software, hardware, theory, and creativity. We intend to explore scientific systems such as membrane/liquid interfaces for separations, solid/solid/gas interfaces for batteries, and solid/liquid/gas interfaces for electrolysis of water, CO_2, and N_2. At the membrane/liquid interface, we will continue to explore solvation, transport, and Donnan potential properties at the interface for desalination membranes. With our newly developed cell, we will track transport rates and interfacial chemistry properties, including the Donnan potential changes, while ions are exchanged through the membrane. Regarding our electrolysis research, our approach will be to continue exploring these properties through model electrode materials (thin films, foils, drop-cast nanoparticles on a conductive substrate) and more applied configurations using nanoparticle composite catalysts dispersed on a carbon and binder support, adhered to a polymer membrane electrolyte (PEM), following the sample procedures found in commercially available cells. For both configurations, time-resolved studies will be employed for water splitting (oxygen evolution and hydrogen evolution), CO2, and nitrogen reduction reactions. We are still iterating on the PEM experimental cells to finalize a design to control electrochemistry and facilitate our simultaneous APXPS and mass spectroscopy measurements. We aim to reveal how the interfacial chemistry is influenced by the double layer, ionic species within the electrolyte and gas reactants and products while probing reaction intermediates and their role in the overall reaction cycle.

The evolution of our technique to further harness time-resolved functionality is especially exciting as it allows us to go beyond basic thermodynamic observations and pursue kinetics and dynamics. When we delve into this realm, particularly as we get to faster time scales of milliseconds to microseconds and eventually nanoseconds, we can push the boundaries of discovery and improve the connectivity between experiments and theory. Going beyond capturing kinetics and dynamics, a temporal data collection strategy, coupled with a digital twin framework, will accelerate scientific insight as data can be continuously collected and analyzed to converge on an understanding of the interface behavior in real time. Through this new functionality, we aim to accelerate our hypothesis explorations by leveraging directed learning models that adapt to the data and direct the conditions to explore. We will be able to rapidly enhance our understanding and ultimately transform how we do science.

For example, with our progression towards capacitive desalination, we aim to integrate our fast electrical pump-x-ray probe time-resolved characterization to reveal the dynamics of the ion diffusion and migration during different frequencies and amplitude of polarization. Through these studies, we look forward to understanding how non-steady-state environments can impact transportation rates and selectivity. We will continue with technical developments and initial proof of principle demonstrations to probe ionic liquid under polarization to try and capture the EDL re-ordering and a solid-state battery under cycling.

Lastly, as I finish my DOE Early Career Award and prepare to transition to the formal LBNL CPIMS program, I want to express my deep gratitude for this opportunity. I am truly thankful and excited for what will be achieved in the future as a result of this experience. Our research has generated many new questions and ideas. I am proud of how it has intersected with many different scientific disciplines, transformed the careers of many former and current group members, and established a framework for expanding scientific directions, techniques, and possibilities. Some of these achievements, which were once thought to be impossible, are now feasible and one day will become the new routine. None of the science discussed above would have been possible without this support. Thank you.

Publications Acknowledging DOE support (2021-2023):

1. Lee, K.-J.; Ye, Y.; Su, H.; Mun, B. S.; Crumlin, E. J., Correlating the Reverse Water−Gas Shift Reaction with Surface Chemistry: The Influence of Reactant Gas Exposure to Ni(100). *ACS Catalysis* **2023,** *13*, 9041 - 9050, doi: 10.1021/acscatal.3c01517.
2. Freiberg, A. T. S.; Qian, S. M.; Wandt, J.; Gasteiger, H. A.; Crumlin, E. J., Surface Oxygen Depletion of Layered Transition Metal Oxides in Li- Ion Batteries Studied by Operando Ambient Pressure X-ray Photoelectron Spectroscopy. *ACS Applied Materials & Interfaces* **2023,** *15* (3), 4743-4754, doi: 10.1021/acsami.2c19008.
3. Jana, A.; Snyder, S. W.; Crumlin, E. J.; Qian, J., Integrated carbon capture and conversion: A review on C2+ product mechanisms and mechanism-guided strategies. *Frontiers in Chemistry* **2023,** *11*, doi: 10.3389/fchem.2023.1135829.
4. Wei, X.; Johnson, G.; Ye, Y.; Cui, M.; Yu, S.-W.; Ran, Y.; Cai, J.; Liu, Z.; Chen, X.; Gao, W.; Bean, P. J. L.; Zhang, W.; Zhao, T. Y.; Perras, F. A.; Crumlin, E. J.; Zhang, X.; Davis, R. J.; Wu, Z.; Zhang, S., Surfactants Used in Colloidal Synthesis Modulate Ni Nanoparticle Surface Evolution for Selective CO2 Hydrogenation. *Journal of the American Chemical Society* **2023,** *in press*, doi: 10.1021/jacs.3c02739.
5. Wesley, T. S.; Hülsey, M. J.; Westendorff, K. S.; Lewis, N. B.; Crumlin, E. J.; Román-Leshkov, Y.; Surendranath, Y., Metal nanoparticles supported on a nonconductive oxide undergo pH-dependent spontaneous polarization. *Chemical Science* **2023**, doi: 10.1039/D3SC00884C.
6. Gokturk, P. A.; Sujanani, R.; Qian, J.; Wang, Y.; Katz, L. E.; Freeman, B. D.; Crumlin, E. J., The Donnan potential revealed. *Nature Communications* **2022,** *13* (1), doi: 10.1038/s41467-022-33592-3.
7. Lee, J. D.; Qi, Z.; Foucher, A. C.; Ngan, H. T.; Dennis, K.; Cui, J.; Sadykov, II; Crumlin, E. J.; Sautet, P.; Stach, E. A.; Friend, C. M.; Madix, R. J.; Biener, J., Facilitating Hydrogen Dissociation over Dilute Nanoporous Ti-Cu Catalysts. *Journal of the American Chemical Society* **2022**, doi: 10.1021/jacs.2c00830.
8. Qian, J.; Crumlin, E. J.; Prendergast, D., Efficient basis sets for core-excited states motivated by Slater's rules. *Phys. Chem. Chem. Phys.* **2022,** *24* (4), 2243-2250, doi: 10.1039/d1cp03931h.
   Carvalho, O. Q.; Crumlin, E. J.; Stoerzinger, K. A., X-ray and electron spectroscopy of (photo)electrocatalysts: Understanding activity through electronic structure and adsorbate coverage. *J. Vac. Sci. Technol. A* **2021,** *39* (4), 30, doi: 10.1116/6.0001091.
9. Barry, M. E.; Gokturk, P. A.; DeStefano, A. J.; Leonardi, A. K.; Ober, C. K.; Crumlin, E. J.; Segalman, R. A., Effects of Amphiphilic Polypeptoid Side Chains on Polymer Surface Chemistry and Hydrophilicity. *ACS Appl. Mater. Interfaces* **2022,** *14* (5), 7340-7349, doi: 10.1021/acsami.1c22683.
10. Ahmed, M.; Blum, M.; Crumlin, E. J.; Geissler, P. L.; Head-Gordon, T.; Limmer, D. T.; Mandadapu, K. K.; Saykally, R. J.; Wilson, K. R., Molecular Properties and Chemical Transformations Near Interfaces. *J. Phys. Chem. B* **2021,** *125* (32), 9037-9051, doi: 10.1021/acs.jpcb.1c03756.
11. Su, H. Y.; Ye, Y. F.; Lee, K. J.; Zeng, J.; Crumlin, E. J., Probing the nickel corrosion phenomena in alkaline electrolyte using tender x-ray ambient pressure X-ray photoelectron spectroscopy. *Journal of Physics D-Applied Physics* **2021,** *54* (37), doi: 10.1088/1361-6463/ac09bb.
12. Aierken, Y.; Agrawal, A.; Sun, M. L.; Melander, M.; Crumlin, E. J.; Helms, B. A.; Prendergast, D., Revealing Charge-Transfer Dynamics at Electrified Sulfur Cathodes Using Constrained Density Functional Theory. *Journal of Physical Chemistry Letters* **2021,** *12* (2), 739-744, doi: 10.1021/acs.jpclett.0c03334.
13. Richter, M. H.; Cheng, W. H.; Crumlin, E. J.; Drisdell, W. S.; Atwater, H. A.; Schmeisser, D.; Lewis, N. S.; Brunschwig, B. S., X-ray Photoelectron Spectroscopy and Resonant X-ray Spectroscopy Investigations of Interactions between Thin Metal Catalyst Films and Amorphous Titanium Dioxide Photoelectrode Protection Layers. *Chemistry of Materials* **2021,** *33* (4), 1265-1275, doi: 10.1021/acs.chemmater.0c04043.
14. Ye, Y. F.; Su, H. Y.; Lee, K. J.; Larson, D.; Valero-Vidal, C.; Bium, M.; Yano, J.; Crumlin, E. J., Carbon dioxide adsorption and activation on gallium phosphide surface monitored by ambient pressure x-ray photoelectron spectroscopy. *Journal of Physics D-Applied Physics* **2021,** *54* (23), doi: 10.1088/1361-6463/abec0a.

Observing the Molecular & Dynamic Pathway of Water Oxidation at the Regulated $SrTiO_3$/Aqueous Interface

Principal Investigator: Tanja Cuk (tanja.cuk@colorado.edu)

Mailing Address: Renewable and Sustainable Energy Institute (RASEI)
University of Colorado, Boulder, 4001
4001 Discovery Drive, Boulder CO 80303

Project Scope:

Chemical transformations have far-reaching impacts for energy utilization, energy storage, and chemical synthesis. The understanding of how chemical transformations occur in real, complex environments is fundamental to our ability to control them and scale them for our needs. Further, at these complex interfaces, chemical transformations occur in a markedly efficient and directed manner and are therefore catalytic or occur with underpinnings which are understandable and tunable. Ultrafast chemistry at heterogeneous, condensed phase interfaces (*e.g.* solid-liquid) develops and applies approaches to reveal how the dynamics of charge across the interface, and between molecular reactants, controls reactivity.

The ultrafast excitation and efficient charge separation at the electron doped (Nb)-$SrTiO_3$/aqueous interface enables triggering the oxygen evolution reaction (OER) at a distinct time point, from which the subsequently downhill and sequential reaction steps can be followed by time-resolved optical spectroscopy in the visible range of electronic transitions, mid-infrared range of vibrational normal modes, and terahertz range of continuum strain (via coherent oscillations in the visible). This platform led to observing the formation and decay of the first electron and proton transfer OER intermediate from a water adsorbed species. By measuring the population dynamics of a meta-stable intermediate, an experimental mapping was made to thermodynamic free-energy descriptors.

The current proposal aims to build kinetic models by connecting reaction dependent population dynamics below nanoseconds to beyond microseconds and discover how the hydration layer and screening modulate the intermediate population. It also aims to build transient optical setups to time-resolve dark, thermochemical steps, such as the formation of the O-O bond. In doing this work, the research advances the design of catalysts for OER by using a model 3d transition metal oxide to experimentally determine to-date theoretical descriptors of activity. The quantitative information on the thermodynamics and kinetics of reaction intermediates will provide the foundation for new chemical models of condensed phase interfaces and advance methods for their *in-situ* spectroscopy.

Recent Progress:

Computationally, often the thermodynamics of intermediate reaction steps differentiate the efficiency of heterogeneous catalysts for product evolution. Yet, when compared to experiment, kinetic models are applied. For example, a material's activity measured by one rate of product evolution is plotted as a function of the calculated formation energies of intermediate chemical forms. A critically important reaction for which this dichotomy between experiment and theory exists is the oxygen evolution reaction (OER) from water. A recent success was to isolate a Langmuir isotherm of the intermediate population the first electron and proton transfer intermediate arising within < 2 ps on the $SrTiO_3$ surface (Figure 1). The intermediate population is of trapped holes measured by emission from the conduction band into unoccupied states in the middle of the semi-conductor bandgap. The isotherm is tuned by the pH of the electrolyte, with a half-rise occurring at pH 11.8. The Langmuir isotherm is modeled by sequential reaction steps to create the intermediate and contains its formation free energy.

The stimulated emission occurred with clear coherent, terahertz oscillations that exhibit a dispersion relationship quantitatively modelled by the acoustic velocity of strain waves in $SrTiO_3$. The magnitude of these oscillations exhibited the same pH dependence as the stimulated emission and like the emission, saturates at relatively low laser fluences (~4% of the surface sites). The phase of these oscillations was modelled by a changing dielectric constant with phenomenological parameters for the formation time and spatial decay of an interfacial continuum strain. The formation time of the continuum strain (1.3 ps) is consistent with the rising exponential kinetics of the emission. It is also consistent with the formation time of a normal mode seen for the oxyl radical, or hole-trapping at a terminal hydroxylated site, Ti-OH^*. Therefore, a similar time constant for hole-trapping is seen across the electromagnetic spectrum. This furthers the assignment of the broad visible emission below the bandgap to molecular distortions of titanium-oxygen bonds.

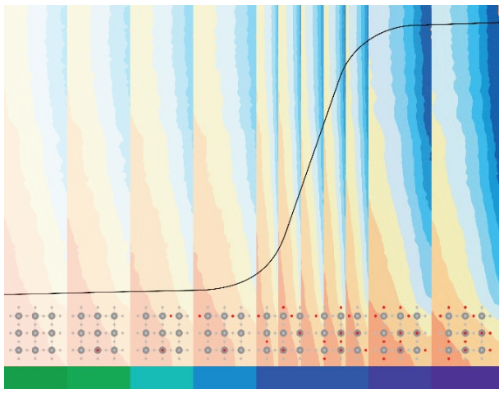

Figure 1. The time-resolved optical data (vertical axis) as a function of pH (horizontal axis) generates a reaction isotherm (black trace). The emission (in blue) counts the intermediate population created by the first proton and electron transfer from an absorbed aqueous species.

More recent work using the broadband visible probe follows the mid-gap signatures of the intermediates from 400 fs through 500 microseconds. The full kinetic model of the emissive population dynamics has been underway. After the initial pH dependent < 2 ps rise followed by a pH-independent rise ~60-100 ps, the population is metastable through microseconds. It then decays bi-exponentially with ~10 μs and ~100 μs time constants. We recently discovered that the population dynamics of the bi-exponential decay map onto their bi-exponential formation. The population with the ~ 10 us decay constant is pH dependent, increasing near pH 11 where the rise of the Langmuir isotherm of the population with the < 2 ps formation constant starts. The full kinetic model will then bracket pH-dependent mechanisms by which these hole-traps can lead to the next reaction steps of OER.

In parallel, we have been characterizing the differently electron doped $SrTiO_3$ surfaces before OER. We have done this through standard surface science techniques such as UHV AFM, XPS and LEED. Importantly, we have also characterized the hydration layer under neutral conditions using ambient pressure XPS (AP-XPS). These experiments describe how water dissociation changes based on the crystal termination, defect structure, and most recently, electron doping. Interestingly, changing the electron doping from 0.1 % Nb to 0.7 % Nb in $SrTiO_3$ increased the water dissociation considerably, creating an almost fully hydroxylated surface. The next steps are to correlate these changes in the hydration layer with the time-resolved optical spectra.

The $SrTiO_3$ surfaces have also been well-characterized post catalysis. These efforts now tie together the scanning methodology used to preserve the surface that optical spectroscopy sees to optical microscopy, scanning transmission electron microscopy, scanning electron microscopy, and XPS. It also puts an upper limit on the oxygen evolution that could come from the $SrTiO_3$ lattice rather than from water with our excitation conditions.

Future Work:

There are several avenues planned for future work based on the recent progress and the spectroscopic techniques currently available. The spectroscopic techniques include the time-resolved optical spectroscopy in the visible and mid-IR regimes. Further, a new way to modulate the photo-electrochemistry is introduced that will probe surfaces with a dynamically changing hole-population controlled by the Schottky junction. In short, the planned projects include:

(1) Given the pH dependence (e.g. the Langmuir isotherm) seen by the visible probe of emission on 0.1% Nb $SrTiO_3$ and the changes in the hydration layer seen for differently doped $SrTiO_3$ by AP-XPS, we plan to collect and analyze the pH-dependence of 0.7% Nb $SrTiO_3$ in the ultrafast and microsecond regimes.

(2) Given that the continuum strain derived from the THz oscillations reflects distortions in the titanium oxygen reaction coordinate, we will revisit mid-IR spectroscopy of the normal mode associated with the oxyl radical. Here, the Fano lineshape sensitive to the librational modes of the electrolyte will allow us to investigate the formation dynamics as a function of the liquid vs. air interface. Recent data has shown that the resonance and anti-resonance of the Fano lineshape can isolate formation dynamics via the coupling constant of the mode to its surroundings.

(3) Thus far, efficient photo-electrochemistry on $SrTiO_3$ has been achieved using a constant potential applied to the electrode, while the current is modulated by the repetitive, ultrafast laser pulse. Recently, we have found a way to synchronize the potential control to the trigger of the ultrafast laser and with the same repetition rate. This advancement should allow us to investigate the population dynamics and surface degradation while dynamically modulating the efficiency of charge-separation and surface hole transfer through the Schottky junction.

Peer Reviewed Publications Resulting from this Project (2021-2023):

1. T. Cuk, “Phenomenology of intermediate molecular dynamics at metal-oxide surfaces,” Annual Review of Physical Chemistry, 2023 (accepted).

2. H. Lyle, S. Singh, E. Magnano, S. Nappini, F. Bondino, S. Yazdi*, and Tanja Cuk*, "Assessing and quantifying thermodynamically concomitant and kinetically hindered degradation during oxygen evolution from water on n-SrTiO3," *ACS Catalysis* 2023 13, 8206.

3. C. Courter, J. Stewart, and T. Cuk* "Moderate electron doping assists in dissociating water on a transition metal oxide surface (n-SrTiO3)" Journal of Physical Chemistry C 2023 127, 4905.

4. I. Vinogradov, S. Singh, H. Lyle, A. Mandal*, J. Rossmeisl, and T.Cuk*, “Free energy difference to create the M-OH* intermediate of the oxygen evolution reaction by time-resolved optical spectroscopy,” *Nature Materials* 2022, 21, 88.

5. S. Singh, H. Lyle, L. D’Amario, E. Magnano, I. Vinogradov*, and T. Cuk*, "Coherent acoustic interferometry during photo-driven oxygen evolution reaction associates strain fields with the reactive oxygen intermediate," *J. Am. Chem. Soc.* 2021, 143, 39, 15984.

6. H. Lyle, S. Singh, M. Paolino, I. Vinogradov, and T. Cuk*, “The electron-transfer intermediates of the oxygen evolution reaction as polarons by in-situ spectroscopy,” *Physical Chemistry Chemical Physics* 2021, 23, 24984.

7. X. Chen* and T. Cuk**,** “One-electron water oxidation intermediate on TiO2 P25 probed by ultrafast attenuated total reflection,” *J. Phys. Chem. C.* 2021, 125, 33, 18204.

Using Ultrafast Entangled Photon Correlations to Measure the Temporal Evolution of Optically Excited Molecular Entanglement (DE-SC0020151)

Scott Cushing
Chemistry and Chemical Engineering, Caltech
1200 East California Blvd, Pasadena CA 91125
scushing@caltech.edu

Project Scope:

The goal of this project is to build an ultrafast entangled photon spectrometer and use it to test theoretical predictions that photoexcited states are modulated by spin-photon interactions. Entanglement of two states describes a specific type of quantum superposition in which measuring one state gives information about a second state. While entanglement is well explored for quantum information and computing systems, its effects on photoexcited states are less understood, especially in the ultrafast domains of molecular vibronic coupling. The grant designs a frequency and temporally resolved entangled photon spectrometer and uses it to test theoretical predictions like enhanced two photon absorption, non-reciprocal Fourier relations, and coupling of photons to spin systems. The end goal of the project is an understanding of how, when, and where entanglement is useful for spectroscopy.

Recent Progress:

Ultrafast Spectroscopy of Entangled Photon States

When the program was initiated, entangled photon spectroscopy of molecules was limited to classical transmission or fluorescence measurements without characterization of the quantum state itself. This was because of the low flux of traditional spontaneous parametric down conversion sources (SPDC) and the low purity of entangled photons states from ultrafast lasers. We therefore designed and created on-chip, periodically poled photonic waveguides and gratings which have a million-time higher efficiency than a traditional nonlinear crystal (10^{-6} compared to 10^{-12}).[1] The chirped gratings create visible-by-eye beams of entangled photons with correlations times of <10 fs with 99% purity, all from a CW laser. We have created periodically poled SPDC sources that cover the UV to NIR wavelength ranges needed for entangled photon spectroscopy, setting records for lithium niobate in terms of wavelength range and efficiency.[2] The sources were used to design a spectrometer that can measure the change in an entangled photon state in terms of both quantum and classical correlations when interacting with a molecule (Figure 1).

Entangled Photon – Molecule Interactions

We used the ultrafast entangled photon spectrometer to measure three excited state interactions that are theorized to be enhanced by entangled photons.

1) Entangled two photon absorption and fluorescence: The linearity of entangled photons in a two (or more) photon nonlinear process is now confirmed, but the magnitude of said enhancement was highly debated. Using the ultrafast entangled photon spectrometer, we were able to put bounds on

the two-photon enhancement at $<10^{-25}$ cm^2 in several molecular systems.[3] More importantly, we were able to prove why other measurements in the field were giving false absorption enhancements comparable to single-photon cross sections ($>10^{-18}$ cm^2) because of resonant scattering processes (Figure 1). Although the entangled enhancement is too low to be practical for spectroscopy and microscopy, the signal being just a few photons per minute, the measurements refined ultrafast single photon detection techniques and advanced theoretical methods.

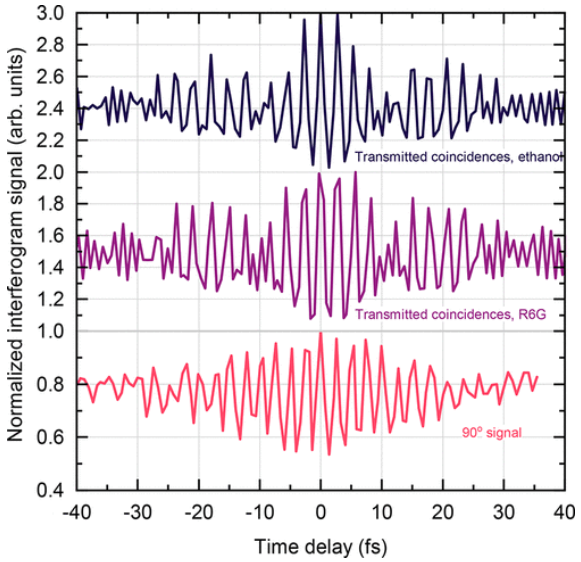

Figure 1. Characterization of the quantum state before, after, and the off-axis signal (top to bottom) interaction with R6G in a two-photon absorption geometry. The asymmetry of the interference pattern's amplitude relates to the quantum state. No change is measured in the quantum state after transmission, only a loss of some classical frequency components. The off-axis signal is purely single photon in nature.

2) Non-reciprocal Fourier relations of entangled photons. In SPDC, two entangled photons are created simultaneously from one pump photon. The combined spectral resolution of the entangled photons therefore depends on the linewidth of the pump laser while their temporal resolution depends on their relative dispersion after being created. This allows for a CW laser with a MHz linewidth to measure <10 fs dynamics, and we confirmed this fact in several molecules.[1,3] The concept is used for single photon, single molecule approaches in the future, described more in the next section.

3) Does an excited spin state preserve the entangled photon state: Finally, we measured whether the superposition of an entangled photon and a spin state preserves the initial entangled state. We performed this experiment using a molecule, indocyanine green (ICG), that has an S_0-S_1-S_2 sequential two-step transition and a single-step S_0-S_2 transition, both of which support absorption and fluorescence. The sequential fluorescence spectrum and its temporal modulation measure whether one entangled photon is enhancing or changing the second entangled photon's sequential absorption event. Specifically, we measure if the modulation of the S_1-S_0 versus S_2-S_0 fluorescence follows the quantum correlations of the entangled state or if it is dephased too quickly, resulting in a classical process, like in Figure 1. Experiments were performed in both entangled pump-probe and fluorescence correlation geometries. In both cases, for a ~20 fs correlation time between entangled photons, it was determined that the entangled photon - spin quantum state was dephased. The results confirm that electronic dephasing processes are important for entangled photon excited state interactions and not just vibronic coupling as usually discussed in molecular qubits.

Entanglement Enables Single Photon, Single Molecule Pump-Probe Measurements

If we consider the entangled photons in the simplest way – practically ignoring entanglement – we are left with two spectrally and temporally correlated single photon pulses. If spectroscopy is performed with one or both photons, and corresponding temporal correlations are measured, the signal must come from one molecule or one molecule and any surrounding interaction. Classical time-resolved, single-molecule-like spectroscopy is therefore possible without precise spatial resolution or incredibly dilute samples. We explored both time-resolved fluorescence and pump-probe spectroscopy as first steps towards realizing single photon – single molecule type spectroscopy. The time resolved fluorescence approach uses entangled correlations produced from CW laser diodes.[4] Better performance characteristics than classical pulsed lasers or CW modulation approaches were achieved. Fluxes millions of times higher than the saturation of modern TCSPC are easily created from the low power CW diode laser without pulsing and without saturating the molecular population. For the pump-probe measurements, we discovered that three entangled photons are needed, the third being used to confirm if the measured signal is correlated with the initial two-photon state that the molecule interacted with. We confirmed this theoretically as well as experimentally. The concept of needing one additional photon will hold for most classical adaptions of entangled ultrafast spectroscopy. While both measurements are early steppingstones to the final single molecule experiments, they represent some of the first experiments where, from a full systems design perspective, entangled photons can beat classical pulsed laser performance.

Future Directions:

Completely On-Chip, Low-Power and Portable Ultrafast Spectroscopy

Using our entangled photon methodology and on-chip photonics, we will build the first completely on-chip ultrafast spectrometers that can be powered by a battery. Entangled photon technology can bring techniques like pump-probe and 2D spectroscopy to an integrated platform at low cost. This is enabled by the ability of entangled photons to convert a low power CW laser diode into a femtosecond time-resolved, ultrafast optical source. Compared to classical on-chip frequency combs and other pulsing schemes, using entangled photons is simpler because the instantaneous power is lower but the time-averaged flux and therefore signal is higher. Additionally, less dispersion management and electro-optics are needed, and periodically poled elements are easily stacked for higher order spectroscopy. From a fundamental science perspective, the on-chip integrated spectrometers are also ideal for exploring how single molecules interact with a continuum under low excitation densities and without needing spatial resolution. In our bulk measurements, we have hit shot noise detection limits at small signals because we are statistically sampling many molecules with few photons. Using on-chip sampling, the coupling efficiency between molecules and photons can be greatly improved, boosting sensitivity. Complete on-chip design therefore has interesting technical and scientific prospects.

Peer-Reviewed Publications Resulting from this Project (2021-2023)

[1] Szoke, S.; He, M.; Hickam, B. P.; Cushing, S. K. Designing High-Power, Octave Spanning Entangled Photon Sources for Quantum Spectroscopy. *J. Chem. Phys.* **2021**, *154* (24), 244201.

[2] Tunable and efficient ultraviolet generation in nanophotonic lithium niobate, E. Hwang, N. Harper, R. Sekine, L. Ledezma, A. Marandi, **S. K. Cushing†**, *Optics Letters*, 48, 3917-3920 (2023). doi.org/10.1364/OL.491528

[3] Hickam, B. P.; He, M.; Harper, N.; Szoke, S.; Cushing, S. K. Single-Photon Scattering Can Account for the Discrepancies among Entangled Two-Photon Measurement Techniques. *J. Phys. Chem. Lett.* **2022**, *13* (22), 4934–4940.

[4] Harper, N.; Hickam, B. P.; He, M.; Cushing, S. K. Entangled Photon Correlations Allow a Continuous-Wave Laser Diode to Measure Single-Photon, Time-Resolved Fluorescence. *J. Phys. Chem. Lett.* **2023**, *14* (25), 5805–5811.

A Synthetic Electronics Route to Scalable and Competitive Molecular Qubit Systems (DE-SC0022089)

Scott Cushing (Lead PI), scushing@caltech.edu
Caltech, 1200 East California Blvd, Pasadena CA 91125

Co-PI's: Ryan Hadt, Theo Agapie (Caltech)
Hai-Ping Cheng (University of Florida)
Wei Xiong, Joel Yuen-Zhou (University of California San Diego)
Gaungbin Dong (University of Chicago)

Project Scope:

The grant focuses on the development of a scalable, molecular qubit on a nanographene architecture. The molecular qubits allow for chemical control of optical and microwave addressable signals. Nanographene allows for the precise relative positioning of multiple molecular qubits on the nanometer scale. The combined molecular qubit and nanographene can then be integrated with a nanophotonic waveguide to increase coupling to the optical and microwave fields. The grant will result in an understanding of molecular qubit dephasing and coupling mechanisms, both within one qubit and between multiple coupled qubits, as well as their interaction with synthetic electronic components. The program's end goal is a systematic evaluation of the advantages and disadvantages of molecular qubit systems for single and multiple qubit applications.

Recent Progress:

Thrust 1: Microwave and optically addressable molecules with multiple qubits.
A combined spectroscopy, synthesis, and theory approach is used to create molecular qubit systems and then understand their coupling and dephasing mechanisms.

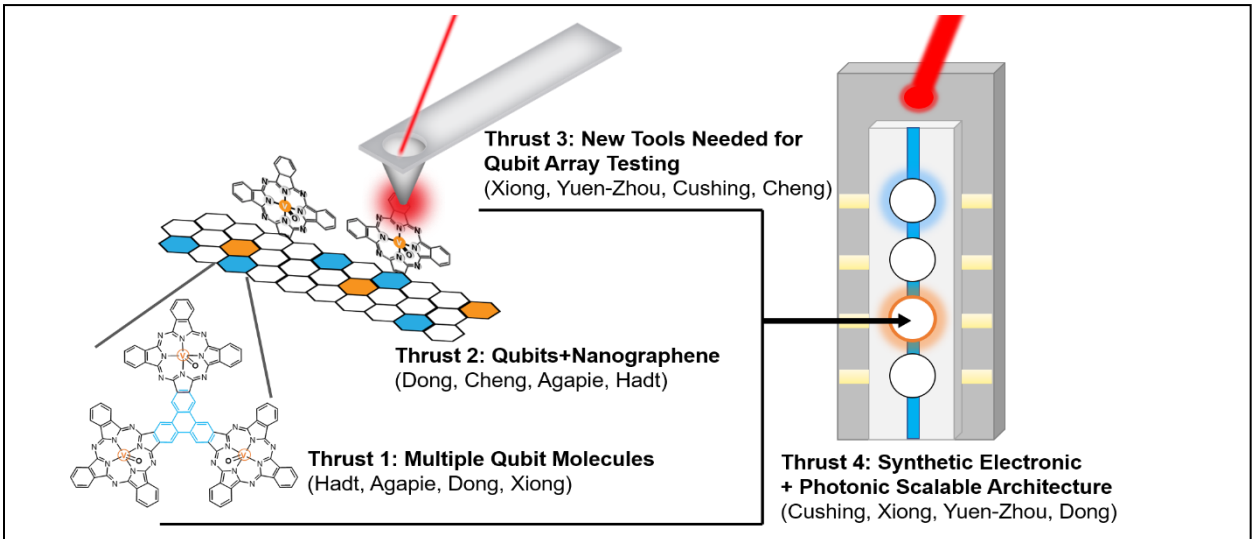

Figure 1. Organization of the research thrusts in this DOE proposal. The research thrusts start with molecular details and progresses into a scalable electronic / photonic architecture.

First, a new modular phenanthroline macrocyclic ligand ($MesN_6$) has been developed for microwave addressable molecular qubits. Primary efforts focused on leveraging the ligand rigidity of $MesN_6$ and the larger electronic energy gap for Cu-centers compared to Co-centers to generate a room temperature coherent S=1/2 qubit. We first demonstrated manipulation of the d-orbital spacing by incorporating different axial ligands. Although axial ligands are detrimental to phase coherence due to new vibrational modes, computational work by the Hadt group suggested that the ligands could actually promote coherence times in Co-centers by increasing the energy gap between the excited and ground state compared to the vibrational mode energy. We have confirmed this counterintuitive design rule using pulsed electron paramagnetic resonance (EPR) measurements. Phase coherence was maximized by both limiting vibrational modes and maximizing the energy gap between the excited and ground state. Synthetic methods were also developed that create molecularly controllable multimetallic systems that are now being used to explore the effects of π-conjugation, distance, and orientation on phase decoherence and coupling strength.

Second, new mechanistic insights were obtained for creating molecular optically addressable qubits. Current molecular analogues of the anionic nitrogen vacancy in diamond suffer from rapid spin-lattice relaxation (T_1) even at sub-liquid nitrogen temperatures. Using an optically addressable S=1 $Cr(o\text{-}tolyl)_4$ molecular qubit as a model system, temperature- and orientation-dependent pulsed EPR spectroscopy revealed that the negative sign of the zero-field splitting is in spin anisotropy.[1] This is important for the development of ligand field models elucidating the specific types of atomic motions that contribute to spin relaxation. Specifically, the T_1 anisotropy of S=1 $Cr(o\text{-}tolyl)_4$ demonstrated that spin relaxation can be driven by rotational motions in low-energy acoustic or pseudoacoustic phonons.

Thrust 2: Molecular qubits on nanographene for atomically precise qubit arrays.
The use of nanographene as an atomically controllable host substrate for the molecular qubits was explored. The use of nanographene allows for easy qubit-qubit coupling control, electronic gating, and nanophotonic integration.

We explored the qubit nanographene system from multiple theoretical fronts. A Clar's goblet-graphene interactions was first studied.[2] This molecule is a radical with unpaired spins and thus a candidate for a spin qubit on nanographene. We find that graphene serves as a reservoir for charge doping and the strength of an external gating field controls the charge transfer level and sign. The doping does not alter the fundamental physical and chemical properties of the nanographene flake. Vanadyl phthalocyanine (VOPc) molecules were then integrated in the nanographene ribbons. Density functional theory was used to obtain ground state atomic configurations and electronic and magnetic structure with the inclusion of spin-orbital interactions. We parameterized a spin Hamiltonian with hyperfine and electric field gradient tensors calculated from density functional theory and then studied spin decoherence due to coupling with a surrounding nuclear spin bath. We then studied an electronic molecular spin of a VOPc molecule attached to edges of zigzag nanoribbons, including the fidelity of two-spin qubits on nanographene in terms of decoherence time and mechanisms to optimize synthetic design.

The theoretical findings were then used to guide synthesis. This included the first successful synthesis of nanographene-conjugated VOPc complexes. The complexes had yet to be synthesized

in literature, even if the sub-components of nanographene and VOPc are common. An important lesson learned from trying to merge these systems in a controllable manner was that the final cyclodehydrogenation step is incompatible with the VOPC part by chemical oxidation methods, so alternative approaches were used. These included on-surface cyclohydrogenation by a STM platform and a cyclodehydrogenation-first-then-VOPC-coupling strategy.

Thrust 3: New spectroscopy and Qubit Nanophotonic Coupling

New techniques were designed to explore the spin-vibronic coupling and magnetic properties of the molecular spin qubit and nanographene candidates. The design of an integrated photonic, electronic, and microwave component that can be used to test or link different qubit centers.

To probe the surface geometry and spin dynamics of the 2D materials, a sum frequency generation (SFG) pump-probe spectroscopy setup was built. We have demonstrated the technique's versatility on various interfacial systems, such as organic-organic polymer heterojunctions TMD-molecule interfaces for first tests.[3] The spectroscopy setup was then applied to determine orientation and framework conformation of the nanographene with conjugated molecules to help guide the various synthetic approaches that were tried. This included developing a repeatable manner to prepare monolayer samples of the nanographene by a matrix-assisted direct transfer method, which is essential for meeting the non-centrosymmetric requirement of SFG. The setup is currently being used to study spin dynamics using direct interfacial charge transfer as a momentum and spin probe. The theoretical framework to describe the time resolved SFG technique in both cases was developed.

A nanophotonic lithium niobate platform was also developed for final integration of multiple nanographene-molecular qubit systems and enhanced coupling to single molecular qubits. Compared to Si nanophotonics, lithium niobate supports a broader wavelength range across the visible spectrum relevant for molecular optical qubits. It also has a strong second-order nonlinearity, allowing easy integration of modulators and other nonlinear interaction elements for optical circuitry. Our work has focused on (1) pushing the lithium niobate transparency range further towards the UV, (2) creating the waveguides, filters, and switches for optical addressing, and (3) integrating electrical contacts and transmission lines for microwave gating of the qubits. The overall goal is to take advantage of the repeatable patterning possible for the nanographene to easily create multiple coupled qubit gates in the future in a compact device.

Future Plans:

All-organic optically addressable qubits

In addition to the integration and experimental testing of multiple qubit centers on nanographene, novel all-organic molecular qubits are being theoretically explored.

In recent years, there has been growing interest in bottom-up molecular design of organometallic molecular complexes, such as studied here, but these systems have yet to reach the utility of NV centers. This is in part due to the difficulty of creating S=1 inorganic molecular centers. As a forward-looking work, we have been theoretically designing a fully organic molecule capable of both qubit initialization and readout via visible light. The open-shell nature of NV centers is

recreated with organic biradicals, and optical addressability is achieved via photoluminescence. We have analyzed the electronic structure of our system and are in the final stages of piecing together the mechanism for operation. Our system provides a metal-free alternative to existing molecular color centers and is experimentally feasible considering recent reports of luminescent organic diradicals being synthesized.

Peer-Reviewed Publications Resulting from this Project (2021-2023)

[1] N. P. Kazmierczak, K. M. Luedecke, E. T. Gallmeier, R G. Hadt, T1 Anisotropy Elucidates Spin Relaxation Mechanisms in an S = 1 Cr(IV) Optically Addressable Molecular Qubit. *J. Phys. Chem. Lett.* (**2023**), 14, 34, 7658–7664.

[2] Adam V. Bruce, Shuanglong Liu, James N. Fry, and Hai-Ping Cheng, Clar's Goblet on Graphene: Field-Modulated Charge Transfer in a Hydrocarbon Heterostructure, *J. Phys. Chem. C* **(2022)**, 126, 12, 5640–5648.

[3] C. Wang, Y. Jing, L. Chen, W. Xiong, Direct Interfacial Charge Transfer in All-Polymer Donor–Acceptor Heterojunctions. *J. Phys. Chem. Lett.*, (**2022**), 13 (37), 8733-8739.

Structural and dynamical evolution of bimetallic nanoalloys across length and time scales: Predicting oxidation effects on metal migration and dissolution at solid–liquid interfaces

Ismaila Dabo (PI) · Materials Science and Engineering, The Pennsylvania State University
Susan B. Sinnott (co-PI) · Materials Science and Engineering, The Pennsylvania State University

1. Project Scope

The goal of this project is to maximize the accuracy and efficiency of quantum-mechanical (electronic-structure) and classical-mechanical (reactive-potential) calculations in predicting the interface stability and time evolution of catalytic nanoalloys under applied voltage and fixed pH. As a first objective, we seek to minimize the computational cost of parameterizing large-scale electrochemical models (*i.e.*, voltage- and pH-dependent surface cluster expansions) using transfer learning from reactive-potential to electronic-structure models. This first task hinges on the hypothesis that reactive potentials can effectively describe correlations between the free energies of different surface configurations (even though they may not predict surface free energies within electronic-structure accuracy). As a second objective, we aim to broaden the range of applications of reactive potentials to enable the efficient modeling of electrochemical interfaces by developing robust algorithms of charge equilibration and surface solvation. In parallel to these two objectives, we are implementing computational tools to automatically generate reactive potentials for nanoalloys in aqueous media. The targeted code developments and their interoperability with widely used open-source software packages (*e.g.*, QUANTUM-ESPRESSO and LAMMPS) are outlined in **Fig. 1**:

- Bayesian selection of configurations for error-bounded cluster expansions (status: implementation). This code exploits Bayesian inference for (1) sampling the configurational space of nanoalloys starting from a pool of configurations (provided by the ICET code) and statistical priors derived from reactive potentials (implemented in LAMMPS), and (2) evaluating the interaction parameters for cluster expansions.
- Electrochemical embedding of electronic-structure models (status: final validation). This code enables (1) the simulation of solid–liquid interfaces using an electronic-structure description of the surface and a continuum treatment of the aqueous environment, and (2) the inclusion of voltage and pH effects in electronic-structure models without explicitly integrating the time evolution of the liquid electrolyte.

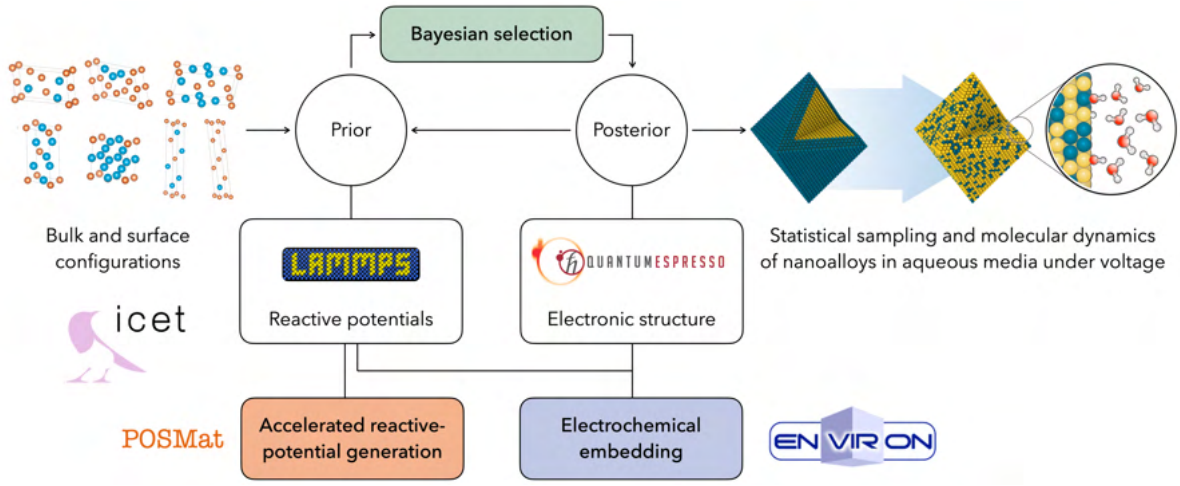

Figure 1 | Targeted software developments. Sampling the configurational space is the main bottleneck in developing large-scale models for electrochemical interfaces. Available acceleration techniques typically rely on simplified statistical kernels (*i.e.*, covariance functions) that do not incorporate physical information. We are implementing algorithms for iterative Bayesian selection, which exploit prior knowledge from available and newly generated reactive potentials to select configurations to be simulated using the electrochemical embedding model, which we developed in the ENVIRON module of QUANTUM-ESPRESSO.

- Accelerated reactive-potential generation for multimetallic surfaces (status: initial conceptualization). This code provides a workflow that augments the capabilities of the POSMAT suite of optimization tools for (1) fitting classical empirical reactive potentials using artificial neural networks to infer interatomic parameters and (2) assessing the sensitivity of these parameters on the choice of the targeted properties.

2. Recent Progress

2.1 Model implementation

We completed a first implementation of the Bayesian selection and tested its efficacy by studying the phase stability of Pt:Ni alloys (whose interatomic-potential parameters are already available). The training data for the cluster expansion included the formation energies of 411 symmetrically inequivalent Pt:Ni bulk structures generated using the ICET software package. The prior distribution was obtained from four interatomic potentials and was used to select optimal configurations via iterative uncertainty minimization. The performance of the resulting Bayesian sampling is compared to that of random sampling in Fig. 2. This comparison showed a two-fold acceleration in error reduction as a function of sample size (Fig. 2a). Errors bars on cluster-expansion parameters were found to systematically decrease while providing reliable upper/lower bounds for these parameters, with the exception of 1 or 2 outliers out of >90 clusters (Fig. 2b).

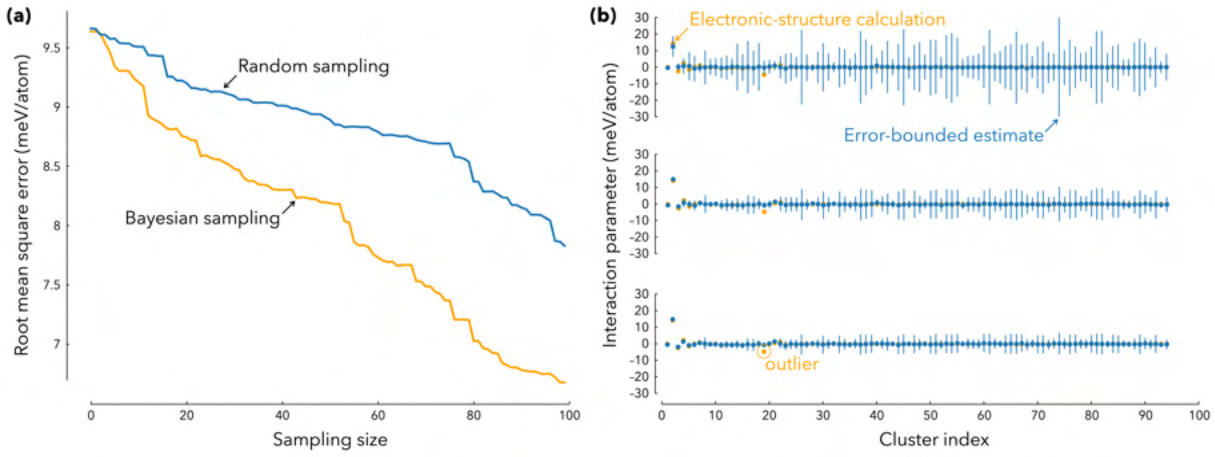

Figure 2 | Performance of Bayesian sampling of configurations to parameterize cluster expansions for Ni:Pt alloys. (a) Rate of convergence of cluster expansions as a function of the sampling size (*i.e.*, the number of configurations computed at the electronic-structure level). The Bayesian approach is found to almost halve sampling-size requirements before plateauing as the number of iterations reaches the total number of Pt:Ni configurations (here, 411 symmetrically unique configurations are considered). The Bayesian prior is constructed using four potentials, namely, EAM (embedded atom model), MEAM (modified embedded atom model), ReaxFF (reactive force-field model), and COMB3 (third-generation charge-optimized many-body model). (b) From top to bottom, evolution of error-bounded estimates for the cluster-expansion interaction parameters, which shows decreasing error bars upon Bayesian configurational sampling with only one statistical outlier (indicated by a circle).

The cluster-expansion energies were then used to run Monte Carlo calculations. By varying the chemical potential of grand-canonical (μVT) simulations, we predicted the phase stability of the Pt:Ni system, finding conclusive agreement with experimental phase diagrams, albeit with an underestimation of the transition temperatures. We are currently repeating the electronic-structure calculations (using refined exchange-correlation functionals) to correct the transition temperatures before addressing the interface stability of Pt:Ni alloys under voltage and pH. The key findings from this first implementation are that (1) exploiting prior knowledge from even a small number of empirical potentials (four) provides a significant (factor-of-two) reduction in computational cost and (2) the performance of the approach is critically dependent on rescaling reactive-potential data to counterbalance the overestimation of the electronic-structure energies. We are now implementing an iterative approach where the rescaling parameter $\alpha = \boldsymbol{F}^{\mathrm{T}}\widetilde{\boldsymbol{F}}/\widetilde{\boldsymbol{F}}^{\mathrm{T}}\widetilde{\boldsymbol{F}}$ is updated to minimize discrepancies between electronic-structure energies ($\boldsymbol{F}$) and rescaled empirical energies ($\alpha\widetilde{\boldsymbol{F}}$).

2.2 Model validation

The charge equilibration model that we developed enables one to describe interfacial charge transfer and simulate realistic redox processes. To test the accuracy of this model, we compared predicted surface-oxide and double-layer structures to data from experiment for both infinite surfaces and finite nanoparticles. Specifically, we studied the stability and dissolution of pre-oxidized platinum nanoparticles using classical molecular dynamics in an explicit solvent (**Fig. 3**). The diameters of the nanoparticles ranged from 1.35 to 2.92 nm with five different monolayer oxygen coverages. Simulations were run at 300 K, 450 K, and 600 K to examine dissolution kinetics in water. The key findings from these simulations were that (1) the rates of dissolution decrease upon increasing the coverage of OH and H adsorbed species (as a result of the dissociation of water molecules), and (2) charging effects and structural fluctuations prevails over nanoparticle size in determining dissolution rates.

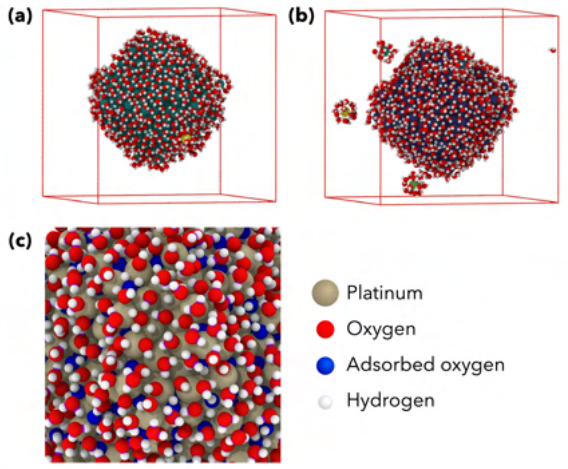

Figure 3 | Molecular dynamics of nanoparticle dissolution. (a) Snapshots of the initial dissolution events for a nanoparticle consisting of 807 platinum atoms over a simulation time of ~3 ns (here, only the water molecules in the proximity of platinum atoms are represented for clarity). (b) Dissociation of water on one of the pre-oxidized facets of the platinum nanoparticle.

In addition to testing the charge equilibration model, we assessed the electrochemical embedding method for predicting the stabillity and activity of (oxyhydr)oxide catalysts containing 3*d* transition metals (*i.e.*, Cr, Mn, Fe, Co, and Ni). This work done in parallel with experimental measurements provided an ideal

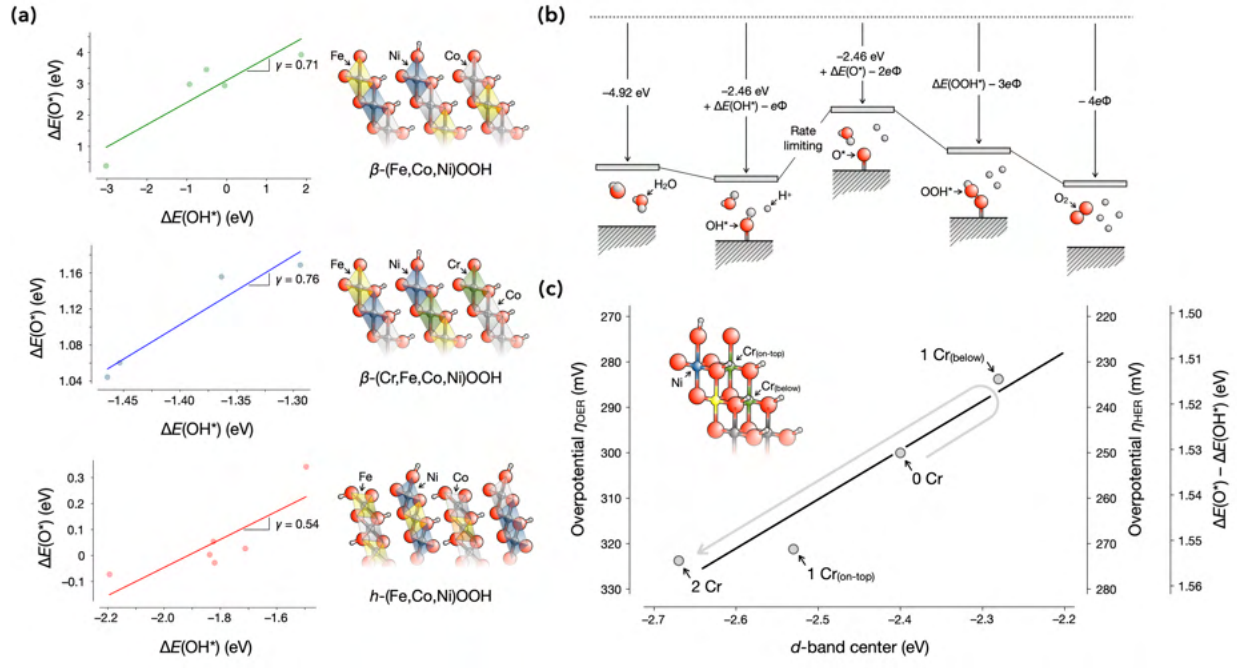

Figure 4 | Modeling multimetallic oxyhydroxides in aqueous media (collaborative work). (a) Trends in O and OH adsorption for (Cr,Fe,Co,Ni)OOH. (b) Reaction intermediates as a function of the applied voltage. (c) Dependence of the overpotentials on the majority-spin population, showing that placing Cr below active Ni sites improves the catalytic activity of the multi-metal electrode.

opportunity to elucidate the influence of local structure on the voltage-dependent activity of multimetal (oxyhydr)oxide catalysts. To assess the influence of the aqueous solvent on the predicted catalytic trends, we applied the electrochemical embedding approach implemented in the `ENVIRON` module of the `QUANTUM-ESPRESSO` code. The key finding from these calculations is that the activity of multimetallic Fe:Co:Ni electrocatalysts can be effectively tuned via subsurface Cr substitution. As part of a second collaboration, we studied the oxidation of *3d* post-transition-metal (Ga) surfaces at elevated temperature, which provided a critical assessment of electronic-structure models in predicting surface oxidation. Beyond oxide systems, we examined the electrochemical stability of sulfide electrodes upon charge/discharge. The key finding from this collaboration is that the embedding models developed for oxides in aqueous media can be adapted to sulfide systems without extensive re-parameterization of the solute–solvent interactions.

3. Future Plans

We will focus on augmenting the precision of electronic-structure models (using meta/generalized-gradient density functionals) to obtain accurate cluster expansions and predict the stability of Pt:Ni and Pt:Pd alloys. The thermodynamic stability of these bimetallic surfaces against metal migration and metal dissolution will be determined using (grand-)canonical Monte Carlo simulations. To evaluate kinetic rates, the charge equilibration model that we previously validated (cf. **Sec 2.2**) will be applied to Pt:Ni and Pt:Pd bimetallic nanoparticles. The formation of local surface motifs and their influence on metal dissolution will be characterized as a function of the applied voltage and surface composition. To further validate the proposed models, a study of cation ordering for mixed oxides of 3*d* transition metals will be carried out. The free energies of different metal terminations of the catalyst will be calculated to assess their voltage-dependent stability in aqueous environment. Predicted stable configurations will be used to estimate voltage-dependent catalytic activity and durability.

5. Peer-reviewed publications resulting from this project (2021-2023)

1. **R. Slapikas**, **I. Dabo**, **S. B. Sinnott**, Atomic-scale modeling of the dissolution of oxidized platinum nanoparticles in an explicit water environment, *Journal of Materials Chemistry A* **11**, 7043-7052 (2023).
2. M. J. Theibault, **C. Chandler**, **I. Dabo**, H. D. Abruña, Transition-metal dichalcogenides as effective catalysts for high-rate lithium–sulfur batteries, *ACS Catalysis* **13**, 3684-3691 (2023).
3. S. McGee, A. Fest, **C. Chandler**, N. N. Nova, Y. Lei, **J. Goff**, **S. B. Sinnott**, **I. Dabo**, M. Terrones, L. D. Zarzar, Direct laser writing of multimetal bifunctional catalysts for overall water splitting, *ACS Applied Energy Materials* **6**, 3756-3768 (2023).
4. F. Turker, C. Dong, M. T. Wetherington, H. El-Sherif, **S. Holoviak**, Z. J. Trdinich, E. T. Lawson, G. Krishnan, C. Whittier, **S. B. Sinnott**, N. Bassim, J. A. Robinson, 2D oxides realized via confinement heteroepitaxy, *Advanced Functional Materials* **33**, 2210404 (2023).
5. **R. Slapikas**, **I. Dabo**, **S. B. Sinnott**, Surface reconstruction of oxidized platinum nanoparticles using classical molecular dynamics simulations, *Computational Materials Science* **209**, 111364 (2022).
6. S. McGee, Y. Lei, **J. Goff**, C. J. Wilkinson, N. N. Nova, C. M. Kindle, F. Zhang, K. Fujisawa, E. Dimitrov, **S. B. Sinnott**, **I. Dabo**, M. Terrones, L. Zarzar, Single-step direct laser writing of multimetal oxygen evolution catalysts from liquid precursors, *ACS Nano* **15**, 9796-9807 (2021).
7. **J. M. Goff**, B. Y. Li, **S. B. Sinnott**, **I. Dabo**, Quantifying multipoint ordering in alloys, *Physical Review B* **104**, 054109 (2021).
8. **J. M. Goff**, F. Marques dos Santos Vieira, N. D. Keilbart, Y. Okada, **I. Dabo**, Predicting the pseudocapacitive windows for MXene electrodes with voltage-dependent cluster expansion models, *ACS Applied Energy Materials* **4**, 3151-3159 (2021).

Charge Carrier Space-Charge Dynamics in Complex Materials for Solar Energy Conversion: Multi-scale Computation and Simulation. Award Number DE-SC0019086

Michel Dupuis
Department of Chemical and Biological Engineering,University at Buffalo, Buffalo USA
mdupuis2@buffalo.edu

- **Project Scope**

Our overall research program deals with timely societal challenges in renewable energy, the efficient and cost-effective conversion of solar energy to electrical and chemical energies. Current conversion efficiencies, including for solar water splitting, are far from the level needed for practical applications. At the most fundamental level, our research addresses how the flow of charge carriers in complex crystalline environments of single phase, multi-phase, and multi-materials semiconductor systems can be tailored to enhance redox reactivity in photo-electro-chemical conversion (PEC). This research is aligned with BES' CSGB Division focus areas of 'charge transport and reactivity' and 'chemistry at complex interfaces.

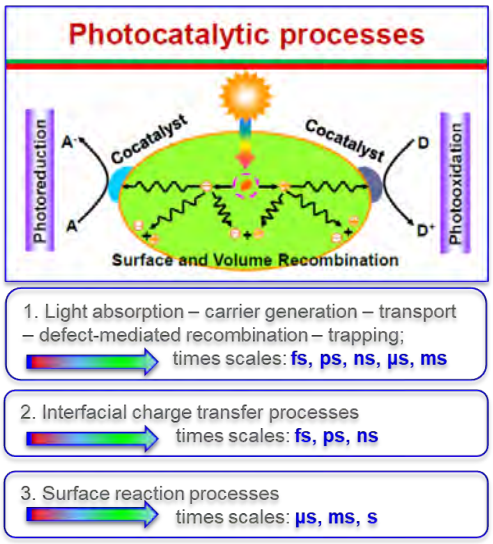

Figure 1. Physics of solar energy-to-fuels conversion: light absorption, carrier transport, carrier utilization.

Solar energy-to-fuels conversion in photo-electro-chemical systems involves 'light absorption', 'carrier generation and transport', and 'carrier reactivity' (Figure 1). Opportunities for computation and simulation in 'light absorption' include material screening and discovery. In 'carrier generation and transport', they include modeling of e^-/h^+ excitation and carrier dynamics in crystalline, single-phase, multi-phase, multi-materials systems. In 'carrier reactivity', they include modeling of e-/h+ carrier utilization in redox reactions.

Figure 2. Computation and simulation opportunities in solar energy-to-fuels conversion.

Past efforts in our group have focused on *Carrier Transport* to understand, characterize, and ultimately control the factors that lead to enhanced separation of photo-generated electron and holes toward higher solar energy-to-fuel conversion efficiency. Our approach combines first-principles atomistic computation and mesoscale kinetics simulation. The computational framework is depicted in Figure 3. At all stages, we validate our computational findings against experimental data. As prototypical systems we investigated semiconductors, doped and undoped, with highest water oxidation efficiency to date, such as bismuth vanadate $BiVO_4$ (BVO), tantalum nitrite Ta_3N_5, and other materials that exhibit the intriguing

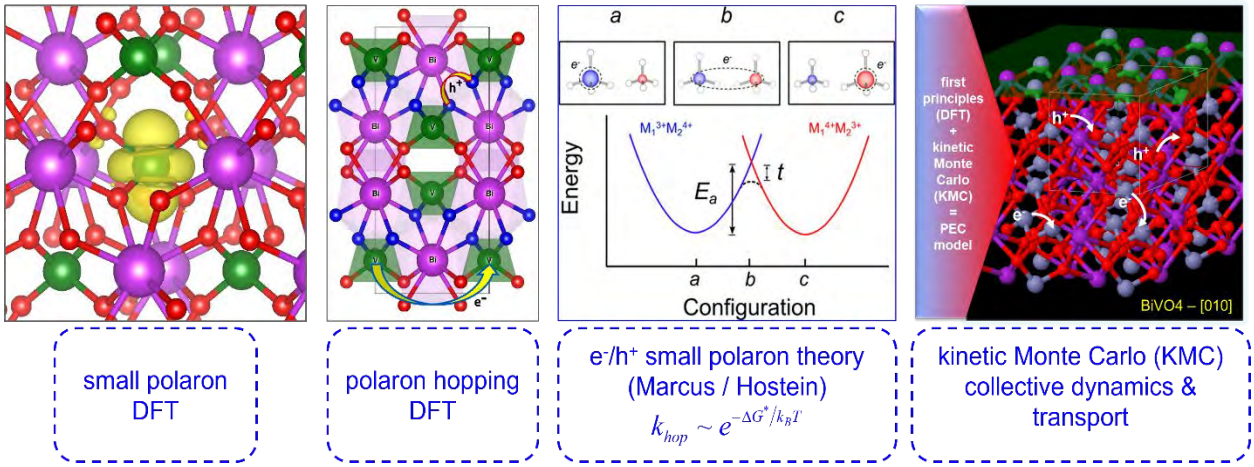

Figure 3 Multiscale modeling framework of carrier transport in semiconductor electrodes of PEC systems. The energy surface diagram is reproduced from Rettie *et al.* [*J. Phys. Chem. Lett. 7, 471 (2016)*] with permission.

phenomenon of *facet selectivity* for selective oxidation and reduction. A notable achievement was the creation of the Python software for Kinetic Monte Carlo (KMC) simulations of charge carrier spatial and temporal distribution. The combined QM+KMC mesoscale modeling has proven essential to understand the nature of intrinsic carrier transport and the role of cation and anion doping in manipulating transport properties. Recent efforts focus on carrier generation upon light absorption and spectroscopic signatures of charge carriers during catalytic utilization.

- **Recent Progress**

We have made significant progress in the computational characterization of exciton structures and dynamics in hematite Fe_2O_3 as a prototypical PEC material. We are also extending this work to $CuFeO_2$. The two systems were selected because there are recent detailed experimental measurements that offer a unique opportunity for cross-validation of theory and experiment. For example, XUV measurements by the Baker's group (Ohio State University and CPIMS investigator) revealed that the electron-hole separation in the exciton is ~ one Metal-ligand chemical bond.[1-3]

✓ *Electronic structure and structure of excitons in hematite Fe_2O_3*: We used DFT and linear-response TDDFT to study the electronic structure of excitons. Upon vertical excitation, the lowest energy exciton is found to have a multi-determinantal wavefunction, describing an electron excited from O *2p* states to Fe *3d* states of the nearest basal plane, possibly supporting a recent XUV-derived exciton structure with radius of a single Fe-O bond. Subsequently, the exciton self-traps into stable electron-hole pair structures whose wavefunctions are well-approximated by a single HOMO-LUMO excitations. Self-trapping yields electron-hole pair structures whereby the electron state (electron polaron-like) is separated from the hole state (hole polaron-like) by 3, 5, 7, 9 … basal planes in structures referred to as Exc-3, Exc-5, Exc-7, and Exc-9 …. The natural transition orbitals (electron-hole states) exhibit

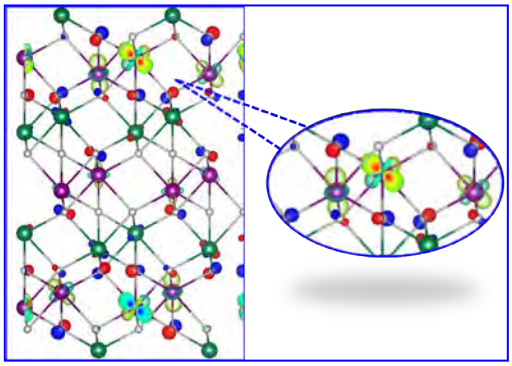

Figure 3. The natural transition states in the vertical lowest energy exciton show the excited electron in the nearest basal plane from the hole.

strong 'localized' character. The hole state is best described as a $(FeO_6)^+$ octahedral moiety carrying ~ 0.65 h^+ charge, and overall ~ 70% of the hole is assigned to O *2p* atomic states, mostly on the four (4) equatorial O atoms of the moiety. The electron state is best described as a $(FeFe)^-$ moiety carrying ~ 0.80 e^- charge in Fe *3d* atomic states. The lattice distortions around the hole site exhibit Fe-O bond shortening due to the removal of electron density from an orbital state with O-Fe-O anti-bonding character. The electron site shows Fe-Fe distance shortening due to excess electron density added to an orbital state with in-phase Fe-Fe interactions. These excitonic structures with increasing electron-hole separation can be viewed as the onset of exciton separation into isolated electron and hole polarons. Hopping amongst the structures will be investigated using Marcus/Holstein theory.

✓ *Exciton dynamics in hematite Fe_2O_3*: We have used the non-adiabatic molecular dynamics approach (NAMD) and the open-source Libra package to study the dynamics of excitons and electron-hole pair lifetime.[4, 5] NAMD is a real-time time-dependent density functional theory (TDDFT) method to get the time evolution of the excited state wavefunction using electron-nuclei coupling evolution. A manuscript describing these results is in preparation.

✓ *Vibrational signatures of reaction intermediates in OER mechanisms*: Recent experiment by the Cuk's group (University of Colorado Boulder and CPIMS investigator) have proposed subsurface vibrations as vibrational signatures of intermediates in water oxidation on perovskite $SrTiO_3$ and other oxides.[6] Calculations for $NaTaO_3$, also a perovskite, support the assertion of vibrational signature, but the position of the peak that depends on the metal (Ti vs Ta here) may prove to be a challenge to qualitative predictions.

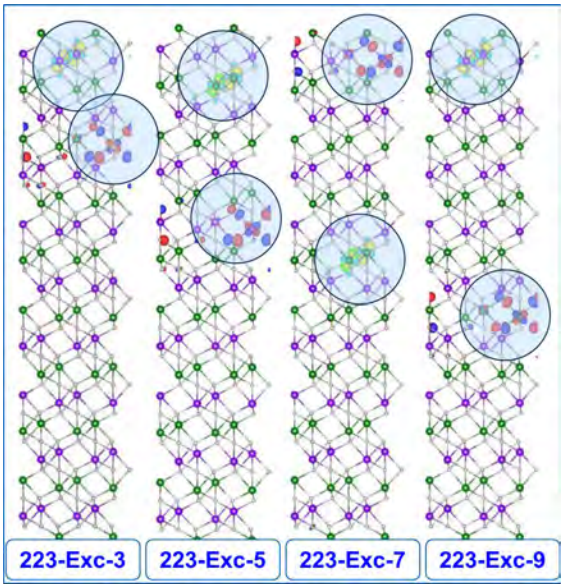

Figure 3. Onset of carrier generation: the *Exc-3, Exc-5, Exc-7, and Exc-9* structures of the lowest energy exciton have electron and hole separated by 3, 5, 7, 9 basal planes.

✓ We presented our research to the community in the form of invited talks (ACS National Fall meeting in 2021, Sanibel Symposium in 2022, WATOC Congress in 2022, ACS Regional NERM meeting in 2022, ASMSD Symposium in 2023, TACC2023 in 2023, U. Arkansas in 2023). Student L. Rassouli received SCGSR fellowship in 2023. We co-authored two review chapters about computational studies of carrier transport in semi-conductor-based PECs and published two papers in 2023. Three other manuscripts are submitted or in preparation:

1/ L. Rassouli and **M. Dupuis**, "Electronic structure of excitons in hematite Fe_2O_3", J. Phys. Chem. C. 2023, *submitted*.

2/ L. Rassouli, M. Shakiba, A. Akimov, and **M. Dupuis**, "Dynamics of excitons, recombination, and relaxation lifetimes in hematite Fe_2O_3", J. Phys. Chem. C, 2023, *in preparation.*

3/ Q. Zhao, T. Liu, Q. Li, J. Yang, and **M. Dupuis**, "Theoretical insight into the role of oxygen and nitrogen vacancies in the oxygen evolution reaction on tantalum oxynitride TaON and nitride Ta_3N_5", *in preparation*.

- **Future Plans**

We are forging ahead with the investigation of exciton dynamics in $CuFeO_2$, a promising cathode material for HER. As a continuation of our earlier work on exciton dynamics in Fe_2O_3, we are starting to investigate the dynamics and rate of exciton hopping leading to exciton separation into isolated electron and hole polarons, the active redox species in photocatalysis. In this work we will adopt and adapt the Marcus/Holstein theory of polaron hoping.

- **References**

1. Husek, J., *et al*., *Surface electron dynamics in hematite (alpha-Fe2O3): correlation between ultrafast surface electron trapping and small polaron formation.* Chemical Science, 2017. **8**(12): p. 8170-8178.
2. Biswas, S., et al., *Highly Localized Charge Transfer Excitons in Metal Oxide Semiconductors.* Nano Letters, 2018. **18**(2): p. 1228-1233.
3. Husek, J., *et al*., *Hole Thermalization Dynamics Facilitate Ultrafast Spatial Charge Separation in CuFeO2 Solar Photocathodes.* Journal of Physical Chemistry C, 2018. **122**(21): p. 11300-11304.
4. Smith, B. and A.V. Akimov, *Modeling nonadiabatic dynamics in condensed matter materials: some recent advances and applications.* Journal of Physics-Condensed Matter, 2020. **32**(7).
5. Smith, B., M. Shakiba, and A.V. Akimov, *Nonadiabatic Dynamics in Si and CdSe Nanoclusters: Many-Body vs Single-Particle Treatment of Excited States.* Journal of Chemical Theory and Computation, 2021. **17**(2): p. 678-693.
6. Herlihy, D.M., *et al*., *Detecting the oxyl radical of photocatalytic water oxidation at an n-SrTiO3/aqueous interface through its subsurface vibration.* Nature Chemistry, 2016. **8**(6): p. 549-555.

- **Peer-Reviewed Publications Resulting from this Project (2021-2023)**

1. N. A. Deskins, P. M. Rao and **M. Dupuis**, "*Charge carrier management in semiconductors: modeling charge transport and recombination*", Springer Handbook of Inorganic Photochemistry 2022.
2. T. Liu and **M. Dupuis**, "*Theory and Computation in Photo-electro-chemical Catalysis: Highlights, Challenges, and Prospects*", Springer Engineering Materials 4288, C.A. Taft and S.R. De Lazaro, Editors, 2022.
3. X. An, T. Yao, Y. Liu, G. Long, A. Wang, Z. Feng, M. Dupuis, and C. Li, "HER on Single-Atom Pt Doped in Ni Matrix under Strong Alkaline Condition", J. Phys. Chem. Letters, 2023, 14, 8121 (2023).
4. Y. Liu, X. Wang, X. Ma, **M. Dupuis**, and C. Li, "DFT electronic structure and vibrational signatures of intermediates in water oxidation on perovskite $NaTaO_3$", J. Phys. Chem. C, 00, 0000 (2023).

Liquid-Liquid Phase Separation in Submicron Aerosol Particles (DE-SC0018032)

Miriam Freedman
Department of Chemistry & Department of Meteorology and Atmospheric Science
205 Chemistry Building, The Pennsylvania State University, University Park, PA 16802
Email: maf43@psu.edu

Project Scope:

The overarching goal of this proposal is to understand how confinement affects phase transitions in aerosol particles. We are specifically interested in liquid-liquid phase separation (LLPS) in aerosol particles composed of salts and organic compounds. In these systems, LLPS can occur due to salting out of the organic component, resulting in an organic-rich phase and a salt-rich phase. As the relative humidity surrounding the particles decreases, the salt concentration within the particle increases, driving the phase separation process. We have previously determined that phase separation is inhibited for particle sizes < 30 nm because small particles cannot overcome the activation barrier needed to form a new phase. Results from these studies have application to understanding myriad processes of aerosol particles in the environment such as heterogeneous chemistry, new particle growth, cloud droplet nucleation, optical properties, etc. At the same time, they have general application to understanding the physical chemistry of this phase transition which results in the formation of an interface within a liquid.

Two broad goals are the focus of the current project. Using a flash freeze flow tube, we have been able to capture and vitrify submicron aerosol particles equilibrated at a given relative humidity, allowing us to capture the dynamics of the phase separation process. Through use of this technique, we have constructed an experimental phase diagram for the phase separation process for a model submicron aerosol system. In addition, we have developed a new parameterization for the relative humidity at which phase separation occurs for submicron aerosol particles. We have also worked to better understand the physical chemistry of liquid-liquid phase separation by working with mixtures of organic compounds combined with salts. To explore the size dependence of the phase separation, we worked with different salts and organic compounds of different oxidation states.

Recent Progress:

Dynamics of the Phase Separation Process. Our main technological advancement from our current CPIMS grant was to develop a system to allow us to flash freeze particles to capture the dynamics of the phase separation process (Kucinski et al. 2020). Our work prior to this development captured images of dry particles, and then inferred the behavior that had occurred in the aqueous state, rather than being able to study the phase separation process as it was occurring. From the TEM images, we observe that at sufficiently high relative humidity (RH), particles are homogeneous. Subsequently, at lower RH, particles begin the phase separation process, starting from multiple nuclei (in the case of nucleation and growth), and then forming a core-shell or partially engulfed structure. Particles can shift from core-shell to partially engulfed depending on their water content.

From the images collected by equilibrating ensembles of particles at different RH values, we can construct diagrams showing the dynamics of the phase separation process (Kucinski et al. 2021). By tracking the phase separation process from the onset to conclusion, defined as where the size dependent morphology is observed, we calculate an average value for the separation

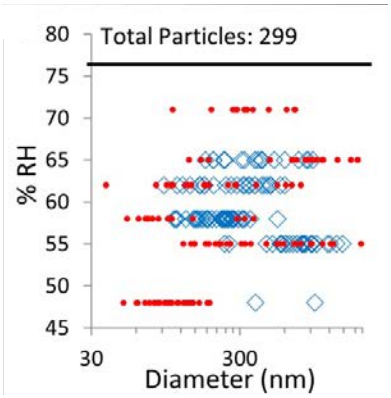

Figure 1. Phase separation process for 2-methylglutaric acid and ammonium sulfate. Red circles are homogeneous particles and blue diamonds are phase separated particles. Black line is the prediction based on studies of supermicron droplets.

relative humidity (SRH). When phase separation occurs by nucleation and growth, we observe that, for most systems, the onset of phase separation occurs at lower RH and over a larger range of RH than expected based on studies of supermicrometer droplets (Fig. 1). The dynamics of phase separation are dependent on thermodynamics and kinetics. In terms of thermodynamics, we observe that phase separation occurs promptly at compositions close to the critical point of the phase diagram, where the activation barrier goes to zero. In terms of kinetics, if the system has a longer equilibration time at the desired RH, then more particles are observed to undergo phase separation. These observations indicate that the lower onset of phase separation and the large range of RH over which phase separation occurs result from the activation barrier for the phase separation process when phase separation occurs via a nucleation and growth mechanism.

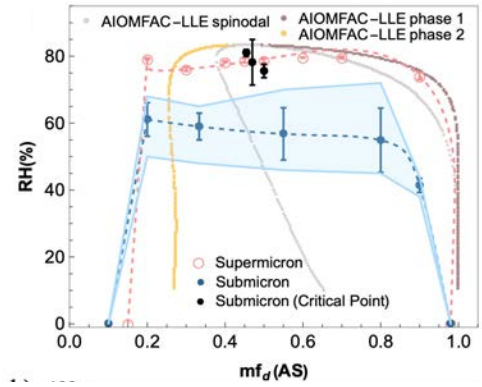

Figure 2. Experimental phase diagram for supermicron and submicron aerosol particles compared with thermodynamic theory.

Experimental Phase Diagram for Submicron Aerosol Particles. With knowledge of the dynamics of the phase separation process, we focused on one system: 2-methylglutaric acid and ammonium sulfate to construct an experimental phase diagram for submicron aerosol particles (Huang et al. submitted; Fig. 2). The thermodynamic theory and optical microscopy of droplets 10s to 100s of micrometers in diameter generally agree well. For submicron particles, the shape of the phase diagram is the same as for optical microscopy, but the binodal curve is shifted downwards. These results show that the SRH occurs at lower values for submicron aerosol particles compared with larger droplets. Equilibration time, however, is important. As the particles are allowed to equilibrate for longer, more of them phase separate. These results suggest that kinetics is extremely important for the phase separation behavior of submicron aerosol particles.

Parameterization of Separation Relative Humidity. Organic compounds in the gas and particle phase evolve in the atmosphere through oxidation pathways, which can result in incorporation of oxygen atoms into an organic compound or fragmentation of that compound, changing its volatility. As a result, many aerosol processes and properties are characterized according to the average oxidation state of the organic compounds in the particle. With respect to liquid-liquid phase separation, we need to understand how the SRH depends on the average oxidation state of the organic compounds. We have worked with a range of different organic compounds mixed with ammonium sulfate to determine how to parameterize SRH as a function of the average oxidation state of the organic compounds. Traditionally, atmospheric chemists have used the number of oxygen atoms to carbon atoms in the organic compound (the O:C ratio) as an approximation for the oxidation state, which is useful for complex mixtures. Our group is proposing, especially for laboratory studies involving known organic compounds, that the octanol-water partition or

distribution coefficient (log K_{ow} = log P or log D at acidic pH) gives a greater understanding of the underlying chemistry. For all metrics, we observe a shift towards lower SRH compared with existing parameterizations.

Role of the Inorganic Component on the Size Dependence. To investigate how the inorganic component of the mixture affects the size dependence of the morphology, we worked with systems consisting of an organic compound, an inorganic compound, and water. Two different organic compounds with different functional groups, diethylmalonic acid and 2,5-hexanediol, and five different salts, ammonium sulfate, ammonium bisulfate, ammonium chloride, sodium chloride, and sodium sulfate were used (Ott et al. 2021). We found that the diameter of the smallest phase separated particle correlated with the cation of the inorganic component (Fig. 3). The use of ammonium resulted in larger values of the diameter of the smallest phase separated particle, and the use of sodium resulted in smaller values. We attributed the difference both to the fact that ammonium can hydrogen bond as well as being more polarizable, both of which would lead to increased interactions with the organic compound, hindering phase separation.

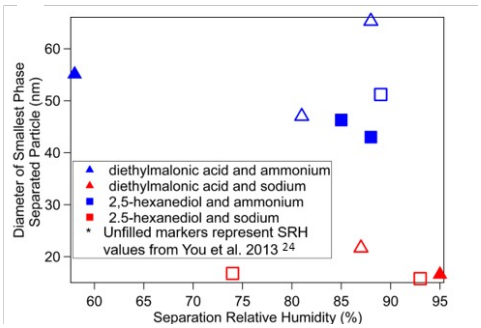

Figure 3. Dependence of the diameter of the smallest phase separated particle vs. SRH color coded by the cation of the inorganic component.

Role of the Organic Oxidation State on the Size Dependence. In addition to the role of the inorganic compound on the size dependence, we also characterized the impact of the oxidation state of the organic compound. We used a range of different aliphatic and organic compounds with acid functional groups mixed with ammonium sulfate. In past studies, we have relied on characterizing the region where both morphologies are found using the diameters of the smallest phase separated particle and the largest homogeneous particle. To more accurately determine this region, we used logistic regression in this study, which allows us to model the probably of phase separation for a given particle diameter. As described above, both the O:C ratio of the organic compound and log K_{ow}= log P and log D at acidic pH were used to describe the organic compounds. As the aliphatic organic compounds become more oxidized, the trend is to increase the diameter at which 50% of the particles are phase separated (Fig. 4). As these organic compounds become more oxidized, they have more/stronger interactions with the solution, and are less likely to be salted out. The few aromatic compounds that worked for this experiment had the opposite trend, which we are still working to understand.

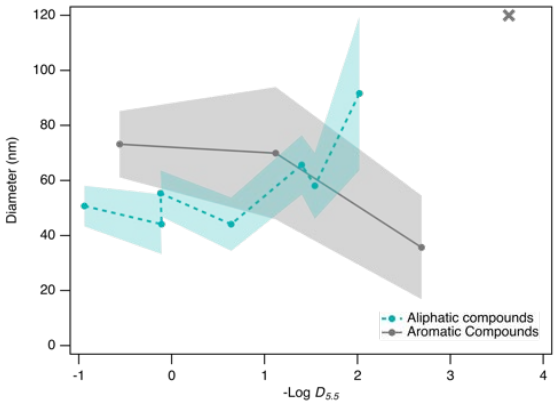

Figure 4. Dependence of the diameter at which 50% of particles are phase separated on the distribution coefficient at pH 5.5. The shaded bounds are for the 20th and 80th percentile for phase separation.

Future Plans:

Partitioning of Particles in Aerosol Particles. We are interested in determining how particles partition within systems that undergo LLPS. We will investigate how polystyrene latex spheres coated in ligands with different functional groups partition within systems that undergo LLPS. After this model system, we will investigate the interactions of mineral dust aerosol with particles that undergo LLPS, which has relevance for internally mixed aerosol particles. Subsequently, we are interested in investigating the partitioning of particles within model systems for respiratory aerosol with relevance to disease transmission.

Impact of Organonitrogen and Organosulfate Compounds on LLPS. To date, the systems in which LLPS has been studied involve organic compounds composed of C, H, and O atoms mixed with salts. Organonitrogen and organosulfate compounds are also present in atmospherically relevant systems, but have not been explored. Furthermore, current parameterizations of SRH are performed using the O:C ratio, and a framework to incorporate heteroatoms beyond oxygen is needed. This project will investigate the impact of organonitrogen and organosulfate compounds on SRH and develop a parameterization for SRH.

References:

T. M. Kucinski, M. A. Freedman, Flash Freeze Flow Tube to Vitrify Aerosol Particles at Fixed Relative Humidity Values, *Analytical Chemistry*, **92**, 5207-5213 (2020).

Q. Huang, K. R. Pitta, K. Constantini, E.-J. E. Ott, A. Zuend, M. A. Freedman, Experimental Phase Diagram and Its Temporal Evolution for Submicron 2-Methylglutaric Acid and Ammonium Sulfate Aerosol Particles, *submitted.*

Peer-Reviewed Publications Resulting from this Project (2021-2023):

E.-J. E. Ott, T. M. Kucinski, J. N. Dawson, M. A. Freedman, Use of Transmission Electron Microscopy for Analysis of Aerosol Particles and Strategies for Imaging Fragile Particles, *Analytical Chemistry*, **93**, 11347-11356 (2021).

E.-J. E. Ott, M. A. Freedman, Influence of Ions on the Size Dependent Morphology of Aerosol Particles, *ACS Earth and Space Chemistry*, **5**, 2320-2328 (2021).

T. M. Kucinski, E.-J. E. Ott, M. A. Freedman, Dynamics of Liquid-Liquid Phase Separation in Submicron Aerosol, *Journal of Physical Chemistry A,* **125**, 4446-4453 (2021).

M. A. Freedman, Q. Huang, K. R. Pitta, Phase Transitions in Organic and Organic/Inorganic Aerosol Particles, *Annual Rev. Phys. Chem. accepted.*

Rational Design of Concentrated Electrolytes for Beyond-Li-ion Batteries with Machine Learning and Quantum Calculations

Mirza Galib (mirza.galib@howard.edu), Department of Chemistry, Howard University, Washington, DC 20069
Bryan M. Wong (bryan.wong@ucr.edu) , Material Science and Engineering Program, UC Riverside, Riverside, CA 92521

Project Scope

Li-ion batteries have made transformative technological advances in portable electronic devices and electric vehicles. However, a limited supply of Li in the Earth's crust has motivated the scientific community to explore other metal cations (e.g., Na, K, Mg, Ca, or Al) as alternatives to Li-ion batteries. One of the most important challenges in developing beyond Li-ion batteries is the design of suitable electrolytes. Ionic liquids are promising electrolytes for beyond Li-ion batteries due to their unique properties, such as high electrochemical and thermal stability.[1,2] However, the vast chemical space of candidate cations and anions makes it difficult to systematically explore all possibilities. To date, most computational work [3,4] has focused on bulk ionic liquids instead of their interfacial properties due to the complexity of simulating electrode-electrolyte interfaces, which requires both quantum mechanics and statistical mechanics. However, interfacial properties, such as the formation and growth of the solid electrolyte interphase (SEI), have a profound impact on the energy density and cycling performance of batteries.[5,6] Our limited understanding of SEI formation[5,6] hinders the rational design of new ionic liquids for these electrochemical systems. To bridge that knowledge gap, this project aims to develop a predictive computational framework that combines ab initio calculations, statistical mechanics, and machine learning to gain molecular-level insights into the composition and dynamics of liquid-electrolyte interface. A comprehensive understanding of the IL-electrode interface and interfacial reactivities leading to the formation of SEI will enable a rational design for selecting the best ionic liquids from an immense chemical space and thereby will facilitate the commercial use of ionic liquids in beyond Li-ion batteries.

Future Plans

Given the complexity of exploring the vast chemical space of ionic liquids through experimental trial and error, computational modeling and high throughput screening represent efficient ways to create predictive models for selecting new prospective ionic liquids. However, when dynamic properties are involved (e.g., diffusion of ions or chemical reactions in a solvated environment), long-time molecular dynamics are needed to sample statistically averaged observables. Unfortunately, non-reactive fixed charge models cannot account for crucial polarization effects, whereas polarizable force fields cannot capture bond formation/dissociation in chemical reactions. Density functional theory (DFT) is the most suitable choice for studying both the reactions and solvation of charged systems, as it includes polarization and bond formation/dissociation. However, the small system sizes (~20 pairs of cations and anions) and limited timescales (~50 ps) in DFT are insufficient to include long-range interactions in ionic liquids, some of which are known to form nanoscale long-range structures.[7] To address this challenge, we aim to develop machine-learned reactive force fields from DFT data sets. These

force fields will include polarization and can capture chemical reactions while preserving the accuracy of DFT. They will also be orders of magnitude faster than the original DFT model enabling the simulation of larger system sizes for longer timescales.

In this project, we will systematically develop machine-learned force fields for ionic liquids in the presence of an electrode. We will explore the chemical space of alkyl and ether-based phosphonium-based cations, along with two commonly used anions ($TFSI^-$ and FSI^-), three commonly used organic solvents (acetonitrile, dimethyl sulfoxide, and methanol), and five metal anodes (Na, K, Ca, Mg, and Al). We will develop machine learning models that can simulate the long-time dynamics for any metal anode-electrolyte-organic solvent combination within the above-mentioned chemical space. Both the electrolyte and electrode will be represented explicitly within full atomistic simulations. We will use DFT-based electronic structure calculations for generating the data set for the machine learning models. Once these models are developed, we will use state-of-the-art statistical mechanics tools to calculate the thermodynamics and kinetics of the elementary steps involved in SEI formation, including thermal and redox decomposition of electrolytes and their migration and adsorption to solid electrodes. Finally, we will analyze the molecular level details of elementary steps informed by the above study within suitable analytical theories and explainable machine learning models to build structure-property relations.

In addition, we will calculate the XANES and EXAFS spectra for the structure and composition of the SEI simulated by our machine-learning model. We will sample structures from long-time molecular dynamics simulations and use a subset of them to calculate the spectral signatures. We will simulate XANES spectra by RT-TDDFT approach[8] using an in-house algorithm developed for periodic systems (by Professor Wong), and the EXAFS by using the multiple scattering formalism. These calculations will help us understand how the local solvation structure of various species affects the computed spectra and also enable us to compare our results to previously published experiments and validate the accuracy of our DFT formalism.

While ionic liquids gained interest decades ago, their full potential remains unexplored due to the high cost of trial-and-error experiments. This project will combine machine learning with state-of-the-art computational tools and leverage that coupling to explore the vast chemical space of ionic liquids for designing next-generation beyond-Li-ion batteries. The framework developed in this work would be easily extendable to larger chemical spaces with additional cation/anion combinations, other anodes based on carbon/alloys, and the cathode-electrolyte interphase.

References

1. Jianming Zheng, Joshua A Lochala, Alexander Kwok, Zhiqun Daniel Deng, and Jie Xiao. Research progress towards understanding the unique interfaces between concentrated electrolytes and electrodes for energy storage applications. Advanced Science, 4(8):1700032, 2017.
2. Huan Liu and Haijun Yu. Ionic liquids for electrochemical energy storage devices applications. Journal of materials science & technology, 35(4):674–686, 2018.

3. Kun Dong, Xiaomin Liu, Haifeng Dong, Xiangping Zhang, and Suojiang Zhang. Multiscale studies on ionic liquids. Chemical reviews, 117(10):6636–6695, 2017.
4. Jónsson, Erlendur. "Ionic liquids as electrolytes for energy storage applications–A modelling perspective." *Energy Storage Materials* 25, 827-835, 2020.
5. Meda Ujwal Shreenag, Libin Lal, M. Sushantha, and Paridhi Garg. "Solid Electrolyte Interphase (SEI), a boon or a bane for lithium batteries: A review on the recent advances." *Journal of Energy Storage* 47: 103564, 2022
6. Wu Haiping, Hao Jia, Chongmin Wang, Ji-Guang Zhang, and Wu Xu. "Recent progress in understanding solid electrolyte interphase on lithium metal anodes." *Advanced Energy Materials* 11(5) :2003092, 2021
7. Hayes Robert, Gregory G. Warr, and Rob Atkin. "Structure and nanostructure in ionic liquids." *Chemical reviews* 115 (13): 6357-6426, 2015.
8. Hanasaki K. , Ali Z. A., Choi M., Del Ben, and Bryan M. Wong, "Implementation of real-time TDDFT for periodic systems in the open-source PySCF software package." *Journal of Computational Chemistry 44* (9): 980-987,2023.

A Cluster Approach to Understanding Solvation Effects on Ion Structure and Photochemistry

Award Number:
PI: Etienne Garand
University of Wisconsin-Madison
Department of Chemistry
1101 University Ave.
Madison WI
Email: egarand@wisc.edu

Project Scope

Many energy transformation, storage, and transport systems consist of interesting environments that differ from conventional bulk "liquid phase", such as porous materials with cavity on the nanometer scale. In such environments, chemical behaviors arising from partial solvation and interfaces can play a dominant role in the observed physical characteristics. Even the fundamental chemical properties of a molecule, such as its structure or its acidity, can differ significantly from those found in the isolated molecule or in the bulk phase.

This project aims to provide a detailed understanding of solvation effects on the structure and chemistry of molecular ions via spectroscopic interrogation of precisely assembled micro-solvated clusters. These clusters have the combined advantages of providing well-defined targets for detailed and systematic studies, as well as containing sufficient complexity to extrapolate our experimental findings to various condensed phase environments. The spectroscopic characterization of these relatively large ions and clusters is made possible by the low-temperature conditions afforded through cryogenic traps, which reduce molecular thermal motions, greatly simplifying spectral analyses and improving the amount of information that can be obtained. Moreover, we have shown that temperature control in such ion traps can be used to efficiently re-condense solvent molecules onto almost any ion. Cluster sizes containing up to 50 water molecules can now be readily produced. This unprecedented versatility and cluster size accessibility enables systematic studies of stepwise solvation of illustrative model systems, making it possible for us to build up a molecular-level understanding of how solvation can influence structures via competitive and cooperative interactions. Such understandings can then be transferred to more complex systems of various sizes to explain observed phenomena, as these models contain all the basic elements of interactions that are present in the larger systems. Finally, results from the proposed studies can serve as crucial benchmarks for theory, where it is still difficult to accurately capture these combinations of non-covalent interactions. Hence, there are several closely interrelated major scientific goals in this proposal.

Specifically, we aim to 1) develop the experimental toolkit necessary to extract molecular structure and non-covalent interaction information from spectroscopy of large solvated ionic clusters. 2) Develop a molecular-based understanding of cooperative and competitive hydrogen-bonding interactions that modulate the conformational space of flexible ions in the presence of water. 3) Understand how the ion species can influence the water hydrogen-bonding network surrounding the entire ionic adduct. 4) Probe how photodissociation yield, branching ratio, and mechanism can change as a function of the solvation environment around an ionic chromophore.

Recent Progress

We conducted a spectroscopic study comparing the conformational structures of the [Gly-Gly-GlyH$^+$]$(H_2O)_{1\text{-}2}$ and [Ala-Ala-AlaH$^+$]$(H_2O)_{1\text{-}2}$ clusters with the goal of determining the effect of the methyl side-chain on the microsolvated structures of these flexible peptides. This is a continuation of our work on the bare protonated peptides, which showed that the relative contribution of each conformational family is highly dependent on the exact amino acid sequence of the tripeptide. These dependencies were rationalized in terms of the electron-donating effect of the methyl side-chain modulating the local proton affinities of the amine and various carbonyl groups in the tripeptide. Therefore, for the next step in our study, we aimed to determine whether the methyl electron-donating effect will persist upon solvation and/or compete with that of the water interactions. The results of our experiments showed that upon microsolvation, the conformation family with all *trans* amide bonds has very similar solvation structures for the two tripeptides. However, in the conformation family with a *cis* amide bond, the two tripeptides differed. This highlighted that the effect of the methyl side-chain can persist, at least in part, with solvation.

We have also studied the vibrational spectra and structures of alkali metal ion (Li^+, Na^+, K^+) complexes with Gly-Gly and Gly-Gly-Gly. Understanding how the electric fields of the metal ions can affect the structure and folding of biomolecules is important as these can directly impact biomolecular functions—as, for example, seen in enzymes, where electrostatic preorganization around the active site is thought to be vital for their catalytic abilities. We were able to assign the most stable conformation of these complexes for the first time, which involves the metal ion coordinating to all available C=O groups and an internal NH$\cdots$NH$_2$ hydrogen-bond in the peptide backbone. Systematic analyses of the spectral shifts of the O-H, N-H, and C=O stretching vibrations across the different metal ions and peptide chain lengths showed that these shifts are largely caused by the electric field of the metal ion, which varies in strength as a function of the square of the distance to each functional group. We also found that as the metal ion-peptide interaction increases in strength (from K^+ to Li^+), the NH$\cdots$NH$_2$ intramolecular hydrogen-bonding became stronger due to polarization of the amide group, i.e., electron density is pulled away from the amide N-H via the amide C=O, making the NH more acidic.

To further scrutinize the impact of electric fields on the structures and vibrations of biomolecules in the presence of water molecules, we studied the sequential solvation of alkali metal ion (Li^+, Na^+, K^+) complexes with Gly-Gly. For Li^+, we found that the first water molecule

binds to the ion and weakens the electric field experienced by the peptide. Consequently, the strength of the internal $NH\cdot\cdot\cdot NH_2$ hydrogen-bond in the diglycine backbone decreases. Moreover, the strength of this hydrogen-bond decreases approximately linearly with the number of water molecules, as a direct result of the decreasing electric field strength. We also found that the addition of just two water molecules is sufficient to alter the energetic ordering of the peptide backbone conformations, leading to a lower energy structure with Li^+ coordinating to the lone pair of the terminal amine group. A comparison of the vibrational frequency predictions of several DFT methods and MP2 showcases the deficiency of DFT methods to accurately describe the strength of hydrogen-bonds. We are currently analyzing the Na^+ and K^+ complexes using a similar framework.

Finally, we have completed the development and testing of a new ion source that will allow us to access more complex intermediates and clusters. Our novel approach uses two mass-selective cryogenic linear quadrupole ion traps that combine processing and filtering capabilities. The main challenge in implementing mass-filtering capabilities in cryogenic ion processing traps lies in the need to use relatively high-pressure gas pulses and the inevitable condensation of solvent molecules onto the cold trap assembly, both of which limit the application of high-amplitude RF voltages. This effectively eliminates the use of conventional approach to quadrupole mass-filtering that relies heavily on scanning the amplitude of the fixed-frequency RF driving voltage. We circumvented this issue by driving the quadrupole ion trap with square-waves instead of the more common sine-waves. The ion motion and stability in square-wave driven devices are governed by similar second-order linear differential Mathieu Equations as sine-waves. However, square-waves can utilize frequency and duty-cycle scanning of fixed-amplitude RF voltage for mass analysis, thus removing the need for high-amplitude voltages. We showed that the clustering and mass-filtering steps can be combined in a mass-selective ion trap that is driven by RF square-waves. Notably, we found that adjustment of the stability boundary during the clustering process allows for preferential formation of a specific cluster size rather than a broad distribution of sizes. We also showed that a specific cluster size can be formed, mass-selected, and then transferred to another ion trap where a second ion processing step can take place. The instrumentation developed here expands the scope of ionic clusters that can be accessed by efficiently post-processing electrosprayed ions.

Future Plans

We plan to continue our study of the effect of metal ion electric field on larger polyalanine peptides that are known to form a-helix secondary structures. One important question that we aim to answer with these studies is how the polarization effects and modulations of the hydrogen bond strength propagate to longer distances. We will also initiate a study of how solvation affects the photodissociation of the nitrate anion, with a focus on the absorption band near 300 nm, which is relevant to atmospheric chemistry. This band corresponds to a nominally forbidden transition and the exact mechanism for the absorption is still not well understood. However, it is known that the presence of water strongly enhances this absorption cross-section.

Peer-Reviewed Publications Resulting from this Project (2021-2023)

6) G. Roesch and E. Garand*, *Tandem Mass-selective Cryogenic Digital Ion Traps for Enhanced Cluster Formation*, **J. Phys. Chem. A,** 127, 7665-7672 (2023)

5) S. L. Sherman, K. C. Fisher, and E. Garand*, *Effects of the methyl side-chains on the microsolvation structure of protonated tripeptides*, **J. Phys. Chem. A**, 127, 6275−6281 (2023)

4) K. A. E. Meyer, K.A. Nickson and E. Garand*, *Impact of the Metal Ion Electric Field on the Structure and Vibrations of Alkali Ion Di- and Triglycine Complexes*, **J. Chem. Phys.** 157, 174301 (2022)

3) S. L. Sherman, K. C. Fisher, and E. Garand*, *Conformational Changes Induced by Methyl Side-Chains in Protonated Tripeptides Containing Glycine and Alanine Residues*, **J. Phys. Chem. A** 126, 4036-4045 (2022)

2) S. L. Sherman, K. A. Nickson, and E. Garand*, *Comment on "Microhydration of Biomolecules: Revealing the Native Structures by Cold Ion IR Spectroscopy"* **J. Phys. Chem. Lett.** 13, 2046-2050 (2022)

1) C.R. Sagan, and E. Garand*, *Anion Resonances and Photoelectron Spectroscopy of the Tetracenyl Anion*, **J. Phys. Chem. A**, 125, 7014-7022 (2021)

Testing the Quadrupolar Solvation Hypothesis of Carbon Capture with Controllably-Polymerizable Ion Gels, 2D-IR Spectroscopy, And Molecular Simulations (Award Number DE-SC0023474)

Sean Garrett-Roe (sgr@pitt.edu), Jennifer Laaser (j.laaser@pitt.edu)
Department of Chemistry, University of Pittsburgh, Pittsburgh, PA 15260
Clyde Daly (cdaly2@haverford.edu), Department of Chemistry,
Haverford College, Haverford, PA 19041

Project Scope

Current technologies for the capture of carbon dioxide from dilute sources are inefficient, approximately eight times above the thermodynamic limit. New technologies are rapidly being developed, but all are hindered by a lack of understanding of the fundamental intermolecular interactions between the CO_2 and the materials.

This project's goal is to develop energy efficient carbon capture materials through the mechanistic understanding of the interactions of CO_2 in polymerizable ionic liquids (PILs), both singly- and doubly-polymerizable ionic liquids (SPILs and DPILs). Our central hypothesis is that carbon dioxide solubility and permeability can be controlled by tailoring CO_2's first solvation shell. This hypothesis is based on our two-dimensional infrared spectroscopy (2D-IR) spectroscopy and molecular dynamics (MD) simulations on carbon capture in ionic liquids, which showed that ions accumulate around the CO_2 forming a quadrupolar solvation shell. We will test this hypothesis by restricting the mobility of the anions through 1) controlled polymerization of cations, anions, or both; 2) varying the PIL structure; and 3) correlating observed bulk film properties (dielectric relaxation, rheology, and CO_2 solubility and permeability) with the molecular dynamics observed in experiment (2D-IR) and MD simulations.

These materials may begin a new generation of low-energy carbon capture membranes, and this mechanistic insight should give design rules for optimizing other next generation carbon capture materials, as well.

Characterization of the bulk transport and solubility of CO2 in CO2-philic singly- and double-polymerized ILs. We will synthesize new materials across several important chemical axes, including the Lewis basicity of the anion, the mobility of the polymerized component, and the effect of free unpolymerized IL component. A wide chemical space of cations and anions will be explored. To test the effect of anion mobility, we will explore the effect of the linker length of the anion, the polymerization of the anions, and the presence or absence of additional free anions.

Characterizing the dynamic properties of the ions and the CO_2 solvation shell. Two complementary spectroscopies can characterize the molecular motions in the membranes. Broadband dielectric spectroscopy (BDS) measures the motion of the ions from tens of nanoseconds to seconds. 2D-IR spectroscopy is sensitive to the dynamics of CO_2's solvation shell

from femtoseconds to hundreds of picoseconds. Temperature-dependent BDS and 2D-IR spectroscopy can measure the local structure and dynamics around the CO_2 using to extract activation energies related to local motion of the CO_2 and its surroundings. These powerful spectroscopies will interrogate the interactions of CO_2 and the surrounding ions in the SPIL and DPIL membranes.

Using bulk and molecular information to provide detailed molecular insights of CO_2 solvation. Molecular dynamics simulations will provide atomistic models of the spectroscopy, transport properties, and thermodynamics. A transferable spectroscopic model based on new machine learning (ML) techniques will connect the 2D-IR spectroscopy and MD simulations. The 2D-IR experiments will validate the molecular dynamics simulations, and the simulations will provide atomistic insights into the origin of the observed behaviors. ML techniques will also guide the selection and optimization of synthetic targets.

Recent Progress

We have synthesized a series of DPIL monomers based on the ethylmethylimidazolium cation and bis(trifluoromethylsulfonyl)imide anion. Broadband dielectric spectroscopy reproduces the dynamics observed in prior work over the 1 to 10^8 Hz range, consistent with hindered mobility of positive and negative charges. We have collected preliminary 2D-IR data on the solvation of CO_2 in these membranes. The 2D-IR spectra show an inhomogeneously broadened antisymmetric stretch with an inhomogeneous linewidth of 7 cm^{-1}. The dynamics of CO_2 are constrained in the membranes, showing spectral diffusion on a 500 ps timescale based on the initial slope of the frequency fluctuation correlation function (FFCF).

Simulations to build a spectroscopic model with polarizable and non-polarizable force-fields have begun. Initial studies support the prior models of a quadrupolar solvation shell but indicate that interactions with the anions are more important than the cations for dictating structure and dynamics of the first solvation shell of CO_2.

Future Plans

Immediate plans are to assess the dynamics of CO_2 in blends of the DPIL and free ionic liquids. This study will assess the impact of the glassy polymeric matrix on the quadrupolar solvation observed in neat ionic liquids. The plasticization of the films by the free ionic liquid component will be measured through the shift in the glass transition temperature, T_g, and the shift in the dielectric relaxations measured in the derivative of the real part of the permittivity measured in BDS. The changes in the local solvation shell will be established through the changes in the observables in 2D-IR spectroscopy – vibrational relaxation time, FFCF, orientational time, and rate of thermal excitation and de-excitation of the bending mode.

Next steps plans include the broadening of the synthetically accessible cationic and anionic monomers to allow additional flexibility in the cast films. Each target compound will be characterized with differential scanning calorimetry, BDS, and 2D-IR spectroscopy. Bulk

transport properties will be determined through both pressure lag techniques and in-situ IR absorption spectroscopy.

In parallel, MD simulations and quantum chemistry will use ML techniques to reparameterize a spectroscopic model of the vibrational frequency of CO_2. The new learned map will be validated against experimental spectroscopic observables (average IR absorption frequency, breadth of the distribution, amount of motional narrowing, orientational correlation time constants, and spectral diffusion time constants).

Future work will train bags of neural networks on the collected observables and literature data to guide the synthesis of other DPIL and SPIL films.

Peer-Reviewed Publications Resulting from this Project (Project start date: 09/2022)

No publications to report.

Interfacial Spectromicroscopy of Water Oxidation at Earth Abundant Solar Photoanodes
DE-SC0023342
Franz M. Geiger, Department of Chemistry, Tech Institute Room KG68, Northwestern University, 2145 Sheridan Road, Evanston, IL, USA, f-geiger@northwestern.edu

Project Scope:
Solar water splitting materials that generate the most photocurrent often leverage Pt-group element (PGEs) catalysts. Among the materials pursued as PGE replacements is the hematite (a-Fe_2O_3) photoanode. Serving both as a thin film semiconductor for light absorption and as a surface catalyst, it is "a unique and obvious choice for solar energy storage via photoelectrochemical water splitting", according to Graetzel.[1] Hematite is an earth-abundant mineral phase, photochemically stable, non-toxic, inexpensive, and readily obtainable in chemically pure form.[1-4] Most recently, Strehle reported 2.35 mA cm^{-2} photocurrent density at +1.23 V_{RHE} which "is higher than any value so far by hematite and other single-material thin-film photoanodes".[5] Still, much fundamental work remains to reach the maximum possible current density of >12 mA cm^{-2} at 0.6 V_{RHE} needed for "the realistic use of a tandem water splitting device".[1] Taking research on photoanodes[6] beyond Edisonian innovation approaches requires fundamental mechanistic studies that link experimental observations with microscopic interpretations of proton-coupled electron transfer (PCET). Our project aims to do so using "*photonic electrochemical microscopy*" as a rapid and label-free new tool.

The guiding hypothesis being tested in this project is that the high overpotential of the oxygen evolution reaction over non-platinum group element electrodes is in part due to the need to flip unfavorably oriented Stern layer water molecules, which point their protons towards the active sites at high pH. Water's oxygen is the electron source for solar energy conversion, but how water interacts with the active site remains poorly studied. Indeed, Priority Research Directions #2, 7, and 11 in BES's 2005 Solar Report contain surprisingly little information on the structure and dynamics of interfacial water.[7] Yet, these are critically important aspects of charged interfaces,[8] including photoelectrodes.[9-11] To fill this gap, we will place on an equal footing novel research on both the active site and the water bound to it. We hypothesize that water reorientation at the active site is a significant source of overpotential (0.5-0.6 V)[1] for water oxidation and the associated transfer of electrons. We will test this hypothesis by imaging, in electrolyte, under bias, and during photoexcitation, the net interfacial water orientation, the Fe^{IV}=O (heme-free "ferryl oxo")[12] active site (reported photocurrents imply >10^{14} such sites cm^{-2}), and the interfacial total potential and energy barriers associated with water flipping during the oxygen evolution reaction (OER). The project also tests weather iridium-, platinum-, and palladium-based electrodes feature a more favorable Stern layer water orientation, which may then support our stated hypothesis and may be useful for improving the performance of the earth-abundant electrodes. Finally, the project also accesses specifically the active sites between 500 and 600 nanometers, where most if not all transition metal oxo (>M=O) groups exhibit sizable charge transfer residences that are readily accessible using nonlinear optical spectroscopic methods that we have developed, and probe the hydrogen bond network strength in the Stern layer using vibrational interfacial spectroscopy.

Using new instrumentation being developed, the major project goals are to elucidate 1) the number density, 2) orientation distributions, and 3) energetics of water molecules in the Stern layer of working electrodes under high pH and ionic strength conditions amenable for the oxygen evolution reaction. Major activities under this project focus on interrogating electrodes made of earth abundant materials, specifically oxide of iron, using novel instrumentation being developed under this grant to further our understanding of the overpotential associated with water oxidation chemistry. To this end, the project entails the construction of several new instruments that provide amplitude and phase resolved spectroscopic data from electrodes under operandi conditions.

Recent Progress:
Year one saw major accomplishments in instrumentation building and spectro-electrochemical studies of hematite electrodes.
1) We designed a custom-built spectro-electrochemical cell by working with engineers at redox.me, a partner of Metrohm, which supplied us with a high-end electrochemical workstation with a true linear-sweep module. The new cell is made entirely out of PEEK (a fluorinated polymer specifically used in electrochemical measurements) and features two optical windows for transmission and reflection spectroscopic modalities of multiple kinds, including video imaging. Using glass slides coated with ~10 nm thin films of fluorine-doped tin oxide (FTO), we deposited 10 nm hematite layers using atomic layer deposition (with Dr. Alex Martinson at Argonne National Laboratory) that feature <100 Ohm sheet resistance. The cyclic voltammograms (CV) obtained with these samples recapitulate published results (Hamann group, Nature Chem. 2016). Using these samples in our new e-chem cell, we have recorded videos of oxygen bubble formation occurring at the exact same locations during multiple replicate CVs. This result has encouraged us to move ahead with second harmonic generation imaging microscopy in an X – shaped cross-beam far-field geometry, with which we observe the spatial and temporal evolution of interfacial structure and electric fields in real time and space while running CV's.
2) To realize second harmonic measurements at the electrode-electrolyte interface, we decided to avoid the aqueous electrolyte, which could be a significant source of phase distortion in our heterodyne detected measurements that are ongoing. We therefore employed a geometry in which we interrogate the interface from the solid side, which means that the fundamental laser light field first transmits through the glass slide, which is coated on one side with the hematite/FTO layer. The fundamental reflects through the sample glass window and along with it, slightly displaced due to refraction, is the second harmonic generation signal that we seek. Transmitted fundamental light also passes through the electrolyte and reflects off the second (back) window that seals the electrochemical cell. That reflection along with the top reflection from the sample window is blocked using custom-built micrometer mounted metal blocks that only allow the fundamental and the second harmonic from the hematite electrode interface to propagate towards the detector. To check alignment, we collected homodyne second harmonic generation signals using 1030 nm pulses (80 fs) at 78 MHz. The SHG intensity is nicely reproducible over several CVs and generally increases sigmoidally as the externally applied potential is raised from -0.4 to +0.9 V vs Ag/AgCl at pH 13 and 1

M NaCl. Otherwise, the information content from this measurement is rather limited. We therefore proceeded towards a heterodyne detection scheme, in which the SHG intensity is for the broken down into its amplitude and fees information, from which the second order nonlinear susceptibility and the interfacial potential drop across the electrode electrolyte interface can be obtained.
3) To this end, we developed an SHG pulse triplet interference detection method to obtain, for the first time, the absolute phase of the SHG response from the hematite electrode under operando CV conditions. Our approach circumvents the need for an arbitrary choice of a reference state, at which the phase would be set to zero. Instead we take the well-known 180° phase flip that occurs with every 60° of azimuthal rotation in z-cut alpha quartz. We build on our recent development of heterodyne detection, in which the SHG single from a sample is interfered with the SHD signal from a local oscillator, a 50 μm thin piece of z-cut alpha quartz. Here, instead of relying on the optical dispersion and air, which is very weak at 10:30 and 515 nm, we employ a fused silica plate having a 1 mm thickness on a rotational stage that is used as a phase shifting unit. This phase shifting unit is placed between the local oscillator source and a second 50 μm thin piece of z-cut alpha quartz (the reference oscillator source), aligned such that its phase relationship to the local oscillator is 180°. We named the resulting module (LO, face shifting unit, RO) the ROLO. We then measure the interference of the signal+ROLO pulse triplet as the phase shifting unit rotates, fit the interferogram ("fringe") to a trigonometric function producing the signal+ROLO phase (and the associated amplitude), and then process the ROLO-only phase (obtained by blocking the signal from the sample using a long-pass filter) to obtain the signal-only phase. This phase is the SHG phase from the electrode-electrolyte interface. The measurement currently takes as little as 10 seconds per fringe. Using this approach, we have successfully recorded the SHG phase and amplitude on multiple hematite electrodes held at pH 13 and 1 M NaCl as we cycle the applied voltage between -0.4 and +0.9 V vs Ag/AgCl. In all cases, we observe a 15 to 20 degree increase in the SHG phase with increasing applied potential and a ca. 40% reduction in the SHG amplitude. We are currently developing the optical model to obtain the second-order nonlinear susceptibility and the total potential from the measured data. This turns out to be challenging, given the non-zero resonance of hematite at the SHG wavelength and its associated SHG phase.
4) We also characterized the hematite electrode characterization at open circuit potential and varying bulk solution pH. This measurement was carried out using homodyne detection and revealed sluggish kinetics on the order of 30 to 60 min when the pH was changed from 2 to 6 to 13. In contrast, fused silica's SHG response to pH jumps is almost instantaneous. The hematite results are consistent with some published data showing similarly sluggish electrokinetic responses of hematite to pH jumps. Yet, we were able to determine a point of zero charge at OCP of pH 6.75 (+/- 0.25), indicated by the observation that the SHG intensity at this pH is invariant with ionic strength. We are currently pursuing measurements using our SHG pulse triplet/ROLO method to determine the potential of zero charge at high ionic strength at various pH values, which is a challenge using traditional e-chem methods unless one works at low (<1 mM) ionic strength.

Future Plans:
Future work includes the full development of our optical model to obtain the second-order nonlinear susceptibility and the total potential from the measured data, which involves challenging experiments and quartz phase referencing techniques. We are also working on building out our spectroscopic SHG microscope, in which we aim to record SHG microscopy images as a function of applied potential while probing the interface with incident light fields having various wavelengths. Finally, we are planning to probe the impact of photoexcitation using 400 nm light as well as the output of a solar simulator on the SHG amplitude and phase as we vary potential, so as to determine if water flipping can be induced photophysically.
References:

1. Sivula, K.; Le Formal, F.; Graetzel, M., Solar Water Splitting: Progress Using Hematite (α -Fe2O3) Photoelectrodes. *ChemSusChem* **2011,** *4*, 432-49.
2. Hardee, K. L.; Bard, A. J., Semiconductor Electrodes: V . The Application of Chemically Vapor Deposited Iron Oxide Films to Photosensitized Electrolysis. *J. Electrochem. Soc.* **1976,** *123*, 1024-6.
3. Faure, G., *Principles and Applications of Geochemistry*. 2nd ed.; Prentice Hall: New Jersey, 1998.
4. Langmuir, D., *Aqueous Environmental Geochemistry*. Prentice-Hall, Inc: New Jersey, 1997.
5. Chnani, A.; Kurniawan, M.; Bund, A.; Strehle, S., Nanometer-Thick Hematite Films as Photoanodes for Solar Water Splitting. *App. Nano Mat.* **2022,** *5*, 2897-2905.
6. Palmisano, L.; Yurdakai, S., *Photoelectrocatalysis: Fundamentals and Applications*. Elsevier: 2022.
7. DOE BES Basic Research Needs for Solar Energy Utilization, please visit https://science.osti.gov/~/media/bes/pdf/reports/files/Basic_Research_Needs_for_Solar_Energy_Utilization_rpt.pdf. **2005**.
8. Gonella, G.; Backus, E. H. G.; Nagata, Y.; Bonthuis, D. J.; Loche, P.; Schlaich, A.; Netz, R. R.; Kühnle, A.; McCrum, I. T.; Koper, M. T. M.; Wolf, M.; Winter, B.; Meijer, G.; Campen, R. K.; Bonn, M., Water at charged interfaces. *Nature Reviews Chemistry* **2021,** *5* (7), 466-485.
9. Shin, S.-J.; Kim, D. H.; Bae, G.; Ringe, S.; Choi, H.; Lim, H.-K.; Choi, C. H.; Kim, H., On the importance of the electric double layer structure in aqueous electrocatalysis. *Nature Comm.* **2022,** *13*, 174.
10. Futera, Z.; English, N. J., Water Breakup at Fe2O3−Hematite/Water Interfaces: Influence of External Electric Fields from Nonequilibrium Ab Initio Molecular Dynamics. *J. Phys. Chem. Lett.* **2021,** *12*, 6818-26.
11. McBriarty, M. E.; Stubbs, J. E.; Eng, P. J.; Rosso, K. M., Potential-Specific Structure at the Hematite‑Electrolyte Interface. *Adv. Functional Mat.* **2017,** *28*, 1705618.
12. Bray, W. C.; Gorin, M. H., Ferryl Ion, a Compound of Tetravalent Iron. *J. Am. Chem. Soc.* **1932,** *54*, 2124-5.

Peer-Reviewed Publications Resulting from this Project (Project Start Date 06/2022): *J.* Chang, H., Lozier, E. H., Ma, E. Geiger, F. M. *Phys. Chem. A* **2023**, 127, 40, 8404–8414.

UNDERSTANDING IONIZING-RADIATION-INDUCED SPECIATION, CHEMISTRY, AND TRANSPORT IN NUCLEAR MATERIALS

Gregory P. Holmbeck (previously Horne)
Center for Radiation Chemistry Research,
Idaho National Laboratory, 1955 N. Fremont Avenue Idaho Falls, ID, 83415, USA.
Gregory.Holmbeck@inl.gov

Project Scope

The research to be presented will cover an overview of three projects supported by the United States Department of Energy Office of Science Solar Photochemistry Program: (i) ***Radiation-Induced Late Actinide Redox Chemistry*** (2019–2022); (ii) ***Understanding Radiation-Induced Iodine Speciation, Chemistry, and Transport in High Temperature Molten Salts*** (2022–2025); and (iii) ***Radiation-Induced Chemistry of Nuclear Materials*** (2023–2026). The overarching aim of these distinct projects is to develop a deep fundamental mechanistic understanding of ionizing-radiation-induced processes occurring in solutions over multiple time and length scales. Investigated solutions range from aqueous to organic to molten salt liquids in the presence and absence of ligands and various redox-active ions and molecules, including the actinides. The ultimate goal of these projects is to utilize the new foundational knowledge gained to construct quantitative multiscale computer models with the capacity to predict radiation-induced behavior in complex systems of relevance to nuclear energy technologies and beyond.

The focus of the concluded ***Radiation-Induced Late Actinide Redox Chemistry*** project, in collaboration with Florida State University, was to evaluate the hypothesis, "*thermodynamic and kinetic measurements of late actinide (americium onwards) radiolytic reactions can be coupled with electrochemical data and modelling of general redox reactions to provide a deeper understanding of the complexities occurring for actinide complexes in solution*." These data will yield greater predictive capabilities for actinide chemical behavior in a variety of applied scenarios, including used nuclear fuel recycling, the implementation of actinide materials in energy and medical technologies, and nuclear forensic analysis.

The goal of the ongoing ***Understanding Radiation-Induced Iodine Speciation, Chemistry, and Transport in High Temperature Molten Salts*** project, in collaboration with Brookhaven National Laboratory (BNL), is to determine the radiation-induced chemistry of fission product iodine in the triumvirate extremes of high-temperature, multi-component ionizing radiation fields, and corrosive molten salts. These fundamental studies are vital to support the accelerated development and deployment of safe, clean nuclear energy technologies based on molten salt reactor (MSR) design concepts. The central hypothesis for this project is, "*the radiation-induced conversion of iodide will yield an extensive suite of transient and steady-state iodine radiolysis products that will alter the bulk chemical and physical properties of the irradiated molten salt system—the speciation, distribution, and chemical transport of which will be dictated by the composition and the availability of multivalent metal cations and metal alloy interfaces.*" To test this hypothesis, we aim to answer the following scientific questions: (i) what are the transient and steady-state iodine species formed by the irradiation of high-temperature molten salts, and what are the fundamental radiation-induced mechanisms responsible for their formation and decay; (ii) how do these radiation-induced iodine species impact the physical and chemical properties of a molten salt system; and (iii) how is the formation, speciation, and transport of these radiolytic

iodine species affected by the presence of multivalent metal cations and metal alloy interfaces? To address these questions, we initiated three synergistic research objectives. The purpose of the first research objective is to determine how: (i) the inclusion of iodine changes the spectroscopic features and physical properties of molten salt mixtures; (ii) iodine speciation in the molten salt and the attendant vapor phase in the absence of radiation fields; and (iii) how this speciation changes in the presence of other solutes. e.g., multivalent metal ions. Our second research objective focuses on understanding the transient and steady-state iodine species formed by the irradiation of high-temperature molten salts, and their fundamental chemical behavior. Finally, the third research objective aims to understand the influence of interfacial processes on determining the final disposition of iodine in high temperature molten salts, notably the structure and chemical speciation of iodine at metal-salt interfaces.

The new ***Radiation-Induced Chemistry of Nuclear Materials*** project, in collaboration with Colorado School of Mines, is directed toward creating a deeper understanding of radiation-induced chemistry in nuclear materials, specifically materials designed for the extraction of actinides and radioisotopes. This project will address two key hypotheses. The first, "*metal ion complexation will alter the radiation-induced reaction kinetics and degradation product distributions of the diglycolamide and di-alkyl-monoamides ligands owing to electron distribution differences, steric effects, and the facilitation of inner- vs. outer-sphere electron transfer mechanisms*." The second, "*complexed radioisotopes will facilitate different radiolytic responses in coordinated ligands owing to the combination of daughter recoil damage and direct radiation effects from the emitted radiation*." The combination of these two hypotheses will help to create a comprehensive understanding of how multi-component radiation fields impact important materials used in radioisotope separation and recovery technologies.

Recent Progress

The ***Radiation-Induced Late Actinide Redox Chemistry*** project concluded at the end of Fiscal Year 22. Over the duration of the project, which was impacted by the COVID pandemic, new rate coefficients were measured—using the BNL Laser-Electron Accelerator Facility (LEAF)[1]—for the intrinsic radiation-induced redox chemistry of trivalent curium, californium, and berkelium ions in acidic aqueous solutions, specifically their reactions with the strongly reducing hydrated electron (e_{aq}^-) and hydrogen atom ($H^\bullet$), and the highly oxidizing hydroxyl ($^\bullet OH$) and nitrate ($NO_3^\bullet$) radicals. Despite their reported redox potentials,[2] all three late actinides exhibited significant reactivity with the investigated transients. These radiation-induced redox reactions resulted in the formation of non-equilibrium actinide oxidation states—di- and tetra-valent—most of which exhibited lifetimes on the order of tens of microseconds. This is more than sufficient time to propagate subsequent radiation chemistry and potentially represents a synthetic avenue for the stabilization and study of these species. Additionally, a series of novel actinide complexes, specifically of plutonium, were synthesized as surrogates to evaluate the impact of non-equilibrium oxidation states on coordination environment and structure. Overall, the research performed during this project highlights the existence of rich, complex, intrinsic late actinide radiation-induced redox chemistry that has the potential to influence the findings of other areas of actinide science.

With regards to ***Understanding Radiation-Induced Iodine Speciation, Chemistry, and Transport in High Temperature Molten Salts***, significant progress has been made in all three of

the aforementioned research objectives. Initial studies on the effect of halide ion identity on metal ion speciation focused on the local structure of divalent nickel ions (Ni^{2+})—a common corrosion product in MSR technologies—dissolved in molten lithium-potassium halide eutectics, specifically chloride (LiCl-KCl), bromide (LiBr-KBr), and iodide (LiI-KI) salts. These salt mixtures were interrogated over a range of temperatures (≤ 600 ºC) using a combination of optical absorption and x-ray spectroscopies. This investigation demonstrated that the coordination environment of Ni^{2+} ions was sensitive to halide identity and temperature. An example of this heterogeneity is shown in **Figure 1A**, wherein the Ni^{2+} ion octahedral state is clearly shown to be favored in iodide salts, while the tetrahedral environment is adopted by the complementary chloride and bromide salts. This behavior was surprising, given the relative size differences between the investigated halides, $I^- > Br^- > Cl^-$. A decrease in Ni^{2+} ion coordination number would have been expected in going from Cl^- to I^- ions. Concerning temperature effects, multiple Ni^{2+} ion coordination geometries were observed upon going from 300–550 ºC, as shown **Figure 1B** for Ni^{2+} ions in molten LiI-KI eutectic. Our preliminary optical spectroscopy results show that Ni^{2+} ions exhibit structural heterogeneity, being present in a mixture of 5-coordinate square pyramidal and 4-coordinate tetrahedral states at 300–400 ºC, and changes above 450 ºC. Further studies of iodide-based salt systems are planned to understand these preliminary findings.

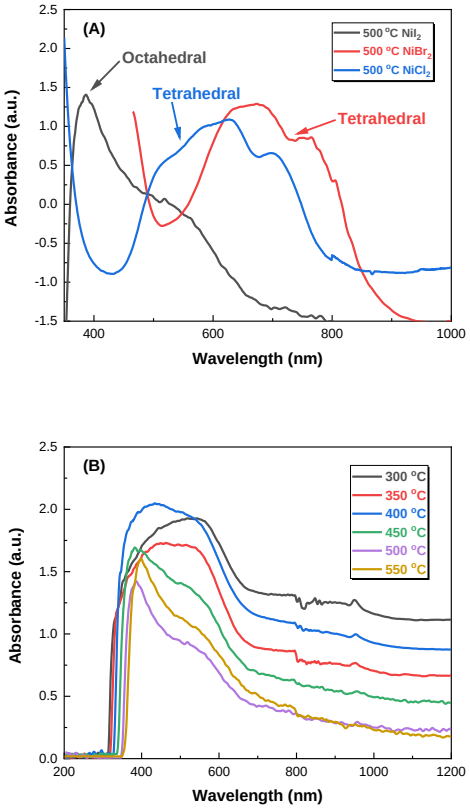

Figure 1. Optical absorption spectra of Ni^{2+} ions in molten chloride, bromide, and iodide salts at 500 ºC **(A)** and in molten LiI-KI eutectic as a function of temperature **(B)**.

Complementary x-ray analyses were performed using the BNL National Synchrotron Light Source II (NSLS-II). Both x-ray absorption fine structure (XAFS) and x-ray absorption near edge structure (XANES) techniques indicated that the observed Ni^{2+} ion coordination state behavior was best correlated with the change in electronegativity of the halide series, which causes the metal-halide bonds to become less polarized (Ni–Cl > Ni–Br > Ni–I). The decrease in electronegativity in going from Cl^- to I^- is manifested as a shift in the absorption edge of the Ni^{2+} ion XANES spectra to lower energies, while the pre-edge feature did not change from 8332.4 eV, as shown in **Figure 2A**.

The intensity ratio of the pre- and main peak changed with increasing ionic radii of the halide anions, indicating a difference in the local coordination environment around the Ni^{2+} ions. This observation is consistent with the trends in metal-halide bond polarizability and ionic radii. With regards to coordination number (C.N.) and bond length (R), preliminary EXAFS analysis are shown in **Figure 2B** for Ni^{2+} ions in LiI-KI eutectic as a function of temperature. These analyses indicate that a transition from a mixture of 6-coordinate and 5-coordinate states to a lower coordinate state was observed upon increasing temperature. This coincided with a shortening of the Ni–I bong length from 2.72 Å (room temperature) to 2.55 Å (500 °C). The reduction in the C.N and bond length is indicative of the weakening of electrostatic interactions between the Ni^{2+} and I^- ions, ultimately reducing the molten salt's local structural distortion. More studies on iodide-based systems such as cobalt iodide (CoI_2) in LI-KI eutectic are planned to further understand changes in local coordination of metal ions in iodide containing molten salts.

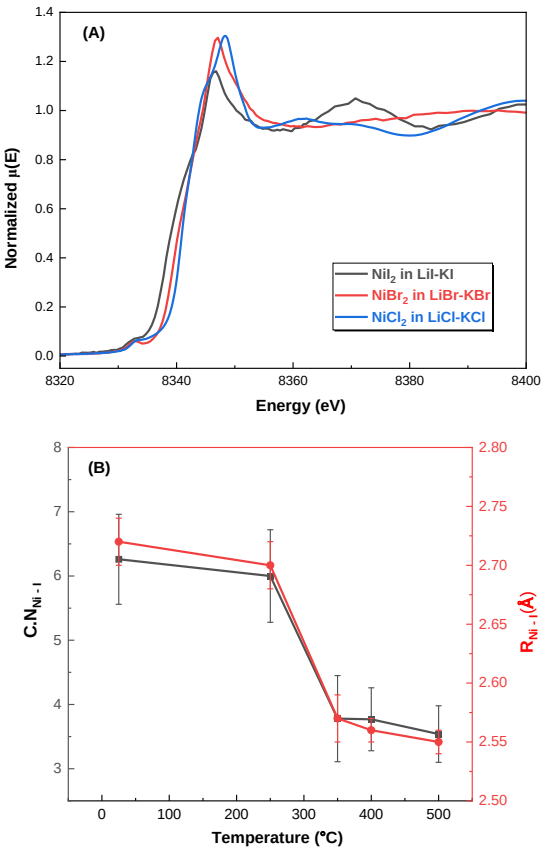

Figure 2. Comparison between normalized XANES spectra of molten Ni^{2+} ion halides eutectics at 500 °C **(A)**. Variation of Ni^{2+} ion coordination number and bond length as a function of temperature in LiI-KI eutectic **(B)**.

Overall, we found that the speciation and local structural heterogeneity demonstrated by Ni^{2+} ions in molten halide salts is directly related to solvent composition owing to the electronegativity of the halide anion. The fundamental structural knowledge gained from these systems will aid in our understanding of radiation effects in iodide containing salt systems in the presence and absence of prototypical MSR corrosion and fission products.

Another aspect of knowledge necessary for a comprehensive understanding of radiation-induced effects on iodine containing molten salts is the impact of iodide species on the thermal phase stability of halide salt mixtures, specifically the solidus and liquidus temperatures. In this study we focused on the impact of I^- ions on LiCl-KCl salt properties by utilizing the FactSage software in conjunction with differential scanning calorimetry (DSC) and high temperature x-ray diffraction (HT-XRD) measurements. This approach provided detailed phase diagram information on solidus and liquidus temperatures, the evolution of crystalline phases as a function of temperature, and the distribution of salt components in the liquid and solid phases for the various pseudo-ternary compositions investigated thus far. Calculated phase diagrams were in good agreement with experimentally determined solidus and liquidus temperatures. For example, the calculated solidus and liquids temperatures for 25KI-33LiCl-42KCl (weight percent, wt.%) were 344.8 and 378.8 ^oC, respectively, while the corresponding experimental DSC measurements were 338.5 and 370.8 ^oC, respectively. Overall, our thermophysical studies thus far show that the addition of 25 wt.% potassium iodide (KI) to LiCl-KCl eutectic increases the melting point of the

mixture by 18.8 °C (from 352–370.8 °C). Furthermore, we discovered that the phase diagrams and equilibrium data calculated by FactSage are in good agreement with the experimental data obtained by DSC and HT-XRD. The theoretical and experimental tools used here are a great combination to gather reliable information on the melting point and thermodynamic phases of the system as a function of temperature. The use of these tools provides the opportunity to further investigate the impact of complex fission product mixtures, such as cesium iodide (CsI), on the thermodynamic phase stability of different molten chloride salt mixtures.

Initial radiation chemistry studies focused on measuring the impact of I^- ions on the fundamental radiation-induced reaction kinetics and speciation occurring in molten chloride salt mixtures, specifically in the LiCl-KCl eutectic mixture. Picosecond, time-resolved electron pulse irradiation measurements were performed as a function of temperature (400–700 °C) using the BNL LEAF. Integrated transient optical detection methods, coupled with spectro-kinetic analysis software (SK-Ana version 3.4) and gas phase density functional theory (DFT) calculations, revealed that in the presence of > 0.1 wt.% I^- ions, a newly observed inter-halide radical anion species ($ICl^{\bullet-}$) was generated in addition to the primary radiation-induced radical species typically found in neat molten LiCl-KCl eutectic salt mixtures, i.e., the solvated electron (e_S^-) and the dichlorine radical anion ($Cl_2^{\bullet-}$), shown in **Figure 3**. This new $ICl^{\bullet-}$ radical anion species is expected to have significant implications for the transport and accumulation of fission-product iodine in MSR environments. Consequently, a deeper understanding of its fundamental chemistry is necessary to support the safe development, deployment, and long-term maintenance of promising MSR technologies.

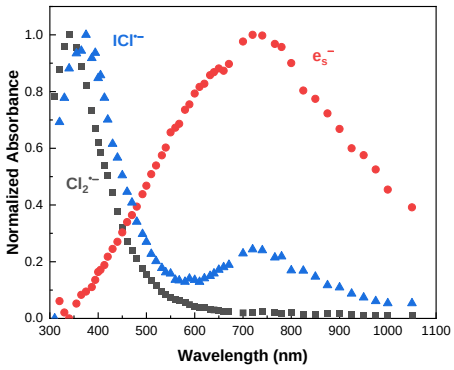

Figure 3. Normalized spectra from the devolution of electron pulse irradiated molten 10 wt.% KI in LiCl-KCl eutectic salt at 400 °C.

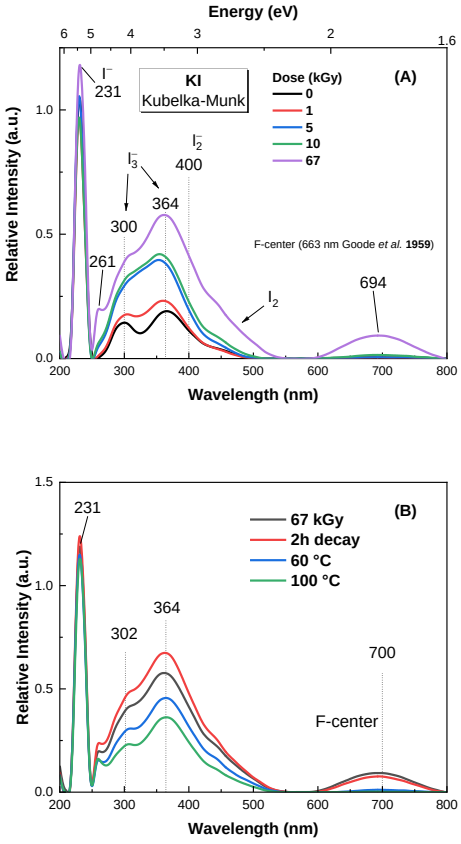

Figure 4. (A) Absorption spectrum for irradiated solid KI salts up to 67 kGy at room temperature. **(B)** Photo- and thermal-bleaching of the radiation-induced primary transients in irradiated solid KI salt.

In parallel to the above time-resolved irradiation studies, solid-state cobalt-60 gamma irradiations were performed up to 100 kGy at ~55 Gy min^{-1} on solid powders of I^- ion containing salts, specifically KI and lithium iodide (LiI). Gamma irradiated salts were interrogated with a combination of room temperature electron paramagnetic resonance (EPR) and diffuse reflectance spectroscopies. A bespoke 3-dimensional (3D) printed sample holder was fabricated for the latter

studies. Typical EPR and diffuse reflectance spectra for these preliminary irradiations are shown in **Figure 4**. EPR spectra indicated the formation and accumulation of both di- and tri-iodide ion species (I_2^- and I_3^-, respectively), as shown in **Figure 4A**. These observations are consistent with previous findings for gamma irradiated chloride mixtures,[3,4] albeit with evidence for a complex equilibrium of inter-and polyhalide species. Pseudo-absorption spectra were obtained from 200–800 nm after Kubelka-Munk treatment (**Figure 4B**), using a previously described experimental arrangement.[3] Interestingly, F-center (trapped electron) signals were only detected at absorbed doses > 67 kGy and found to be relatively unstable, as subsequent bleaching experiments found that a temperature of only 60 °C was needed to completely release the electrons from their F-center vacancies (λ ~ 700 nm), as shown in **Figure 4B**.

Under research objective three we studied the effects of doping transition metals (such as iron (Fe), chromium (Cr), and Ni ions) in iodine containing salts and investigated the formation of new phases. In situ temperature transmission mode synchrotron XRD studies of KI, LiI, and nickel iodide (NiI_2) in LiCl-KCl eutectic salt mixtures were characterized at different concentrations, up to 10 wt.% iodide content. These studies were performed at the BNL NSLS-II. Typical date for 5 wt.% NiI_2 dissolved in LiI-KI eutectic is shown in **Figure 5**. Our analysis showed that the NiI_2 phase recovers after cooling below the melting temperature of the salt mixture (**Figure 5A**). Development of new phases after thermal cycling was not detected in the XRD spectra. Atomic pair distribution function (PDF) data (**Figure 5B**) showed that the long-range order between LiI and KI was destroyed above the melting point of the LiI-KI eutectic, i.e., ≥ 290 °C. This information provides an initial insight into the correlation between changes in the speciation and thermophysical properties of a molten salt due to transition metal ions originating from the corrosion of structural materials.

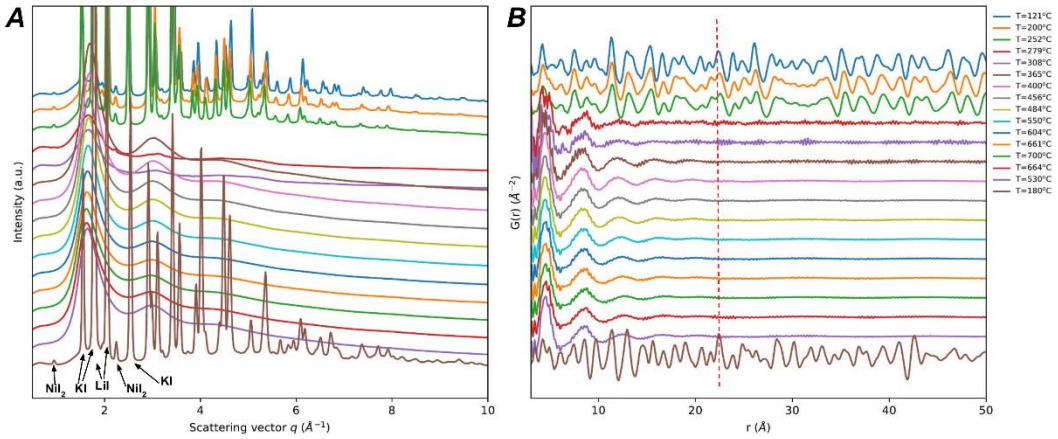

Figure 5. (A) Variation of XRD spectra with temperature, in which NiI_2, KI, and LiI reflections are highlighted with arrows in the low q-region of the cooled spectrum. **(B)** Variation of PDF spectra with temperature.

With regards to the new ***Radiation-Induced Chemistry of Nuclear Materials*** project, experiments are underway to probe the impact of metal ion complexation and molecular architecture on the gamma radiation-induced behavior of diglycolamide ligands and their reusling distribution of degradation products.

Future Plans

Although the ***Radiation-Induced Late Actinide Redox Chemistry*** project has concluded, there are several manuscripts in preparation for submission between 2023 and 2024, including:

1. B.M. Rotermund, S.P. Mezyk, J.M. Sperling, N. Beck, H. Wineinger, A.R. Cook, T.E. Albrecht-Schönzart, and G.P. Horne*, Chemical Kinetics for the Reaction of Californium(III) with Select Radiation-Induced Inorganic Radicals ($Cl_2^{\bullet-}$ and $SO_4^{\bullet-}$), *Journal of Physical Chemistry Letters*, **2023**, submitted.
2. D. Gomez Martinez, J.M. Sperling, N.B. Beck, H.B. Wineinger, J.P. Brannon, T.E. Albrecht-Schönzart, Synthesis and Characterization of a Neodymium and Americium Complex Synthesized Under Identical Conditions, *Inorganic Chemistry*, **2023**, submitted.
3. B.M. Rotermund, Z.K. Huffman, N.B. Beck, J.M. Sperling, D. Grödler, G.P. Horne, T.E. Albrech-Schönzart. A Comprehensive Synthesis of Lanthanide Diglycolamide Complexes and Explorations Into Americium and Curium Diglycolamides, **2024**, in preparation.
4. H.J. Culbertson, C. Celis-Barros, C.D. Pilgrim, J.R. McLachlan, A.R. Cook, S.P. Mezyk, and G.P. Horne, Elucidating the Impact of Neptunium and Plutonium Complexation on TBP, DEHBA, and DEH*i*BA Radiation-Induced Reaction Kinetics, **2024**, in preparation.

For the ongoing ***Understanding Radiation-Induced Iodine Speciation, Chemistry, and Transport in High Temperature Molten Salts*** project several future research avenues are in the process of being investigated to further address the previously outlined hypotheses and scientific, in addition to exploring new research avenues that have arisen from the first year's activities. Research objective one will build upon our foundational knowledge of Ni^{2+} ion speciation in different halides. We plan to investigate temperature-driven speciation of other major corrosion products, such as Cr^{3+}/Cr^{2+}, and Fe^{3+}/Fe^{2+}. We will apply a combination of optical absorption and x-ray absorption spectroscopy techniques to elucidate the effect of halide ion on the coordination environment of these metal cations. The chemistry of Cr^{3+}/Cr^{2+} and Fe^{3+}/Fe^{2+} redox couples will be investigated using combined spectroscopy and electrochemistry techniques. The kinetics of these metal ions will be correlated in I^- and Cl^- ion systems, to provide a deeper understanding of the impact of halide ion identity/properties on the diffusion of species in molten salt systems. This work will be correlated with interfacial corrosion studies, which will also explore the L3 edge of the I^- ion using XAS to probe the interaction of I^- ions with alkali and transition metal cations in molten salts. In addition, the temperature dependent phase evolution of molten chloride salts in the presence and absence of I^- ions and anticipated MSR fission products, such as Cs^+ ions, will be investigated using FactSage, DSC analysis, and high temperature XRD. This study will provide greater insight into phase formation, phase transition temperatures, and the distribution of the salt's components between the liquid and solid phase, as dictated by the presence of iodine species.

Under research objective two, the fundamental chemical behavior of the $ICl^{\bullet-}$ radical anion will be further elucidated with respect to its reactivity with multivalent metal cations, such as Ni^{3+}/Ni^{2+}, Cr^{3+}/Cr^{2+}, and Fe^{3+}/Fe^{2+} ions. This new knowledge will provide critical insight into the underlying mechanisms of molten salt radiolysis and support the continued development of multi-scale modeling methods. Furthermore, a new high-temperature steady-state electron beam irradiation capability, which has been recently tested at the Idaho Accelerator Center, will be employed to investigate the chemical behavior of steady-state radiolysis products arising from the irradiation of I^- ion containing molten salts in the presence and absence of metal cation solutes. Additional chemical kinetics, relevant to I^- ion transients in irradiated molten salts, will be measured and incorporated into the existing FACSIMILE computer models. These kinetic data, combined with the physical properties of the salts to be measured by this project will be incorporated into a preliminary Monte Carlo simulation of the radiation chemical tracks formed in

molten salt mixtures. The yields from this preliminary model will be evaluated against existing data to target additional areas for further model development/refinement. Finally, solid-state irradiations will be performed on KI-LiI eutectic salt mixtures to close the gap in time between the aforementioned electron pulse and steady-state radiolysis studies. The decrease in thermal energy of the system will allow for the assessment of primary radicals through EPR, which would otherwise rapidly decay via fast combination processes at room temperature. Controlled annealing will provide information on $I_2^{\bullet-}$ radical anion formation and recombination to yield the triiodide anion (I_3^-) and thermal exchange between the various iodide species involved, i.e., I_2, $I_2^{\bullet-}$, and I_3^-. The second phase of solid-state experimentation will involve the inclusion of stoichiometric concentrations of different halide ions (Cl^- or Br^-) to evaluate their effect on the iodine speciation and the precipitation of metal ions in non-stoichiometric mixtures, i.e., radiolytic reduction.

For research objective three, electrochemical impedance spectroscopy (EIS) and linear polarization resistance (LPR) experiments are planned to elucidate the mechanisms of corrosion with respect to time and provide an estimation of corrosion rates in LiCl-KCl eutectic salt mixtures, complementing baseline static corrosion studies. Following baseline corrosion studies, electron microscopy characterization (i.e., scanning and transmission electron microscopy techniques) will be employed to characterize the salt-alloy interfacial corrosion mechanisms in the presence and absence of I^- ions, assessing microstructural and chemical compositional changes observed within the mesoscale and nanoscale length scales. These characterization studies will specifically consist of direct imaging of the interface after salt exposure, electron diffraction studies to image changes in grain size distribution and crystallographic structure, elemental analysis to generate two-dimensional images of species to document preferential dissolution of alloying elements, and electron energy loss spectroscopy to characterize the evolution of the oxidation states of the alloying and salt species.

Finally, the new ***Radiation-Induced Chemistry of Nuclear Materials*** project will focus initially on elucidating the impacts of metal ion complexation on the radiation-induced behavior of ligands designed for deployment in nuclear energy technologies, starting with the diglycolamide class of minor actinide extractants. These first experiments will leverage time-resolved electron pulse and steady-state alpha and gamma irradiation techniques to understand how the degradation mechanisms of the simplest diflycolamide, N,N,N′,N′-tetra(methyl)diglycolamide (TMDGA), are influenced by the complexation of minor actinides (americium and curium) and lanthanide surrogates. From this foundation, changes in DGA molecular architecture on radiation-induced metal complex behavior will then be investigated.

References

1. Wishart, J. F., Cook, A. R., and Miller, J. R. The LEAF Picosecond Pulse Radiolysis Facility at Brookhaven National Laboratory. *Review of Scientific Instruments* **2004**, *75 (11)*, 4359.
2. Bard, A. J., Parsons, R., and Jordan, J. Standard Potentials in Aqueous Solution. Marcel Dekker Inc., New York, **1985**.
3. Ramos-Ballesteros, A., Gakhar, R., Horne, G.P., Iwamatsu, K., Wishart, J.F., Pimblott, S.M., and LaVerne, J.A., Gamma radiation-induced defects in KCl, MgCl2, and ZnCl2 salts at room temperature. *Physical Chemistry Chemical Physics* **2021**, *23*, 10384.
4. Ramos-Ballesteros, A., Gakhar, R., Woods, M.E., Horne, G.P., Iwamatsu, K., Wishart, J.F., Pimblott, S.M., and LaVerne, J.A., Radiation-induced long-lived transients and metal

particle formation in solid KCl-$MgCl_2$ mixtures. *The Journal of Physical Chemistry C* **2022**, *126 (23)*, 9820.

Peer-Reviewed Publications

Radiation-Induced Late Actinide Redox Chemistry (2019–2022)

1. B. Rotermund, J. Sperling, G.P. Horne, N. Beck, H. Wineinger, Z. Bai, C. Celis-Barros, D. Gomez Martinez, and T. Albrecht-Schönzart*, Co-Crystallization of Plutonium(III) and Plutonium(IV) Diglycolamides with Pu(III) and Pu(IV) Hexanitrato Anions: A Route to Redox Variants of $[Pu^{III,IV}(DGA)_3]^{x+}$. *Inorganic Chemistry* **2023**, *62 (32)* 12905. DOI: https://doi.org/10.1021/acs.inorgchem.3c01590.
2. G.P. Horne*, B.M. Rotermund, T.S. Grimes, J.M. Sperling, D.S. Meeker, P.R. Zalupski, N. Beck, D. Gomez Martinez, A. Beshay, D.R. Peterman, B.H. Layne, J. Johnson, A.R. Cook, T.E. Albrecht-Schönzart, and S.P. Mezyk*, Transient Radiation-Induced Berkelium(III) and Californium(III) Redox Chemistry in Aqueous Solution. *Inorganic Chemistry* **2022**, *61 (28)*, 10822. DOI: https://doi.org/10.1021/acs.inorgchem.2c01106.
3. G.P. Horne*, T.S. Grimes, P.R. Zalupski, D.S. Meeker, T.E. Albrecht-Schönzart, A.R. Cook, and S.P. Mezyk*, Curium(III) Radiation-Induced Reaction Kinetics in Aqueous Media. *Dalton Transactions* **2021**, *50*, 10853. DOI: https://doi.org/10.1039/D1DT01268A.

Understanding Radiation-Induced Iodine Speciation, Chemistry, and Transport in High Temperature Molten Salts (2022–2025)

1. J.K. Conrad*, K. Iwamatsu, M.E. Woods, R. Gakhar, B. Layne, A.R. Cook, and G.P. Horne*, Impact of iodide ions on the speciation of radiolytic transients in molten LiCl–KCl eutectic salt mixtures. *Physical Chemistry and Chemical Physics* **2023**, *25*, 16009. DOI: https://doi.org/10.1039/d3cp01477k.

Spectroscopic elucidation of molecular-level interactions in water-mediated proton transport, interfacial reactions of HOCl, and macroscopic properties of ionic liquids with cryogenic ion chemistry DE-SC0021081 (ABM), DE-SC0021065 (KDJ) and DE-SC0021012 (MAJ)

Program Managers: Dr. Marat Valiev and Dr. Gregory Fiechtner

K. D. Jordan (jordan@pitt.edu), Dept. of Chemistry, University of Pittsburgh, Pittsburgh, PA
A. B. McCoy (abm@uw.edu), Dept. of Chemistry, University of Washington, Seattle, WA
M. A. Johnson (mark.johnson@yale.edu), Dept. of Chemistry, Yale University, New Haven, CT

Program Scope

The long-standing goal of our integrated theory/experiment approach is to create composition- and temperature-controlled systems that are sufficiently large display spectral signatures that are found in the condensed phase and used to infer local structural motifs and interactions between solutes (typically ions) and the surrounding solvent. By identifying the smallest assembly and composition that gives rise to a particular macroscopic observable, we can then systematically decompose the origins of the response to specific features of the assembly at the molecular level using accurate theoretical calculations that treat the entire ensemble under ansatz of a "super-molecule". When these assemblies are cooled near 10 K, they typically yield well defined spectral signatures that can be associated with specific structures, thus enabling us to establish the spectral response of particle intermolecular scaffolds. Understanding the mechanical origins of spectral responses in these systems often requires application of theoretical analyses beyond those typically applied to polyatomic molecules. These breakdowns of the commonly used paradigms are especially pronounced in strongly H-bonded systems involving solvation of electrolytes where floppy intermolecular motions can drive extreme anharmonic coupling between high frequency oscillators and the soft modes that act to break H-bonds. In the past two years, we significantly expanded the capability of the Yale instrument by incorporating a scheme to enable us to follow the evolution of spectral patterns with increasing temperature. Implementation of this important experimental parameter is non-trivial in cluster spectroscopy because one can no longer rely on photodissociation of weakly bound "tags" to obtain linear vibrational spectra.

IA. Microscopic mechanism underlying the shape of the OH stretch + HOH bend (SB) combination band in the infrared spectrum of water

A useful example of how well-defined cluster systems can reveal the molecular-level origin of spectral features associated with bulk water (D_2O) is found in the explanation of the shape of the band appearing near 4000 cm^{-1} that is derived from the DOD bend-OD stretch (SB) combination band (Fig. 1a), described in ref. 8. The band contour is dramatically different than that of the well-known, diffuse OD stretching band upon which it is based, and we traced this effect to the anharmonic coupling at play in molecules associated with specific network sites in the water cage. This difference was traced to the behavior of the mixed second derivative of

the electric dipole moment with respect to the OD stretch displacement and the DOD bond angle:

$$\frac{d^2\mu}{dr_{\mathrm{OD}}d\theta}\Delta r_{\mathrm{OD}}\Delta\theta = \frac{\partial}{\partial\theta}\left(\frac{\partial\mu}{\partial r_{\mathrm{OD}}}\right)\Delta r_{\mathrm{OD}}\Delta\theta.$$

In essence, the intensity of the OD fundamental is not strongly dependent on the bond angle, which is needed to drive oscillator strength in the combination band. As a result, the combination band is most representative of the populations of OD(H) oscillators embedded in different H-bond environments, modified by the spectral linewidths.

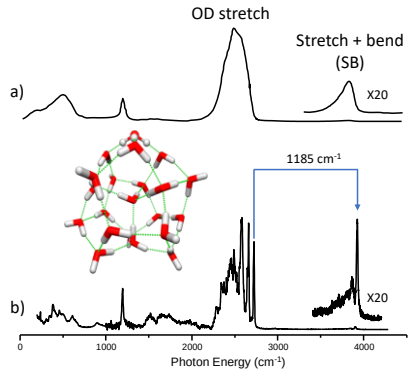

Fig. 1. a) Vibrational spectrum of ambient bulk D_2O, and b) H_2-tagged spectrum of the $D_3O^+\cdot(D_2O)_{20}$ cluster. SB denotes the combination band arising from excitation of one quantum in the OD stretch with one quantum of the DOD bend.

IB. Cluster models for the local environments of hydrated ions

We continued to refine our understanding of the potential energy landscape that controls the motion of "excess protons" in water in several complementary studies. In one study, the theoretical component of our team (complemented by CPIMS colleague Xantheas) established that a cyclic isomer is an intermediate on the low-energy pathway for interconversion of the well-known "Zundel" and "Eigen" forms of the protonated water hexamer (ref 13). This species is important because it may play a role in the interconversion of the well known "Zundel" and "Eigen" forms of this species. We also carried out a detailed investigation(ref. 5) of the local mechanics that drive the spectral response of water molecules in the vicinity of an excess proton. In a separate, theory/experiment effort(ref. 6), we reported how the competition for docking in the first coordination shell around alkali metal cations explains the metal-ion dependence of the effective acidity displayed by HNO_3. That study emphasized how asymmetric solvation of ions, which is significant at the air-water interface, leads to "reaction" electric fields that in turn control chemical behaviors of both water and proximal acids. Another example of the symbiotic effects of the local reaction field was explored in ref. 7, which focused on how the acidity of a particular water molecule bound to the anionic carboxylate head group is strongly enhanced by the shape of the surrounding network. This class of systems requires advanced theoretical methods to handle the extreme anharmonicities in play. The Jordan theory team addressed the inherent multidimensionality of these mechanics by introducing a two-dimensional, vibrationally adiabatic treatment in Ref. 12. Finally, we expanded our experimental capabilities that explore time-dependent changes in the chemical composition of size-selected clusters as a function of temperature or alternatively, internal energy. To demonstrate the latter, we followed the kinetics of protonated water hexamers relax into either Eigen or Zundel forms after selective vibrational excitation of the Zundel isomer in Ref. 10.

II. Plans for the next year

IIA. Elucidate the pathways for long range, water-mediated proton translocation on a prototypical organic scaffold in a temperature controlled, finite system

(b)

One important focus for the next year will be to experimentally determine the number of water molecules required to translocate protons between protomers of an organic scaffold. For this purpose, we will focus on the two protomers of para-aminobenzoic acid (denoted 4-ABA) depicted at the top of Fig. 2. This system was chosen because the two protomers (protonation at the amino vs acid functionalities) have dramatically different electronic spectra in the UV. This enables facile determination of the location of the excess proton in a mixed ensemble without requiring a mass "tag". In preliminary experiments, we photodepleted a large fraction of the O-protomers of size-selected 4-ABA-$(H_2O)_n$ clusters held in a trap at a variable temperature, T. We then monitored the spontaneous recovery of this proton accommodation motif after 100 ms as a function of *n* and T. The results are presented in Fig. 2b, indicating that only three water molecules are required to execute transfer with an onset of about 100 K. The challenges for the next year are to theoretically simulate such low kinetics and refine the measurements to follow the time evolution of the interconversion using two independently tunable uv lasers.

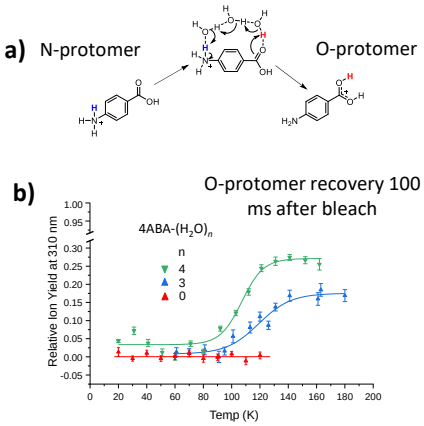

Fig. 2. a) Schematic pathway for transfer of a proton between the two protomers of para-aminobenzoic acid, b) temperature dependence of the recovery of the O-protomer following a uv bleach for n, the number of attached water molecules.

IIB. Clarify temperature-dependent H-bonding interaction between cations in carboxyl-functionalized ionic liquids (ILs)

We will continue our ongoing program to establish the local, molecular-level interactions that are responsible for the macroscopic behaviors of functionalized ILs. Our current focus in on the "double H-bond" motif between carboxyl functionalized cations depicted in Fig. 3a. These cations are synthesized by IL specialist, Prof. Ralf Ludwig, at the University of Rostock. Preliminary results demonstrate that the low temperature IR spectra of the bulk IL (Fig. 3b) are already present in the surprisingly small cluster consisting of two cations and one NFt_2 anion. Our next measurements will establish the alkyl chain length dependence of the vibrational signatures and then monitor the temperature dependence of the cluster spectra using an IR-UV double resonance scheme.

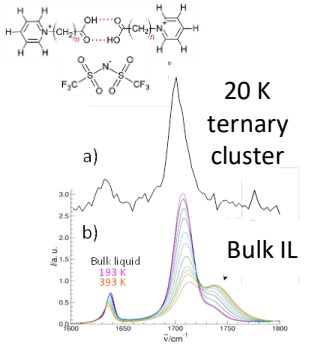

Fig. 3. Structure shows the carboxyl functionalize cationic IL, which exhibits the temperature dependent vibrational spectra shown in b). Trace a) presents the spectrum of the cold cluster consisting of only cations and one anion.

Papers in the past two years under this grant

1. "Coupling of torsion and OH-stretching in tert-butyl hydroperoxide. I. The cold and warm first OH-stretching overtone spectrum," Anne S. Hansen, Rachel M. Huchmala, Emil Vogt, Mark A. Boyer, Trisha

Bhagde, Michael F. Fansco, Casper V. Jensen, Alexander Kjaersgaard, Henrik G Kjaergaard, Anne B. McCoy and Marsha I. Lester, J. Chem. Phys., Vol. 154, 164306 (2021). DOI link: https://doi.org/10.1063/5.0048020.

2. "Coupling of torsion and OH-stretching in tert-butyl hydroperoxide. II. The OH-stretching fundamental and overtone spectra," Emil Vogt, Rachel M. Huchmala, Casper V. Jensen, Mark A. Boyer, Anne S. Hansen, Alexander Kjaersgaard, Marsha I. Lester, Anne B. McCoy and Henrik G Kjaergaard, J. Chem. Phys., Vol. 154, 164307 (2021). DOI link: https://doi.org/10.1063/5.0048022.

3. "Applications of Lasers in Mass Spectrometry," Timothy L. Guasco and Mark A. Johnson in Emerging Trends in Chemical Applications of Lasers, M. R. Berman, L. Young , and H.-Dai, eds. (2021).

4. "Infrared spectroscopic signature of a hydroperoxyalkyl radical (•QOOH)," Anne A. Hansen, Trisha Bhagde, Yujie Qian, Alyssa Cavazos, Rachael M. Huchmala, Mark A. Boyer, Coire F. Gavin-Haner, Stephen J. Klippenstein, Anne B. McCoy and Marsha I. Lester, J. Chem. Phys., Vol. 156, 014301 (2022). DOI link: https://doi.org/10.1063/5.0076505

5. Rachel M. Huchmala and Anne B. McCoy, "Exploring the Origins of Spectral Signatures of Strong Hydrogen Bonding in Protonated Water Clusters, J. Physical Chemistry A, Vol. 126, pp. 1360-1368 (2022). DOI link: https://doi.org/10.1021/acs.jpca.1c10036.

6. "Vibrational Signatures of HNO_3 Acidity When Complexed with Microhydrated Alkali Metal Ions, $M^+ \cdot (HNO_3)(H_2O)_{n=5}$ (M = Li, K, Na, Rb, Cs), at 20 K," Sayoni Mitra, Thien Khuu, Tae Hoon Choi, Rachel M Huchmala, Kenneth D Jordan, Anne B McCoy, Mark A Johnson, J. Physical Chemistry A, Vol. 126, pp. 1640-1647 (2022). DOI link : https://doi.org/10.1021/acs.jpca.1c10352

7. "Water Network Shape-Dependence of Local Interactions with the Microhydrated $-NO_2-$ and $-CO_2-$ Anionic Head Groups by Cold Ion Vibrational Spectroscopy," Sayoni Mitra, Joanna K Denton, Patrick J Kelleher, Mark A Johnson, Timothy L Guasco, Tae Hoon Choi, Kenneth D Jordan, J. Phys. Chem. A, Vol. 126, pp. 2471-2479 (2022). DOI link: https://doi.org/10.1021/acs.jpca.2c00721

8. "Character of the OH Bend–Stretch Combination Band in the Vibrational Spectra of the "Magic" Number $H_3O^+(H_2O)_{20}$ and $D_3O^+(D_2O)_{20}$ Cluster Ions," Nan Yang, Rachel M Huchmala, Anne B McCoy, Mark A Johnson, J. Phys. Chem. Letters, Vol. 13, pp. 8116-8121 (2022). DOI link: https://doi.org/10.1021/acs.jpclett.2c02318

9. "Microhydration of the metastable N-protomer of 4-aminobenzoic acid by condensation at 80 K: H/D exchange without conversion to the more stable O-protomer," Thien Khuu, Santino J Stropoli, Kim Greis, Nan Yang, Mark A Johnson, J. Chem. Phys., Vol. 157, pp. 131102 (2022). DOI link: https://doi.org/10.1063/5.0119027

10. "Observation of Slow Eigen-Zundel Interconversion in $H^+(H_2O)_6$ Clusters upon Isomer-Selective Vibrational Excitation and Buffer Gas Cooling in a Cryogenic Ion Trap," Thien Khuu, Abhijit Rana, Sean C. Edington, Nan Yang, Anne B. McCoy, Mark A. Johnson, J. Am. Soc. Mass Spectrom. Vol. 34, 4, pp. 737-744 (2023) **DOI:** 10.1021/jasms.3c00007

11. "High-resolution vibrational predissociation spectroscopy of $I^- H_2O$ by single-mode CW infrared excitation in a 3D cryogenic ion trap," Payten Harville, Sean Edington, Olivia C. Moss, Meng Huang, Anne B. McCoy, Mark A. Johnson, Molecular Physics Issue Dedicated to Prof. Dr. Dieter Gerlich, Vol. NA, 14, pp. NA. DOI Link: 10.1080/00268976.2023.2174784

12. "Two-Dimensional Adiabatic Model for Calculating Progressions Resulting from Stretch–Rock Coupling in Vibrational Spectra of Anion–Water Complexes," Elva V. Henderson and Kenneth D. Jordan, J. Phys. Chem. Lett., Vol. 12, 27, pp 6326–6329 (2021). DOI link :10.1021/acs.jpca.2c00721

13. "Isotope Effects in the Zundel–Eigen Isomerization of $H^+(H_2O)_6$," Jacob M. Finney, Tae Hoon Choi, Rahcel M. Huchmala, Joseph P. Heindel, Sotiris S. Xantheas, Kenneth D. Jordan and Anne B. McCoy, vol. 14, 20, 4666–4672 DOI Link: https://doi.org/10.1021/acs.jpclett.3c00952

14. "Exploring the Origins of the Intensity of the OH Stretch-HOH Bend Combination Band in Water," Rachel M. Huchmala and Anne B. McCoy, J. Phys. Chem. A, Vol. 127, 32, 6711-6721 DOI: 10.1021/acs.jpca.3c02980

Femtosecond X-ray Probes of Coherence in Ultrafast Photoinduced Electron and Proton Transfers

DE-SC0023249 previously DE-SC0019277

Munira Khalil[1,*], Elisa Biasin[2], Niranjan Govind[2], Robert W. Schoenlein[3]
[1]Department of Chemistry, University of Washington, Seattle, WA, 98195
[2]Physical and Computational Sciences Directorate, Pacific Northwest National Laboratory, Richland, WA 99352
[3]Linac Coherent Light Source, SLAC National Accelerator Laboratory, Menlo Park, CA 94025
[*]mkhalil@uw.edu

Project Scope

The development of ultrafast X-ray free electron laser (XFEL) sources like the Linac Coherent Light Source (LCLS), have demonstrated the ability to probe electron density with atom-specificity in solution at high spatial and temporal resolution. These advances in ultrafast X-ray methods open the possibility of connecting coherent beating observed in ultrafast optical and multidimensional measurements with atomic and electronic motion with element and orbital specificity. The central goal of this proposal is to develop and demonstrate advanced X-ray probes of coherent vibronic and electronic motion during electron and proton transfers with atomic resolution to directly visualize and quantify how coherent solute-solvent motions and the charge flow between electron/proton donor-acceptor sites control intramolecular electron and proton motion on the 0.3 – 500 femtosecond (fs) time scale. In pursuit of this goal, we have identified three thrusts to guide our research program.

1. Identify (the effects of) coherent solute-solvent interactions that couple short lived charge transfer states using ultrafast X-ray solution scattering and advanced non-equilibrium molecular dynamics (MD) simulations.
2. Reveal an atomic level description of coherent vibronic motion/coupling between donor and acceptor sites in ultrafast photoinduced electron and proton transfers with advanced X-ray spectroscopies and simulations of X-ray signals.
3. Understand the role of heteroatomic valence charge correlation, charge migration and electronic motion in intramolecular H-bonded complexes with advanced nonlinear X-ray spectroscopic methods.

This proposal brings together an experienced team of experimentalists (Khalil, Biasin, and Schoenlein) and theorist (Govind) to perform and simulate fs X-ray experiments.

Recent Progress

Developing an atomic description of coherent solvent motion in ultrafast electron transfer processes. The interaction of a solute with its solvent environment plays an essential role in determining the outcome of an electron transfer process in solution. While the importance of specific solute-solvent interactions such as hydrogen bonds is now increasingly recognized, the lack of structural probes at an atomic level has so far impeded their direct investigation. Recently, the advent of free electron lasers has made it possible to probe solute-solvent interactions on the relevant sub-Å length and sub-ps time scales. In our previous work,[1] we established that

femtosecond x-ray solution scattering can be employed to monitor coherent translational motions of solvent molecules in the first solvation shell around a solute molecule upon its photoexcitation. We now leverage this insight to study the solvent shell dynamics in a series of different solvents, which interact with the solute trans-$[(NC)_5Fe^{III}(\mu\text{-}CN)Ru^{II}(pyridine)_4(\mu\text{-}NC)Fe^{III}(CN)_5]^{4-}$ (FeRuFe) to different degrees. Upon photoexcitation of FeRuFe, an electron transfers from the Ru to the Fe, and electron density is shifted to the cyano ligands of the reduced Fe, which results in a strengthening of hydrogen bonds. Based on our previous studies, we then expect a solvent shell contraction for hydrogen bonding solvents. In a recent LCLS beamtime, we tested this hypothesis by photoexciting FeRuFe in solution while probing the systems structural dynamics using x-ray scattering, and its electronic dynamics using x-ray emission spectroscopy. We used the solvents water, methanol, and acetonitrile, which have a decreasing tendency to form hydrogen bonds in this order as measured by their Gutmann acceptor numbers. As shown in Figure 1, we observe that stronger hydrogen-bonding solvents exhibit a shorter lifetime of the contracted solvent shell, in line with their shorter-lived excited states. We are currently working to quantify coherent solvent motion in this data, and to separate dipolar and hydrogen bonding interactions. We conducted molecular dynamics simulations of FeRuFe in water which accurately reproduce the observed scattering signals, demonstrating that Ru-O and Fe-O atomic pairs are the primary contributors to our scattering signal. Simulations in methanol and acetonitrile are currently underway and will help with the identification of solvent coherences.

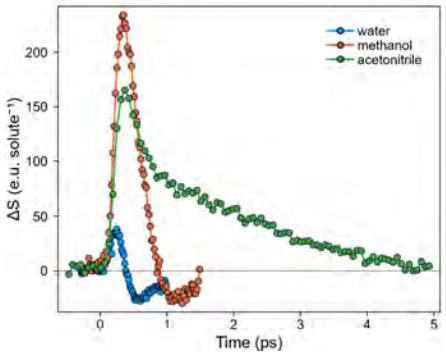

Figure 1. Femtosecond x-ray solution scattering probed at 0.3 $Å^{-1}$, monitoring dynamics of the first solvation shell upon photoexcitation of FeRuFe. The initial positive amplitude represents a contraction of the solvation shell, which subsequently re-expands on a timescale that depends on the solvent.

Development of QM-derived accurate excited state force fields. The FeRuFe molecule described above represents a prototypical system for studying long-range electron-transfer reactions and understanding the role played by specific solute–solvent interactions in modulating the excited state dynamics. To tackle this problem, while achieving a statistically meaningful description of the solvent and of its relaxation, one needs a computational approach capable of handling large polynuclear transition metal complexes, both in their ground and excited states, as well as the ability to follow their dynamics in several environments up to nanoseconds. In collaboration with M. Pastore (Université de Lorraine, France) and G.Prampolini (Istituto di Chimica dei Composti OrganoMetallici, Italy), we have developed a mixed quantum classical approach, which combines large-scale molecular dynamics (MD) simulations, based on an accurate quantum mechanically derived force field (QMD-FF) and self-consistent QMD polarized point charges to describe FeRuFe in different solvent (water, acetonitrile, and methanol). We demonstrated the reliability of the QMD-FF/MD approach in sampling the solute conformational space and capturing the local solute-solvent interactions by comparing the results with higher-level QM-MM/MD reference data. In water, solvent molecules are much more closely bound and structured around the cyano ligands, whereas a more uniform density is settled around the aromatic substituents. Conversely, the less polar and aprotic solvent (MeCN) shows less bounded solvent molecules around the cyano groups and an increased density in the region surrounding the pyridine ligands. MeOH solvation structure appears to be an intermediate case, where solvent molecules

tend to settle at larger distances and are more loosely bound with respect to water, as indicated by the wider density region. The IR spectra calculated along the classical MD trajectories in different solvents correctly predict the red-shift of the CN stretching band in the aprotic medium (acetonitrile) and the subtle differences measured in water and methanol, respectively. By explicitly including the solvent molecules around the cyanide ligands and calculating the thermal averaged UV-vis absorption spectra using TDDFT/TDA calculations, the experimental solvatochromic shift is quantitatively reproduced going from water to methanol, while it is overestimated for acetonitrile. This discrepancy can likely be traced back to the lack of important dispersion interactions between the solvent cyano groups and the pyridine substituents in our microsolvation model. The results have been submitted to the *Journal of Chemical Theory and Computation* and are under review. The proposed protocol will be applied to study excited state non-equilibrium solvation dynamics of FeRuFe and this will allow us to interpret the ultrafast scattering data that we have collected for the complex.

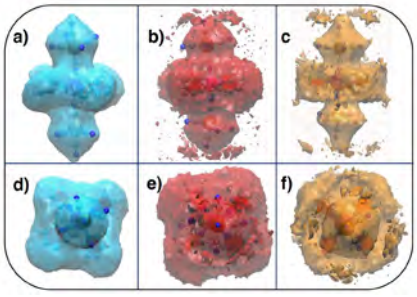

Figure 2. The spatial density functions (SDFs) of solute solvent interactions in FeRuFe on the electronic ground state are shown in the figure for the three different solvents, water (blue: a, d), methanol (red: b, e), and acetonitrile (orange: c, f), respectively.

Measuring time-dependent electronic delocalization on short lived charge transfer states. As mentioned in previous sections, the FeRuFe molecule acts as an excellent model system for investigating electronic delocalization during electron transfer processes. Previous work has shown that the binding of the Ru center ($[L_4Ru^{II}\{NC\text{-}Fe^{III}(CN)_5\}_2]^{4-}$), where L can be either pyridine or 4-methoxypyridine, controls the extent of electron delocalization in the electronic ground state. The synthetic modulation provides an additional parameter to tune the excited state dynamics, a concept that holds potential significance in applications such as molecular wires. To probe the excited state dynamics, we employed X-ray absorption near-edge structure (XANES) spectroscopy. The time resolved XANES experiments were conducted at the Linac Coherent Light Source (LCLS) at the Stanford Linear Accelerator (SLAC) National Laboratory in the X-ray Pump Probe (XPP) Hutch. A 3.5 μJ, 40 fs fullwidth at half-maximum (FWHM), 800 nm laser pulse with a 100−120 μm $1/e^2$ diameter focus, excites FeRuFe to the MMCT state. The sample concentration was 40 mM for FeRuFe-MeOpy and 34.4 mM for FeRuFe-py in methanol. Subsequent difference XANES spectra at the Fe K-edge for both derivatives are shown in Figure 3, highlighting three prominent features: 1s → t_{2g} (A), 1s → e_g (B), and 1s → ligand π* (C), each shifted from their respective ground state positions, demarcated by horizontal lines. The data quality of FeRuFe-MeOpy (right panel) was somewhat constrained due to time limitations during data acquisition. Consequently, we are in the process of requesting additional beamtime. From the FeRuFe-py data, kinetic trace fittings at different transition energies identified two distinct components of 270 fs and 2.0 ps. The 270 fs component corresponds to back electron transfer (BET), while the 2.0 ps component is attributed to vibrational cooling. To quantify the electron delocalization in a more quantitative manner on the ground and excited electronic states, we are in the process of running Quantum Mechanics/Molecular Mechanics (QM/MM) calculations on FeRuFe molecules.

QM/MM Simulations: The pyridine FeRuFe system was solvated in a 65x65x65 $Angstrom^3$ box with 3821 methanol molecules. The FeRuFe complex was represented quantum mechanically (QM) at the hybrid density functional level of theory (DFT). The PBE0 hybrid

density functional along with the 6-311G** basis set for the organic ligands and the Stuttgart basis set with effective core potentials for the metal atoms were utilized, while methanol solvent is treated using classical force fields (MM). All QM/MM simulations were performed with the NWChem computational chemistry code. Since the FeRuFe system has a -4 charge, four Na^+ cations were added to the box to balance the charge. The GAFF2 non-bonding and bonding forcefield parameters were assigned to the methanol solvent atoms, bonds, bond angles, and dihedral angles. PARM99 atom charges from the AMBER parameter database were assigned to the methanol atoms. GAFF2 non-bonding Lennard-Jones (LJ) parameters were assigned to the ligands in the pyridine FeRuFe complex, and the Fe LJ parameters from CLAYFF were used for the Fe and Ru (since the solvent interacts only with the ligands, the accurate LJ parameterization of the metal atoms is not crucial). The solvent was NVT equilibrated with the pyridine FeRuFe geometry held fixed for 500 ps at 298.15 K with a time step of 2 ps (SHAKE was used to constrain the hydrogen-bearing bonds). After the initial equilibrations, the solvated FeRuFe geometry was allowed to relax for 500 fs with NVT dynamics, at a temperature of 298.15 K, and a reduced time step of 0.25 fs. Following this initial relaxation of the FeRuFe complex and solvent system, the solvated FeRuFe and methanol system is continuing to be evolved with NVT dynamics to gather statistics and snapshot structures for further structural (e.g., RDF) and spectroscopic analyses. We have up to 10 ps of trajectory thus far. We are setting up the planned trajectory for the 4-methoxypyridine FeRuFe system, which will follow an almost identical procedure as that of the pyridine FeRuFe system above. These will be followed by excited state simulations at the time-dependent density functional theory (TDDFT) to study electron delocalization along the lines of our earlier study on the FeRu mixed-valence system in water. We will compute the ground and excited-state XANES at the Fe K and Ru L3 edges and monitor the hole densities as the system evolves in the metal-to-metal charge transfer (MMCT) excited state.

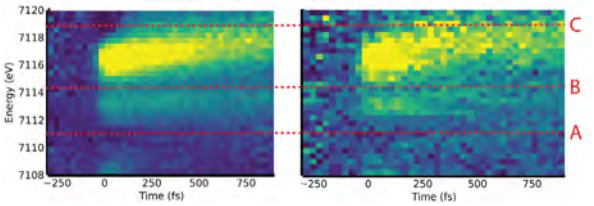

Figure 3. Transient XANES on FeRuFe-py (left) and FeRuFe-MeOpy (right) displaying the blue shifts in peaks B and C on the MMCT excited state.

Tracking electron delocalization and non-equilibrium vibrational relaxation on mixed valence excited states. The mixed-valence chemistry of multi-nuclear transition metal complexes has been a crucial tool for understanding electron transfer processes in catalysis, in nature (such as in metalloenzymes), and in next generation functional materials. Ground state mixed valency has been widely studied since the introduction of the Creutz-Taube ion in the late 1960s, but less studied are systems in which mixed valency only arises in their excited electronic states which could exhibit unique excited state reactivity. We have recently investigated the excited state dynamics of a bimetallic complex, $[Ru^{II}(tpy)(bpy)(\mu\text{-}CN)Ru^{II}(bpy)_2(NCCH_3)]^{3+}$ with time-resolved infrared and X-ray spectroscopies in order to track electron delocalization and form a quantitative description of excited state mixed valency from the perspectives of both the CN bridge and the Ru metal centers. The primary results from these studies are summarized in Figure 4. A metal-to-ligand-charge-transfer transition is excited by 400 nm laser light and subsequent delocalization of the hole across both metal centers and the CN bridge occurs. The transient infrared measurement was analyzed by global analysis (right panel) which identified three main components which decay on 300 fs, 6 ps, and 700 ps timescales. All of these components exhibit excited state absorption features that are red shifted with respect to the ground state CN mode which corresponds to additional electron density present in CN π^* orbitals compared to the ground

state, even after removal of one of the metal centered t_{2g} electrons by the laser excitation. The peak of the excited state absorption feature blue shifts from 2056 cm^{-1} to 2073 cm^{-1} on a 6 ps timescale corresponding to vibrational relaxation of the CN bridging mode in the excited mixed valence state. Finally, the third component corresponding to the lowest triplet excited state in its lowest vibrational state decays back to the ground state on a 700 ps timescale. Turning now to the transient X-ray measurements, which were done at the Swiss X-ray Free Electron laser, we measured the 2p3d resonant inelastic X-ray scattering (RIXS) spectrum of the Ru-Ru dimer in its ground and mixed valence excited state. The full RIXS difference map (laser pumped - ground state) is shown in the left panel of Figure 4, where the appearance of a positive feature at 2838 eV, 280 eV corresponds to the formation of a hole in the Ru t_{2g} orbitals. The negative feature at 2841 eV, 282 eV and the positive feature at 2842 eV, 284 eV correspond to the e_g orbitals shifting to higher energies. Cuts of this difference map, and the ground state map (not pictured) were taken along the diagonal corresponding to constant emission energy which resulted in high energy resolution fluorescence detected X-ray absorption spectra. By fitting the ground state and the difference spectrum, the excited state spectrum was reconstructed and the energy separation between the t_{2g} and e_g peaks is measured to be 2.86 eV which is significantly reduced when compared to model Ru complexes with t_{2g} holes (~3.8 eV or higher). Based on previous X-ray work with a FeRu dimer,[1] this suggests a high degree of delocalization between the Ru centers. Additionally, the ratio between the A and B peak is expected to be 1:8 if no delocalization is present due to the number of possible transitions, but a ratio of ~1:12 is found. This suggests that there is a significant contribution from the CN ligand in the Ru t_{2g} orbitals which reduces the intensity of the feature and is another indication of delocalization. A manuscript of the above work is currently being prepared with plans to submit for publication by the end of this calendar year. Earlier this year we published work in *Inorganic Chemistry* where solution phase Ru model complexes were measured with 2p3d RIXS and the spectral information contained within the resulting RIXS maps were described in detail.[14] This work was vital in the development of this new X-ray spectroscopy and to facilitate the understanding of more complex chemical systems such as the transient 2p3d RIXS of the Ru-Ru dimer.

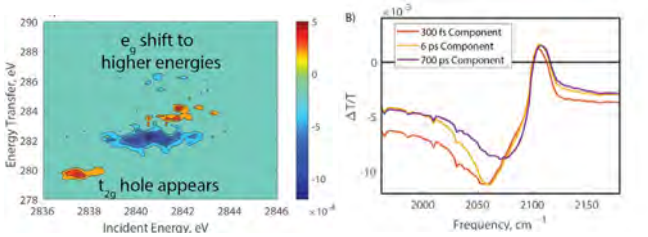

Figure 4. Transient RIXS map (left panel) and transient IR spectral analysis (right panel) characterizing the mixed valence excited state of the Ru-Ru dimer.

Understanding RIXS signatures of intramolecular H-bonding on ground and excited states. Excited-state intramolecular proton transfer (ESIPT) is a fundamental chemical process with several applications in optoelectronics and biological systems. Ultrafast ESIPT involves coupled electronic and atomic motions and has been primarily studied using femtosecond optical spectroscopy. 10-hydroxybenzo[h]quinoline (HBQ) is a molecular system containing an intramolecular hydrogen bond. ESIPT in HBQ takes place within 13 fs as revealed by previous optical spectroscopic studies. The photophysics of HBQ can be tuned synthetically or by exchanging the solvent, making it an ideal model system to study ESIPT processes and the mechanisms influencing them. X-ray spectroscopy is particularly useful for understanding the electronic structure because its element-specificity enables direct, individual probes of the proton-donating and -accepting atoms. We have previously reported a computational study to resolve the

ESIPT in HBQ utilizing TDDFT combined with ab-initio molecular dynamics (AIMD) and time-resolved X-ray absorption spectroscopy (XAS) computations to track the ultrafast excited-state dynamics. Our results revealed clear X-ray spectral signatures of coupled electronic and atomic motions during and following ESIPT at the oxygen and nitrogen K-edge.[5] We are extending this study and computing the resonant inelastic X-ray scattering (RIXS) signatures on the ground and excited states. In the RIXS processes, an incoming X-ray photon ($\hbar\omega_{in}$) leads to excitation into a core-excited state (CES). Relaxation from the CES leads to emission of a photon with an energy of $\hbar\omega_{out}$. The energy transfer ($E_{trans} = \hbar\omega_{out} - \hbar\omega_{in}$) contains information about the valence electronic structure. By measuring the emitted X-rays RIXS enables the observation of optically dark states that could otherwise not be seen. Building on the framework of the previous computational study of the dynamics of HBQ we calculated XAS and UV-Vis spectra of HBQ in the enol and keto ground state. Using the Kramers-Heisenberg equation we calculated the RIXS spectra for both tautomers at the oxygen and nitrogen K-edge. The resulting spectra are presented in Figure 5. To be able to track the excited state dynamics and changes in the potential energy landscape throughout the ESIPT process, we have performed excited state calculations for several geometries along the excited state trajectory. In the next step we will simulate the RIXS spectra for these geometries. By eventually comparing the calculated RIXS spectra to experimental time-resolved RIXS data, we will be able to benchmark the theory approach and gain detailed insights into the potential energy surface along the reaction trajectory.

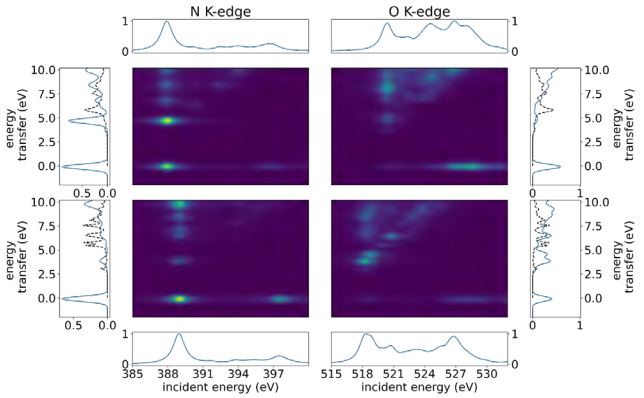

Figure 5. Calculated RIXS maps of HBQ in its enol (top) and keto (bottom) form at the nitrogen (left) and oxygen (right) K-edge.

Nuclear Quantum Effects in Proton Transfer Reactions. Excited-state intramolecular proton transfer (ESIPT) is a key component of natural and artificial processes. Ultrafast ESIPT processes occurring on the sub-100 fs time scale often involve coupled electronic and atomic motions as observed through ultrafast optical transient absorption and multidimensional spectroscopy. We have recently computationally investigated the excited-state dynamics and corresponding spectral signatures of the ultrafast ESIPT process in 10-hydroxybenzo[h]quinoline (HBQ), an intramolecularly H-bonded compound, with multi-edge transient X-ray absorption spectroscopy. HBQ, exhibits strong intramolecular hydrogen bonding and undergoes tautomerization following near-UV excitation and has been widely studied by experiments and theory. In the electronic ground state, HBQ is energetically stable only in the enol form when dissolved in nonpolar solvents. Upon photoexcitation ($S_0 \rightarrow S_1$) in the near UV, the molecule is excited to an enol* (E*) state and the proton moves from the oxygen to the nitrogen atom to form the keto* (K*) state. The timescale of the barrierless ESIPT on the S1 state in HBQ has been experimentally determined to be 13±5 fs. Our excited-state molecular dynamics simulations at the TDDFT theory level on the S1 state, which is dominated by the HOMO-to-LUMO excitation, yielded a proton transfer of 14±6 fs, consistent experimental measurements. Our results revealed clear X-ray spectral fingerprints of coherent atomic motions coupled to local electronic changes around the proton donor and acceptor

atoms, shedding light on the non-equilibrium vibronic dynamics. These excited-state dynamics simulations did not include nuclear quantum effects (NQEs) for the proton transfer since this involved a barrierless process. However, in order to treat HBQ derivatives containing NO_2 electron acceptor groups, which allow for a systematic variation of the barrier heights between the enol and keto tautomers in the ground and electronic excited states, NQEs have to be included in the dynamics and barrier computations. To accomplish this, we have combined ab initio calculations, within the DFT and TDDFT framework, with semiclassical ring-polymer approaches. We have implemented this protocol by interfacing the NWChem computational chemistry program with the i-PI simulation software, which includes implementations of ring-polymer algorithms for dynamics and barrier computations. We are currently performing extensive tests using well-characterized molecular systems like malonaldehyde, aminopropenal, and 6-hydroxy-2-formylfulvene (HFF). These simulations will be further extended to the QM/MM environment to treat proton transfer in explicit solvent environments.

X-ray pump X-ray probe spectroscopy in solution reveals core-valence interactions. The further development of XFELs is enabling new coherent nonlinear experiments in the condensed phase utilizing pairs of X-ray pump and X-ray probe (XPXP) pulses. A first step towards nonlinear X-ray experiments in solution, is the demonstration of XPXP core level transient absorption spectroscopy. We recently performed the first core-level transient absorption XPXP experiment at the Fe K-edge, guided by prior computational study.[15] Two chief challenges in XPXP experiments are resolving the ultrashort core-hole lifetimes and differentiating a large ensemble of novel electronic states generated by Auger-Meitner cascades. In an initial study,[4] we first calculated XPXP signals using an electron cascade Monte-Carlo simulation to predict electronic states for TDDFT based Fe K-edge XANES of a solvated transition metal complex, $K_4Fe^{II}(CN)_6$. Our study showed that the novel electronic states prepared by a fs X-ray pulse provide a unique measurement of key chemical signatures, such as the effect of 3p-3d electron interactions on the ligand-field energy splitting (Fig. 6a). The 1s→3p absorption transition serves as reliable and accessible reporter on those interactions due to its spectral isolation and strong dipole oscillator strength. We recently performed a two-color X-ray pump X-ray probe experiment, at the CXI instrument at LCLS. As calculated, the experiment directly probes core-valence interactions in a model metal-ligand charge transfer system $[Fe^{II}(CN)_6^{4-}]$ The first X-ray pulse generates a 1s hole in the metal center, which is subsequently filled by the ensuing Auger-Meitner cascade, resulting in a distribution of holes in both the 3p and valence shells. Informed by Monte-Carlo simulations of the cascade and TDDFT calculations of the predicted ensemble of electronic states, the X-ray probe pulse is tuned resonantly with the 1s-3p (*K*β) transition. The 3p energy shifts in response to the interactions between 3p and valence orbitals: loss of electron density in either the 3p or valence orbitals increase the *K*β energy. Specifically, our

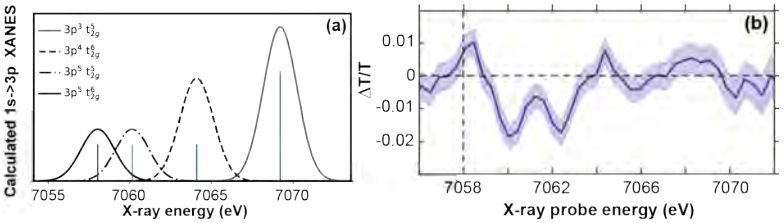

Figure 6. Calculated shifts in 1*s*→3*p* transition energy and oscillator strengths as function of holes in the 3*p* and 3*d* states following a removal of a 1*s* Fe core hole and subsequent electron cascade dynamics in $K_4Fe^{II}(CN)_6$. (b) Experimental fs XPXP difference signal for the same complex collected when the X-ray pump and probe pulses are overlapped in time. The vertical dashed line represents the atomic Kβ line. Negatively going peaks centered at 7.060 and 7.063 keV correspond to the additional 1*s*→3*p* absorption due to 3*p* holes resulting from the Auger-Meitner cascade.

calculations (Fig. 6a) predict that each successive hole in the valence results in the *K*β blue shifting by ~2.1 eV relative to the atomic *K*β transition. A larger shift (~6 eV) results from additional holes in the 3*p*. These shifts report directly on the strength of interaction between the valence electrons and the high lying core electrons. We directly measure those shifts by spectrally monitoring the drop in transmission of the probe as a function of pump fluence. Fig. 6(b) displays XPXP data collected when the X-ray pump and X-ray probe pulses are overlapped in time showing multiple peaks to the blue of the *K*β transition (vertical line), in agreement with the predictions of additional hole formation in the t_{2g}orbitals.

Future Plans

Calculations of non-linear X-ray signals – attosecond X-ray pump X-ray probe experiments. The development of LCLS-II makes the generation of high repetition rate multi-color attosecond X-ray pulses on the sample feasible. Our ultimate goal is to perform multi-pulse, multi-color attosecond X-ray pump X-ray probe experiments in solution. The goals of this experiment will be to probe electronic correlations and coherent charge migration in intramolecular H-bonded organic and transition metal complexes. As a first step, we will calculate single core hole XANES (SCH-XANES) signals on HBQ in solution to map the valence charge migration between the donor acceptor sites. We will also explore SCH-XANES spectroscopy to investigate valence charge and magnetic correlations in a model 3*d* transition-metal mixed-valence heterodimer, $Mn^{II}Fe^{III}$, dissolved in CH_3CN. Our previous calculations on SCH XES (metal VtC emission in the presence of a ligand core hole) showed rich spectral signatures that directly reflect the chemical bonding between the metal center and ligand. In our proposed SCH-XANES investigations, we expect the Fe L-edge XANES spectrum to undergo dramatic changes at A, B and C, features following the creation of a Mn 2*p* core hole and charge migration across the hydrogen bonds of the mixed valence dimer. The change in the Fe L-edge XANES will report on 3*d*-3*d* correlations between the two metal centers.

Ru 2*p*4*d* RIXS probes of coherent electron transfer dynamics. In a recent experimental work on model Ru(II) and Ru(III) complexes in solution, we demonstrated Ru 2p4d resonant inelastic X-ray scattering (RIXS) to probe the valence excitations, and our work revealed novel insights into the chemical bonding. With the development of fs tender X-ray beamlines at XFELs around the world, we will perform fs 2p4d RIXS on the Ru center in various synthetic analogues of the molecule FeRuFe (described earlier). The goal of these experiments will be to spatially resolve coherent signals during ultrafast long range electron transfer.

Experimental femtosecond RIXS maps of excited state proton transfer processes. Following the calculations described previously, we have applied for beamtime at LCLS-II, to perform O and N K-edge transient RIXS experiments on a model intramolecular hydrogen-bonded molecule and tis analogues. The goal of these experiments will be to measure coupled electronic and atomic motions during the ultrafast rearrangement of an intramolecular hydrogen bond.

Peer-Reviewed Publications Resulting from this Project (2021-2023)

1. Biasin, E.; Fox, Z. W.; Andersen, A.; Ledbetter, K.; Kjær, K. S.; Alonso-Mori, R.; Carlstad, J. M.; Chollet, M.; Gaynor, J. D.; Glownia, J. M.; Hong, K.; Kroll, T.; Lee, J. H.; Liekhus-

Schmaltz, C.; Reinhard, M.; Sokaras, D.; Zhang, Y.; Doumy, G.; March, A. M.; Southworth, S. H.; Mukamel, S.; Gaffney, K. J.; Schoenlein, R. W.; Govind, N.; Cordones, A. A.; Khalil, M. Direct observation of coherent femtosecond solvent reorganization coupled to intramolecular electron transfer. *Nat. Chem.* **2021,** *13* (4), 343-349 DOI: 10.1038/s41557-020-00629-3.

2. Biasin, E.; Nascimento, D. R.; Poulter, B. I.; Abraham, B.; Kunnus, K.; Garcia-Esparza, A. T.; Nowak, S. H.; Kroll, T.; Schoenlein, R. W.; Alonso-Mori, R.; Khalil, M.; Govind, N.; Sokaras, D. Revealing the bonding of solvated Ru complexes with valence-to-core resonant inelastic X-ray scattering. *Chem. Sci.* **2021,** *12* (10), 3713-3725 DOI: 10.1039/D0SC06227H.
3. Gu, B.; Cavaletto, S. M.; Nascimento, D. R.; Khalil, M.; Govind, N.; Mukamel, S. Manipulating valence and core electronic excitations of a transition-metal complex using UV/Vis and X-ray cavities. *Chem. Sci.* **2021,** *12* (23), 8088-8095 DOI: 10.1039/d1sc01774h.
4. Liekhus-Schmaltz, C. E.; Ho, P. J.; Weakly, R. B.; Aquila, A.; Schoenlein, R. W.; Khalil, M.; Govind, N. Ultrafast x-ray pump x-ray probe transient absorption spectroscopy: A computational study and proposed experiment probing core-valence electronic correlations in solvated complexes. *J. Chem. Phys.* **2021,** *154* (21), 214107 DOI: 10.1063/5.0047381.
5. Loe, C. M.; Liekhus-Schmaltz, C.; Govind, N.; Khalil, M. Spectral Signatures of Ultrafast Excited-State Intramolecular Proton Transfer from Computational Multi-edge Transient X-ray Absorption Spectroscopy. *J. Phys. Chem. Lett.* **2021**, 9840-9847 DOI: 10.1021/acs.jpclett.1c02483.
6. Nascimento, D. R.; Biasin, E.; Poulter, B. I.; Khalil, M.; Sokaras, D.; Govind, N. Resonant Inelastic X-ray Scattering Calculations of Transition Metal Complexes Within a Simplified Time-Dependent Density Functional Theory Framework. *J. Chem. Theory Comput.* **2021,** *17* (5), 3031-3038 DOI: 10.1021/acs.jctc.1c00144.
7. Tetef, S.; Govind, N.; Seidler, G. T. Unsupervised machine learning for unbiased chemical classification in X-ray absorption spectroscopy and X-ray emission spectroscopy. *Phys. Chem. Chem. Phys.* **2021,** *23* (41), 23586-23601 DOI: 10.1039/D1CP02903G.
8. Liekhus-Schmaltz, C.; Fox, Z. W.; Andersen, A.; Kjaer, K. S.; Alonso-Mori, R.; Biasin, E.; Carlstad, J.; Chollet, M.; Gaynor, J. D.; Glownia, J. M.; Hong, K.; Kroll, T.; Lee, J. H.; Poulter, B. I.; Reinhard, M.; Sokaras, D.; Zhang, Y.; Doumy, G.; March, A. M.; Southworth, S. H.; Mukamel, S.; Cordones, A. A.; Schoenlein, R. W.; Govind, N.; Khalil, M. Femtosecond X-ray Spectroscopy Directly Quantifies Transient Excited-State Mixed Valency. *J. Phys. Chem. Lett.* **2022**, 378-386 DOI: 10.1021/acs.jpclett.1c03613.
9. Driscoll, D. M.; Shiery, R. C.; D'Annunzio, N.; Boglaienko, D.; Balasubramanian, M.; Levitskaia, T. G.; Pearce, C. I.; Govind, N.; Cantu, D. C.; Fulton, J. L. Water Defect Stabilizes the Bi3+ Lone-Pair Electronic State Leading to an Unusual Aqueous Hydration Structure. *Inorg. Chem.* **2022,** *61* (38), 14987-14996 DOI: 10.1021/acs.inorgchem.2c01693.
10. Ghosh, S.; Agarwal, H.; Galib, M.; Tran, B.; Balasubramanian, M.; Singh, N.; Fulton, J. L.; Govind, N. Near-Quantitative Predictions of the First-Shell Coordination Structure of Hydrated First-Row Transition Metal Ions Using K-Edge X-ray Absorption Near-Edge Spectroscopy. *J. Phys. Chem. Lett.* **2022,** *13* (27), 6323-6330 DOI: 10.1021/acs.jpclett.2c01532.
11. Tetef, S.; Kashyap, V.; Holden, W. M.; Velian, A.; Govind, N.; Seidler, G. T. Informed Chemical Classification of Organophosphorus Compounds via Unsupervised Machine Learning of X-ray Absorption Spectroscopy and X-ray Emission Spectroscopy. *J. Phys. Chem. A* **2022,** *126* (29), 4862-4872 DOI: 10.1021/acs.jpca.2c03635.

12. Nascimento, D. R.; Govind, N. Computational approaches for XANES, VtC-XES, and RIXS using linear-response time-dependent density functional theory based methods. *Phys. Chem. Chem. Phys.* **2022,** *24* (24), 14680-14691 DOI: 10.1039/D2CP01132H.
13. Dhakal, D.; Driscoll, D. M.; Govind, N.; Stack, A. G.; Rampal, N.; Schenter, G.; Mundy, C. J.; Fister, T. T.; Fulton, J. L.; Balasubramanian, M.; Seidler, G. T. The evolution of solvation symmetry and composition in Zn halide aqueous solutions from dilute to extreme concentrations. *Phys. Chem. Chem. Phys.* **2023,** *25* (34), 22650-22661 DOI: 10.1039/D3CP01559A.
14. Poulter, B. I.; Biasin, E.; Nowak, S. H.; Kroll, T.; Alonso-Mori, R.; Schoenlein, R. W.; Govind, N.; Sokaras, D.; Khalil, M. Uncovering the 3d and 4d Electronic Interactions in Solvated Ru Complexes with 2p3d Resonant Inelastic X-ray Scattering. *Inorg. Chem.* **2023,** *62* (25), 9904-9911 DOI: 10.1021/acs.inorgchem.3c00919.
15. Weakly, R. B.; Liekhus-Schmaltz, C. E.; Poulter, B. I.; Biasin, E.; Alonso-Mori, R.; Aquila, A.; Boutet, S.; Fuller, F. D.; Ho, P. J.; Kroll, T.; Loe, C. M.; Lutman, A.; Zhu, D.; Bergmann, U.; Schoenlein, R. W.; Govind, N.; Khalil, M. Revealing core-valence interactions in solution with femtosecond X-ray pump X-ray probe spectroscopy. *Nat. Commun.* **2023,** *14* (1), 3384 DOI: 10.1038/s41467-023-39165-2.

Measuring Vibronic Coupling and Ultrafast Charge Delocalization on Nanocrystal Surfaces Using Ligand-Specific Vibrational Probes

DE-SC0021232

Munira Khalil[1,*], Brandi Cossairt[1]
[1]Department of Chemistry, University of Washington, Seattle, WA, 98195
[*]mkhalil@uw.edu

Project Scope

The central goal of this proposal is to directly quantify how vibronic couplings between the excitonic states of nanocrystals (NCs) and their passivating ligands dictate charge delocalization and non-radiative relaxation on the ultrafast timescale as a function of ligand identity and nanocrystal size and structure. Several studies point to the importance of ligand NC interactions and their effects on the overall nanoparticle exciton dynamics. Despite the large experimental and theoretical effort in NC photophysics, it remains a challenge to quantitatively connect ultrafast spectroscopy of NCs to microscopic interfacial interactions, which is crucial for validating theoretical models of charge/electron transfer at the NC interface. This presents a significant knowledge gap for developing predictive design principles to harness molecular energy capture or electron transfer in NC-catalyst assemblies and is the motivation for the proposed work.

In the proposed work, Cossairt will develop a series of atomically precise CdSe NCs (nanoclusters and larger quantum dots) with functionalized carboxylate ligands and other vibrational tags. Ultrafast nonlinear vibrational spectroscopy by the Khalil group on these NCs with precisely placed IR-active tags will allow us to definitively correlate how modifications in surface chemistry determine the nature of ligand-exciton vibronic coupling and the subsequent charge delocalization timescales and pathways.

The collective synthetic and spectroscopic experiments will inform on how the magnitude of the vibronic coupling changes as a function of NC size and structure, surface dipole, ability of the ligand to accept the electron/hole, CdS shell thickness of CdSe/CdS heterostructures and distance from the NC surface. Using multidimensional electronic-vibrational spectroscopy to map vibronic couplings as a function of the excitonic states in the atomically precise ligand-NC platforms will allow us to develop and test models of interfacial charge transfer at the ligand-NC interface.

Recent Progress

Measuring ligand binding energies on the surfaces of InP MSCs. Capping ligands, such as long chain aliphatic carboxylates, are anchored to nanocrystal surfaces in multiple binding confirmations and facilitate charge stabilization for colloidal stability. In this work, we measured relative binding energies of multiple carboxylate ligand motifs of myristate functionalized InP magic-sized clusters (MSCs) to characterize the surface ligand structure. Through temperature-dependent Fourier transform infrared spectroscopy (FTIR) combined with a Markov chain Monte Carlo (MCMC) global fitting routine, we found that the energy difference between the monodentate and free ligand matches well with the carboxylate stretching frequency. This implies

that the ligand vibrational energy is integral is ligand dissociation, accounting for energy variances between bound and freed ligand states. We also found that coordination with one surface indium atom does not significantly decrease the binding energy compared to a carboxylate in the bidentate *syn-anti* geometry. Moreover, the MCMC global fit model provides empirical insights into the nuances of surface ligand binding, potentially guiding subsequent endeavors in nanocrystal surface modification for photocatalysis.

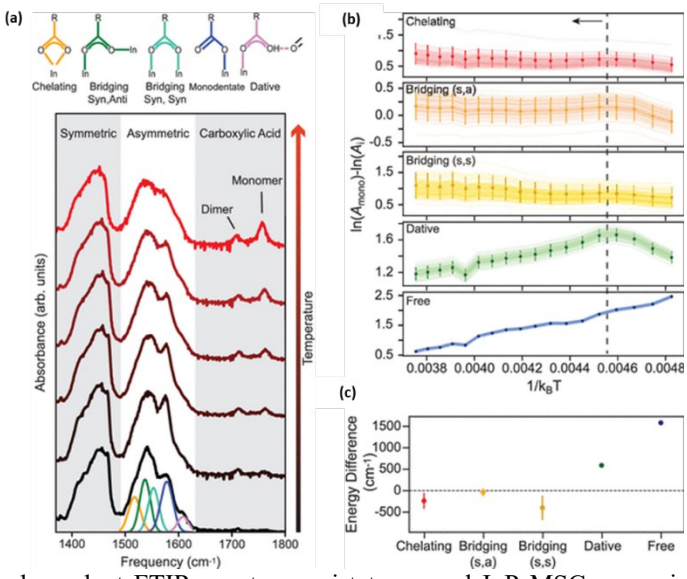

Figure 1. (a) Temperature dependent FTIR spectra myristate-capped InP MSCs spanning from 25°C (bottom)to 100°C (top). (b) Differences of the log of peak areas with respect to the monodentate binding motif .(c) Extracted slopes from linear regressions of the 45−110°C regime in (b).

Effect of a redox-mediating ligand shell on photocatalysis by CdS quantum dots. Having prepared a library of CdS nanocrystals with electron- and hole-delocalizing ligands, we hypothesized that we could increase the activity of quantum dot photocatalysts by directing the photoinduced charge transfer these redox-mediating ligands. To test this hypothesis, we studied CdS quantum dots with hole-mediating ferrocene (Fc) derivative ligands and performed a reaction where the slow step is hole transfer from the quantum dot to substrate. In our model reaction, a photoredox-generated α-amino radical is coupled to a vinyl sulfone to afford an allylic amine. Surprisingly, we found that a hole-shuttling Fc inhibits catalysis but confers much greater stability to the catalyst by preventing a build-up of destructive holes. We also found that dynamically bound Fc ligands can promote catalysis by surface exchange and creation of a more permeable ligand shell. Finally, we found that trapping the electron on a phenazine-1-carboxylic acid ligand dramatically increases the rate of reaction. These

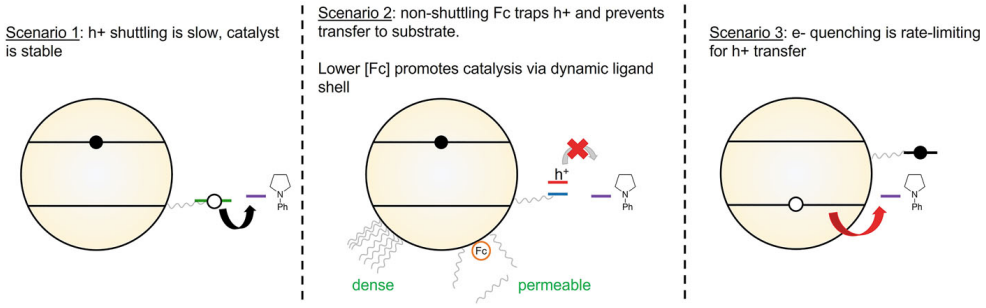

Figure 2. Diagram depicting different charge transfer pathways and effects on catalysis.

results have major implications for understanding the rate-limiting processes for charge transfer from quantum dots and the role of the ligand shell in modulating it.

Future Plans

Ultrafast IR spectroscopy on nanocrystals. We are actively working to baseline the relaxation dynamics of ligands anchored to the surface of oleate capped CdS nanocrystals with ultrafast IR spectroscopy, which monitors exciton dynamics via vibronic coupling between ligands and the nanocrystal surface. Small CdS NCs (~3 nm) exhibit broad symmetric (~1400-1475 cm^{-1}) and asymmetric (~1500-1600 cm^{-1}) carboxylate IR absorption bands. To test the hypothesis that vibronic coupling between ligands and nanocrystals is sensitive to specific ligand structure, we photoexcited the 1S exciton of CdS with 400 nm and directly probed the mid-IR symmetric and asymmetric carboxylate stretching frequencies. Qualitative analysis of the differential mid-IR spectra clearly indicates that multiple carboxylate motifs experience a change in extinction following generation of electron-hole pairs from the 1S exciton transition, leading to a broad photoinduced absorption signal that spans the symmetric and asymmetric bands at 100 fs. However, within 210 ± 60 fs vibrational relaxation occurs within the excited state manifold and the photoinduced absorption feature becomes localized to two narrow bands at ~1480 cm^{-1} and ~1540 cm^{-1} and persists beyond 2000 femtoseconds. This is a significant result, because amongst a manifold of different carboxylate binding motifs that exhibit an immediate vibrational response after exciton generation, specific motifs uniquely mediate thermalization of electronic charge carriers generated by photoexcitation of the 1S exciton resonance. Thus, ligand-nanocrystal vibronic coupling is sensitive to specific binding motifs that comprise the carboxylate symmetric and asymmetric stretches in CdS nanocrystals. Future directions are centered around understanding the dynamics of ligands with different magnitudes of vibronic coupling, specifically hole-mediating ligands like ferrocene.

Peer-Reviewed Publications Resulting from this Project (2021-2023)

1. Klein, M. D.; Bisted, C. H.; Dou, F. Y.; Sandwisch, J. W.; Cossairt, B. M.; Khalil, M. Measuring Relative Energies of Ligand Binding Conformations on Nanocluster Surfaces with Temperature-Dependent FTIR Spectroscopy. *J. of Phys. Chem. C* **2023**, *127* (34), 16970-16978. DOI: 10.1021/acs.jpcc.3c03951.

2. Dou, F. Y.; Harvey, S. M.; Mason, K. G.; Homer, M. K.; Gamelin, D. R.; Cossairt, B. M. Effect of a redox-mediating ligand shell on photocatalysis by CdS quantum dots. *J. Chem. Phys.* **2023**, *158* (18). DOI: 10.1063/5.0144896.

Title: Chemical Kinetics and Dynamics at Interfaces

Principal Investigators: Elisa Biasin, Patrick Z. El-Khoury, John L. Fulton, Bruce D. Kay, Greg A. Kimmel, Xue-Bin Wang

Project Scope

The experimental Chemical Kinetics and Dynamics at Interfaces program aims to provide a fundamental, molecular-level understanding of the condensed phase chemistry that underpins chemical structure, transport, and reactivity in condensed phases and at interfaces. Our program has three research subtasks that use distinct experimental approaches to explore interrelated scientific objectives that have resulted in 69 publications since 2021.[1-69]

Subtask 1: Fundamentals of Ion and Ion Cluster Solvation Structure, Dynamics, and Reactivity under Complex Aqueous Environments (Elisa Biasin, John Fulton, and Xue-Bin Wang, PIs).

The goal of this subtask is to understand the fundamental interactions, reactivity, and dynamics of ions and ionic systems in aqueous solutions under ambient and extreme conditions of concentration, pH, and temperature. Ion–water and cation–anion interactions underlie all aqueous chemistry and a multitude of energy, environmental, and biological processes. Many of these processes are specifically relevant to DOE objectives in areas such as mixed hazardous waste processing, power plant chemistry, geologic carbon dioxide sequestration, energy production, catalysis, and atmospheric science. Obtaining the relevant molecular-level energetics and structures of complex hydrated ions and their reactivity requires the development and use of sophisticated experimental techniques coupled to state-of-the-art computational studies. To achieve our vision, we employ two distinct yet synergistic experimental approaches: (1) magnetic-bottle and velocity-map imaging photoelectron spectroscopy and (2) development and use of advanced X-ray spectroscopy and scattering techniques. The first approach allows for the investigation of multiply charged anions and solvated complex anions at well-defined temperatures, and the second enables the investigation of solvation in bulk liquid environments and chemical dynamics in time-resolved fashion. All experiments require close coupling with theoretical methods such as molecular dynamics and electronic structure calculations to test and refine structural models that are used to interpret the experimental results. In this subtask, we aim at understanding ion–ion and ion–solvent specific interactions, the structure of contact and solvent-separated ion pairs, and the reactivity and dynamics of intra- and inter-molecular hydrogen-bonded systems. The expected outcome is a deep understanding of ion solution chemistry and related complex molecular systems through the application of advanced chemical physics methods including the development of novel experimental techniques and through the promotion of the synergy between the experimental and theoretical CPIMS programs at PNNL.

Subtask 2: Imaging Local Optical Fields and Chemistry at Complex Interfaces (Patrick El-Khoury, PI; Alan Joly and Oliva Primera-Pedrozo, co-investigators).

This subtask involves creating tailored nanoscopic light sources to drive and monitor chemical reactions at increasingly complex interfaces, ultimately with joint nanometer spatial and femtosecond temporal resolution. Our proposed research aims to expose the various mechanisms that underpin interfacial chemical transformations, with particular emphasis on understanding the role of distinct heterogeneous local environments on chemistry. Using a suite of experimental

near-field microscopies, most prominently tip-enhanced Raman scattering, we address plasmon-driven photo(electro)chemistry from the perspective of the molecules and local optical fields. Our approach can be distilled into several generalized objectives, including (1) investigating the fundamentals of plasmon-driven chemical transformations and reactivity at interfaces using both prototypical and realistic molecular systems, and (2) developing novel complementary nano-imaging and nano-spectroscopy approaches and advanced theoretical treatments to gain unprecedent insights into molecule–plasmon interactions at solid–air and solid–liquid interfaces.

Subtask 3: Physical and Chemical Processes in Water, Oxides, and Amorphous Solids (Bruce Kay and Greg Kimmel, PIs; Scott Smith, Loni Kringle, and Zdenek Dohnálek, co-investigators).

This subtask investigates physical and chemical phenomena occurring at the surface and within the bulk of ices, oxides, and amorphous materials. We employ molecular beam techniques to create nonequilibrium, compositionally tailored systems of adsorbates that we probe and characterize using a wide range of experimental ultrahigh vacuum (UHV) techniques including temperature programmed desorption, inert gas permeation, electron- and photon-stimulated desorption, and reflection absorption IR spectroscopy. The microscopic details of physisorption, chemisorption, and reactivity of these materials are important for unraveling the kinetics and dynamic mechanisms at heterogeneous interfaces (i.e., gas–solid, gas–liquid). These same molecular processes are also germane to understanding dissolution, precipitation, and crystallization kinetics in condensed phase multicomponent systems that are prevalent in chemical processing, nuclear waste storage, and in the environment. This research is relevant to solvation and liquid solutions, glasses, and deeply supercooled liquids, heterogeneous catalysis, and environmental chemistry. Amorphous solid water (ASW) is of special importance for many reasons, including its use as a model for liquid water, solutions, and other glassy materials. Oxide interfaces are important in the subsurface environments, in nuclear materials, and in catalysis. A key element of our approach is the use of well-characterized systems to obtain a quantitative understanding of elementary processes that will lead to understanding the complex chemistry occurring at surfaces and interfaces.

Recent Progress

Subtask 1 Fundamentals of Ion and Ion Cluster Solvation Structure, Dynamics, and Reactivity under Complex Aqueous Environments

- *Determined the primary gas-phase hydration shell of hydroxide contains four water molecules.* In contrast to previous experiments that suggested three water molecules in the first solvation of shell of hydroxide, our experiments found four, thus reconciling experiment and theory.[56] Furthermore, the structural motifs involved were similar to those previously identified in aqueous hydroxide solution studies, suggesting similarities in water coordination structures around hydroxide ions in clusters and solutions. The fine vibrational progression in the spectrum of cryogenically cooled $OH^-(H_2O)$ clusters unambiguously showed appreciable vibrational couplings among the shared proton, O-O stretching and proton bending modes, thus providing a critical benchmark for accurate description of the multidimensional potential energy surface for the HO• + HOH → HOH + •OH reaction.[1]

- *Illustrated the first two water molecules being sufficient to annihilate photochemistry of the pyruvate anion (PA^-).* Isolated PA^- is quite photoactive and can generate CO_2, CO, CH_3^-, $CH_3^•$

and a slow electron upon ultraviolet (UV) irradiation, but it is inactive in aqueous solutions. Our study shows that PA^- photochemical reactivity is significantly reduced with the addition of a single H_2O molecule and is eliminated with the addition of a second H_2O.[30]

- *Investigated electronic and solvation structures of biologically important anions.* All four mononucleotides, the smallest DNA building blocks, can exist as dianions $[dNMP\text{-}2H]^{2-}$ (N = A, G, C, or T) in the gas phase with each proton respectively detached from phosphate and nucleobase.[26] We found that these negatively charged groups provide the preferable sites to which the surrounding waters and cations bind.[41, 53] We quantitatively measured hydridic-to-protonic dihydrogen bond strength,[39] examined its influence on organizing the surrounding water network in hydrated dodecaborate clusters,[38] and probed cyclodextrin-dodecaborate complexes that have wide applications in biomedicinal treatments, separation sciences, and supramolecular chemistry.[9, 70]

- *Lone-pair stability and the hydration structure about aqueous Bi^{3+}.* A new concept in ion solvation was reported.[34] A hydrogen bonding defect, which forms between the first and second hydration shell, stabilizes the lone pair electronic configuration of the Bi^{3+} cation leading to a highly asymmetric structure with a short ion–water bond in the first shell.

- *Precise ion–water structures for alkali metals, halides, transition metals, and lanthanides.* Comprehensive extended X-ray absorption fine structure (EXAFS) and XRD studies of Na^+ and K^+ show that DFT-based MD (SCAN), quantitatively reproduces ion–water structure, whereas previous functionals do not.[71] In the case of Br^- and I^-, multibody potential energy functions provide quantitative representation of halide−water interactions enabling affordable MD simulations with CCSD(T) accuracy.[31] X-ray absorption near-edge spectroscopy (XANES) analysis of the full series of ten different first-row transition metal, M^{2+} and M^{3+}, ions quantitively benchmarks high-level theory time-dependent density-functional theory (TDDFT) predictions of XANES.[35] Subsequently high-level theory (G_0W_0@PBE0) was used to predict their vertical ionization potentials. At the "Gadolinium Break," the lanthanide series undergoes a transition from nine- to eight-coordinate configuration although exact symmetry is the subject of much debate. A new variation of EXAFS spectroscopy involving analysis of long-range photoelectron multiple scattering was used to fingerprint the complex, first-shell symmetry.[15, 33, 66]

- *Solvent reorganization coupled to photoinduced proton-coupled electron transfer (PCET).* Ultrafast X-ray scattering studies have been employed to probe the reorganization of water molecules upon photoinduced metal-to-ligand charge transfer in a Ru-polypyridyl complex in aqueous solution under two different pH. At acidic conditions, solvent reorganization coupled to protonation of the metal complex have been captured. Analysis and interpretation of the data through comparison with MD simulations are underway.

Subtask 2: Imaging Local Optical Fields and Chemistry at Complex Interfaces

- *State-of-the-art ambient AFM-optical setup.* In the past 3 years, we completed the development of a flexible AFM optical platform that can be used to perform several linear and nonlinear spectroscopic as well as spatio-spectrally resolved microscopic and nanoscopic measurements.[5, 50] This setup is equipped with several continuous wave and ultrafast broad band and tunable narrow band lasers that are required to perform different spectroscopic measurements. A subtle yet important aspect of our design has to do with the ability to deliver/collect the incident and scattered signals using different optical axes. For instance, side-

excitation bottom collection is very helpful in the quest to suppress background signals in nano-extinction and coherent nonlinear nano-optical measurements. The capabilities of this platform have been separately described in several recent publications from our group that are summarized in recent review/perspective articles.[5, 50]

- *Nanometric plasmonic reactors.* In the quest to push the spatial resolution of ambient nano-optical measurements to the 1-few nanometer length scale, we identified several plasmonic constructs that may be used to monitor plasmon-induced chemistry on the same length scale.[5, 50] Plasmonic silver nanocubes serve particularly well for this purpose.[72] Namely, the interaction between the metallic probe and the nanocubes results in regions of high optical field enhancement. In effect, nano-optical images of both bare and chemically functionalized silver cubes trace the edges of the cubes. The redundant nature of the measurements along the edge otherwise of symmetric plasmonic nanostructures (such as nanocubes) illustrates the reproducibility of our observations. These measurements and constructs are suitable for imaging solid–air interfaces, but we have found that silver nanoparticles (and tips) are unstable in water. For in-liquid measurements, gold nanostructures and nanoparticles are more appropriate. We very recently showed that gold nanoplates may be used for both chemical and chemical reaction imaging in solution with a (record) spatial resolution of < 3 nm.[58] These and other structures are now routinely used as platforms for in-liquid TERS and (non)linear nano-optical measurements more generally.
- *TERS in solution.* In the last cycle, we advanced theoretical models that may be used to forward-simulate TERS images and to explain several of their salient features.[57] Our principle focus was on being able to reliably assign spectra to specific species throughout the course of a plasmon-induced chemical transformation, an effort of particular relevance to the proposed research. To date, we used prototypical molecular reporters, namely thiophenol derivatives, to establish the principles. We found that molecular orientation, multipolar Raman scattering, molecular charging, and optical rectifications all affect the recorded spectra and images in ways that are not fully appreciated.[57] Most recently, we also found that the solvent affects local chemistry, e.g., in the case of water leading to plasmonic hydrolysis reactions that are not observed at solid–air interfaces under ambient laboratory conditions.[58] We also found that the water medium affects the nature of the plasmonic fields in ways that are not understood. Gaining a detailed understanding of the effect of water on plasmonic chemistry and on the operative fields in nano-optical measurements is the subject of on-going work.

Subtask 3: Physical and Chemical Processes in Water, Oxides, and Amorphous Solids

- *Demonstrated reversible structural transformations in deeply supercooled water.* Using our laser heating technique, we investigated the structural transformations in supercooled water.[11, 40, 59, 60, 73] Previously, an unresolved question was whether liquid water at ambient conditions was connected by a thermodynamically reversible path to water heated just above it glass transition temperature at 136 K. While intense disagreements over MD simulations were eventually resolved, the behavior for real water was still in doubt. Our experimental results showed that water at high and low temperatures are reversibly connected.[73] Furthermore, we showed that over a wide temperature range (130 K < T < 245 K), water's structure (for both H_2O[73] and D_2O[40]) could always be decomposed into a linear combination of just two components, which corresponds to the behavior predicted by the liquid-liquid critical point hypothesis. We also

showed that the structural relaxation, while complex, was always fast compared to the time required to crystallize the water.[11]

- *Investigated the structure and reactions of water adsorbed on oxide surfaces.* In these studies, we examined the interactions of water with rutile TiO_2(110) and anatase TiO_2(101) and the role of surface and near-surface defects in those interactions.[46, 55, 63] We collaborated with Chris Mundy from the CPIMS molecular theory and modelling program to investigate the structure and reactivity of submonolayer water coverages on reduced rutile TiO_2(110) using azimuth- and polarization-resolved IR and *ab initio* MD.[46] While hydrogen-bonded chains formed at low coverage as expected from previous work,[74] we also found that defect electrons mediated the dissociation of some of the adsorbed water into terminal and bridging hydroxyl pairs (OH_t and OH_b, respectively). In contrast to rutile TiO_2(110), oxygen vacancies are not stable on the surface of anatase TiO_2(101), instead they reside in subsurface. However, we found that these subsurface vacancies also lead to some water dissociation into OH_t and OH_b pairs.[55] We also use IR spectroscopy to investigate the structure of thin water layers on nearly stoichiometric anatase TiO_2(101).[63] Those results showed that while the density of Ti_{5c} binding sites for water is very similar on anatase TiO_2(101) and rutile TiO_2(110), differences in the distance adjacent between Ti_{5c} sites on the two surfaces leads to very different structures for the water adlayer.
- *Probed crystallization of acetonitrile nanoscale films.* In a series of papers we used IR spectroscopy and temperature programmed desorption to investigate the effects of deposition temperature, film thickness, and the underlying substrate on the morphology, structure, and crystallization kinetics of vapor-deposited acetonitrile films.[16, 75, 76] Previously, we investigated the structure of multilayer (~bulk) and monolayer films on Pt(111) and graphene.[75, 76] More recently, we found that the crystallization kinetics of amorphous acetonitrile films have a unique thickness dependence with the thinner films crystallizing much slower than the thicker ones.[16] The experiments also showed that decane layers at both the substrate and vacuum interfaces can also affect the crystallization rates. The overall results suggested that the crystallization kinetics are complicated, indicating the possibility of multiple nucleation and growth mechanisms.

Future Plans

Subtask 1: Fundamentals of Ion and Ion Cluster Solvation Structure, Dynamics, and Reactivity under Complex Aqueous Environments

- *Effects of cation lone-pair electrons on the hydration structure of multivalent cations (Fulton).* The central part of this effort will explore how the lone-pair chemistry of aqueous ions such as Pb^{2+} and Bi^{3+} affect their hydration structure. Both Pb^{2+} and Bi^{3+} have a pair of nonbonding valence electrons that interact only weakly with water leading to a highly asymmetric structure. We will probe the water hydration structure with EXAFS and use XANES to look at the lone-pair electronic state. A further objective is to determine how nuclear quantum effects (NQEs) subtly modulate the first- and second-shell structure of these species.

In a previous study, we showed that water ordering around the Bi^{3+} ion is dominated by the lone-pair electronic state of Bi that creates an unusual hydration structure.[34] A non-uniformity or defect in the water structure occurs, in the presence of two or more water solvation shells, that stabilizes the stereochemically active Bi^{3+} lone-pair electronic configuration over that of the centro-symmetric state. The conventional picture of a broad ion–water distribution with a high

degree of disorder is incorrect since the hydrating water is well ordered about a discrete set of distances within the first coordination sphere.

Based on this finding, the proposed work focuses on the structure of Pb^{2+} that is the isoelectronic neighbor of Bi^{3+}. Pb^{2+} is important in some photovoltaic devices and as a contaminant in the environment. We seek to determine whether aqueous Pb^{2+} mimics the unusual structure of Bi^{3+} through EXAFS measurements coupled with hybrid-DFT calculations. We will also evaluate the electronic state of Pb^{2+} with XANES measurements and TDDFT calculations to assess the lone-pair electronic state as well as explore spin orbit effects on the ion–water structure. Finally, the water "defect" that stabilizes the lone-pair configuration is quite similar in some ways to how water bonds to hydronium (H_3O^+) for which NQEs are known to be important. This led to some preliminary EXAFS measurements and path-integral MD studies (with Greg Schenter) that showed structural differences between Bi^{3+} in H_2O versus D_2O. Whereas monovalent ions are known to show weak NQEs, there are no reports for divalent cations. Hence another objective is to understand the role of NQEs in Pb^{2+} hydration through EXAFS measurements using H_2O and D_2O.

- *Long-range (1–5 nm) ion and water correlations (Fulton, Biasin).* We will use SAXS measurements to probe the long-range ordering of ions in water from 1–5 nm. The overwhelming majority of scattering studies (X-rays, neutrons, photoelectrons, EXAFS) in the literature have only probed the local structure about ions up to approximately 0.5 nm. However, electrostatic forces order ions to much longer distances. The size domain up to 5 nm reaches length scales that (1) can be quantitatively related to important thermodynamic properties such as ion activity coefficients and osmotic coefficients and (2) are important to the formation of prenucleation clusters at near-saturation conditions and to long-range ion ordering that affects mesoscale processes.

An outcome from the previous period was the discovery of pre-peaks for divalent cations in the X-ray structure function, S(Q), that are correlated with long-range periodic ordering of anions and cations.[77] From our experimental SAXS measurements and theory, we have confirmed that at low concentrations the ions conform to a simple Debye-Hückel distribution, while at higher concentrations there is an abrupt onset to periodically ordered ion–ion nanodomains. We have found that this Kirkwood transition occurs at moderate concentrations (0.5–1 m) for monovalent cations and to remarkably low concentration for trivalent cations (0.005 m).

We will investigate the long-range ordering in mixed electrolytes, high-concentration electrolytes, and ionic liquids. Most biological and geological systems involve mixed electrolytes, yet the interplay of effects involving the presence of a monovalent salt (e.g., NaCl) on the Kirkwood transition of a divalent salt (e.g., $CaCl_2$) is unknown. Several mixed salt systems (monovalent, divalent, and trivalent) will be explored by SAXS to determine the correlations length and the lattice spacing of the periodically ordered nanodomains from the SAXS pre-peak spectrum. While our previous studies involved single electrolyte solutions up to about 5 m, we plan to extend systems to much higher concentrations such as 20 m $ZnCl^2$ that is of relevance to battery storage. In a similar vein, we will explore ordering in certain types of ionic liquids relevant to separations and catalysis. The objective for both types of systems is to interpret the structures from the point of view of the periodically ordered nanodomains using the SAXS pre-peak spectrum.

- *Tracking electron and proton transfer dynamics and the effect of solute-solvent H-bonding interactions with X-ray Free Electron Lasers (Biasin)* We plan to achieve a molecular-level understanding of light-induced electron transfer (ET) and proton-coupled electron-transfer (PCET) reactions, which are ubiquitous in chemistry, by studying metal-based donor-acceptor complexes. Particularly, we aim at considering explicitly the interaction of such molecular systems with the surrounding solvent by directly visualizing how local microenvironmental effects control electron transfer, stabilization of charge separated states, and excited-state PCET reactions on the picosecond timescale. We will achieve this by utilizing state-of-the-art time-resolved x-ray spectroscopy and scattering methods at X-ray Free Electron Laser facilities, such as the Linac Coherent Light Source (LCLS). Time-resolved X-ray Solution Scattering (XSS) directly probes, at atomic spatial and temporal scales, the photoinduced changes of all the atom-pair distances. These observables can be directly compared with the atomic positions calculated by MD simulations, enabling direct tracking of photoinduced structural dynamics and the accompanying changes in the solvation shell structure.[78] In particular, XSS is uniquely sensitive to coherent motions of the first-solvation shell solvent molecules upon changes in solute-solvent hydrogen bonding.[79] The structural dynamics measured by XSS can be correlated to the electronic dynamics measured by X-ray spectroscopy methods, which are element-specific and uniquely capture the signatures of ET and excited-state protonation.

We will apply these methods to study photoinduced dynamics in metal-based photosensitizers linked to electron and proton donor/acceptor sites that can form hydrogen bond interactions with – and eventually be (de)protonated by – the surrounding solvent molecules, as a function of solvent properties such as polarity, H-bond ability, and acidity. By combining x-ray transient signals with state-of-the-art MD and TDDFT calculations, we will correlate specific solute-solvent interactions with the structural and electronic excited state dynamics and achieve a mechanistic understanding of the effect of solvent structure and dynamics in i) driving the ET and PCET processes, and ii) stabilizing charge separated state – which are fundamental intermediates in solar conversion and catalytic processes.

We already have preliminary results obtained by investigating the photoinduced PCET in $[Ru(bpy)_2(bpz)]^{2+}$ (where bpz = 2,2′-bipyrazine, bpy = 2,2′-bipyridine) with ultrafast XSS at LCLS, and we are currently investigating the ultrafast nitrogen K-edge X-ray absorption on the same molecule at the chemRIXS instrument at LCLS. In the future, we will turn our attention to molecular dyads comprised of a photosensitizer linked to quinone electron and proton donor/acceptor. In these systems, ET proceeds from the photogenerated MLCT state, with an additional excited-state process prior to the formation of the charge separated state and eventually the protonation step. While it is well established that quinones can form hydrogen bonds the with solvent molecules, and that this modulates the ET and PCET behavior beyond the expected dipolar response, the mechanistic details of the observed kinetics are unclear. We will utilize ultrafast X-ray methods as detailed above to shed light on these mechanisms. We will furthermore explore the possibility that protonation leads to stabilization of the charge separated state in these systems.

- *Cluster model investigation of ion solvation, hydrogen bonding interactions, and excited state induced reactivity (Wang).* The experimental capabilities that we have developed give us the opportunity to attack a broad range of fundamental chemical physics problems pertinent to ionic solvation, solution chemistry, homogeneous/heterogeneous catalysis, aerosol chemistry, biological processes, and material synthesis. The ability to cool and control ion temperature, when combined with wavenumber energy resolution velocity mapping imaging will enable us to study different isomer populations and conformation changes of environmentally important hydrated clusters. Another major direction will employ gaseous clusters to model ion-specific interactions in solutions, ion transport, inert compound activation, ion-receptor interactions in biological systems, and the initial stages of nucleation processes relevant to atmospheric aerosol formation.

Specifically, we plan to extend anion solvation beyond normal Hofmeister anions to include large nm-sized superchaotropes. We will investigate how the solvent water network responds to these anions at such weak ion-water interaction regimes. Other complex and polyatomic anions we are proposing to study include those that have been used in redox flow batteries. We will probe how their redox potentials evolve as a function of the degree of solvation. Microscopic solvation of anions holds a key role to connect their gas-phase intrinsic properties to their solution phase physiochemical behaviors, as demonstrated in our recent work on the actinic chemistry of the pyruvate anion.[30] We will systematically investigate how water molecules modulate the electronic structures of anions and influence their subsequent photochemistry. In addition, gas-phase anion photoelectron spectroscopy (PES) will be used to probe proton transfer reactions induced by electron detachment in acid-base hydrogen bonded clusters. Gas-phase PES will also be utilized to precisely measure electron affinities of the electron donor/acceptor units and clusters. This will allow us to quantify thermodynamic driving forces in seeking the optimal speciation and to model the dependence on solvent environments in PCET.

Subtask 2: Imaging Local Optical Fields and Chemistry at Complex Interfaces

Our recent work provides the foundation to advance the existing understanding of plasmon-driven chemistry with the ultimate goal of visualizing both local optical fields and interfacial chemistry with record spatio-temporal resolution. Indeed, there are several proposed research directions that rely on the unique methods that were developed by our group throughout the past few years. An important initial direction entails taking advantage of our multimodal nano-imager to separately probe local fields and molecular reactivity at increasingly complex interfaces. Prior to describing the proposed measurements and their limitations, it is important to note that our envisioned research directions are designed with several hypotheses in mind, including:

1. Local and nonlocal optical fields lead to different products in plasmonic chemical reactions.
2. The formation of anions at plasmonic junctions due to plasmonic decay leads to resonance Raman scattering that may easily be confused with the onset of plasmonic chemistry.
3. The solvent (e.g., water) affects the (non)local character of the junction plasmon, and hence, leads to distinct products in plasmon-induced chemical reactions.
4. Selectivity (or lack of) in plasmonic chemistry depends on the local availability of reactants.

5. Molecular and plasmon resonances, which vary on the few nanometer length scale, alter the pathways of plasmonic (photo)chemical transformations.

- *Chemical reaction nano-imaging.* The following proposed set of measurements will be used to advance our understanding of plasmonic chemistry by addressing the above-outlined hypotheses. We will chiefly employ TERS to visualize and identify molecules that are chemisorbed or physiosorbed onto plasmonic metal substrates and nanostructures. In going through the ensuing proposed measurements, it is important to recognize that there is much more to TERS than chemical (reaction) imaging.[5] Namely, these measurements are also sensitive to (i) the (non)local nature of the local optical field (hypotheses 1, 3, 5), (ii) molecular resonances (hypotheses 2, 5), and (iii) plasmonic resonances of the tip, the nanostructures on the substrate, and the gap plasmons that develop when the two are closely positioned (hypothesis 5). Hypothesis 4 can otherwise be tested using carefully prepared hybrid molecular-plasmonic substrates and through a direct comparison between TERS measurements performed at solid-air *vs* solid-liquid interfaces.

Silver/gold nanocubes as well as silver/gold nanoplates will primarily be used as prototypical substrates for our proposed measurements. In addition, we will use state-of-the art (direct write) nano-lithographic techniques to etch nano-patterns into continuous gold and silver films. These include helium ion lithography and AFM-based pulsed-force lithography.[20, 80] The advantage of the latter is that patterns can be introduced in the TERS setup, without sample transfer and the need for correlative measurements or fiducial marks to locate nanoscale features. In addition, AFM-written nanojunctions drawn into continuous films were recently found to support highly localized and enhanced plasmonic fields,[20] wherein chemical reactions can be tracked with a spatial resolution of ~1 nm under ambient laboratory conditions.

We have several approaches to the chemical functionalization of our nano-reactors, including methods as simple as drop casting/substrate immersion and as sophisticated as electrospray deposition and soft-landing.[81] Some sample preparation methods are molecule-agnostic (e.g., electrospray), whereas others are optimal for molecules with specific functional group like thiols and amines (e.g., substrate immersion). The molecules themselves are selected with specific questions in mind. For instance, we previously found that 4,4'-dimercaptostilbene and biphenyl-4,4'-dithiol were found to induce the transition between local and tunneling plasmons in the TERS geometry,[82] while their monothiol analogues, which differed by a single atom, have a dramatically different optical response. The difference in the local optical response can be tracked through both TERS and nano-extinction. These molecules, interrogated at solid-air *vs* solid-liquid interfaces can help up test hypotheses 1, 3, and 5. The onset of tunneling is also associated with optical rectification and molecular charging,[83] and all of these effects can be suppressed using the choice of tapping *vs* contact mode feedback in TERS.[81] In this regard, 4-mercaptobenzonitrile, which features a nitrile resonance that is sensitive to rectified local optical fields[83, 84] may be used to track tunneling plasmons. Overall, mixtures of molecules that act as nanoscopic probes of their local environments will be used to ascertain the (non)local character of the operative plasmonic field, its resonance, as well as its dependence on the molecule(s) at the gap and otherwise presence/absence of a solvent (e.g. water) medium. Once the local optical field properties are established, we will first use prototypical molecular systems that undergo, e.g., molecular charging (4-nitrothiophenol), dimerization reactions (4-nitrothiophenol and 4-aminothiophenol), and hydrolysis (4-mercaptobenzoic acid) reactions in the TERS geometry.

Once again, mixtures of reactive and probe molecules may be used to accomplish both multimodal optical field imaging as well as chemical reaction imaging in the same measurement.

Motivated by recent (unpublished) observations of highly selective oxidation reactions of aromatic amines in the TERS geometry, we are also interested in furthering our existing understanding of the role of molecular orientation *vs* the local availability of oxygen on the outcome of a plasmonic oxidation reaction. Whereas the role of molecular orientation on chemistry can be established using a combination of experiment and theory, the first requires correlated electron microscopy and potentially electron energy loss spectroscopy. The latter will be performed here at PNNL in collaboration with electron microscopy experts.

- *Correlated TERS-nano-extinction measurements.* This objective is conceived with hypotheses 1, 2, and 5 in mind. Namely, we propose to track local molecular and local field resonances that vary over the few nanometer using novel approaches to nano-extinction, to understand how spatially varying resonances alter local chemistry, as visualized *via* correlated TERS mapping. Nano-extinction measurements can be performed directly, at least at solid-air interfaces. These measurements however require side-excitation, which is not currently possible using our in-liquid AFM head and liquid cell design. In particular, optical aberrations in the incidence and back-scattered geometry preclude reliable in-liquid nano-extinction measurement and spectral nano-imaging more generally using our current approach. We are currently working on overcoming the existing challenges by (i) developing a new liquid cell that allows side excitation-bottom collection, and (ii) incorporating a deformable mirror in the incidence path to correct for optical aberrations. Whereas the 3D printed prototypes of (i) can easily be accomplished, on-the shelf deformable mirrors with wavefront sensors will be used to accomplish (ii).

Despite the reduced backgrounds in nano-extinction measurements that take advantage of the side-excitation side-collection geometry, the metallic response is likely to dominate the overall scattered signals. Selectively tracking molecular extinction in hybrid molecule-metallic constructs has proven to be truly challenging and requires more finesse. Multiple approaches are envisioned to overcome this challenge. The first is based on excitation wavelength-dependent photoluminescence measurements, which yield an excitation spectrum at every tip position. This is similar to conventional UV-Vis but takes advantage of background-free molecular luminescence signals. Notwithstanding the need for a fluorophore and careful sample engineering (e.g., decoupling molecules from the metal), this is a promising method that allows single molecule detection sensitivity even without plasmonic antennae. In this regard, it is possible to record tip-only enhanced excitation-tunable photoluminescence spectra, as we recently demonstrated for related tip-enhanced linear and nonlinear photoluminescence.[21, 67]

In the absence of fluorescence or photoluminescence more generally, excitation wavelength-dependent tip-enhanced Raman scattering is a second envisioned approach to molecular nano-extinction measurements. In a previous study, we found that TERS may be used to track distinct multipolar plasmonic resonances of gold nanorods that fall within the Stokes scattering window.[57] Tuning the excitation wavelength across the (modified) extinction spectrum of the molecule is another approach to extracting background-free molecular nano-extinction spectra, akin to the first approach that we describe above. Dissecting the information content in resonance Raman scattering however requires careful treatment. The same is true for assigning the spectra in resonant TERS spectral imaging measurements to test hypothesis 2. This requires

establishing protocols for simulating resonance Raman scattering, which is an effort we will undertake in the near future.

A third possible approach to molecular nano-extinction is motivated by recent observations from our group, wherein we tracked the extinction of single layers of 2D excitonic materials through correlated hyperspectral absorption, reflectance, and excitation-tunable parametric 4-wave mixing.[51] Beyond excitation tunable electronic 4-wave mixing, it is also possible to (simultaneously) record other nonlinear responses from hybrid molecular-metallic constructs that can also inform us on molecular and metallic resonances over a broad spectral region. Overall, all three major approaches discussed in this sub-section can be performed using a single optical platform.

TERS and nano-extinction measurements are typically performed using contact mode or hybrid contact mode-tapping AFM feedback. Using the latter method of choice, it is possible to record current at every position of the tip relative to the sample. We have recently established an approach that allowed simultaneously recorded tip-sample distance dependent force (A), current (B), and nano-Raman (C) signals. These measurements will be used to better understand the different plasmonic regimes that are operative in TERS, and the effect of the transition between classical and quantum regime on the observations in TERS chemical as well as chemical reaction nano-imaging. This requires a detailed analysis of nano-Raman spectra from molecules beneath the tip, as discussed in the next sub-section. We will use familiar molecular reporters, such as 4-nitrothiophenol to answer questions at the interface of the above discussed TERS and nano-extinction measurements, and to directly test hypotheses 1, 2, and 5. We will also test the possibility of performing nano-optical measurements using negative force values (attractive regime) to take advantage of optimal enhancement prior to the onset of tunnel rectification and molecular charging. Indeed, even though one of our goals is to take advantage of quantum plasmons to drive desired (redox) chemistry, an important more general goal of our work entails analytical/non-invasive TERS measurements for ultrasensitive chemical detection and imaging.

- *Advanced simulations of TERS chemical images.* In the past several years, we developed the protocols required to forward simulate our TERS chemical images using a combination of FDTD and static/dynamic density functional theory simulations.[57, 85-87] Our formalism treats ensemble-averaged as well as single-molecule Raman scattering on equal footing, and it has been benchmarked using various non-resonant TERS reporters. The existing approaches can already be used to test hypotheses 4 and 5. We will now extend our approach to treat both non-resonant as well as resonant Raman scattering in the TERS geometry, to bridge the gap between our existing protocols and those required to test hypothesis 2. Throughout this cycle, we will also extend the numerical TERS approach to account for our observations in nano-extinction measurements in support of objective 2. Our overall goal is to rigorously understand the electronic and vibrational signatures that are associated with molecular charging at plasmonic nanojunctions, and thus, to disentangle the TERS signatures of physical changes from chemical transformations at interfaces. Both periodic calculations and large molecular systems may be used to this end. For instance, modeling Ag_n-molecule complexes (systems with $n > 79$) can be reliably tackled using the recently developed AIMD module in NWChem.[88] The same models may also be used to rigorously test the accuracy of 3D molecular orientation measurements via TERS. This will be achieved through a direct comparison between the experimentally inferred molecular orientation and minimum energy geometries from density functional theory calculations of molecules on large metallic clusters and metal surfaces. This objective is key to

advancing a quantitative optical field mapping protocol through an inversion of experimentally recorded TERS spectra and images. It will be accomplished in close collaboration with PNNL CPIMS theory PIs.

Subtask 3: Physical and Chemical Processes in Water, Oxides, and Amorphous Solids

- *Investigate the structure of nanoscale supercooled water films versus temperature*: Recently, we have investigated the structure and relaxation rates of supercooled water.[11, 40, 59, 60, 73] Those experiments used water films that were ~15 nm thick (i.e., 50 ML) and sought to understand the properties of bulk water. While 15 nm might not seem to be thick enough to converge upon bulk behavior, experiments with films half or twice as thick yielded similar results, as did experiments on Pt(111) and graphene/Pt(111), all of which suggested the influence of the substrate was minimal. Furthermore, MD simulations investigating the structure of water near various substrates typically show convergence to bulk structure for distances more than ~1 nm from the surface, and experiments on confined water, where the distance to the nearest interface is typically less than 1 nm, have been used for years to provide insights into the properties of bulk liquid water. Nonetheless, we expect the substrate to influence both the structure and kinetics for water films that are sufficiently thin.

We plan to investigate the structure, relaxation rates, and crystallization kinetics of nanoscale water films versus temperature as a function of decreasing film thickness. Our expectation is that for thinner films, the properties of the substrate will begin to influence the structure and relaxation rates. For example, water films on a hydrophobic surface, such as graphene, might be expected to have faster relaxation due to the lack of strong bonds anchoring some water molecules to the surface. In contrast, such anchors could hinder relaxation on hydrophilic surfaces. Because our previous experiments on ice nucleation in the transiently heated water films suggested it occurred via bulk nucleation,[89, 90] we also expect crystallization to slow as the films get thinner and the total volume decreases. For water in confinement, crystallization can be completely avoided, and we will investigate if this is also true for the transiently heated thin films.

- *Measure the self-diffusion in supercooled H_2O and D_2O from 130 to 270 K*. Among water's numerous anomalous properties, the question of whether the behavior of water above its reputed glass transition at ~136 K is that of a true supercooled liquid is still hotly debated. One argument is that the glass transition is too weak to be from the unfreezing of translational and rotational degrees of freedom expected in a supercooled liquid but instead is the result of rotational transitions only, and various experimental results have been interpreted as supporting this explanation. We plan to use isotopically layered nanoscale water film to study diffusive mixing with infrared spectroscopy and measurements of the desorption kinetics of the water isotopomers in the mixed films. These experiments will be conducted using isothermal and "normal" heating rates (e.g. < 10 K/s) for 130 K < T < 160, and transient heating for 190 K < T < 270 K.

Previously, we have measured the growth rate of crystalline ice over a wide temperature range in no man's land.[91] The diffusivity was calculated from the growth rate data using the Wilson-Frenkel model, which relates the crystalline growth rate of a material to the liquid mobility of molecules at the liquid–solid interface. The extracted self-diffusivity varied smoothly by ~11 orders magnitude from 126 to 262 K suggesting thermodynamic continuity. However, the Wilson-Frenkel model, while plausible, is not a direct measurement of the diffusivity. Our measurements of the self-diffusion will allow us to test the validity of the Wilson-Frenkel model.

Investigate proton mobility and exchange mechanisms in supercooled liquid water and ASW. Understanding proton exchange and mobility is of great importance in a wide range of scientific research areas including astrochemistry, biology, and fuel cell technology. The transport of protons has long been described by a Grotthuss or "structural" diffusion mechanism where a proton is passed between adjacent water molecules in a series of hops. In prior work we used simultaneous dosing of D_2O and H_2O from two molecular beams onto a substrate held at 20 K to create an amorphous film of unreacted D_2O embedded in an H_2O matrix. The metastable system was heated to ~130 K where H/D exchange could be observed.[92] We demonstrated that isotopic exchange was controlled by protons at either the substrate or vacuum interface moving through the films to the reactant layer. To quantify the proton transport kinetics, we will use molecular beams to create isotopically layered films where proton mobility rate through the films will be measured by varying the thickness of the water films and the selective placement of the reactant layer. Charge carriers can also be deposited on the underlying substrate or generated at the vacuum interface using electron beam exposure. This work will focus on quantifying various aspects of the H/D mobility and exchange reaction kinetics and energetics. We will also extend these measurements into the supercooled liquid temperature regime using pulsed laser heating techniques. A key question here is will we be able to observe direct H/D exchange at higher temperatures that does not require an external source of mobile protons.

- *Investigate the transport mechanisms in supercooled liquids near the glass transition temperature.* Understanding the behavior of supercooled liquids at and near their glass transition remains an important scientific challenge. The glass transition is typically defined to occur when molecules are moving too slowly to sample the available configurational space on a laboratory timescale (~100 s). At the glass transition temperature, T_g, the supercooled liquid's structure is said to be "frozen," and the material is called a glass. When the glass is heated above T_g, the previously inaccessible configurational degrees of freedom become accessible and the rotational and translational properties of the supercooled liquid reemerge. Transport behavior in a supercooled liquid is often characterized as either "strong" (Arrhenius) or "fragile" (super Arrhenius). Strong liquids are characterized by having a single activation barrier suggesting a constant transport mechanism over the entire temperature range. Fragile liquids are characterized by an activation barrier that increases sharply with decreasing temperature, which suggests a transport mechanism that involves cooperative rearrangement of an increasing number of molecules near T_g. While the fragile or strong designations are useful for grouping liquids with similar behavior, a full molecular-level understanding is still lacking.

We will employ inert gas permeation techniques and isotopic substitution to measure the diffusivity and stability of molecular glasses and supercooled liquids near T_g. In a permeation experiment, an amorphous film deposited on top of an inert gas layer is heated to temperatures near its T_g, whereupon it transforms into a supercooled liquid, and the inert gas can begin to diffuse through the overlayer. We have previously shown that the transport of the inert gas is directly related to the diffusivity of the supercooled liquid itself. In preliminary experiments, we measured the diffusivity/permeation of Kr through various isotopes of methanol at temperatures near and just above T_g (103 K). The results showed two surprising features. First, the magnitude of the isotope effect is much larger than expected. The difference in diffusivity between CH_3OH and CD_3OD is greater than a factor of two. Based on mass scaling, one would expect the isotope effect to be no greater than ~1.05, although nuclear magnetic resonance measurements report an isotope effect of 1.4 near 150 K. Second, the unexpectedly large isotope effect is observed by the substitution of the methyl hydrogen (C-H), not the hydroxyl. Typically, intermolecular

interactions are dominated by hydrogen bonds, therefore one might expect substitution of the OH hydrogen to have the largest effect. These results suggest that the diffusion mechanism involves strong translational–rotational coupling and point to the methyl group as affecting the mobility. We will collaborate with Greg Schenter and Britta Johnson in the CPIMS molecular theory and modelling group to develop theoretical models to account for these observations and better understand the transport mechanisms for methanol near T_g.

The properties and stability of glasses depend on a combination of structural, kinetic, and thermodynamic factors. For example, we have previously shown that the deposition temperature affects the stability of vapor deposited glasses of toluene and ethylbenzene.[93] The permeation method provides a direct measure of the onset temperature for the transition from an amorphous solid to supercooled liquid, which is a measure of the glass stability. Our results are consistent with previous research on stable glasses that are formed at deposition temperatures ~0.85 T_g, where the enhanced stability is attributed to increased surface mobility leading to the formation of more compact amorphous structures during growth near T_g. We will investigate stable glass formation in other systems and the mechanisms for the onset of molecular translational motion that accompanies the glass to supercooled liquid transition. Recent work has shown that in some systems the transition from stable glass to supercooled liquid proceeds from a surface-initiated growth front. The mechanism is similar to the one we have observed in the crystallization of ASW films. We will investigate whether the glass to supercooled liquid transition is surface initiated or homogenously throughout the film.

- *Investigate Relaxation in Metastable systems*. The transition from a metastable-homogenized mixture to a phase-separated system will depend on the relative molecular interaction energies of the species and the energetic barriers for molecular mobility. For example, a binary mixture of water and a hydrocarbon of specific composition can be created at low temperature by simultaneous dosing from two molecular beams. Upon heating, the transformation into a phase-separated mixture will be followed using IR spectroscopy. In a hydrocarbon-rich system, the initially isolated water molecules dispersed in a hydrophobic solvent would become mobile and begin to aggregate. As this happens, the OH-stretch intensity should dramatically increase as water molecules begin to cluster. Experiments with various hydrophobic/water compositions and concentrations will be studied. Initial studies will focus on hydrocarbon (C_6-C_{10})/water and/or hydrocarbon/alcohol systems. In water rich systems, there is the question of whether the solvation of hydrophobic solutes can either hinder or accelerate crystallization. At issue is how the solvation structure around the solute plays a role in ice nucleation. Experiments will also be conducted using the pulsed-heating technique, and will focus on how small solutes such as linear alkanes (C_nH_{2n+2}) and their corresponding alcohols ($C_nH_{2n+1}OH$), affect the structure of supercooled water. The effects will be monitored primarily through their influence on the OH-stretch vibrations of the water in the solutions. Because the structure and dynamics of water around hydrophobic molecules affect, among other things, the formation of clathrate hydrates and biological processes such as membrane formation and protein folding, it is important to develop a detailed understanding of the factors influencing them. These interaction energies are what determine the structure and activity of proteins and lipids in aqueous environments and are needed to understand various biological processes at a molecular level.

Peer-Reviewed Publications Resulting from this Project (2021-2023)

[1] W. J. Cao, S. S. Xantheas, and X. B. Wang,"Cryogenic Vibrationally Resolved Photoelectron Spectroscopy of $OH^-(H_2O)$: Confirmation of Multidimensional Franck-Condon Simulation Results for the Transition State of the OH + H_2O Reaction," J. Phys. Chem. A **125**, 2154-2162 (2021).
[2] W. J. Cao, H. H. Zhang, Q. Q. Yuan, X. G. Zhou, S. R. Kass, and X. B. Wang,"Observation of Conformational Simplification upon *N*-Methylation on Amino Acid Iodide Clusters," Journal of Physical Chemistry Letters **12**, 2780-2787 (2021).
[3] W. J. Cao, H. H. Zhang, Q. Q. Yuan, X. G. Zhou, S. R. Kass, and X. B. Wang,"Observation and Exploitation of Spin-Orbit Excited Dipole-Bound States in Ion-Molecule Clusters," Journal of Physical Chemistry Letters **12**, 11022-11028 (2021).
[4] K. T. Crampton, A. G. Joly, and P. Z. El-Khoury,"Surface plasmon polariton pulse shaping via two-dimensional Bragg grating pairs," Nanophotonics **10**, 959-965 (2021).
[5] P. Z. El-Khoury,"Tip-Enhanced Raman Scattering on Both Sides of the Schrodinger Equation," Accounts Chem. Res. **54**, 4576-4583 (2021).
[6] M. Gabel, P. Z. El-Khoury, and Y. Gu,"Imaging Charged Exciton Localization in van der Waals $WSe_2/MoSe_2$ Heterobilayers," Journal of Physical Chemistry Letters **12**, 10589-10594 (2021).
[7] M. Gabel, B. T. O'Callahan, C. Groome, C. F. Wang, R. Ragan, Y. Gu, and P. Z. El-Khoury,"Mapping Molecular Adsorption Configurations with < 5 nm Spatial Resolution through Ambient Tip-Enhanced Raman Imaging," Journal of Physical Chemistry Letters **12**, 3586-3590 (2021).
[8] C. Y. Jia, L. C. Wu, J. L. Fulton, X. R. Liang, J. J. De Yoreo, and B. H. Guan,"Structural Characteristics of Amorphous Calcium Sulfate: Evidence to the Role of Water Molecules," Journal of Physical Chemistry C **125**, 3415-3420 (2021).
[9] Y. R. Jiang *et al.*,"Gaseous cyclodextrin-*closo*-dodecaborate complexes $\chi CD \bullet B_{12}X_{12}^{2-}$ (χ = α, β, and γ; X = F, Cl, Br, and I): electronic structures and intramolecular interactions," Phys. Chem. Chem. Phys. **23**, 13447-13457 (2021).
[10] Z. J. Jing *et al.*,"Developing Ideal Metalorganic Hydrides for Hydrogen Storage: From Theoretical Prediction to Rational Fabrication," ACS Mater. Lett. **3**, 1417-1425 (2021).
[11] L. Kringle, W. A. Thornley, B. D. Kay, and G. A. Kimmel,"Structural relaxation and crystallization in supercooled water from 170 to 260 K," Proceedings of the National Academy of Sciences of the United States of America **118**, e2022884118 e2022884118 (2021).
[12] C. J. Lee, M. A. Sharp, R. S. Smith, B. D. Kay, and Z. Dohnálek,"Adsorption of ethane, ethene, and ethyne on reconstructed Fe_3O_4(001)," Surf. Sci. **714**, 121932 10 (2021).
[13] Z. D. Li, P. Z. El-Khoury, and D. Kurouski,"Tip-enhanced Raman imaging of photocatalytic reactions on thermally-reshaped gold and gold-palladium microplates," Chem. Commun. **57**, 891-894 (2021).
[14] Z. D. Li, J. Rigor, N. Large, P. Z. El-Khoury, and D. Kurouski,"Underlying Mechanisms of Hot Carrier-Driven Reactivity on Bimetallic Nanostructures," Journal of Physical Chemistry C **125**, 2492-2501 (2021).
[15] R. C. Shiery, J. L. Fulton, M. Balasubramanian, M. T. Nguyen, J. B. Lu, J. Li, R. Rousseau, V. A. Glezakou, and D. C. Cantu,"Coordination Sphere of Lanthanide Aqua Ions Resolved with Ab Initio Molecular Dynamics and X-ray Absorption Spectroscopy," Inorg. Chem. **60**, 3117-3130 (2021).

[16] R. S. Smith, M. Tylinski, G. A. Kimmel, and B. D. Kay,"Crystallization kinetics of amorphous acetonitrile nanoscale films," Journal of Chemical Physics **154**, 144703 12 (2021).
[17] C. K. Su *et al.*,"Materials Engineering of Violin Soundboards by Stradivari and Guarneri," Angew. Chem.-Int. Edit. **60**, 19144-19154 (2021).
[18] C. F. Wang, and P. Z. El-Khoury,"Imaging Plasmons with Sub-2 nm Spatial Resolution via Tip-Enhanced Four-Wave Mixing," Journal of Physical Chemistry Letters **12**, 3535-3539 (2021).
[19] C. F. Wang, and P. Z. El-Khoury,"Multimodal Tip-Enhanced Nonlinear Optical Nanoimaging of Plasmonic Silver Nanocubes," Journal of Physical Chemistry Letters **12**, 10761-10765 (2021).
[20] C. F. Wang, B. T. O'Callahan, A. Krayev, and P. Z. El-Khoury,"Nanoindentation-enhanced tip-enhanced Raman spectroscopy," Journal of Chemical Physics **154**, 241101 4 (2021).
[21] C. F. Wang, M. Zamkov, and P. Z. El-Khoury,"Ambient Tip-Enhanced Photoluminescence with 5 nm Spatial Resolution," Journal of Physical Chemistry C **125**, 12251-12255 (2021).
[22] F. F. Wang, Z. B. Hu, X. B. Wang, Z. R. Sun, and H. T. Sun,"Assessment of DFT methods for the prediction of detachment energies and electronic structures of complex and multiply charged anions," Comput. Theor. Chem. **1202**, 113295 9 (2021).
[23] L. Wang, J. Hang, Q. Q. Yuan, W. J. Cao, X. G. Zhou, S. L. Liu, and X. B. Wang,"Electron Affinity and Electronic Structure of Hexafluoroacetone (HFA) Revealed by Photodetaching the $HFA^{\bullet-}$ Radical Anion," J. Phys. Chem. A **125**, 746-753 (2021).
[24] J. Warneke, and X. B. Wang,"Measuring Electronic Structure of Multiply Charged Anions to Understand Their Chemistry: A Case Study on Gaseous Polyhedral closo-Borate Dianions," J. Phys. Chem. A **125**, 6653-6661 (2021).
[25] Q. Q. Yuan, W. J. Cao, M. Valiev, and X. B. Wang,"Photoelectron Spectroscopy and Theoretical Study on Monosolvated Cyanate Analogue Clusters ECX^-•Sol (ECX^- = $NCSe^-$, $AsCSe^-$, and $AsCS^-$; Sol = H_2O, CH_3CN)," J. Phys. Chem. A **125**, 3928-3935 (2021).
[26] Q. Q. Yuan, L. Chomicz-Manka, S. Makurat, W. J. Cao, J. Rak, and X. B. Wang,"Photoelectron Spectroscopy and Theoretical Investigations of Gaseous Doubly Deprotonated 2′-Deoxynucleoside 5′-Monophosphate Dianions," Journal of Physical Chemistry Letters **12**, 9463-9469 (2021).
[27] Q. Q. Yuan, M. Rohdenburg, W. J. Cao, E. Aprà, J. Landmann, M. Finze, J. Warneke, and X. B. Wang,"Isolated $B_2(CN)_6^{2-}$: Small Yet Exceptionally Stable Nonmetal Dianion," Journal of Physical Chemistry Letters **12**, 12005-12011 (2021).
[28] M. Zalibera *et al.*,"Metallofullerene photoswitches driven by photoinduced fullerene-to-metal electron transfer," Chem. Sci. **12**, 7818-7838 (2021).
[29] E. T. Baxter *et al.*,"Functionalization of Electrodes with Tunable $EMIM_xCl_{x+1}^-$ Ionic Liquid Clusters for Electrochemical Separations," Chem. Mat. **34**, 2612-2623 (2022).
[30] W. J. Cao, Z. B. Hu, X. G. Peng, H. T. Sun, Z. R. Sun, and X. B. Wang,"Annihilating Actinic Photochemistry of the Pyruvate Anion by One and Two Water Molecules," J. Am. Chem. Soc. **144**, 19317-19325 (2022).
[31] A. Caruso, X. Y. Zhu, J. L. Fulton, and F. Paesani,"Accurate Modeling of Bromide and Iodide Hydration with Data- Driven Many-Body Potentials," Journal of Physical Chemistry B **126**, 8266-8278 (2022).
[32] K. T. Crampton, A. G. Joly, and P. Z. El-Khoury,"Uncovering surface plasmon optical resonances in nanohole arrays through interferometric photoemission electron microscopy," Appl. Phys. Lett. **120**, 081102 6 (2022).

[33] D. M. Driscoll, R. C. Shiery, M. Balasubramanian, J. L. Fulton, and D. C. Cantu,"Ionic Contraction across the Lanthanide Series Decreases the Temperature-Induced Disorder of the Water Coordination Sphere," Inorg. Chem. **61**, 287-294 (2022).
[34] D. M. Driscoll *et al.*,"Water Defect Stabilizes the Bi^{3+} Lone-Pair Electronic State Leading to an Unusual Aqueous Hydration Structure," Inorg. Chem. **61**, 14987 (2022).
[35] S. Ghosh, H. Agarwal, M. Galib, B. Tran, M. Balasubramanian, N. Singh, J. L. Fulton, and N. Govind,"Near-Quantitative Predictions of the First-Shell Coordination Structure of Hydrated First-Row Transition Metal Ions Using K-Edge X-ray Absorption Near-Edge Spectroscopy," Journal of Physical Chemistry Letters **13**, 6323-6330 (2022).
[36] J. Han, L. Wang, W. J. Cao, Q. Q. Yuan, X. G. Zhou, S. L. Liu, and X. B. Wang,"Manifesting Direction-Specific Complexation in $HFIP_{-H}{\bullet}H_2O_2^-$: Exclusive Formation of a High-Lying Conformation," Journal of Physical Chemistry Letters **13**, 8607-8612 (2022).
[37] M. Hetzert, Q. Q. Yuan, W. J. Cao, X. B. Wang, J. Hempelmann, R. Dronskowski, and U. Ruschewitz,"$Li_2\ SeC_2Se\ {\bullet}2NH_3$: A Crystalline Ammoniate with a $^-Se\text{-}C{=}C\text{-}Se^-$ Dianion," Inorg. Chem. **61**, 18769-18778 (2022).
[38] Y. R. Jiang, Z. J. Cai, Q. Q. Yuan, W. J. Cao, Z. B. Hu, H. T. Sun, X. B. Wang, and Z. R. Sun,"Highly Structured Water Networks in Microhydrated Dodecaborate Clusters," Journal of Physical Chemistry Letters **13**, 11787-11794 (2022).
[39] Y. R. Jiang *et al.*,"Unraveling hydridic-to-protonic dihydrogen bond predominance in monohydrated dodecaborate clusters," Chem. Sci. **13**, 9855-9860 (2022).
[40] L. Kringle, W. A. Thornley, B. D. Kay, and G. A. Kimmel,"Isotope effects on the structural transformation and relaxation of deeply supercooled water," Journal of Chemical Physics **156**, 084501 10 (2022).
[41] S. Makurat, Q. Q. Yuan, J. Czub, L. Chomicz-Manka, W. J. Cao, X. B. Wang, and J. Rak,"Guanosine Dianions Hydrated by One to Four Water Molecules," Journal of Physical Chemistry Letters **13**, 3230-3236 (2022).
[42] A. B. C. Mantilla, C. F. Wang, Y. Gu, Z. D. Schultz, and P. Z. El-Khoury,"Multipolar Raman Scattering vs Interfacial Nanochemistry: Case of 4-Mercaptopyridine on Gold," J. Am. Chem. Soc. **144**, 20561-20565 (2022).
[43] A. C. Morales *et al.*,"Atmospheric emission of nanoplastics from sewer pipe repairs," Nat. Nanotechnol. **17**, 1171-+ (2022).
[44] B. T. O'Callahan, and P. Z. El-Khoury,"A Closer Look at Tip-Enhanced Raman Chemical Reaction Nanoimages," Journal of Physical Chemistry Letters **13**, 3886-3889 (2022).
[45] L. M. Obloy, P. Z. El-Khoury, and A. N. Tarnovsky,"Excited-State-Selective Ultrafast Relaxation Dynamics and Photoisomerization of trans-4,4′-Azopyridine," Journal of Physical Chemistry Letters 10863-10870 (2022).
[46] N. G. Petrik, M. D. Baer, C. J. Mundy, and G. A. Kimmel,"Mixed Molecular and Dissociative Water Adsorption on Hydroxylated TiO2(110): An Infrared Spectroscopy and Ab Initio Molecular Dynamics Study," Journal of Physical Chemistry C **126**, 21616-21627 (2022).
[47] V. Prabhakaran *et al.*,"Integrated photoelectrochemical energy storage cells prepared by benchtop ion soft landing," Chem. Commun. **58**, 9060-9063 (2022).
[48] A. Rodriguez, A. Krayev, M. Velicky, O. Frank, and P. Z. El-Khoury,"Nano-optical Visualization of Interlayer Interactions in WSe_2/WS_2 Heterostructures," Journal of Physical Chemistry Letters **13**, 5854-5859 (2022).

[49] P. Vester *et al.*,"Tracking structural solvent reorganization and recombination dynamics following e^- photoabstraction from aqueous I^- with femtosecond x-ray spectroscopy and scattering," Journal of Chemical Physics **157**, 224201 17 (2022).
[50] C. F. Wang, and P. Z. El-Khoury,"Multimodal (Non)Linear Optical Nanoimaging and Nanospectroscopy," Journal of Physical Chemistry Letters **13**, 7350-7354 (2022).
[51] C. F. Wang, and P. Z. El-Khoury,"Resonant Coherent Raman Scattering from WSe_2," J. Phys. Chem. A 5832-5836 (2022).
[52] C. F. Wang, B. T. O'Callahan, B. W. Arey, D. Kurouski, and P. Z. El-Khoury,"High-Resolution Raman Nano-Imaging with an Imperfect Probe," Journal of Physical Chemistry C **126**, 4089-4094 (2022).
[53] Q. Q. Yuan, W. W. Feng, W. J. Cao, Y. C. Zhou, L. J. Cheng, and X. B. Wang,"Sodium Cationization Enables Exotic Deprotonation Sites on Gaseous Mononucleotides," Journal of Physical Chemistry Letters **13**, 9975-9982 (2022).
[54] F. S. Yang *et al.*,"On-Surface Single-Molecule Identification of Mass-Selected Cyclodextrin-Supported Polyoxovanadates for Multistate Resistive-Switching Memory Applications," ACS Appl. Nano Mater. **5**, 14216-14220 (2022).
[55] K. C. Adamsen *et al.*,"Origin of hydroxyl pair formation on reduced anatase TiO_2(101)," Phys. Chem. Chem. Phys. **25**, 13645-13653 (2023).
[56] W. J. Cao, H. Wen, S. S. Xantheas, and X. B. Wang,"The primary gas phase hydration shell of hydroxide," Sci. Adv. **9**, eadf4309 8 (2023).
[57] P. Z. El-Khoury,"High spatial resolution ambient tip-enhanced (multipolar) Raman scattering," Chem. Commun. **59**, 3536-3541 (2023).
[58] P. Z. El-Khoury,"Tip-Enhanced Raman Chemical and Chemical Reaction Imaging in H_2O with Sub-3-nm Spatial Resolution," J. Am. Chem. Soc. **145**, 6639-6642 (2023).
[59] L. Kringle, B. D. Kay, and G. A. Kimmel,"Dynamic heterogeneity and Kovacs' memory effects in supercooled water," J. Phys. Chem. B **127**, 3919-3930 (2023).
[60] L. Kringle, B. D. Kay, and G. A. Kimmel,"Structural relaxation of water during rapid cooling from ambient temperatures," Journal of Chemical Physics **159**, 064509 11 (2023).
[61] D. Leshchev *et al.*,"Revealing Excited-State Trajectories on Potential Energy Surfaces with Atomic Resolution in Real Time," Angew. Chem.-Int. Edit. **e202304615**, e202304615 (2023).
[62] A. Nimmrich *et al.*,"Solvent-Dependent Structural Dynamics in the Ultrafast Photodissociation Reaction of Triiodide Observed with Time-Resolved X-ray Solution Scattering," J. Am. Chem. Soc. **145**, 15754-15765 (2023).
[63] C. R. O'Connor, M. F. C. Andrade, A. Selloni, and G. A. Kimmel,"Elucidating the water-anatase TiO_2(101) interface structure using infrared signatures and molecular dynamics," Journal of Chemical Physics **159**, 104707 14 (2023).
[64] O. M. Primera-Pedrozo *et al.*,"Influence of surface and intermolecular interactions on the properties of supported polyoxometalates," Nanoscale **15**, 5786-5797 (2023).
[65] M. Reinhard *et al.*,"Ferricyanide photo-aquation pathway revealed by combined femtosecond Kβ main line and valence-to-core x-ray emission spectroscopy," Nat. Commun. **14**, 2443 (2023).
[66] T. J. Summers, J. A. Sobrinho, A. de Bettencourt-Dias, S. D. Kelly, J. L. Fulton, and D. C. Cantu,"Solution Structures of Europium Terpyridyl Complexes with Nitrate and Triflate Counterions in Acetonitrile," Inorg. Chem. **62**, 5207-5218 (2023).

[67] C. F. Wang, A. B. C. Mantilla, Y. Gu, and P. Z. El-Khoury,"Ambient Tip-Enhanced Two Photon Photoluminescence from CdSe/ZnS Quantum Dots," J. Phys. Chem. A **127**, 1081-1084 (2023).
[68] Q. L. Wang, Z. B. Qin, G. L. Hou, Z. Yang, M. Valiev, X. B. Wang, X. F. Zheng, and Z. F. Cui,"Properties of Gaseous Deprotonated L-Cysteine S-Sulfate Anion cysS-SO_3^-: Intramolecular H-Bond Network, Electron Affinity, Chemically Active Site, and Vibrational Fingerprints," Int. J. Mol. Sci. **24**, 1682 11 (2023).
[69] T. Yang, Z. Y. Li, X. B. Wang, and G. L. Hou,"Quantitative Descriptions of Dewar-Chatt-Duncanson Bonding Model: A Case Study of Zeise and Its Family Ions," ChemPhysChem **24**, 7 (2023).

References

[70] Z. P. Li, Y. R. Jiang, Q. Q. Yuan, J. Warneke, Z. B. Hu, Y. Yang, H. T. Sun, Z. R. Sun, and X. B. Wang,"Photoelectron spectroscopy and computational investigations of the electronic structures and noncovalent interactions of cyclodextrin-*closo*-dodecaborate anion complexes χ-CD•$B_{12}X_{12}^{2-}$ (χ = α, β, γ; X = H, F)," Phys. Chem. Chem. Phys. **22**, 7193-7200 (2020).
[71] T. T. Duignan *et al.*,"Quantifying the hydration structure of sodium and potassium ions: taking additional steps on Jacob's Ladder," Phys. Chem. Chem. Phys. **22**, 10641-10652 (2020).
[72] A. Bhattarai, I. V. Novikova, and P. Z. El-Khoury,"Tip-Enhanced Raman Nanographs of Plasmonic Silver Nanoparticles," Journal of Physical Chemistry C **123**, 27765-27769 (2019).
[73] L. Kringle, W. A. Thornley, B. D. Kay, and G. A. Kimmel,"Reversible structural transformations in supercooled liquid water from 135 to 245 K," Science **369**, 1490-1492 (2020).
[74] G. A. Kimmel, M. Baer, N. G. Petrik, J. VandeVondele, R. Rousseau, and C. J. Mundy,"Polarization- and Azimuth-Resolved Infrared Spectroscopy of Water on TiO2(110): Anisotropy and the Hydrogen-Bonding Network," Journal of Physical Chemistry Letters **3**, 778-784 (2012).
[75] M. Tylinski, R. S. Smith, and B. D. Kay,"Morphology of Vapor-Deposited Acetonitrile Films," J. Phys. Chem. A **124**, 6237-6245 (2020).
[76] M. Tylinski, R. S. Smith, and B. D. Kay,"Structure and Desorption Kinetics of Acetonitrile Thin Films on Pt(111) and on Graphene on Pt(111)," Journal of Physical Chemistry C **124**, 2521-2530 (2020).
[77] E. O. Fetisov, C. J. Mundy, G. K. Schenter, C. J. Benmore, J. L. Fulton, and S. M. Kathmann,"Nanometer-Scale Correlations in Aqueous Salt Solutions," Journal of Physical Chemistry Letters **11**, 2598-2604 (2020).
[78] E. Biasin *et al.*,"Femtosecond X-Ray Scattering Study of Ultrafast Photoinduced Structural Dynamics in Solvated $Co(terpy)_2^{2+}$," Phys. Rev. Lett. **117**, 013002 6 (2016).
[79] E. Biasin *et al.*,"Direct observation of coherent femtosecond solvent reorganization coupled to intramolecular electron transfer," Nat. Chem. **13**, 8 (2021).
[80] P. Z. El-Khoury, Y. Gong, P. Abellan, B. W. Arey, A. G. Joly, D. H. Hu, J. E. Evans, N. D. Browning, and W. P. Hess,"Tip-Enhanced Raman Nanographs: Mapping Topography and Local Electric Fields," Nano Lett. **15**, 2385-2390 (2015).
[81] P. Z. El-Khoury, G. E. Johnson, I. V. Novikova, Y. Gong, A. G. Joly, J. E. Evans, M. Zamkov, J. Laskin, and W. P. Hess,"Enhanced Raman scattering from aromatic dithiols electrosprayed into plasmonic nanojunctions," Faraday Discuss. **184**, 339-357 (2015).

[82] P. Z. El-Khoury, D. H. Hu, V. A. Apkarian, and W. P. Hess,"Raman Scattering at Plasmonic Junctions Shorted by Conductive Molecular Bridges," Nano Lett. **13**, 1858-1861 (2013).
[83] P. Z. El-Khoury, and Z. D. Schultz,"From SERS to TERS and Beyond: Molecules as Probes of Nanoscopic Optical Fields," Journal of Physical Chemistry C **124**, 27267-27275 (2020).
[84] C. F. Wang, B. T. O'Callahan, D. Kurouski, A. Krayev, Z. D. Schultz, and P. Z. El-Khoury,"Suppressing Molecular Charging, Nanochemistry, and Optical Rectification in the Tip-Enhanced Raman Geometry," Journal of Physical Chemistry Letters **11**, 5890-5895 (2020).
[85] A. Bhattarai, A. G. Joly, W. P. Hess, and P. Z. El-Khoury,"Visualizing Electric Fields at Au(111) Step Edges via Tip-Enhanced Raman Scattering," Nano Lett. **17**, 7131-7137 (2017).
[86] E. Aprà, A. Bhattarai, K. T. Crampton, E. J. Bylaska, N. Govind, W. P. Hess, and P. Z. El-Khoury,"Time Domain Simulations of Single Molecule Raman Scattering," J. Phys. Chem. A **122**, 7437-7442 (2018).
[87] E. Aprà, A. Bhattarai, and P. Z. El-Khoury,"Gauging Molecular Orientation through Time Domain Simulations of Surface-Enhanced Raman Scattering," J. Phys. Chem. A **123**, 7142-7147 (2019).
[88] P. Z. El-Khoury, and E. Aprà,"Spatially Resolved Mapping of Three-Dimensional Molecular Orientations with ∼2 nm Spatial Resolution through Tip-Enhanced Raman Scattering," Journal of Physical Chemistry C **124**, 17211-17217 (2020).
[89] G. A. Kimmel, Y. T. Xu, A. Brumberg, N. G. Petrik, R. S. Smith, and B. D. Kay,"Homogeneous ice nucleation rates and crystallization kinetics in transiently-heated, supercooled water films from 188 K to 230 K," Journal of Chemical Physics **150**, 204509 204509 (2019).
[90] Y. T. Xu, N. G. Petrik, R. S. Smith, B. D. Kay, and G. A. Kimmel,"Homogeneous Nucleation of Ice in Transiently-Heated, Supercooled Liquid Water Films," Journal of Physical Chemistry Letters **8**, 5736-5743 (2017).
[91] Y. T. Xu, N. G. Petrik, R. S. Smith, B. D. Kay, and G. A. Kimmel,"Growth rate of crystalline ice and the diffusivity of supercooled water from 126 to 262 K," Proceedings of the National Academy of Sciences of the United States of America **113**, 14921-14925 (2016).
[92] R. S. Smith, N. G. Petrik, G. A. Kimmel, and B. D. Kay,"Communication: Proton exchange in low temperature co-mixed amorphous H_2O and D_2O films: The effect of the underlying Pt(111) and graphene substrates," Journal of Chemical Physics **149**, 081104 (2018).
[93] R. S. Smith, R. A. May, and B. D. Kay,"Probing Toluene and Ethylbenzene Stable Glass Formation Using Inert Gas Permeation," Journal of Physical Chemistry Letters **6**, 3639-3644 (2015).

Drawing electronic structure on the nanoscale using switchable molecular interfaces (DE-SC0021950)

Sarah B. King
sbking@uchicago.edu
929 E 57th Street, Chicago, IL 60637

Project Scope Inhomogeneity on the nanoscale is an omnipresent problem in materials for advanced energy technologies. Depending on the degree of variation, and how it effects the electronic structure and properties of a material, the impact of these variations can range from a decrease in the efficiency of an electronic device to a complete misunderstanding of a catalytic mechanism and poor catalytic selectivity. Atomically thin, two-dimensional materials are particularly sensitive to this inhomogeneity problem due to the realities of their synthesis and preparation, yet are also uniquely suited to tuning and healing at the nanoscale level due to their responsiveness to the external environment.[1–3] The long-term goal of the research program is to not only understand how particular structural motifs modify the electronic structure and electronic and phononic dynamics of 2D materials, but also design ways heal or modify these motifs for specific functionality such as directional charge and phonon transport. In the funded project we use time-resolved microscopies to uncover how nanostructures, and their modifications, determine the electronic structure, phonon dynamics, and functionality of two model 2D materials, black phosphorus and indium selenide. Through interfacing 2D materials with photoswitchable molecules we will use patterned light illumination of photoswitchable molecular interfaces to apply local strain or electrostatic doping on 2D materials drawing new electronic structure on the nanoscale and encode charge transport or modify antiferroelectricity in both 2D materials.

Recent Progress We have made progress on the funded project in three main directions: (1) elucidating the nanoscale variation of black phosphorus electronic structure on the nanoscale, (2) demonstrated how structural variation in black phosphorus modifies coherent phonon transport and (3) developed the methodology for imaging antiferroelectric domains in 2D materials and showed the long-range antiferroelectricity of β'-In_2Se_3.

Nanoimaging of the Edge-Dependent Optical Polarization Anisotropy of Black Phosphorus Black phosphorus (BP), a corrugated orthorhombic 2D material, has in-plane optical absorption anisotropy critical for applications, such as directional photonics, plasmonics, and waveguides.[4] Using polarization-dependent photoemission electron microscopy we were able to directly visualize the anisotropic optical absorption of BP. We find the edges of BP flakes have a shift in their optical polarization anisotropy from the flake interior due to the 1D confinement and symmetry reduction at flake edges that alter the electronic charge distributions and transition dipole moments of edge electronic states, confirmed with first-principles calculations. Our work was recently corroborated using edge-dependent photoluminescence imaging where in the work they observed edge-specific excitons of black phosphorus where the symmetry was similarly modified by the confinement of the exciton to the flake edge.[5] These newly observed edge states of black phosphorus create an opportunity for selective excitation of edge states of black phosphorus with polarized light. This work has been published in Nano Letters.[6]

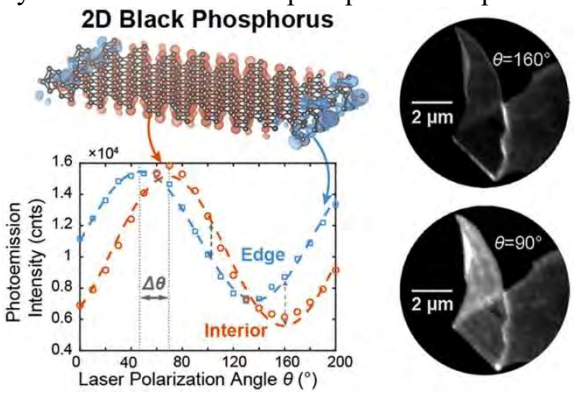

Figure 1 Edges and interior regions of 2D black phosphorus flakes have a pronounced phase shift in their polarization-dependent photoemission electron microscopy intensities enabling selective photoexcitation with specific laser polarizations.

Influence of lattice anisotropy on coherent phonon transport in Black Phosphorus Phonon transport in solids determines how heat can be utilized or dissipated in materials. Conventional methods for investigating phonon transport use experimental techniques that spatially average over material morphology, limiting investigation to macroscopic perturbations to the lattice. However, as electronic devices continue to shrink, material boundaries increasingly contribute to phonon dynamics, which demand experimental methods that can resolve the interplay between intrinsic lattice dynamics and the extrinsic impact of morphology. Using ultrafast electron microscopy we have been able to directly interrogate the phonon dynamics of two-dimensional black phosphorus (BP) on the nanoscale. BP has intrinsic anisotropic phonon transport with distinct phonon velocities along the two principal crystal directions, zigzag (ZZ) and armchair (AC).[7] In our experiments, we directly observe the coherent acoustic phonon (CAP) dynamics and their group velocities as a function of propagation direction. Our experiments confirm previous non-localized measurements of the phonon group velocity along the ZZ and AC directions. However, they also show that edge-launched CAPs which propagate 31° relative to the AC lattice direction have an anomalously low group velocity, significantly lower than the group velocities of the ZZ and AC modes, which deviate from common mode-averaged models that do not account for lattice anisotropy. Using a Gaussian Approximation Potential,[8] a machine learning potential, in calculations with a >8000 atom supercell, we find that an avoided crossing of the transverse acoustic (TA) and longitudinal acoustic (LA) phonon modes driven by lattice corrugation results in the anomalously low LA group velocities we observe in our nanoscale experiments. This suggests that corrugated materials are an ideal model platform to explore morphology and directional control of heat transport, particularly for miniaturized optoelectronic and thermoelectric applications. This work has been submitted and is available on ChemRxiv.[9]

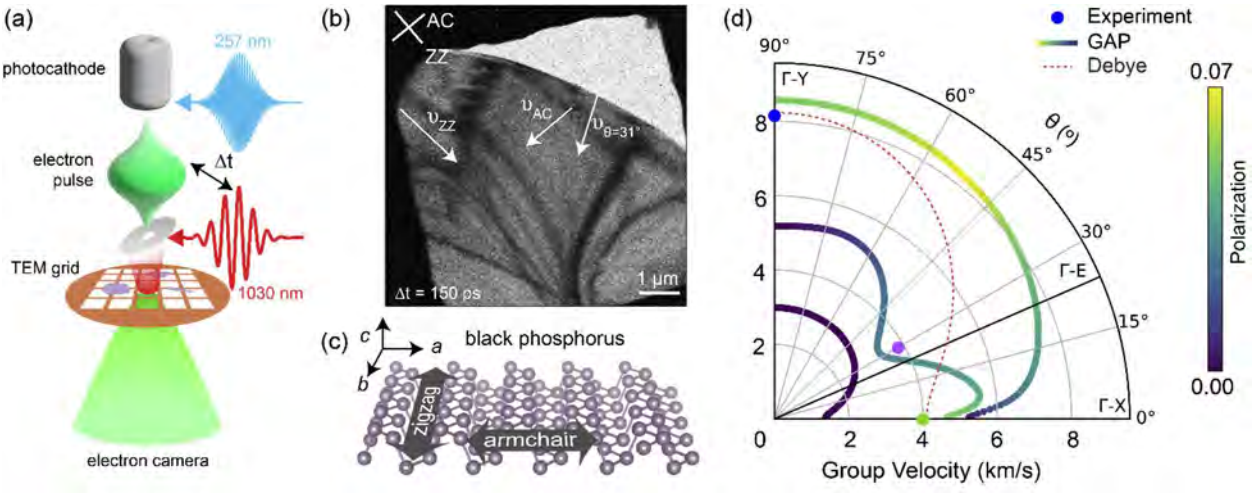

Figure 2 (a) Schematic of the ultrafast electron microscope. (b) A representative TEM bright-field image at a pump probe time delay of 150 ps. (c) crystal structure with the zigzag (ZZ) and armchair (AC) axes labeled. (d) Group velocity of each of the three acoustic phonon modes as a function of angle in real-space, θ, from experimental results and a Debye model.[10,11] The shading of the GAP calculations indicates the degree of polarization of the phonon mode where high polarization indicates a longitudinal phonon mode.

Imaging In-Plane Antiferroelectric domains of β'-In_2Se_3 Measuring the domain structure of in-plane antiferroelectric materials has been notoriously challenging. High-spatial resolution techniques are required making macroscale electrical or spectroscopic techniques unsuitable. While piezo-force-microscopy can image ferroelectric materials, antiferroelectric materials (and nonferroelectrics in general) only have PFM contrast from weak second-order electrostrictive effects, meaning that domain contrast is frequently not

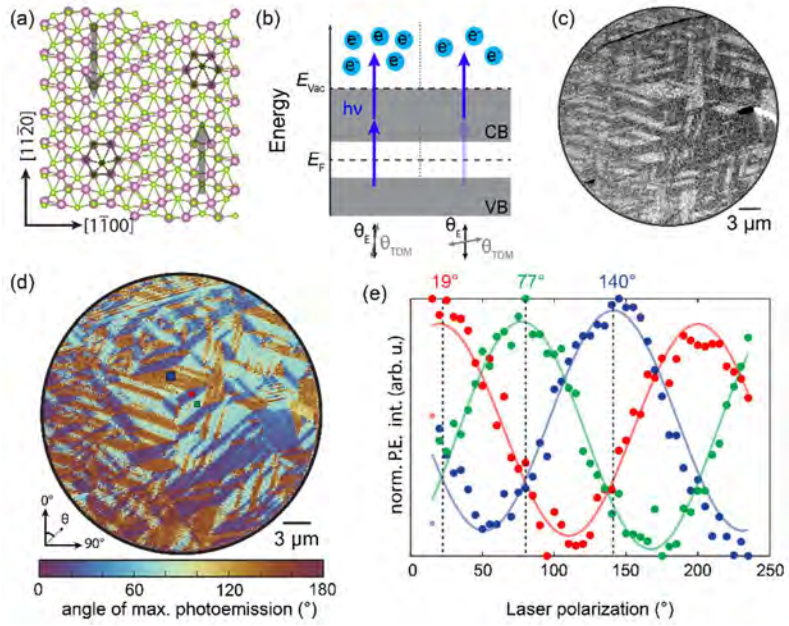

Figure 3 (a) Atomic structure of a single supercell of β'-In_2Se_3. (b) Energy level diagram of polarization-dependent PEEM experiment. Variation in the alignment of the laser polarization with a material's local transition dipole moment results in the variation in the number of electrons photoemitted as a function of space. (c) Difference image from PD-PEEM experiment with 400 nm illumination for 140° - 50° (d) Map of the local transition dipole moment for each pixel in the PEEM data. (e) Photoemission intensity vs laser polarization from the three regions indicated by the colored squares in (d) showing 60° shifts between domains, where 0° is vertical in the plane of the image and positive angles correspond to clockwise rotation.

observed.[12] Even if PFM can observe antiferroelectric domains, the phase contrast cannot be used to determine the directions of antiferroelectric domains and the structural relationships between domains, limiting our experimental capabilities for imaging antiferroelectric domains at both the nano- and mesoscales. In recent work, we have shown that polarization-dependent photoemission electron microscopy can image in-plane antiferroelectric domains on the nanoscale and used that to image the antiferroelectric domain structure of β'-In_2Se_3 across length scales ranging from 10s of nm to 30 μm. We show that the long-range order of β'-In_2Se_3 antiferroelectric domains makes it a good candidate for applications that require robust in-plane antiferroelectric polarization and control. This work is in preparation and will be submitted in the coming weeks.

Future Plans

Ultrafast dynamics on the nanoscale In the coming year our experiments are largely focused on the ultrafast electron dynamics of β'-In_2Se_3 and black phosphorus on the nanoscale. Given the strong spatial variation in the potential energy surfaces of both materials we anticipate significant modification in the ultrafast electron and charge dynamics on the nanoscale in both materials.

Interfacial strain modification Our collaborators in the Levin group at the University of Chicago have already synthesized the spyropyran molecules that we are going to be using for molecularly applied strain to β'-In_2Se_3 and black phosphorus. We have done initial spin-coating and photo-switching experiments but optimizing the molecular addition to 2D materials is going to be an upcoming focus. We have also established a collaboration with Prof. Stephan Wu at the University of Rochester to fabricate macroscale strain devices via overgrowth of a secondary material. We are going to investigate these materials as a possibility for local strain patterning and modification of the properties of β'-In_2Se_3 and black phosphorus.

Peer-Reviewed Publications Resulting from this Project (2021-2023)

Joshi, P.P., Li, R., Spellberg, J.L., Liang, L., and King, S.B. (2022). Nanoimaging of the Edge-Dependent Optical Polarization Anisotropy of Black Phosphorus. Nano Lett *22*, 3180–3186. 10.1021/acs.nanolett.1c03849.

References

1. Das, S., Robinson, J.A., Dubey, M., Terrones, H., and Terrones, M. (2015). Beyond Graphene: Progress in Novel Two-Dimensional Materials and van der Waals Solids. Annu Rev Mater Res *45*, 1–27. 10.1146/annurev-matsci-070214-021034.

2. Raja, A., Chaves, A., Yu, J., Arefe, G., Hill, H.M., Rigosi, A.F., Berkelbach, T.C., Nagler, P., Schüller, C., Korn, T., et al. (2017). Coulomb engineering of the bandgap and excitons in two-dimensional materials. Nat Commun *8*, 15251. 10.1038/ncomms15251.

3. Raja, A., Waldecker, L., Zipfel, J., Cho, Y., Brem, S., Ziegler, J.D., Kulig, M., Taniguchi, T., Watanabe, K., Malic, E., et al. (2019). Dielectric disorder in two-dimensional materials. Nat Nanotechnol *14*, 832–837. 10.1038/s41565-019-0520-0.

4. Liu, H., Du, Y., Deng, Y., and Ye, P.D. (2015). Semiconducting black phosphorus: synthesis, transport properties and electronic applications. Chem Soc Rev *44*, 2732–2743. 10.1039/c4cs00257a.

5. Biswas, S., Wong, J., Pokawanvit, S., Yang, W.-C.D., Zhang, H., Akbari, H., Watanabe, K., Taniguchi, T., Davydov, A.V., Jornada, F.H. da, et al. (2023). Edge-Confined Excitons in Monolayer Black Phosphorus. ACS Nano. 10.1021/acsnano.3c07337.

6. Joshi, P.P., Li, R., Spellberg, J.L., Liang, L., and King, S.B. (2022). Nanoimaging of the Edge-Dependent Optical Polarization Anisotropy of Black Phosphorus. Nano Lett *22*, 3180–3186. 10.1021/acs.nanolett.1c03849.

7. Carvalho, A., Wang, M., Zhu, X., Rodin, A.S., Su, H., and Neto, A.H.C. (2016). Phosphorene: from theory to applications. Nat Rev Mater *1*, 4475 16. 10.1038/natrevmats.2016.61.

8. Deringer, V.L., Caro, M.A., and Csányi, G. (2020). A general-purpose machine-learning force field for bulk and nanostructured phosphorus. Nat Commun *11*, 5461. 10.1038/s41467-020-19168-z.

9. Joshi, P.P., Unruh, D., Gage, T.E., Li, R., Liu, H., Liang, L., Arslan, I., Chan, M.K.Y., and King, S.B. (2023). Anomalous reduction in black phosphorus phonon velocities driven by lattice anisotropy. ChemRxiv. 10.26434/chemrxiv-2023-r0qq2-v2.

10. Chen, Z., Wei, Z., Chen, Y., and Dames, C. (2011). Anisotropic Debye model for the thermal boundary conductance. Phys. Rev. B *87*, 125426. 10.1103/physrevb.87.125426.

11. Tao, Y., Cai, S., Wu, C., Wei, Z., Lu, X., Zhang, Y., and Chen, Y. (2022). Anisotropic phonon transport in van der Waals nanostructures. Phys. Lett. A *427*, 127920. 10.1016/j.physleta.2022.127920.

12. Xu, C., Mao, J., Guo, X., Yan, S., Chen, Y., Lo, T.W., Chen, C., Lei, D., Luo, X., Hao, J., et al. (2021). Two-dimensional ferroelasticity in van der Waals β’-In2Se3. Nat Commun *12*, 3665. 10.1038/s41467-021-23882-7.

Probing Electrolyte Dynamics Near Electrode Surfaces

PI: Amber T. Krummel
Colorado State University, 200 W. Lake Street, Fort Collins, CO 80525
amber.krummel@colostate.edu

1. Project Scope

In order to broadly apply electrification across the chemical industry, an understanding of fundamental physical and chemical processes of electrolytes near electrode surfaces is required. More specifically, work towards understanding how classes of liquid electrolytes support chemical species, catalyst function, and ultimately chemical transformations must be undertaken. The primary goal of this project will be to address the question: How are electrolyte dynamics influenced by external applied biases near electrode surfaces? The completion of this project will produce unique insights and new knowledge of how two classes of electrolytes—organic electrolytes and water-in-salt (WIS) electrolytes—behave near electrode surfaces. Completion of this project will yield the discovery of guiding design principles of electrode/electrolyte pairs that drive specific outcomes in practice. Therefore, the scientific community will be poised to design new complex fluid-electrode systems optimized for specific applications in the energy-water and catalysis science paradigms.

Approach: Two-dimensional infrared (2D IR) spectroscopy and 2D IR imaging will be used to generate a picture of the interplay between electrolyte mixtures and electrodes. 2D IR spectroscopy and 2D IR imaging are promising tools to gain a new vantage point with which to observe fundamental chemical dynamics at play in the complex environment near electrode surfaces. Two classes of electrolytes will be investigated in this project: 1. Organic liquid electrolytes and 2. Water-in-Salt electrolytes. Comparative studies will allow the influence electric fields near electrodes have on electrolyte mixtures to be determined. Molecular details of dissolution processes in model electrochemical cells will be observed. The project will leverage model electrochemical cells designed specifically to allow observation of the dynamics of electrolyte mixtures near electrodes.

2. Recent Progress & Current Efforts

The start date of this project was August 1, 2023. In the past two months we have focused on designing a model organic electrolyte system and a water-in-salt electrolyte system. Measurements of the bulk fluids have been initiated.

3. Future Plans

The first year of this project is focused on using 2D IR spectroscopy to investigate the bulk characteristics of the electrolyte solutions. In addition, we will determine which objective set will be best for our broad bandwidth, tunable, mid-infrared light produced in our recently upgraded 100 kHz 2D IR microscope.

4. Publications

Given the August 1, 2023 start date of this project, no publications have been produced.

Structure and Dynamics of Solvate Ionic Liquid Electrolytes: Experiments, Modeling and Applications in Energy Storage

Award Number: DE-SC0023440

Daniel Kuroda, Louisiana State University (Principal Investigator)
Revati Kumar, Louisiana State University (co-Investigator)
Daniel Abraham, Argonne National Laboratory (National Laboratory Collaborator)

Project Scope

In recent years, the urgent need to reduce our dependence on fossil fuels has led to the rapid rise of the renewable energy sector and its associated technologies, namely rechargeable batteries. The latter have proven to be very useful, but the increasing demand has underlined the need to improve the energy retention performance after several charge/discharge cycles, a better capacity/cost ratio, etc. Until now, the main focus in lithium batteries has been on the electrode components; however, the optimization of the electrolyte is also becoming increasingly important in these battery technologies. One of the problems with electrolytes is that the anion coordination causes the lithium ion to migrate in the opposite direction due to the presence of negatively charged clusters, resulting in less efficient diffusional lithium transport in the electrolyte. To reduce the lithium-anion coordination, the use of solvate ionic liquids has been proposed. Solvate ionic liquids (SILs) are electrolytes with ionic liquid-like properties consisting of a lithium salt and a glyme (oligoether) molecule that forms a complex cation with the lithium.[1, 2] Unlike the typical organic solvents, i.e., carbonates, used in conventional lithium batteries, glyme-based electrolytes are inherently electrochemically stable. In addition to their excellent stability, glymes can be easily manufactured with different numbers of units, allowing us to use the glyme chain length as a tunable parameter to alter the properties of the SIL. Hence, combining glymes of different chain lengths in different ratios offers another tunable handle of the electrolyte properties. Another important component in these electrolytes is the lithium salt. It has been previously shown that fluorinated anions, such as TFSI, FSI and BETI, are particularly stable and form solvate ionic liquids. Hence, fluorinated lithium salts are good candidates for battery electrolytes. Moreover, the utilization of binary salt solutions has proven to be advantageous to overcome the limitations of single-component systems.[3] Finally, the enhanced properties of different SILs can be combined to create mixtures with improved physico- and electro-chemical properties. The ultimate goal, beyond the initial two years of this project, is to determine design principles for optimal battery performance by building machine learning models that combine molecular level data from experiments and simulations with device operando data when using SILs mixtures for lithium batteries.

Recent Progress

Develop a new high conductivity and low viscosity SIL-based electrolyte

This subproject investigates the effect of the composition on SIL models with spectroscopic characterization and computer simulations to relate electrolyte chemistry and structure to the transport of ionic species. In particular, the study focuses on investigating various molecular interactions, such as coulombic and chelation, within glyme-based lithium electrolytes. It was hypothesized that the mixture of SILs should promote the presence of "defects" in the ionic network, resulting in an enhanced ionic conductivity when compared to pure SILs. To test this hypothesis, we measured many mixtures of SILs using differential scanning calorimetry (**Figure 1**). While the pure SILs show distinct phase transitions, the mixtures of SILs do not present the same thermodynamic phase transition, as they behave like glasses when mixed. This result

confirms our hypothesis that the ionic network is severely perturbed by the presence of the second SIL. Moreover, the mixtures have very different conductivities and viscosities (**Figure 1**), indicating that the presence of the second SIL significantly affects the molecular structure of the resulting electrolyte.

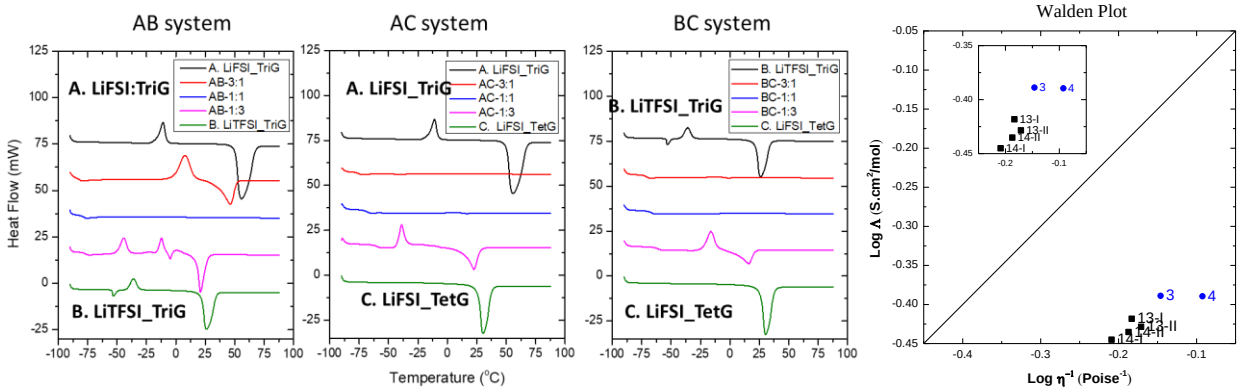

Figure 1. *Differential Scanning calorimetry of a pure SILs and their mixtures. Left panel shows the thermograms of mixtures from mixing only the salts: LiTFSI-triglyme (1:1 molar ratio) and LiFSI-triglyme (1:1 molar ratio). Middle panel shows the thermograms of mixtures from mixing only the solvents: LiFSI-triglyme (1:1 molar ratio) and LiFSI-tetraglyme (1:1 molar ratio). Right panel shows the thermograms of mixtures from mixing both salts and solvents: LiTFSI-triglyme (1:1 molar ratio) and LiFSI-tetraglyme (1:1 molar ratio). Walden plot of viscosity and conductivity for pure SILs (blue circles) and their mixtures (black squares).*

In addition to the real SILs, we are using a model SIL to test the hypothesis that a mixture of SILs should promote the presence of "defects" in the ionic network, resulting in an improved ionic conductivity when compared to pure SILs. To perform this study, we measured many mixtures of model SILs composed of lithium thiocyanate and glymes of different lengths. Our studies reveal, as expected, that the chelating power of the glyme significantly affects the ionic speciation of the compound forming the SIL (**Figure 2**). Furthermore, it is observed that the SIL formed with a mixture of glymes reaches the "ideal" conductivity, while the pure SIL never reaches the ideal conductivity curve (**Figure 2**). We have identified the ionic species, which include ion pairs and aggregates.

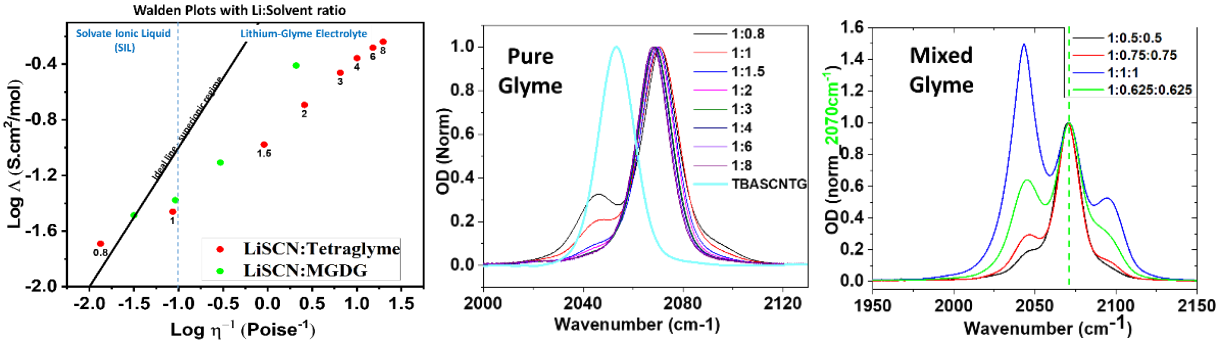

Figure 2. *Left Panel: Walden plot of viscosity and conductivity for SILs composed of a pure tetraglyme (red circles) and 1:1 molar ratio of monoglyme and diglyme mixtures (green circles). Center and right panels: FTIR spectra as a function of the lithium salt concentration for SILs composed of a pure tetraglyme (center) and 1:1 molar ratio of monoglyme and diglyme mixtures (right).*

Development of a new high fidelity classical force field.

We use a joint experimental-molecular simulation based approach to investigate these SILs at the molecular level. To perform accurate molecular simulations on the length and time scales relevant

to the systems, one needs efficient yet accurate force fields. It has been previously shown for other organic electrolytes that of-the-shelf classical force fields do not provide a good representation of lithium systems. As a first step, we tested conventional force fields on data from ab initio molecular dynamics (AIMD) simulations of lithium sulfonylimide in diglyme. The AIMD simulations results shown a Li+ solvation of about four oxygen atoms, as seen from the various radial distribution functions in **Figure 3**. A comparison with a modified classical PCFF force field (which is a class2 force-field that was developed for glymes) reveals a sizeable difference between the classical and AIMD simulations. The PCFF force field does a poor job of recovering the solvation environment around the Li+ ion and gives rise to an overcoordinated Li+ ion. Hence, we have developed a new force field to model the lithium sulfonylimide salts in different glymes using the force matching algorithm on the data from AIMD simulations. The first generation force field, developed using the data on 1.5 M lithium TFSI in diglyme, shows great promise as it is able to capture the solvation environment around the lithium ion. This is evidenced by the various radial distribution functions produced by our newly develop force field in comparison with AIMD and more conventional ones (**Figure 3**). Furthermore, it is transferable to glymes of different chain lengths and salt concentrations, despite being parameterized to data for the 1.5 M sodium sulfonylimide in diglyme system, as it can recover the experimental fraction of bound glymes (see **Figure 3** left panel) as a function of salt concentration (especially at mole fractions of around 0.5, where SIL formation is expected). We are also exploring the different solvation environments around the Li+ ion in the different glymes.

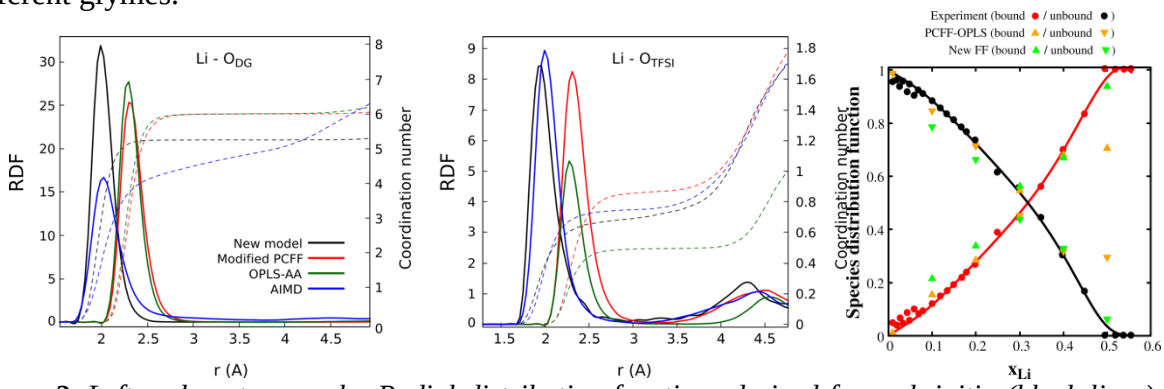

***Figure 3**. Left and center panels: Radial distribution functions derived from ab initio (black lines) and classical (red, green and black lines) molecular dynamics simulations. The panels contains the radial distribution function between the lithium atom and oxygen atom of glymes (left) and between the lithium atom and oxygen atoms of TFSI (middle). (Right) Fraction of bound and unbound glymes as a function of the mole fraction of the salt for the triglyme system.*

Future Plans

Experimental: Our next studies will focus on investigating the effect of mixing more "dissimilar" ions, such as triflate and BETI. In addition, we plan to extend the characterization of the mixtures to their electrochemical properties. Note that these parameters are key to generating observables that can serve as predictors for future multidimensional modeling of the system. In addition, we plan to start measuring some of the "good" SIL electrolyte candidates under operando conditions. Computational: Our next set of studies will focus on the solvation environments in mixed glymes systems at different mole fractions as well as different salt concentrations of the lithium sulfonylimide salts such as those of triflate, BETI etc. Our previous work on sodium-based electrolytes have shown that the cation-anion force field parameters parameterized for one of the sulfonylimides are transferable to other anions that are chemically similar.[4] We will also validate the transferability in these Li+ systems as well. These simulations will give us a detailed picture

of the distribution of solvation environments in these systems. We will connect these results to the experimental observations, including DSC thermograms, electrochemical and physicochemical properties, and device level information.
To get a more complete picture of the effect of solvation on battery performance, our next set of studies will concentrate on elucidating the electrolyte degradation mechanisms. To this end, we will carry out ab initio molecular dynamics/metadynamics simulations in which an additional electron is introduced to mimic the reducing environment near the electrode in the actual battery.

As previously mentioned in the introduction, the ultimate goal is to design batteries with improved performance metrics. This is beyond the two-year scope of the project. We plan to combine the data at different scales, from the molecular to the mesoscale and ultimately to the device level, to develop an explainable machine learning framework for predicting the optimal electrolyte composition for these battery technologies. We also plan to extend this formalism to other non-aqueous electrolytes relevant to the energy sector.

References

1. Eyckens, D.J. and L.C. Henderson, *A Review of Solvate Ionic Liquids: Physical Parameters and Synthetic Applications.* Frontiers in Chemistry, 2019. **7**: p. 263.
2. Mandai, T., et al., *Criteria for solvate ionic liquids.* Physical Chemistry Chemical Physics, 2014. **16**(19): p. 8761-8772.
3. Xia, L., et al., *Lithium Bis(fluorosulfony)imide-Lithium Hexafluorophosphate Binary-Salt Electrolytes for Lithium-Ion Batteries: Aluminum Corrosion Behaviors and Electrochemical Properties.* Chemistryselect, 2018. **3**(7): p. 1954-1960.
4. Li, K., et al., *Effect of anion identity on ion association and dynamics of sodium ions in non-aqueous glyme based electrolytes-OTf vs TFSI.* Journal of Chemical Physics, 2021. **154**(18).

Peer-Reviewed Publications Resulting from this Project (2021-2023)

None

Photo-Electrochemistry of Hybrid Nanoelectrodes

Christy F. Landes[1] and Stephan Link[2]

[1]*Department of Chemistry, Department of Electrical and Computer Engineering*
University of Illinois Urbana-Champaign, Champaign, IL 61820 USA
[2]*Department of Chemistry, Department of Electrical and Computer Engineering*
Rice University, Houston, TX 77005 USA
cflandes@illinois.edu, slink@rice.edu

U.S. Department of Energy, Office of Science, Basic Energy Sciences, CPIMS Program
Award No. DE-SC0016534

1. Program Scope

The goal of this project is to electrochemically create plasmonic-polymer heterostructures and characterize how energy and charge transfer between the constituents can be regulated and hence exploited to execute unique photo-electrochemical transformations. One challenge for exploiting localized surface plasmon resonances (LSPR) for energy harvesting is the active modulation of plasmonic characteristics over a wide range as the LSPR is typically fixed when size, shape, elemental composition, and dielectric environment are determined. To overcome this challenge, diverse external stimuli, such as electrochemical potentials and photothermal heating, can be applied to plasmonic nanoparticles, while further incorporation of functional soft materials to produce plasmonic nanohybrids can be exploited for enhanced plasmonic modulation at the nanoscale interface. However, understanding the underlying mechanisms that govern active plasmon modulation, especially occurring at heterojunctions, is complicated by competing processes such as photothermal heating, interfacial charge vs. resonance energy transfer (RET), conformational changes of interfacial adsorbates, and electrochemical charge density tuning. To address these challenges, well-defined model systems are needed, giving us a way to understand the interplay between these factors and how to control them. The central hypothesis of this study is that diverse external stimuli applied to plasmonic nanoparticles and their hybrids will enable us to distinguish underlying mechanisms for plasmon energy conversion. State-of-the-art single-particle and single-molecule spectroscopic techniques were employed to read out the optical properties of hybrid nanoelectrodes. Further, redox events associated with molecular affinity or electric field hot spots, which are typically localized to dimensions much smaller than the diffraction limit of light, were investigated. Specifically, the following three aims are pursued:

1) Understand mechanistic principles that control RET efficiency in hybrids of plasmonic nanoelectrodes/acceptor molecules under applied electrochemical potentials.

2) Determine the factors that govern plasmon modulation by electrochemical potentials

when analyzing photoluminescence (PL) vs. dark-field scattering (DFS).

3) Modulate the plasmon response of hybrid nanoelectrodes with stimuli-responsive polymers.

2. Recent Progress

Hybridizing plasmonic particles with a diverse range of molecular/polymer acceptors provides an alternative route for energy dissipation at the nanoscale soft interface, creating an enhanced modulation driven by external-stimuli. As a model system, we used methylene blue (MB) as its redox chemistry is suitable for investigating optical modulation when applying an electrochemical potential. We investigated the RET pathway for MB on single AuNRs and studied plasmon damping that was dependent on the electrochemically controlled chemical states of MB (**Reference 1**). Through single-particle spectro-electrochemistry we manipulated the AuNR Fermi level and controlled the redox chemistry between MB and leucomethylene blue (LMB) at negative and positive bias, respectively. Based on this system, we revealed that the plasmonic signal modulation by consecutive sweeping of an applied voltage bias was enhanced in the presence of MB compared to its absence, indicating the generation of an additional damping factor (**Figure 1a**). Statistical quantification through correlation measurements between the plasmonic modulation depths (−ΔΓ) for bare AuNRs and AuNRs-MB provided clear evidence for this additional damping pathway, importantly showing that the change in plasmon linewidths –ΔΓ depends on initial resonance energy E_{res} (**Figure 1b**). In this study, because each spectrum was correlated (charge density tuning, before and after MB adsorption, and redox reaction), extra damping contributions by MB adsorbates could be systematically quantified from the total plasmon linewidth Γ. η_{RET} calculated from the additional linewidth broadening as a function of initial E_{res} revealed that plasmon damping was maximized when the E_{res} of the AuNRs overlapped with the π→π* transition dipole energy of MB (**Figure 1c**), confirming RET as the additional damping mechanism. Furthermore, the applied potentials gave rise to dipole coupling at lower energies through

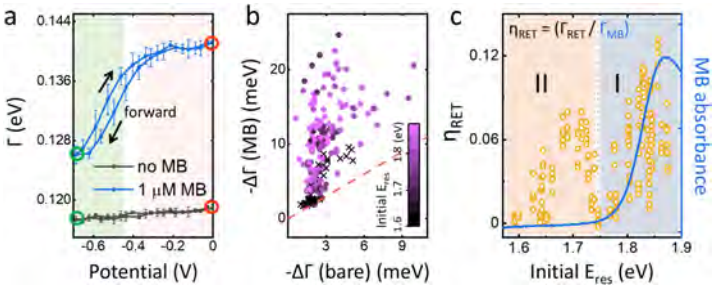

Figure 1. (a) Mean changes between cyclovoltammetry traces and associated standard deviations in linewidth Γ for a single bare AuNR (grey) and AuNR-MB (blue) as a function of applied potential. Green and red shaded regions correspond to redox potentials for LMB and MB, respectively. (b) Correlations between the plasmonic modulation depths of -ΔΓ for bare AuNRs and AuNRs-MB. Red dashed lines indicate a 1:1 correlation, visualizing no difference. (c) η_{RET} calculated from Γ_{RET} / Γ_{MB} as a function of initial resonance energy E_{res}, showing two distinct regions for increased η_{RET}. Region I (blue) and Region II (orange) indicate RET to MB monomer and oligomers, respectively.

electrochemical oxidative oligomerization of MB, as confirmed by time dependent-density functional theory calculations of vertical transition energies for MB monomers and its oligomers.

We additionally studied plasmonic modulation with single-particle PL and DFS during electrochemical charge density tuning (**Reference 2**). The PL spectrum arises as the light that is absorbed by the AuNR creates hot carriers that relax though nonradiative and radiative decay, creating intraband and interband PL modes at lower and higher energies, respectively (**Figure 2a**). Applying a stepwise potential, analysis of the single-particle photon counts vs. time traces shows that PL is more strongly modulated than DFS, suggesting the presence of an additional mechanism (**Figure 2b**). The modulation in DFS can be fully understood through a charge density-dependent elastic scattering cross-section. Intriguingly, we found that changes in the PL of a single AuNR during charge density tuning of intraband PL can be attributed to changes in the Purcell factor enhancing PL as well modifications to the adsorption cross-section. In addition, modulation of interband PL provides an extra constructive observable, enabling the establishment of dual channel sensing (PL and DFS) in spectro-electrochemical measurements.

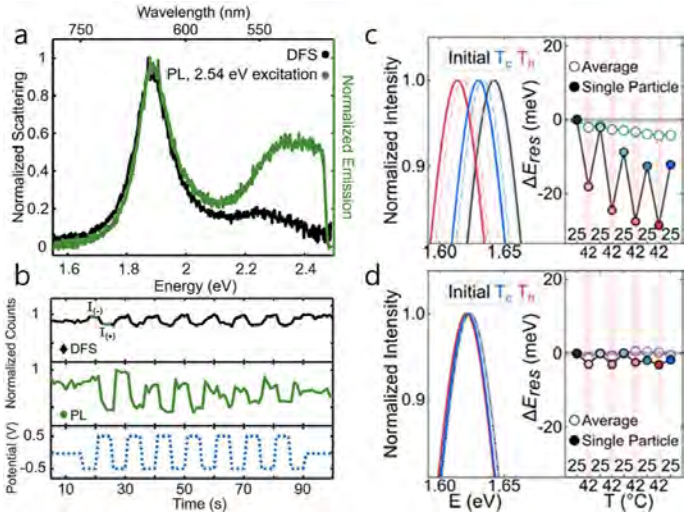

Figure 2. (a) DFS (black) and PL (green) of a single AuNR in 100 mM $NaNO_3$ at open circuit potential. (b) DFS (top, black) and PL (middle, green) photon counts vs. time traces during the application of a step wise potential cycling from −0.5 to 0.5 V vs. a quasi-reference electrode (bottom, blue). Lorentzian fits of the longitudinal plasmon resonance of representative single particles, and corresponding ΔE_{res} (filled circles, right) for (c) thin and (d) thick polymer shells at successive cold and hot temperatures, T_c and T_h. The solid lines indicate the initial (black), final T_c (25°C, blue), and final T_h (42°C, red) measurements. The dashed lines indicate the intermediate T_c and T_h measurements. The average ΔE_{res} of all single particles (open circles, right) is included for comparison. The vertical red bars indicate T_h.

Finally, we investigated temperature-induced polymer dynamics for thermoresponsive poly(N-isopropylacrylamide) (pNIPAM) coated on AuNRs (**Reference 3**). A coil-to-globular phase transition at elevated temperatures was read out through a few meV spectral shifts of the plasmon resonance due to the polymer's refractive index difference associated with its change in conformation (**Figure 2c**). Repeated heating and cooling, achieved through optically heating the surrounding water with a 1064 nm laser, furthermore allowed us to capture hysteresis in polymer expansion and collapse. We observed a broad polymer collapse distribution with a thicker polymer shell and attributed

it to a two-step phase transition likely due to a density gradient in the polymer network (**Figure 2d**). This work confirms the sensitivity of single-particle DFS to report on small changes in polymer conformation and its ability to resolve microscopic heterogeneity.

The common important progress in all these projects is that if interparticle and intraparticle heterogeneity using single nanoparticle spectroscopies can be resolved, it is possible to elucidate the underlying mechanisms that govern active tuning of the LSPR in hybrid nanoelectrodes. The outcomes gained from this work will lead to the rational design of optimized plasmonic photo-electrocatalysts.

3. Future Plans

The main focus of future studies is to understand the role of interfacial RET in plasmon-assisted chemistry at plasmonic-soft material interfaces, enabling efficient utilization of the plasmon energy. Based on the overall mechanistic insight into RET from our previous projects, we will further study polymerization following plasmon excitation while applying electrochemical potentials, as a means to finally carry out important plasmon-enhanced photocatalytic chemical reactions. One of our model reactions will be the polymerization of MB on single AuNRs. We will tune the RET efficiency by changing the energetics of the constituent materials. We hypothesize that efficient energy transfer opens an alternative pathway for MB oxidation by generating excitons in MB adsorbates, which are required for its polymerization through N-to-ring connection under an applied potential. We expect that the RET-enhanced MB polymerization will result in selective growth onto individual nanoelectrodes, and lower the anodic threshold needed to polymerize the MB subunits. This insight will inform reaction conditions to enable optimal plasmonic and polymeric design parameters for scalable hybrid materials, and eventually highly efficient energy conversion from photons through plasmons and excitons to nanoscale chemistry.

4. Peer-Reviewed Publications Resulting from this Project (2021-2023)

1) H. Oh, E. K. Searles, S. Chatterjee, Z. Jia, S. Lee, S. Link, C. F. Landes *Energy Transfer Driven by Electrochemical Tuning of Methylene Blue on Single Gold Nanorods*. ACS Nano 17, 18280–18289 (2023).

2) E. K. Searles, E. Gomez, S. Lee, B. Ostovar, S. Link, C. F. Landes *Single-particle photoluminescence and dark-field scattering during charge density tuning.* J. Phys. Chem. Lett. 14, 318–325 (2023).

3) C. Flatebo, C. Dutta, B. Ostovar, S. Link, C. F. Landes *Heterogeneity and Hysteresis in the Polymer Collapse of Single Core–Shell Stimuli-Responsive Plasmonic Nanohybrids.* J. Phys. Chem. C 125, 18270–18278 (2021).

Understanding and Controlling Photoexcited Molecules in Complex Environments

DE-SC0020121
David Limmer
University of California, Berkeley
dlimmer@berkeley.edu

1. Project Scope

The major goals of this project concern the study of nonadiabatic dynamics in complex, condensed phase environments. Specifically, we aim to develop a perspective and accompanying set of tools to predict the efficiencies, yields and mechanisms of photoinduced reactions. Progress in this area is historically complicated by the lack of formal and numerical tools capable of describing small, nonequilibrium and quantum systems generally, and especially when there exists a hierarchy of time and energy scales characterizing their dynamics. The specific goals below address both of these points by synergistically building numerical tools to study concrete chemical systems, and using those tools to benchmark and hypothesis test simplifying theories.

The first goal is to develop effective models for condensed phase quantum dynamics that are accurate and provide fundamental insight into diverse sets of problems. Our effort here is aimed at making physically motivated simplifications to reduce complex systems into simple representations, and to propose equations of motion that tractable and physically consistent thermodynamic constraints. Simple representations are deduce and derived by considering natural locality and energetic scales. Effective equations of motion employ such compact representations and unite them with descriptions of additional environmental degrees of freedom. The result is a compromise between exact quantum mechanical evolution with explicit wavepacket propagation or electron correlation for some degrees of freedom with quantum master equation models for the environment that obey weak coupling and Markovian approximations consistently.

The second goal is to develop importance sampling algorithms for nonadiabatic and nonequilibrium processes. These will be used synergistically with the effective models for condensed phase quantum dynamics developed in the first goal. The basis for these algorithms is transition path sampling, which has been widely used in simulations of thermal reactions in condensed phases to provided assumption free calculations of rate constants, and importantly to admit systematic understanding of the mechanisms of reactions. Their use away from equilibrium has been recently pioneered, and their extension into fundamental quantum dynamical processes has been limited. This is because the initial algorithms required detailed balance dynamics, which is not satisfied away from equilibrium or in many existing approximation to quantum dynamics. We aim to develop generalizations of transition path sampling algorithms for studying rare nonadiabatic dynamics like those associated with rare relaxation pathways during photoisomerization or improbable energy transfer routes in couple chromophores. These will be based on stochastic unravellings of quantum master equations.

2. Recent Progress.

Quantum rate theory. We have developed a method of calculating rates and detailing reaction pathways in weakly coupled open quantum systems we call quantum transition path. Quantum transition path theory generates an ensemble of reactive trajectories for a quantum system, each trajectory consisting of a series of jumps between energy eigenstates, with the committor, the

probability to complete the reaction, assigned to each eigenstate. This allows us to identify the jump between two eigenstates when the committor exceeds fifty percent, the transition eigenstates, as a quantum equivalent to the classical transition state. We applied quantum transition path theory to investigate the dependence of conical intersection dynamics on the coupling between diabatic electronic states [1]. Conical intersections, where the Born-Oppenheimer approximation breaks down necessitating quantum mechanical treatment, are critical components of photoswitches. They provide a means for ultrafast relaxation and facilitate thermal isomerization. By identifying ensembles of barrier crossing pathways and transition eigenstates, we found that, when the diabatic electronic states in our model were weakly coupled, the thermal barrier crossing reaction was dominated by deep tunneling mechanisms. At large coupling, the barrier crossing reaction was dominated by traversing around the conical intersection. The latter mechanism was, unsurprisingly, associated with a higher rate. A similar change in regime in relaxation mechanisms following vertical excitation was observed when increasing diabatic electronic coupling. Given weak coupling, the system committed to relaxing into one of two metastable wells of the conical intersection early in evolution due to dephasing effects. Given strong coupling, the system committed due to dissipation, with the final decision made at the height of the barrier. Larger diabatic coupling resulted in a higher photoyield, implying a tradeoff. Larger photoyield is achievable by increasing diabatic coupling, but the rate of thermal isomerization also increases.

Quantum transition path theory also allowed us to investigate polaritonic systems, whose nature remains a subject of debate, elucidating a possible explanation for rate enhancements and suppressions observed in experiment [2]. Experiments have shown that, when the natural frequency of a dark microcavity matches the bond frequency of molecules inside that cavity, bond breaking reaction rates may be enhanced or suppressed. By identifying the dominant reaction pathways in a model polariton system and inspecting the transition eigenstates, we found that resonance between the vacuum photon mode and vibrational mode resulted in transition eigenstates with mixed light-matter character. These states interacted differently with the thermal bath, resulting in suppression of the barrier crossing reaction. This mechanism is entirely a quantum dynamical phenomenon, which explains why it has not been identified in classical studies and highlights the importance of applying quantum methods when attempting to understand and manipulate reactions dependent on polaritonic effects.

Chiral induced spin selectivity. We have studied photo-induced electron transfer processes in complex environments employ suitably adapted quantum master equations. First we studied a phenomena known as chirality induced spin selectivity [3,4]. Specifically, we proposed a mechanism by which spin-polarization can be generated dynamically in chiral molecular systems undergoing photoinduced electron transfer. The proposed mechanism explains how spin-polarization emerges in systems where charge transport is dominated by incoherent hopping, mediated by spin-orbit and electronic exchange couplings through an intermediate charge transfer state. We derive a simple expression for the spin polarization that predicts a non-monotonic temperature dependence, consistent with recent experiments, and a maximum spin-polarization that is independent of the magnitude of the spin-orbit coupling. We validated this theory using approximate quantum master equations and the numerically exact hierarchical equations of motion. A subsequent study demonstrated that spin recombination could transiently produce a spin polarization, but only if though a process mediated by an intervening bridge. Super-exchange mechanisms that recombine radical pairs by contrast do not produce a spin polarization.

Energy transfer and nonphotochemical quenching in natural light harvesting. We have made significant progress learning how to decode nonadiabatic dynamics through a new experimental technique, two-dimensional electronic-vibrational spectroscopy (2DEV). 2DEV spectroscopy has been recently developed by my colleague at Berkeley, Graham Fleming, and has emerged as an experimental technique that can directly observe the correlated motion of electronic and nuclear degrees-of-freedom. This has shown great promise in uncovering mechanisms of photoisomerization and energy transfer dynamics. We studied the role of vibronic coupling mechanisms in a model energy transfer system through simulations of 2DEV spectroscopy [5,6]. We considered two forms of nonadiabatic dynamics, through the consideration of energetic electron-phonon coupling and additionally Hertzberg-Teller coupling. In simulations of the 2DEV spectra we found a means of uncovering the impact of vibronic coupling on energy transfer dynamics. We expanded these generic insights into a novel understanding the mechanistic function of a natural light-harvesting system, light-harvesting complex II (LHCII), where vibronic signatures were suggested to be involved in energy transfer. In this comparison, we directly assign the vibronic coupling mechanism in LHCII as arising from Herzberg-Teller activity and show how this coupling modulates the energy transfer dynamics in this photosynthetic system.

More detailed studies of vibrationally assisted energy transfer dynamics requires accurate and computationally affordable methods. We recently developed a method for simulating exciton dynamics in protein-pigment complexes, including the effects of charge transfer as well as radiative processes [7]. The method combines the hierarchical equations of motion (HEOM), which are used to describe quantum dynamics of excitons exactly, and the Nakajima-Zwanzig quantum master equation, which is used to describe slower charge transfer and radiative processes. As an example, this combined HEOM/QME is used to study the charge transfer quenching processes in LHCII, a protein postulated to control non- photochemcial quenching in many plant species. Using the HEOM/QME approach, we find good agreement between our calculation and experimental measurements of the LHCII excitation lifetime. Furthermore our calculations reveal that the exciton energy funnel plays an important role in determining quenching efficiency in LHCII, a conclusion we expect to extend to other proteins which perform excitation quenching.

Iin collaboration with my colleague at Berkeley, Graham Fleming, we also studied how quenching processes are dynamically controlled using phenomenological rate equations [8,9]. To do so, we developed a formal response theory for actinic light conditions on photosynthetically active organisms, predicting non-photochemical quenching responses that agreed well with experiments. In the alga Nannochloropsis oceanica we observed an ability to respond rapidly to sudden increases in light level which occur soon after a previous high light exposure. This ability implies a kind of memory. In a follow up study to our initial efforts, we explored the xanthophyll cycle in N. oceanica as a photoprotective memory system. By combining snapshot fluorescence lifetime measurements with a biochemistry-based quantitative model we showed that both short-term and medium-term “memory” arises from the xanthophyll cycle. In addition, the model enabled us to characterize the relative quenching abilities of the three xanthophyll cycle components. Given the ubiquity of the xanthophyll cycle in photosynthetic organisms, we expect the model developed will be of utility in improving our understanding of vascular plant photoprotection with important implications for crop productivity.

4. Future Plans.

Our future plans concern two major directions. First, we aim to continue developing quantum transition path theory and transition path sampling for use in non-adiabatic reactions. We have begun generalizing the concept of a commitment probability to instances where quantum interference plays a role. This requires lifting some of the approximations that have been used in our initial formulations. In particular, we have to relax the secular approximation that decouples coherences and populations. Using partially secularized master equations offer a simple means of doing this. We will aim to use this perspective to uncover novel coherent control schemes for photochemistry. Second, we have undertaken more molecular studies in spin-orbit mediated electron transfer. Specifically, we have parameterized fully atomistic models of donor-acceptor complexes in explicit solution to study the detailed roles of inner- and outer-sphere contributions to these processes.

5. Publications.

1. M. C. Anderson, A. J. Schile, and D. T. Limmer. "Nonadiabatic transition paths from quantum jump trajectories." *The Journal of Chemical Physics* 157, no. 16 (2022).

2. M. C. Anderson, E. J. Woods, T. P. Fay, D. J. Wales, and D. T. Limmer. "On the mechanism of polaritonic rate suppression from quantum transition paths." *Journal of Physical Chemistry Letters*, 14, 30, 6888–6894 (2023)

3. T. P. Fay, and D. T. Limmer. "Spin selective charge recombination in chiral donor–bridge–acceptor triads." *The Journal of Chemical Physics* 158, no. 19 (2023).

4. T. P Fay, and D. T. Limmer. "Origin of chirality induced spin selectivity in photoinduced electron transfer." *Nano letters* 21, no. 15 : 6696-6702 (2021)

5. E. A. Arsenault, A. J. Schile, D. T. Limmer, and G. R. Fleming. "Vibronic coupling in light-harvesting complex II revisited." *The Journal of chemical physics* 155, no. 9 (2021).

6. E. A. Arsenault, A. J. Schile, D. T. Limmer, and G. R. Fleming. "Vibronic coupling in energy transfer dynamics and two-dimensional electronic–vibrational spectra." *The Journal of chemical physics* 155, no. 5 (2021).

7. T. P. Fay, and D. T. Limmer. "Coupled charge and energy transfer dynamics in light harvesting complexes from a hybrid hierarchical equations of motion approach." *The Journal of Chemical Physics* 157, no. 17 (2022).

8. A. H. Short, T. P. Fay, Thien Crisanto, J. Hall, C. J. Steen, K. K. Niyogi, D. T. Limmer, and G. R. Fleming. "Xanthophyll-cycle based model of the rapid photoprotection of Nannochloropsis in response to regular and irregular light/dark sequences." *The Journal of chemical physics* 156, no. 20 (2022).

9. A. H. Short, T. P. Fay, T. Crisanto, R. Mangal, K. K. Niyoga, D. T. Limmer, and G. R. Fleming. "Kinetics of the Xanthophyll Cycle and its Role in the Photoprotective Memory and Response." *Nature Communications,* in press (2023).

Tailoring the selective transport pathway of rare earth elements in solid ionic channels guided by in situ characterization and predictive modeling

DE-SC0022231
Chong Liu (chongliu@uchicago.edu), University of Chicago
George Schatz (g-schatz@northwestern.edu), Northwestern University
Matthew Tirrell (mtirrell@uchicago.edu), University of Chicago
Hua Zhou (hzhou@anl.gov), Argonne National Laboratory

Project Scope

This project aims to understand and control the transport behavior in confinement using rare earth elements (REEs) as model systems. We propose to build two-dimensional solid ionic channels with controllable dimensions and chemistry to modulate the desolvation, coordination, and transport of rare earth ions based on their differences in Lewis acidity and ionic radius. There are two key aspects in understanding the transport of rare earth ions. The first is to create a precise model to extract the molecular level binding configuration and transport pathway. The second is to unveil the emerging behaviors of rare earth ions and water in confinement (such as cooperative ion transport and pairing). We aim to gain a holistic picture of ion transport in confinement by connecting the thermodynamics and kinetics of binding in single flakes to the transport behavior in a single channel and in a macroscopic membrane with an ensemble of channels. This understanding will allow us to achieve selective transport by design using synthetic tools.

Recent Progress

Probing and manipulating the transport of rare earth ions in 2D solid-state ionic channels

The long-range confinement in rigid solid ionic channels, with confinement dimensions at the Angstrom scale and material dimensions at tens to hundreds of nanometers, could induce coupling and amply the thermodynamic and kinetic energy differences among incorporated species.

The Liu group uses synthetic tools to construct 2D solid ionic channels and probe the behavior of ion and water in such confinement via correlative characterization. First, hydrated layered MnO_2 was selected as one of our model solid ionic channels. This is because buserite MnO_2 can provide the optimal confinement dimension (free spacing of ~6.8 Å from the interlayer lattice spacing of ~9.6 Å), which is comparable to or smaller than the first hydration shell diameter of rare earth ions. The hard base nature of the channel chemistry from the terminating oxygen can provide a strong affinity to REEs. We find that different REE ions can induce different solid-state phase transformations in MnO_2, balancing dehydration and coordination, and can be divided into two groups.[1] Group I (La^{3+} to Nd^{3+}) expands the buserite phase to a new water-rich phase with an interlayer spacing of ~11.1 Å, while Group II (Eu^{3+} to Yb^{3+}) maintains the buserite phase with an interlayer spacing of ~9.7 Å, and Sm^{3+} is on the border with an interlayer spacing of ~10.0 Å. These results are in quantitative agreement with the results of density functional theory calculations of the Schatz Group. It is interesting that lanthanides prefer to interact with water in its first shell rather than the MnO_2 layers (Figure 1). The significantly different structural responses promote separation across Group I and Group II lanthanides, preferring Group II elements due to

the enlarged dehydration energy barriers and unfavorable coordination for Group I REEs entering and residing in a narrower channel that is occupied by Group II REEs. Importantly, to induce structural features for separation among Group I lanthanides, we designed a pinning strategy to use co-ions to fix MnO_2 at the buserite phase with narrower interlayer spacing during the entire ion transport pathway of REEs via electrochemical intercalation. The pinning was proven effective in increasing the enrichment factor by ~ 3-fold.

The dimension and chemistry of the 2D solid ionic channels are critical and unique for governing the transport behavior of ions and water molecules. Therefore, the Liu and Tirrell Groups developed synthetic tools aiming to build a library of building blocks using MoS_2-based materials for 2D solid ionic channels. We target to build channel dimensions ranging from Angstroms to nanometers using small molecules, oligomers, and polymers as spacers. This bottom-up strategy allows us to connect the thermodynamics and kinetics of a single flake to a single channel and, finally, to an ensemble of channels. For acetic acid functionalized MoS_2 (MoS_2-COOH) channels, a strong interplay among REE ions is discovered where single element uptake shows a monotonic increase with atomic number; however, a volcano shape uptake trend is observed for REEs with competition in mixtures, indicating change in the entrance and binding energies for minor ions by dominating ions.[2]

Computation and modeling for the binding and transport of rare earth ions

The Schatz group is involved in electronic structure, molecular dynamics and other calculations to study lanthanide ions interacting with the layered materials with the goal of understanding structural and energetic factors that determine ion uptake and transport. This year, we primarily focused on lanthanide diffusion through MoS_2 membranes that are functionalized with acetate, and in the uptake of lanthanides by MnO_2 layered materials (Figure 1).[1-2] As a side project, we collaborated with a group in Korea to study the transport of ions through peptide-based nanotubes to study the relationship between potential of mean force (PMF) results and molecular dynamics results in determining ion transport.

To study the separation of lanthanides within MoS_2-COOH membranes, we have developed an all-atom model of the 2D bilayer channel, including explicit water and ions and where interactions are based on empirical potentials from the literature. To validate the model, we performed a series of thermodynamic integration (TI) and umbrella sampling simulations to obtain the hydration free energy (HFE) and the PMF for lanthanide cations, the results of which are consistent with experimental measurements. Subsequently, we simulated ion transport from the feed into the channel by applying high pressure to a piston wall. Notably, the flux of cations into the permeate

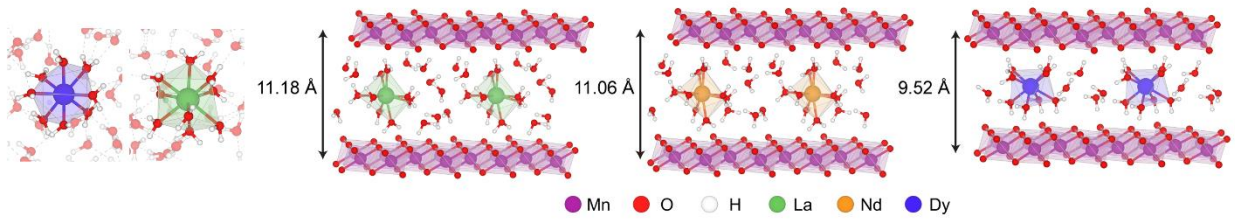

Figure 1. Coordination configuration of REE ions in bulk water and in 2D MnO_2 solid ionic channels.

accurately reproduced the experimentally observed volcano-shaped behavior of lanthanide cations where Sm^{3+} is the peak. Furthermore, our investigations indicate that Sm^{3+} ions with moderate hydration free energy and intermediate affinity for channel interaction exhibit the smallest dehydration volume during the permeation process, resulting in the highest observed permeability. This provides constructive guidance for the precise design of selective 2D materials.

We have used density functional theory to elucidate the molecular and electronic structure of hydrated lanthanides confined within the MnO_2 interlayer region, choosing La^{3+} and Nd^{3+} to represent light lanthanides and Dy^{3+} as a heavy lanthanide. The results show that the optimized structures of La and Nd prefer to form a water-rich phase of hydrated MnO_2, while Dy prefers the buserite phase, and our interlayer spacings and water coordination numbers are in agreement with experiment. Calculated binding energies for the lanthanide ions show systematically stronger binding as atomic number increases, a result that is consistent with measured uptake results.

Correlative Characterization

Zhou made significant progress on advanced synchrotron surface-sensitive X-ray characterizations of rare earth ion adsorption on the MoS_2 monolayer model system, including grazing incidence X-ray absorption spectroscopy (GIXAS) and surface X-ray diffraction (SXRD) measurements. As demonstrated in Figure 2, SXRD technique crystal truncation rod (CTR) method has been favorably applied to surface functionalized MoS_2 monolayer samples to determine those surface group distributions. Our CTR measurements and phase-retrieval based analysis have derived the total electron density profile, including surface-functionalized group and surface-adsorbed REEs, such as the cysteine group and attached Sm^{3+} ion, as illustrated. Furthermore, we have also utilized the GIXAS technique to investigate the surface coordination environment of thiol functionalized monolayer MoS_2, which can be combined with SXRD results to build an accurate surface structure model to understand the REE transport processes.

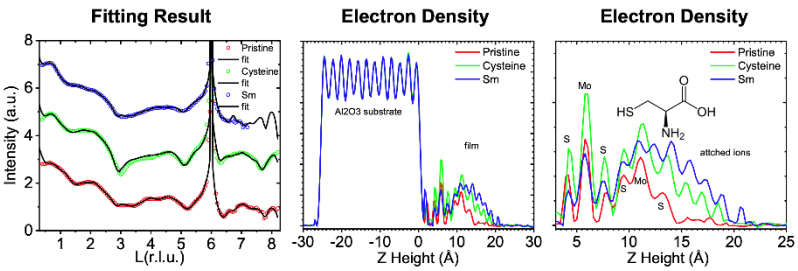

Figure 2. SXRD characterization of MoS_2 monolayer with REE adsorption. Left, CTR scans of bare, cysteine decorated and Sm^{3+} adsorbed MoS_2 monolayer grown on Al_2O_3 substrate. Middle, Total electron density profiles of the respective samples. Right, Zoom-in view of surface region of the electron density profiles.

Liu and Tirrell have also developed anomalous X-ray diffraction (AXRD) and anomalous small angle X-ray scattering (ASAXS) characterization. AXRD was proved to be able to distinguish between ion storage sites in 3D confined Prussian Blue Analogues, and ASAXS was demonstrated to provide chemical, structural, and spatial information simultaneously. Combined with synchrotron X-ray diffraction, absorption, and atomic resolution transmission electron microscopy (TEM), we aim to detail the binding and transport in confinement.

Future Plans

The Liu group will keep expanding the family of oxide- and sulfide-based 2D solid ionic channels and probing the effects of channel dimension, interface chemistry, and interlayer species on the transport properties of water and ions.[3] Liu will also build devices for single channel characterization and transport measurement. The single channel will be fabricated on SiN TEM grid with a window area of tens of microns. Channel materials will be transferred to the window for both material characterization and ion transport measurement. This device allows us to resolve the atomic resolution spatial distribution of rare earth ions and their location correlations in competition.

The Tirrell group will investigate the effect of charge distribution (especially the pairing of positively and negatively charged functional groups) on REE ion uptake in bulk polymer matrix and confinement.

For the Schatz group, further work will be done with polarizable force fields for the MD calculations, and we will consider extending the MD calculations to consider other 2D channel materials, such as lanthanide uptake in V_2O_5, which is an important layered material alternative to MnO_2. In addition, Schatz will use electronic structure calculations to study binding energy changes associated with electrochemical intercalation in redox active membranes.

Zhou will perform resonant anomalous CTR scans to acquire element specific REE ion distribution to systematically quantify the magnitude of REE ion binding with the functionalized group (e.g., sulfur or others) on the MoS_2 basal plane. Moreover, we will utilize the quick GIXAS capability at NSLS-II to measure under wet conditions to obtain more accurate local coordination data in the upcoming beamtime runs. The in-parallel quantitative comparison with theoretical simulations is our ongoing effort with the Schatz group.

References

1. S. Zou, W. C. Jeon, M. Wang, Y. Han, G. Yan, G. T. Hill, H. Zhou, G. C. Schatz, C. Liu. Pinning angstrom-size channel for separation of rare earth elements. Submitted.
2. M. Wang, Q. Xiong, N. H. C. Lewis, M. Wang, O.-S. Lee, G. Yan, D. Ying, Y. Han, F. Shi, H. Zhou, G. C. Schatz, C. Liu. Lanthanide transport in angstrom-scale MoS_2-based two-dimensional channel. Submitted.
3. Y. Han, G. T. Hill, P. Smeets, X. Hu, G. Yan, S. Zou, F. Shi, H. Zhou, C. Liu. Uncovering the predictive pathways of lithium and sodium interchange in layered oxides. Under review.

Peer-Reviewed Publications Resulting from this Project (Project start date: 09/2021)

Namho Kim Ji Hye Lee, Yeonho Song, Jeong-Hyung Lee, George C. Schatz, Hyonseok Hwang. Molecular dynamics simulation study of the protonation state dependence of glutamic acid transport through a cyclic peptide nanotube. J. Phys. Chem. B, 127, 6061-72 (2023).

Qiming He, Yijun Qiao, Carlos Medina Jimenez, Ryan Hackler, Alex B. F. Martinson, Wei Chen, Matthew V. Tirrell. Ion Specificity Influences on the Structure of Zwitterionic Brushes. Macromolecules, 56, 1945−1953 (2023).

Elucidating the Mechanisms of Formation of Zeolites Using Data-Driven Modeling and Experimental Characterization

DE-SC0023213 (previously DE-SC0020201)

Valeria Molinero[1] (valeria.molinero@utah.edu)
Subramanian K.R.S. Sankaranarayanan[2] (skrssank@uic.edu)
Jeffrey D. Rimer[3] (jrimer@central.uh.edu)

[1]Department of Chemistry, The University of Utah, Salt Lake City, UT 84112. [2]Department of Mechanical and Industrial Engineering, University of Illinois Chicago, IL 60607. [3]Department of Chemical and Biomolecular Engineering, University of Houston, Houston, TX 77204

Project Scope.

Zeolites are the main solid catalysts in the chemical industry and also used extensively as adsorbents and detergent builders. These porous silicate crystals have an outstanding number of polymorphs: 255 realized to date and 300,000 more proposed. The topological diversity of zeolites is at the core of their expanding use as shape-selective catalysts and adsorbents. It is also the source of the most enduring challenge in zeolite synthesis: how to selectively produce one among the many competing crystals. Organic molecules are used as structure-directing agents (SDA) in the synthesis of silica zeolites. The premise is that molecules that fit tightly into the pores stabilize the crystals, promoting their formation. However, the same SDA can result in zeolites with various sizes and dimensionalities of pores upon changes in temperature, ratio of silica to organics, and even water content in the synthesis mixture. The diversity of outcomes indicates that stabilization of the pores by SDA cannot predict the crystal produced in the synthesis. To date, the molecular mechanisms by which organic SDAs direct the crystallization towards a specific zeolite polymorph are not known. Understanding these mechanisms is key to realize new zeolites for catalysis and separations and is the focus of this project. Our overarching goal in this project is to synergistically integrate experimental characterization and synthesis of zeolites, deep learning, and molecular simulations to elucidate the molecular processes involved in the formation and transformation of zeolites and their interfaces.

Recent Progress.

1. Development of models and methods.

1.1. Development of all-atom silica force-fields based on long- and short-ranged interactions.

We developed and deployed a reinforcement learning (RL) approach based on a tree search and operating in a continuous action space (Manna et al. *Nature Communications* 2022). We use that approach to find optimal potential parameters or coefficients concurrently trained to multiple different sets of target silica properties of several crystalline polymorphs Traditionally, these searches are time-consuming, and do not scale well with the search dimensionality. To address this challenge, we introduce a multi-reward RL approach to train a silica model based on the long-range BKS functional form as well as the short-range Soules potential. Our all-atom ML-BKS based on a combination of coulomb and short-ranged two-body interactions concurrently captures the structure, energetics, and density of 21 polymorphs of silica, including 17 zeolites, and the equation of state, and elastic constants of quartz. We perform a comprehensive comparison of ML-

BKS on several crystalline and amorphous properties and demonstrate that our model outperforms several previous well-studied empirical models in capturing the experimental structure and properties of silica polymorphs and amorphous silica (Koneru et al. *nPJ Computational Materials* (2023)).

The Soules potential offers a more efficient formulation than BKS *via* shorter-range two-body interactions. We machine-learned the Soules parameters (ML-Soules), following the approach developed for ML-BKS. We achieved significant improvement in energetic predictions but observed minor improvement in Si-O-Si angular properties. To address this issue, we are evaluating Tersoff formalism that have explicit 3-body dependence and developing an in-house Symbolic Regression workflow to identify and introduce additional 2-body and 3-body terms that can capture the angular variations in the silica polymorphs.

1.2. Development of coarse-grained models for zeolite synthesis.

The formation of silica zeolites involves hydrolysis and condensation reactions that drive the polymerization of silicates in the presence of water and ions. The polymerization drives the demixing of a hydrated silica phase, within which the zeolite crystals nucleate. That process involves barriers due to chemistry (catalyzed by hydroxide) and potentially barriers for nucleation, making the modeling of the whole process impossible even with advance sampling methods (each opening and closing of the bonds is a rare event). This issue has stalled the development of force fields to model the polymerization and crystallization involved in zeolite synthesis. As the evolution of the reaction is orthogonal to the reaction coordinate of the phase transition, we address this challenge by modeling silica as a monatomic bead, without explicit O atoms, which enables orders of magnitude faster reconstruction than the silica network, compared to experiments.

We developed the reactive coarse-grained (Rx-CG) TS+W model, that represents silica, SDA and water by single particles that interact through short-range anisotropic interactions (Dhabal et al. *Journal of Physical Chemistry C* (2021)). TS+W is the first model that captures the three fundamental steps of hydrothermal synthesis of zeolites: (1) demixing of the initial aqueous solution of the silica source and SDA through polymerization of silica, (2) crystallization of the zeolite from the resulting hydrated amorphous phase, and (3) dehydration of the zeolite at temperatures above those of HS and below the one of melting of the crystal.

As we have previously demonstrated that mesophases that result from the frustrated attraction between the cationic SDAs and anionic silicates can be part of the free energy landscape in the synthesis of zeolites, we developed an implicit solvent reactive coarse-grained model (implicit Rx-CG) with tunable mesophase stability to investigate the nucleation pathway of zeolite Z1 with respect to mesophase stability and synthesis temperature (Bertolazzo et al. *Journal of Physical Chemistry C* 126, 3776-3786, 2022). The implicit Rx-CG model can stabilize a wide range of zeolites through changes in the structure directing agent and its ratio to silica. Moreover, it predicts relative energies of zeolites comparable to those reported in experiments. To determine the relative stability of possible competing zeolites, we evaluate the energy of Silicalite-1, BEA, AFI, CHA and AST in the implicit solvent model model and compare with the relative energies reported in experiments. The level of agreement in the difference in energy between zeolites is comparable to DFT, i.e. slightly underestimated when compared to the experiment.

1.3. Graph attention neural network fingerprinting workflow for classification of zeolites and mesophases during their nucleation and growth.

One of the challenges of studying the mechanisms of formation of zeolites in simulations is the detection of the crystals as they emerge from the amorphous precursors. We introduce a new fingerprinting method that learns the graphical and structural features of a crystal network through a graph convolutional (GCN) architecture with attention to the environments around an atom based on their proximity. Characterization of zeolitic frameworks and their evolution in molecular simulations of synthesis mixtures is essential to provide key insights on the role of local subcritical networks in nucleation pathways and on inter-zeolite transformations. CEGANN performs accurate classification and is effective in distinguishing the zeolite nucleus from the amorphous phase during the formation of zeolites. CEGANN successfully characterizes the amorphous, mesophase and crystalline phases individually, and accurately detects the transition between phases along simulations (Banik et al. *npj Computational Materials* (2023))

2. Mechanisms of synthesis of zeolites.

2.1. Influence of mesophase stability on the nucleation of a zeolite in model systems.

Zeolites and mesoporous silicas form under comparable conditions of synthesis, and in some cases the two phases are observed at the same conditions. Metastable or unstable mesophases can arise in the free energy landscape of synthesis of zeolites due to frustrated attraction between the silicates and organic structure directing agents (SDA). We used molecular simulations with the Rx-CG models and nucleation theory to investigate whether these mesophases could facilitate the nucleation and polymorph selection of zeolites by providing a pre-ordering of silica and the SDA that would diminish the barrier for nucleation of the porous crystal. We found that mesophases can occur and decrease the nucleation barrier for the zeolite, resulting in multi-step non classical mechanisms of nucleation. However, our analysis demonstrated that mesophases facilitate nucleation only at relatively low driving forces compared to those under the conditions of synthesis of zeolites in laboratory experiments (Bertolazzo et al. *Journal of Physical Chemistry C* (2022))

2.2. Mechanisms of nucleation of zeolites.

The hydrothermal synthesis of zeolites involves the polymerization of silica to produce ~5-10 nm disordered precursors that evolve into a “secondary amorphous phase” with order and solubility intermediate between that of the zeolite and primary amorphous phase. The origin and structure of this “secondary amorphous phase” have been long-standing puzzles. We used nucleation theory with experimental literature data to compute the barriers for nucleation and critical crystal size. We found that at temperatures of hydrothermal synthesis the nucleation barrier is comparable to the thermal energy and the critical nucleus for the formation of the zeolite contains ~3 SiO2 units, i.e. not enough to distinguish between crystal polymorphs. The negligible barriers for nucleation lead to spinodal-like crystallization to produce multiple tiny zeolitic crystallites that compete to grow inside each precursor nanoparticle. We term this disordered arrangement of competing crystallites the “zeolitic mosaic”. Our analysis suggests that amorphous precursors are close to their glass transition temperature, resulting in extremely slow dynamics of the restructuring of the silica network that controls the crystallization rate. The combination of glassy dynamics and spinodal-like crystallization explains the very slow and seemingly continuous evolution of the nanoparticles from amorphous to single crystal zeolite and reconciles why a first-order

crystallization transition appears as a continuous development of structural motifs. (Bertolazzo et al. *Journal of Physical Chemistry Letters* (2022).

Our molecular simulations of zeolite synthesis with our Rx-CG models are consistent with the theoretical predictions. The simulations reproduce the polymerization of silica in the presence of the SDA to produce amorphous glassy precursors that develop multiple small crystallites of zeolite (the structure we dubbed the zeolitic mosaic) that slowly coarsens ordering the channels and producing nanozeolites. Our simulations indicate that Consistent with the experiments, our simulations show that embryonic zeolites that do not appear crystalline in XRD have pore size distribution almost indistinguishable from the crystalline ones, which explains their catalytic activity.

2.3. Finding the smaller zeolite nanoparticle size that could be synthesized.

How small can a zeolite be and still keep the open framework structure that gives it its selectivity? We addressed this question using molecular simulations with the Rx-CG model and thermodynamic analysis. We showed that amorphous precursors as small as 4 nm can crystallize zeolites, in agreement with recent experiments. Interfacial forces dominate the structure of smaller particles, resulting in size-dependent compact isomers that have ring and pore distributions different from open framework zeolites. The instability of zeolites smaller than 4 nm precludes a classical mechanism of nucleation from solution – a conclusion that we have reached also through the direct study of the mechanism of nucleation using molecular simulations (Dhabal et al. *Angewandte Chemie International Edition* (2022))

2.4. Mechanisms of growth of zeolites.

Zeolites with one-dimensional channels and large pores have been suggested to have excellent coking properties. However, their slow synthesis hinders their application in large industrial processes. We investigated the mechanism of growth of zeolite SSZ-24 (AFI) using laboratory synthesis, high-resolution imaging, molecular simulations, and computer vision. Our transmission Electron Microscopy (TEM) reveals that the nascent crystals are rounded, and they develop anisotropic shape -longer along the direction of the 1D pores- in the later stages of synthesis. Our large-scale molecular simulations of growth of AFI from the amorphous precursors explain those results, demonstrating that at low crystallization driving force the AFI crystals grow preferentially along the channels, while at high driving force they grow equivalently in all directions. We use computer vision to generate simulated TEM images from the simulations that have excellent agreement with those obtained in the experiments. We are currently investigating the molecular mechanisms of growth of AFI from the amorphous precursor and from solution, which are important at different stages of the synthesis.

3. Zeolite-zeolite interfaces and interzeolite transformations.

Zeolite-zeolite develop in the formation of intergrowths (stacking disordered materials featuring alternating layers of different zeolites) as well as during interzeolite transformation through cross-nucleation of one zeolite on the surface of another during seeded synthesis or spontaneously in a multi-stage synthesis process. We address interzeolite transformations through an integrated approach involving experimental synthesis and characterization, molecular simulations, and search algorithms. Our focus has been on the cross-nucleation of zeolites CHA, MWW and AFI, which are structurally distinct in the dimensionality and order of the channels and their structural

building blocks, but are all synthesized with the same structure directing agent, N,N,N-trimethyl-1adamantammonium (TMAda).

3.1. Emergence of MWW from CHA.

We examined in laboratory experiments a newly discovered interzeolite transformation in borosilicate growth media involving the initial synthesis of zeolite CHA in the presence of TMAda. Parametric analysis revealed synthesis conditions where CHA undergoes partial interconversion to MWW. Powder X-ray diffraction patterns of solids extracted at periodic times of hydrothermal treatment reveal that interzeolite conversion is not complete, and reaches a point where a binary mixture of CHA and MWW is obtained. Scanning electron microcopy images of solids extracted at periodic synthesis times show that MWW crystals seemingly emerge from the center of CHA crystals. This poses an intriguing fundamental question: is there a potential epitaxial relationship between zeolite frameworks CHA and MWW that drives this structural transition? These questions will be explored computationally in this next year of the project.

3.2. Cross nucleation between zeolites CHA and AFI.

The use of seeds of zeolite CHA has been recently shown to be effective at decreasing the synthesis time for AFI. We achieved for the first time an interzeolite transformation using molecular simulations: the cross-nucleation of AFI' on CHA. AFI' shares with AFI the size and order of the 1D channels. We find that the structural commonalties between the (100) planes of these zeolites strongly promote cross-nucleation. Epitaxy is manifested in the regular orientation of the emerging crystal's channels relative to the seed crystal's pores and a promotion of the nucleation rate. When the cross nucleation occurs at the CHA-amorphous interface, we find that CHA and AFI are connected by an ordered interfacial transition layer that does not have the order of either zeolite. The simulations reveal that the interactions governing intergrowths involve those between the silica in the frameworks and not those between the SDA particles. We expect a variety of pure and non-pure silica zeolite combinations to meet this criterion, suggesting a diverse landscape of topology combinations between zeolites, that we will explore with by combining all-atom modeling and machine learning methods (see below).

3.3. Optimization of the synthesis of CHA and AFI.

We investigated the conditions of laboratory synthesis of the CHA – AFI system, focusing on establishing an understanding under what synthesis conditions each zeolite framework crystallizes. To this end, we developed an experimental workflow involving synthesis and characterization of CHA and AFI to complement the simulation studies and explore previously undiscovered relationships between structurally similar zeolite frameworks. We successfully synthesized zeolite SSZ-13 (CHA type) using TMAda as SDA, following protocols previously reported by Rimer. We modulated the TMAda:SiO_2 molar ratio and synthesis time to optimize the synthesis recipe for highly crystalline CHA-type zeolite, obtaining a fully crystalline product, as evidenced by PXRD. We employed a seed-assisted approach using CHA crystals to significantly reduce the crystallization time of AFI. The PXRD reveals peaks corresponding to both CHA and AFI phases (with AFI as the dominant phase). Based on the results of our simulations, we posit that the binary mixture contains intergrowths between CHA and AFI, which will be analyzed in the future using more advanced characterization techniques (e.g., electron microscopy).

3.4. Interface optimization to understand interlayer growth in zeolites.

Predicting compatibility of zeolite/zeolite interfaces has long remained a challenging problem. The phase space of possible interfacial configurations is huge especially when the unit cell sizes modeling the interfaces grow larger. We recently introduced the CASTING ML workflow, an RL-based scalable framework for crystal structure, topology, and potentially microstructure prediction. CASTING employs an reinforcement learning-based continuous search space decision tree (MCTS -Monte Carlo Tree Search) algorithm with three important modifications (i) a modified rewards scheme for improved search space exploration (ii) a "windowing" or "funneling" scheme for improved exploitation and (iii) adaptive sampling during playouts for efficient and scalable search. We demonstrate the accuracy, speed of convergence, and scalability of CASTING to discover new metastable crystal structures and phases that meet the target objective, using a set of representative examples ranging from metals such as Ag to covalent systems such as C and multicomponent systems. We are extending the CASTING workflow to search for zeolite/zeolite interfaces and guide the experimental search of IZT. Our initial efforts involve deploying CASTING with the machine-learned all-atom models of silica to explore phase space and minimize interface energy and strain in zeolite crystals.

Future Plans.

1. To elucidate the interplay between glassy dynamics, negligible nucleation barriers, and nanoconfinement in the development of crystallinity in precursor nanoaggregates. We will investigate the synthesis of selected zeolites through synergistic combination of experiments, molecular simulations, data science analysis, and computer vision. On the experimental side, we will focus on establishing detailed kinetic phase diagrams that systematically map the synthesis conditions leading to pure phases CHA, MWW and AFI. These zeolites have distinct building units and dimensionality of the pores but are all synthesized with the same structure-directing agent (SDA), TMAda. On the simulations side, we have been successful in synthesizing AFI' (which subtly differs from AFI in the conformation of hexagons tiling its pores) and will investigate its mechanisms of formation from silica-TMAda aggregates at various conditions of driving force, determined by the temperature and ratio of silica to SDA in the precursor aggregates.

2. To determine whether the organization of SDA in dense precursors of zeolite synthesis encodes the selection of the zeolite polymorph. We will pursue the identification of computational synthesis conditions that lead to competition of AFI and MWW and use the competition as testing ground for our machine learning methods to identify and classify distinct amorphous orders in the precursors. The competing polymorph model with be used to study polymorph selection through neuroevolutionary learning. Our preliminary efforts have focused on interfacing the "Learning to Grow" L2G workflow developed by Whitelam at TMF with LAMMPS to facilitate exploration of synthesis variables in polymorph selection. As an initial test, we have deployed the L2G-LAMMPS workflow to identify time-dependent synthesis protocols that allow for polymorph control in carbon. We will extend this workflow to study polymorph selection in silica zeolites and zeolitic MOFs.

3. To investigate the classical and non-classical molecular mechanisms of growth of zeolites from solution. We will investigate the growth of AFI' zeolite at late conditions of synthesis, where the nucleation has been completed and the crystals grow by attachment of oligomers from solution and nanoparticles at various stages of crystallization. We will address the mechanisms of growth from these dilute solutions, with emphasis on how the zeolite interface develops when the

oligomers do not have the order of building blocks of the growing zeolite. We will also initiate the study of growth by amorphous and partially crystallized nanoparticles, to understand how are the processed and incorporated into the growing crystal.

4. To control and predict cross-nucleation between zeolites. We will explore experimental combinations of inorganic and organic structure-directing agents through the guidance of modeling that identifies molecules with both high and moderate selectivity for AFI, MWW and CHA. We will then examine the mechanisms of zeolite crystallization through time-resolved studies, focusing on the pathways leading to zeolite intergrowth structures. We anticipate that regions of overlapping phase boundaries will provide optimal conditions for achieving intergrowth structures. The impact of seeding will also be assessed to determine if interzeolite transformations can lead to unique zeolite structures. Collectively, these findings will be used in combination with ML methods with the accurate force fields we have developed for silica in year 1, to predict the feasibility of cross-nucleation between pairs of zeolites and to assess whether intergrowths can connect through matching surfaces or through an interfacial transition layer (ITL). The simulations and data science analyses will focus on assessing plausible molecular mechanisms that explain the emergence of MWW from the CHA cubes as well as continuing the development of interface optimization methods to be able to predict the structure of the ITL when it forms and weigh its cost through the use of the accurate silica force fields we developed already.

5. Optimization of models using symbolic regression. Our work to-date has focused on exploring physics-based models of silica and demonstrated that while improved predictions can be obtained *via* reparameterization using ML workflows, there is still a ceiling limit that is dictated by the pre-defined functional forms. We seek to address this by implementing Symbolic Regression to discover physically meaningful corrections to the functional forms of inter-atomic potentials (delta learning) discussed in the previous sections. During the training process, SR does an unconstrained search on the function space spanned by a collection of given function building blocks, e.g., mathematical operators, analytic functions, material property variables, constants, etc., to find the most appropriate solution (with minimum training error). Traditionally, this search is guided by evolutionary methods *i.e.* genetic programming, but improved optimization schemes, for instance, Monte Carlo tree search (MCTS), can also be used. Our preliminary work in this area shows significant promise: using Cu as a representative system, we show that one can obtain significantly improved predictions in energies and forces in the far-from-equilibrium configurations using the SR obtained functional forms. We are further developing our workflow to focus on multi atomic system such as those of silica, where we are extending the delta learning concepts to explore new improved functional forms for Si-Si, Si-O and O-O interactions. Advances in symbolic regression with three body forms are also key to develop a new generation of high fidelity reactive coarse-grained models with which to investigate the synthesis of a broader range of zeolites.

Publications from this project, 2021-2023:

- Aditya Koneru, Henry Chan, Sukriti Manna, Troy Loeffler, Debdas Dhabal, Andressa A. Bertolazzo, Valeria Molinero and Subramanian Sankaranarayanan. ***Multi-Reward Reinforcement Learning Based Development of Inter-atomic Potential Models for Silica***. *nPJ Computational Materials*, 9 (1) 125 (2023)

- Suvo Banik, Debdas Dhabal, Henry Chan, Sukriti Manna, Mathew Cherukara, Valeria Molinero, Subramanian KRS Sankaranarayanan. *CEGANN: Crystal Edge Graph* ***Attention Neural Network for multiscale classification of materials environment****. npj Computational Materials*, 9 (1) 23 (2023)
- Debdas Dhabal, Andressa A. Bertolazzo and Valeria Molinero. ***What is the Smallest Zeolite that Can Be Synthesized?*** *Angewandte Chemie International Edition*, 61 (29) e202205095 (2022)
- Andressa A. Bertolazzo, Debdas Dhabal, and Valeria Molinero. ***Polymorph selection in zeolite synthesis occurs after nucleation***. Journal of Physical Chemistry Letters 13 (4), 977-981 (2022)
- Andressa A. Bertolazzo, Debdas Dhabal, Laura JS Lopes, Samantha K Walker and Valeria Molinero. ***Unstable and metastable mesophases can assist in the nucleation of porous crystals.*** *Journal of Physical Chemistry C* 126 (7), 3776-3786 (2022)
- Koneru, A.; Batra, R.; Manna, S.; Loeffler, T. D.; Chan, H.; Sternberg, M.; Avarca, A.; Singh, H.;Cherukara, M. J.; Sankaranarayanan, S. K. R. S. ***Multi-reward Reinforcement Learning Based Bond-Order Potential to Study Strain-Assisted Phase Transitions in Phosphorene****. Journal of Physical Chemistry Letters*, 13 (7), 1886 (2022)
- Manna, S.; Loeffler, T. D.; Batra, R.; Banik, S.; Chan, H.; Varughese, B.; Sasikumar, K.; Sternberg, M.; Peterka, T.; Cherukara, M. J.et al. ***Learning in continuous action space for developing high dimensional potential energy models****.* Nature Communications, 13 (1), 368 (2022)
- Leonid Pereyaslavets, Ganesh Kamath, Oleg Butin, Alexey Illarionov, Michael Olevanov, Igor Kurnikov, Serzhan Sakipov, Igor Leontyev, Ekaterina Voronina, Tyler Gannon, Grzegorz Nawrocki, Mikhail Darkhovskiy, Ilya Ivahnenko, Alexander Kostikov, Jessica Scaranto, Maria G Kurnikova, Suvo Banik, Henry Chan, Michael G Sternberg, Subramanian KRS Sankaranarayanan, Brad Crawford, Jeffrey Potoff, Michael Levitt, Roger D Kornberg, Boris Fain. ***Accurate determination of solvation free energies of neutral organic compounds from first principles.*** *Nature Communications* 13 (1), 1-7 (2022)
- Srinivasan, S.; Batra, R.; Chan, H.; Kamath, G.; Cherukara, M. J.; Sankaranarayanan, S., ***Artificial Intelligence Guided De Novo Molecular Design targeting COVID-19.*** *ACS Omega*, 6, 19, 12557–12566 (2021)
- Debdas Dhabal, Andressa A. Bertolazzo, Valeria Molinero. ***Coarse-grained model for the hydrothermal synthesis of zeolites.*** *Journal of Physical Chemistry C* 125 (48), 26857-26868 (2021)

Disentangling nonlinear spectroscopy to control nonequilibrium energy transport

Award Number: DE-SC0024154
PI: Andrés Montoya-Castillo
Department of Chemistry, University of Colorado Boulder
Cristol Chemistry, 215 UCB, Boulder, CO 80309
Andres.MontoyaCastillo@colorado.edu

Program Scope: This proposal aims to develop and apply the next generation theoretical and simulation tools required to simulate and elucidate the nonlinear spectra that reports on energy and charge flow in complex molecular systems. Our research will yield insights into how specific molecular motions can be used to dynamically tune bright and dark transitions to endow commonly used chemical building blocks in energy conversion systems – whether natural or artificial – with controllable optical properties. This will ultimately enable us to develop design principles for the manipulation and control of commonly used and easy to manipulate chemical building blocks, such as porphyrins. Importantly, our results will also delineate how to tune the optical and transport properties of chromophores included in larger chemical scaffolds that can facilitate directional energy transfer.

To achieve this, we will develop and apply methods to:
(1) Predict nonlinear spectra of chromophores beyond the Condon limit (i.e., where nuclear motions dynamically modulate the strength of dark and bright transitions).
(2) Efficiently capture the signatures of nonadiabatic energy transfer in nonlinear spectra.
(3) Leverage physics-based machine learning to diagnose and manipulate energy transfer mechanisms.

Our methodological advances in Aims 1 and 2 will enable us to faithfully account for intermolecular interactions and accurately and efficiently capture the quantum dynamics of the excitations that determine the nonlinear spectral responses. These are crucial advances that facilitate assigning spectral features to specific interactions and predicting how chemical changes (group additions and substitutions, molecular topology, and solvent interactions) can be used to tune energy transport. Our advances in Aim 3 will enable us – and other researchers – to quickly determine if and which physically transparent model can be used to decipher the energy transfer pathways revealed by the spectroscopy. This would be a critical breakthrough that would enable researchers to identify systems that require one to deploy advanced methods to simulate and interpret their spectroscopy while accelerating the theory-experiment feedback loop that optimizes materials properties for technological applications.

We will initially apply our techniques to predict and elucidate the energy transfer processes revealed by the multidimensional optical spectra of photosynthetic and chlorophyll-carotenoid complexes that are crucial in photoprotection, and porphyrins in solution and in polymeric form, as these are highly tunable and critical ingredients in natural and artificial energy conversion and electrocatalysis. We will then leverage the resulting insights to develop design principles for directed energy transport and tunable optoelectronic properties in porphyrin systems for applications in energy conversion and catalysis. Our proposed advances will be broadly applicable and offer a promising tool to interrogate and manipulate the optical and transport properties of systems ranging from biological dyes, to disordered organic semiconductors, and perovskites.

Recent Progress: We have completed the first two manuscripts related to this project.

The first paper[1] outlines our theory and simulation strategy for capturing the linear optical spectra of dilute chromophore solutions beyond the Condon limit with atomistic simulations. We derive this theory by exploiting the expectation that the non-Condon fluctuations of the transition dipole should obey Gaussian statistics in many condensed phase systems. Our theory introduces novel quantities that enable one to quantify the nuclear modulations of both the energy gap and the transition dipole and goes beyond state-of-the-art and widely adopted theories based on the harmonic approximation of the potential energy surfaces and perturbative treatments of non-Condon effects, allowing us to account for arbitrarily strong non-Condon effects and disordered chemical environments. Importantly, our theory is directly compatible with first-principles atomistic simulations, which means that it incorporates realistic molecular interactions, finite-temperature effects, and disorder in solution. We demonstrate that our theory can predict the spectra of system that exhibit strong non-Condon effects, such as phenolate in various solvents and reveals two independent mechanisms for apparent peak splitting. We further introduce simple tools to identify how intramolecular vibrations, solute-solvent interactions, and environmental polarization effects impact the prominence of dark transitions in optical spectra.

The second paper[2] introduces a highly efficient theory to reduce the cost of simulating 2D spectral. To achieve this, we offer a discrete-time reformulation of multitime generalized quantum master equations that greatly reduce their computational cost and complexity, while ensuring that their interpretability remains intact. We illustrate the advantages of our method by simulating 2D spectra for the energy transfer dimer model, leading to computational savings of 10-10^3. Importantly, this method enables the decomposition of multitime correlation functions and 2D spectra into 1-, 2-, and 3-time correlations, showing how and when the system enters a Markovian regime where further measurements are unnecessary to predict future spectra. We anticipate that this advance will enable the efficient generation and analysis of 2D spectra when coupled with any user's dynamical method of choice.

Future plans: Our work over the next year will focus on completing our work on the origin of the spectral splitting of the Q-bands of free-base porphyrins. We will also generalize our theory to capture the nonlinear optical spectra of dilute solutions of chromophores in the condensed phase beyond the Condon limit. We will illustrate the theory on model chemical systems, such as free-base porphyrins at first. More specifically, we will develop a set of analysis tools that will enable the fast and easy diagnosis of the presence of significant non-Condon effects based on the nonlinear spectra of materials. We will then develop techniques to interrogate the effect of non-Condon fluctuations on the nonadiabatic energy transfer properties and the associated spectra of model dimers and trimers.

References:

1. Z. R. Wiethorn, K. Hunter, T. Zuehlsdorff, A. Montoya-Castillo. "Beyond the Condon limit: Condensed phase optical spectra from atomistic simulations" arXiv:2310:04333 (2023)
2. T. Sayer, A. Montoya-Castillo. "Efficient formulation of multitime generalized quantum master equations: Taming the cost of simulating 2D spectra." arXiv:2310.20022 (2023)

Peer-Reviewed Publications Resulting from this Project (Project start date: MM/YYYY): No publications to report.

What is the Matter Within Polaritons: Molecular Control of Collective Hybrid States

DE-SC0021941

Andrew J Musser

Department of Chemistry and Chemical Biology

Cornell University

Baker Laboratory, Ithaca, NY 14850

ajm557@cornell.edu

Project Scope. This project started in August 2021 and aims to develop a systematic spectroscopic understanding of the ultrafast photophysics of organic exciton-polaritons and the basis of this behavior (or lack thereof) in the properties of the active material. Exciton-polaritons have attracted significant recent attention for their potential to alter molecular photophysical pathways and open new applications in photochemistry. Reports of significantly enhanced charge and energy transport, changes to spin photophysics, and altered photoisomerization suggest great promise to exploit polaritons to non-synthetically improve the properties of organic semiconductors. Yet the field has been unable to reproduce some headline results, and there is a lack of fundamental understanding of how strong light-matter coupling can induce many of the reported effects. Our project aims to fill this critical gap by supplying a detailed photophysical picture of organic exciton-polaritons and their relaxation processes. Through correlations between the molecular properties of the active layer and the polariton dynamics, we will build a systematic understanding of if and how the 'matter' in these light-matter hybrid states matters. In addition to the intrinsic ultrafast dynamics of exciton-polaritons, we are extending this analysis to polariton-mediated energy transport and photoinduced electron transfer to identify what molecular control knobs exist for optimization.

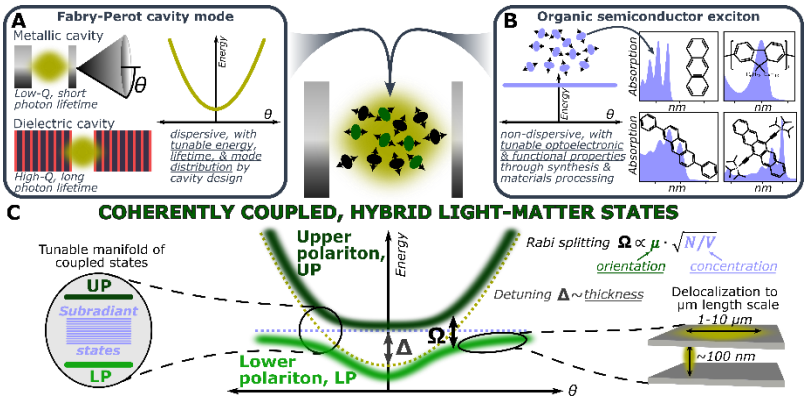

Figure 1. Basic principle of collective light-matter coupling to form polaritons. Easily tunable **A** photonic states and **B** organic semiconductors can hybridize to form **C** mixed polariton states. We seek to establish how the tuning parameters in **A** and **B** impact the collective properties.

Recent Progress. Early in the project, we published a collaborative study on the ultrafast energy transport dynamics of organic exciton-polaritons using transient absorption microscopy (TAM) [2]. This was the first work in the organics field to capture the coherent transport regime (within the cavity photon lifetime), and we demonstrated a new method to distinguish polaritonic features

from optical artefacts through control of the cavity quality factor. Crucially, we revealed that the quality factor likewise impacts the velocity of transport – this unexpected effect points to a complex interplay of bright and dark states on even ultrafast timescales.

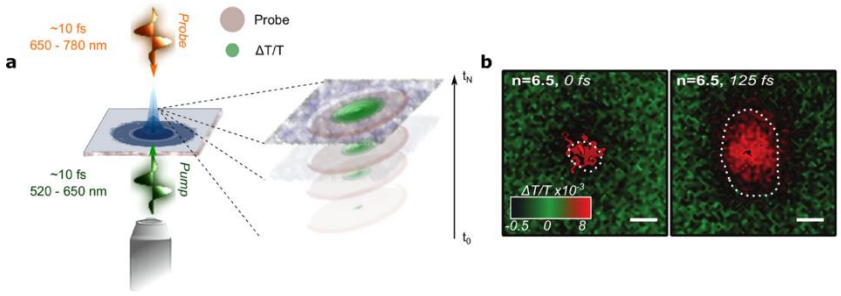

Figure 2. Ultrafast TAM of exciton-polaritons. a Concept of ultrafast TAM experiment, which can deliver ~10 fs temporal resolution and ~10 nm spatial precision. **b** Ultrafast expansion of polariton population in a high-Q BODIPY cavity, recorded by TAM. Adapted from [2].

This year we published a review article laying out some of the critical questions facing the field that demand more systematic experimental investigation [3]. One of the key material properties we have identified that is widely overlooked is disorder. In a work recently posted to arXiv and currently under review [1], we systematically controlled the degree of order in conjugated polymer films to investigate the impact of linewidth on the microcavity electronic structure. Based on our observations, we developed a new approach to model the strong coupling in broad absorbers based on explicitly accounting for inhomogeneous broadening in a simple Tavis-Cummings framework. This result reveals an alternative description for the electronic structure of the cavity – likewise found by more advanced models – in terms of weakly mixed 'grey' states, and it highlights the major shortcomings of current descriptions of ultrastrong coupling.

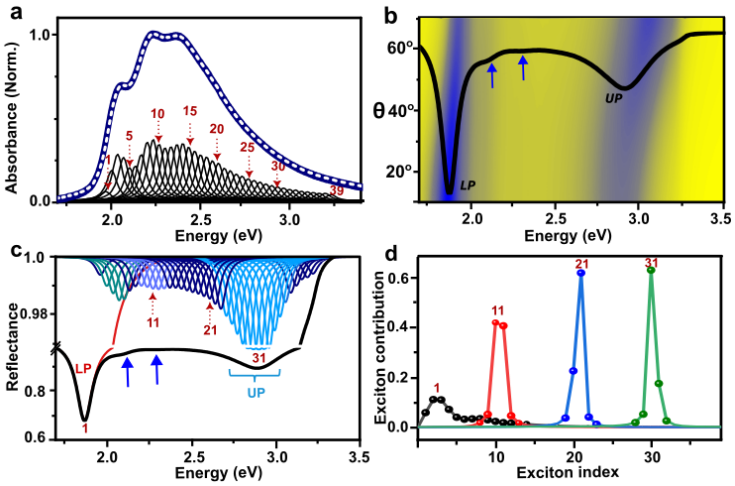

Figure 3. a Optical spectrum and multi-oscillator decomposition of P3HT thin film, resulting in **b** modelled polariton dispersion with subtle intermediate bands (arrows) reporting on 'grey' states. Decomposition of eigenstates by **c** reflectance (photon content) and **d** exciton contributions reveals the degree of state mixing. From [1].

To lay the groundwork for more systematic explorations of polariton-mediated energy transport, we have begun to explore materials platforms where we can control inter-site coupling without strongly affecting the optical spectra. In one study [4], we explored the excitation dynamics in films of lead-halide perovskite quantum dots (QDs) with different ligand treatments, which alters the connectivity between QDs. We observed that confinement with individual QDs leads to the formation of bound polaron pairs, while the weak connectivity induced through ligand treatment results in the formation of large polarons with significantly longer-range transport and longer lifetime.

Future Plans

In the coming year we are refining our ultrafast optical tools to perform higher time-resolution transient absorption and photoluminescence measurements on organic exciton-polaritons. We are further building a high-throughput TAM experiment to study the materials dependence of long-range polariton transport. Building on our findings regarding molecular disorder, we are developing a set of materials platforms in which we can systematically tune the electronic disorder to determine what impact is has on crucial polaritonic dynamics.

References

[1] A. George, T. Geraghty, Z. Kelsey, S. Mukherjee, G. Davidova, W. Kim, A.J. Musser, 'Controlling the Manifold of Polariton States Through Molecular Disorder', under review, arXiv: 2309.13178.

Peer-Reviewed Publications Resulting from this Project (Project start date: 08-2021)

[2] R. Pandya, A. Ashoka, K. Georgiou, J. Sung, R. Jayaprakash, S. Renken, L. Gai, Z. Shen, A. Rao & A.J. Musser. 'Tuning the Coherent Propagation of Organic Exciton-Polaritons through Dark State Delocalization', Advanced Science 2022, 2105569.

[3] T. Khazanov, S. Gunasekaran, A. George, R. Lomlu, S. Mukherjee, A.J. Musser. 'Embrace the Darkness: An Experimental Perspective on Organic Exciton-Polaritons', Chemical Physics Reviews 2023, in press.

[4] J. Kim, Y. Xu, M. Li, M. Cotlet, Q. Yu, A.J. Musser, 'Small to Large Polaron Behavior Induced by Controlled Interactions in Perovskite Quantum Dot Solids', ACS Nano 2023, in press.

DE-SC0023503: Signatures of Entropic and Quantum Charge Effects at Operando Solid/Liquid Interfaces

Tod A Pascal
Department of Nano and Chemical Engineering, University of California San Diego
9500 Gilman Dr, MC 044, La Jolla, CA 92093
tpascal@ucsd.edu

Project Scope

This project proposes to develop a multi-scale computational platform for elucidating the complex physics, local structure and dynamics of electrolytes next to electrodes *operando*, i.e., operating at finite bias. Our central hypothesis is that the structure and dynamics of molecules at solid/liquid interfaces is strongly influenced by solvent-induced entropic forces and quantum charge fluctuations. To test this hypothesis, we propose to generate realistic structural models of the interface *operando* and probe the associated electronic structure by leveraging simulations of the core-level X-ray response. These emerging experimental spectroscopic techniques promises to fundamentally reshape our understanding of the forces that inform functional solid/liquid interfaces, if we can elaborate accurate and efficient computational schemes of interpreting the spectroscopy from first principles. By exploiting the unique 1:1 mapping of X-ray spectroscopy to validate thermodynamically relevant computer simulations, we uncover physical principles for predictive design strategies for optimizing the performance of electrochemical cells.

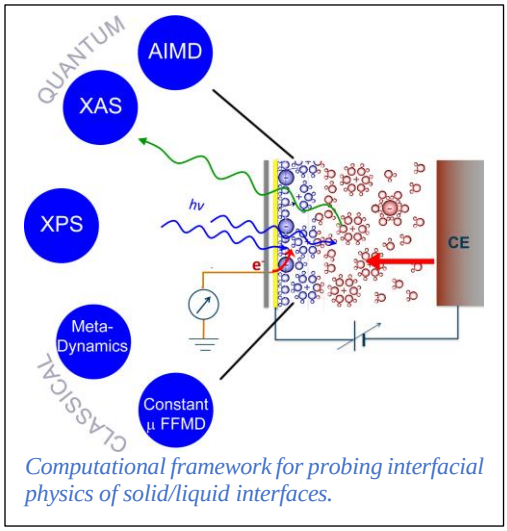

Computational framework for probing interfacial physics of solid/liquid interfaces.

Recent Progress

We have developed a first-principles approach for simulating the X-ray adsorption spectra (XAS), under applied bias and for complex materials and applied it to obtain insights into:

Electrochemical reduction of CO_2 by MoS_2

The interconversion of electrical and chemical energy is central to many emerging technologies, including decarbonization by reducing CO_2 to products of value. Conversion of electrical to chemical energy at acceptable rates, is fundamentally enabled by electrocatalysis, through the manipulation of electrical charge at material interfaces to drive the desired reactions. However, despite numerous developments in electrocatalysis, even the most studied reactions have reached a point where significant gaps of knowledge are impeding further progress. We have thus developed a first-principles computational framework, including an efficient approach for simulating XAS at applied bias, that allows us to define the fundamental electronic features during electrocatalytic transformations, by advancing the capabilities of XAS to track active states simultaneous to the reaction. We found that in the case of electrochemical reduction of CO_2 on transition-metal dichalcogenide nanosheets, catalyst-molecule interactions modulate the electronic states of the electrocatalyst, incorporating electron injection and altered S 3p-Mo 4d hybridization physics. Following the evolution of the measured and simulated XAS spectra reveals a detailed mechanism, first involving the formation of S vacancies electrochemically at

low negative bias, followed by CO_2 binding to the active state and electrochemical conversion at the most negative potentials.

Dynamics of Li ions in graphite, as a function of concentration

The reversible lithiation and delithiation of graphite anodes underlies the operation of modern Lithium-ion batteries and developing a fundamental understanding of this process is a long-desired goal of computational electrochemistry. We advanced an approached based on ab-initio molecular dynamics simulations, free energy and entropy calculations and simulated XAS to probe the electronic states of Lithium at various loadings in graphite, which represents unique structures in the cathode as the battery discharges. We found that the stability of the Lithium ions, as determined by their charge state and ion mobility, are mostly determined by charge fluctuations and anharmonic vibrations in the carbon host. Moreover, these nanoscale physics present as unambiguous features in the Carbon K-edge XAS spectra, such that including these effects are required to reproduce the experimentally measured spectra. Thus, we show that far from being "static" measurements, XAS in fact encodes subtle thermodynamic effects and can be used to elucidate complex dynamics when coupled with first-principles simulations.

iv. Surface structure and $BaTiO_3$ as a function of applied field.

Future Plans

We have made progress in developing a computational framework that incorporates dynamic charge reorganization physics at interfaces and in predicting the associated core-level, electronic structure response. This has been applied to model systems comprising main-group elements (i.e., cathodes comprising carbon and simple oxides). Extending this to more complex, extended interfaces require going beyond simple pair potentials and incorporating many-body effects. We are thus exploring the use of convoluted neural networks, trained from ab-initio MD simulations, to describe the interactions at these interfaces in a general way. We are also developing an approach for simulating transitions from occupied p-orbitals to unoccupied d orbitals (i.e., L-edge XAS), as a way of directly probing the electronic states on transition metal ions, critical for developing a more complete picture of electrocatalytic reduction and evolution reactions.

Peer-Reviewed Publications Resulting from this Project (08/2022-Present)

- Abbasi P, Fenning DP and Pascal TA*, "Investigation of local distortion effects on X-ray absorption of ferroelectric perovskites from first principles simulations", Nanoscale, 15 (11), 5193-5200, 2023
- Kumar K, Jamnuch S, Majidi L, Misal S, Ahmadiparidari A, Dato M, Sterbinsky GE, Wu T, Salehi-Khojin A, Pascal TA* and Cabana J*, "Active states during the reduction of CO_2 by an MoS_2 electrocatalyst", J. Phys. Chem. Lett. 2023, 14, 13, 3222–3229
- Jamnuch S and Pascal TA*, "Electronic signatures of Lorentzian dynamics and charge fluctuations in lithiated graphite structures", Nature Communications, 14, 2291 (2023)
- Woodahl C, Jamnuch S, Amado A, Amado A, Uzundal CB, Berger E, Manset P, Zhu Y, Li Y, Fong D, Connell J, Hirata Y, Kubota Y, Owada S, Tono K, Yabashi M, Matsuda I, te Velthuis SGE, Tapavcevic S, Drisdell WS, Schwartz CP, Freeland JW, Pascal TA*, Zong A and Zuerch M*, "Probing Lithium Mobility at a Solid Electrolyte Surface", Nature Materials, 22, 848–852 (2023)
- Devlin SW, Jamnuch S, Xu Q, Chen AC, Qian J*, Pascal TA* and Saykally RJ*, "Agglomeration Drives the Reversed Fractionation of Aqueous Carbonate and Bicarbonate at the Air-Water Interface", JACS, 2023, 145, 41, 22384–22393

Facilitating and Inhibiting Clathrate Hydrate Formation (DE-SC0021241)

PI: Amish Patel
Department of Chemical and Biomolecular Engineering, University of Pennsylvania,
311A Towne Building, 220 S 33rd Street, Philadelphia, PA 19104
E-mail: pamish@seas.upenn.edu

Project Scope

The properties of interfacial liquid molecules, particularly those near heterogeneous surfaces, can be very different from those in the bulk. These differences can, in turn, lead to novel emergent properties, such as the ability to facilitate or inhibit crystal nucleation. However, identifying the distinguishing characteristics of interfacial molecules that directly influence their emergent macroscopic properties can be challenging. We seek to address this challenge by developing novel computational methods, and by using such methods to uncover the molecular characteristics of a surface that enable it to preferentially interact with crystals (relative to their coexisting liquids) [1].

At low temperatures and high pressures, small guest molecules, such as methane or carbon dioxide, stabilize ice-like structures called clathrate hydrates [2]. Our oceans contain staggering amounts of natural gas in the form of clathrate hydrates, which are a source of tremendous excitement as well as grave concern. Natural gas hydrates are also a source of great frustration due to their tendency plug oil and gas pipelines. Although surfaces are instrumental in both stimulating and suppressing clathrate formation, what enables a surface to heterogeneously nucleate clathrates or kinetically inhibit them remains poorly understood. We are developing specialized simulation techniques to uncover the molecular underpinnings of favorable surface – clathrate interactions over diverse thermodynamic conditions, and to shed light on how "clathrate-philicity" enables certain surfaces to facilitate, and others to inhibit clathrate formation.

Recent Progress

Methodological Advances: We developed techniques for biasing orientational order parameters [3] that discriminate between water molecules that belong to a crystalline phase, such as clathrate or ice, and those that are in the liquid phase. Using these techniques, we then interrogated the thermodynamic preference of a surface for the crystal (relative to the liquid) [1]. The presence of multiple components (water, guests) and phases (crystalline solid, aqueous solution and vapor mixture) makes clathrate formation a particularly challenging process to study; we therefore make use of the closely related, but somewhat simpler problem of ice formation as a stepping stone for testing our methods, ideas and hypotheses.

Characterizing Surface Crystal-philicity: To characterize the relative preference of a surface for a crystalline phase (e.g., ice or clathrate) over liquid water, (i.e., surface crystal-philicity), we generalized a technique, called Surface Wetting and Interfacial Properties using Enhanced Sampling (SWIPES), which we had developed for characterizing surface hydrophobicity [4]. In this generalization of SWIPES, the number of crystal-like waters confined between surfaces of interest are biased to systematically increase surface-crystal contact (Figure 1). The free energy associated with the process is estimated and quantifies surface crystal-philicity; a negative

(favorable) free energy corresponds to a crystal-philic surface, whereas positive a free energy corresponds to a crystal-phobic surface [1]. To develop and refine this generalization of SWIPES, we characterized the ice-philicity of model surfaces. Building upon our initial success in using SWIPES to characterize surface ice-philicity, we have also started to use SWIPES to grow empty clathrates and characterize the corresponding the free energetics.

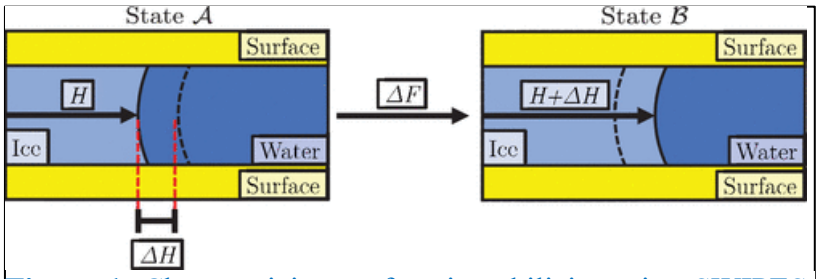

Figure 1. Characterizing surface ice-philicity using SWIPES. In going from state $\mathcal{A}$ to state $\mathcal{B}$, the ice–liquid interface advances by a distance, ΔH, and the system free energy changes by ΔF. During this process, the solid surface of interest (yellow) is brought into contact with ice (light blue) at the expense of liquid water (dark blue).

Molecular Underpinnings of Surface Ice-philicity: Using our generalization of the SWIPES method, we chose to initially characterize the ice-philicity of a family of model surfaces that have perfect lattice match with ice but vary in their polarities. We found that surface ice-philicity increased with polarity for these lattice matched surfaces. Interestingly, ice-philicity was relatively insensitive to polarity for the non-polar surface but was highly sensitive to polarity for the most polar surfaces (Figure 2, blue) [1]. We also studied a family of surfaces, which are not lattice matched with ice, and found that their ice-philicity remained constant over wide range of surface polarities (Figure 2, red). These results highlight the importance of both polarity and lattice matching in conferring surface ice-philicity [1].

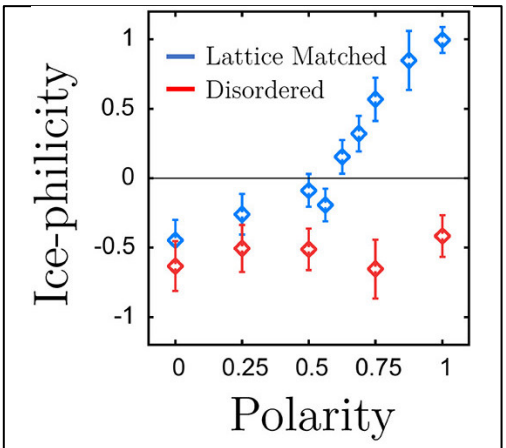

Figure 2. Surface ice-philicity as a function of polarity for both the lattice-matched family of surfaces (blue) and the disordered family of surfaces (red).

Future Plans

In the future, we will build on both the conceptual and methodological advances made thus far to uncover the molecular characteristics of a surface that enable it to interact favorably or unfavorably with clathrate hydrates. These studies will also serve as a starting point for our investigations into the mechanistic pathways of heterogeneous clathrate nucleation and clathrate growth inhibition.

References

1. SM Marks, Z Vicars, AU Thosar and AJ Patel. "Characterizing Surface Ice-philicity Using Molecular Simulations and Enhanced Sampling", *J. Phys. Chem. B* **127**, 6125–6135 (2023).
2. NJ English and JMD MacElroy. “Perspectives on molecular simulation of clathrate hydrates: Progress, prospects and challenges”, *Chem. Engg. Sci.*, **121**,133–156, (2015).

3. AH Nguyen and V Molinero “Identification of clathrate hydrates, hexagonal ice, cubic ice, and liquid water in simulations: the CHILL+ algorithm” *J. Phys. Chem. B*, **119**, 9369–9376 (2015).
4. H Jiang, S Fialoke, Z Vicars, and AJ Patel. " Characterizing Surface Wetting and Interfacial Properties using Enhanced Sampling (SWIPES)", *Soft Matter*, **15**, 860–869 (2019).

Peer-Reviewed Publications Resulting from this Project (Project start date: 09/2020)

1. SM Marks, Z Vicars, AU Thosar and AJ Patel. "Characterizing Surface Ice-philicity Using Molecular Simulations and Enhanced Sampling", *Journal of Physical Chemistry B* **127**, 6125–6135 (2023).
2. AU Thosar, Y Shalom, I Braslavsky, R Drori and AJ Patel. "The Accumulation of Antifreeze Proteins on Ice is Determined by Adsorption", *Journal of the American Chemical Society* **145**, 17597–17602 (2023).

Understanding molecular scale chemical transformations at solid-liquid interfaces – computational investigation of electrolyte oligomerization and the role of additives

Jim Pfaendtner
NC State University, Chemical and Biomolecular Engineering
915 Partners Way | Raleigh, NC 27606 | pfaendtner@ncsu.edu

Program Overview. Understanding the molecular and nanoscale mechanisms of chemical reactions occurring at a liquid/solid interface is critically important to a huge range of processes. Compared with homogenous chemistry in a bulk condensed or gas phase, the modeling toolkit for predicting an interface-mediated reaction mechanism is far less developed, with many researchers falling back on individual reaction-by-reaction studies guided by chemical intuition. The proposed work will develop new computational approaches that address time scale limitations with a suite of enhanced sampling tools.

To date, our project has focused on a systematic study of reaction mechanisms of electrolyte degradation and liquid water interfaces within lead halide perovskite. We have used MD to study electrolyte behavior under different types of interface functionalization, electron transfer in early stages of electrolyte degradation, implemented a reaction coordinate optimization scheme in an automated approach that will greatly facilitate the use of this approach for determining reaction mechanisms in liquids at interfaces, studied facet-specific degradation of perovskites and

Selected Recent Progress and Future Directions. The formation of a solid electrolyte interphase (SEI) at the electrode/ electrolyte interface substantially affects the stability and lifetime of lithium-ion batteries (LIBs). One of the methods to improve the lifetime of LIBs is by the inclusion of additive molecules to stabilize the SEI. To understand the effect of additive molecules on the initial stage of SEI formation, we have published several studies investigating the decomposition and oligomerization reactions of a fluoroethylene carbonate (FEC) additive on a range of oxygen-functionalized graphitic anodes to those of an ethylene carbonate (EC) organic electrolyte. Recently, a series of density functional theory (DFT) calculations augmented by ab initio molecular dynamics (AIMD) simulations reveal that EC decomposition on an oxygen-functionalized graphitic ($11\bar{2}0$) edge facet through a nucleophilic attack on an ethylene carbon site (CE) of an EC molecule (S2 mechanism) is spontaneous during the initial charging process of LIBs. However, decomposition of EC through a nucleophilic attack on a carbonyl carbon (CC) site (S1 mechanism) results in alkoxide species regeneration that is responsible for continual oligomerization along the graphitic surface. In contrast, FEC prefers to decompose through an S1 pathway, which does not promote alkoxide regeneration. Including FEC as an additive is thus able to suppress alkoxide regeneration and results in a smaller and thinner SEI layer that is more flexible toward lithium intercalation during the charging/discharging process. In addition, we find that the presence of different oxygen functional groups at the surface of graphite dictates the oligomerization products and the LiF formation mechanism in the SEI. Ongoing work on this project involves the inclusion of solvent and additional ionic effects.

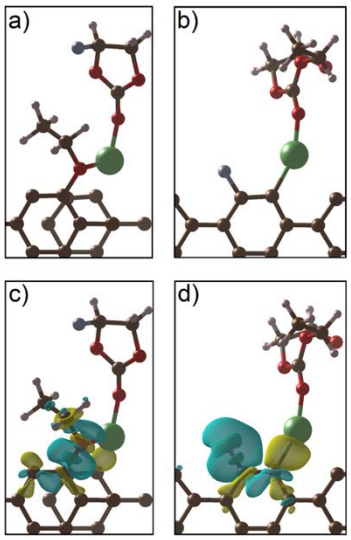

Figure 1: Adsorption configuration of (a) ethoxide-Li-FEC and (b)EC·on pristine graphite ($11\bar{2}0$) surfaces; charge density difference distributions for (c) ethoxide-Li-FEC and (d) EC·. From DOI: 10.1021/acsami.0c18414

Building on our studies understanding mechanisms at liquid/solid interfaces, we have recently completed an interesting investigation of the role of surface structure on dissolution of lead halide perovskites. The degradation of CH3NH3PbI3 (MAPbI3) hybrid organic inorganic perovskite (HOIP) by water has been the major issue hampering its use in commercial perovskites solar cells (PSCs), as MAPbI3 HOIP has been known to easily degrade in the presence of water. Even though there have been numerous studies investigating this phenomenon, there is still no consensus on the mechanisms of the initial stages of dissolution. Here, we attempt to consolidate differing mechanistic interpretations previously reported in the literature through the use of the first-principles constrained ab initio molecular dynamics (AIMD) to study both the energetics and mechanisms that accompany the degradation of MAPbI3 HOIP in liquid water. By comparing the dissolution free energy barrier between surface species of different surficial types, we find that the dominant dissolution mechanisms of surface species vary widely based on the specific surface features. The high sensitivity of the dissolution mechanism to surface features has contributed to the many dissolution mechanisms proposed in the literature. In contrast, the dissolution free energy barriers are mainly determined by the dissolving species rather than the type of surfaces, and the type of surfaces the ions are dissolving from is inconsequential toward the dissolution free energy barrier. However, the presence of surface defects such as vacancy sites is found to significantly lower the dissolution free energy barriers. Based on the estimated dissolution free energy barriers, we propose that the dissolution of MAPbI3 HOIP in liquid water originates from surface defect sites that propagate laterally along the surface layer of the MAPbI3 HOIP crystal.

Completion of this project required an extraordinary amount of compute power due to the requirements for using ab initio MD to model the water/perovskite interface. Thus, further details of mechanism such as multiple ion dissolution or multi-species dissolution are not thought to be accessible while DFT calculations are required. Ongoing work in our lab is developing machine-learning based potentials that can reproduce the accuracy of DFT but provide significant increases in computational speed. First to replicate these results and later to advance the study of reactions at interfaces.

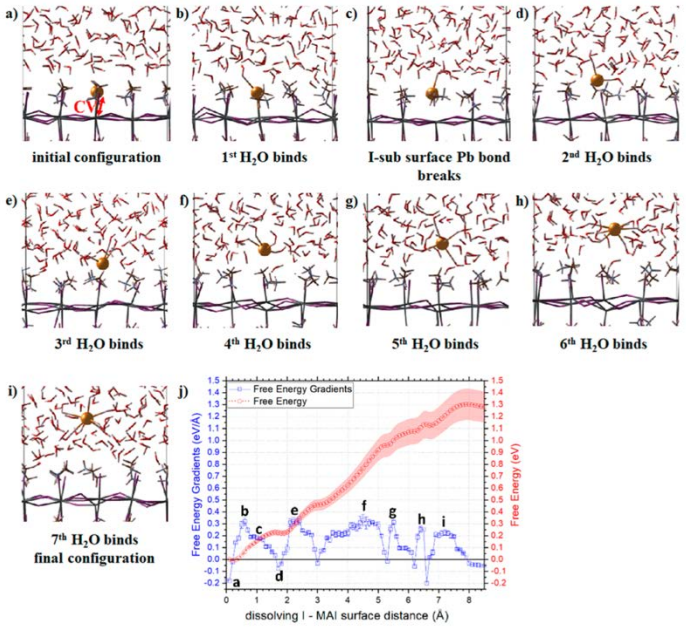

Figure 2: (a−i) Sequence of events for I− ion dissolution from the MAI-terminated surface of MAPbI3 HOIP, and (j) free energy gradient average (left axis) and corresponding free energy barrier (right axis) of I− ion dissolution from the MAI surface into liquid water as estimated by blue-moon simulations. The upper and lower barriers of the force are represented by the blue lines on the force line, while the red shaded area shows the error bars of the free energy from thermodynamic integration. Letters a−i in panel (j) correspond to key stages in the I− ion dissolution, for which the configurations are shown in panels (a−i). The dissolving iodide ion is shown in orange, the red and white lines represent water molecules, while the cage-like structure in the lower half of panels (a−i) colored in purple, gray, and brown lines represents the MAPbI3 HOIP slab. From DOI: 10.1021/acsnano.3c04601.

Probing Condensed-Phase Structure and Dynamics in Hierarchical Zeolites and Nanosheets for Catalytic Upgradation of Biomass (Award #: DE-SC0018211)

Neeraj Rai
330 Swalm Chemical, Mississippi State University, Mississippi State, MS, 39762
Email: neerajrai@che.msstate.edu

Program Scope

Understanding complex reactions at the molecular level in systems characterized by multi-scale collective coupling across time and space is a significant scientific challenge. This project is guided by the hypothesis that interactions of oligomers, solvents and active sites can be tailored by a suitable choice of solvent and also of pore architecture of solid-acid catalysts to promote chemical transformations during catalytic conversion of biomass. The architecture is determined by the choice of hierarchical zeolites, which provide large channels for macromolecule diffusion and small pores for catalysis. A multi-scale computational approach is used to elucidate physical and chemical interaction across multiple spatial and temporal scales. One of the expected outcome is a better understanding of the fundamental interactions of reactant and solid acid catalysts in the presence of solvents, enabling rational design of catalytic systems that can upgrade biomass in a selective and energy efficient manner. Another outcome will be the development of sampling tools essential to detangle interactions in complex, reactive phenomena.

Recent Progress

Effect of Water Models on Structure & Dynamics of Lignin: As the structural and transport properties of biopolymers in the aqueous phase depend on the water model's accuracy; it is important to investigate the sensitivity of aqueous phase lignin solvation and transport properties to different water models. In this project, we used the three-center point charge flexible model (SPC/Fw), the three-center rigid TIP3P, and the four-center rigid TIP4P/Ew. SPC/Fw and TIP4P/Ew correctly predict densities and energetic properties and provide a reasonable estimate of the diffusion and dielectric constant. These water models perform better than TIP3P. However, the accuracy comes with a higher computational cost. TIP4P/Ew has one additional interaction site compared to the TIP3P model, and flexible SPC/Fw necessitates using a smaller integration time step. Although the native lignin is heterogeneous, a large body of previous computational work has used homogeneous lignin. In our work, we used both homogeneous and heterogeneous models of lignin. In Fig. 1, we show the self-diffusion coefficient of hardwood and softwood lignin, respectively, at different temperatures for the three water models. The diffusion constant of lignin, irrespective of the source, is significantly higher in TIP3P than in SPC/Fw and TIP4P/Ew. Hardwood lignin shows higher diffusivity in TIP4P/Ew water model than SPC/Fw for all temperatures except at 420 K. Sim-

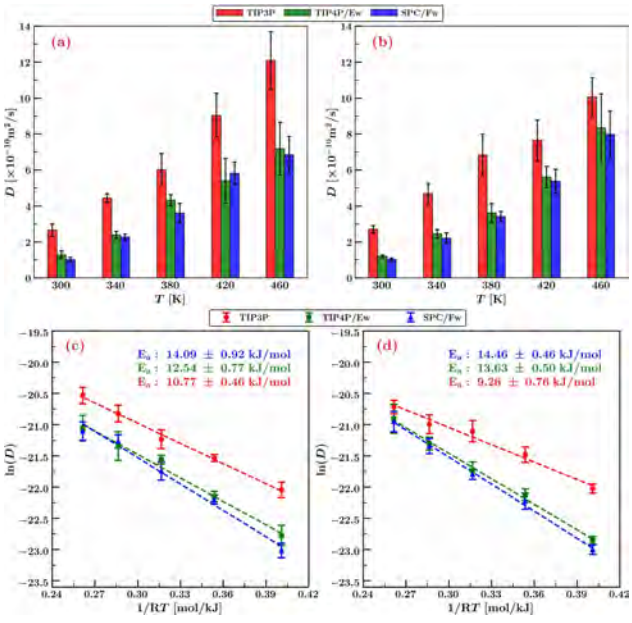

Figure 1. Self-diffusion coefficient of (a) hardwood lignin and (b) softwood lignin. Arrhenius plot of (c) hardwood lignin and (d) softwood lignin. The mean and the standard error of the mean are reported for five independent runs. The dashed lines represent linear fit for ln(D) vs. $1/RT$.

ilarly, softwood lignin has higher diffusivity in TIP4P/Ew than SPC/Fw at all temperatures. The general trend in the self-diffusivity is as follows: TIP3P > TIP4P/Ew > SPC/Fw. In Fig. 1, we also show the Arrhenius plot for hardwood and softwood models, respectively. It is evident from the graphs that the Arrhenius equation fits the data reasonably well over the range of temperatures considered in the present work. As expected, the hardwood and softwood lignin has the highest activation energy for SPC/Fw. The activation energy in the TIP3P water model is ~3 kJ/mol and ~ 5 kJ/mol smaller than in SPC/Fw model, respectively, for hardwood and softwood lignin. Softwood lignin has a slightly higher activation energy barrier than hardwood lignin for TIP4P/Ew and SPC/Fw, whereas the opposite is true for TIP3P. (**See Reference 1 for more details.**)

Effect of Solvent Quality on Structure & Dynamics of Lignin: Here, we examined the structure and dynamics of lignin in water/methanol mixtures using all-atom molecular dynamics (MD) simulations. Methanol, one of the cheapest and readily available green solvents produced from biomass components by demethoxylation, has been widely used in organosolv pretreatment and lignin depolymerization due to its low boiling point and ease of recovery. Prior computational work on lignin conformation suggests that lignin undergoes morphological transition due to the change of external conditions during solubilization. Morphological transition can provide information regarding self-aggregation during fractionation and "solvolytically or catalytically competent conformation" for depolymerization. Conformational changes of lignin can be elucidated by the framework of "solvent quality". Here, we investigated the structure of two lignin types (linear softwood and linear hardwood) in the binary mixtures of methanol and water. Thus we aimed to provide detailed molecular insights into the solvation of lignin in methanol and their binary mixtures with water as cosolvent at three different temperatures (300, 340, and 380 K). Through careful analysis of trajectory and molecular interactions, we rationalize the role of solvent in the structure and dynamics adopted by the lignin polymers.

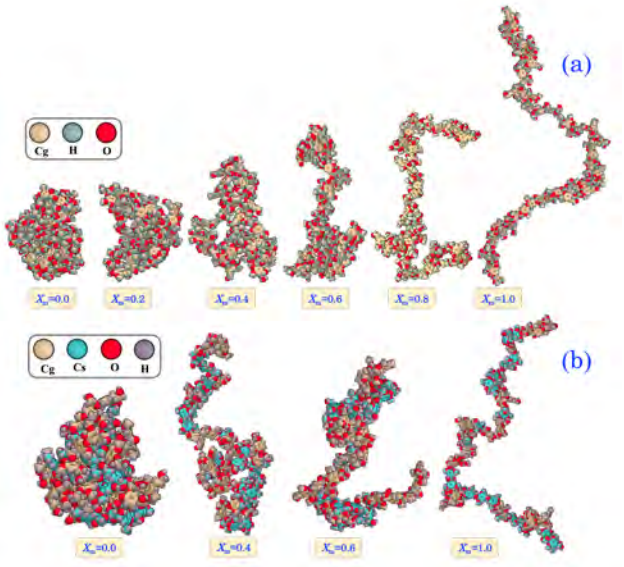

Figure 2. The representative snapshot of lignin polymer conformation at $T = 300$ K for different solvent compositions (water and methanol). (a) Softwood lignin, and (b) hardwood lignin. X_m represents methanol mole fraction in the solution.

In dilute solutions, the polymer conformation is a strong function of the solvation environment. In Figure 2, we show the representative polymer conformation in binary solution as a function of methanol mole fraction at $T = 300$ K. Due to the strong intermolecular hydrogen bond network in pure water, these lignin polymers (hardwood and softwood) adopt a collapsed structure to minimize the surface area (see Figure 2). As methanol concentration is increased, the polymer chains adopt a more extended conformation. We quantify the equilibrium lignin polymer structure via polymer theory. To evaluate the impact of different solvent environments on the lignin structure, we analyze the radius of gyration, mass fractal dimension, solvent accessible surface area (SASA), and end-to-end distance. (**See Reference 2 for more details.**)

Liquid Phase Diffusion of Complex Molecules in Zeolite Nanopores: It has been shown that Lewis acidic β-zeolite with large hydrophobic pores can be an effective catalyst for isomerization of glucose in an aqueous medium and epimerization reaction in the methanol solution.rai2013role Since glucose molecule contains a large number of hydroxyl groups, it can be effectively solvated by the water molecules leading to large solubility of glucose in water. This begs an important question: how does the glucose molecule diffuse from the solution phase to the hydrophobic zeolite pores? Furthermore, what are the thermodynamic driving forces for glucose transport? To understand the kinetics of glucose loading, we carry out molecular dynamics simulations that closely mimic the experimental approach. Our approach enables us to examine the equilibrium loading and the transient behavior that provides kinetics of the adsorption process. Furthermore, we examine the effect of the solvent and interface on the diffusion of aqueous glucose in all silica β-zeolite framework. A better understanding of the transport of glucose molecules and their local environment will help design catalytic processes for converting monomers of cellulose to valuable chemicals.

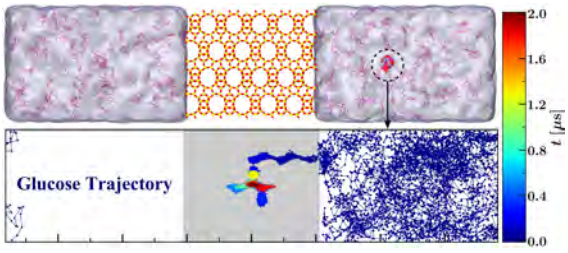

Figure 3. Trajectory of selected glucose in the microsecond-long molecular dynamics simulation.

In Fig. 4, we show the number of adsorbed species as a function of time at the liquid/zeolite interface and the interior of the zeolite framework for TIP3P and TIP4P/Ew, respectively. Interfaces are defined both sides of slab along the **a**-vector (Fig. 4A). We observed that the interfacial region reaches equilibrium concentration faster than the zeolite's interior part. Both water models show a virtually similar number of adsorbed species at the interface. The average number (from 1.5 to 2.0 μs) of glucose molecules adsorbed at the interface are 2.6 ± 0.2 and 2.4 ± 0.2 /nm^2, and for water 73 ± 1 and 70 ± 1, /nm^2, respectively, for TIP4P/Ew and TIP3P. Although both water models exhibit similar behavior at the interface, the behavior in the interior region is different. For the TIP3P water model, initially, a large water uptake (approx. 12/u.c.) takes place, but as the glucose molecules enter the pores, they replace water inside the zeolite slab. In contrast, for TIP4P/Ew, water uptake takes place gradually until 1.0 μs; after that, partial desorption takes place from the zeolite's interior. The average number of water molecules adsorbed in the interior region of the zeolite are 3.9 ± 0.2 and 6.35 ± 0.2 per unit cell, respectively, for TIP4P/Ew and TIP3P. The differences in the initial water uptake for TIP3P and TIP4P are largely because the boiling point of the water model is much lower than that for TIP4P/Ew (365.3 vs. 393.4 K). As shown in Fig. 4(C), glucose molecules took approx-

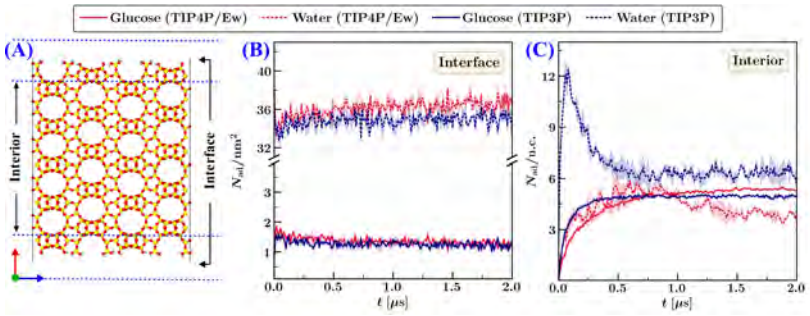

Figure 4. Definition of slab interface and inside (A), number of adsorbed species per unit cell as a function of time at the interface (B), and number of adsorbed species per unit area as a function of time inside of the slab (C). Interface dimension: the length of each interface is 1.8 nm, which consists of 1.2 nm liquid region at the liquid/zeolite interface, density starts changing 1.2 nm away from zeolite surface), plus 0.6 nm zeolite side of the interface (half of a unit cell along **a**-vector).

imately two times longer time to reach the saturation loading for TIP4P/Ew compared to the TIP3P model (1.0 vs. 0.5 μs). The average number of glucose molecules adsorbed in the zeolite pores is 5.37 ± 0.04 and 4.95 ± 0.07 per unit cell, respectively, for TIP4P/Ew and TIP3P water models. The average glucose loading is qualitatively similar despite significantly different kinetics of glucose adsorption for TIP4P/Ew and TIP3P models suggesting that equilibrium loading is governed by the zeolite and glucose interactions. The average number of water molecules per glucose molecule in the zeolite interior is quite different for TIP4P/Ew and TIP3P models (0.72 vs. 1.28). We attribute this to the higher cohesive energy density of the TIP4P/Ew model compared to the TIP3P model. The qualitatively similar adsorption loading of glucose molecules inside the zeolite pores suggests that glucose adsorption is not very sensitive to the water model employed in the simulation. (**See Reference 3 for more details.**)

Lignin Interaction with the Zeolite Nanosheet: Using atomistic molecular dynamics simulations, we investigated the structure and dynamics of model softwood lignin polymer on a nanosheet with the MFI topology in the liquid phase. At the thermodynamic conditions (near ambient temperature & pressure) considered in the present work, we find that water in the pure water system does not diffuse into the nanosheet pores. However, as we increase methanol concentration, we find that not only methanol readily diffuses into the zeolite nanopores, but interestingly, it also facilitates the diffusion of water molecules. The solvent composition significantly influences the contact between lignin and the surface; for example, higher methanol concentration lowers the contact between lignin and the surface as lignin adopts an extended conformation in methanol, resulting in a large number of lignin segments are well-solvated away from the interfacial region. Although the surface contact is the highest for pure water case, lignin adopts a very compact structure, and it can promote recondensation on the surface. Adding a suitable solvent (for lignin) can help lignin adopt an extended conformation and help lignin fragments diffuse into the solvent phase post-catalytic depolymerization on the catalytic surface.When lignin polymer is anchored on the surface through hydrogen bonds, the chain dynamics slow down dramatically (an order of magnitude) as we decrease methanol concentration. At the higher temperature (T = 330 K), the hydrogen bond between the lignin and the surface silanol group increased. We also find an enrichment of the methanol molecules at the surface of the nanosheet, and the residence time of the methanol molecules in the interfacial region is larger than water molecules. Overall, our study provides a molecular perspective of lignin polymer will interact with the zeolite surface, which is the first step for the catalytic conversion to valuable chemicals. (**See Reference 4 for more details.**)

Future Plans

In the next few months, we aim to complete the simulations for the diffusion of lignin in the large pore zeolites.

Peer-Reviewed Publications Resulting from this Project (2021-2023)

1. M. M. Huda, N. Jahan, W. N. Wilson, and N. Rai “Effect of water models on structure and dynamics of lignin in solution", *AIP Advances*, **11**, 065024, 2021
2. N. Jahan, M. M. Huda, Q. X. Tran, and N. Rai “Effect of Solvent Quality on Structure and Dynamics of Lignin in Solution", *J. Phys. Chem. B*, **126**, 5752–5764, 2022
3. M. M. Huda, C. Saha, N. Jahan, W. N. Wilson, and N. Rai “Insights into Sorption and Molecular Transport of Aqueous Glucose into Zeolite Nanopores", *J. Phys. Chem. B*, **126**, 1352–1364, 2022
4. M. M. Huda, and N. Rai “Effect of Solvent on the Interaction of Lignin with a Zeolite Nanosheet in the Condensed Phase", *J. Phys. Chem. B*, **127**, 6767–6777, 2023

Harnessing Electrostatics for the Conversion of Organics, Water and Air: Driving Redox on Particulate Liquids Earthshot (DROPLETS)

DE-FOA-0003003

PI: Prof. Joaquín Rodríguez López
Department of Chemistry, University of Illinois Urbana-Champaign
600 S Mathews Ave, Urbana, IL, 61801, USA
e-mail: joaquinr@illinois.edu

Project Scope

The **overall objective** of DROPLETS is to explore an unconventional, straightforward, and underutilized approach based on microdroplet-enabled redox reactions towards H_2 production, CO_2 activation, and the synthesis of redox species for long-duration energy storage (LDES). In recent years, it has been established that the scope of chemical reactions in aqueous microdroplets produced in a variety of formats significantly departs from that in bulk solutions. Such microdroplets can dramatically accelerate chemical reactions or accomplish complex chemical transformations with simple experimental setups. Although these experiments have unambiguously demonstrated a new pathway for chemical reactions, a concerted team effort to understand their **fundamental principles** leverages their unique properties towards energy applications and CO_2 conversion. To this point, DROPLETS pursues three objectives: 1) the splitting of water to generate renewable hydrogen and oxygenated precursors, 2) the development of water oxidation-driven processes for the electrosynthesis of molecules for LDES and CO_2 capture, and 3) the exploration of mechano-electric effects in the synthesis of organic molecules and precursors for LDES.

DROPLETS strives to achieve simplicity and lower the energy input and reactor cost for complex chemical reactions, a key advantage to simultaneously achieve multiple Earthshots, including the Hydrogen Shot, the Long Duration Storage Shot, and the Carbon Negative Shot. This project also features **efficiency in collaborative science**, the use of advanced characterization techniques, and a forward-looking plan for data management. DROPLETS ensures that the scientific diversity of the project's research is also reflected in the **human diversity** of its trainees and scientists. This is accomplished by means of a promotion of inclusive and equitable research (PIER) plan that trains a diverse team and builds a thriving community with equitable access to scientific resources, including two Hispanic-serving institutions. Continuous training, mobility grants, community building through established partners, an annual retreat with components for safety, ethics, data management, and creativity awards, ensure an overall benefit to America's ability to successfully accomplish Earthshots.

Recent Progress

The DROPLETS project just started on 10/15/2023. Pre-award, we have started developing concepts for driving and measuring electrochemical processes at sonicated microdroplet reactors based on microemulsions of water in hexadecane. This strategy to generate microdroplets and study reactions within them has been reported very recently to generate reactive oxygen species and hydrogen [1]. In parallel, we have focused on using this system to understand the role that oxygenation has on the formation of hydrogen peroxide within the droplets and how concepts of electrocatalysis under the confinement of the microdroplet can be tested using this species as a probe. **Figure 1** shows an example of electrochemical detection of hydrogen peroxide using Pt ultramicroelectrode probes on solutions resulting from the sonication of aqueous/oil droplets in a proportion of 1/10 under gas sparging. These results first establish the possibility of swiftly using electrochemical probes to measure products within extracts from phase separation of the sonicated emulsions. Second, they show clear dependencies on the increase of peroxide signal as a function of sonication time, and more importantly as a function of presence of oxygen in the solution. Notice that the control in **Figure 1** consists of sonicated water in the absence of the microemulsion structure, which shows only background signal. This suggests strongly that the observed effects are not simply due to well-known cavitation effects induced by ultrasonication. Instead, we are interested in exploring the electric field effects reported previously on these type of systems [2]. To this end, we are developing methodologies to test trends in the generation of hydrogen peroxide as we make aspects of the generated microdroplets develop a distinct environment for the formation of such field.

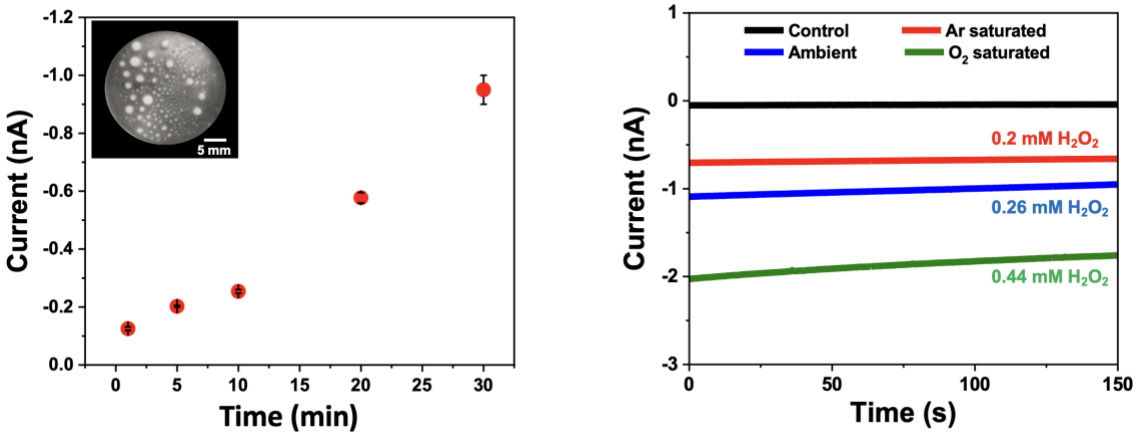

Figure 1. Measurement of hydrogen peroxide generation on water/hexadecane microdroplets using a Pt 12.5 micron radius ultramicroelectrode (left) as a function of sonication time (n=3 for every point), and (right) showing the limiting current and equivalent H_2O_2 concentration under different conditions of aeration. The control is a sample of sonicated water.

Future Plans

The DROPLETS project has formally started recently, so the bulk of our activities towards the Earthshot objectives will be reported in future presentations. Our kickoff meeting took place on 10/18/2023 and we have started assembling our team into subtasks. Each member of our team carries unique research capabilities to address specific research inquiries related to the complex microdroplet chemistry problem. To this point, we will systematically address three key scientific questions:

Scientific Question 1. How does droplet reactivity depend on electrical quantities such as charge and internal electric field? We will use an innovative approach using state-of-the-art operando methods to control charge injection, probe electric fields, and image species distribution. We will accomplish this through nanoelectrochemical methods, high-rate fluorescence spectroscopy imaging, quadrupole trap, single particle methods, and imaging/spectroscopy under the electron microscope.

Scientific Question 2. How do confined electrical quantities impact electrocatalytic principles within microdroplets? We will introduce a strong materials-driven component to microdroplet electrochemistry by using concepts of nanoelectrochemistry. We will test the hypothesis that spontaneously generated electric fields drive electrocatalytic reactions depending on particle size, shape, and targeted distribution of reactants and products within the droplets.

Scientific Question 3. To what extent can the convergence of mechanochemical and electrical activation be leveraged within microdroplets to enable novel redox pathways? Microdroplets are deformable reactors. We will explore how mechanochemical activation at microdroplets might enable new energy transduction mechanisms. These studies will create new prospects for complex redox transformations while leveraging the benefits of deformable interfaces.

The DROPLETS team is:

PI: Dr. Joaquín Rodríguez López[1], Professor of Chemistry
Co-PI(s): Qian Chen[1], Paul Kenis[1], Christy Landes[1], Jeffrey S. Moore[1], Lisa Olshansky[1], Charles Schroeder[1], Hong Yang[1], David W. Flaherty[2], Víctor Ramos-Sánchez[3], Michael I. Jacobs[4], Rajeev Assary[5]
[1]University of Illinois Urbana-Champaign, Urbana, IL, 61801
[2]Georgia Institute of Technology, Atlanta, GA, 30332
[3]Northern Arizona University, Flagstaff, AZ, 86011
[4]Texas State University, San Marcos, TX, 78666
[5]Argonne National Laboratory, Lemont, IL, 60439

References.

[1] Chen, X., Xia, Y., Zhang, Z., Hua, L., Jia, X., Wang, F., Zare, R. N. *J. Am. Chem. Soc.* **2023**, *145, 39,* 21538–21545

[2] Xiong, H., Lee, J. K., Zare, R. N., Min, W. J. *Phys. Chem. Lett.* **2020***, 11(17),* 7423-7428.

Peer-Reviewed Publications Resulting from this Project (Project Start date 10/15/2023)
No publications to report.

Molecular Theory and Modeling 16249

Greg Schenter, Shawn Kathmann, Christopher Mundy, Marat Valiev,
Sotiris Xantheas, Britta Johnson, and Pauline Simonnin

Pacific Northwest National Laboratory
902 Battelle Blvd, Mail Stop J7-10
greg.schenter@pnnl.gov

Project Scope

The Molecular Theory and Modeling Program at Pacific Northwest National Laboratory (PNNL) seeks a fundamental understanding of important processes such as solvation, transport, and reaction in complex condensed-phase and interfacial environments. This research provides a basis for the development of new and improved energy technologies and the control of environmental impacts of energy use. Our diverse team has focused on processes in aqueous solutions, interfacial water, ionic liquids, and molecular frameworks. We systematically connect processes in simple to increasingly more complex systems and advance the fundamental understanding of molecular systems through the development of molecular modeling methods. Our work includes the construction of models of molecular interactions based on empirical forms as well as explicit electronic structures. We combine the method development with appropriate statistical and dynamical sampling techniques to elucidate the fundamental properties and behavior of well-characterized systems for benchmarking by experimental measurement. With an established knowledge of fundamental processes, we further provide the necessary foundation to control and design processes in more complex systems where complexity is due to heterogeneity in space and/or time scales. This allows us to identify intrinsic properties of systems that control collective response and to connect frameworks that impact understanding of complex macroscopic phenomena.

Our approach is based on three pillars of investigation:

1. Advancing Descriptions of Molecular Interaction: we advance molecular simulation techniques, including descriptions of intermolecular interactions, analysis of response, and generation of ensembles, to better understand molecular phenomena.

2. Connecting Theoretical Frameworks: we strive to develop methods to connect multiple time and spatial scales, ensuring consistency between techniques.

3. Integrating Simulations and Experiment: we seek to simulate experimentally measured signals to understand molecular phenomena more effectively. Experimental signals include EXAFS, XANES, x-ray and neutron diffraction, SAX, WAX, infrared, Raman, and photoelectron spectroscopies.

We undertake a fundamental, integrated approach spanning the above three pillars that develops a systematic connection between models of molecular interactions and collective behavior of molecular systems, leading to improved knowledge of complex collective behavior at the mesoscale. A common element in many DOE problem areas is the need to understand complex molecular processes that often involve the collective response of weak intermolecular interactions. Since these processes typically involve hydrogen bonding, understanding aqueous-phase systems specifically and hydrogen-bonded liquids more generally is a major focus of this program. Figure 1 represents our approach of understanding complexity and ensuring consistency between various theoretical frameworks. We study processes involving the solvation and speciation of ions as well as chemical reactivity using theoretical and computational approaches for well-characterized model systems. This approach allows us to identify the essential ingredients that will affect the properties of realistic systems. PIs on the theory program engage in close collaborations with the CPIMS experiment team at PNNL. Specific interactions are illustrated in Figure 2.

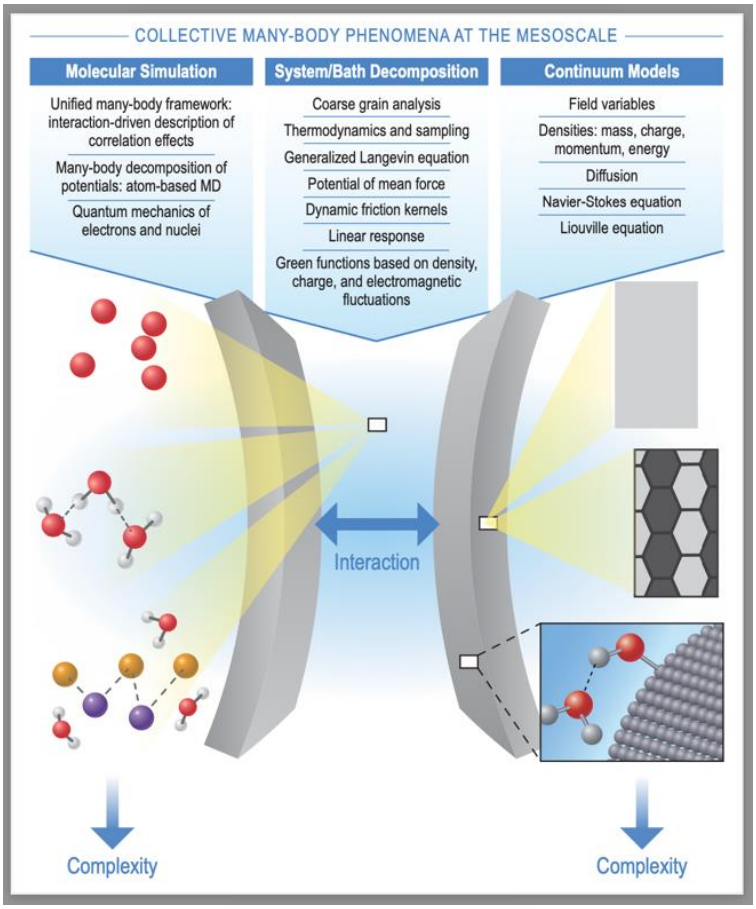

Figure 1. The path towards understanding complexity and complex systems is the coupling of frameworks. Members of our research team contribute unique expertise to each of these areas in our exploration of collective many-body phenomena at the mesoscale. Progress in all three areas advances fundamental understanding of increasingly complex condensed-phase and interfacial molecular processes.

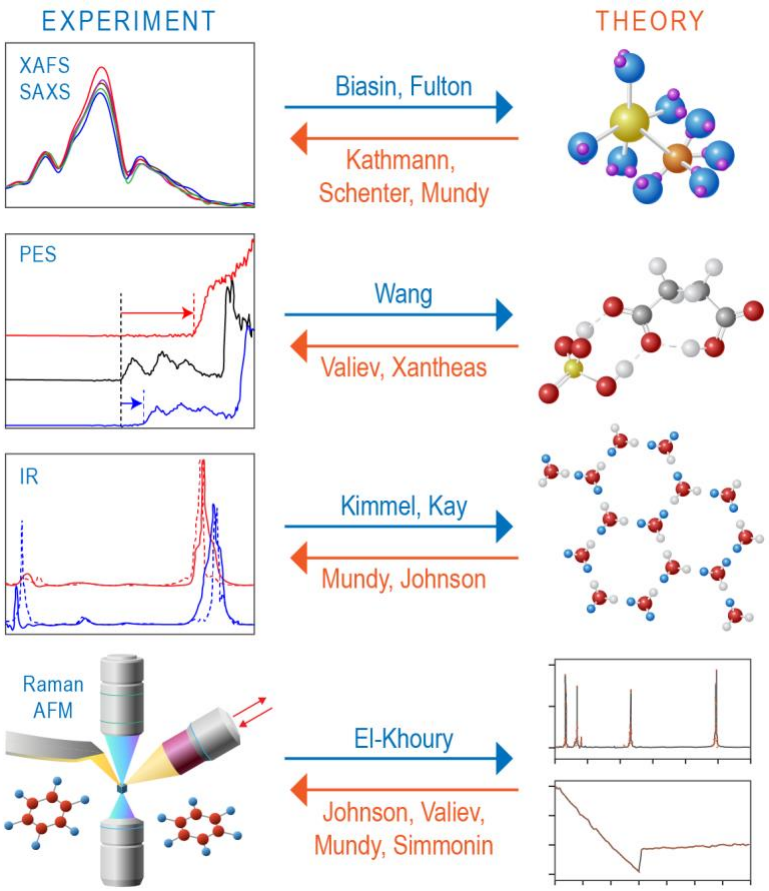

Figure 2. The close collaboration between the Experimental (FWP 16248) and Theory (FWP 16249) programs allows for the theoretical modeling and simulation of quantitative experimental data. This interaction allows for mechanistic molecular-level interpretation of experimental data obtained using X-ray absorption fine structure, photoelectron, tip-enhanced Raman and infrared spectroscopies (XAFS, PES, TERS, and IR).

Recent Progress

1. Advancing Descriptions of Molecular Interaction

- We constructed a ~5M entry database of water cluster minima $(H_2O)_n$, n=3-25 (Cartesian coordinates and relative energies accessible via https://sites.uw.edu/wdbase/). This was generated using an improved version of the Monte Carlo temperature basin paving (MCTBP) global optimization procedure in conjunction with the ab initio based, flexible, polarizable Thole-Type Model interaction potential for water.
- We developed a mixed time slicing ring polymer molecular dynamics (MTS-RPMD) code that works with the CP2K programming suite. This code allows the user to run atomistic RPMD simulations in which individual particles in the simulations can be quantized to various degrees. its potential for treating large, condensed phase systems.
- With an Office of Science Graduate Student Researcher (SCGSR) we established a unique picture of “birth” of the solvated electron from a charge transfer to solvent state (CTTS) via

iodide. The salient picture is that we see the evolution from "trap seeking" to "trap digging" supporting experimental conjecture. In additional work we introduce an automated diabatization that enables fast and effective screening of the CTTS acceptor space in bulk solution. Our procedure introduces "natural charge-transfer orbitals" that provide a means to isolate orbitals that are most likely to participate in a CTTS excitation. Projection of these orbitals onto solvent-centered virtual orbitals provides a criterion for defining the most important solvent molecules associated with a given excitation and can be used as an automated subspace selection algorithm for projection-based embedding of a high-level description of the CTTS state in a lower-level description of its environment.

- We assigned the complete IR spectrum of the protonated water cluster $H^+(H_2O)_{21}$. We developed a new protocol for the calculation of the IR spectra of complex systems, which combines the fragment-based coupled-cluster method and anharmonic vibrational quasi-degenerate perturbation theory. We demonstrated its accuracy toward the complete and accurate assignment of the IR spectrum of the $H^+(H_2O)_{21}$ cluster. Revelation of the spectral signature of the excess proton offers deeper insight into the nature of charge accommodation in the extended hydrogen-bonding network in aqueous clusters.
- We extended Badger's rule to describe the generality between structure and spectra in aqueous hydrogen bonds. We established a correlation between the ratios for both the equilibrium OH bond length/harmonic frequency and the vibrationally averaged bond length/anharmonic frequency in water, hydronium water, halide water clusters, and liquid water. We demonstrate that this simple correlation for both harmonic and anharmonic systems can be modeled by the response of an OH bond to an external field. Our findings indicate a relationship between the molecular structure of the hydrogen-bonded network and the ensuing dynamics, probed by vibrational spectroscopy. In the future, we will further probe the relationship between hydrogen bond strength and energetics.
- We determined the structure of gas phase monohydrated nicotine. We reported a joint experimental–theoretical study of the structure and infrared spectra of gas phase monohydrated nicotine and nornicotine and assigned their protonation sites. We will continue this work by exploring the proton transfer rates in aqueous nicotine.

2. Connecting Theoretical Frameworks

- We continued our analysis of intrinsic and collective properties of electrolytes. We demonstrated the differences between quantum-based interaction potentials (qDFT) and classical empirical potentials for determining both intrinsic and collective properties of electrolyte systems. The unique response to ions afforded by qDFT methods (as compared to classical force fields) provides a qualitatively different picture regarding our understanding of solvation and screening in electrolytes.
- We provided simulation and experimental evidence for anomalous correlations in electrolytes. We demonstrated that measurement via small angle X-ray scattering (SAXS) the prepeak structure of concentrated electrolytes provides an excellent proxy for the measurement of screening lengths of electrolytes as a function of concentration. Using

molecular simulation with Kirkwood-Buff forcefields we were able to quantify anomalous screening of concentrated electrolytes through bulk measurements.

- We constructed reduced models for the initial stages of nucleation in $CaCO_3$ We provided a theoretical procedure to construct reduced molecular models of the initial stages of nucleation of calcium carbonate based on the PMFs between combinations of ion–ion interactions. Through this protocol we can construct a statistical mechanical theory of speciation leading to nucleation.
- We previously worked on development and applications of cDFT. We developed new dual space methodology, implemented open source code, and demonstrated its accuracy for the problems of solvation of ions and nanoparticles.
- With an Office of Science Graduate Student Researcher (SCGSR), we established a molecular-level framework for predicting the reduction potentials and rate constants of electron transfer for ethylene carbonate at the electrode–electrolyte interface in a condensed-phase environment. This work demonstrates the need to carefully treat the solvation environment when computing reduction potentials and electron transfer rate constants. Our results suggest that the common workflows for predicting reduction potentials in ethylene carbonate do not account for all the necessary thermodynamic steps.
- Dr. Pauline Simonnin (new staff) performed her doctoral studies with Dr. Benjamin Rotenberg, where she developed methodologies to study multiphase flow in nanoconfined materials. In pores where the size of molecules is comparable to the confinement length, continuous hydrodynamics fail to describe the flow, and interfacial behavior is neglected. She developed nonequilibrium MD tools, allowing the study at the molecular level of one-phase and multiphase flows in nanopores of clay materials, varying surface charge and salt concentration.

3. Integrating Simulations and Experiment

- We explored nanometer-scale correlations in aqueous salt solutions by interpreting measurements using synchrotron X-ray diffraction at low Q (<1.5 $Å^{-1}$). Features in this region indicate nanometer-scale oscillatory behavior and are reproduced with classical MD simulations. We analyzed the concentration dependence of these features and are developing an analysis of correlation and interaction in concentrated electrolytes.
- Electric fields and vibrational response of carboxylate head group to divalent metal cation. We exploited gas-phase cluster ion techniques to provide insight into the local interactions underlying divalent metal ion-driven changes in the spectra of carboxylic acids at the air–water interface. This established that direct metal complexation or deprotonation can account for the interfacial behavior. These effects can be described via the water network-dependent local electric field along the C–C bond that connects the head group to the hydrocarbon tail as the key microscopic parameter that is correlated with the observed trends.
- We quantified the hydration structure of sodium and potassium ions. The hydration structure around Na^+ and K^+ alkali cations as measured by EXAFS is sensitive to and requires a higher level of electron correlation (e.g., SCAN and RPA) compared to lower levels (revPBE-D3). We showed that better treatment of electron correlation leads to smaller fluctuations in the mean error of the ion-water cluster binding energies.

- Accurate quantification of electric fields and potentials in condensed phases and interfaces is essential to control and exploit chemical and physical transformations. We explored the connections between experimental vibrational Stark, electrochemical, X-ray, and electron spectroscopic probes of these potentials and fields, outline relevant conceptual difficulties, and underscore the advantage of electron holography as a basis to better understand electrostatics in matter.
- We used qDFT MD to interpret ultrahigh vacuum surface experiments using IR probes to investigate the structure of D_2O on TiO_2 (110) surfaces with and without vacancy defects. We showed on the defect-free surface, molecular D2O adsorption occurs, however, with defects dissociation can occur.
- Electric potentials and fields experienced by the ions in small metastable NaCl clusters and cubic crystals in vacuum and aqueous electrolyte solutions were used to characterize features underlying condensed-phase nucleation. We show how the potentials and fields of these crystals can be classified into various subgroups corresponding to corners, edges, faces, and interior sites. The differences between the interior and face potentials are correlated with the interfacial surface energy. A key result of this work is the identification of the electric potential as a possible order parameter to understand nucleation pathways.
- Improving our experimental and theoretical knowledge of electric potentials at liquid–solid boundaries is essential to achieve a deeper understanding of the driving forces behind interfacial processes. Electron holography has proved successful in probing solid–solid interfaces but requires knowledge of the materials' mean inner potential (MIP,V_o), which is a fundamental bulk material property. We provided the first quantitative MIP determination of liquid water V_o = 4.48 ± 0.19 V, whose precise MIP lays the foundation for nanoscale holographic potential measurements in liquids and provides a benchmark to improve quantum mechanical descriptions of aqueous systems and their interfaces in, e.g., electrochemistry, solvation processes, and spectroscopy.
- We investigated how electronic structure changes are connected to solvation and hydrogen bond properties of molecular clusters to interpret photoelectron spectroscopy.

Some key publications are summarized here:

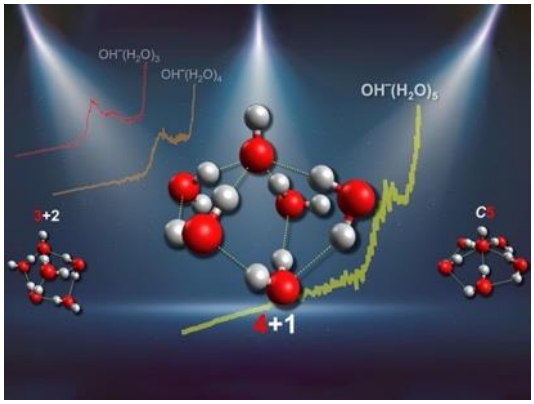

Cao, W, H Wen, SS Xantheas, and XB Wang, "The Primary Gas Phase Hydration Shell of Hydroxide," *Science Advances* **9**, eadf4309 (2023). DOI: https://doi.org/10.1126/sciadv.adf4309

The number of water molecules in hydroxide's primary hydration shell has been long debated to be three from the interpretation of experimental data and four from theoretical studies. Here, we provide direct evidence for the presence of a fourth water molecule in hydroxide's primary hydration shell from a combined study based on high-resolution cryogenic experimental photoelectron spectroscopy and high-level quantum chemical computations.

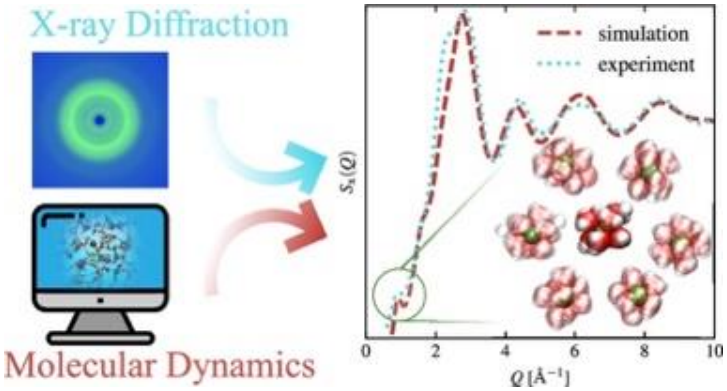

Fetisov, EO, CJ Mundy, GK Schenter, CJ Benmore, JL Fulton, and SM Kathmann, "Nanometer-Scale Correlations in Aqueous Salt Solutions," J Phys Chem Lett 11, 2598 (2020). DOI: https://doi.org/10.1021/acs.jpclett.0c00322

The X-ray diffraction of various alkaline-earth chloride electrolytes was measured, simulated, analyzed, and interpreted. The detected prepeaks are quantitatively reproduced with MD simulations. We confirm the existence of small quasi close-packed lattice structures at high concentrations arising mainly from correlations between Ca–Ca hydration complexes. How intermediate-range correlation arises in electrolytes going from very dilute to concentrated solutions to the ordered crystalline phase enables a better understanding of their liquid structure, the role of water, the existence of local super arrangements, and the interpretation of time-dependent small-angle X-ray scattering signals during homogeneous nucleation, growth, and coagulation.

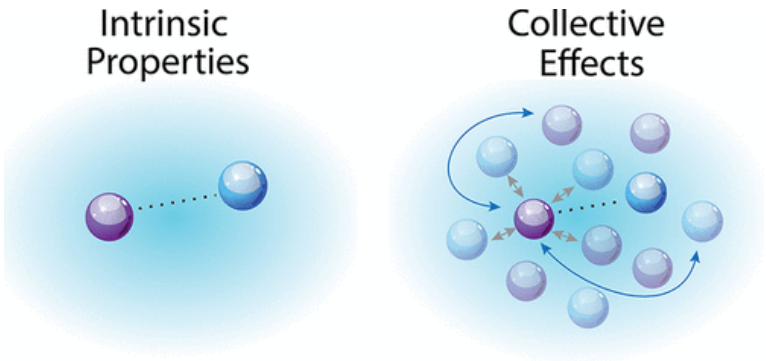

Duignan, TT, SM Kathmann, GK Schenter, and CJ Mundy, "Toward a First-Principles Framework for Predicting Collective Properties of Electrolytes," Accounts of Chemical Research 54, 2833 (2021). DOI: https://doi.org/10.1021/acs.accounts.1c00107

We make the case that understanding electrolyte solutions requires a faithful QM representation of the short range (SR) nature of the ion–ion, ion–water, and water–water interactions. However, the number of molecules that is required for collective behavior makes the direct application of high-level QM methods that contain the best SR physics untenable, making methods that balance accuracy and efficiency a practical goal. We demonstrate that accurately describing the SR interaction is imperative for predicting both intrinsic properties, namely, at infinite dilution, and collective properties of electrolyte solutions.

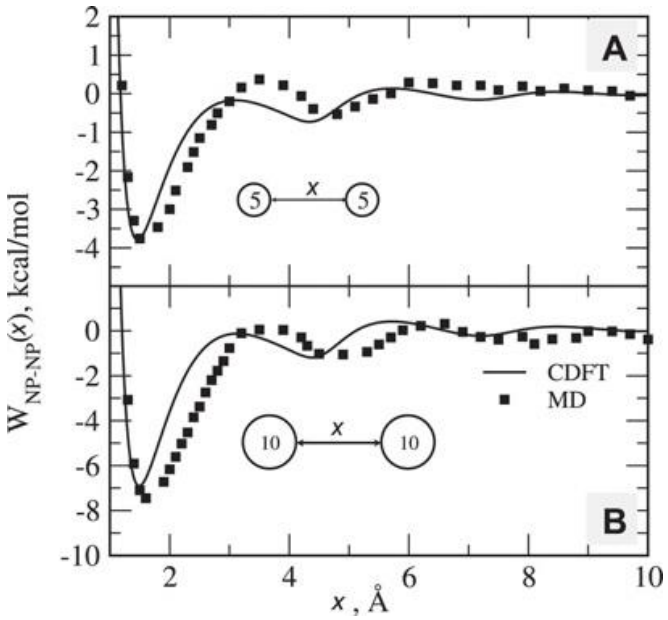

Chuev, G, M Dinpajooh, and M Valiev, "Molecular-Based Analysis of Nanoparticle Solvation: Classical Density Functional Approach," Journal of Chemical Physics 157, 184505 (2022). DOI: https://doi.org/10.1063/5.0128817

Proper statistical mechanics understanding of nanoparticle solvation processes requires an accurate description of the molecular structure of the solvent. Achieving this goal with standard molecular dynamics (MD) simulation methods is challenging due to large length scales. An alternative approach to this problem can be formulated using classical density functional theory (cDFT), where a full configurational description of the positions of all the atoms is replaced by collective atomic site densities in the molecule. Using an example of the negatively charged silica-like system in an aqueous polar environment represented by a two-site water model, we demonstrate that cDFT can reproduce MD data at a fraction of the computational cost. An important implication of this result is the ability to understand how the solvent molecular features may affect the system's properties at the macroscopic scale.

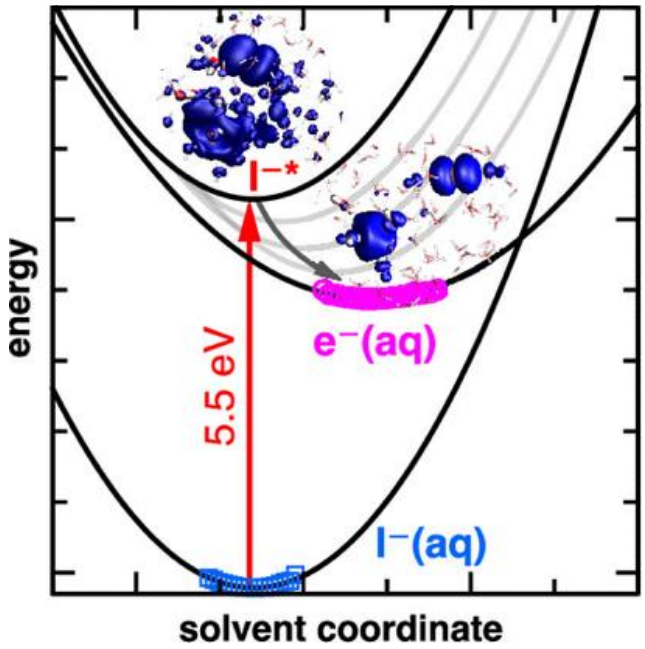

Carter-Fenk, K, BA Johnson, JM Herbert, GK Schenter, and CJ Mundy, "Birth of the Hydrated Electron Via Charge-Transfer-to-Solvent Excitation of Aqueous Iodide," J Phys Chem Lett 14, 870 (2023). DOI: https://doi.org/10.1021/acs.jpclett.2c03460

A primary means to generate hydrated electrons in laboratory experiments is excitation to the charge-transfer-to-solvent (CTTS) state of a solute such as I^- (aq), but this initial step in the genesis of e^-(aq) has never been simulated directly using ab initio molecular dynamics. We report the first such simulations, combining ground- and excited-state simulations of I^- (aq) with a detailed analysis of fluctuations in the Coulomb potential experienced by the nascent solvated electron. The methodology used here should be applicable to other photochemical electron transfer processes in solution, an important class of problems directly relevant to photocatalysis and energy transfer.

Future Plans

1. Advancing Descriptions of Molecular Interaction

We will continue to explore Many-Body decomposition of molecular interaction. This will enhance our understanding of the relation between molecular interaction in clusters and molecular interaction in extended systems. We will continue to create simulation protocols that balance efficiency and accuracy. This includes the development of empirical, semi-empirical electronic structure, electronic density functional theory, and conventional wave-function electronic structure. We will explore the utility of machine learning techniques to understand molecular interaction and enhance statistical sampling. We will extend our exploration of ion–water and ion–ion interactions of more complex systems. We will incorporate quantum effects for complex aqueous systems, and to develop molecular descriptors of complex processes in aqueous systems.

We will continue to investigate the correlation between the strength of hydrogen bonds and associated spectroscopic features and account for quantum nuclear effects in the generation of ensembles and characterizing response to understand fundamental phenomena and interpret experimental measurement. This will establish enhanced understanding of the correlation between the strength of hydrogen bonds and associated spectroscopic features.

2. Connecting Theoretical Frameworks

We will focus on two classes of systems. The common element of these two classes is to formulate a detailed understanding of the aqueous response to both molecular (ions or solutes) and macroscopic interfaces (nanoparticles, colloids). We will continue to explore the role of finite electrolyte concentration on both dynamical and equilibrium properties. The additional complexity of finite electrolyte concentrations necessitates the formulation of reduced descriptions of interactions ion–ion correlations that capture the phenomena of screening. These reduced descriptions will focus on developing new collective variables to efficiently describe the system. These collective variables will enable the connection of molecular detail to effective models of interaction that will be used to study both bulk and interfacial phenomena.

We will continue to explore optimal descriptors and reaction coordinates for fundamental processes. This includes coordination number, electric fields, and local vibrational response as an order parameter. We will explore reduced descriptions of phenomena based on three dimensional fields as order parameters. This includes density, charge, and multipole fields. Fields describing

3. Integrating Simulations and Experiment

We will continue to explore the connection between simulated ensembles and response to direct experimentally measured signals. We will continue to utilize X-ray spectroscopy measurements such as EXAFS and XANES to benchmark local structure and fluctuations about ions in solution. We will continue to utilize x-ray and neutron diffraction measurements to characterize long range correlation. We will continue to explore the relation between SAX and WAXS signals and models of molecular interaction and the balance between short range and long-range driving forces. We will continue to explore the progression of structures and fluctuations with increasing concentration and reduced water content. We will continue to explore the use of x-ray techniques to characterize and capture the initial stages and progression of nucleation in solution. We will continue to explore the use of photoelectron spectroscopy to probe intramolecular hydrogen bonds.

Peer-Reviewed Publications Resulting from this Project (2021-2023)

1. Cao, WJ, SS Xantheas, and XB Wang, "Cryogenic Vibrationally Resolved Photoelectron Spectroscopy of OH-(H2O): Confirmation of Multidimensional Franck-Condon Simulation Results for the Transition State of the OH + H2O Reaction," Journal of Physical Chemistry A 125, 2154 (2021). DOI: https://doi.org/10.1021/acs.jpca.1c00848
2. Carter-Fenk, K, CJ Mundy, and JM Herbert, "Natural Charge-Transfer Analysis: Eliminating Spurious Charge-Transfer States in Time-Dependent Density Functional Theory Via Diabatization, with Application to Projection-Based Embedding," Journal of Chemical Theory and Computation 17, 4195 (2021). DOI: https://doi.org/10.1021/acs.jctc.1c00412
3. Chuev, GN, MV Fedotova, and M Valiev, "Renormalized Site Density Functional Theory," Journal of Statistical Mechanics-Theory and Experiment 2021, 033205 (2021). DOI: https://doi.org/10.1088/1742-5468/abdeb3
4. Chuev, GN, MV Fedotova, and M Valiev, "Renormalized Site Density Functional Theory for Models of Ion Hydration," Journal of Chemical Physics 155, 13 (2021). DOI: https://doi.org/10.1063/5.0060249
5. Duignan, TT, SM Kathmann, GK Schenter, and CJ Mundy, "Toward a First-Principles Framework for Predicting Collective Properties of Electrolytes," Accounts of Chemical Research 54, 2833 (2021). DOI: https://doi.org/10.1021/acs.accounts.1c00107
6. Gibson, LD, J Pfaendtner, and CJ Mundy, "Probing the Thermodynamics and Kinetics of Ethylene Carbonate Reduction at the Electrode-Electrolyte Interface with Molecular Simulations," Journal of Chemical Physics 155, 11 (2021). DOI: https://doi.org/10.1063/5.0067687
7. Kathmann, SM, "Electric Fields and Potentials in Condensed Phases," Physical Chemistry Chemical Physics 23, 23836 (2021). DOI: https://doi.org/10.1039/d1cp03571a
8. Liu, J, JR Yang, XC Zeng, SS Xantheas, K Yagi, and X He, "Towards Complete Assignment of the Infrared Spectrum of the Protonated Water Cluster H+(H2O)21," Nature Communications 12, 10 (2021). DOI: https://doi.org/10.1038/s41467-021-26284-x
9. Yuan, QQ, WJ Cao, M Valiev, and XB Wang, "Photoelectron Spectroscopy and Theoretical Study on Monosolvated Cyanate Analogue Clusters ECX-•Sol (ECX- = NCSe-, AsCSe-, and AsCS-; Sol = H2O, CH3CN)," Journal of Physical Chemistry A 125, 3928 (2021). DOI: https://doi.org/10.1021/acs.jpca.1c03336
10. Chuev, G, M Dinpajooh, and M Valiev, "Molecular-Based Analysis of Nanoparticle Solvation: Classical Density Functional Approach," Journal of Chemical Physics 157, 184505 (2022). DOI: https://doi.org/10.1063/5.0128817
11. Heindel, JP, MV Kirov, and SS Xantheas, "Hydrogen Bond Arrangements in (H2O)(20, 24, 28) Clathrate Hydrate Cages: Optimization and Many-Body Analysis," Journal of Chemical Physics 157, 094301 (2022). DOI: https://doi.org/10.1063/5.0095335
12. Mato, J, D Tzeli, and SS Xantheas, "The Many-Body Expansion for Metals. I. The Alkaline Earth Metals Be, Mg, and Ca," Journal of Chemical Physics 157, 084313 (2022). DOI: https://doi.org/10.1063/5.0094598
13. Petrik, NG, MD Baer, CJ Mundy, and GA Kimmel, "Mixed Molecular and Dissociative Water Adsorption on Hydroxylated TiO2(110): An Infrared Spectroscopy and Ab Initio Molecular

Dynamics Study," Journal of Physical Chemistry C 126, 21616 (2022). DOI: https://doi.org/10.1021/acs.jpcc.2c07063
14. Santis, GD, N Takeda, K Hirata, K Tsuruta, SI Ishiuchi, SS Xantheas, and M Fujii, "Structure of Gas Phase Monohydrated Nicotine: Implications for Nicotine's Native Structure in the Acetylcholine Binding Protein," J Am Chem Soc 144, 16698 (2022). DOI: https://doi.org/10.1021/jacs.2c04064
15. Takeda, N, K Hirata, K Tsuruta, GD Santis, SS Xantheas, S Ishiuchi, and M Fujii, "Gas Phase Protonated Nicotine Is a Mixture of Pyridine- and Pyrrolidine-Protonated Conformers: Implications for Its Native Structure in the Nicotinic Acetylcholine Receptor," Physical Chemistry Chemical Physics 24, 5786 (2022). DOI: https://doi.org/10.1039/d1cp05175j
16. Valiev, M, GN Chuev, and MV Fedotova, "Cdftpy: A Python Package for Performing Classical Density Functional Theory Calculations for Molecular Liquids," Computer Physics Communications 276, 108338 (2022). DOI: https://doi.org/10.1016/j.cpc.2022.108338
17. Cao, W, H Wen, SS Xantheas, and XB Wang, "The Primary Gas Phase Hydration Shell of Hydroxide," Sci Adv 9, eadf4309 (2023). DOI: https://doi.org/10.1126/sciadv.adf4309
18. Carter-Fenk, K, BA Johnson, JM Herbert, GK Schenter, and CJ Mundy, "Birth of the Hydrated Electron Via Charge-Transfer-to-Solvent Excitation of Aqueous Iodide," J Phys Chem Lett 14, 870 (2023). DOI: https://doi.org/10.1021/acs.jpclett.2c03460
19. Finney, JM, TH Choi, RM Huchmala, JP Heindel, SS Xantheas, KD Jordan, and AB McCoy, "Isotope Effects in the Zundel-Eigen Isomerization of H+(H2O)6," J Phys Chem Lett4666 (2023). DOI: https://doi.org/10.1021/acs.jpclett.3c00952
20. Heindel, JP, KM Herman, and SS Xantheas, "Many-Body Effects in Aqueous Systems: Synergies between Interaction Analysis Techniques and Force Field Development," Annual Review of Physical Chemistry 74, 337 (2023). DOI: https://doi.org/10.1146/annurev-physchem-062422-023532
21. Herman, KM, E Apra, and SS Xantheas, "A Critical Comparison of Ch···Π Versus Π···Π Interactions in the Benzene Dimer: Obtaining Benchmarks at the CCSD(T) Level and Assessing the Accuracy of Lower Scaling Methods," Physical Chemistry Chemical Physics 25, 4824 (2023). DOI: https://doi.org/10.1039/d2cp04335a
22. Herman, KM and SS Xantheas, "An Extensive Assessment of the Performance of Pairwise and Many-Body Interaction Potentials in Reproducing Ab Initio Benchmark Binding Energies for Water Clusters n=2-25," Physical Chemistry Chemical Physics 25, 7120 (2023). DOI: https://doi.org/10.1039/d2cp03241d
23. Wang, Q, Z Qin, GL Hou, Z Yang, M Valiev, XB Wang, X Zheng, and Z Cui, "Properties of Gaseous Deprotonated L-Cysteine S-Sulfate Anion [cysS-SO3]-: Intramolecular H-Bond Network, Electron Affinity, Chemically Active Site, and Vibrational Fingerprints," Int J Mol Sci 24, 1682 (2023). DOI: https://doi.org/10.3390/ijms24021682
24. Legg, BA, MD Baer, J Chun, GK Schenter, S Huang, Y Zhang, Y Min, CJ Mundy, and JJ De Yoreo, "Visualization of Aluminum Ions at the Mica Water Interface Links Hydrolysis State-to-Surface Potential and Particle Adhesion," J Am Chem Soc 142, 6093 (2020). DOI: https://doi.org/10.1021/jacs.9b12530
25. Palmer, BJ, J Chun, JF Morris, CJ Mundy, and GK Schenter, "Correlation Function Approach for Diffusion in Confined Geometries," Physical Review E 102, 022129 (2020). DOI: https://doi.org/10.1103/PhysRevE.102.022129

26. Kowalski, K, R Bair, NP Bauman, JS Boschen, EJ Bylaska, J Daily, WA de Jong, T Dunning, N Govind, RJ Harrison, M Keceli, K Keipert, S Krishnamoorthy, S Kumar, E Mutlu, B Palmer, A Panyala, B Peng, RM Richard, TP Straatsma, P Sushko, EF Valeev, M Valiev, HJJ van Dam, JM Waldrop, DB Williams-Young, C Yang, M Zalewski, and TL Windus, “From Nwchem to Nwchemex: Evolving with the Computational Chemistry Landscape,” Chemical Reviews 121, 4962 (2021). DOI: https://doi.org/10.1021/acs.chemrev.0c00998
27. Nakouzi, E, AG Stack, S Kerisit, BA Legg, CJ Mundy, GK Schenter, J Chun, and JJ De Yoreo, “Moving Beyond the Solvent-Tip Approximation to Determine Site-Specific Variations of Interfacial Water Structure through 3d Force Microscopy,” Journal of Physical Chemistry C 125, 1282 (2021). DOI: https://doi.org/10.1021/acs.jpcc.0c07901
28. Nakouzi, E, S Yadav, BA Legg, S Zhang, JH Tao, CJ Mundy, GK Schenter, J Chun, and JJ De Yoreo, “Visualizing Solution Structure at Solid-Liquid Interfaces Using Three-Dimensional Fast Force Mapping,” Jove-Journal of Visualized Experiments 174, e62585 (2021). DOI: https://doi.org/10.3791/62585
29. Kumawat, N, A Tucs, S Bera, GN Chuev, M Valiev, MV Fedotova, SE Kruchinin, K Tsuda, A Sljoka, and A Chakraborty, “Site Density Functional Theory and Structural Bioinformatics Analysis of the Sars-Cov Spike Protein and Hace2 Complex,” Molecules 27, 799 (2022). DOI: https://doi.org/10.3390/molecules27030799
30. Dhakal, D, DM Driscoll, N Govind, AG Stack, N Rampal, G Schenter, CJ Mundy, TT Fister, JL Fulton, M Balasubramanian, and GT Seidler, “The Evolution of Solvation Symmetry and Composition in Zn Halide Aqueous Solutions From Dilute to Extreme Concentrations,” Physical Chemistry Chemical Physics 25, 22650 (2023). DOI: https://doi.org/10.1039/d3cp01559a
31. Mato, J, SY Willow, JC Werhahn, and S Xantheas, “The Back Door to the Surface Hydrated Electron,” The Journal of Physical Chemistry Letters, 14, 8221 (2023). DOI: https://doi.org/10.1021/acs.jpclett.3c01479
32. Mejia-Rodriguez D, E Apra, J Autschbach, NP Bauman, EJ Bylaska, N Govind, JR Hammond, K Kowalski, A Kunitsa, A Panyala, B Peng, JJ Rehr, H Song, S Tretiak, M Valiev, and FD Vila, “NWChem: Recent and Ongoing Developments,” Journal of Chemical Theory and Computation (2023). DOI: https://doi.org/10.1021/acs.jctc.3c00421
33. Fetisov EO, MD Baer, JI Siepmann, GK Schenter, SM Kathmann, and CJ Mundy, "The Statistical Mechanics of Solution-Phase Nucleation: CaCO_3 Revisited," Foundations of Molecular Modeling and Simulation, pp 101-122, Springer (2021).

Quantum Simulation of the Identity and Dynamics of Chemical Bonds in Liquids
DE-SC0017800

Principal Investigator: Benjamin J. Schwartz
Dept. Chem. & Biochem., UCLA, Los Angeles, CA, USA
E-mail: schwartz@chem.ucla.edu

Project Scope: For simple solution-phase chemical reactions, such as the photodissociation of a diatomic molecule, is it appropriate to assume that the potentials energy surfaces of the molecule are the same in solution as in the gas phase? If not, what modifications need to be made because of the solute-solvent interactions to understand the electronic structure and reactivity of molecules in solution? When the solvent determines the outcome of a chemical reaction, how does it induce quantum decoherence? This project uses theoretical methods, including mixed quantum/classical simulations in combination with machine learning algorithms, along with the novel development of quantum umbrella sampling and pseudopotentials to make the solution-phase chemical calculations as accurate and efficient as possible, including non-adiabatic dynamics on electronic excited states.

Most of the work to date has focused on simple solutes, such as Na_2, Na_2^+ and NaK^+, where the only valence electrons are the bonding electrons, allowing the theoretical methods we use to accurately describe the electronic structure, even in solution environments. To date, we have explored solvents including liquid Ar as an example of a solvent that is weakly interacting, and liquid tetrahydrofuran (THF), which is an example of a medium-polarity solvent that can form weak dative bonds between the oxygen lone pairs and the empty valence orbitals on alkali metal cations. In previous work funded by this award, we found that the interactions with the solvent not only control the bond dynamics of the solute, but that the solvent can actually become part of the chemical identity of the solute.[1] This is because local specific interactions between the solvent and solute, such as those in liquid THF, are enough to complete change the chemical nature of the solute, even though each interaction only has the energetic strength comparable to that of a hydrogen bond. If the solvent coordinates the solute in different ways, the new solute (which includes the locally coordinating solvent molecules) can have different bond lengths, vibrational spectra and electronic structure.[2] The questions listed above build on this previous work, allowing us to delve deeply into the best ways to think about solvent effects on chemical reactivity.

Recent Progress: Recently, we have used quantum simulation methods to extend our previous work by examining how solvent-induced changes in chemical identity affect the breaking of chemical bonds on the electronic excited state. We found that for a diatomic solute that normally undergoes a photodissociation reaction in the gas phase, Na_2^+, the chemistry following photoexcitation in THF solution is entirely different: the solution-phase dynamics involve a two-step process whose first step is best described as a photoisomerization reaction involving rearrangement of the locally-coordinated solvent molecules, followed by a second quasi-dissociative step that can take place only after the solvent isomerization is complete. Because motions of the coordinated solvent molecules, rather than the solute photofragments, dominate the early-time dynamics, the solution-phase reaction needs to be described by a 2-dimensional

potential energy surface involving collective motion of the first-shell solvent molecules rather than the simpler one-dimensional potential energy curves that describe the gas-phase photoreactivity. The results indicate that the solvent can play an intimate role in chemical reactions involving bond breaking or formation, potentially requiring a whole new formalism beyond what is typically used for gas-phase reactivity.

Due to Pauli repulsion of the datively-bound THF molecules, the Na_2^+ bonding electron has its excited-state node oriented parallel to the Na–Na bond axis, similar to the structure of a π bonding MO. The fact that the initial photoexcitation produces an excited-state wavefunction with more π than σ^* character gives little driving force to separate the Na^+ ions in the Franck-Condon region. Yet, if trajectories are run for a time much longer than necessary for the gas-phase dissociation reaction, the Na^+ ions in liquid THF eventually do separate.

To investigate this, we constructed a 2-D free energy surface based both on the distance between the Na^+ fragments and the geometry of the datively-bonded THFs that determine the solute chemical identity. Figure 1 shows this 2-D energy surface following photo-excitation of Na_2^+, where one axis is the datively-bonded solvent molecular geometry (defined as '0' when the solvent arrangement is 'see-saw' and as '1' when the arrangement is 'tetrahedral') and the other is the distance between photofragment centers of mass. Superimposed on the energy surface is an orange curve showing the time-averaged behavior of the nonequilibrium ensemble. Clearly, the initial motion of the photoexcited system is entirely along the THF geometry coordinate: Franck-Condon excitation now leads solely to photoisomerization instead of photodissociation. Only after the isomerization is complete and the node in the excited-state wavefunction rotates from the π to σ^* position can dissociation begin to occur. Thus, the change in chemical identity by placing the molecule in the weakly-interacting solvent thus changes the chemical reactivity upon photoexcitation. Our current work is aimed at exploring how the molecular identity changes on-the-fly following excitation (i.e., if additional molecules become coordinated or some coordination bonds break during the reaction), thus changing the energetic driving force for the photoreaction.

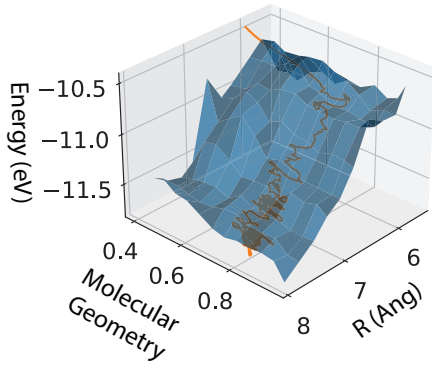

Fig. 1: 2-D Free energy surface describing the photoexcitation of Na_2^+ in THF; see Ref. [B] for details.

We also recently completed a study of the Na_2^+ photoexcitation in liquid Ar, a solvent that does not have local specific interactions with the solute. To understand the role that different solvent motions play at and away from equilibrium for the Na_2^+/Ar system, we analyzed the solvent fluctuations that affect the quantum mechanical energy gap of the solute. Figure 2 plots the natural logarithm of the distribution of solvent-induced changes in solute energy gap, creating an effective solvation free energy surface similar to those used in the Marcus theory of electron transfer. The left panel shows that the way the solvent affects the solute's electronic structure is quite different when the solute is at equilibrium on the electronic ground state (squares), electronic excited state (triangles) and during the nonequilibrium dissociation dynamics (vertical lines). None of the three free energy surfaces are parabolic, indicating that the solvent

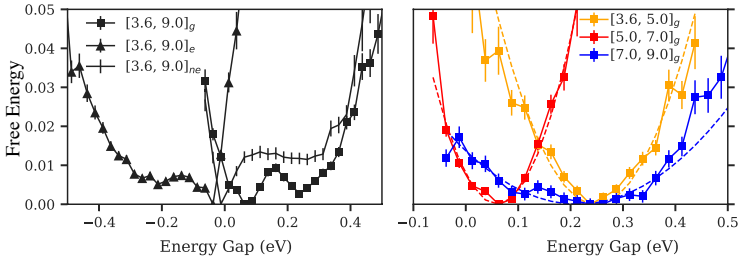

Fig. 2: Marcus-like solvation free energy surfaces for the dissociation of Na_2^+ in liquid Ar. Each of the free energy surfaces can be described by a few parabolas corresponding to fluctuations of the solvent at different solute bond lengths.[A]

fluctuations that underlie these surfaces are not Gaussian. This means that linear response cannot be used to describe the dynamics of this simple molecule in liquid Ar.

Remarkably, however, all of the free energy surfaces can be well described as the sum of two or three parabolic surfaces, as shown for the ground state in the right panel of Fig. 2. In this case, the parabolic surfaces result from restricting the solute bond distance between 3.6 and 5.0 Å (yellow squares), 5.0 and 7.0 Å (red squares), and for nearly-dissociated Na_2^+ with bond distances greater than 7.0 Å (blue squares). The fact that these solvation free energy surfaces fit to parabolas with different curvatures at distinct Na_2^+ bond lengths suggests that the solute encounters unique solvent environments as it dissociates. In other words, the solvent motions that modulate the solute energy gap fluctuate in one particular way when the bond length is small, and suddenly fluctuate in a different way as the bond extends. The way the fluctuations change with bond length is different for the equilibrium ground-state, equilibrium excited-state, and during the nonequilibrium dynamics. This is remarkable because the liquid Ar solvent in this system can undergo only translational motions, meaning that the same solvent motions affect the solute's quantum energy gap differently as the bond length changes. Thus, rather than experiencing a continuous change of solvent environments, the dissociating solute encounters a small handful of discrete, distinct environments. We are currently sorting out the reasons why these discrete environments occur (see Ref. [A]), but we suspect that this idea of a few discrete solvent environments may underlie a great deal of solution-phase reactivity.

Finally, we have used molecular simulations to examine the quantum decoherence that accompanies solution-phase chemical bond breaking. For Na_2^+, the wavefunction of the bonding electron is a superposition of positional quantum states centered on each atom. In vacuum, this coherence is conserved indefinitely, with half the bonding electron associated with each atom as the distance between them approaches infinity. In liquid Ar, interactions with the solvent environment break the local symmetry, causing the electron to collapse onto a single positional quantum state and localize on one of the two atomic photofragments. We have used machine learning (ML) to focus on isolating the subset of solvent motions that cause decoherence.

Using a Balanced Random Forest (BRF) classifier model, we are able to predict whether decoherence will occur and which atom the electron will collapse on to with ~90% accuracy given an optimized feature space of dimensionality five. We deduce from the feature importance analysis that there are two primary requisites for decoherence. First, decoherence only occurs at longer Na–Na bond distances: if the bond is too short, excited Na_2^+ behaves as a single quantum entity, so there is no way for interactions with the environment to break the local symmetry and cause decoherence. Second, the solvent motions that promote electron localization involve asymmetric collisions on each Na^+ fragment: simultaneous collisions on

the two fragments do not lead to decoherence. This suggests that for quantum computing and other applications involving entanglement, the existence of strong collisions between the entangled system and the environment is not necessarily problematic; only dissimilar collisions need to be avoided.

Future Plans: We are current extending all of the above studies to the excited-state dynamics of the NaK^+ molecule. What makes this system interesting is its broken symmetry: because the electron affinities of Na^+ and K^+ are different, dissociation of the molecule in the gas phase produces $K^+ + Na^0$ on the electronic ground state and $K^0 + Na^+$ on the lowest electronic excited state. In THF solution, however, we have performed thermodynamic integration calculations to show that the thermodynamically stable product on the excited state becomes $K^+ + Na^0$ because the solvation free energy of K^+ is larger than that of Na^+, leading to a curve crossing that does not exist in the gas phase. Our preliminary results, however, suggest that the solvent is unable to achieve equilibrium during the photodissociation dynamics, leading to a branching ratio where both sets of products are observed, although the $K^+ + Na^0$ product (which is not the most thermodynamically stable) appears to be kinetically preferred. This provides yet another example where the presence of a solvent can change the outcome of a reaction both thermodynamically and kinetically. In liquid Ar, we plan to explore whether asymmetric interactions with the solvent can change the localization from that expected in the gas phase.

References:

[1] D. R. Widmer and B. J. Schwartz, "Solvents Can Control Solute Molecular Identity," *Nature Chemistry* **10**, 910-6 (2018); DOI: 10.1038/s41557-018-066-z.

[2] D. R. Widmer and B. J. Schwartz, "The Role of the Solvent in the Condensed-Phase Dynamics and Identity of Chemical Bonds: The Case of the Sodium Dimer Cation in THF," *J. Phys. Chem. B* **124**, 6603-16 (2020); DOI: 10.1021/acs.jpcb.0c03298.

Peer Reviewed Publications Resulting from this Project (2022-3):

[A] A. Vong and B. J. Schwartz, "Bond Breaking Reactions Encounter Distinct Solvent Environments, Causing Breakdown of Linear Response," *J. Phys. Chem. Lett.* **13**, 6783-91 (2022); DOI: 10.1021/acs.jpclett.2c01656.

[B] A. Vong, K. J. Mei, D. R. Widmer and B. J. Schwartz, "Solvent Control of Chemical Identity Can Change Photodissociation into Photoisomerization," *J. Phys. Chem. Lett.* **13**, 7931-8 (2022); DOI: 10.1021/acs.jpclett.2c01955.

[C] W. A. Narvaez, S. J. Park and B. J. Schwartz, "Competitive Ion Pairing and the Role of Anions in the Behavior of Hydrated Electrons in Electrolytes," *J. Phys. Chem. B* **126**, 7701-8 (2022); DOI: 10.1021/acs.jpcb.2c04463.

[D] S. J. Park, W. A. Narvaez and B. J. Schwartz, "Ab Initio Studies of Hydrated Electron:Cation Contact Pairs: Hydrated Electrons Simulated by Density Functional Theory are too Kosmotropic," *J. Phys. Chem. Lett.* **14**, 559-66 (2023); DOI: 10.1021/acs.jpclett.2c03705.

[E] S. J. Park and B. J. Schwartz, "How Ions Break Local Symmetry: Simulations of Polarized Transient Hole Burning for Different Models of the Hydrated Electron in Contact Pairs with Na^+," *J. Phys. Chem. Lett.* **14**, 3014-22 (2023); DOI: 10.1021/acs.jpclett.3c00220.

[F] K. J. Mei, W. Borrelli and B. J. Schwartz, "Using Machine Learning to Understand the Causes of Quantum Decoherence in Solution-Phase Bond Breaking Reactions," submitted (2023).

Next generation solar cells Probed at the Interface with Exceptional precision (PIE): Towards new device design
Award Number – AWD-02-0000-2003

Craig Schwartz
NEXCL, University of Nevada, Las Vegas, Las Vegas, NV 89154, craig.schwartz@unlv.edu
Keith Lawler
NEXCL, University of Nevada, Las Vegas, Las Vegas, NV 89154, keith.lawler@unlv.edu

Project Scope

A viable solar cell technology needs to be affordable, efficient and stable. Hybrid organic-inorganic halide perovskite-based solar cells have reached power conversion efficiency levels comparable to the mature first-generation silicon-based technology (~26 %) with total costs for the solar cell stack (not accounting for system cost, installation etc.) predicted to be half the cost of silicon solar cells.[1] The key remaining challenge for this new technology is stability and more precisely, interfacial stability. The electronic structure at interfacial junctions between different material components of these cells play a key role in device function and efficiency, but the way that functional interfaces form and dynamically evolve under operating conditions is presently not well understood. Using a variety of methods, including recently developed soft X-ray second harmonic generation (SXSHG) with interfacial sensitivity, the goal of this project is to develop an in-depth fundamental understanding of interfacial electronic structure and dynamics in photovoltaic systems. These insights will enable the rational design of more efficient and stable devices.

This project will leverage the soft X-ray energy range and high repetition rate of LCLS-II, which recently saw first light and should start user experiments in late 2024. The upgraded facility will make it possible to study halide perovskite interfaces, with a focus on two challenging interface problems: i) two-dimensional (2D) layered passivation of three-dimensional (3D) perovskite light absorbers to overcome atmospheric surface degradation, and ii) trap-assisted tunneling pathways in recombination junctions for CIGS/perovskite tandem devices, which are critical for achieving tandem operation to enhance the overall power conversion efficiency. Prior to anticipated experimental time at LCLS-II, the project will include studies of simpler Si-based solar cell interfaces at other X-ray free electron laser (XFEL) facilities, specifically studying selective contact junctions for harvesting photogenerated electrons or holes. We will study the band bending at these junctions that enables selective charge carrier transport, and we will attempt to probe interfacial trap states that limit transport efficiency.

These XFEL measurements boast elemental selectivity and ultrafast time resolution, so eventual time-resolved measurements will explore charge transport limitations at an atomic level including elemental diffusion. Ultimately, this will enable understanding of elemental composition and dynamics of buried interfaces in photovoltaic systems, identifying key pathways that create inefficiencies. It is important to note that solar energy is one of the leading forms of carbon free energy and is particularly important to the state of Nevada due to the large number of hot and sunny days. This project will train several students in Nevada in cutting edge projects of importance to the Department of Energy.

Recent Progress

We have collected the first soft X-ray second harmonic generation (SXSHG) data of silicon-based solar cell materials. This initial result allowed us to understand the junctions between silicon, the native SiO_2 layer, and overlayer materials including TiO_2, Al_2O_3, and LiF/Al designed for surface passivation or electron-selective transport. When the incident XFEL pulse was resonant with the SiO_2 2*p* core level, as verified with XPS measurements, we observed clear SXSHG signal for all overlayer samples. By contrast, the bare Si/SiO_2 sample showed no detectable SXSHG. These results demonstrate that SXSHG is highly sensitive to the asymmetric potential induced by the overlayer materials that leads to band bending at the junction (**Figure 1**). A spread of extracted $\chi^{(2)}_{eff}$ values for different samples suggests that, with better statistics, the SXSHG response may be proportional to the degree of band bending at each interface. We note that XPS measurements of the SiO_2 layer in the LiF/Al overlayer sample yielded no signal, because the LiF/Al layer was too thick, yet the same sample yielded ample SXSHG signal. This demonstrates the utility of SXSHG measurements in probing buried interfaces that cannot be accessed by traditional surface science techniques. We have beamtime in December at SACLA in Japan to continue these studies (see below). Complementary studies to be done at LCLS-II have been planned but will need to wait for LCLS-II user operations.

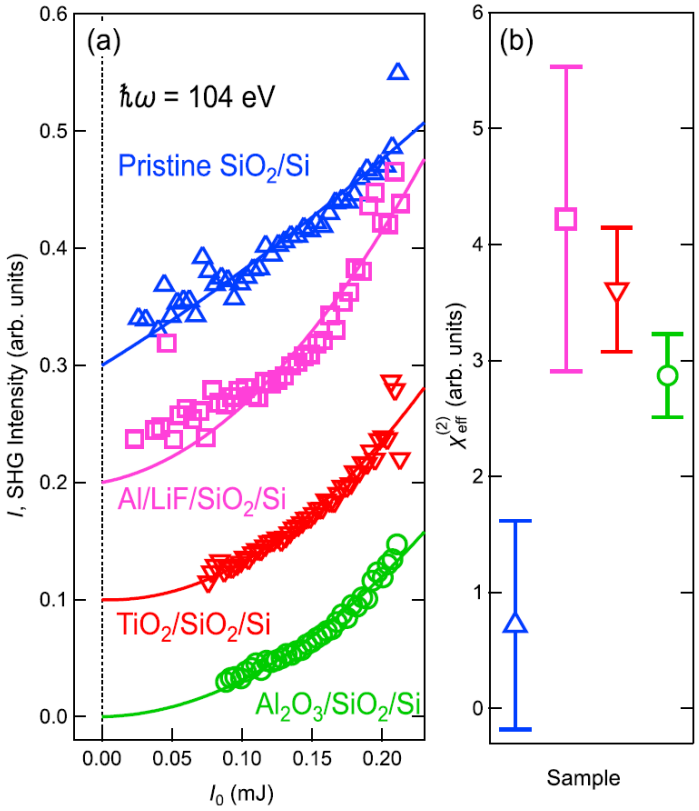

Figure 1: (a) SXSHG intensity as a function of input power for four Si samples with different overlayers, when resonant to the L-edge of the SiO_2 layer. **(b)** Extracted $\chi^{(2)}_{eff}$ values for each sample.

The delay in LCLS-II commissioning caused us to delay hiring, but we finished hiring junior staff in June 2023. Our national lab partner, Carolin Sutter-Fella at LBL, along with the postdoctoral fellow hired for this work, has begun investigation of the formation of 2D molecules Phenethylammonium iodide (PEAI) and 4-Fluoro-Phenethylammonium iodide (F-PEAI) on 3D thin films of $CsFAPb(I,Br)_3$ (FA= formamidinium) with in situ photoluminescence (PL) and in situ diffraction. The 2D molecules are hydrophobic in nature and act as a passivation layer for the 3D perovskite thin film. It was found that the *n*=1 2D perovskite phase as a reaction between PbI_2 from the 3D film and the 2D molecule forms primarily instead of higher order *n* (*n* is the number of inorganic lead halide octahedra separating the 2D molecules). The activation energy for this reaction was higher when using F-PEAI resulting in slower kinetics and thinner quasi-2D layers. Possibly F-PEAI exhibits stronger intermolecular interactions than PEAI. Heat treatment at 100 °C for 30 min was found to further promote growth of the quasi-2D perovskites

rather than degrading it. These insights will enable future design of operando measurements, as described below. The materials from this effort will be taken to LCLS-II for study by SXSHG in the long term.

Future Plans

A follow-up experiment on Si-based photovoltaic interfaces is scheduled at SACLA for December 5-10, 2023. We plan to use a reconfigured experimental apparatus to collect full SXSHG spectra as a function of input photon energy. Focusing on $TiO_2/SiO_2/Si$ samples, we hope to demonstrate sensitivity to the direction of band bending within the SiO_2 layer. These samples can be prepared as either electron-selective or hole-selective contacts by varying the synthesis procedure, so we will directly compare both types. The TiO_2 overlayer will induce band bending in the conduction band and core level states of SiO_2, but the effect on the core levels should be smaller due to electronic screening. Therefore, the resonant excitation from core to conduction band should shift to higher energy for upwards band bending (hole-selective contact) and to lower energy for downwards band bending (electron-selective contact). Collecting full SXSHG spectra will reveal this shift in absorption onset, although we expect the magnitude of the shift is small (sub-eV). We have demonstrated sub-sampling of input energies due to jitter of the XFEL beam at SACLA in prior studies,[2,3] and hope to use the same analysis here to resolve the SXSHG spectral shift. It is difficult to detect the direction of band bending with established characterization methods, so a successful demonstration of SXSHG sensitivity to the polarity of the band bending in these samples will constitute a significant advance.

Another scientific challenge for selective contact junctions is characterizing the surface states that form at the interface. These are electronic states that appear in the mid-gap due to the crystal truncation at the interface, that can act as trap states or recombination pathways for charge carriers. These states are difficult to detect due to their low density and confinement to the interface. The interfacial sensitivity of SXSHG should enhance signal from these states, and their position within the band gap means there will be little background to obscure their signal, even if small. The same SXSHG spectra described above should, in principle, be able to detect these states in the form of spectral features below the main absorption edge. The band gap in Si, however, is only 1.12 eV, so high energy resolution will be needed to observe these features. Thus, this remains a secondary goal, with our primary aim to demonstrate sensitivity to upwards vs. downward band bending.

In parallel to these experiments on Si samples, we will perform in situ investigation of the formation of 2D molecules (PEAI, F-PEAI, TMAI, TMABr) on $FAPbI_3$ and $CsFAPbI_3$ thin films with in situ photoluminescence and in situ diffraction. The concentration of the 2D molecules will be varied between 10 mM and 40 mM dissolved in isopropyl alcohol. In addition, $FAPbI_3$ and $CsFAPbI_3$ thin films will be grown Pb-rich and Pb-stoichiometric before 2D deposition on top. The hypothesis is that Pb-stoichiometric films will show self-limited 2D growth with better control over the number of inorganic slabs in between the organic cations. The measurements on formation of 2D/3D interfaces will be followed by operando measurements i.e. continued photoluminescence and diffraction while exposing the stack to 85□C in inert atmosphere for several minutes to hours. The device synthesis efforts of our planned studies into trap-assisted tunneling pathways in recombination junctions for CIGS/perovskite tandem devices will commence following the completion of these 2D/3D interface formation experiments.

While part of our studies necessarily depend on the status going forward with LCLS-II, we will be able to make the following measurements in the near future. We will characterize the partial solar cell stacks we grow by both XPS (using the Molecular Foundry at LBL's lab source) and X-ray absorption spectroscopy (using the Advanced Light Source at LBL). We will then perform SXSHG measurements on these solar cell stacks to understand how these interfaces work and evolve over time. These measurements may be performed initially at SACLA, which would largely limit us to static characterization of low energy edges (i.e. I N-edges, Cs N-edges, Pb O-edges) due to the low repetition rate. Longer term, we will be able to work at the higher energies enabled by LCLS-II, and work towards measuring a solar cell in situ. In the event of further delays of LCLS-II though, the focus will shift more towards synthesis than characterization as needed.

References

(1) Park, N.-G.; Grätzel, M.; Miyasaka, T.; Zhu, K.; Emery, K. Towards Stable and Commercially Available Perovskite Solar Cells. *Nat Energy* **2016**, *1* (11), 1–8. https://doi.org/10.1038/nenergy.2016.152.

(2) Berger, E.; Jamnuch, S.; Uzundal, C. B.; Woodahl, C.; Padmanabhan, H.; Amado, A.; Manset, P.; Hirata, Y.; Kubota, Y.; Owada, S.; Tono, K.; Yabashi, M.; Wang, C.; Shi, Y.; Gopalan, V.; Schwartz, C. P.; Drisdell, W. S.; Matsuda, I.; Freeland, J. W.; Pascal, T. A.; Zuerch, M. Extreme Ultraviolet Second Harmonic Generation Spectroscopy in a Polar Metal. *Nano Lett.* **2021**, *21* (14), 6095–6101. https://doi.org/10.1021/acs.nanolett.1c01502.

(3) Uzundal, C. B.; Jamnuch, S.; Berger, E.; Woodahl, C.; Manset, P.; Hirata, Y.; Sumi, T.; Amado, A.; Akai, H.; Kubota, Y.; Owada, S.; Tono, K.; Yabashi, M.; Freeland, J. W.; Schwartz, C. P.; Drisdell, W. S.; Matsuda, I.; Pascal, T. A.; Zong, A.; Zuerch, M. Polarization-Resolved Extreme-Ultraviolet Second-Harmonic Generation from $LiNbO_3$. *Phys. Rev. Lett.* **2021**, *127* (23), 237402. https://doi.org/10.1103/PhysRevLett.127.237402.

Peer-Reviewed Publications Resulting from this Project (Project start date: 09/2022)

1. M. Horio, T. Sumi, J. Bullock, Y. Hirata, M. Miyamoto, B. R. Nebgen, T. Wada, T. Senoo, Y. Tsujikawa, Y. Kubota, S. Owada, K. Tono, M. Yabashi, T. Iimori, Y. Miyauchi, M. W. Zuerch, I. Matsuda, C. P. Schwartz, and W. S. Drisdell, *Detecting Driving Potentials at the Buried SiO2 Nanolayers in Solar Cells by Chemical-Selective Nonlinear x-Ray Spectroscopy*, Applied Physics Letters **123**, 031602 (2023).

Probing Interfacial Electron Dynamics (PIED) - A Multimodal Study to Advance Solar Photochemistry

Award Number – AWD-02-0000-2011

Craig Schwartz
NEXCL, University of Nevada, Las Vegas, Las Vegas, NV 89154, craig.schwartz@unlv.edu
Keith Lawler
NEXCL, University of Nevada, Las Vegas, Las Vegas, NV 89154, keith.lawler@unlv.edu
Walter Drisdell
Chemical Sciences Division, Lawrence Berkeley National Laboratory, Berkeley, CA, 94720, wsdrisdell@lbl.gov
Carolin M. Sutter-Fella
Molecular Foundry, Lawrence Berkeley National Laboratory, Berkeley, CA, 94720, csutterfella@lbl.gov

Project Scope

Photoelectrochemical (PEC) devices can convert abundant and cheap solar energy directly into value added chemicals or stored electric energy. Current PECs involve integrating several different materials in layers, for example a photovoltaic-grade light absorber, selective transport layer, and electrocatalyst layer. The electronic structure at the interfaces between these layers controls charge transport and device function, but can also lead to losses due to trap states or recombination pathways that are difficult to characterize. The aim of this project is to study these functional interfaces at the atomic length and ultrafast time scales to gain a deeper understanding of charge transport at these (often buried) interfaces. We will leverage the interfacial sensitivity and time resolution of the recently developed Soft X-ray Second Harmonic Generation (SXSHG) technique, coupled with supporting measurements and theory, to interrogate the electronic structure at these interfaces with unprecedented detail. Further development of the SXSHG technique, through studies of other materials and systems, is another goal.

Inspired by recent halide perovskite-based PEC device for syngas production [1,2], we have selected several different interfaces to study, including those responsible for charge carrier transport within the PEC system: (i) metal catalyst/$BiVO_4$, (ii) inorganic/halide perovskite, and (iii) organic/halide perovskite interfaces. Each of these interfaces serves a different function, controlled by the interfacial electronic structure. SXSHG measurements, supported by laser induced fluorescence and X-ray absorption spectroscopy, will reveal the structure and dynamics of these functional interfaces and determine sources of charge transport limitations at an atomic level. Ultimately, this will enable understanding of interfaces in both elemental composition and time resolution, determining where charge carrier losses in device interfaces are located and their cause at the molecular scale. This fundamental understanding will guide the development and integration of next generation PEC components.

With the commissioning of LCLS-II, the collection of full SXSHG spectra will be accelerated temporally by orders of magnitude, thus enabling new classes of previously infeasible measurements including time-resolved SXSHG. This proposal will also develop the nascent technique of SXSHG to exploit the new capabilities of LCLS-II and combine time resolved SXSHG pump-probe measurements with steady-state measurements to create a complete picture of the dynamics at an interface. Overall, this project addresses the DOE core goals of increasing the spatial and/or temporal ability to probe interfaces and understanding the mechanisms of

multiscale processes at interfaces to advance the design of integrated multicomponent systems.

Recent Progress

The delay in the commissioning of LCLS-II has delayed this project, and we purposely delayed hiring. Thus, our primary recent progress has focused on assembling a research team, starting our first researcher in April 2023 and staffing up more fully as of June 2023. During the interim time, other milestones related to SXSHG development have been accomplished.

As SXSHG is a relatively novel technique and there have been no comprehensive reviews of the technique, we took this opportunity to review the field of nonlinear optics in the soft X-ray region as well as discuss the future of soft X-ray nonlinear optics, focusing on new lasers and light sources that will be developed shortly. This is set to be published in a book entitled Nonlinear X-Ray Spectroscopy for Materials Science. [3,4]

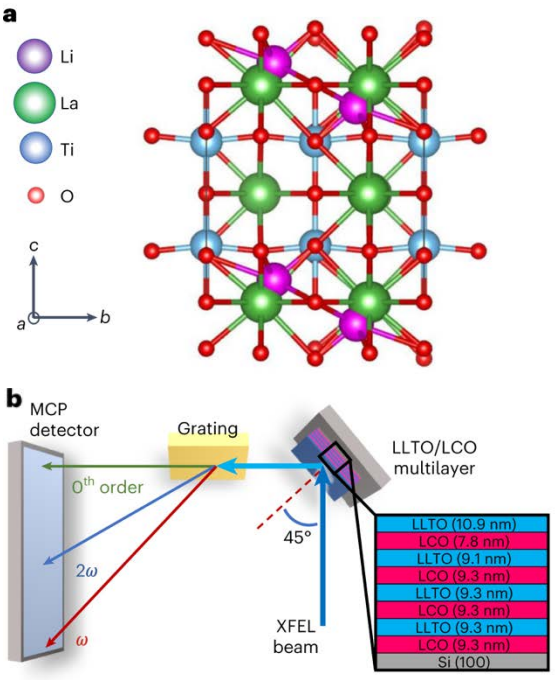

Figure 1 – a – crystal structure of LLTO and its constituent elements. b – Experimental setup for XUV-SHG and layered structure consisting of repeating LLTO and LCO layers [5].

We also further developed the application of SXSHG on solid interfaces with a study of battery materials. Current lithium-ion battery technology exhibits many issues such as safety hazards and dendrite formation. These issues may be overcome with the use of a solid-state electrolyte such as lithium lanthanum titanium oxide (LLTO) [Fig. 1] which has an ionic conductivity comparable to liquid electrolytes. However, like with the halide perovskite-based PEC devices of interest to this proposal, challenges remain with solid-state electrolytes in regard to their interfacial interactions, in particular with lithium electrodes. Stacks of LLTO and lithium-cobalt oxide (LCO) cathodes in conjunction with a Li metal anode were studied by FEL SXSHG (~70 eV) and XAS probes [5]. This work showed that the cause of high interfacial resistance in the case of LLTO is due to a lack of rattling modes at the surface as compared to the bulk. This allows for the design of mitigation strategies for high resistance at surfaces of batteries such as various coating techniques.

The high repetition rate of LCLS-II makes liquids an ideal system to study for the development of SXSHG because these samples constantly refresh, minimizing sample damage concerns. We have already taken SXSHG data at LCLS on the liquid water surface at the oxygen K-edge, as well as on solutions of $Fe(NO_3)_3$ at the Fe M-edge at SACLA. By comparing surface spectra to bulk spectra, we expect to be able to understand the differences between bulk and surface effects. We have several more X-ray experiments scheduled on these systems. We are also excited to participate in the commissioning of LCLS-II.

Developing time-resolved capabilities in is a key goal for free electron laser work, especially with the high repetition rate promised of LCLS-II likely enabling time-resolved SXSHG. Observing the time-resolved magnetic and charge dynamics in the bulk of magnetically

ordered materials provides an ideal platform for such developments given the operating parameters of current soft X-ray FELs. To that extent, we participated in time-dependent studies on ferromagnetically ordered $La_{2/3}Ca_{1/3}MnO_3$ (LCMO) at FERMI operating at the Mn M-edge. Some of the data collected during this beam time is currently being analyzed by our students; the tools developed and student training serve as preparation for the analysis of the much more complex time-resolved data that will be taken at LCLS-II on halide perovskite-based PEC devices.

We also studied the effect of the most predominantly used solvents (dimethylformamide, DMF, dimethyl sulfoxide, DMSO) for halide perovskite thin film fabrication. [6] Multimodal in situ photoluminescence (PL) and wide angle X-ray scattering experiments revealed significant differences in the crystallization pathway of DMF-pure precursors versus DMF-rich (DMF/DMSO=4/1) ones. One of the major findings was that addition of 20 vol% DMSO suppresses crystalline intermediate phases and helps the formation of photoactive α-perovskite. While DMF-pure precursors resulted in compositionally distinct initial perovskite phases; homogeneous perovskite composition was found when DMSO was added. This in situ data combined with insights from DFT explains the benefit of mixed DMF:DMSO precursor solutions. We have now begun halide perovskite layered device fabrication. The first target is partial solar cell stacks of formamidinium lead iodide ($FAPbI_3$) perovskite with an electron selective layer (SnO_2) on ITO or FTO coated glasses. Our hypothesis is that the SnO_2/$FAPbI_3$ interface is not stable due to oxygen vacancies in the SnO_2 layer. Therefore, different alkali metal interlayers between the SnO_2 and $FAPbI_3$ have been tested. In situ PL, in situ diffraction collected at the Advanced Light Source (ALS), and X-ray photoelectron spectra were taken to study the formation of this SnO_2/$FAPbI_3$ interface with and without interlayers. Data analysis is in progress.

Our team has also begun theoretical modelling efforts of SXSHG data, with the first project supporting analysis of the first SXSHG measurements on liquid water. These efforts are on-going, with student training and method development being undertaken in preparation for future simulations of PEC devices and other liquid SXSHG development projects.

Future Plans

During initial commissioning and operation of LCLS-II, it will likely not be running at maximum capabilities. In that case, we think there is a reasonable chance that we will be given time to develop SXSHG on liquid samples, rather than PEC devices, as studies of solid samples would benefit tremendously from LCLS-II operating optimally. Thus, in the near term, we will develop time-resolved SXSHG experiments on liquid samples to assist with LCLS-II commissioning.

Simultaneously, we will continue developing partial PEC device to study at LCLS-II as well as at the Advanced Light Source (ALS) and in our labs. We are planning to perform depth profiling analyses of the SnO_2/$FAPbI_3$ stacks with and without the above-mentioned alkali metal interlayers. To do so, our junior researchers will get trained on XPS/UPS measurements to extract compositional and electronic band structure information at the electron extraction interface. To prove our hypothesis regarding the SnO_2/$FAPbI_3$ interface stability we will also test a high-quality atomic layer deposited (ALD) SnO_2 layer which allows for tuning of the oxygen vacancies.

In an upcoming beamtime at the ALS, we will do angle dependent grazing incident diffraction measurements to probe the SnO_2/$FAPbI_3$ interface (with and without interlayers). Driven by the hypothesis that strain at this interface influences stability, the goal is to understand this interface and its stabilization with interlayer designs. We also anticipate ALS beamtime to measure standard X-ray absorption spectra and X-ray reflectivity on these samples, which will

support our planned LCLS-II experiments.

We have begun applying theoretical methods to the study of complicated condensed matter SXSHG spectra, starting with liquids. Additionally, modeling of ultrafast processes is underway for complicated condensed matter dynamics. Ultimately, these two models – the study of ultrafast phenomena and the study of interfaces – will be combined with the study of PEC devices via SXSHG computationally to understand devices dynamically. Long term, this will be used to develop better PEC devices.

References

[1] A. M. K. Fehr, A. Agrawal, F. Mandani, C. L. Conrad, Q. Jiang, S. Y. Park, O. Alley, B. Li, S. Sidhik, I. Metcalf, C. Botello, J. L. Young, J. Even, J. C. Blancon, T. G. Deutsch, K. Zhu, S. Albrecht, F. M. Toma, M. Wong, and A. D. Mohite, *Integrated Halide Perovskite Photoelectrochemical Cells with Solar-Driven Water-Splitting Efficiency of 20.8%*, Nat Commun **14**, 1 (2023).

[2] V. Andrei, B. Reuillard, and E. Reisner, *Bias-Free Solar Syngas Production by Integrating a Molecular Cobalt Catalyst with Perovskite–BiVO4 Tandems*, Nat. Mater. **19**, 2 (2020).

[3] I. Matsuda, C. P. Schwartz, W. S. Drisdell, and R. Arafune, *Future Prospects*, in *Nonlinear X-Ray Spectroscopy for Materials Science* (Nature Publishing Group, London, 2023).

[4] C. P. Schwartz and W. S. Drisdell, *Nonlinear Soft X-Ray Spectroscopy*, in *Nonlinear X-Ray Spectroscopy for Materials Science* (Nature Publishing Group, London, 2023).

[5] C. Woodahl, S. Jamnuch, A. Amado, C. B. Uzundal, E. Berger, P. Manset, Y. Zhu, Y. Li, D. D. Fong, J. G. Connell, Y. Hirata, Y. Kubota, S. Owada, K. Tono, M. Yabashi, S. G. E. te Velthuis, S. Tepavcevic, I. Matsuda, W. S. Drisdell, C. P. Schwartz, J. W. Freeland, T. A. Pascal, A. Zong, and M. Zuerch, *Probing Lithium Mobility at a Solid Electrolyte Surface*, Nat. Mater. **22**, 7 (2023).

[6] M. Singh, M. Abdelsamie, Q. Li, T. Kodalle, D.-K. Lee, S. Arnold, D. R. Ceratti, J. L. Slack, C. P. Schwartz, C. J. Brabec, S. Tao, and C. M. Sutter-Fella, *Effect of the Precursor Chemistry on the Crystallization of Triple Cation Mixed Halide Perovskites*, Chem. Mater. **35**, 7450 (2023).

Peer-Reviewed Publications Resulting from this Project (Project start date: 09/2022)

1. Woodahl, C.; Jamnuch, S.; Amado, A.; Uzundal, C. B.; Berger, E.; Manset, P.; Zhu, Y.; Li, Y.; Fong, D. D.; Connell, J. G.; Hirata, Y.; Kubota, Y.; Owada, S.; Tono, K.; Yabashi, M.; te Velthuis, S. G. E.; Tepavcevic, S.; Matsuda, I.; Drisdell, W. S.; Schwartz, C. P.; Freeland, J. W.; Pascal, T. A.; Zong, A.; Zuerch, M. *Probing Lithium Mobility at a Solid Electrolyte Surface*, Nat. Mater. 2023, 1–5. https://doi.org/10.1038/s41563-023-01535-y.
2. M. Singh, M. Abdelsamie, Q. Li, T. Kodalle, D.-K. Lee, S. Arnold, D. R. Ceratti, J. L. Slack, C. P. Schwartz, C. J. Brabec, S. Tao, and C. M. Sutter-Fella, *Effect of the Precursor Chemistry on the Crystallization of Triple Cation Mixed Halide Perovskites*, Chem. Mater. 2023. https://doi.org/10.1021/acs.chemmater.3c00799.
3. C. P. Schwartz and W. S. Drisdell, *Nonlinear Soft X-Ray Spectroscopy*, in *Nonlinear X-Ray Spectroscopy for Materials Science* (Nature Publishing Group, London, 2023).
4. I. Matsuda, C. P. Schwartz, W. S. Drisdell, and R. Arafune, *Future Prospects*, in *Nonlinear X-Ray Spectroscopy for Materials Science* (Nature Publishing Group, London, 2023).

DE-SC0007347 **Princeton University**

UNDERSTANDING SURFACES AND INTERFACES OF (PHOTO-)CATALYTIC OXIDE MATERIALS WITH FIRST PRINCIPLES THEORY AND SIMULATIONS

Annabella Selloni,
Department of Chemistry, Princeton University
Email: aselloni@princeton.edu

Project Scope

The overall goal of this project is to characterize and understand the surfaces and aqueous interfaces of TiO_2 and other (photo-)catalytically active oxide materials using first-principles based and machine learning assisted molecular simulations.

Recent Progress

Proton transfer at the IrO_2-water interface from molecular simulations with machine learning potentials **-** Heterogeneous electrocatalysts for the oxygen evolution reaction (OER) operate via inner-sphere processes that are highly sensitive to the composition and structure of the catalyst's aqueous interface. We investigated the proton transfer mechanisms at the aqueous interface of rutile IrO_2, one of the most efficient catalytic materials for the OER, using large scale molecular dynamics simulations with ab-initio based machine learning potentials. The intrinsic proton affinities of the different IrO_2(110) surface sites were characterized by calculating their acid dissociation constants, which yielded a point of zero-charge in good agreement with experiments. A large fraction (≈ 80%) of adsorbed water dissociation is predicted, together with a short lifetime (≈ 0.5 ns) of the resulting terminal hydroxyls, due to rapid proton exchanges between adsorbed H_2O and OH species at adjacent surface Ir sites. This rapid surface proton transfer supports the suggestion that the rate-determining step in the OER may not involve proton transfer across the double layer into solution, but rather depend on the concentration of oxidized sites formed by the deprotonation of terminal and bridging hydroxyls, as indicated by recent experiments. [Ref. 1 in the list of peer-reviewed publications.]

Water Dissociation at the Water-Rutile TiO_2(110) Interface from Ab-initio based Deep Neural Network Simulations. The equilibrium fraction of water dissociation at the TiO_2-water interface has a critical role in the surface chemistry of TiO_2 but is difficult to determine both experimentally and computationally. Among TiO_2 surfaces, rutile TiO_2(110) is of special interest as the most abundant surface of TiO_2's stable rutile phase. While surface-science studies provided detailed information on the interaction of rutile TiO_2(110) with gas-phase water, studies of the TiO_2(110) – liquid water interface have been scarce. In this work, we characterized the structure of the aqueous TiO_2(110) interface using nanosecond time scale molecular dynamics simulations with deep neural network potentials that accurately reproduced the DFT results for water/TiO_2(110) over a wide range of water coverages. Simulations on TiO_2(110) slab models of increasing thickness provided insight into the dynamic equilibrium between molecular and dissociated adsorbed water at the interface, with an estimated equilibrium water dissociation fraction of 22 ± 6 %. This value is much larger than the average dissociation estimated for the aqueous anatase TiO_2(101) interface, consistent with the higher water photooxidation activity that is experimentally observed on rutile than on anatase. [Ref. 5.]

Water-amorphous TiO_2 interface. Amorphous titanium dioxide (a-TiO_2) is widely used as a coating material in applications such as electrochemistry and self-cleaning surfaces where its interface with water has a central role. However, little is known about the structures of the a-TiO_2 surface and aqueous interface, particularly at the microscopic level. In this work, we constructed a model of the a-TiO_2 surface via a cut-melt-and-quench procedure based on molecular dynamics simulations with deep neural network potentials (DPs) trained on density functional theory data. After interfacing the a-TiO_2 surface with water, we investigated the structure and dynamics of the resulting system using a combination of DP-based molecular dynamics (DPMD) and ab initio molecular dynamics (AIMD) simulations. Both AIMD and DPMD simulations show that the distribution of water on the a-TiO_2 surface lacks distinct layers normally found at the aqueous interface of crystalline TiO_2, leading to a 10 times faster diffusion of water at the interface. Bridging hydroxyls resulting from water dissociation decay several times more slowly than terminal hydroxyls (OH_t), due to fast proton exchanges between adsorbed H_2O and OH_t species at adjacent surface Ti sites. [Ref. 3].

Future Plans

Characterizing the carboxylic acid-covered anatase TiO_2 water interface. The adsorption of atmospheric carboxylic acids on titania surfaces is relevant to applications such as self-cleaning windows and photocatalysis. While these acids have been found to readily adsorb forming molecularly ordered structures on the rutile TiO_2 (110) surface under ambient conditions, less is known about the adsorption of carboxylic acids on anatase TiO_2 under similar conditions. We will combine deep learning-assisted molecular dynamics (DPMD) simulations and enhanced sampling methods to investigate the interface of formic and acetic acid-covered anatase TiO_2 with water. Long timescale (ns) DPMD simulations show that the adsorption coverage, adsorption mode, and carboxylic acid tail all play a role in the stability of the interface. Moreover, the computed desorption-free energies suggest that the desorption of both formic and acetic acid is facile. This indicates that, in contrast to the rutile TiO_2 (110) surface, molecularly ordered carboxylic acid layers may not form on the anatase TiO_2 (101) surface.

Electron Transfer at the Aqueous ZrO_2 Interface - Electron transfer (ET) across the aqueous interfaces of metal oxides is ubiquitous in fundamental energy processes and radiation chemistry. In particular, one of the most effective materials for enhancing the yield of H_2 during water radiolysis is ZrO_2. We will investigate the pathways for ET from the conduction band of ZrO_2 to aqueous species at the interface and in solution via *ab initio* molecular dynamics (AIMD), using the computational approach recently developed for MgO (see ref. 11). We expect that the results from this study, especially in comparison to those previously obtained for MgO, will elucidate the capability of ZrO_2 to enhance the radiolytic yield of hydrogen.

Cation exchange at the muscovite-water interface. The aqueous interface of muscovite mica, a common phyllosilicate, plays a prominent role in environmental, bio-, and geo-chemistry, including possibly aiding the formation of abiotic precursors for life to originate on Earth. Muscovite mica (nominal composition $KAl_2(Si_3Al)O_{10}(OH)_2$), in its bulk phase, is composed of alternating aluminosilicate and K^+ layers and easily splits apart at the K^+ layers leaving half the

K^+ ions on each surface maintaining charge neutrality and short-range K^+ ordering. The interactions of these surfaces with water are yet to be fully resolved. Our aim is to develop a deep potential model (DP) that can be subsequently used to understand the mica-water interface at long timescales using deep potential molecular dynamics simulations (DPMD) with *ab initio* accuracy. In particular, we seek to determine if the surface K^+ become mobile when exposed to water resulting in their complete hydration, coupled with the replacement of water/hydronium in the empty surface cavities vacated by them. This understanding of the local interfacial structure and possible ion hydration coupled with water exchange will provide broad insights into mineral-water interactions that could be relevant even to decarbonization technologies.

Peer-Reviewed Publications Resulting from this Project (2021-2023)

1. A.S. Raman, A. Selloni, Acid-Base Chemistry of a Model IrO_2 Catalytic Interface*, J. Phys. Chem. Lett.* **2023**, *14*, 7787−7794.
2. J. Kang, X. Chen, R. Si, X. Gao, S. Zhang, G. Teobaldi, A. Selloni, L-M. Liu, L. Guo, Activating Bi p-orbitals in Dispersed Clusters of Amorphous BiOx for Electrocatalytic Nitrogen Reduction, *Angew. Chem*. **2023**, *135,* e202217428.
3. Z. Ding, A. Selloni, Modeling the aqueous interface of amorphous TiO_2 using deep potential molecular dynamics, *J. Chem. Phys*. **2023**, *159*, 024706.
4. Lee, T.H.; Selloni, A., Deep and Shallow Gap States in Reduced and n-Type Doped *m*-ZrO_2, *J Phys Chem* C **2023**, *127*, 13936-13944.
5. B. Wen, M. F. Calegari Andrade, L.M. Liu, A. Selloni, Water Dissociation at the Water-Rutile TiO_2(110) Interface from *Ab-initio* based Deep Neural Network Simulations, *Proc. Nat. Acad. Sci.* **2023**, *120,* e2212250120.
6. Lee, T.H.; Selloni, A. Structure and Stability of Oxygen Vacancy Aggregates in Reduced Anatase and Rutile TiO2, *J Phys Chem* C **2023**, *127*, 627-634.
7. A.S. Raman, A. Selloni, "Modeling the Solvation and Acidity of Carboxylic Acids Using an ab *initio* Deep Neural Network Potential", *J Phys Chem* A **2022**, *126*, 7283-7290.
8. J. Kang, Y. Xue, J. Yang, Q. Hu, Q. Zhang, L. Gu, A. Selloni, L.-M. Liu and L. Guo, "Realizing Two-Electron Transfer in Monolayer $Ni(OH)_2$ Nanosheets for Energy Storage", *J. Am. Chem*. Soc. **2022**, *144*, 8969-8976
9. Lee, T.H.; Ferri, M.; Piccinin, S.; Selloni, A. Theoretical Insights in Photo-electrochemical Water Reduction on Delafossite $CuRhO_2$, *ACS Energy Letters* **2022**, *7,* 1528-1533.
10. Lee, T.H.; Ferri, M.; Piccinin, S.; Selloni, A. Structure, Electronic Properties and Defect Chemistry of Delafossite $CuRhO_2$ Bulk and Surfaces, *Chem. Mater*. **2022**, *34*, 1567-1577.
11. Ding, Z; Goldsmith, Z.K; Selloni, A. Pathways for Electron Transfer at MgO-Water Interfaces from *Ab-Initio* Molecular Dynamics, *J. Am. Chem*. Soc. **2022**, *144*, 2002-2009.
12. Hu, Q.; Xue, Y.; Kang, J.; Scivetti, I.; Teobaldi, G.; Selloni, A.; Guo, L.; Liu, L.M.; Structure and Oxygen Evolution Activity of β-NiOOH: Where Are the Protons? *ACS Catalysis* **2022**, *12,* 295-304.
13. Zhao, F.; Wen, B.; Niu, W.; Chen, Z.; Yan, C.; Selloni, A.; Tully, C. G; Yang, X.; Koel, B. E; Increasing Iridium Oxide Activity for the Oxygen Evolution Reaction with Hafnium Modification, *J. Am. Chem. Soc***, 2021**, *143*, 15616-15623
14. B. Wen, and A. Selloni, Hydrogen Bonds and H_3O^+ Formation at the Water Interface with

Formic Acid Covered Anatase TiO_2, *J Phys Chem Lett.* **2021,** *12*, 6840-6846.
15. G. Zeng, B. Wen, and A. Selloni, Structure and Stability of Pristine and Carboxylate-Covered Anatase TiO_2 (001) in Aqueous Environment, *J Phys Chem* C **2021**, *125*,15910-15917.
16. A. Rushiti, C. Hattig, B. Wen, A. Selloni, Structure and Reactivity of Reduced Spinel $CoFe_2O_4$ (001)/(100) Surfaces, *J. Phys. Chem. C* **2021,** *125*, 9774-9781.
17. A.J. Tanner, B. We, J. Ontaneda, Y. Zhang, R. Grau-Crespo, H.H. Fielding, A. Selloni, G. Thornton, Polaron-Adsorbate Coupling at the TiO_2(110)-Carboxylate Interface, *J. Phys. Chem. Letters* **2021,** *12*, 3571-3576.
18. N.G. Petrik, Y. Wang, B. Wen, Y. Wu, R. Ma, A. Dahal, F. Gao, R. Rousseau, Y. Wang, G.A. Kimmel, A. Selloni, Z. Dohnalek, Conversion of Formic Acid on Single- and Nano-Crystalline Anatase TiO2(101), *J. Phys. Chem. C* **2021,** *125*, 7686-7700.
19. A.J. Tanner, B. We, Y. Zhang, L.M. Liu, H.H. Fielding, A. Selloni, G. Thornton, Photoexcitation of Bulk Polarons in Rutile TiO_2, *Physical Review B* **2021,** *103*, L121402.
20. Z. Ding, A. Selloni, Hydration structure of flat and stepped MgO surfaces, *J. Chem. Phys*. **2021**, *154*, 114708

ADVANCING ATOMISTIC UNDERSTANDING OF ELECTRONIC ENERGY TRANSFER

AWARD NUMBER: DE-SC0024267

Liang Shi (PI), lshi4@ucmerced.edu, University of California Merced
Christine Isborn (co-PI), cisborn@ucmerced.edu, University of California Merced
Henrik Larsson (co-PI), larsson@ucmerced.edu, University of California Merced
Britta Johnson (co-PI), britta.johnson@pnnl.gov, Pacific Northwest National Lab

Project Scope

Our collaborative project aims to elucidate the effects controlling the dynamics of electronic energy transfer (EET) between chromophores by advancing atomistic scale understanding through simulations that span from simple models that can be solved exactly to condensed phase atomistic dynamics. A process of fundamental importance in both natural and artificial light-harvesting systems, EET is heavily influenced by the multifaceted interactions between electronic and nuclear degrees of freedom in condensed phases, such as energetic disorder caused by structural heterogeneity, electronic polarization from surrounding molecules, and energy fluctuation due to nuclear motions. The interplay of these factors involving multiple energy and time scales is complex, and the experimental spectra used to probe EET (e.g., two-dimensional electronic spectroscopy) are often difficult to interpret, sometimes leading to controversies. Theoretical modeling has been useful in revealing the EET pathways and mechanisms as well as dissecting experimental spectra, often with assumptions that neglect atomistic detail. However, the complexity of the real molecular systems may render these assumptions invalid, and bridges between atomistic simulations and quantum dynamics methods must be built to better understand their regimes of validity.

Our research will use atomistic simulations to provide deeper insights into factors controlling EET that are often overlooked in model simulations, including the environmental correlations between chromophores, the fluctuating excitonic couplings in complex environments, and the state mixing between bright and dark states. Large-scale electronic structure methods will be validated against correlated wavefunction methods, and molecular dynamics (MD) simulations will be performed with force fields derived from electronic structure calculations and validated against ab initio MD. Key advancements in our approach over standard techniques will be the incorporation of the couplings between electronic excitation and nuclear motions derived from atomistic MD simulations and going beyond linear coupling terms within a vibronic Hamiltonian. The effect of these couplings on EET will be examined by various dynamical simulation methods, ranging from classical simulations with phenomenological quantum corrections, to semi-classical ring-polymer molecular dynamics (RPMD) simulations, to quasi-exact state-of-the-art quantum dynamics methods based on tensor network states. The complementary expertise of the team members enables the comparison between high-level theories with atomistic details and more efficient, but more approximate, fully atomistic methods.

The methods developed here will provide additional atomistic physical information and the thorough comparison and analysis of dynamical approaches will provide the simulation community with reliable protocols for modeling EET with atomistic details. The gained physical insights will be useful for the further improvement of EET efficiency in artificial light-harvesting systems.

This partnership between the University of California Merced (UCM) and Pacific Northwest National Laboratory (PNNL) will be beneficial to the training of diverse student populations at UCM, a Hispanic-serving institution with a large number of first-generation college students. The proposed activities, including graduate student summer internships at PNNL, professional and technical workshops, and mentor/mentee training, will expose under-represented minority students in STEM fields to national lab and DOE career pathways, increase their hands-on training on energy-related science, and strengthen their mentoring networks and relationships.

Recent Progress

This is a new project. Initial work is underway.

Future Plans

Since atomistic details are essential to the molecular design and morphology engineering for improved EET efficiency, we aim to examine the many factors affecting EET at the atomistic level, using first-principles simulations and quantum dynamical methods with careful benchmarking against high-level methods, to bridge the gap between experimental spectra and underlying molecular mechanisms that govern EET in complex environments. We will use higher-level dynamical methods to benchmark lower-level dynamical methods (e.g., using fully quantum methods to benchmark RPMD) with model Hamiltonians parametrized from atomistic simulations, and eventually use the well-benchmarked affordable methods (e.g., classical MD with quantum correction) to perform atomistic simulation of EET in complex systems. To achieve this goal, we will integrate the complementary expertise of theorists at the University of California Merced (UCM) and Pacific Northwest National Laboratory (PNNL). The proposed multi-level atomistic modeling of EET will leverage Shi's expertise on the simulations of organic semiconductors and chromophores in solution, Isborn's expertise on GPU-accelerated excited-state electronic structure calculations of condensed phases, Larsson's expertise on high-level multireference electronic structure and molecular quantum dynamics, and Johnson's expertise on quantum and semi-classical dynamics. Key to our success is that our team has strengths in modeling techniques that range from "exact" methods for model systems, to large-scale electronic structure (hundreds of atoms), to complex condensed phase dynamics, allowing us to connect approximate methods and higher-level methods. The PIs also have extensive experience modeling spectroscopy from different perspectives. The validated atomistic methods then will be utilized to examine several key factors

controlling EET and their manifestation in optical spectroscopy, in direct comparison with available experimental spectra.

In this project, we will illuminate how three factors control EET: environmental correlations between chromophores, fluctuating excitonic couplings, and state mixing between bright and dark states. These factors are often ignored in simulations of EET, especially with model Hamiltonians, due to the lack of atomistic details. As a team with diverse expertise in theoretical methods, ranging from "exact" quantum dynamics methods to atomistic molecular simulations, we will employ atomistic classical MD simulations and electronic-structure calculations to obtain realistic and quantitative descriptions of these factors, fuse these atomistic details into model vibronic Hamiltonians beyond those commonly adopted, and use "exact" quantum dynamics methods to benchmark approximate semi-classical and classical atomistic simulation methods for EET.

Peer-Reviewed Publications Resulting from this Project (Project start date: 08/2023)

No publications to report.

Title: Ultranano, Single-Atom Catalysts for Chemical Transformations
Award Number: DE-SC0020258
Principal Investigator: Mary Jane Shultz
Address: Laboratory for Water and Surface Studies, Pearson Chemistry Laboratory, Tufts University, 62 Talbot Ave, Medford, MA 02155
E-mail: Mary.Shultz@Tufts.edu

Project Scope

The core objective of this project is to advance understanding of molecular-scale dynamics at ultranano (< 2 nm) scale oxide particle surfaces. The motivation for using such structures is they are small enough that they resemble large molecules hence are essentially defect free yet are sufficiently large that they have properties resembling those of their solid-state counterparts. The current focus is on titania, we dub these TiUNP (titania ultranano particles). One of the grand challenges for understanding chemical reactions on these ultra-small particles is probing their surfaces, particularly under reaction conditions. Thus, a second objective of the proposed work is to advance a recently invented instrument to push the frontiers for probing interactions and reactions on these complex, nanoscale surfaces. The third goal is to generate a molecular-level picture of interactions and transformations to rationally modify the surfaces and ultimately to control the products. A prime target is reduction of CO_2 in aqueous solutions.

Methods

Reproducible synthesis addresses one of the grand challenges in nano science.[1] In this project we use wet chemical methods starting with molecular precursors: $TiCl_4$ or $Ti(OR)_4$ where R is typically isopropyl or isobutyl, hydrolyzing in water or acidified water at ambient conditions. The key to limiting particle size is controlling pH; Coulombic repulsion constrains growth. Following hydrolysis, the solution is dialyzed increasing the pH whereupon the particles Ostwald ripen to a size controlled by surface charge. Experimental data: XAFS, UV-Vis absorption, and UV-Vis reflection absorption support a model in which these particles form an isomorphic anatase truncated square bipyramid structural series of increasing size with increasing pH. Particles have large area [101] facets and smaller [001] faces. Principles of catalysis indicate that the small area, square [001] face is the high energy face. We leverage this high energy by hydrolyzing in an aqueous solution containing a small concentration of a target dopant; a concentration that nets one dopant atom per particle. The dopant stabilizes the [001] face so is located there (see below). Successful doping is signaled by lack of deliquescence of the doped oxide and by a red-shifted color relative to the hydrated dopant ion. We label these particles as dopant·TiUNP. To date, Fe·TiUNP is the most thoroughly characterized.

Characterization of Fe·TiUNP with XAFS shows that iron is incorporated is a single-atom and is located in the [001] face.[2] This location is consistent with kinetic characterization data.[3-5] As a wide band gap semiconductor, TiUNP reactions are driven by readily available sunlight. Due to the wide bandgap, titania has the potential to mineralize a wide range of organic molecules dissolved in water. The efficiency of undoped titania is limited by competition between direct electron-transfer to dissolved molecular oxygen and reduction of water generating hydrogen gas – the hydrogen evolution reaction (HER). The latter releases hydroxyl radicals that homogeneously oxidize the targeted organic molecules albeit with low efficiency due to many alternative $OH^{\cdot}$ deactivation pathways. The result is a low oxidation efficiency (oxidations/photon absorbed). Kinetic data shows that the Fe·TiUNP slightly lowers the

reduction potential of the photo generated electron, quenching HER leaving the direct electron transfer pathway without competition. The result is an Fe·TiUNP oxidation efficiency more than three times that of undoped TiUNP.[4]

We leveraged electron localization at the iron site to successfully capture a single atom of several elements: Pt, Ir, and Ni. Each of these elements is more electronegative than either Ti or Fe, so enhance charge separation/electron transfer to molecular oxygen. The result is that platinum decorated, iron doped TiUNP (Pt-Fe·TiUNP) is 40% photo efficient and Ni-Fe·TiUNP is 35% efficient: unprecedented levels. XAFS data indicates that Pt is captured as Pt(IV) and Ni as Ni(II). Combining the positive oxidation state with high electronegativity nets more efficient charge transfer to molecular oxygen. Furthermore, the two-element combination can support greater than one-electron transfer, likely also playing a role in the enhanced efficiency.

Recent Progress

Recently, we found that the Ostwald ripening process during and after dialysis requires time: a few hours at room temperature. Alowing ripening, recently we successfully doped all fourth-period transition elements (except Sc) plus the Cr and Cu groups. Since each of these elements have a unique electron configuration so they are expected to support different chemistry. In concert with this expectation, recent diffuse reflectance UV-Vis data shows several interesting results. (i) With the exception of Fe and Cu, the band-edge of these materials are very close to that of undoped titania and is essentially the same as that of bulk titania. Since the band edge is expected to blue shift as the particles become smaller, this result is unexpected. We attribute the edge states to valence O band to localized surface Ti atom *d* states. That the edge is near to that of bulk titania is consistent with more confined bulk states at the surface. (ii) Elements other than Fe and Cu have unfavorable one-electron reduction potentials compared with Ti, hence have little impact on the edge adsorption. In contrast Fe(III) and Cu(II) both have very favorable one-electron reduction potentials. Thus, the edge O-band to dopant absorption is significantly red of the Ti band, consistent with a picture in which Fe captures the photo generated electron. Thus Cu·TiUNP is also expected to enhance oxidation of organic molecules dissolve in water. Indeed, pilot data indicates that Cu·TiUNP has greater efficiency than undoped TiUNP though less than that of Fe·TiUNP. We conjecture that Cu is less efficient due to lowered adsorption of molecular oxygen; a conjecture consistent with more favorable oxygen transport by iron heme compared with Cu heme in living creatures. (See future plans for evaluating the oxidation efficiency conjecture.)

The third (iii) observation is that below the band edge, the absorption-reflection spectrum of all the elements examined reflects localized $d \rightarrow d$ transitions in the dopant. All are red shifted relative to their hydrated ion analogue. This indicates that the crystal field around the ion is weaker in the particles than the octahedral field of six hydrating water molecules. In part, this weaker field effect is due to the lower symmetry: S_4 in anatase, C_{2v} or lower at the surface. One impact of the weaker field is that Fe(III) in TiUNP reversibly captures molecular oxygen while in hemoglobin if iron becomes oxidized to Fe(III) it is unable to deliver oxygen to target organs. We conjecture that this is due in part to high spin d^5 Fe(III) in the lattice compared with low spin hydrated or heme captured Fe(III). Again, this high spin configuration is a direct result of the weaker crystal field in the titania lattice.

Future Plans

The immediate plan is to evaluate the conjectures listed above. The key question is whether TiUNP doped with elements other than Fe (i) quench HER and (ii) enhance oxidation via adsorption of molecular oxygen. Both can be evaluated using kinetic characterization. The first step is to determine if the doped particles enhance oxidation of organic molecules in water relative to undoped TiUNP. If not, the model needs to be rethought. If yes, then evaluate whether particles oxidize organic molecules when dissolved oxygen is displaced with nitrogen. Residual oxidation in the absence of molecular oxygen indicates that HER remains active. Since Fe·TiUNP passes this test and pilot data suggests that Cu·TiUNP does as well, if the remaining dopants do not, the HER potential must be right at the band edge (remain active via the OH· mechanism). These data are expected to aid in mapping charge flow in these doped particles.

The next planned phase is to focus on one core goal of this project: can these particles reduce CO_2 in aqueous solution? Our conjecture is that if the solution is purged of molecular oxygen, then CO_2 acts as the electron acceptor. We have pilot data indicating that Fe·TiUNP can indeed reduce CO_2 to formic acid. To select particles for more advanced surface probe techniques, the plan is to expand CO_2 reduction investigation to the remaining fourth period elements. We conjecture that elements that readily form chelation compounds (Cu and Co specifically) also capture CO_2 and reduce it. If several the doped TiUNPs successfully reduce CO_2, we will select the most favorable for surface spectroscopy characterization.

In brief, the surface spectroscopy, sum frequency generation (SFG), is a $\chi^{(2)}$ process hence is forbidden in any environment with a macroscopic center of inversion. The planned method is to make a thin film of the doped TiUNP particles. The bulk gas and substrate phases are centrosymmetric, hence generate no SFG signal; molecules adsorbed to such a film are SFG active.[5-7] The recently invented nonlinear interferometer not only enhances the sensitivity of SFG, it also produces both high spectral and high phase resolution data.[8-10] We thus expect to successfully detect adsorption of CO_2 to the particle surface as follows. CO_2 is a linear molecule with a center of inversion hence physiosorbed CO_2 is SFG inactive. However, stronger adsorption bends CO_2. Bent CO_2 lacks a center of inversion thus is expected to produce two vibrational resonances: at about 1700 cm^{-1} and nearer to 1300 cm^{-1}. SFG is quite powerful in this work since it can probe the surface under reaction conditions. For example, if CO_2 is physiosorbed, bending only upon accepting an electron, this can be detected by irradiating the sample while probing with SFG. We plan to use our newly acquired broadband, ultrafast SFG system for these measurements thus acquiring a whole spectrum under identical conditions.

Impact

Creating ultranano solids represents a new paradigm in catalyst research. Unfortunately, the elegant suite of atomic-level UHV probe techniques do not lend themselves to probing these extremely small particles, particularly at buried interfaces such as the particle-water interface. The only method that yields molecular-level information on such interfaces is the vibrational spectroscopy sum frequency generation, SFG. The Shultz laboratory created a nonlinear interferometer to transform nonlinear SFG into a linear analytical technique. This project not only uses this new instrument to probe CO_2 reduction, but it also seeks to create a new mode: difference phase interference, DPI. It is expected to be a generally applicable tool thus impacting many problems involving dynamic, soft, nanoscale irregular interfaces. Finally,

the overarching goal of reducing CO_2 to value added materials is expected to have a global impact.

References

1. Yan, Huan; Su, Chenliang; He, Jun; Chen, Wei, "Single-atom catalysts and their applications in organic chemistry" *J. Mat. Chem. A* **2018**, *6*, 8793-8814, 10.1039/C8TA01940A. 10.1039/c8ta01940a
2. Anderson, Nick; Xu, Tongzhou; Ouyang, Mengyao; Davies, Rebecca; Marmolejos, Joam; Bisson, Patrick J.; Shultz, Mary Jane, "Photosynthesis of a Photocatalyst: Single-Pt-Atom Decorated Fe·TiO_2" *J. Phys. Chem. A* **2021**, *125*, 88-98. 10.1021/acs.jpca.0c08527
3. Dukes, Faith Marie, *Photocatalytic Studies of Metal Doped Titanium Dioxide*, Ph.D. Thesis, Department of Chemistry, Tufts University, 2013.
4. Dukes, Faith M.; Iuppa, Elizabeth; Meyer, Bryce; Shultz, Mary Jane, "Differing Photo-Oxidation Mechanisms: Electron Transfer in TiO_2 vs. Iron-Doped TiO_2" *Langmuir* **2012**, *28*, 16933-16940. DOI: 10.1021/la303848g
5. Asong, Nkengafeh; Dukes, Faith; Wang, Chuan-Yi; Shultz, Mary Jane, "Iron doped TiO_2 probed by methanol adsorption and sum frequency generation" *Chem. Phys.* **2007**, *339*, 86-93.
6. Wang, Chuan-Yi; Groenzin, Henning; Shultz, Mary Jane, "Comparative Study of Acetic Acid, Methanol, and Water Adsorbed on Anatase TiO_2 Probed by Sum-Frequency Generation Spectroscopy" *J. Am. Chem. Soc.* **2005**, *127*, 9736-9744.
7. Wang, Chuan-Yi; Groenzin, Henning; Shultz, Mary Jane, "Molecular Species on Nano-Particle Anatase TiO_2 Film Detected by Sum Frequency Generation: Trace Hydrocarbons and Hydroxyl Groups" *Langmuir* **2003**, *19*, 7330-7334.
8. Shultz, Mary Jane; Bisson, Patrick; Wang, Jing; Joam Marmolejos; Davies, Rebecca G.; Gubbins, Emma; Xiong, Ziqing, "High Phase Resolution: Probing Interactions in Complex Interfaces with Sum Frequency Generation" *Biointerphases* **2023**, *to appear*.
9. Wang, Jing; Bisson, Patrick J.; Marmolejos, Joam M.; Shultz, Mary Jane, "Nonlinear Interferometer: Design, implementation and absolute sum frequency measurement " *J. Chem. Phys.* **2017**, *147*, 064201:1-8, 2017 JCP Editors' Choice innovative and influential article 2017. 10.1063/1.4997736
10. Wang, Jing; Bisson, Patrick; Marmolejos, Joam M.; Shultz, Mary Jane, "Measuring Complex Sum Frequency Spectra with a Nonlinear Interferometer" *J. Phys. Chem. Let.* **2016**, *7*, 1945-1949. 10.1021/acs.jpclett.6b00792

Peer-reviewed Publications (2021-2023):

1. Shultz, Mary Jane; Bisson, Patrick; Wang, Jing; Joam Marmolejos; Davies, Rebecca G.; Gubbins, Emma; Xiong, Ziqing, "High Phase Resolution: Probing Interactions in Complex Interfaces with Sum Frequency Generation" *Biointerphases* **2023**, *to appear*.
2. Davies, Rebecca G.; MacInnis, Allyson E.; Bisson, Patrick J.; Shultz, Mary Jane, "Robust, Reproducible Silica Scaffold for Liquid Flow Applications" *Appl. Eng. Mater.* **2023**, *1*, 1752-1758. 10.1021/acsaenm.3c00149
3. Anderson, Nick; Xu, Tongzhou; Ouyang, Mengyao; Davies, Rebecca; Marmolejos, Joam; Bisson, Patrick J.; Shultz, Mary Jane, "Photosynthesis of a Photocatalyst: Single-Pt-Atom Decorated Fe·TiO_2" *J. Phys. Chem. A* **2021**, *125*, 88-98. 10.1021/acs.jpca.0c08527

Thesis: Anderson, Nicholas J., *One good dopant deserves another: leveraging engineered defect sites towards the facile synthesis of ultra-nano, hybrid single atom doped TiO_2* Ph.D. Thesis, Department of Chemistry, Tufts University, 2023.

Patents:
1. Shultz, Mary Jane; Davies, Rebecca; MacInnis, Allyson; Bisson, Patrick, Unidirectional, Interconnected Super-Micropore Silica Support, Patent No. 63/369,370
2. Shultz, Mary Jane; Anderson, Nicholas J.; Xu, Tongzhou; Bisson, Patrick, Photocatalysts and Methods of Making and Using the Same, Patent No. USA, 12/2/2021. PCT/US63/120,628

An Atomic-scale Approach for Understanding and Controlling Chemical Reactivity and Selectivity on Metal Alloys (#SC0004738)

E. Charles H. Sykes (charles.sykes@tufts.edu)
Department of Chemistry, Tufts University, 62 Talbot Ave, Medford, MA 02155

Program Scope:

Catalytic hydrogenations and dehydrogenations are critical steps in many industries including agricultural, chemicals, foods and pharmaceuticals. In the petroleum refining industry, for instance, catalytic hydrogenations are performed to produce light, hydrogen rich products like gasoline. Hydrogen activation, uptake, and reaction are also important phenomena in fuel cells, hydrogen storage devices, materials processing, and sensing. Typical heterogeneous catalysts involve nanoparticles composed of expensive noble metals or alloys based on metals like Pt, Pd, and Rh. Our goal is to alloy these reactive metals, at the single atom limit, with more inert and often much cheaper hosts and to understand how the local atomic geometry affects reactivity.

The CPIMS program has supported Sykes lab work in developing a new class of model alloy catalysts that we have termed *Single-Atom Alloys* (SAAs) and understanding their ability to activate small molecules and enable spillover of species like hydrogen atoms, alkyl, or alkoxy groups to the support where ultra-selective reactions can occur. Spurred on by our fundamental studies, we and many research groups around the world have now shown that our SAA concept is valid in real catalysts working under ambient conditions. For example, SAAs have been shown to catalyze selective hydrogenation, dehydrogenation, C-C coupling, NO reduction, oxygen reduction, CO_2 reduction among many other reactions. Our goal is to study the ability of SAAs to perform C-H activation chemistry and dehydrogenation reactions, as well as probing the effect of surface structure on reactivity, and combining two different SAAs in one surface to enable trifunctional chemistry.

Recent Progress *A: Reactivity Trends in Copper-Based Single-Atom Alloys for Formic Acid Decomposition*

The complexity of heterogeneous catalysts makes cross comparison of the reactivity of different metal catalysts difficult. However, single-atom alloys, with their atomically dispersed active sites in the inert host metal surface, make this problem tractable. We compared and contrasted the reactivity of four different Cu-based SAAs for formic acid decomposition, an important industrial process for on-site hydrogen production. According to previous model catalyst studies, a general trend in the decomposition rate for monometallic surfaces has been established (Pt(111) > Pd(111) > Rh(111) > Ni(111)). The trend can be understood by carefully investigating the reaction pathway, which the formic acid decomposition proceeds stepwise via either the dehydration ($HCOOH \rightarrow CO + H_2O$) or dehydrogenation pathway ($HCOOH \rightarrow CO_2 + H_2$). The formate pathway is generally most common given the high activation barrier to break a C-H bond as compared to an O-H bond. And the reason that Pt and Pd are considered to be optimal candidates for this reaction is that they have intermediate binding strength for the formate so that the subsequent C-H activation would not be required to surpass a high activation barrier. Selectivity is another important aspect to consider as model catalysts studies show that the dehydration pathway, which

produces CO to poison the active sites and leads to significant performance loss, can occur on Pt(111), Pd(111) and Pd(100) surfaces.

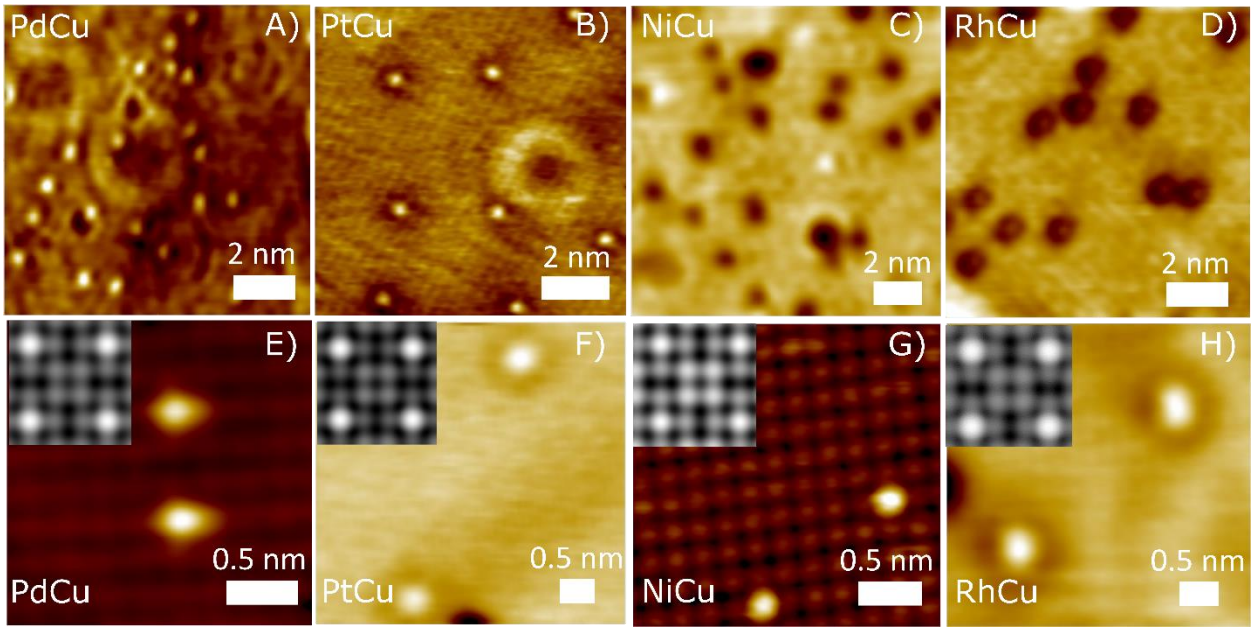

Fig.1 Experimental and DFT-simulated STM images of highly dispersed single-atom alloys. A) PdCu(100) SAA B) PtCu(100) SAA. C) NiCu(100) SAA. D) RhCu(100) SAA; High resolution image of individual E) Pd atoms in Cu(100) host. F) Pt atoms in Cu(100) host. G) Ni atoms in Cu(100) host. H) Rh atoms in Cu(100) host. Inset shows DFT simulated STM images of single atoms in Cu(100). In these images, Pd and Pt atoms appear as protrusions, while Ni and Rh appear as depressions.

We performed a systematic investigation of the reactivity of Cu-based SAAs (SAA=Pd, Pt, Ni and Rh) towards formic acid decomposition using a combined simulations and surface science approach. We have found that the reactivity trend of these SAAs is: RhCu(100) > NiCu(100) > PtCu(100) > PdCu(100), which is distinctly different from the aforementioned trend on monometallic surfaces. Crucially, monometallic Rh and Ni are not generally considered good candidates for formic acid decomposition as they bind carboxyl or formate intermediates too strongly, which hinders further reaction steps. On the other hand, our data shows that in the single atom regime, RhCu shows the highest reactivity towards this reaction. DFT results reveal that the isolated dopant metal sites bind adsorbates moreweakly than their monometallic surface counterpart, thereby destabilizing formate and lowering the activation barrier of the subsequent C-H activation step. Moreover, these RhCu alloy nanoparticle catalysts show significant reactivity increase over other counterparts and high stability under 20-hour-stream. Overall, this study shows that candidates which are not considered to be optimum catalysts in their bulk phase may show promising catalytic behavior in the single-atom regime.

Recent Progress *B: Double-Atom Alloys for C-H activation and C-C coupling*

Single Atom Alloys (SAAs), a subclass of single atom catalysts where active metal dopants are atomically dispersed in the inert metal host, have shown their potential for industrial relevant reactions in the past decade. However, it is difficult for one single-atom site to cover all the reaction steps with high efficiency in a multistep reaction, which necessitates the introduction of second dopant to develop multi-functional catalysts.

In this project, we extended this model catalysts approach to investigate the synergistic effect between isolated Rh and Pd sites in RhPdCu(100), denoted as double-atom alloy(DAA) system, by tracking 1,3-butadiene formation from methyl iodide (CH3I). Using a combined STM and CO reflection absorption infrared spectroscopy (RAIRS) characterization approach, we managed to visualize isolated Rh and Pd atom sites in Cu(100) and observed two distinct monocarbonyl peaks on the Pd and Rh sites. TPD spectra shows 1,3-butadiene desorbs ~70 K lower from 0.2% Rh 0.2% PdCu DAA surface compared to 0.4% PdCu(100) while no 1,3-butadiene desorption observed for 0.4% RhCu(100). The formation of 1,3-butadiene involves C-H activation and C-C coupling and we can understand the role of Rh and Pd sites by examine methane (C-H activation capability) and ethane formation (C-C coupling capability) on RhCu SAA and PdCu SAA from methyl iodide. Methane and ethane traces indicate that the synergistic effect in the RhPdCu DAA originates from Rh sites catalyzing the C-H activation step while Pd sites catalyze the C-C coupling step. Together, we have shown that our surface science approach is a powerful tool to visualize two isolated dopant sites and correlate atomic-scale surface structure with observed reactivity and selectivity, which should be generalizable to the rational DAA catalyst design for industrial relevant reactions.

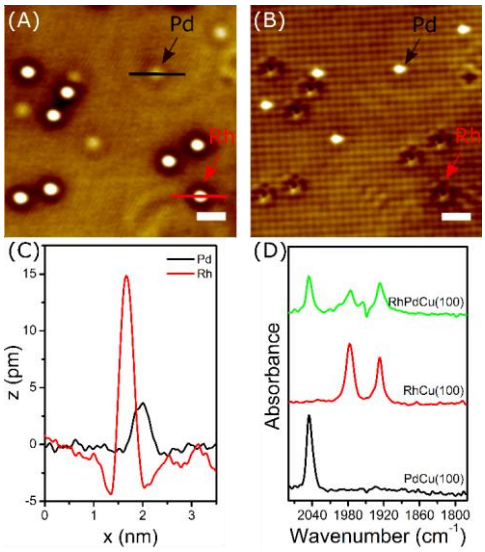

Fig. 2 Characterization of RhPdCu(100) DAA using STM and RAIRS. A) STM image of RhPdCu(100) before acquiring atomic resolution where Rh atoms appear as bright protrusions and Pd atoms appear as shallow protrusions. B) STM image of RhPdCu(100) at the exact same area after acquiring atomic resolution where Rh atoms appear as donuts shape features and Pd atoms appear as protrusions. C) Apparent height profile of Pd and Rh atom acquired from Fig.1A. D) RAIRS of saturation CO exposures on PdCu(100), RhCu(100) and RhPdCu(100). All spectra were obtained at 240 K

Future Plans: Despite the many heterogenous catalysis groups that have taken up SAAs there are only a few performing UHV surface science work on SAAs. Our combined theory, surface science, and microscopy approach offers the opportunity to study the atomic-scale composition and structure of active sites and relate this information to their ability to activate, spillover and react industrially relevant small molecules. We continue to work closely with theorists (Montemore at Tulane, Stamatakis at Oxford University, and Michaelides at Cambridge University) enabling us to predict and test new SAA combinations in well-defined environments. These studies enable us to guide the growing heterogenous catalysis community working on Single-Atom Alloy catalysts.

The goal of the latest work is to extend this approach to selective epoxidation reactions by identifying SAAs that have favorable energetics for O_2 activation and weak binding of the dissociated O atoms,

which are key factors in active and selective oxidation reactions. Industrially, the direct oxidation of ethylene by oxygen on Ag catalysts can reach ~85% selectivity by using promotors such as Cl and Cs, but must be operated at low conversion to maintain selectivity and avoid total combustion of ethylene to carbon dioxide. We hypothesize that the SAA concept will enable the design of alloy surfaces that reduce the O_2 dissociation barrier, thereby enabling higher conversions, and also potentially reducing catalyst the operating temperature so that less ethylene oxide is lost to decomposition on the catalyst support. Guided by a theorical prediction that single atoms in Ag should have a negligible O_2 dissociation barrier while also binding the O significantly more weakly than pure metal we have demonstrated facile uptake and release of O_2 from 1% doped Ag(111). This exciting result is analogous to the H_2 activation and spillover work that inspired the development of a range SAA hydrogenation catalysts and bodes well for selective epoxidation chemistry.

Peer-Reviewed Publications Resulting from this Project (2021-2023)

1) Stick or Spill? Scaling Relationships for the Binding Energies of Adsorbates on Single-Atom Alloy Catalysts R Réocreux, ECH Sykes, A Michaelides, M Stamatakis ***The Journal of Physical Chemistry Letters*** 13 (31), 7314-7319, 2022. Sykes lab contribution to this manuscript was funded solely by CPIMS.
2) Observation and Characterization of Dicarbonyls on a RhCu Single-Atom Alloy Y Wang, J Schumann, EE Happel, V Çınar, ECH Sykes, M Stamatakis, ... ***The Journal of Physical Chemistry Letters*** 13 (27), 6316-6322, 2022. Sykes lab contribution to this manuscript was funded solely by CPIMS.
3) Tuning the Product Selectivity of Single-Atom Alloys by Active Site Modification RT Hannagan, Y Wang, R Réocreux, J Schumann, M Stamatakis, ... ***Surface Science*** 717, 121990, 2022. Sykes lab contribution to this manuscript was funded solely by CPIMS.
4) Periodic Trends in Adsorption Energies around Single-Atom Alloy Active Sites J Schumann, Y Bao, RT Hannagan, ECH Sykes, M Stamatakis, ... ***The Journal of Physical Chemistry Letters*** 12 (41), 10060-10067, 2021. Sykes lab contribution to this manuscript was funded solely by CPIMS.
5) First-principles design of a single-atom–alloy propane dehydrogenation catalyst RT Hannagan, G Giannakakis, R Réocreux, J Schumann, J Finzel, ...***Science*** 372 (6549), 1444-1447, 2021. The Sykes lab contribution to this manuscript was funded solely by CPIMS.
6) "Directing reaction pathways via in situ control of active site geometries in PdAu single-atom alloy catalysts" M. Ouyang, K. G. Papanikolaou, A. Boubnov, A. S. Hoffman, G. Giannakakis, M. Stamatakis, M. Flytzani-Stephanopoulos, E. C. H. Sykes ***Nature Communications*** 2021, 12. Sykes's contribution to this manuscript was funded by CPIMS, co-author Giannakakis was funded in part by the IMASC EFRC.

Understanding the Effect of Interfacial Ions on the Atomistic Structure and Chemical Reactivity at Solid-Liquid Interfaces

Award Number: DE-SC0024654

Tibor Szilvási
Department of Chemical & Biological Engineering
The University of Alabama
Tuscaloosa, AL 35487
Email: tibor.szilvasi@ua.edu

Program Scope

Interfacial ions play a critical role in various applications such as electrocatalysis, energy storage, water desalination, electricity generation, and environmental and biological processes including dissolution and crystallization. Despite such importance, simulation of interfacial ions is rare and oversimplified because it requires simulations at excessive length and time scale and the interfacial ion concentrations may differ from measured bulk ion concentrations by orders of magnitude questioning the validity of simulation results. The aim of this research is to overcome these shortcomings of existing simulation methods in order to establish a reliable computational framework to study interfacial ions and understand the effect of interfacial ions on atomistic structure and reactivity at solid-liquid interfaces.

Recent Progress

Our recent efforts have focused on assembling our research team and generating initial results related to our research plans. We have hired two graduate students and a postdoctoral fellow will join our team. Our initial results show that it is possible to train machine learning interatomic potentials at least within 1.0 meV/atom and 0.04 eV/A error compared to Density Functional Theory (DFT) calculations for bulk water and graphene-water interfaces including dissolved Na^+ and SO_4^{2-} ions at the 0.2-2.0 M range. We also made progress to set up our protocol to calculate the chemical potential of ions that will be used to estimate the difference in ion concentration between the bulk and the interface to obtain realistic structural information about interfaces in the presence of interfacial ions.

Future Plans

Our immediate future plan is to validate our computational protocols against benchmark-quality experimental results on interfacial molecular structures. Then, we will elucidate fundamental questions on how the presence of interfacial ions influence the structure of the solid-liquid interface and how applied potential, surface termination, and generated electric field affect the concentration of ions at the interface. We will establish how the choice of cation and anion influence the interfacial water structure and whether there is a distinctive effect of the size of the ion on interfacial ion concentrations. We will also gain insights into interfacial pH and how it is affected by the nature of the surface and applied potential. Long-term plans include to obtain detailed understanding on how electrochemical reactivity change in the presence of interfacial ions as well as how interfacial pH influences electrocatalytic reactions.

Peer-Reviewed Publications Resulting from this Project (Project start date: 09/2023)

No publications to report.

Understanding Rate Constants of Hydrated Electron Reactions

Award # DE-SC0021114; PI: Ward H. Thompson
Department of Chemistry, University of Kansas, Lawrence, KS 66045; wthompson@ku.edu

Project Scope

Solvated electrons are among the most powerful reducing agents in nature and as such, are important in systems ranging from nuclear reactors to radiation therapy. Solvated electrons produced by ionizing radiation create radicals and ions, which can participate in the corrosion of fuel cladding and reactor structures in nuclear reactors and can also lead to similar reactive species that react with macromolecules in tissue. Thanks to the very large extinction coefficient of hydrated electrons in the visible (20,000 M^{-1} cm^{-1} at 720 nm) their reaction rates with soluble scavengers can be measured quite easily using pulse radiolysis/transient absorption. Thus, thousands of rate constants have been reported, with many of the reactions of the form

$$e^-_{aq} \; + \; S\,(aq) \; \longrightarrow \; S^-\,(aq). \tag{1}$$

However, not every important rate constant can be measured, making it critical to have a reliable theory for making estimates. It is not generally appreciated that no such theory exists. This project, carried out in close collaboration with Prof. David M. Bartels of the Univ. of Notre Dame and the Notre Dame Radiation Lab, aims to uncover the molecular-level origins of the failure of Marcus electron transfer theory to describe Rxn. (1) and elucidate the reaction mechanism(s) to aid in the development of new theoretical descriptions.

Recent Progress

Our work in the present grant period has improved our understanding of hydrated electron reactions, but also substantially changed the direction of our investigations. The initial hypothesis for the origin of non-Marcus theory behavior of the hydrated electron was that its unique solvation structure leads to non-Gaussian behavior. However, our first mixed quantum-classical MD (MQC-MD) study of the hydrated electron showed that this is not the case.[1] This induced a re-evaluation of our approach and ultimately a significant change in direction of the work. We turned our attention to direct simulation of hydrated electron reactions for substrates where the reduction is rapid enough to feasibly simulate with AIMD.[4] This has generated (and continues to generate) new insights into the chemistry. Meanwhile, we were able to make some contributions to hydrated electron modeling through one-electron pseudopotentials,[2,3] as well as a study of the hydrated proton in water.[5]

The Hydrated Electron Exhibits Gaussian Statistics. As noted above, we initially hypothesized that the nearly constant activation energy for e^-_{aq} reduction reactions was due to non-Gaussian behavior of the hydrated electron. The implication was that this non-Gaussian behavior made the free energy curves governing the reaction non-harmonic. Our first efforts on the project were to test this through MQC-MD simulations of the hydrated electron alone using one-electron pseudopotentials. We used two limiting descriptions, between which the actual hydrated electron behavior is expected to lie, to draw a firm conclusion. The first was the Turi-Borgis (TB) pseudopotential,[6] a cavity model known to have the most limited inter-

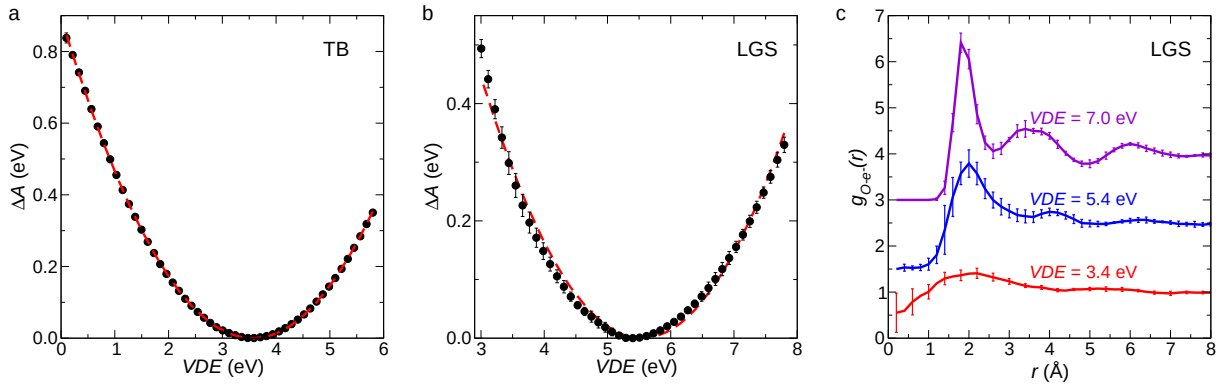

Figure 1: Free energy of the hydrated electron versus VDE for the a) TB and b) LGS pseudopotentials; simulation results (black circles) and results from Gaussian fits to the VDE distributions (red dashed lines) are shown.[1]. c) Origin of non-Gaussian behavior for LGS: The $e^-_{aq}\cdots$O RDFs at different VDE values show the transition from a cavity to a non-cavity structure (top to bottom).

actions with water molecules and thus might be expected to exhibit non-Gaussian statistics through strong interactions with a small number of waters. The second was the Larsen-Glover-Schwartz (LGS) pseudopotential,[7] a non-cavity model that describes the electron as more delocalized and fluxional, a property that can lead to non-Gaussian behavior due to a change in system character (two or more arrangements or configurations of the system).

We carried out extensive umbrella sampling calculations of the free energy as a function of the electron vertical detachment energy (VDE), a proxy for a collective solvent coordinate corresponding to removal of the electron. To our knowledge these are the first calculations of this kind. The resulting VDE distributions and corresponding free energy profiles are shown in Fig. 1a,b for both the TB and LGS pseudopotentials. The TB results clearly give a harmonic free energy surface over a range of 6 eV (575 kJ/mol) in the VDE. The LGS model, on the other hand, shows distinctly non-Gaussian behavior which gives deviations from a harmonic description of the free energy. However, these deviations are quite modest and certainly not significant enough to explain the nearly constant activation energy observed in the hydrated electron reactions. This conclusion is further emphasized by the fact that we showed the non-Gaussian behavior arises from a transition between cavity and non-cavity behavior as the VDE changes within the LGS model, as illustrated in Fig. 1c. This fluxional behavior is generally regarded as more extreme than that of the actual hydrated electron. Thus, we must conclude that the failure of Marcus theory for hydrated electron reactions is *not* due to non-Gaussian behavior (*i.e.*, anharmonic behavior of the free energy surfaces).

The e^-_{aq} Partial Molar Volume. We also investigated the hydrated electron partial molar volume (V_M), which is a quite sensitive measure of its structure and solvation. We used the Kirkwood-Buff (KB) approach to calculate V_M,[2] which had not previously been done. We applied it to three pseudopotentials – the TB and LGS models mentioned above and the TBOpt model developed as an improvement of the TB description; the results show V_M is a sensitive measure of the fidelity of hydrated electron descriptions. We found, consistent with more primitive approaches, that the TB pseudopotential gives a positive V_M in agreement with

experiment[8] ($V_M^{expt} = 26 \pm 6$ cm^3/mol.), while the LGS and TBOpt models predict $V_M < 0$. More importantly, because the KB method relates V_M to an integral of the electron-water radial distribution function (RDF), it provides key insight into the connection between V_M and the hydrated electron solvation structure though the contributions to V_M from different regions of the RDF. Results are presented in *Fig. 2*, where the contributions to V_M from the cavity region and first, second, and third solvation shells are shown for the three pseudopotentials. The results show that the second and even third solvation shell have a significant effect on the value of V_M, challenging the traditional interpretation of V_M as a measure of the cavity size.

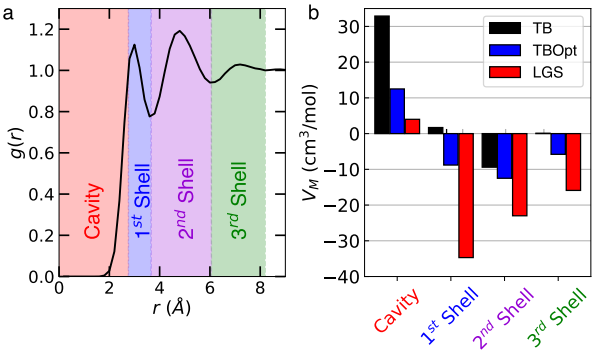

Figure 2: a) Definitions of the regions contributing to V_M based on the RDF (black line). b) The estimated contributions to the partial molar volume from each region for the TB (black), TBOpt (blue), and LGS (red) models.[2].

An Empirically Optimized Hydrated Electron Pseudopotential. Much work has been devoted to developing and evaluating one-electron pseudopotentials for the hydrated electron, motivated, at least in part, by arguments over the structure of the excess electron in water. This now appears settled in favor of a cavity structure, but the flurry of validation work has spurred the development of new pseudopotentials and revealed a number of strengths and weaknesses of extant ones. Traditionally, pseudopotentials have been derived by fitting them to *ab initio* calculations of an electron interacting with a single water molecule. We presented a proof-of-concept demonstration of an alternative approach in which the pseudopotential parameters are determined by optimizing them to reproduce key experimental properties.[3] Specifically, we developed a new pseudopotential, using the existing TBOpt model as a starting point, which accurately describes the hydrated electron vertical detachment energy and radius of gyration; these two properties have been accurately measured, and also provide some tension within the description, *i.e.*, pseudopotentials can accurately predict one of these properties but often not both. In addition, this empirically optimized model displays a significantly modified solvation structure, which improves, *e.g.*, the prediction of V_M and the temperature dependence of the electronic absorption energy.

Proton Transport in Water. The overlapping issues between e^-_{aq} and a hydrated proton motivated a collaboration with Axel Gomez and Prof. Damien Laage at École Normale Supérieure (Paris, FR), who are studying the transport of excess protons in water.[5] The work used neural network potentials trained on DFT calculations and including nuclear quantum effects. The simulations agree with experimental data (including vibrational spectra) on the excess proton diffusion (including isotope effect). The transport mechanism was found to be doubly-gated by hydrogen-bond (HB) exchanges. The first is an HB break around the proton acceptor creating a stable Zundel-like species, but without proton delocalization; the second completes the transfer *via* HB formation with the proton donor.

Ab Initio *MD Simulations Reveal Mechanistic Details.* Following our demonstration that non-Gaussian behavior cannot explain the failure of Marcus theory for hydrated electron reactions, we turned our attention to direct investigations of the reactions. We began with the reaction $e^-_{aq} + CO_2 \rightarrow CO_2^-$, which has been previously studied experimentally and theoretically. We carried out the most extensive AIMD simulations of the reaction to date, propagating more than 400 five-ps trajectories at two temperatures (298 and 373 K). This yielded 73 reactive trajectories at each temperature, which was sufficient to estimate the rate constants. This sampling also permitted new insight into the reaction mechanism.[4] We found k_r to be weakly dependent on temperature, consistent with the small activation energy of the observed bimolecular rate constant. In examining the mechanism, we see: 1) There is no long-range electron transfer. 2) Solvent reorganization accompanies the reaction. 3) Significant vibrational excitation of the CO_2^- bending and symmetric stretching modes is generated by the reaction. This last item is the primary observation that appears to be at odds with Marcus theory

Future Plans

We are continuing to use AIMD simulations to explore Rxn. (1) for different substrates to understand the general properties of the reaction mechanism and the effects of the reaction exergonicity. These insights should shed light on the failure of Marcus theory to describe these important reactions.

Peer-Reviewed Publications Resulting from this Project (2021-2023)

[1]Neupane, P.; Katiyar, A.; Bartels, D. M.; Thompson, W. H. "Investigation of the Failure Of Marcus Theory for Hydrated Electron Reactions", *J. Phys. Chem. Lett.* **2022,** *13,* 8971–8977.

[2]Neupane, P.; Bartels, D. M.; Thompson, W. H. "Relation between the Hydrated Electron Solvation Structure and Its Partial Molar Volume", *J. Phys. Chem. B* **2023,** *127,* 5941–5947.

[3]Neupane, P.; Bartels, D. M.; Thompson, W. H. "Empirically Optimized One-Electron Pseudopotential for the Hydrated Electron: A Proof-of-Concept Study", *J. Phys. Chem. B* **2023,** *127,* 7361–7371.

References

[4]Neupane, P.; Bartels, D. M.; Thompson, W. H. "Exploring the Unusual Reactivity of the Hydrated Electron with CO_2", *J. Phys. Chem. B* **2023,** *submitted.*

[5]Gomez, A.; Thompson, W. H.; Laage, D. "Proton Transport in Water is Doubly-Gated by Hydrogen-Bond Exchanges", **2023,** *submitted.*

[6]Turi, L.; Borgis, D. "Analytical Investigations of an Electron-Water Molecule Pseudopotential. II. Development of a New Pair Potential and Molecular Dynamics Dimulations", *J. Chem. Phys.* **2002,** *117,* 6186–6195.

[7]Larsen, R. E.; Glover, W. J.; Schwartz, B. J. "Does the Hydrated Electron Occupy a Cavity?", *Science* **2010,** *329,* 65–69.

[8]Janik, I.; Lisovskaya, A.; Bartels, D. M. "Partial Molar Volume of the Hydrated Electron", *J. Phys. Chem. Lett.* **2019,** *10,* 2220–2226.

Excitons in Low-Dimensional Perovskites

Award #DE-SC0019345

William A. Tisdale
Department of Chemical Engineering
Massachusetts Institute of Technology, Cambridge, MA 02139
tisdale@mit.edu

Program Scope

The goal of this research effort is to obtain a deeper understanding of strongly bound excitonic states in low-dimensional halide perovskites. Experiments will address how excitons in these quantum-confined materials move, how they interact with the polar lattice, and how their behavior can be manipulated through chemical or structural modification. There is a particular focus on intrinsic exciton physics in 2D and 0D perovskite nanomaterials, and emergent excitonic phenomena in perovskite nanomaterial assemblies.

Recent Progress

Quantification of exciton fine structure splitting in a two-dimensional perovskite compound. Applications of two-dimensional (2D) perovskites have significantly outpaced the understanding of many fundamental aspects of their photophysics. The optical response of 2D lead halide perovskites is dominated by strongly bound excitonic states. However, a comprehensive experimental verification of the exciton fine structure splitting and associated transition symmetries remains elusive. We employed low temperature magneto-optical spectroscopy to reveal the exciton fine structure of $(PEA)_2PbI_4$ (here PEA is phenylethylammonium) single crystals. We observe two orthogonally polarized bright in-plane free exciton (FX) states, both accompanied by a manifold of phonon-dressed states that preserve the polarization of the corresponding FX state. Introducing a magnetic field perpendicular to the 2D plane, we resolve the lowest energy dark exciton state, which although theoretically predicted, has systematically escaped experimental observation (in Faraday configuration) until now. By orienting the 2D crystal on its edge, we were also able to observe the out-of-plane Z-polarized exciton state. These results corroborate standard multiband, effective-mass theories for the exciton fine structure in 2D

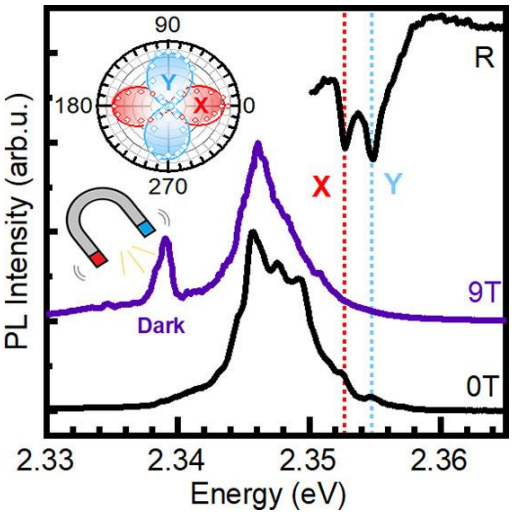

Figure 1. Photoluminescence spectra of a 2D perovskite compound under no magnetic field and under high magnetic field, showing brightening of the dark exciton state. Inset = orthogonal polarization of the two in-plane bright exciton states. *Published work from this award* (Posmyk *et al.*, ***J. Phys. Chem. Lett.*** (2022)).

perovskites and provide valuable quantification of the fine structure splitting in $(PEA)_2PbI_4$.

Discovery of enhanced lattice dynamics in a single-layered hybrid perovskite. Layered hybrid perovskites exhibit emergent physical properties and exceptional functional performances, but the coexistence of lattice order and structural disorder severely hinders our understanding of these materials. One unsolved problem regards how the lattice dynamics are affected by the dimensional engineering of the inorganic frameworks and their interaction with the molecular moieties. We addressed this question by using a combination of spontaneous Raman scattering, terahertz spectroscopy, and molecular dynamics simulations. This approach reveals the structural dynamics in and out of equilibrium and provides unexpected observables that differentiate single- and double-layered perovskites. While no distinct vibrational coherence is observed in double-layered perovskites, an off-resonant terahertz pulse can drive a long-lived coherent phonon mode in the single-layered system. This difference highlights the dramatic change in the lattice environment as the dimension is reduced, and the findings pave the way for ultrafast structural engineering and high-speed optical modulators based on layered perovskites.

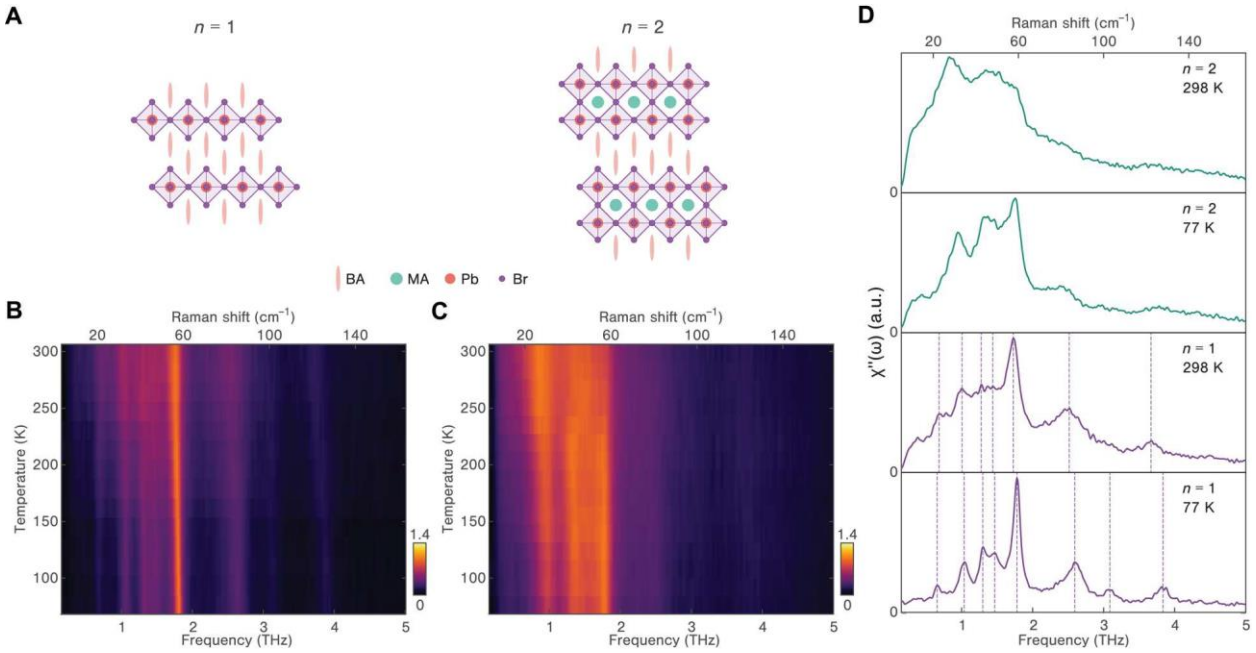

Figure 2. Crystal structure and spontaneous Raman responses of 2D LHPs. (**A**) Schematic illustration of crystal structure for both single-layer (n = 1) and double-layer (n = 2) bromide perovskites. BA, butylammonium; MA, methylammonium; Pb, lead; Br, bromide. (**B** and **C**) Temperature-dependent Raman spectra of n = 1 and n = 2 2DHPs from 77 to 298 K. (**D**) Selected Raman spectra of n = 1 (bottom) and n = 2 (top) 2DHPs at 77 K (bright purple and green) and 298 K (light purple and green). All the phonon modes are indicated by dashed lines. a.u., arbitrary units. *Published work from this award* (Zhang *et al.*, ***Sci. Adv.*** (2023)).

Future Plans

A key focus for the coming year is visualization of exciton and charge carrier transport in 2D and 3D halide perovskites. Using funds from this award we have purchased a Montana Instruments Cryostation Microscope, which enables high stability optical microscopy at cryogenic

temperatures. Using spatially resolved transient photoluminescence, we will study exciton and carrier diffusivity in single crystal and thin film (polycrystalline) perovskite materials as a function of temperature. A key goal is to probe the mechanism of transport and assess the potential interplay between polaron formation and exciton diffusivity.

Peer-Reviewed Publications Resulting from this Project (2021-2023)

1. "Power-Dependent Photoluminescence Efficiency in Manganese-Doped 2D Hybrid Perovskite Nanoplatelets" S.K. Ha, W. Shcherbakov-Wu, E.R. Powers, W. Paritmongkol, W.A. Tisdale ***ACS Nano*** 15, 20527-20538 (2021).
2. "Temperature-Independent Dielectric Constant in $CsPbBr_3$ Nanocrystals Revealed by Linear Absorption Spectroscopy" W. Shcherbakov-Wu, P.C. Sercel*, F. Krieg, M.V. Kovalenko, W.A. Tisdale* ***J. Phys. Chem. Lett.*** 12, 8088-8095 (2021).
3. "State of the Art and Prospects for Halide Perovskite Nanocrystals" A. Dey *et al.* (*multi-author review*) ***ACS Nano.*** 15, 10775-10981 (2021).
4. "Colloidal Nano-MOFs Nucleate and Stabilize Ultra-Small Quantum Dots of Lead Bromide Perovskites" L. Protesescu, J. Calbo, K. Williams, W.A. Tisdale, A. Walsh, M. Dinca; ***Chem. Sci.*** 12, 6129-6135 (2021).
5. "Tuning the Excitonic Properties of the 2D $(PEA)_2(MA)_{n-1}Pb_nI_{3n+1}$ Perovskite Family *via* Quantum Confinement" M. Dyksik, S. Wang, W. Paritmongkol, D.K. Maude, W.A. Tisdale, † M. Baranowski, † P. Plochocka; † ***J. Phys. Chem. Lett.*** 12, 1638-1643 (2021).
6. "Quantification of exciton fine structure splitting in a two-dimensional perovskite compound" K. Posmyk, N. Zawadzka, Mateusz Dyksik, A. Surrente, D.K. Maude, T. Kazimierczuk, A. Babinski, M.R. Molas, W. Paritmongkol, M. Maczka, W.A. Tisdale, Paulina Plochocka, M. Baranowski ***J. Phys. Chem. Lett.*** 13, 4463-4469 (2022).
7. "Light Emission in 2D Silver Phenylchalcogenolates" W.S. Lee, Y. Cho, E.R. Powers, W. Paritmongkol, T. Sakurada, H.J. Kulik, W.A. Tisdale ***ACS Nano*** 16, 20318–20328 (2022).
8. "Uniaxial Strain Engineering *via* Core Position Control in CdSe/CdS Core/Shell Nanorods and Their Optical Response" D. Kim, W. Shcherbakov-Wu, S.K. Ha, W.S. Lee, W.A. Tisdale ***ACS Nano*** 16, 14713-14722 (2022).
9. "Robust estimation of charge carrier diffusivity using transient photoluminescence microscopy" N.N. Wong, S.K. Ha, K. Williams, W. Shcherbakov-Wu, J.W. Swan, W.A. Tisdale ***J. Chem. Phys.*** 157, 104201 (2022).
10. "Giant Nonlinear Optical Response *via* Coherent Stacking of in-Plane Ferroelectric Layers" N. Mao, Y. Luo, M.-H. Chiu, C. Shi, X. Ji, T.S. Pieshkov, Y. Lin, H.-L. Tang, A.J. Akey, J.A. Gardener, J.-H. Park, V. Tung, X. Ling, X. Qian, W.L. Wilson, Y. Han, W.A. Tisdale, J. Kong ***Adv. Mater.*** 2210894 (2023).
11. "Fine Structure Splitting of Phonon-Assisted Excitonic Transition in $(PEA)_2PbI_4$ Two-Dimensional Perovskites" K. Posmyk, M. Dyksik, A. Surrente, K. Zalewska, M. Smiertka, E. Cybula, W. Paritmongkol, W.A. Tisdale, P. Plochocka, M. Baranowski ***Nanomaterials*** 13, 1119 (2023).

12. "1D Hybrid Semiconductor Silver 2,6-difluorophenylselenolate" T. Sakurada, Y. Cho, W. Paritmongkol, W.S. Lee, R. Wan, A. Su, W. Shcherbakov-Wu, P. Müller, H.J. Kulik, W.A. Tisdale ***J. Am. Chem. Soc.*** 145, 5183-5190 (2023).
13. "Lead Halide Perovskite Nanocrystals with Low Inhomogeneous Broadening and High Coherent Fraction through Dicationic Ligand Engineering" M. Ginterseder, W. Sun, W. Shcherbakov-Wu, A.R. McIsaac, D.B. Berkinsky, A.E.K. Kaplan, L. Wang, C. Krajewska, T. Sverko, C.F. Perkinson, H. Utzat, W.A. Tisdale, T. van Voorhis, M.G. Bawendi ***Nano Letters*** 23, 1128-1134 (2023).
14. "Dipole-Dependent Waveguiding in an Anisotropic Metal-Organic Framework" R. Wan, D. Mankus, W.S. Lee, A.K.R. Lytton-Jean, W.A. Tisdale, M. Dincă ***J. Am. Chem. Soc.*** 145, 19042-19048 (2023).
15. "Discovery of enhanced lattice dynamics in a single-layered hybrid perovskite" Z. Zhang, J. Zhang, Z.-J. Liu, N.S. Dahod, W. Paritmongkol, N. Brown, A. Stollmann, W.S. Lee, Y.-C. Chien, Z. Dai, K.A. Nelson, W.A. Tisdale, A.M. Rappe, E. Baldini ***Science Adv.*** 9, eadg4417 (2023).
16. "Exciton Fine Structure in 2D Perovskites: The Out-of-Plane Excitonic State" K. Posmyk, M. Dyksik, A. Surrente, D.K. Maude, N. Zawadzka, A. Babiński, M.R. Molas, W. Paritmongkol, M. Mączka, W.A. Tisdale, P. Plochocka, M. Baranowski ***Adv. Opt. Mater.*** 2300877 (2023).

Modeling phase transitions in liquids with interfaces with Artificial Intelligence and Local Molecular Field theory (DE-SC0021009)

Principal Investigator: Pratyush Tiwary

University of Maryland, Department of Chemistry and Biochemistry

College Park, MD 20740

Email: ptiwary@umd.edu

1. **Project Scope:** Our overarching objective is to combine chemical intuition with Artificial Intelligence (AI) for predictive modeling of complex problems in condensed phase systems involving generic phase transitions. Of specific interest to us is studying nucleation, which is crucial for scientific and technological progress, aligning with DOE and Basic Energy Sciences objectives. Nucleation's role in energy and environmental challenges is significant, but its atomic scale understanding and control is challenging. Integrating AI methods like deep variational information bottleneck and Diffusion Probabilistic Models with statistical mechanics approaches, we aim to develop computational methods for enhanced sampling and understanding of both nucleation thermodynamics and kinetics, together with size and supersaturation effects. We will apply these methods to practical systems like Sodium Chloride and colloidal anisotropic systems, surpassing current computational capabilities. Our goal is to provide new insights and solutions for nucleation complexities particularly in solvated systems with static/fluctuating interfaces.

2. **Recent Progress:** In the 2021-2023 grant period, we aimed to advance our understanding of nonuniform polar liquids in two key areas: (i) the thermodynamics and kinetics of ionic and apolar solutes in solvation, and (ii) the mechanisms of nucleation and growth at solid-liquid and liquid-vapor interfaces. We integrated Local Molecular Field (LMF) theory for handling long-range Coulomb interactions with Artificial Intelligence (AI) based sampling methods for managing short-range forces. Specifically,

   Aim 1: We successfully combined LMF with AI-based sampling methods to gain insights into both short and long length scales, enabling a more comprehensive understanding of these complex systems.

   Aim 2: We applied this hybrid approach to investigate crystal nucleation, a process with unresolved questions and complex multi-dimensional reaction coordinates. Our work provided valuable insights into different nucleation mechanisms and their system-dependent characteristics.

   Aim 3: We explored the potential of AI in extracting valuable information from complex data relevant to energy sciences and chemical physics, contributing to new insights in these areas.

During this funding period, we have achieved significant research output, including seven peer-reviewed publications. Additionally, we have developed open-source software for enhanced molecular dynamics and provided ready-to-run notebooks to facilitate the use of our methods within the scientific community. Our research findings can be summarized as follows:

(a) *Identification of Reaction Coordinates:* We developed a deep learning approach, State Predictive Information Bottleneck (SPIB), for identifying reaction coordinates from molecular simulation data, which aids in understanding high-dimensional data from MD simulations. This approach connects to the committor in chemical physics, providing a versatile tool for various applications.
(b) *Enhancing MD Simulations for Nucleation:* We applied SPIB-based RAVE (Reweighted Autoencoded Variational Bayes for Enhanced sampling) to enhance molecular dynamics simulations of crystal nucleation from the melt and in solvents. This allowed us to study nucleation events efficiently and non-classical transitions in various molecular systems.
(c) *Combining LMF Theory with SPIB:* We investigated the combination of LMF theory with SPIB for capturing both short and long-range forces. The results showed the effectiveness of this approach for different systems, depending on the nature of long-range interactions and solvents.
(d) *Recovering Physics from Data with AI:* We developed two AI-based approaches for extracting meaningful information from condensed matter and molecular datasets. One approach connects deep neural network reaction coordinates to mechanistic processes, while the other uses fundamental dynamics constraints for latent representation learning, outperforming existing methods.

3. **Future Plans:** Our future plans will build up on the success achieved in the first three years. Specific aims include

Aim 1: Develop automated methods for enhanced sampling and understanding of solvent-mediated nucleation and other phase transitions. Key advancements in this aim include utilizing Graph Neural Networks to characterize phases without human-engineered features, employing generative AI frameworks like diffusion models for free energy calculations, and coupling LMF-RAVE with Dynamical Nucleation Theory to calculate nucleation mechanisms and rates beyond thermodynamics.

Aim 2: Apply the methods developed in Aim 1 to practical systems involving nucleation and phase transitions. Specifically, investigate nucleation modes for different systems, such as NaCl (homogeneous and on vibrating carbon nanotubes), 1,3,5-tris(4-bromophenyl)-benzene (TBB) for both homogeneous and template-induced heterogeneous nucleation, and colloidal anisotropic systems. These diverse systems will help validate the wide applicability of the simulation methods and address experimental observations that existing computational approaches cannot currently explain.

4. Peer-Reviewed Publications Resulting from this Project (2021-2023):

1. Wang, D.; Tiwary, P. State predictive information bottleneck. The Journal of Chemical Physics 2021, 154, 134111.

2. Zou, Z.; Tsai, S.-T.; Tiwary, P. Toward automated sampling of polymorph nucleation and free energies with the SGOOP and metadynamics. The Journal of Physical Chemistry B 2021, 125, 13049–13056.

3. Wang, D.; Zhao, R.; Weeks, J. D.; Tiwary, P. Influence of long-range forces on the transition states and dynamics of NaCl ion-pair dissociation in water. The Journal of Physical Chemistry B 2022, 126, 545–551.

4. Beyerle, E. R.; Mehdi, S.; Tiwary, P. Quantifying Energetic and Entropic Pathways in Molecular Systems. The Journal of Physical Chemistry B 2022, 126, 3950–3960.

5. Kulik, H. J.; Tiwary, P. Artificial intelligence in computational materials science. MRS Bulletin 2022, 1–3.

6. Zou, Z.; Beyerle, E. R.; Tsai, S.-T.; Tiwary, P. Driving and characterizing nucleation of urea and glycine polymorphs in water. Proceedings of the National Academy of Sciences 2023, 120, e2216099120.

7. Gao, A.; Remsing, R. C.; Weeks, J. D. Local Molecular Field Theory for Coulomb Interactions in Aqueous Solutions. The Journal of Physical Chemistry B 2023

Structural Dynamics in Complex Liquids Studied with Multidimensional Vibrational Spectroscopy (DE-SC0014305)

Andrei Tokmakoff

Department of Chemistry, James Franck Institute, and Institute for Biophysical Dynamics
The University of Chicago, 929 E 57th Street, Chicago, IL 60637
E-mail: tokmakoff@uchicago.edu

Project Scope

The aim of our research program is to understand the role of water in influencing the properties of complex aqueous solutions and electrolytes using ultrafast two-dimensional IR spectroscopy. Our recent spans the molecular dynamics of water, aqueous protons and electrolyte solutions in the bulk, in confinement, and near interfaces. Our primary new efforts involve the studying the dynamics of water in microstructured complex fluids and water reorganization during phase separation to gain insight into the molecular origins of the closely related topics of solubility and hydrophobicity. This work also helps support our studies of water and electrolytes within the electrical double layer at an electrode interface.

Recent Progress

Protons in water including water in zeolites

Over many years the DOE has supported our work to understand excess protons and strong hydrogen bonds in water. The structure and dynamics of hydrated protons are fundamental to numerous energy transduction, transport, and storage processes, and these properties can be strongly modulated by interfacial and confinement effects. The hydration behavior of zeolites, aluminosilicate materials with strong Brønsted acid sites (BAS) inside sub-nanometer pores, is a broad topic of interest because zeolites are among the most widely used industrial solid acid catalysts, and the presence of water can have a large effect on the catalytic behavior.

By preparing zeolites with stoichiometric ratios of water molecules per BAS, we studied changes in the water structure and protonation state under tight confinement as a function of water cluster size using IR spectroscopy. In our most recent study, we reported the linear and 2D IR spectra of ZSM-5 zeolites over the hydration range of 0 to 8 equivalents of H_2O per BAS. We assigned IR spectral signatures to protonated zeolite Brønsted acid sites and protonated water cluster states, finding that the BAS is deprotonated in clusters with 2 or more H_2O molecules. Comparison with *ab initio* molecular dynamics simulations revealed further details about the proton charge migration and delocalization as a function of hydration. The experimental methodologies developed in this work provides a route to high quality 2D IR spectroscopy measurements of highly scattering particles such as zeolites and other solid materials.

Phase separation in binary liquid mixtures and thermoresponsive polymers

Understanding aqueous solubility, miscibility, and hydrophobicity hold broad importance in our basic understanding of aqueous solutions; however, much of our current understanding remains empirical. Our most recent research efforts seek to address these topics through the study of liquid-liquid phase separation in complex aqueous fluids. Our approach centers on using IR spectroscopy to monitor water reorganization during phase separation in binary liquid mixtures, where water's hydrogen-bonding network dynamically restructures around and reshapes its dissolved constituents as the components phase separate. This study is facilitated using thermoresponsive polymers exhibiting a lower-critical solution temperature (LCST) which demix via a structural collapse and subsequent aggregation originating from the hydrophobic ordering of solvating waters. We are investigating such polymers that are rich in amide groups, such as poly-N-isopropylacrylamide (PNIPAM) and elastin like peptides (ELPs).

In practice, solvent-solute interactions are difficult to study due to the overwhelming response from bulk solvent. The most common approach for studying these interactions relies on high solute concentrations or indirect vibrational probes which can either influence the intrinsic interactions due to deformation of bulk solvent or evoke unwarranted models. Our approach is to employ intermolecular cross peaks within a 2D IR spectrum, which originate from short range vibrational coupling between water and the solvent of interest, and thus report on the solvent local to the solute of interest.

As a starting point to understand the origin and interpretation of water-amide cross-peaks, we have chosen to start with a simple molecule that can mimic these behaviors, N-methylacetamide (NMA). The structure of NMA resembles the pendant amide groups in PNIPAM and ELPs, which are a primary source of the vibrational coupling with water due to their hydrogen bonding sites. Studies of NMA in water and other hydrogen bonding solvents illustrate how different hydrogen bonding configurations between solvent and amide give rise to unique spectral characteristics that can be time-resolved to reveal their dynamics.

Technology: Amplification of BBIR

The spectral coverage and time resolution in 2D IR spectroscopy is closely tied to technological capabilities for generating and manipulating short, broadband, and intense pulses of mid IR radiation. This is a particularly important consideration for 2D IR studies of H bonding systems including water and hydrated protons, where the vibrational transitions can span hundreds of wavenumbers and relax on ultrafast timescales. Our group developed and utilized a broadband IR (BBIR) probe source generated by laser filamentation in N_2 gas, providing unique capabilities for broadband 2D IR spectroscopy. Using this BBIR source, we can detect spectral transients from 1000 to 4000 cm^{-1} with <100 fs time resolution and spectral coverage far exceeding typical 2D IR capabilities. While it is an excellent probe source, the generated BBIR pulses are relatively weak, approximately 1 nJ, far less than the microjoule energies required to excite molecular vibrations. As a result, the excitation bandwidth in 2D IR experiments has been restricted to 200-400 cm^{-1}, limiting the capabilities for extracting proper intensities and

linewidths for broad spectral features spanning >400 cm^{-1}. To extend the capacity for broadband excitation in 2D IR spectroscopy, we developed a strategy for amplifying the BBIR pulses using optical parametric amplification (OPA). The device uses the broad phase matching bandwidth of GaSe, pumped at 2 μm and seeded with BBIR, to produce signal and idler pulses that each span >1000 cm^{-1} and together cover the mid IR. Both amplified pulses reach several microjoules in energy and the signal was compressed to 34 fs. Using the signal pulse for excitation and detection, we demonstrated proof of principle 2D IR spectroscopy with simultaneous excitation of molecular vibrations spanning 1000 cm^{-1}, improving the spectral coverage along the excitation axis by a factor of 2 compared to current capabilities.

Vibrational probing of water and electrolytes in the electrical double layer

In addition, DOE has supported our efforts to study the structure of water and ions within the electrical double layer near an electrified solid-liquid interface. This is the functional region of an electrochemical system, and its properties are of fundamental importance for wide ranging technologies, including water remediation, *in situ* sensing, and important catalytic processes such as CO_2 reduction and water splitting. Our understanding of the solution structure at the electrode-electrolyte interface is centered on long-standing Debye-Hückel and Gouy-Chapman mean field theories that apply to the dilute limit, but these fail at realistic concentrations and provide no insight into the dynamics of the solution. Importantly, there are few experimental techniques that can probe the solvation dynamics in the double layer of an active electrochemical cell, and how they might differ from the bulk solution.

To approach this problem, we have developed new methods that allow us to measure 2D IR spectra of vibrational probes functionalized on an active electrode. This has centered on the development of an electrode that is compatible with ultrafast IR spectroscopy in ATR mode and features plasmonic enhancement of the vibrational spectrum, necessary to achieve monolayer sensitivity. The electrode we developed is built on Si ATR substrates, and consists of a 20 nm thick layer of ITO topped with a 1-2 nm thick layer of Al_2O_3, both deposited via ALD. The ITO layer provides the necessary conductivity for the electrode while minimizing IR absorption while the thin Al_2O_3 layer acts as an adhesion layer for the 10-12 nm layer of Au that we subsequently sputter coat onto the device. The Au provides the ability to functionalize the surface with a monolayer that can serve as a vibrational probe of the solution via thiol linkages, while simultaneously enhancing the sensitivity through the plasmonic modes in the nanostructured Au. We can observe how the probe vibrations shift in response to the application of a bias potential to the electrode, and isolate effects such as the mixing of the vibrational states with the plasmons and vibrational non-Condon effects and see how these change with the application of the bias potential. This new experimental platform opens new capabilities for studying the solution structural dynamics near the electrified interface, how they depend on the bias potential and the composition and concentration of the electrolyte, and how they differ from the bulk solution.

Future Plans

Upon completion of our studies of NMA, our primary efforts will turn to interpreting the spectroscopy of amide-rich thermoresponsive polymers in water as a function of temperature through the LCST. Experiments are planned as a function of polymer molecular weight, concentration, and ionic strength. Interpretation of these experiments will draw from molecular dynamics simulations using mixed quantum-classical modeling of the amide I carbonyl vibration and water O-H stretch. Additionally, we are also designing experiments to investigate the dynamics of phase separation following a laser temperature jump across the LCST and rapid microfluidic mixing techniques to monitor the process with an increase of ionic strength.

Peer-Reviewed Publications Resulting from this Project (2021-2023)

- "Infrared Compatible Rapid Mixer to Probe Millisecond Chemical Kinetics," Ram Itani, Max Moncada Cohen, and Andrei Tokmakoff, *Review of Scientific Instruments*, **94** (2023) 034102. https://doi.org/10.1063/5.0121817
- "Amplification of mid-IR continuum for broadband 2D IR spectroscopy," John H. Hack, Nicholas H. C. Lewis, William B. Carpenter, Andrei Tokmakoff, *Optics Letters*, **48** (2023) 960-963. https://doi.org/10.1364/OL.481088
- "Proton dissociation and delocalization under stepwise hydration of zeolite HZSM-5," John H. Hack†, Xinyou Ma†, Yaxin Chen, James P. Dombrowski, Nicholas H. C. Lewis, Chenghan Li, Harold H. Kung, Gregory A. Voth, and Andrei Tokmakoff, *The Journal of Physical Chemistry C*, accepted. https://doi.org/10.1021/acs.jpcc.3c03611
- "From Networked to Isolated: Observing Water Hydrogen Bonds in Concentrated Electrolytes with Two-Dimensional Infrared Spectroscopy," Nicholas H. C. Lewis, Bogdan Dereka, Yong Zhang, Edward J. Maginn, and Andrei Tokmakoff, *Journal of Physical Chemistry B* **126** (2022) 5305–5319. https://doi.org/10.1021/acs.jpcb.2c03341
- "Lineshape Distortions in Internal Reflection 2DIR Spectroscopy: Tuning Across the Critical Angle," Nicholas H. C. Lewis and Andrei Tokmakoff, *Journal of Physical Chemistry Letters*, **12** (2021) 11843–11849. https://doi.org/10.1021/acs.jpclett.1c03432
- "Characterization of Acetonitrile Isotopologues as Vibrational Probes of Electrolytes," Bogdan Dereka, Nicholas H. C. Lewis, Jonathan H. Keim, Scott A. Snyder, Andrei Tokmakoff, *The Journal of Physical Chemistry B*, **126** (2022) 278–291. https://doi.org/10.1021/acs.jpcb.1c09572.

The Molecular Building Block Sampling Approach for Polymorphic Free Energy Calculations
DE-SC0024283

Dr. Omar Valsson, Assistant Professor
Department of Chemistry
University of North Texas
1155 Union Circle #305070
Denton, TX 76203-5017

Project Scope:
This proposal aims to develop new atomistic simulations methodology for polymorphic free energy calculations. Polymorphism, the possibility of molecular crystals to have two or more crystalline phases with different molecular agreements (e.g., packing and orientation of molecules) but identical in the chemical formulation, has immense scientific and practical importance in chemistry and materials science. Therefore, it is a vital task in the academic scientific field and industry to identify different polymorphs and obtain their thermodynamic properties, such as their relative populations. However, tackling molecular crystals is among the most challenging computational chemistry tasks, especially for flexible molecules exhibiting conformational polymorphism. In this project, we will develop a novel enhanced sampling method for molecular dynamics simulations called the *Molecular Building Block Sampling Approach* for tackling challenging temperature-mediated polymorphic transition in molecular crystals that state-of-the-art crystal structure prediction methods cannot describe. This free energy method will give us access to thermodynamic properties such as free energy landscapes and relative stabilities of polymorphs at finite temperatures. The novelty of the technique lies in biasing directly local order parameters that can describe both the inter-molecular and intra-molecular degrees of freedom of the molecular building blocks of the crystal. This is a shift compared to conventional enhanced sampling methods that employ global collective variables that describe the state of the whole system. The outcome of this research program will be a novel enhanced sampling method for tackling challenging polymorphic transition that can be applied to a wide range of experimentally relevant molecular crystal systems. All methodological development resulting from the proposed project will be made publicly available in open-source codes such as the PLUMED enhanced sampling code.

Recent Progress:
This is a new award, with an official start date of July 1, 2023.

In preliminary result, obtained previously, we have implemented an initial version of the Molecular Building Block Sampling Approach in the PLUMED enhanced sampling code. We have applied the method to a prototypical case of sodium atomic crystal undergoing transitions between the liquid phase and the solid BCC phase. In this case, the molecular building blocks are the individual atoms in the crystal. We observe a significant enhancement in the transitions between the liquid and solid (BCC) phases, as compared to unbiased simulations, that allows us to obtain converged estimates of free energy profiles.

Future Plans:
In the next step we will develop and extend the Molecular Building Block Sampling Approach to be applied to molecular crystals. Initially, we will consider prototypical test cases such as water/ice1h system, urea crystals, and other test cases that have a well-known phase behavior. To improve the performance of the method, we will consider various strategies, such as: usage of a localized wavelet-based bias potential; improved stochastic optimization methods to update the bias potential; and improved reweighting procedures. We will then consider more challenging cases, such as *p*-aminobenzoic acid and the ROY molecular that exhibits rich conformational polymorphism. We will also develop data-driven machine learning methods to construct local order parameters.

Peer-Reviewed Publications Resulting from this Project (Project start date: 07/2023):
There are no publications to report as this is a new award.

Catalysis Driven by Confined Hot Carriers at the Liquid/Metal/Zeolite Interface

DE-SC0020300
Bin Wang, Professor, Conoco-DuPont Professor
School of Sustainable Chemical, Biological and Materials Engineering, University of Oklahoma,
100 E. Boyd St. Norman, OK 73019-1004
Email: wang_cbme@ou.edu

Project Scope

To achieve high reaction selectivity, one needs to control on a catalyst surface the dissociation and formation of specific chemical bonds toward a certain desirable product. Achieving this bond selectivity is challenging for conventional thermal reaction approaches, in which dissipation of thermal energy increases the probability for transformation of all chemical bonds at the interface. Introduction of energetic charge carriers, through plasmonic photoexcitation, can in principle improve the reaction selectivity to an unprecedented level by tuning the orbital occupation associated with a specific chemical bond and driving targeted bond dissociation and association. However, to rationally design a reaction system with high efficiency based on this concept, some fundamental challenges remain: (i) precise manipulation of charge transfer at the interfaces, (ii) track the dynamic nature of the complex interfacial systems, and (iii) the inherently coupled physicochemical process between the electronic and atomic degrees of freedom at the interface.

Our vision is to develop "all-optically controlled activation and targetted excitation (ALLOCATE)" to promote interfacial chemistry. Specifically we want to provide fundamental understanding of the nature of the interfaces between light-sensitive solid materials and a dielectric media (e.g., a microporous cavity, a thin film of insulator, and a solvent), at which the chemical reactions are driven by highly energetic electrons and/or holes; these energetic charge carriers are generated upon photoexcitation of plasmonic nanoparticles. In this hybrid material, the electrons and the holes modify the electronic properties of the active sites or directly serve as the active sites.

Recent Progress

Benchmark excitation calculations. Light-induced hot carriers derived from Localized surface plasmon resonances (LSPR) have been proposed to drive chemical transformation through different mechanisms: (i) direct intramolecular excitation, (ii) direct interfacial charge transfer and (iii) indirect hot electron or hot hole transfer. Because of the complexities involving electron, vibration, and reaction, ambiguities of the plasmonic catalysis mechanism exist even for intuitively simple reactions. We started with a prototype system – dissociation of dimethyl disulfide molecule, $(SCH_3)_2 \rightarrow 2SCH_3$, on a single-crystalline silver or copper surface. It was shown experimentally that the assistance from LSPR can reduce the threshold photon energy into the infrared (IR) region. The reaction was previously studied at 5 K in ultra-high vacuum, which thus effectively removed the thermal and entropy effects on the reaction and provided a good basis for better understanding of plasmon-induced photocatalysis. It was observed that the S-S cleavage could be triggered by photons of threshold energy of 1.59 eV on Ag when LSPRs are present in the system, clearly manifesting the role of plasmonic excitation. The values changed to 1.27 eV on Cu (111). However, the contributions from the direct interfacial charge transfer and intramolecular excitation could not be distinguished.

We thus reexamined the plasmon-induced dissociation of $(SCH_3)_2$, beyond the ground-state DFT calculations, and reported that a combined, direct interfacial charge transfer could quantitatively explain the different thresholds and maximum-yield energy on Ag and Cu. Our calculations show that the intramolecular excitation proposed in the literature is unlikely to be feasible. Instead, the calculated threshold energy (1.60 eV for Ag and 1.23 eV for Cu) agrees well with experiments and clearly show that the plasmon-induced molecular dissociation most likely follows a metal-mediated direct interfacial charge transfer mechanism. We present energy profiles for the reaction at the ground- and excited-states and address how IR/visible light irradiation in the presence of LSPRs can reduce the reaction barrier. Our results thus help identify the reaction mechanism and provide insights for further improving plasmon-assisted photocatalytic reactions. The method applied here, due to the excellent agreement between theory and experiments, was adopted to investigate reactions over a few interfaces between light-sensitive solid materials and a dielectric media (microporous zeolite, a thin film of semiconducting Cu_2O, and a polar solvent) in the following three cases.

Mechanistic study of CO_2 reduction at a hybrid plasmonic catalyst. We applied the same method to investigate plasmonic reverse water-gas shift reactions over Cu_2O supported on a plasmonic metal such as Al, Ag, and Au. We first calculated it over the pristine Cu_2O surface and found the barrier was very high, rendering it difficult to interpret some published experimental works of the same system. We thus decided to investigate the potential role of defects such as oxygen vacancies in this reaction and indeed find that oxygen vacancies can reduce the reaction energy of CO_2 reduction to much lower endothermic values than the pristine (111) surface. This reduction in reaction energy also results in a significant decrease of the reaction activation barrier (i.e., from 3.2 eV on the pristine surface to 0.9–1.2 eV on oxygen-deficient surfaces). This remaining barrier can be eliminated by plasmonic energetic electrons (Figure 1).

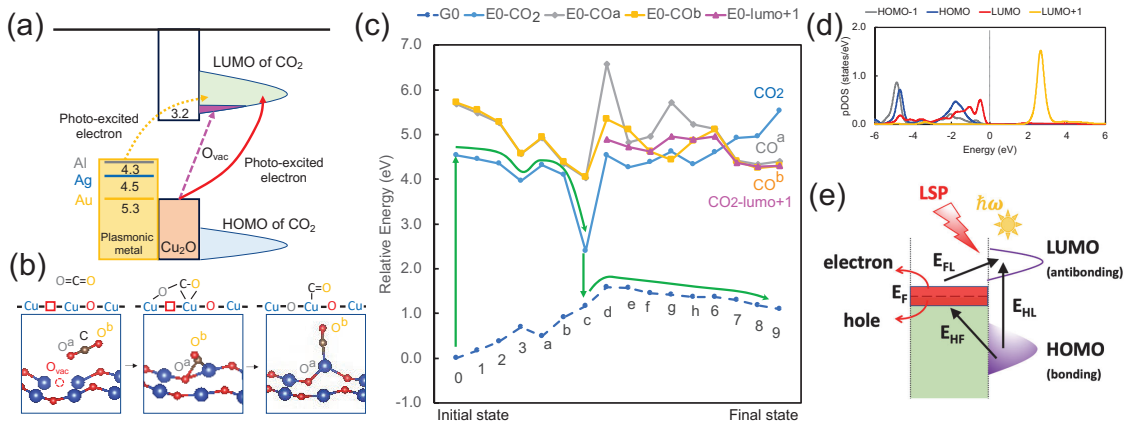

Figure 1. Recent work on mechanistic study of plasmonic CO_2 study over Cu_2O. (a) plasmon-induced CO_2 reduction on a hybrid catalyst consisting of a plasmonic metal (Al, Ag or Au) and an oxide thin film (Cu_2O). (b) Mechanism of C–O bond cleavage over an oxygen vacancy in Cu_2O, (c) reaction profile along the reaction coordinates at the ground state and excited states, (green arrows) showing that the molecular reaction will likely proceed along an excited state between the Fermi level and the LUMO and return to the ground state when approaching the transition state structures. (d) Projected molecular orbitals showing orbital occupation at the transition state where the LUMO is almost fully occupied due to the interfacial charge transfer. (e) schematic for comparison of different excitation scenarios.

The extent of reduction in the activation energy on oxygen-deficient surfaces with and without the energetic electrons can be attributed to the different population of the antibonding states in CO_2. That is, only a few low-lying antibonding states of CO_2 can be occupied through interfacial transfer of the excess electrons associated with oxygen vacancies, leading to a limited level for decreasing the activation energy. Instead, the highly energetic electrons generated by light irradiation can populate antibonding states of CO_2 more extensively, leading to further reduction of the activation barriers. We find that, after excitation, the system will likely travel on an excited energy profile and then return to the ground state to complete the reaction (Figure 1). Moreover, we find that the formation of oxygen vacancies on Cu_2O is feasible via hydrogenation, as the intrinsic activation energy for this formation ranges from 0.9 to 1.1 eV. The energetic electrons, however, have no impact on the intrinsic barrier of this vacancy formation step. Our studies thus reveal that the major impact of plasmon-induced energetic electrons is to drive the CO_2 dissociation at the oxygen vacancies.

Plasmon-modulated Lewis acid catalysis. In this second case study, we investigated the active sites in microporous materials under light illumination and proposed to combine this microporous zeolite with a plasmonic metal. Using different probing molecules, such as NH_3 and pyridine, and their adsorption in Sn-beta. we investigated the interaction between molecules with zeolites under the effect of highly energetic charge carriers. Using the heat adsorption of NH_3 as the measure for the interaction between molecules and zeolites (Si-BEA, Sn-BEA, Zr-BEA and Ti-BEA), we find that Sn-BEA is the best candidate for tunning the interaction between molecules and zeolites by the highly energetic electrons, because of the more localized hot electrons, followed by Ti-BEA. The mid-gap states on Sn-BEA and Ti-BEA help to localize more electrons on the active site, leading to more pronounced charge redistribution between zeolites and adsorbed molecules; this electron localization results in the decrease in the interaction between molecules with zeolites. This plasmon-modulated Lewis acid strength may have strong impact in catalysis. We are working on epoxidation of ethylene over Sn-BEA and Ti-BEA integrated with the hot carriers. We hypothesize that by manipulating the acid strength of the Lewis acid sites, we can tune the Sn-O and Ti-O bond strength, so that the oxygen can be transferred from the active sites to the adsorbed olefines. More results from this ongoing work will be reported soon.

Solvent-induced local environment effect in plasmonic catalysis: Solvents that form chemical interaction with reactants and may also affect the plasmonic catalysis. We used NH_3 decomposition on Ru-doped Cu as a probe reaction since NH_3 is a promising hydrogen-carrier for H_2 storage and transportation. A few polar solvents, such as water, methanol and phenol, were selected to study the effect of the local environment induced by solvents around the surface-adsorbed NH_3. We find that H-bonds formed between these solvents and NH_3 increase the excitation energy of an electron from the Fermi level of the system to the LUMO of NH_3 and reduce the excitation energy of an electron from the HOMO of NH_3 to the Fermi level. We also find that changing the basicity of the solvents can alter the LUMO of NH_3 to different levels, resulting in the change in the electronic excitation to LUMO. That is, the higher the basicity of the solvent, the higher required energy to populate the LUMO of NH_3. This observation that the hydrogen bonding between solvents and reactants can modify the plasmonic excitation energy provides a valuable route for controlling the selectivity of channeling the photonic energy into a targeted molecular orbital for specific reactions. We are in the process of calculating the reaction profile of NH_3 decomposition at the excited states and revealing the underlying mechanism.

Future Plans

We are calculating the reaction profile of the plasmonic dissociation of NH_3 at the ground and excited states. This system is fundamentally interesting and practically important. Our calculations can provide insights into the mechanisms by comparing with the experimental results available in the literature. At that point, we may further extend this research to a broad range of molecular hydrogen carriers. Note in most of them, the limiting factor is the slow dehydrogenation kinetics, which can benefit from channeling the photon energy into the targeted chemical bonds. This selective channeling of photon energy into particular molecular orbitals is also the key hypothesis and motivation of this research. We are investigating molecules with multiple functional groups and catalysts with discrete energy levels (e.g., single atom catalysts) to illustrate this concept and achieve all-optically controlled activation and targetted excitation (ALLOCATE).

Peer-Reviewed Publications Resulting from this Project (2021-2023)

1. Le, T.; Salavati-fard, T.; Wang, B.*, Plasmonic Energetic Electrons Drive CO_2 Reduction on Defective Cu_2O. *Acs Catalysis* **2023,** *13* (9), 6328-6337.
2. Le, T.; Wang, B.*, Solvent-Induced Local Environment Effect in Plasmonic Catalysis. *Nanoscale Advances* **2023,** DOI: 10.1039/D3NA00835E.
3. Salavati-fard, T.; Wang, B.*, Plasmon-Assisted Direct Interfacial Charge Transfer Enables Molecular Photodissociation on Metal Surfaces. *Acs Catalysis* **2022,** *12* (20), 12869-12878.
4. Peiris, E.; Hanauer, S.; Le, T.; Wang, J. L.; Salavati-fard, T.; Brasseur, P.; Formo, E. V.; Wang, B.; Camargo, P. H. C., Controlling Selectivity in Plasmonic Catalysis: Switching Reaction Pathway from Hydrogenation to Homocoupling Under Visible-Light Irradiation. *Angewandte Chemie-International Edition* **2022,** *62* (4), e202216398.
5. Benson, G.; Costa, V. Z.; Border, N.; Yumigeta, K.; Blei, M.; Tongay, S.; Watanabe, K.; Taniguchi, T.; Ichimura, A.; Santosh, K. C.; Salavati-fard, T.; Wang, B.; Newaz, A., Giant Effects of Interlayer Interaction on Valence-Band Splitting in Transition Metal Dichalcogenides. *Journal of Physical Chemistry C* **2022,** *126* (20), 8667-8675.
6. Le, T.; Shao, Y. H.; Wang, B.*, Plasmon-Induced CO_2 Conversion on $Al@Cu_2O$: A DFT Study. *Journal of Physical Chemistry C* **2021,** *125* (11), 6108-6115.
7. Mou, T.; Quiroz, J.; Camargo, P. H. C.; Wang, B.*, Localized Orbital Excitation Drives Bond Formation in Plasmonic Catalysis. *Acs Applied Materials & Interfaces* **2021,** *13* (50), 60115-60124.
8. Le, T.; Wang, B.*, First-Principles Study of Interaction between Molecules and Lewis Acid Zeolites Manipulated by Injection of Energized Charge Carriers. *Industrial & Engineering Chemistry Research* **2021,** *60* (39), 14124-14133.
9. Salavati-fard, T.; Wang, B.*, Significant Role of Oxygen Dopants in Photocatalytic PFCA Degradation over h-BN. *Acs Applied Materials & Interfaces* **2021,** *13* (39), 46727-46737.
10. Ramakrishnan, S. B.; Mohammadparast, F.; Dadgar, A. P.; Mou, T.; Le, T.; Wang, B.; Jain, P. K.; Andiappan, M., Photoinduced Electron and Energy Transfer Pathways and Photocatalytic Mechanisms in Hybrid Plasmonic Photocatalysis. *Advanced Optical Materials* **2021,** *9* (22), 2101128.
11. Ramakrishnan, S. B.; Tirumala, R. T. A.; Mohammadparast, F.; Mou, T.; Le, T.; Wang, B.; Andiappan, M., Plasmonic photocatalysis. In *Catalysis*, **2021**; pp 38-86.
12. Le, T., Effects Of Non-Equilibrium Charge Carriers On Photocatalytic Reactions Over Hybrid Plasmonic Catalyst, PhD dissertation, University of Oklahoma, 2023

Polariton Reaction Dynamics: Exploiting Strong Light-Matter Interactions for New Chemistry

Award # DE-SC0022948
Prof. Marissa L. Weichman, weichman@princeton.edu
Frick Chemistry Laboratory, Princeton University Department of Chemistry
Washington Road, Princeton, NJ 08544

Project Scope

The aim of this effort is to survey elementary reactions under vibrational strong coupling (VSC) in order to advance mechanistic understanding of cavity-altered molecular reactivity. The recent experimental literature has reported dramatically modified reaction rates, branching ratios, and equilibrium constants of thermal ground state reactions under VSC of reactant vibrational modes.[1-3] These early reports have spurred excitement as a potentially powerful new avenue to achieve vibrational mode-selective chemistry. However, the mechanisms underlying cavity-altered chemistry remain unexplained. The emerging models for polariton chemistry cannot be validated with the current laboratory data, as a large gap presently exists between the complexity of polaritonic systems being approached experimentally and theoretically. We therefore aim to assemble a new body of experimental work directly surveying strongly-coupled reaction trajectories on easily-modeled reactive surfaces.

Our initial focus is on the elementary solution-phase reactions of polaritonic organic molecules. We target a suite of hydrogen (H)-abstraction reactions of the form:

$$RH + X\cdot \rightarrow R\cdot + XH$$

where $X\cdot$ is a small molecular or atomic radical (e.g. the cyano radical, CN), and RH is an organic molecule (e.g. chloroform, cyclohexane) present in excess and under VSC. This class of reactions has not yet been studied under cavity coupling, and offers distinct advantages for disentangling the complexities of polariton chemistry. H-abstraction processes are ubiquitous across chemistry, well-studied outside of cavities, and accessible to detailed theoretical interpretation of reaction pathways. These are typically exothermic, elementary processes with small energy barriers. The combination of kinetic and thermodynamic favorability makes H-abstraction reactions well-suited to resolve ultrafast solution-phase dynamics. We use ultrafast transient absorption spectroscopy to follow the photolysis-initiated ground state chemical reactivity of molecules under VSC. Our experiments represent the first reported studies of laser-induced chemistry and ultrafast bimolecular reaction dynamics under strong light-matter coupling.

Recent Progress

We have recently performed experiments on the ultrafast H-abstraction reactions of the cyanide radical with both chloroform (CN + $CHCl_3$) and cyclohexane (CN + C_6H_{12}) under vibrational strong coupling of the C−H stretching mode of $CHCl_3$ and C_6H_{12}, respectively.[4,5]

Vibrational strong coupling in dichroic microcavities. Our spectroscopic studies of solution-phase intracavity reaction dynamics require the development of microfluidic cavities to enable VSC in the infrared while preserving transparency for UV photolysis and ultrafast spectroscopy at visible and ultraviolet wavelengths. We use custom dichroic dielectric mirrors coated for reflectivity at mid-IR wavelengths and maximum transparency in the optical. We couple intense vibrational modes of intracavity species to the microcavity by compressing the cavity length until an optical mode is degenerate with the desired molecular feature and the Rabi splitting is observed on resonance at normal incidence. We have demonstrated vibrational polaritons in C–H stretching modes of both chloroform and cyclohexane, where strong coupling conditions are straightforward

to access due to high intracavity absorber concentrations. We confirm that the dispersive behavior of these polaritonic systems behaves expected when the cavity length is detuned.

Ultrafast spectroscopy. Our ultrafast laser system is configured for 250 nm pump, broadband white light (320-700 nm) probe transient absorption (TA) measurements. We use this TA setup to track reaction kinetics under VSC through the electronic signatures of reactant complex formation and decay following UV photolysis. We additionally use tunable mid-IR light from a second OPA to monitor the static cavity transmission spectrum in the infrared and ensure that the cavity coupling conditions and collective Rabi splitting remain consistent throughout our ultrafast TA measurements of chemistry.

CN + $CHCl_3$ reaction kinetics under VSC. We first report TA measurements of the CN + $CHCl_3$ reaction under VSC of $CHCl_3$.[4] CN is synthesized *in situ* via ultrafast photolysis of ICN near 250 nm, initiating chemistry at a precise starting time. Free CN is formed on a few-100 fs timescale and can be identified via the appearance of a strong absorption feature at 390 nm. CN then undergoes complexation with $CHCl_3$ solvent on a timescale of ~4 ps, indicated by broadening and shifting of its absorption spectrum to the blue. The solvent-complexed CN feature appears as a broad feature at 340 nm, which grows in on a timescale of ~2.5 ps. Following complexation, CN has a high proclivity to remove an H atom from the nearby solvent molecule on a timescale of ~1400 ps. We have examined the growth and decay dynamics of the 340 and 390 nm CN features outside of cavities in a microfluidic cell composed of uncoated CaF_2 windows; in a ~50 μm long microcavity composed of dielectric mirrors tuned for VSC of the C−H stretching mode of $CHCl_3$; and in dielectric microcavities tuned off-resonance with any vibrational modes of the reacting mixture. In all cases, we observe reaction rates consistent with the extracavity rates that appear to be unimpacted by cavity coupling conditions.

CN + C_6H_{12} reaction kinetics under VSC. We followed up our CN + $CHCl_3$ study by targting analogous H-abstraction experiments for the CN + cyclohexane system. We wanted to rule out the possibility that no cavity effects appeared in CN + $CHCl_3$ because the Rabi splitting achievable in $CHCl_3$ (~25 cm^{-1}) was too small to modify chemistry. By contrast, in cyclohexane one can access considerably larger absolute Rabi splittings due to the larger C–H stretching transition dipoles. Using various dilutions of our reactant mixture, we can tune the collective cavity-coupling strength for the strongest IR-active C–H stretching mode of cyclohexane from 55 to 85 cm^{-1}. We record ultrafast reaction rate constants in extracavity, on-resonance, and off-resonance cavity coupling conditions over this range of coupling strengths. Again, we find no cavity-dependence of the solvent complexation or H-abstraction dynamics of CN radicals in C_6H_{12}.

Conclusions and outlook. While we have not yet found evidence of cavity-altered chemistry in H-abstraction reaction systems, our work demonstrates that we can directly track ultrafast solution-phase reaction dynamics inside microcavities under VSC. We argue that our null results for cavity-alteration of the CN + $CHCl_3$ and CN + C_6H_{12} reactions helps shed light on what properties may make certain reactions susceptible to modulation with VSC in the first place. The polariton chemistry community is increasingly reaching the consensus that VSC influences chemical reactions by altering vibrational dynamics. In particular, a growing body of theoretical and experimental work implicates cavity-mediated intramolecular vibrational relaxation (IVR) channels as one key mechanism by which VSC may operate on reactive trajectories.[6-8] The most compelling examples of VSC-altered chemistry report rate reductions,[3] potentially because cavity-mediated IVR processes drain energy away from the reaction coordinate. In contrast, the highly exothermic H-abstractions we examine here possess a negligible activation barrier and proceed rapidly on their ground vibrational surfaces. We should therefore perhaps not expect that cavity-

mediated IVR pathways would significantly perturb reaction rates. Our report of the negligible impacts of VSC on H-abstraction reaction dynamics is therefore consistent with the proposal that cavity-mediated IVR may be an important mechanism in polariton chemistry.

Future Plans

In future work, we plan to consider a wider class of condensed-phase reactive processes under VSC, targeting systems that may be more likely to demonstrate cavity-altered behavior. One future avenue is to move on from the low-barrier reaction regime towards systems with higher barriers in which vibrational dynamics are more likely to dominate reactivity and thus may be more susceptible to perturbation by VSC. Drawing inspiration from the vibrationally-driven chemistry literature, we will consider VSC of *endothermic* bimolecular reactions that only proceed following vibrational pumping.[9,10] In such a system, one could directly compare the relative reactive propensities of pumped bare molecular vibrational states versus pumped vibrational polaritons.

References

[1] R.F. Ribeiro, L.A. Martínez-Martínez, M. Du, J. Campos-Gonzalez-Angulo, and J. Yuen-Zhou, "Polariton chemistry: controlling molecular dynamics with optical cavities," *Chemical Science* **9**, 6325 (2018).
[2] F. Herrera and J. Owrutsky, "Molecular polaritons for controlling chemistry with quantum optics," *Journal of Chemical Physics* **152**, 100902 (2020).
[3] W. Ahn, J.F. Triana, F. Recabal, F. Herrera, and B.S. Simpkins, "Modification of ground-state chemical reactivity via light-matter coherence in infrared cavities," *Science* **380**, 1165 (2023).
[4] A.P. Fidler, L. Chen, A.M. McKillop, and M.L. Weichman, "Ultrafast dynamics of CN radical reactions with chloroform solvent under vibrational strong coupling," *J. Chem. Phys. Emerging Investigators Special Collection* (2023).
[5] L. Chen, A.P. Fidler, A.M. McKillop, and M.L. Weichman, "Exploring the impact of vibrational strong coupling strength on CN + C_6H_{12} reaction dynamics via ultrafast spectroscopy " *Nanophotonics* (submitted).
[6] B.S. Simpkins, A.D. Dunkelberger, and J.C. Owrutsky, "Mode-specific chemistry through vibrational strong coupling (or a wish come true)," *J. Phys. Chem. C* **125**, 19081 (2021).
[7] D.S. Wang and S.F. Yelin, "A roadmap toward the theory of vibrational polariton chemistry," *ACS Photonics* **8**, 2818 (2021).
[8] J.A. Campos-Gonzalez-Angulo, Y.R. Poh, M. Du, and J. Yuen-Zhou, "Swinging between shine and shadow: Theoretical advances on thermally activated vibropolaritonic chemistry," *J. Chem. Phys.* **158**, 230901 (2023).
[9] J.Y. Shin, M.A. Shaloski, F.F. Crim, and A.S. Case, "First evidence of vibrationally driven bimolecular reactions in solution: Reactions of Br atoms with dimethylsulfoxide and methanol," *J. Phys. Chem. B* **121**, 2486 (2017).
[10] T. Stensitzki, Y. Yang, V. Kozich, A.A. Ahmed, F. Kossl, O. Kuhn, and K. Heyne, "Acceleration of a ground-state reaction by selective femtosecond-infrared-laser-pulse excitation," *Nat. Chem.* **10**, 126 (2018).

Peer-Reviewed Publications Resulting from this Project (Project start date: 07/2022)

- A. P. Fidler, L. Chen, A. M. McKillop, and M. L. Weichman, "Ultrafast dynamics of CN radical reactions with chloroform solvent under vibrational strong coupling", *J. Chem. Phys. Emerging Investigators Special Collection* (in press), featured article.

Nonequilibrium properties of driven electrochemical interfaces

Award Number: DE-SC0018094

Adam P. Willard (awillard@mit.edu)
77 Massachusetts Ave.
Room 6-231
Cambridge, MA 02139

Project Scope:

The goal of this proposal is to develop new theoretical models and simulation methods for studying the nanoscale properties of electrochemically active electrode-electrolyte interfaces.

Electrochemical interfaces play a fundamental role in the energy sciences due to their ability to facilitate the interconversion of electrical and chemical energies. The microscopic chemical processes that enable this interconversion are sensitive to the chemical, physical, and compositional properties of their anisotropic molecular environment. The models and methods we develop are designed to expand our capability to study these properties using molecular simulation so that their effects can be more accurately accounted for when analyzing and interpreting experimental data.

The prevailing theoretical approaches to most electrochemical analysis are based on continuum-level models, such as those pioneered by Gouy, Chapman, Stern, and Grahame. These models describe the electrode-electrolyte interface as a set of smoothly varying one-dimensional fields, typically describing the electrostatic potential or the density profiles of various chemical species. While continuum models provide an efficient and intuitive framework for studying and understanding the macroscopic behavior of electrochemical systems, they lack a detailed description of the interfacial molecular environment and its influence on molecular scale chemical processes. Over these scales - generally nanoseconds and nanometers - the discrete molecular nature of the electrolyte is clearly apparent. Theoretical models of interfacial electrochemistry that incorporate effects molecular structure and dynamics can dramatically improve our ability to extract detailed mechanistic insight from existing and emerging electrochemical experiments.

The goals of this project is to (1) develop a better understanding of the fluctuating disordered molecular environments that are inherent to electrode-electrolyte interfaces and (2) identify the fundamental role that these fluctuations play in shaping the rates and mechanisms of electrochemical reactions. Our approach utilizes all-atom and coarse-grained molecular dynamics simulations that can include reactive electrode boundary conditions with tunable potentials. This project is organized around three specific research objectives:

Objective 1: To develop methods for performing and analyzing atomistic simulations of driven electrochemical interfaces.

Objective 2: To characterize the molecular scale fluctuations of the electric double-layer in and out of equilibrium.
Objective 3: To model the role of interfacial solvent fluctuations on inner-sphere electrochemical reactions.

This project addresses important scientific challenges in theoretical electrochemistry. Nanoscale properties of the electrode-electrolyte interface are known to influence the rates and mechanisms of interfacial chemical reactions, as well as the transport of reactive species to and from the interface. Advances in our fundamental understanding of the electrode-electrolyte interface will allow us, and others, to more effectively leverage this influence and can thus lead to improvements of existing energy technologies or catalyze the development of new ones.

Recent Progress:
Modeling solid surface vibrations with the generalized Langevin equation:
The atomic vibrations of a solid surface can have a significant influence on the rates and mechanisms of surface chemical processes. Quantifying this influence is challenging because it is difficult to isolate experimentally and difficult to model theoretically. All-atom simulation has the potential to provide useful physical insight into the interplay between the molecular dynamics of surface-bound molecules and the vibrations of the underlying atomic surface. However, the characteristics of the latter are known to depend on the size of the simulation cell, and approximating the full spectrum of surface phonon modes necessitates the simulation of prohibitively large systems.

Recently, we have developed an approach to modeling the effects of atomic surface vibrations on the dynamics of surface-bound molecules. In this approach, the influences of atomic surface vibrations are described by a memory kernel and simulated using the generalized Langevin equation (GLE). The memory kernel can be developed to represent surface modes with wavelengths well beyond that of a typical simulation cell, thereby eliminating a common source of finite-size effects.

To highlight the capabilities of this approach, we have studied when and how the properties of the memory kernel affect molecular adsorption and surface scattering. In order to parameterize the memory kernel we use data taken from atomistic simulations. We show that the qualitative properties of the memory kernel are independent of the atomistic model details, such as force field parameters. As illustrated in Fig. 1, we have demonstrated the ability of this approach to reproduce the results of all-atom simulation and its ability to overcome system size effects in the simulation of molecular sticking coefficients.

Modeling the effects of external electric fields on the neat air-water interface:
In collaboration with Professor Heather Allen (Ohio State University), we have been studying the influence of electric fields on the molecular structure of the liquid water-air interface. [insert reference] This influence provides insight into the physical characteristics of the interface that may not be apparent under unbiased conditions.

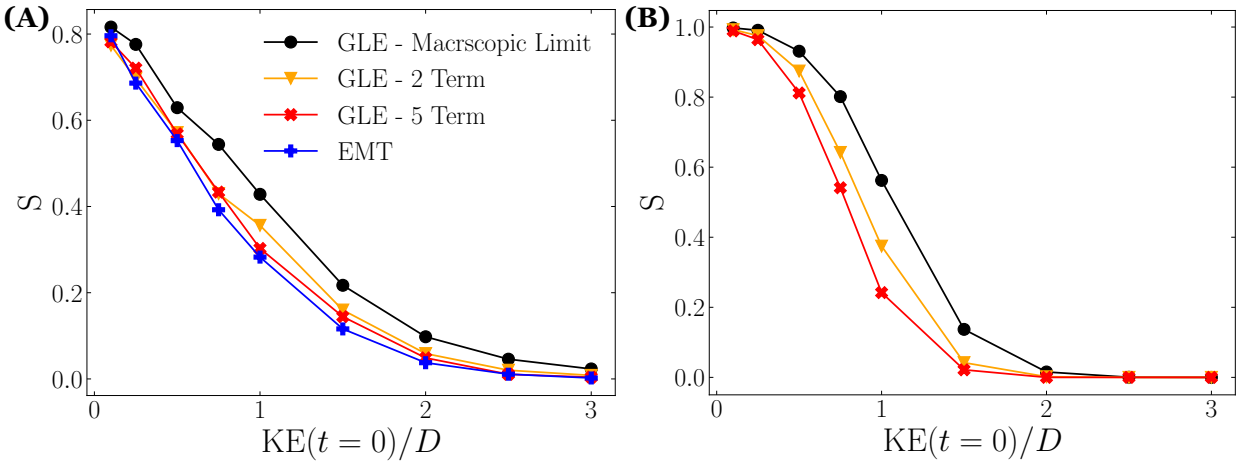

Figure 1. Sticking probabilities S as a function of the ratio of the incident kinetic energy to the well depth $\mathrm{KE}(t=0)/D$, where D denotes the strength of molecule-surface interactions. (A) Results for Morse PES with $D = 6.62\mathrm{eV}$. (B) Results for Morse PES with an increased well-depth, $D = 30.62\mathrm{eV}$. The blue curve uses an all-atom simulation using an EMT forcefield to treat the metal degrees of freedom. The red and orange curves use the GLE parameterized from a 4x4x4 EMT simulation to treat the metal. The red curve uses only two damped sinusoids to fit the memory kernel, while the orange curve uses a five term fit give a more accurate estimation of the memory kernel and power spectrum. The black curve corresponds to the extrapolated macroscopic limit of the LGLE, wherein the surface site motion is coupled to only to the Debye mode.

Water's molecular structure can be indirectly probed via second harmonic generation (SHG) spectroscopy, which displays a distinct dependence on the strength and direction of an external field. By comparing this dependence to literature theory and the results of classical MD simulation, we conclude that the application of a field may induce an over-screening effect whereby the excess population of OH- or H3O+ at the interface differs from expectations derived from classical electrostatics.

Future Plans:

Extending the GLE approach to model surface molecular diffusion:

In our previous application of the GLE to surface chemical phenomena [cite], we applied the effects of the memory kernel to a single active solid surface atom. We are now developing an approach in which the effects of the memory kernel are applied to the surface-bound molecule, thereby enabling the evaluation of the influence of surface phonons on molecular surface diffusion. We plan to apply this method to explore the dependence of this influence on the nature of the molecule-surface coupling.

Tracking electrolyte relaxation in space and time:

When an electrolyte solution is subject to an external bias, such as due to the sudden change in an electrode potential, its structure will evolve to reach a new equilibrium. Understanding this evolution, and how it manifests over molecular length and time scales, is important to our ability to analyze and predict the behavior of electrochemical systems. We plan to carry out non-equilibrium simulations and track the evolution of

the electrostatic potential profile as the system returns to equilibrium. Comparing the mean (Poisson) potential to the potential experienced by different species (Madelung potential) yields different qualitative relaxation timescales. This appears to indicate that these two similar properties report differing physical properties.

Peer-Reviewed Publications Resulting from this Project (2021-2023):

1. K.H. Myint, W. Ding, and A.P. Willard. "The influence of spectator cations on solvent reorganization energy is a short-range effect." *J. Phys. Chem. B*, 125, no. 5 (2021): 1429-1438.

2. B. Huang, K.H. Myint, Y. Wang, Y. Zhang, R.R. Rao, J. Sun, S. Muy, Y. Katayama, J.C. Garcia, D. Fraggedakis, J.C. Grossman, M.Z. Bazant, K. Xu, A.P. Willard, and Y. Shao-Horn. "Cation-dependent interfacial structures and kinetics for outer-sphere electron-transfer reactions." *J. Phys. Chem. C*, 125, no. 8 (2021): 4397-4411.

3. B. Huang, R.R. Rao, S. You, K.H. Myint, Y. Song, Y. Wang, W. Ding, L. Giordano, Y. Zhang, T. Wang, S. Muy, Y. Katayama, J.C. Grossman, A.P. Willard, K. Xu, Y. Jiang, and Y. Shao-Horn. "Cation-and pH-dependent hydrogen evolution and oxidation reaction kinetics." *JACS Au,* 1, no. 10 (2021): 1674-1687.

4. Y. Shen, A.P. Willard. "Directed walk in probability space that locates mean field solutions to spin models." *Physical Review E,* 106, no. 4 (2022): 044132.

5. K. Ray, A. Limaye, K.C. Ng, A. Saha, S. Shin, B. Biswas, M-P Gaigeot, S. Pezzotti, A.P. Willard, and H.C. Allen. "Second-harmonic generation provides insight into the screening response of the liquid water interface." *J Phys. Chem. C*, 127, no. 30 (2023): 14949-14961.

6. A. Farahvash, M. Agrawal, A. Peterson, and A.P. Willard. "Modeling Surface Vibrations and Their Role in Molecular Adsorption: A Generalized Langevin Approach." *J. Chem. Theo. Comp.,* 19, no. 18 (2023): 6452-6460.

Condensed Phase and Interfacial Molecular Science at Lawrence Berkeley National Laboratory

Musahid Ahmed (mahmed@lbl.gov), Monika Blum (mblum@lbl.gov), Ethan J. Crumlin (ejcrumlin@lbl.gov), Phillip L. Geissler (1974-2022), Teresa Head-Gordon (thg@berkeley.edu), David Limmer (dlimmer@berkeley.edu), Kranthi Mandadapu (kranthi.k.mandadapu@gmail.com), Richard Saykally (RJSaykally@lbl.gov), and Kevin Wilson (krwilson@lbl.gov)

Chemical Sciences Division, Lawrence Berkeley National Laboratory
1 Cyclotron Road, Berkeley, CA 94720

The CPIMS program at LBNL seeks to expand the fundamental science base that underlies current and future problems in energy sciences, which include both energy production and its environmental impacts. The program is not focused on device-level technologies but rather basic science, with the expectation that any new technological advances are enabled by the long-term commitment to uncover the fundamental principles that control transformations in heterogeneous systems, in particular, those in aqueous solutions.

The program supports Department of Energy's Basic Energy Sciences mission: "…to better assess, mitigate and control the efficiency, utilization, and environmental impacts of energy use by providing the molecular basis for understanding chemical, physical, and electron-driven processes in aqueous media and at interfaces."

The LBNL CPIMS program is organized into three subtasks:

Subtask 1. Solvation and Reactivity in Spatially Heterogeneous Liquid Environments
Subtask 2: Adsorption and Reactivity at Solid-Liquid Interfaces
Subtask 3: Heterogeneous Dynamics of Assembly and Structural Relaxation in Liquids

Subtask 1: Solvation and Reactivity in Spatially Heterogeneous Liquid Environments

Musahid Ahmed, Monika Blum, Phillip L. Geissler (1974-2022), Teresa Head-Gordon, David Limmer, Richard Saykally, and Kevin Wilson (Subtask Leader)

Project Scope:
Subtask 1 aims to elucidate the fundamental principles that govern adsorption of solutes to a "prototypical" interfaces (*e.g.*, air/water). Ongoing and future work focuses on understanding the asymmetry in cation/anion adsorption, with a long-term objective to fully characterize the molecular forces that drive simple solutes to and from an interface. This provides a robust predictive framework for our second objective, which is to understand how chemical reactions and solvent dynamics are altered when bulk symmetry is broken by an interface. We focus on how nano-confinement alters solvent properties and dynamics, as well as transition states. At larger length scales we examine chemical reactions confined in micron-sized compartments to determine how the presence of an interface alters overall reaction rates and mechanisms. Unique sample

environments (liquid jets and droplets) are envisioned to access short-lived intermediates and interfacial reactions.

Recent Progress:

Solvation and Interfacial Dynamics: Experiments and computer simulations have established that liquid water's surfaces can deviate in important ways from familiar bulk behavior. Even in the simplest case of an air-water interface, distinctive layering, orientational biases, and hydrogen bond arrangements have been reported, but an overarching picture of their origins and relationships has been incomplete. Prior to his death, Phill Geissler and coworkers showed that a broad set of such observations can be understood through an analogy with the basal face of crystalline ice. Simulations demonstrated that there are a number of structural similarities between water and ice surfaces, suggesting the presence of domains at the air-water interface with ice-like features that persist over 2-3 molecular diameters. Most prominent is a shared characteristic layering of molecular density and orientation perpendicular to the interface. Lateral correlations of hydrogen bond network geometry point to structural similarities in the parallel direction as well. These results bolster and significantly extend previous conceptions of ice-like structure at the liquid's boundary and suggest that the much-discussed quasi-liquid layer on ice evolves subtly above the melting point into a quasi-ice layer at the surface of liquid water.

The solvated electron is a fundamental reaction intermediate in physical, chemical, and biological processes. The Head-Gordon lab in collaboration with the Havenith group have followed the birth and time evolution of the solvated electron with state-of-the-art, solvent-sensitive kinetic terahertz spectroscopy and molecular simulations. From optical-pump terahertz-probe spectroscopy, they identified a broadband feature, ultra-short lived (<200\ fs), and centered at ~180 cm^{-1} corresponding to a particle in a box with a radius of 22 Å, *i.e.*, "excitonic" molecular precursors of the solvated electron that are instantaneously generated upon photoexcitation. (Fig. 1) Due to the sensitivity of the experimental setup we were able to probe this solvation cavity part without the ion-specific effect, which is a direct probe of the hydrogen bond strength of the cavity and the trace of the birth of a solvated electron in water. As supported by AIMD, we conclude that the hydrogen bond strength is considerably weakened around the electron, which facilitates localization and gives rise to an increase in entropy – in contrast to what was observed before for addition of salts or alcohols.

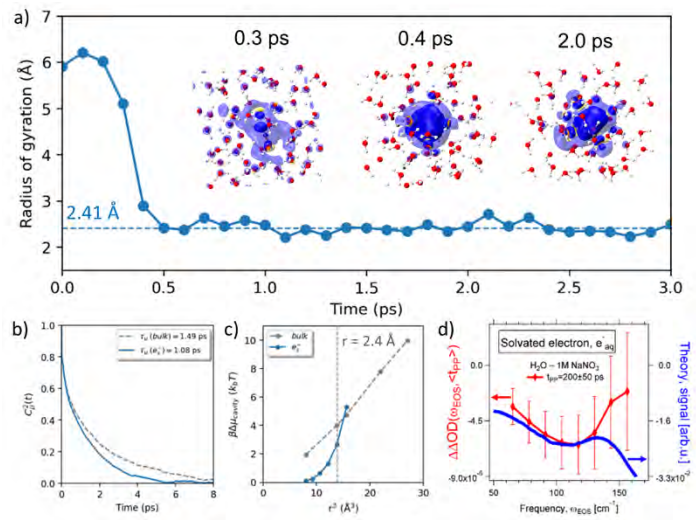

Fig. 1. (a) Time evolution of Rg of electron spin density in neat water with one excess electron and the structures of spin density for some key snapshots. (b) Theoretical water re-orientation lifetime for the water molecules in bulk and in the hydration shell of a single excess electron. (c) Free energy of cavity formation for bulk water and the electron cavity. (d) difference between the transient optical densities, ΔΔOD, in pure water and a 1M NaNO3 aqueous solution at 5°C, (red curve), and the corresponding results from the AIMD simulations (blue curve).

Building on the comprehensive models for the interfacial behavior of a simple prototypical anion (*e.g.*, thiocyanate) at

the air/water and graphene/water interfaces developed jointly by the Saykally and Geissler groups, Saykally and coworkers extended their measurements to several simple oil/water interfaces (*e.g.* toluene, heptane, nonane, etc.), seeking to establish general governing principles. In collaboration with Ilan Benjamin (UC Santa Cruz), it has been shown that ion adsorption at these systems is governed by a different mechanism; adsorption is driven by *entropy* in the form of "water fingers" protruding from the liquid hydrocarbons into the water phase, whereas adsorption at both air/water and graphene/water interfaces was found to be e*nthalpy* driven.

Extending the understanding of anion adsorption from monovalent to polyvalent ions, Saykally and coworkers performed nonlinear optical studies of the carbonate and bicarbonate ions at the air/water interface, confirming earlier X-ray photoelectron spectroscopy (XPS) studies that showed the doubly charged carbonate ion to be adsorbed much more strongly than the singly charged bicarbonate. In collaboration with theory groups from LBL and U.C. San Diego, this surprising result was confirmed and shown to be a consequence of ion pairing of the carbonate with sodium cations, which mitigates the image charge repulsion and facilitates the observed surface adsorption. Future work will explore the generality of this unexpected behavior.

Seeking to extend these studies to cations, the Saykally group has also performed nonlinear spectroscopy studies of the guanidinium ion, determining that the Gibbs free energy of adsorption to the air/water interface is of the same magnitude as that for the thiocyanate anion. Using free energy calculations and thermodynamic integration, the Limmer group evaluated the interfacial partitioning coefficient of guanidinium from its free energy of adsorption. Within the simulations the guanidinium cation exhibited a single minimum directly at the Gibbs dividing surface, and a broad shallow minimum away from the Gibbs dividing surface. This has been compared to measurements from the Saykally group fit with a Langmuir adsorption isotherm. It is only with the combination of both contributions to the surface excess that quantitative agreement between theory and experiment is found. In both simulation and experiment, observations of the temperature dependence of the specific adsorption enabled a thermodynamic decomposition into energetic and entropic contributions to the free energy.

Ahmed and coworkers used XPS, a surface sensitive technique and near-edge X-ray fine structure (NEXAFS) spectroscopy, which is bulk sensitive, to study the solvation of ammonium nitrate (NH_4NO_3). Aerosolized solutions of NH_4NO_3 were introduced into a photoelectron spectrometer via an aerodynamic lens, and interrogated with soft X-ray photons, the resulting electrons detected via velocity map imaging. Density functional theory calculations were performed to compare the measured binding energies of NH_4^+ and NO_3^- solvated in water. The results reveal that the nitrate anion has a slight propensity for the surface, while both ammonium and nitrate ions are present in equal measure in the bulk. This work sets the stage for an in-depth study of aqueous ammonium nitrate and its solvation dynamics, which is postulated to occur due to bifurcated hydrogen bonding networks in solution.

Ahmed and coworkers developed a detailed picture of the photoionization dynamics of aqueous histidine by tuning the pH of the aqueous solution from which aerosols are generated. Assignment of the experimental C1s and N1s photoelectron spectra allows for the determination of the protonation state of histidine in these aqueous aerosols and is confirmed by density functional calculations. It is anticipated that this methodology will find increased application in probing

micro-heterogeneity in aqueous co-solvent and ionic solutions and will also become a tool for probing surface chemistry of aqueous aerosols.

In ongoing work examining acid-base equilibria at aerosol surfaces, the Ahmed group used XPS and NEXAFS spectroscopy to probe nicotine in hydrated vaping aerosols. They show that, unlike the behavior observed in bulk water, nicotine in the core of aqueous particles was partially protonated when the pH of the nebulized solution was 10.4, with a fraction of free-base nicotine (α_{FB}) of 0.34. Nicotine was further protonated by acidification with equimolar addition of benzoic acid (α_{FB} = 0.17 at pH 6.2). This is in contrast to the degree of nicotine protonation at the particle surface which is significantly lower $0.72 < \alpha_{FB} < 0.80$ over the same pH range. The presence of propylene glycol and glycerol shuts down the protonation of nicotine at the surface ($\alpha_{FB} = 1$), while not significantly affecting its acid-base equilibrium in the particle core. This study contributes to a growing body of evidence illustrating differential acid-base properties due to reduced hydration of ionic species at the surface of aerosol particles with respect to their core, and to bulk aqueous conditions.

Blum and co-workers investigated aqueous NaCl solutions with ambient pressure XPS (APXPS) and a novel colliding micro flat jet-system. This flat jet system was recently commissioned by Blum at the Advanced Light Source. Na 2s, Cl 2p and O1s core levels have been measured for a 0.7 M aqueous NaCl solution at different information depths ranging from 2.3 to 5.1 nm in solution. At an information depth of ~ 2.3 nm the measurements revealed that Na^+ and Cl^- are enriched, while further into the bulk (~ 5.1 nm information depth) both ion concentrations decrease. The group also completed a similar study on aqueous $CaCl_2$, which showed an enhanced Cl^- ion concentration at the surface and subsurface compared to the Ca^{2+} ions.

***Trace Gas Solvation and Reaction at Liquid Interfaces*:** The molecular details of the interaction of incoming gas phase solutes with the liquid-vapor interface are strikingly complex with intricate fluctuations aiding the chemical and physical processes. To address this complexity Wilson and coworkers completed a series of measurements examining the reactive uptake kinetics of ozone on levitated droplet arrays. Multiphase kinetics are quantified using single droplet mass spectrometry. A detailed kinetic model was formulated that includes surface and bulk kinetics to explain the observed results. A key feature of the model is to include the preferential solvation of ozone at the air-water interface obtained from molecular simulations. The Wilson group followed up these experimental and kinetic modeling studies with an additional paper deriving closed formed expressions for predicting multiphase kinetics and uptake coefficient at aqueous interfaces that include explicit contributions from chemistry occurring at the surface and in the bulk regions of the droplet. These efforts provided the groundwork for a more extensive and ongoing theory-experiment collaboration (detailed below) with the Limmer group. In other completed work the Wilson group used their newly developed colliding droplet reactor to measure kinetics in micro-confinement. The study focused on the reaction of dopamine with resorcinol, where it was found that oxidation at the interface of the droplet played a large role in accelerating the reaction kinetics in microdroplets by 4-10x relative to the kinetics observed at the macroscale.

To develop a robust and general molecular description of trace gas uptake and reaction, the Limmer group proposed a continuum statistical mechanical framework for the adsorption of solutes by incorporating some molecular details from molecular dynamics simulations into stochastic differential equations and the Fokker-Planck equation. Specifically in collaboration with the Wilson group, Limmer and coworkers developed a method to compute the nature of spatial dependence of friction near the air-water interface. The variation of diffusion constant in the interfacial region plays an important role in controlling the nature of the physical processes taking place at the interface that make them distinct from the processes in bulk solution. The fast-varying friction requires underdamped dynamics, and together with the fluctuations of the liquid-vapor interface make these systems challenging. By combining stochastic differential equations with molecular dynamics simulations, the friction near the interface can be obtained iteratively. Using the coordinate dependent friction along with free energy profiles of obtained from classical molecular dynamics simulation, several interfacial properties can be computed like the mass accommodation coefficient, residence time distribution and reactive uptake coefficient. This approach has been demonstrated for the interfacial reaction of ozone (Fig. 2) with iodide in aqueous solution for which Wilson's group is making measurements in parallel.

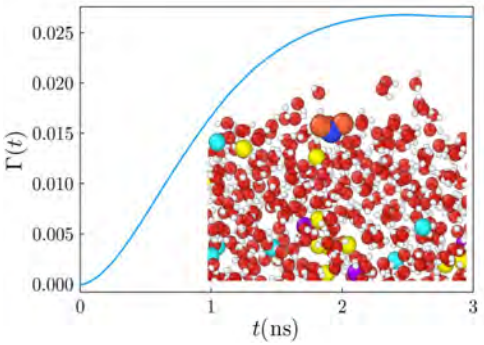

Fig. 2. Ozone adsorbed to an aqueous solution of NaI, and the resultant predicted uptake coefficient vs. time.

Blum and co-coworkes examined CO_2 capture mechanisms in water/solvent mixtures as a function of both concentration and time. In addition to the air water/solvent interface, the bulk liquid is of interest as well since past studies showed that the reaction products "sink" below the reaction surface. Ethanolamines are of interest as a solvent, since primary, secondary, and tertiary amines involve reaction mechanisms that operate on different time scales. For example, monoethanolamine and diethanolamine are very reactive and form carbamate by direct reaction with CO_2 via a Zwitterion mechanism. The tertiary amine (triethanolamine) only forms bicarbonate ions and protonated amines by the base-catalyzed hydration of CO_2. In this study the group concentrated on primary and secondary aqueous ethanolamine solutions with different CO_2 loadings and collected C 1s and N 1s core level spectra at two different information depths. The data revealed a nearly linear decrease of pure amine and a liner increase of protonated amine with increasing CO_2 loading. Furthermore, an increased difference between the protonated and carbamate amine concentrations for the secondary amine solution with increasing CO_2 loading is noticeable while it is less extended in the primary amine solution. In contrast to previous studies, we find a slight tendency for the reaction products to linger at the liquid-vapor interface especially with increasing CO_2 loading. This is an indicator for the slowing down of the CO_2 capturing mechanism over time.

Future Directions:

Interfacial Solvation. The Broadband DUV-SHG experimental approach will be used by Saykally and coworkers to measure charge-transfer-to-solvent (CTTS) spectra of other surface-enhanced ions, emphasizing the study of multiply charged ions and concomitant counterion effects on the spectra, as described above for the case of the carbonate system. The long-term goal is to develop a complete model of ion adsorption to aqueous interfaces with the Limmer group. Studies of ion

adsorption will be extended to water-metal interfaces, seeking to quantify entropy and enthalpy effects. The use of the Trieste FERMI soft X-ray free electron laser facility will be extended to the study of liquid interfaces with atom-selective and surface-selective nonlinear spectroscopy, using the liquid sheet generation technology developed by the Koralec group at SLAC. The carbonate system, previously investigated by our group using X-ray absorption spectroscopy, will be the first target system of study.

The oxidation of SO_2 in aqueous aerosol droplets is one of the main sulfate sources in the atmosphere. In particular, aqueous ammonium sulfate aerosols represent a significant component of the atmospheric aerosol population, with important implications for cloud formation and global radiation balance. Ammonium and sulfate are also important components in planetary atmospheres and can act as mimics for ice. Ahmed and coworkers will couple XPS, NEXAFS, X-Ray scattering, and Raman spectroscopy to track the chemical bonding environments and structure of ammonium sulfate aerosols. Initial results suggest that the surface chemistry of aerosol droplets differs from that expected in the bulk, requiring the consideration of multiple ion species, *e.g.*, HSO_4^- and SO_4^{2-} to describe the measured behaviors. Changing the pH of the bulk solution appears to dramatically affect the surface, with significant suppression of surface sulfate as pH increases. Additionally, the rapid drying and cooling associated with the introduction of aqueous aerosols into a vacuum environment for measurement leads to the development of a state with behaviors between those of the solvated and dry states, allowing a novel avenue for investigating the fundamental interactions between ammonium sulfate and water, especially at surfaces, with both atmospheric and planetary implications. Ahmed is collaborating with Jenny Bergner (UC Berkeley and LBNL) to understand how these aerosols can act as mimics of interstellar ice and with Jin Qian (LBNL) who is calculating XPS spectra to interpret the experimental results.

Wilson and Blum will collaborate on studying the surface reactivity of thiosulfate and partitioning behavior, in general, of sulfates at the air-water interface. The Wilson group will complete thiosulfate reactions with gas phase O_3 in levitated droplets to measure the heterogeneous reaction kinetics in order to fully understand the multiphase reaction mechanism. The terminal products of the reaction are expected to be sulfate and S_2O_6. One substantial unknown is the surface activity of thiosulfate itself compared to its reaction products (*e.g.*, sulfate). Using APXPS the surface partitioning of thiosulfate and sulfate will be measured and incorporated in kinetic models to explain the surface reactivity of O_3 with thiosulfate. Additional complementary studies are envisioned where dissolved O_3 will be mixed with thiosulfate in the colliding flat jet system *in situ* or alternatively an aqueous thiosulfate jet will be exposed to O_3 (from the gas phase) and in both cases the sulfur-containing reaction products will be detected and quantified at the air-water interface.

Recently, a large amount of experimental work has shown that aqueous microdroplets are capable of accelerating the rates of many different types of reactions by one to six orders of magnitude relative to the bulk liquid. Of particular interest are many observations of redox chemistry occurring at accelerated rates in microdroplets. For redox chemistry to occur in a microdroplet, one must produce an oxidizing agent and/or a reducing agent. Considering most microdroplet chemistry is done in liquid water, the most likely redox agents are hydroxyl radicals (oxidation) and solvated electrons (reduction). Because the solvated electron is highly reactive, and if it were produced would rapidly reduce any available species such as an organic molecule or even protons produced by water autoionization. We note that no experiment has determined the fate of the

electron, even though the knowledge of its fate is a critical requirement of any proposed mechanism for most redox chemistry. Overall, the reduction of a proton by loss of electrons from hydroxide ion is the simplest redox chemistry that can occur in a microdroplet and therefore will be the focus of future experimental work by Wilson and theoretical work by Head-Gordon.

Technique Development. Blum will build on her expertise with colliding liquid flat jets and integrate a liquid-liquid planar jet to study buried interfaces. An example study will be a water-hydrophobic surface, e.g. water-alkane, to study the solvation structure in the aqueous phase via the O 1s core level and the solvation structure in the organic phase via the C 1s core level. Reliable, thin, liquid-liquid heterostructures have recently been demonstrated and characterized, and are ideal for X-ray and IR spectroscopies, as the thickness of each individual layer can be controlled.

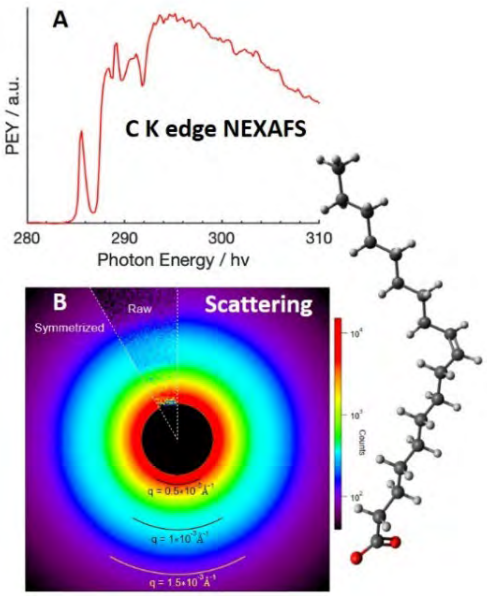

Fig. 3. (A) C K-edge NEXAFS spectra, and (B) X-ray scattering from a 1 µm oleic acid aerosol. On the right is a schematic of the oleate anion.

X-ray scattering is a valuable method for providing information both on structural changes during phase transitions and on dimensions of crystallization nuclei at the relevant, nanometer length scale. Performed at resonance (*i.e.*, at an absorption edge) conditions using soft X-ray radiation, the technique allows for probing chemical composition of the system under study. Ahmed and coworkers, in collaboration with Wilson's group, have developed new techniques for multi-modal and *in-situ* probing of aerosol chemistry and also processes such as crystallization and growth as described above. The formation and nucleation of particles from gas-phase precursors, physical and chemical processes on the particle surface and in the bulk span a range of temporal and spatial scales. These aerosols can exist in different phase states: solid, liquid, and highly viscous, which can change the atmospheric fate of these particles. In viscous, diffusion-limited aerosols, species at the aerosol surface are expected to react more rapidly than molecules residing in the nanoparticle interior, forming steep chemical gradients. Surface-sensitive techniques, such as soft XPS, coupled with X-ray scattering will probe phase changes and structure simultaneously and will be of enormous benefit. Fig. 3A shows the C K-edge NEXAFS spectra from 1-µm-diameter oleic acid aerosol generated via a condensation monodisperse aerosol generator. At a chosen wavelength from this NEXAFS spectra, we perform X-ray scattering (Fig 3B). In the figure are shown the range of q-space accessible in the C soft X-ray region. These images will change as chemistry occurs on the aerosol and will allow us to capture diffusion dynamics and reaction kinetics under study within the timescale of the measurement (10 – 30s).

Trace Gas Uptake and Reaction. Together the Limmer and Wilson groups will examine trace gas uptake and reaction at non-aqueous interfaces. The model system to be investigated is inspired by previous measurements of the heterogeneous reaction of Cl_2 with alkenes (Zeng and Wilson, *Chemical Science*, 12(31), 10455-10466 (2021)). In that previous study, the effective uptake

coefficient increased by 10x in the presence of non-reactive spectator molecules containing oxygenated functional groups (*e.g.,* alcohols). Key questions to be explored thru molecular simulation and theory are: (1) does the mass accommodation coefficient and the solvation energies of Cl_2 change in the presence of unreactive spectator molecules? and (2) if these changes occur how do they impact the observed reactive uptake coefficient?

Blum will expand the studies to aqueous tertiary amine solutions to investigate the Zwitterion mechanism and base-catalyzed hydration of CO_2. In addition, Blum and co-workers will perform *in-situ* CO_2 capture measurements, *i.e.,* surrounding the amine solution with CO_2 during the measurement or utilizing the colliding jet system and mixing the amine solutions with CO_2 moments before the measurement. This should give the opportunity to detect possible short-lived reaction intermediates.

Photochemistry at Liquid Interfaces. Together the Wilson and Limmer groups will work to understand photochemical processes at liquid-vapor interfaces. The nature of the liquid-vapor interface is often very different than the bulk liquid due to the presence of instantaneous fluctuations and inherent inhomogeneity that can result in a marked difference in the dynamics and properties of the solute particles. One of these manifestations is shown in different rates of photochemical reactions near the interface compared to bulk phase. The different reactivities have drawn attention in the field of heterogeneous interfacial chemistry and atmospheric chemistry. We will elucidate the nature and reason for these differences with tools from semi-classical mechanics and non-equilibrium statistical mechanics aided by electronic structure theory calculations. First, we will examine the photodissociation dynamics of phenol (the O-H bond breaking), which experimentally exhibit remarkably faster rates near the air-water interface (R. Kusaka, S. Nihonyanagi, T. Tahara, Nat. Chem. 13, 306–311 (2021), V. Vallet, et al., Faraday Discuss. 127, 283–293 (2004)). Major differences in the reactivity in bulk water and near the interface should depend upon the different hydrogen bonding environments of solvent water molecules. The potential energy surfaces, both ground and excited states, can be obtained from electronic structure theory calculations. From these calculations, we will extract the force field (Lennard-Jones) parameters, bond, angular and dihedral frequencies by fitting. We hypothesize that the charges on the atoms would be a linear combination of the gas phase charges and charges with a continuum solvent model. The exact coefficients can be optimized by checking the solvation energies from the free energy profile compared with experimental values.

Trajectory based semiclassical approaches have been applied widely for the efficient and accurate treatment of dynamics for nonadiabatic processes. We will be using explicit molecular dynamics with semiclassical framework, like one recently developed quasi classical methods, multistate mapping Hamiltonian approach to surface hopping (J. E. Runeson, D. E. Manolopoulos, arXiv preprint arXiv:2305.08835 (2023), J. R. Mannouch, J. O. Richardson, J. Chem. Phys. 158 (2023)), that allows us to incorporate *ab initio* potentials in the adiabatic basis (J. C. Tully, J. Chem. Phys. 93, 1061–1071 (1990)). The electronic degrees of freedom are mapped into a spin-1/2 coherent states and their classical limit is obtained with a Wigner transformation. The nuclei will be treated as classical degrees of freedom as in molecular dynamics simulations and system modes as quantum degrees of freedom, a reasonable choice for photochemical reactions and a signature of most semiclassical methods. This quasiclassical approach would be a great candidate as it marries the surface hopping approach with spin mapping Hamiltonian and makes the method deterministic

rather than traditional surface hopping methods which are stochastic. It produces correct long time population estimations of the electronic states, assuming ergodicity. The real- time population dynamics and correlation functions would be calculated by generating classical trajectories from mapping the Hamiltonian with surface hopping, with the potential gradients and nonadiabatic coupling vector coming from electronic structure calculations. This project will give us details of the effect of solvent environment that drives the difference in reactivities and will provide insights into experimental findings. It will also be useful for studying photochemical reactions taking place in atmospheric aerosols.

Once these theoretical methods have been developed to understand phenol photochemistry at the air-water interface, Wilson, Limmer and coworkers together will address the photochemistry of nitrate at aqueous interfaces. There is substantial uncertainty as to the mechanism of HONO formation produced by the photochemistry of nitrate in aqueous aerosols in pristine marine environments. Wilson's group will make detailed measurements of the photolysis rate of NO_3^- in levitated droplets, while the Limmer group will explore the same reaction using the molecular simulations and the techniques outlined above, with the goal a molecular detailed picture of the photochemical surface reaction. Key questions to be addressed are how the presence of spectator ions (*i.e.* chloride) alter the observed photochemical transformation at the air-water interface?

Subtask 2: Adsorption and Reactivity at Solid-Liquid Interfaces

Monika Blum, Ethan J. Crumlin, Phillip L. Geissler (1974-2022), Teresa Head-Gordon (Subtask Leader), David Limmer, and Richard Saykally

Program Scope

Reactivity at interfaces poses a remarkable series of challenges for experiment and theory to elucidate the sequence of chemical transformations at the molecular scale.[1] While considerable knowledge about electrochemical reactions has been organized around Sabatier's principle and manifested in modern day volcano plots using Density Functional Theory (DFT), a number of idealized assumptions are made including a perfect electrode surface, a single reaction mechanism, a single adsorbate site, and a continuum treatment of solvent. However, under *in-situ* conditions, the metal surfaces restructure and chemical transformations can be driven through multiple intermediates that are difficult to characterize within the fluctuations and dynamics of the continuously reorganizing solvent environment. Hence, there is a current knowledge gap in molecular detail that demands new methods for experimental observations of the reactive intermediates and improved computational modeling of the adsorbate-metal interaction with complete solvent environments,[2] and to clarify the steps leading from reactants to products at the ensemble level for the mechanistic chemistry at an active electrode. Subtask 2 aims to advance technical capabilities towards this end and, by applying them, to reveal general physical roles of solvent reorganization, spatio-temporal substrate heterogeneity, and nonequilibrium driving in dictating the routes and efficiencies of solid-liquid reactivity.

Progress Report:

Adsorption to Electrochemical Interfaces. To understand the complex nanoparticle - electrolyte interface, Blum and co-workers have utilized APXPS at the Advanced Light Source in the soft X-ray range (< 2 keV) to study adsorption processes. First measurements on Au nanoparticles (NPs) in an aqueous environment revealed an hydroxyl layer at the solid-liquid interface combined with

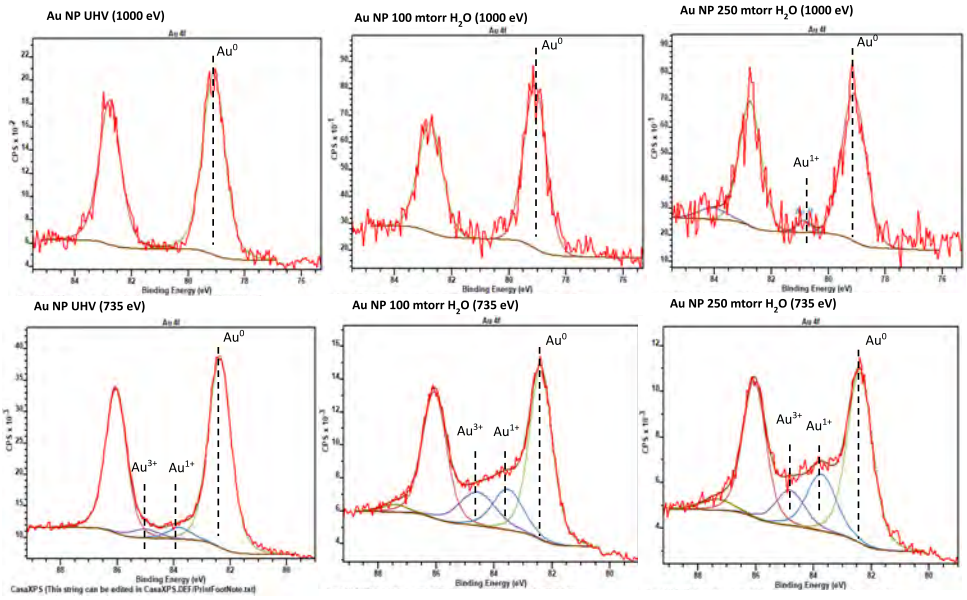

Fig. 4**:** APXPS Au 4f spectra of Au NPs under UHV , 100 mTorr, and 250 mTorr at both 1000 eV (top row; probing the Au NP core) and 735 eV (bottom row; probing the NP-liquid interface) excitation energies.

metal-oxides formation, which is clearly focused on the surface through formation of Au^{+1} and Au^{+3} species and little to no oxidation toward the core of the nanoparticle (see Fig. 4).

In addition, Blum has built on her recent cross-collaboration with the Gessner group in the DOE-AMOS program and their joint work[3] on photoinduced charge dynamics of Au NPs on TiO_2 substrate with time-resolved X-ray photoelectron spectroscopy and performed proof-of-principle measurements to study the additional influence of water and electrolytes on the NPs-liquid interface, the electron transfer between nanoparticles and substrates. The preliminary experimental results showed a clear H_2O pressure dependent photoinduced Au 4f shift.

Head-Gordon and co-workers performed a benchmark study using RPBE and the meta-GGA functionals SCAN, RTPSS, and B97M-rV to examine their ability to reproduce experimental surface relaxation properties, and CO adsorption energies and site preferences, on the M(111) where M = Pt, Cu, Ag, Au metal surfaces. Disappointingly, all DFT functionals considered did not predict the CO adsorption site preference on Pt and Cu – the atop site for all metals observed at low CO adsorbate coverage – instead predicting stronger binding to multi-coordinated metal sites (Fig. 5A, B). But as is standard in nearly all electrocatalysis computational work, DFT functionals are evaluated at 0 K, while all electrochemical surfaces, adsorbants, and reactions are experimentally produced at finite temperatures. Although thermodynamic corrections in the harmonic regime have been used, they can't account for the genuine configurational entropy that is manifest in all catalytic experiments as surfaces relax.

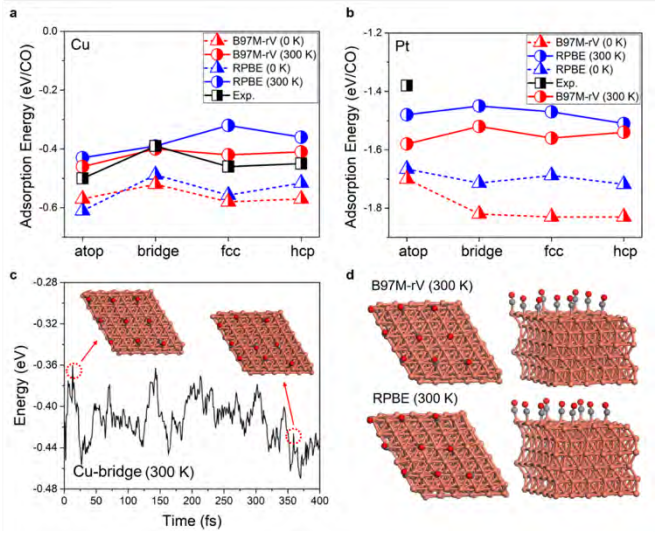

Fig. 5. Thermal effects on the adsorption energies for 25% CO coverage on Cu(111) and Pt(111) surfaces illustrating the importance of ensemble effects. Calculated and experimentally observed adsorption energies for CO on atop, bridge, fcc, and hcp sites at 0 K and 300 K for (a) Cu(111) and (b) Pt(111). (c) Binding energy vs. time for B97M-rV, illustrating CO adsorbed on Cu(111) surface at the bridge site for the first 100 fs at 300 K, but moving to the atop due to the strong energetic preference for CO binding at this site. (d) Representative geometries from two different perspectives of the CO adsorbed on Cu(111) at the atopsite for both B97M-rV and RPBE, showing deviations from linearity of M-C=O angle at 300K.

We used AIMD in the NVT/NPT ensembles to better simulate the statistical fluctuations and surface relaxations under ambient conditions (Fig. 5).[4] We found that the good agreement for RPBE at 0K worsened with experiment at finite temperature, whereas B97M–rV better reproduced experimental bulk and surface relaxation properties, and in turn the CO adsorption energies and site preferences on the M(111) surfaces. Thermalization exposes the importance of dispersion interactions, for which the B97M-rV functional accurately predicts the weak binding energetics for the Ag(111) and Au(111) metals and were found to be a mixture of chemisorbed and physisorbed CO species. Finally, because the B97M–rV functional also provides an excellent description of bulk water, it reveals its potential feasibility for better theoretical predictions at the solid-liquid interface.

Molecular dynamics (MD) simulation engines are based on a potential energy function that links the system configuration with its energy and its evolution in time and space through forces. It has been the holy grail for machine learning (ML) to ultimately yield a high-quality *ab initio* (AI) potential energy surface (PES) for chemical reactivity that will replace very expensive AIMD calculations. At present there has been mostly an arms race in machine learning models that strive to reach new levels of accuracy with reduced data requirements on several established and static benchmark data sets at the CCSD(T) or expensive hybrid DFT functional for small molecules and non-reactive systems. But the true translational goal of ML potentials is to perform MLMD for reactive systems for complex chemical applications which has not materialized in full view yet.

The Head-Gordon lab has moved beyond benchmarking to realize the promise of ML toward true chemical application work. Our results speak to three main points: (1) the QM reference data will always be small scale and a long period of gestation using active learning is always required to develop the ML PES; it is important to emphasize that this undertaking of active learning is often ignored in the cost-benefit analysis. (2) the actual new data often required is unintuitive, i.e., mostly unphysical regions of the PES, because the ML model requires a “negative design” component to learning. This addresses the point that almost all data construction is based on chemical intuition as to what is important. Here we have utilized metadynamics as an ergodic sampler to rapidly find this data. and (3) at some point further active learning training is counterproductive in wall time and simply running in a hybrid AIML mode becomes beneficial. For example, using the deviation among multiple ML models to recognize a data outlier, and now replace that time step with an ab initio call directly instead of retraining. We show that this maintains ML speeds of 2-3 orders of magnitude over AIMD without disrupting the trajectory, which we illustrate with reconstruction

of the free energy surface of several reactions in which the transition state has changed from the 0 K result.

We have demonstrated our complete approach to a complex reactive chemistry for hydrogen combustion which has at least 19 reaction channels and show that we can reconstruct the free energy surface with new insight into barriers at high temperatures. We believe that this is an approach that ultimately proves that ML speeds with AIMD accuracy are possible on complex systems involving chemical reactivity which we will explore in future plans. (Guan, X.; Heindel, J.P.; Ko, T.; Yang, C.; Head-Gordon, T., Using machine learning to go beyond potential energy surface benchmarking for chemical reactivity. *Nature Comp. Sci.* **2023**. In press.).

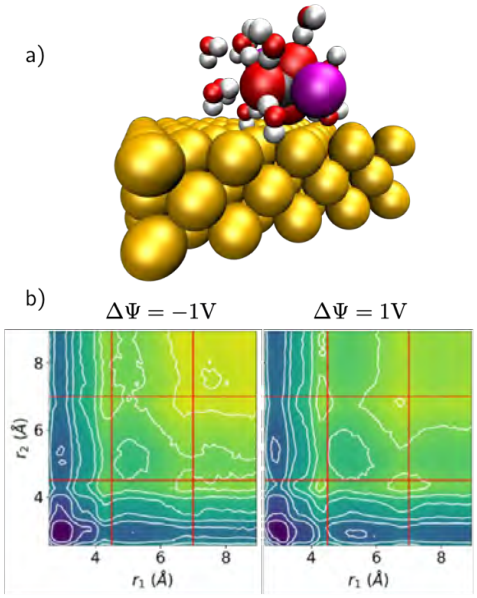

Fig, 6. Na_2CO_3 ion pairing near an electrified interface under a constant applied potential.

Water structure near electrode interfaces may play an important role in controlling CO_2 electroreduction. Together with the Baker group at Ohio State University, the Limmer group have studied the emergent structure of water in the presence of carbonate derived electrolytes. Using plasmon-enhanced vibrational sum frequency generation spectroscopy, the Baker group identified an interfacial water subpopulation with large electric fields along their OH bonds, when Na_2CO_3 ions are present near the electrode under applied potential. The Limmer group employed molecular dynamics simulations to show that the approach of aqueous Na_2CO_3 to electrodes is coupled to the formation of structured and oriented ion complexes, and that the emergent water population is associated with the first solvation shell of these complexes. This structuring near the interface was quantified using free energy calculations, Fig. 6, for the dissociation of the two Na^+ cations relative to CO_3^{2-}. This water subpopulation is seen even when the sole source of CO_3^{2-} is its in-situ generation from CO_2 indicating that the interfacial species investigated here are likely ubiquitous in CO_2 electroreduction contexts. (Submitted to J. Colloid and Interface Science, 2023)

These electrolyte simulations were made possible by a methodological advance concerning the Drude oscillator potentials, a popular and computationally efficient class of polarizable models. Postdoc Amr Dodin working with Geissler showed that existing force fields that place all non-Coulomb forces on the Drude core and none on the shell inadvertently couple the dipole to non-Coulombic forces. This introduces errors where interactions with neutral particles can erroneously induce atomic polarization, leading to spurious polarizations in the absence of an electric field, exacerbating violations of equipartition in the employed Carr–Parinello scheme. A suitable symmetrization of the interaction potential that correctly splits the force between the Drude core and shell can correct this shortcoming, improving the stability and numerical performance of Drude oscillator-based simulations. The symmetrization procedure is straightforward and only requires the rescaling of a few force field parameters.[5]

Future Plans:

The Nitrogen Reduction Reaction (NRR). The nitrogen reduction reaction (NRR) is of profound importance for society as a whole since the production of ammonia underpins the world's food

supply in its use for producing fertilizer. Head-Gordon's recent work on the nitrogenase enzyme showed that undercoordinated Fe is a key factor to adsorb and activate the N_2 molecule.[6] There is new evidence that aqueous microdroplets containing small molecular FeO catalysts can distort at interfaces. Blum will provide FTIR and APXPS experiments to understand the mechanism to produce ammonia on the catalyst surface while being exposed to different relative humidities and N_2 pressures. The experiments will gain insight into the electronic, chemical, and vibrational structure of the catalyst - H_2O/N_2 interface. In case the experiments require a full water film on the metal-oxide surface or higher N_2 pressure, Blum will collaborate with Crumlin to utilize the tender APXPS setup at the ALS. The NRR is a very complex reaction requiring the use of AIMD simulations and multi-reference electronic structure, and this may also open up to include some machine learning strategies. We will also calculate electric fields to understand both local and non-local interfacial contributions to nitrogen activation and subsequent catalysis.[6]

Machine-learned Models for Reactivity at the Solid-Liquid Interface. The Head-Gordon lab has recently reported a new deep learning message passing NN that takes inspiration from Newton's equations of motion to learn interatomic potentials and forces. With directional information from trainable force vectors, and physics-infused operators that are inspired by Newtonian physics, the entire model remains rotationally equivariant. NewtonNet shows excellent performance on the prediction of several reactive and non-reactive high quality ab initio data sets including single small molecules and a large set of chemically diverse molecules. Recently we have developed a new ML data acquisition strategy for chemical reactivity, and a hybrid NewtonNet-physics model idea, and used it to complete application to learning the free energy transition state of several reaction channels for hydrogen combustion. (Guan, X.; Heindel, J.P.; Ko, T.; Yang, C.; Head-Gordon, T., Using machine learning to go beyond potential energy surface benchmarking for chemical reactivity. *Nature Comp. Sci.* **2023**. In press.)

Simulating charge transfer reactions at electrochemical interfaces presents a unique set of hurdles. It is crucial to capture (1) the movement of charges within the metal electrode, electrolyte solution, and between the two phases, (2) how this changes when an electric potential is applied to the electrodes and the total number of electrons in the system fluctuate, and (3) the specific and dynamically shifting chemical bonding and adsorption interactions within the electrolyte and between the electrolyte and electrode as charge transfer reactions take place. Additionally, describing reactions necessitates sampling a large ensemble of infrequent reactive events, which demands highly efficient computational methods. The Limmer group is currently developing simulation methodologies that will combine constant potential molecular dynamics simulations with neural-network based reactive forcefields (using reactive FFs developed in the Head-Gordon group), and Limmer and Head-Gordon will also use ML potentials, enabling the simulation of heterogeneous charge transfer reactions at working electrodes with accuracy approaching near ab initio methods, all at costs comparable to classical molecular dynamics. The Crumlin group will provide experimental results detailing the solid/liquid electrochemical interface using tender APXPS to iteratively validate and refine the ML models developed. This novel simulation technique empowers the use of robust tools from statistical mechanical rate theories to investigate electrochemical reactions at the atomic scale.

Interfacial Chemistry and Potentials. The Crumlin group will continue their work understanding the interfacial chemistry and potential profiles of electrified interfaces at the solid/liquid interface. As particular salt combinations or additives are introduced into electrolytes to tailor electrochemical reactions, revealing the fundamental mechanism governing these interactions is

critical to enhancing their control to improve selectivity, stability, and reactivity. We will continue our efforts to explore the solid/liquid interface and experimentally determine an electrodes chemical and potential profile transformation under applied potentials and detail these behaviors in collaboration with Head-Gordon and Limmer groups. A primary focus of our investigations will revolve around decoding the electrode/electrolyte interaction during the nitrogen reduction reaction. Metallic Fe and FeO_x will serve as the primary electrodes with a series of M-hydroxide electrolytes to probe the cation influence (M = Li, Na, K, Rb, Cs) to understand the interfacial environments influence on the NRR. This investigation will complement and expand upon the work performed by Blum/Head-Gordon previously described above. To reach these goals, we will employ our conventional Dip and Pull technique for model thin film electrodes, as well as develop a 2-chamber operando electrochemical cell that will be able to accommodate nanoparticle electrocatalysts and higher nitrogen partial pressures.

Nanofluidics. In addition, the Limmer group is actively pursuing studies concerning the electrokinetic effects in nanofluidic systems. When fluids are confined to small scales, interfacial boundary conditions become important, and molecular driving forces for specific ion adsorption can fundamentally alter streaming currents and permeabilities. Building off of previous experimental work from the Saykally group, the Limmer group aims to simulate how ionic concentration profiles are altered under flow conditions and how these distributions enhance proton transfer processes on rigid substrates.

Subtask 3: Heterogeneous Dynamics of Assembly and Structural Relaxation in Liquids

Musahid Ahmed, Ethan J. Crumlin, Phillip L. Geissler (1974-2022), Teresa Head-Gordon, Kranthi Mandadapu (Subtask Leader), and Kevin Wilson

Program Scope

Heterogeneities that can profoundly influence energy-related transformations extend well beyond spatial nonuniformity that is part of subtasks 1 and 2. As the simplest example, mixtures (e.g. co-solvents) introduce compositional heterogeneity, whose diverse physical and chemical consequences are familiar but, in many cases, poorly understood. More subtly, driven systems or out-of-equilibrium systems are unavoidably heterogeneous in time, since the departure from equilibrium lends a direction to time – that of increasing entropy – that is absent at equilibrium. Subtask 3 focuses on such non-spatial heterogeneities, by focusing on exemplary phenomena related to self-assembly of molecules in liquid solutions, the slow and heterogeneous dynamics of liquids exhibiting glassy dynamics, microheterogeneity and transient non-equilibrium transport of ions at and across membranes and interfaces. All of the mentioned forms of heterogeneity, which move beyond the “simple” spatial heterogeneity imposed by interfaces addressed in Subtask 1, pose significant difficulties for computer simulation, and most severely, heterogeneities in time, requiring advanced theoretical and computational methods addressed by Geissler, Head-Gordon and Mandadapu. Wilson and Ahmed are developing new experimental strategies to test the mechanisms and theoretical advances.

Recent Progress

Self-Assembly. Wilson and Geissler addressed aspects of assembly and reactivity of amphiphilic interfaces. To that end, they have completed a comprehensive set of experiments aimed at understanding the self-assembly mechanism in a system driven by photochemistry focusing on

alkyl oxoacids (e.g. 2-oxodecanoic acid, 2-OOA, Fig. 7). From past work in Veronica Vaida's group (University of Colorado, Boulder), it is known that photoexcitation of 2-OOA forms oligomeric compounds (Fig. 7). The formation of these photochemical products is accompanied by a highly monodisperse nanoscale structure with a radius ~80-100 nm. Using mass spectrometry, they have quantified the molecular building blocks and their formation kinetics. Mass spectra reveals peaks that are consistent with the multi-tailed reaction products. As the reaction proceeds, it is observed that 2-OOA is consumed and the dimer products appear, which coincide with the appearance of monodisperse, radius of ~80 nm structures (measured by dynamic light scattering, Fig. 7). Using electrospray ionization mass spectrometry (ESI-MS), it is also observed that the nanoparticle composition is enriched in double tailed products at m/z = 315, 317 and 385 over those corresponding to single-tailed products and the precursor. In collaboration with Miriam Freedman's group (Penn. State University), preliminary evidence from cryo-electron microscopy shows that the structures are spherical and have a phase separated morphology (Fig. 7). The formation of monodisperse, phase separated particles is unexpected and it is currently unclear how to connect the formation of these structures with the relatively simple set of molecular building blocks that are produced photochemically.

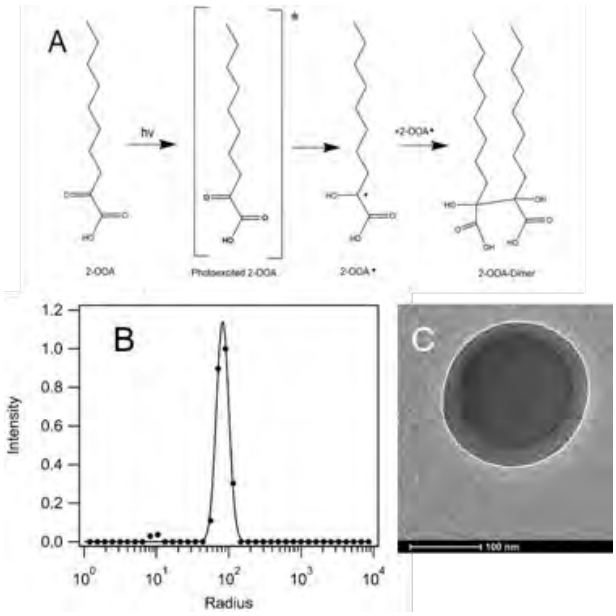

Fig. 7. (A) Cartoon of dimer formation during the photochemistry of 2-OOA. (B) Dynamic light scattering determination of particle size in solution. (C) Cryo-electron microscope image of phase separated droplet produced photochemically from 2-OOA.

Theoretical work was initiated by Geissler's group with the aim of developing a molecular mechanism to explain the formation of these nanostructures. In preliminary work they have

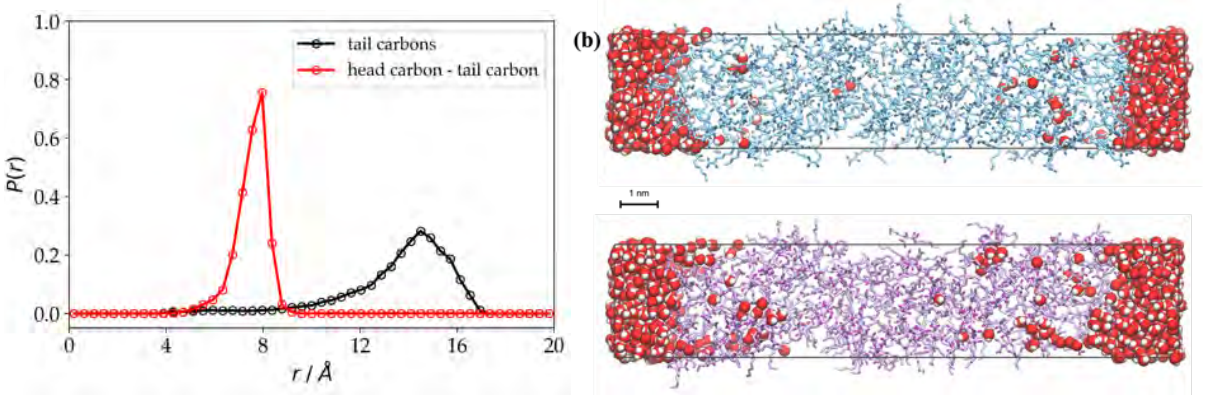

Fig. 8. All-atom molecular dynamics simulations of 2-OOA and its double-tailed dimer. (a) Probability distribution of intramolecular distances for the dimer in aqueous solution, indicating a tail-tail separation nearly twice that of head-tail, as expected for a splayed configuration. (b) Coexistence between liquid water and condensed phases of the single-tailed (top) and double-tailed (bottom) species feature alternating head-rich and tail-rich layers that persist ~10nm into the bulk.

examined the basic building blocks for this mesoscale assembly, as well as pertinent macroscopic phases and extended interfaces, using all-atom molecular dynamics simulations. In idealized drawings, the double-tailed dimer species resembles textbook head-tail amphiphiles, but its typical intramolecular structure differs qualitatively, both in solution and in its condensed phase. Specifically, the tails are splayed with high probability (as indicated by distributions of head-tail and tail-tail distances), resulting in a roughly linear tail-head-tail arrangement (Fig. 8). This preference, which strains micelle-like and lamella-like motifs, likely has a strong impact on both the thermodynamics and kinetics of assembly. It is also observed that interfaces between water and the condensed organic phase generate head-rich and tail-rich layers that oscillate coherently with distance from the interface for tens of nm (Fig. 8). How these geometric features shape dynamical pathways of aggregation remain a central question in this work.

Head-Gordon studied how self-assembled micelles alter solvated proton dynamics relative to the bulk phase. This is a critical factor in our understanding of important chemical and biological processes including proton transport at membrane surfaces, for synthetic membranes used in fuel cells and separations, and the acidic interfacial chemistry of aerosols, particularly those originating from marine environments. While the effect of hydronium concentration on solvated proton dynamics has been investigated in bulk solutions, it is not clear what the status is near interfaces and under confinement. To that end, the properties of the water network in concentrated HCl acid pools in nanometer-sized non-ionic reverse micelles (RMs) were probed with TeraHertz (THz) absorption, dielectric relaxation (DR), and reactive force field simulations. With this study, Head-Gordon identified a critical micelle size in which solvated proton complexes undergo a change in mechanism from Grotthuss forward shuttling to one that favors local oscillatory hopping. This is due to a preference for high acid concentrations of hydroniums to adsorb to the interface that causes a “traffic jam”, short-circuiting the Grotthuss hydrogen-bonding motif that decreases the forward hopping rate even as the micelle size increases.

Glass Dynamics. Mandadapu addressed the development of an advanced theory to understand the strongly heterogeneous glassy dynamics in liquids, where even basic driving forces for vitrification remain sharply debated. This work connects intermolecular structure and microscopic motion to the abstract building blocks of dynamical facilitation theory, a perspective founded on the notion of dynamic heterogeneity. To that end, Mandadapu and his student developed a theory for localized excitations, which are central to the molecular rearrangements in supercooled liquids. Building on this work, Mandadapu and coworkers have now proposed a complete theory for the onset temperature for emergence of glassy dynamics in supercooled liquids. The dynamics of glass formers exhibit a dramatic slowdown below an onset temperature that delineates the high-temperature and supercooled liquid regimes. For two-dimensional (2D) glass formers, the theory proposes that the onset temperature is described by a Kosterlitz-Thouless transition, driven by the elastic excitations underlying the glassy dynamics. Analogous to dislocation-mediated melting in 2D solids, the onset temperature indicates the unbinding of dipoles leading to a loss of elastic modulus of supercooled liquids at intermediate time scales. The theory explains the elastic behavior of supercooled liquids at intermediate timescales observed in experiments and simulations of 2D glass formers and is relevant to systems under extreme confinement.

Hydrogen Bonding, Phase Changes, and Organic Framework growth. The hydrogen-bond network within a composite solvent system can involve co-solvation with the solution exhibiting significant differences from pure substances, depending on the concentration of each component. Ahmed and coworkers focused on using poly-alcohols, particularly glycerol, to develop an

understanding of the molecular heterogeneities that appear upon their interaction in aqueous co-solvent systems. These poly-alcohols show significant deviation from ideal behavior upon mixing with solvents, and ions in the bulk environment, which is directly a result of micro heterogeneity and liquid-liquid phase separation and solid-solid phase changes, respectively. This complex behavior provides a rich tapestry to test hydrogen bond dynamics, probe solvation and confinement, and map nucleation and crystallization events. The hydrogen bond network of glycerol-water aerosols generated from an aqueous solution with different mixing ratios, is probed directly using XPS. The carbon and oxygen X-ray spectra reveal contributions from gas and condensed phase components of the aerosol. It is shown that water suppresses glycerol evaporation up to a critical mixing ratio. A dielectric analysis using terahertz spectroscopy coupled with IR spectroscopy of the bulk solutions provides a picture of the microscopic heterogeneity prevalent in the hydrogen bond network when combined with the photoelectron spectroscopy analysis. The hydrogen bond network is comprised of three intertwined regions. At low concentrations, glycerol molecules are surrounded by water forming a solvated water network. Adding more glycerol leads to a confined water network, maximizing at 22 mol%, beyond which the aerosol resembles bulk glycerol. This microscopic view of hydrogen bonding networks holds promise in probing evaporation, diffusion dynamics and reactivity in aqueous aerosols.

Ahmed and coworkers focused on developing a molecular-level understanding of phase changes in hydrogen-bonded solid-state systems, which are of paramount importance in fields spanning thermal science to medical therapeutics. Focusing on polyols, which have recently emerged as prime targets for deployment, Ahmed probed the hydrogen-bond network of neopentyl glycol (NPG) with terahertz time domain spectroscopy, and attenuated total reflection spectroscopy in the far and mid infrared regions augmented by electronic structure calculations. A picture emerged where vibrational spectroscopy can exquisitely probe a crystalline to amorphous solid-solid phase transition, while spectroscopy in the mid infrared region provided a molecular picture of the phase transition. These methods are then applied to understand the thermal properties and phase changes in NPG upon incorporation of bis(trifluoromethane)-sulfonimide lithium salt, to demonstrate that vibrational spectroscopy can directly probe the disruption of hydrogen-bond networks in plastic crystals.

Ahmed also applied a multimodal approach to study complex aspects of growth dynamics of metal-organic frameworks, which are described by complex free energy landscapes analogous to the case of dynamics in glassy liquids. This approach includes using wide-angle X-ray scattering (WAXS), Raman spectroscopy, mid-infrared (MIR) spectroscopy, and far-infrared (FIR) spectroscopy to investigate the growth kinetics of Co-MOF-74 across various length scales using microscopic volumes of reagents confined either in a capillary or a chip-based reactor. Theoretical Raman and Infrared spectra were calculated by Jin Qian (GPCP program) to interpret the experimental results. It was found that synthesis of the metal-organic framework with microscopic volumes leads to monodisperse, micron-sized crystals, in contrast to those typically observed under bulk reaction conditions. Reduction in the volume of reagents within the microchip reactor was found to accelerate the reaction rate.

Future Plans

Micelles, Foams and Self-Assembly. The Head-Gordon lab has proposed that the Grotthuss mechanism dominates for either smaller RMs and/or weaker acid concentrations, whereas at the other extreme there is a cross-over to oscillatory hopping due to a proton traffic jam. Her lab will continue their theoretical work to test the generality of this new mechanism by now extending it

to new surfactants with anionic or cationic head groups that will have different types of interactions with the water pools (and anything dissolved in it) than when using surfactants with polar head groups. Different classes of reverse micelles will clearly involve different molecular interactions with different magnitudes (Coulombic field effects, hydrogen bond interactions, etc.) and with different spatial distribution functions, different hydrogen-bond lifetimes, and as a result different proton transfer times (rattling and forward Grotthuss hopping). Hence the IR and THz region of the water spectrum is highly affected by its hydrogen-bonding environment and is thus an excellent probe for these systems and ideally suited for studies that will be conducted by Ahmed. using tools described earlier.

Alkyl Polyglycoside (APG) surfactants are characterized by an alkyl tail and glucoside head groups. They are synthesized from carbohydrates, oils, and alcohols, derived from renewable resources. Their ability to form foams in aqueous solutions with additives are being increasingly seen as alternatives to PFAS based fire-fighting foams. Ahmed has embarked on a collaboration with Dr. Katie Hinnant from the Naval Research Laboratory to study the hydrogen bonding and foaming abilities of these novel surfactants. Surfactants can orient into different shapes rather than spherical; however, the formation of non-spherical micelles suggests additional interactions working to reduce opposing forces between surfactant head groups. For APG surfactants specifically, it has been suggested that the altered shape is due to inter-surfactant hydrogen bonding, between the APG surfactant molecules in solution. The OH groups on the glucoside rings of APGs represent strong hydrogen bond donors, which have the capacity to H-bond with surrounding water molecules in solution or other APG molecules. H-bonding between surfactant head groups may alter micelle shape and effect solution and foam properties. However, it is difficult to isolate surfactant hydrogen bonding from surfactant-water and water-water H-bonding. We will use vibrational and aerosol-based X-Ray spectroscopy coupled with judicious use of X-Ray scattering techniques to understand the underlying dynamics of surfactant molecule interactions. We believe that vibrational spectroscopy (particularly Raman) could be the initial screening tool to probe the chemical systems of interest. This is due to the fact that the low frequency region (40-300 cm^{-1}) is sensitive to low amplitude lattices and extended modes, which will allow for the identification of structural changes and particle formation, while the fingerprint and mid IR region will be sensitive to functional groups and water bonding. Preliminary results obtained on dilute APG solutions along with a hydrotropic additive (sodium p-toluene sulfate) with Raman, ATR-FTIR, aerosol based XPS and NEXAFS and a white light surface profilometer developed by our group suggest that indeed, our methods will be able to provide unique insights into surfactant chemistry and foam stability.

Microheterogeneity in Exotic Solvents & Hydrogen Bonded Organic Frameworks. Deep eutectic solvents (DES) are considered as alternatives to conventional organic solvents and ionic liquids in many applications owing to their versatile characteristics. DESs consist of a hydrogen bond donor and an acceptor and to-date model studies have focused on mixtures of choline chloride (ChCl) and poly-alcohols. At specific compositions, these form a eutectic mixture, which resembles many characteristics of ionic liquids and organic solvents due to complicated inter- and intramolecular hydrogen-bond networks. Charge transfer and delocalization effects and the consequences on the hydrogen-bond network remain unresolved and controversial. Furthermore, hydration tends to make an already complex system even more difficult to understand. Similar to the glycerol/water system, nano-structuring, and phase separations are also invoked in DESs. We will focus on coupling X-ray spectroscopy (especially NEXAFS), X-ray scattering, and vibrational spectroscopy, in collaboration with the Wilson group, to provide a unique view of the

microstructure and dynamics in DES systems. We will start with the classic DES, glyceline (composed of ChCl and glycerol) phase system to understand how the changes in the hydrogen-bond network lead to a eutectic mixture at specific concentrations. Beyond using THz time-domain spectroscopy and chip-based ATR-FTIR spectroscopy and X-ray spectroscopies, we propose to use Raman spectroscopy and X-ray scattering to shed new light into the underlying structure and dynamics. Probes, which allow us to access low-frequency regions of the Raman spectrum up to

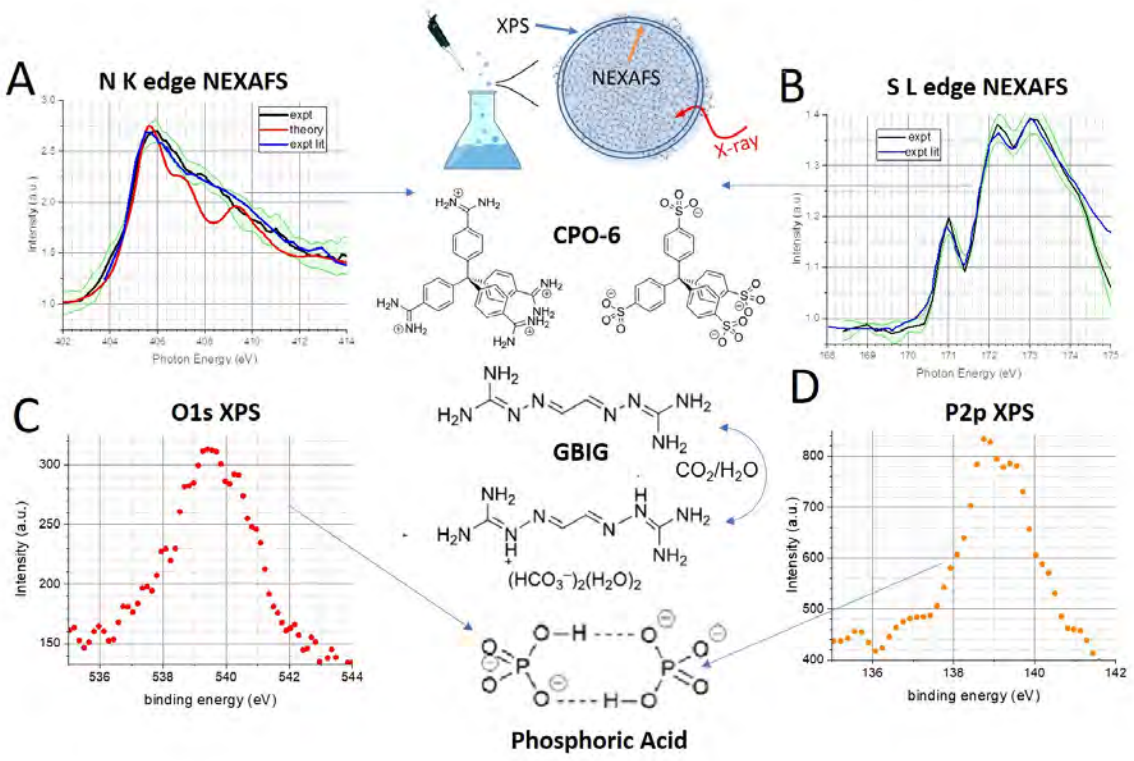

Fig 9. Schematic depicting ammonium sulfate aerosols with XPS and NEXAFS detecting surface and bulk respectively. (A) N L-edge NEXAFS spectra generated from an ammonium sulfate aerosol (in black with errors constrained in green). The red line is a theoretical calculation using TDDFT (10.1039/D2CP04077H), and the blue line is the data from literature generated using liquid jets (10.1021/jacs.7b07207). (B) S $L_{2,3}$-edge NEXAFS spectra generated from an ammonium sulfate aerosol (in black with errors constrained in green). The blue line is data collected from sulfate aerosols deposited on a filter and measured using scanning transmission X-ray microscopy (10.1029/2007JD008954). Also shown in the figure are molecular structures for the CPO-6 precursors, the crystallization pathway for GBIG, and the hydrogen bonding in a phosphoric acid dimer.

40 cm^{-1}, will be coupled with X-ray spectroscopy at the Cl $L_{2,3}$-, C K-, N K-, and O K-edges of glyceline in order to unravel the local electronic structure of the mixtures. Raman spectroscopy will be used to probe both the hydrogen-bond networks of the mixture using low-frequency modes, and probe intermolecular and intramolecular interactions in glyceline using the fingerprint and C-H and O-H stretching regions of the spectrum. Theory will play a crucial role in allowing us to decipher the electronic structure of these hydrogen bonded systems and corresponding disruption of these bonds.

Ahmed will extend the methodology employed to study deep eutectic solvents to study hydrogen bonded organic frameworks (HOFs). HOFs are porous solids that are self-assembled by organic

molecules through hydrogen bond interactions. Since hydrogen bonding is much weaker than the covalent and electrostatic bonds that drive the formation and stability of MOFs and covalent organic frameworks (COFs), the design rules for synthesizing these networks are still emerging and not clear at present. However, the reversible nature and the weakness of the hydrogen bond, coupled with the ability to select the molecular backbone and hydrogen bonding moieties does allow synthesis in benign and green solvents (even water) and easy separation, purification and regeneration. Hence there has been an explosion of studies recently to try and understand the underlying kinetics and mechanisms of formation, and phase change dynamics that occur upon the input of external stimuli. However, fundamental understanding is still lacking at the molecular level and connecting structural details to the bulk crystal has proven elusive. We seek to understand hydrogen bonding in two systems which have garnered enormous interest recently in which we understand the X-ray spectroscopy of some of their constituent moieties. The first system is prepared from cationic tetra-amidinium or anionic tetra-sulfonates components of Crystalline Porous Organic Salt-6 (CPO-6, Fig. 9), while the second is based on the formation of a bicarbonate salt upon incorporation of CO_2 on to a glyoxal-bis(iminoguanidine) (GBIG, Fig. 9) salt.

The study of HOF dynamics may also answer fundamental and controversial questions on the nature of hydrogen bonding, such as the invocation of anti-electrostatic forces in their formation. Phosphate-based systems are an ideal system to try and decipher what leads to anion-anion interactions and how hydrogen bonding can actually stabilize complexes and larger systems. Evidence is garnered from X-ray crystallography in the solid state as to how hydroxy-anions dimerize and subsequently polymerize by overcoming long-range electrostatic repulsion. The short-range hydrogen bonds that form between the anionic donor and acceptor are what is termed an anti-electrostatic hydrogen bond. However, an unequivocal observation of anti-electrostatic hydrogen bonding in phosphate solutions is lacking, and we hypothesize that X-ray spectroscopy coupled to vibrational spectroscopy could be a path forward. We will continue the preliminary measurements of aqueous phosphoric acid solutions that we have taken in collaboration with the Wilson group, where we tracked changes in the XPS and NEXAFS spectra (Fig. 9) while varying concentrations and pH to track the feasibility of the approach. A determination of NEXAFS spectra particularly to understand ion partitioning between the core and surface of the aerosol, in conjunction with theory will be required to understand the nature of hydrogen bonding in these aerosols, which will be addressed in a collaboration with Martin Head-Gordon and Kevin Carter-Fenk.

Glass Dynamics. Developing a self-consistent microscopic theory for the emergence of glassy dynamics in supercooled liquids is an important and open problem in condensed phase matter. There exist three central questions in being able to develop such a theory: (1) what is the onset temperature below which localized excitations or particle rearrangements exist? (2) what is the energy cost or barrier to such arrangements? (3) why do localized excitations lead to other excitations in their vicinity, namely dynamical facilitation, leading to super-Arrhenius behaviors in the relaxation dynamics of supercooled liquids? In the last year, Mandadapu and co-workers have provided answers to the first two questions. However, the third and last question remains unanswered; Mandadapu and Hasyim (a graduate student supported by CPIMS) are on the verge of answering this question. Briefly, they have constructed a model demonstrating the emergence of dynamical facilitation using the Markov-state formalism by means of the quadrupole-quadrupole interactions, the central elements leading to the emergence of localized excitations. Their preliminary results demonstrate super-Arrhenius behaviors of relaxation times, one of the most important properties of supercooled liquids. Much work needs to be done to understand the

anomalous diffusive behavior, the role of phonons in the relaxation behaviors, finite system size effects in the intermediate scattering and bond relaxation functions, and breakdown of Stokes-Einstein relationships. Their preliminary results show promise, and if successful, this work leads to a self-consistent microscopic theory for understanding glassy dynamics that is in line with the observations in experiments and molecular simulations. A new post-doctoral researcher is also hired to understand the consequences of the aforementioned microscopic theory for glassy dynamics in confined systems. To that end, the post-doc will be advised jointly with Kevin Wilson in applying this theory towards understanding the role of glassy heterogeneous dynamics confined in droplet systems and thin films. Work will focus on identifying the nature of the energy barriers in spherical liquid droplets to understand the role of free surfaces in reducing these barriers. Wilson and Mandadapu will also plan to design an experimental test bed in studying the relaxation dynamics of finite size objects.

Non-Equilibrium Transport. Understanding the behaviors of interfaces subjected to chemical and electrical potential gradients presents unique challenges associated with far from equilibrium phenomena. One of the primary challenges is to resolve the driving forces for electrochemical transport, specifically when the interfaces are embedded in electrolyte solutions at high salt concentrations. Furthermore, the thin nature of interfaces presents another challenge in terms of their mechanical behaviors: membranes have sufficiently small bending modulus and are subjected to shape transformations. Crumlin and Mandadapu propose to study coupled non-equilibrium transport processes occurring on thin interfaces. Within the CPIMS effort, Mandadapu was instrumental in developing a generalized formalism to treat transport phenomena in multicomponent electrolyte solutions. Mandadapu and co-workers have also recently developed a mesoscale self-consistent framework for understanding the coupling between electrical and mechanical behaviors of generic membranes. While the aforementioned theories now exist, we are at a crucial state to be able to test the applicability of these theories to understand transport phenomena in realistic systems. To this end, Crumlin and Mandadapu propose a joint experimental-theoretical collaboration towards applicability of these theories to membrane systems that are of utility to generic energy devices that involve ion-exchange membranes.

One of the major challenges in understanding the coupled electrical and chemical transport phenomena associated with interfaces is related to the measurement of membrane electrical potential. Traditionally, this requires constructing a closed electrochemical circuit, subjecting the membrane to electrolyte solutions which are then in contact with electrodes. Understanding or resolving the membrane potential involves studying the electrochemical reactions associated with electrolytes, a procedure that also involves resolving the associated electrical double layers. This process introduces more phenomenological parameters and does not represent a direct measurement of the membrane potential. Crumlin and co-workers resolved this problem by applying a novel method based on APXPS, and correlating the shifts in electron binding energies to the local electrical potentials. With this, they were able to successfully apply the method to perform the first direct measurement of the Donnan potential at membrane-electrolyte interfaces at various concentrations. Crumlin and Mandadapu will now apply the experimental and theoretical methods to study time resolved transport measurements across ion-exchange membranes subjected to electrolyte solutions with varying positive ionic species (Na, K, Rb, Cs) and concentrations. Using APXPS, we will measure the membrane potentials in time that is associated with the uptake and diffusion of salts across the membrane and compare it with the theoretical predictions.

Publications Acknowledging DOE support (2021-2023):

1. Ahmed, M.; Blum, M.; Crumlin, E. J.; Geissler, P. L.; Head-Gordon, T.; Limmer, D. T.; Mandadapu, K. K.; Saykally, R. J.; Wilson, K. R., Molecular Properties and Chemical Transformations Near Interfaces. *J. Phys. Chem. B* **2021,** *125* (32), 9037-9051.

2. Hao, H.; Pestana, L. R.; Qian, J.; Liu, M.; Xu, Q.; Head-Gordon, T., Chemical Transformations and Transport Phenomena at Interfaces. *WIRES: Comp. Mol. Sci.* **2022,** *13* (2), e1639.

3. Borgwardt, M.; Mahl, J.; Roth, F.; Wenthaus, L.; Brausse, F.; Blum, M.; Schwarzburg, K.; Liu, G. J.; Toma, F. M.; Gessner, O., Photoinduced Charge Carrier Dynamics and Electron Injection Efficiencies in Au Nanoparticle-Sensitized TiO_2 Determined with Picosecond Time-Resolved X-ray Photoelectron Spectroscopy. *J. Phys. Chem. Lett.* **2020,** *11* (14), 5476-5481.

4. Li, W.-L.; Lininger, C. N.; Chen, K.; Welborn, V. V.; Rossomme, E.; Bell, A. T.; Head-Gordon, M.; Head-Gordon, T., Critical Role of Thermal Fluctuations for CO Binding on Electrocatalytic Metal Surfaces. *J. Am. Chem. Soc. Au* **2021,** *1* (10), 1708-1718.

5. Dodin, A.; Geissler, P. L., Symmetrized Drude Oscillator Force Fields Improve Numerical Performance of Polarizable Molecular Dynamics. *J. Chem. Theory Comput.* **2023,** *19* (10), 2906–2917.

6. Li, W.-L.; Li, Y.; Li, J.; Head-Gordon, T., How Thermal Fluctuations Influence the Function of the FeMo-cofactor in Nitrogenase Enzymes. . *Chem. Catal.* **2023**.

7. Weeraratna, C.; Tang, X.; Kostko, O.; Rapp, V. H.; Gundel, L. A.; Destaillats, H.; Ahmed, M., Fraction of Free-Base Nicotine in Simulated Vaping Aerosol Particles Determined by X-ray Spectroscopies. *J. Phys. Chem. Lett.* **2023,** *14* (5), 1279-1287.

8. Rovelli, G.; Wilson, K. R., Elucidating the Mechanism for the Reaction of o-Phthalaldehyde with Primary Amines in the Presence of Thiols. *J. Phys. Chem. B* **2023,** *127* (14), 3257–3265.

9. Novelli, F.; Chen, K.; Buchmann, A.; Ockelmann, T.; Hoberg, C.; Head-Gordon, T.; Havenith, M., The Birth and Evolution of Solvated Electrons in the Water. *Proc. Natl. Acad. Sci.* **2023,** *120* (8), e2216480120.

10. Lahiri, N.; Song, D.; Zhang, X.; Huang, X.; Stoerzinger, K.; Carvalho, O. Q.; Adiga, P. l.; Blum, M.; Rosso, K., Interplay between Facets and Defects during the Dissociative and Molecular Adsorption of Water on Metal Oxide Surfaces. *J. Am. Chem. Soc.* **2023,** *145* (5), 2930-2940.

11. Guan, X.; Heindel, J. P.; Ko, T.; Yang, C.; Head-Gordon, T., Using Machine Learning to Go Beyond Potential Energy Surface Benchmarking for Chemical Reactivity. *Nat. Comput. Sci.* **2023**.

12. Fraggedakis, D.; Hasyim, M. R.; Mandadapu, K. K., Inherent State Melting and the Onset of Glassy Dynamics in Two-Dimensional Supercooled Liquids. *Proc. Natl. Acad. Sci.* **2023,** *120* (14), e2209144120.

13. Devlin, S. W.; Jamnuch, S.; Xu, Q.; Chen, A. A.; Qian, J.; Pascal, T. A.; Saykally, R. J., Agglomeration Drives the Reversed Fractionation of Aqueous Carbonate and Bicarbonate at the Air-Water Interface. *J. Am. Chem. Soc.* **2023**.

14. Devlin, S. W.; Bernal, F.; Riffe, E. J.; Wilson, K. R.; Saykally, R. J., Spiers Memorial Lecture: Water at Interfaces. *Faraday Discuss.* **2023,** *Advance Article*.

15. Brown, E.; Rovelli, G.; Wilson, K. R., pH Jump Kinetics in Colliding Microdroplets: Accelerated Synthesis of Azamonardine from Dopamine and Resorcinol. *Chem. Sci.* **2023,** *Advance Article*.

16. Ahmed, M.; Lu, W., Probing Complex Chemical Processes at the Molecular Level with Vibrational Spectroscopy and X-ray Tools. *J. Phys. Chem. Lett.* **2023,** *14*, 9265–9278.

17. Adiga, P.; Wang, L.; Wong, C.; Matthews, B. E.; Bowden, M. E.; Spurgeon, S. R.; Sterbinsky, G. E.; Blum, M.; Choi, M.-J.; Tao, J.; Kaspar, T. C.; Chambers, S. A.; Stoerzinger, K. A.; Du, Y., Correlation Between Oxygen Evolution Reaction Activity and Surface Compositional Evolution in Epitaxial La 0.5 Sr 0.5 Ni 1− x Fe x O 3− δ Thin Films. *Nanoscale* **2023,** *15*, 1119-1127.

18. Zhang, X. Q.; Kirilin, A. V.; Rozeveld, S.; Kang, J. H.; Pollefeyt, G.; Yancey, D. F.; Chojecki, A.; Vanchura, B.; Blum, M., Support Effect and Surface Reconstruction in In_2O_3/*m*-ZrO_2 Catalyzed CO_2 Hydrogenation. *ACS Catal.* **2022,** *12* (7), 3868-3880.

19. Wilson, K. R.; Prophet, A. M.; M.D., W., A Kinetic Model for Predicting Trace Gas Uptake and Reaction. *J. Phys. Chem. A* **2022,** *126* (40), 7291–7308.

20. Willis, M. D.; Wilson, K. R., Coupled Interfacial and Bulk Kinetics Govern the Timescales of Multiphase Ozonolysis Reactions. *J. Phys. Chem. A* **2022,** *126* (30), 4991-5010.

21. Weeraratna, C.; Kostko, O.; Ahmed, M., An Investigation of Aqueous Ammonium Nitrate Aerosols with Soft X-ray Spectroscopy. *Mol. Phys.* **2022,** *120* (1-2), SI.

22. Thomas, N.; Mandadapu, K. K.; Agrawal, A., Electromechanics of Lipid-Modulatedgating of Potassium Channels. *Math. Mech. Solids* **2022,** *27* (7), 1284-1300.

23. Petzoldt, P.; Eder, M.; Mackewicz, S.; Blum, M.; Kratky, T.; Gunther, S.; Tschurl, M.; Heiz, U.; Lechner, B. A. J., Tuning Strong Metal-Support Interaction Kinetics on Pt-Loaded TiO_2 (110) by Choosing the Pressure: A Combined Ultrahigh Vacuum/Near-Ambient Pressure XPS Study. *J. Phys. Chem. C* **2022,** *126* (38), 16127-16139.

24. Pestana, L.-R.; Head-Gordon, T., Evaporation of Water Nanodroplets on Heated Surfaces: Does Nano Matter? . *ACS Nano* **2022,** *16* (3), 3563–3572.

25. Odendahl, N. L.; Geissler, P. L., Local Ice-Like Structure at the Liquid Water Surface. *J. Am. Chem. Soc.* **2022,** *144* (25), 11178-11188.

26. Lu, W.; Zhang, E.; Qian, J.; Weeraratna, C.; Jackson, M.; Zhu, C.; Long, J.; Ahmed, M., Probing Growth of Metal–Organic Frameworks with X-ray Scattering and Vibrational Spectroscopy. *Phys. Chem. Chem. Phys.* **2022,** *24*, 26102.

27. Lu, W.; Zhang, E.; Amarasinghe, C.; Martin, A.; Kaur, S.; Prasher, R.; Ahmed, M., Probing Hydrogen-Bond Networks in Plastic Crystals with Terahertz and Infrared Spectroscopy. *Cell Rep. Phys. Sci.* **2022,** *3* (8), 100988.

28. Li, W.-L.; Hao, H.; Head-Gordon, T., Optimizing the Solvent Reorganization Free Energy by Metal Substitution for Nanocage Catalysis. *ACS Catal.* **2022,** *12* (7), 3782–3788.

29. Hoffmann, L.; Jamnuch, S.; Schwartz, C. P.; Helk, T.; Raj, S. L.; Mizuno, H.; Mincigrucci, R.; Foglia, L.; Principi, E.; Saykally, R. J.; Drisdell, W. S.; Fatehi, S.; Pascal, T. A.; Zuerch, M., Saturable Absorption of Free-Electron Laser Radiation by Graphite Near the Carbon K-edge. *J. Phys. Chem. Lett.* **2022,** *13 CoverArticle*, 8963-8970 ACS Editor's Choice.

30. Hasyim, M. R.; Batton, C. H.; Mandadapu, K. K., Supervised Learning and the Finite-Temperature String Method for Computing Committor Functions and Reaction Rates. *J. Chem. Phys.* **2022,** *157*, 184111.

31. Hao, H.; Leven, I.; Head-Gordon, T., Can Electric Fields Drive Chemistry for an Aqueous Microdroplet? *Nature Commun.* **2022,** *13* (1), Article number: 280.

32. Devlin, S. W.; McCaffrey, D. L.; Saykally, R. J., Characterizing Anion Adsorption to Aqueous Interfaces: Toluene-Water versus Air-Water. *J. Phys. Chem. Lett.* **2022,** *13* (1), 222-228.

33. Devlin, S. W.; Benjamin, I.; Saykally, R. J., On the Mechanisms of Ion Adsorption to Aqueous Interfaces: Air-Water vs. Oil-Water. *Proc. Natl. Acad. Sci. U.S.A.* **2022,** *119* (42), e2210857119.

34. Ye, Y.; Su, H.; Lee, K.-J.; Larson, D.; Valero-Vidal, C.; Blum, M.; Yano, J.; Crumlin, E. J., Carbon Dioxide Adsorption and Activation on Gallium Phosphide Surface Monitored by Ambient Pressure X-ray Photoelectron Spectroscopy. *J. Phys. D: Appl. Phys.* **2021,** *54* (23), 234002.

35. Weeraratna, C.; Amarasinghe, C.; Lu, W. C.; Ahmed, M., A Direct Probe of the Hydrogen Bond Network in Aqueous Glycerol Aerosols. *J. Phys. Chem. Lett.* **2021,** *12* (23), 5503-5511.

36. V., J.; Hargus, C.; Ben-Mohse, A.; Aghazadeh, A.; D., H. H.; Mandadapu, K. K.; Alivisatos, A. P., Anomalous Nanoparticle Surface Diffusion in LCTEM is Revealed by Deep Learning-Assisted Analysis. *Proc. Natl. Acad. Sci.* **2021,** *118* (10), Article Number e2017616118.

37. Sui, X.; Xu, B.; Yu, J.; Kostko, O.; Ahmed, M.; Yu, X. Y., Studying Interfacial Dark Reactions of Glyoxal and Hydrogen Peroxide Using Vacuum Ultraviolet Single Photon Ionization Mass Spectrometry. *J. Atmos.* **2021,** *12* (3), 338.

38. Sui, X.; Xu, B.; Yao, J.; Kostko, O.; Ahmed, M.; Yu, X. Y., New Insights into Secondary Organic Aerosol Formation at the Air-Liquid Interface. *J. Phys. Chem. Lett.* **2021,** *12* (1), 324-329.

39. Schwartz, C. P.; Raj, S. L.; Jamnuch, S.; Hull, C. J.; Miotti, P.; Lam, R. K.; Nordlund, D.; Uzundal, C. B.; Pemmaraju, C. D.; Mincigrucci, R.; Foglia, L.; Simoncig, A.; Coreno, M.; Masciovecchio, C.; Gianessi, L.; Poletto, L.; Principi, E.; Zuerch, M.; Pascal, T. A.; Drisdell, W. S.; Saykally, R. J., Angstrom-Resolved Interfacial Structure in Buried Organic-Inorganic Junctions. *Phys. Rev. Lett.* **2021,** *127* (9), 096801.

40. Rogers, J. R.; Espinoza Garcia, G.; Geissler, P. L., Membrane Hydrophobicity Determines the Activation Free Energy of Passive Lipid Transport. *Biophys. J.* **2021,** *120* (17), 3718-3731.

41. Omar, A. K.; Klymko, K.; GrandPre, T.; Geissler, P. L., Phase Diagram of Active Brownian Spheres: Crystallization and the Metastability of Motility-Induced Phase Separation. *Phys. Rev. Lett.* **2021,** *126*, 188002.

42. Nguyen, D.; Casillas, S.; Vang, H.; Garcia, A.; Mizuno, H.; Riffe, E. J.; Saykally, R. J.; Nguyen, S. C., Catalytic Mechanism of Interfacial Water in the Cycloaddition of Quadricyclane and Diethyl Azodicarboxylate. *J. Phys. Chem. Lett.* **2021,** *12* (12), 3026–3030.

43. Moritz, C.; Geissler, P. L.; Dellago, C., The Microscopic Mechanism of Bulk Melting of Ice. *J. Chem. Phys.* **2021,** *155* (12), 124501.

44. Li, W. L.; Head-Gordon, T., Catalytic Principles from Natural Enzymes and Translational Design Strategies for Synthetic Catalysts. *ACS Cent. Sci.* **2021,** *7* (1), 72-80.

45. Leven, I.; Hao, H.; Tan, S.; Guan, X.; Penrod, K. A.; Akbarian, D.; Evangelisti, B.; Hossain, J.; Islam, M.; Koski, J. P.; Moore, S.; Aktulga, H. M.; Duin, A. C. T. v.; Head-Gordon, T., Recent Advances for Improving the Accuracy, Transferability, and Efficiency of Reactive Force Fields. *J. Chem. Theory Comput.* **2021,** *17* (6), 3237−3251. .

46. Kostko, O.; Xu, B.; Ahmed, M., Local Electronic Structure of Histidine in Aqueous Solution. *Phys. Chem. Chem. Phys.* **2021,** *23* (14), 8847-8853.

47. Kersell, H.; Chen, P.; Martins, H.; Lu, Q.; Brausse, F.; Liu, B.-H.; Blum, M.; Roy, S.; Rude, B.; Kilcoyne, A., Simultaneous Ambient Pressure X-ray Photoelectron Spectroscopy and Grazing Incidence X-ray Scattering in Gas Environments. *Rev. Sci. Instrum.* **2021,** *92* (4), 044102.

48. Karagoz, B.; Tsyshevsky, R.; Trotochaud, L.; Yu, Y.; Karslıoğlu, O.; Blum, M.; Eichhorn, B.; Bluhm, H.; Kuklja, M. M.; Head, A. R., NO_2 Interactions with MoO_3 and CuO at Atmospherically Relevant Pressures. *J. Phys. Chem. C* **2021,** *125* (30), 16489-16497.

49. Karagoz, B.; Blum, M. A.; Head, A. R., Oxidation of $Cu_2O(111)$ by NO_2: An Ambient Pressure X-ray Photoelectron Spectroscopy Study. *J. Phys. D: Appl. Phys.* **2021,** *54* (19), 194002.

50. Hasyim, M. R.; Mandadapu, K. K., A Theory of Localized Excitations in Supercooled Liquids. *J. Chem. Phys.* **2021,** *155* (4), 044504.

51. Hargus, C. H.; Epstein, J. M.; Mandadapu, K. K., Odd Diffusivity of Chiral Random Motion. *Phys. Rev. Lett.* **2021,** *127* (17), 178001.

52. GrandPre, T.; Klymko, K.; Mandadapu, K. K.; Limmer, D. T., Entropy Production Fluctuations Encode Collective Behavior in Active Matter. *Phys. Rev. E* **2021,** *103* (1), 012613.

53. Goodacre, D.; Blum, M.; Buechner, C.; Jovic, V.; Franklin, J. B.; Kittiwatanakul, S.; Söhnel, T.; Bluhm, H.; Smith, K. E., Methanol Adsorption on Vanadium Oxide Surfaces Observed by Ambient Pressure X-ray Photoelectron Spectroscopy. *J. Phys. Chem. C* **2021,** *125* (42), 23192-23204.

54. Cox, S. J.; Mandadapu, K. K.; Geissler, P. L., Quadrupole-Mediated Dielectric Response and the Charge-Asymmetric Salvation of Ions in Water. *J. Chem. Phys.* **2021,** *154*, 244502.

55. Chen, K.; Li, W.-L.; Head-Gordon, T., Linear Combination of Atomic Dipoles to Calculate the Bond and Molecular Dipole Moments of Molecules and Molecular Liquids. *J. Phys. Chem. Lett.* **2021,** *12* (51), 12360–12369.

56. Brausse, F.; Borgwardt, M.; Mahl, J.; Fraund, M.; Roth, F.; Blum, M.; Eberhardt, W.; Gessner, O., Real-Time Interfacal Electron Dynamics Revealed Through Temporal Correlation in X-ray Spectroscopy. *Struct. Dyn.* **2021,** *8* (4), 044301.

57. Adams, E. M.; Hao, H.; Leven, I.; Rüttermann, M.; Wirtz, H.; Havenith, M.; Head-Gordon, T., Proton Traffic Jam: Effect of Nanoconfinement and Acid Concentration on Proton Hopping Mechanism. *Angew. Chem. Int. Ed.* **2021,** *60* (48), 25419-25427.

Electron and Photo-Induced Processes for Molecular Energy Conversion

James F. Wishart, Matthew J. Bird, Diane E. Cabelli, Andrew R. Cook,
David C. Grills, John R. Miller
Chemistry Division, Brookhaven National Laboratory, Upton, NY 11973-5000
wishart@bnl.gov, mbird@bnl.gov, cabelli@bnl.gov, acook@bnl.gov, dcgrills@bnl.gov,
jrmiller@bnl.gov

Project Scope

Radiation chemistry is extremely important for the energy and environmental future of our nation and the world. It touches our daily lives in very direct ways through nuclear power, radiation treatment of advanced materials, pollution abatement, sterilization of food and medicine, and its positive and negative consequences for human health. It also has a large impact in scientific studies as a technique for understanding chemical reactivity in general, by approaching it from a different but complementary direction than photochemistry, electrochemistry, and other techniques. In this role it has widespread application across the programmatic interests of the Department of Energy and the commercial interests of our nation.

The Electron and Photo-Induced Processes for Molecular Energy Conversion (EPIP) Group conducts research in fundamental radiation chemistry and equally important, it applies radiation chemistry techniques to general questions of chemical reactivity relevant to energy science, including radical chemistry and charge separation, recombination, transfer and transport processes. The work is conducted in three thrusts. Thrust 1 (*Radiation Chemistry and Dynamics in Non-aqueous Media*) investigates radiation chemistry in organic solvents and ionic liquids, by elucidating the primary radiolysis products, their relaxation dynamics and reactivity, and mastering their conversion into strong reductants or oxidants to enable radiolysis studies of general chemical reaction mechanisms. Radiolysis techniques provide unique insights into the redox thermodynamics and reactivity of transient species; we employ them to obtain redox potentials without supporting electrolyte, and to elucidate thermodynamics, rates and reaction mechanisms of important radical transients and charge transfer processes. Thrust 2 (*Charges and Excitons in Molecular Systems*) investigates charge transport, separation, and recombination, including highly delocalized charges in conjugated molecules for efficient solar energy conversion in nonpolar media, and production of triplet ion pairs. Delocalization can reduce electronic coupling matrix elements between molecules, and such reduced couplings could be used to make a better, stronger Marcus inverted region for electron transfer. Thrust 3 (*Accelerator Center for Energy Research, ACER*) develops and operates unique instrumental capabilities to support our science. These include the picosecond Laser Electron Accelerator Facility (LEAF) with advanced nanosecond mid-IR detection (PR-TRIR) and 15 ps optical-fiber single-shot (OFSS) detection, the 2 MeV electron Van de Graaff with UV-Vis, mid-IR and microwave conductivity detection, and two ^{60}Co sources. These resources provide powerful and rare capabilities to BNL programs, external collaborators, and users in energy research, and unique research on biological processes involving free radicals.

Thrust 1: Radiation Chemistry and Dynamics in Non-aqueous Media

Electron and energy transfer and transport, and the reactions of free radicals, are key processes in energy-related research, including solar photocatalysis, organic solar cells, nuclear fuel processing, and energy storage (batteries), etc. Radiation chemistry techniques such as pulse

radiolysis (PR), which utilizes high-energy electron pulses from an electron accelerator, and the complementary technique of gamma radiolysis, provide a unique route to many of the reactive charged and radical intermediate species involved in these processes. Coupling radiolysis with advanced and unique experimental detection capabilities (see Thrust 3), we study a variety of fascinating systems that were previously inaccessible for technical reasons, with a strong emphasis on non-aqueous media, including organic and ionic liquids.

The radiation chemistry of non-aqueous media is generally far less understood than that of water because of their more complex molecular structures and greatly varied environments. The initial processes in these liquids that define the range of subsequent chemistry, such as ion fragmentation, recombination, and charge capture, are explored by our group using radiolysis techniques to gain fundamental kinetic and mechanistic insight. Understanding the radiation chemistry of organic solvents and ionic liquids as well as we understand that of water would empower the use of PR for investigations of general chemical reactivity in these solvents. Thrust 1 thus investigates a range of fundamental radiation chemistry processes in non-aqueous media, which underpin the work conducted throughout our entire FWP.

Recent Progress

Characterization and Mechanisms of Ultrafast Excess Charge Capture in Non-aqueous Media

The fundamental processes of ultrafast excess charge capture by solutes following ionization are not well characterized, and yet they are crucial for predicting and controlling products. The unexpected phenomenon of ultrafast, sub-10 ps hole (solvent radical cation) capture by solutes,[1] even in hole-fragmenting liquids such as THF, is of particular interest, as it is a powerful method for rapidly attaching holes to the conjugated molecules studied in Thrust 2, and it also has implications for the stability of metal extractants in used nuclear fuel (UNF) reprocessing. Key questions under investigation include the timescale and mechanism of this process, the effect of charge delocalization and energetics on yields, and how it compares to the related phenomenon of ultrafast pre-solvated electron capture. Ionic liquids (ILs) provide a uniquely tunable environment with slow solvation dynamics on multiple timescales. Taking advantage of this, we will probe the timescale of electron solvation dynamics and scavenging kinetics, quantifying the reactivity of intermediate solvation states. We will also extend the work to ask whether a similar separation of timescale might be observed for pre-solvated hole capture.

Ultrafast hole capture after radiolysis is relatively unknown. Here we examined hole capture in THF,[1] a solvent where the initially-formed solvent radical cation is known to transfer H^+ to another THF in ~0.5 ps. Because of this rapid fragmentation, solute radical cations are usually not observed, thus providing a stringent test of the mechanism and rate of ultrafast hole capture. Contrary to this expectation, radical cations of 9,9-dihexyl-2,7-dibromofluorene (Br_2F) were produced in THF with radiolysis yields up to G = 2.23/100 eV absorbed. While a bit more than half of this was the result of direct solute ionization, the remainder were captured from $THF^{+\bullet}$ prior to its solvation and fragmentation, much faster than the ~10 ps resolution provided by Optical Fiber Single-Shot (OFSS) detection after radiolysis. Such sudden $Br_2F^{+\bullet}$ production is commensurate to observations of pre-solvated or dry electron capture in water and a few organic liquids including THF. The yield of holes scavenged from THF was interpreted with a similar formalism as for pre-solvated electrons, finding C_{37} = 1.7 M (the concentration at which 37% of holes escape capture, Fig. 1). This result can be accounted for by capture of holes by solutes adjacent to $THF^{+\bullet}$, however mechanisms such as delocalized holes or rapid hopping may play a role. At low temperature (-72 °C) where THF is still a liquid, the yield of capture from $THF^{+\bullet}$ more than doubles, suggesting that the timescale for capture is longer than 0.5 ps and indicating that capture of nearly all solvent holes would be possible if they were longer lived. This work surprisingly shows that holes, which must reside on molecules, can be captured rapidly and efficiently, similar to dry electrons, which are commonly regarded to move rapidly as they are not attached to molecules.

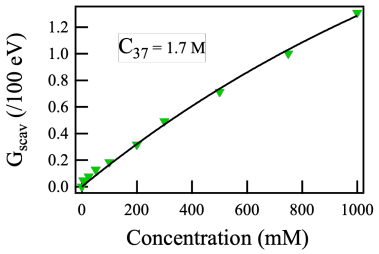

Figure 1. Yield of $Br_2F^{+\bullet}$ produced by capture of a hole from $THF^{+\bullet}$, fit: $G_{scav} = G_{THF}\left(1 - e^{-[S]/C_{37}}\right)$ with G_{THF} = 2.9/100 eV

We have also examined ultrafast hole capture in alkanes, important because of their widespread use in used nuclear fuel (UNF) reprocessing and because they offer unique insight into questions of hole delocalization. It is well known that radical cations of alkanes are unusually delocalized across the entire carbon-carbon backbone through sigma-bonds; calculations suggest this extends to chains as long as hexadecane. OFSS measurements show that pre-solvated hole capture was efficient in alkanes from pentane through hexadecane. Despite the different length of the alkanes, yields of $Br_2F^{+\bullet}$ made in < 10 ps by capture from the solvent as a function of concentration were found to be essentially identical in all liquids (Fig. 2). We find that not only do the differences in delocalization not impact capture, but unsurprisingly neither do the different viscosities of the liquids. These yields are large, and a global fit to the data in Fig. 2 find C_{37} ~ 210 mM. While measurements for pre-solvated electrons are not known in alkanes, this value is very likely quite similar. At 210 mM, it is clear that pre-solvated hole capture must be considered when concentrations approach or exceed this amount, for example in UNF reprocessing, discussed below. While results cannot definitively identify the mechanism for pre-solvated hole capture, they are suggestive that an initial delocalized hole prior to localization and solvation may be responsible. Delocalization could cover some number of alkane carbon atoms, and not care strongly about chain length, predicting a spherical capture distance ~ 1.23 nm in < 10 ps. On the other hand, resonant hole transfer or hopping prior to relaxation would be expected to have two main problems. First, the number of hops in pentane would be much greater than in hexadecane.

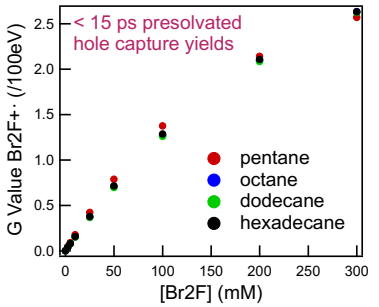

Figure 2. Yield of presolvated hole capture from n-dodecane radical cations.

At the same time, the reorganization energy of hole relaxation on pentane is much larger than in hexadecane. While it is possible for both of these issues to conspire to result in the same pre-solvated hole capture across alkanes, the coincidence would be surprising.

Radiation Chemistry Relevant to Used Nuclear Fuel (UNF) Extraction[2,3,16,17,19]

The first part of this effort was collaborative with Idaho National Laboratory (G. Holmbeck) and California State University at Long Beach (S. Mezyk). The overall goal was twofold: first to provide a basis for understanding radiation-induced damage to the organic phase of proposed new extraction systems for UNF, and second to provide reaction rates for early-time species following radiolysis, which is required input for multi-scale modelling of these complex systems. At BNL, we used pulse radiolysis to measure reactions of dodecane radical cations ($DD^{+\bullet}$) with the organic-phase metal complexants TODGA, CMPO, HONTA, DEHBA, DEHiBA, and the classic TBP, both in neat dodecane and with varied conditions including added *n*-octanol, metal oxides, and contact with acidic water phases. BNL also provided computational support to help understand reaction pathways. Experiments at INL determined damage yields to complexants with dose. Together, these data provided clues to how damage to complexants occurs.

Degradation of the novel carbon/hydrogen/oxygen/nitrogen-only extractant HONTA was found to be likely due to oxidation by $DD^{+\bullet}$ followed by subsequent fragmentation. An important finding from pulse radiolysis experiments was an order-of-magnitude increase in the hole transfer rate when HONTA was complexed to a metal, increasing total HONTA oxidation and likely degradation.[2] Enhanced hole transfer reaction rates from $DD^{+\bullet}$ were also observed with UO_2 complexes of the butyramides DEHBA and DEH*i*BA, but not with the classic PUREX complexant TBP, due to substantial differences in reaction mechanism.[3] As with HONTA, the enhanced rate of hole transfer to the butyramides may indicate an additional path for degradation. Curiously, radioprotection of CMPO appeared to be afforded by complexing HNO_3 extracted from the aqueous phase to a single oxygen of the complexant phosphate group, possibly acting as a sink for excited states formed by recombination of $CMPO^{+\bullet}$ with electrons, that might otherwise have resulted in dissociation and radical production. TODGA was surprisingly found to be protected from damage by the presence of *n*-octanol, (added to suppress 3rd phase formation) when contacted with an HNO_3/H_2O phase, otherwise it led to greater degradation. Pulse radiolysis experiments showed that while *n*-octanol reacted with most $DD^{+\bullet}$, thereby protecting TODGA from being oxidized and possibly fragmenting, the potentially-damaging alcohol radical left after its fragmentation was rendered inert by co-extracted HNO_3/H_2O in the organic phase. TODGA was also found to be protected when in metal complexes formed from extraction from water, likely by reaction with coextracted nitrate ions, similar to CMPO. Key findings of these works are the differences in reaction rate and correlated damage of free and complexed extractants, as well as the effects of other species extracted from aqueous phases.

Important questions remained following this work, namely whether the interaction of $DD^{+\bullet}$ with free extractants like TODGA was by hole transfer (HT) or proton transfer (PT), what the impact of pre-solvated hole capture might be, and what is the fate of TODGA at short times in these systems? Many decomposition and addition products of TODGA following radiolysis have been reported in the literature, but the extent to which these are made as a direct consequence of early time reactions of TODGA is not known. To address these questions, at BNL we extended the previous studies by first using OFSS to measure the reaction of $DD^{+\bullet}$ with TODGA using OFSS. We found that at the large concentrations of TODGA typically used, about half of the DD

holes disappeared faster than 10 ps. This is a clear indication that pre-solvated hole capture is the mechanism, and not proton transfer. Further diffusive reaction was resolved, but it was rapid, also pointing to HT. Because HT is the mechanism, we sought to transfer the holes from TODGA to lower IP scavenger to provide another measure of HT yield. While results showed this technique worked quantitatively with *p*-xylene used instead of TODGA, we were able to transfer at most ~10% of holes from TODGA to tritolylamine (TTA). This suggests that on short timescale, $TODGA^{+\bullet}$ is decomposing, possibly by backbone scission or proton transfer. When we extrapolate the yield/dose of this damage upon production of $TODGA^{+\bullet}$ to the large gamma doses used by the INL team, it could account for a large fraction of all TODGA damage seen in the gamma radiolysis studies. This suggests that while the myriad of products reported may be made at long times, the initial damage may be due to radiolytic oxidation of TODGA, much of which occurs in under 10 ps.

Radiation-Induced Radical Chemistry in Organic Solvents

For organic solvents to be as useful as water for clean, mechanistic PR applications, it is often critical that the complex mixture of highly reactive solvent-derived radicals is scavenged. Our goal is to develop solvent class-based radical scavenging techniques that will either convert the primary radicals into useful secondary reductants or oxidants, or convert them into benign secondary radicals. This work impacts a wide range of applications, including PR studies of the mechanisms of solar fuels catalysis with transition metal complex catalysts. Acetonitrile (CH_3CN) is often the solvent of choice for solar fuels catalysis and other redox processes, and it is a primary solvent for our work. Other important solvents are also being investigated, including *N*,*N*-dimethylformamide, ILs, and alkyl carbonates.

Solvated Electron in Acetonitrile: Radiation Yield, Absorption Spectrum, and Equilibrium Between Cavity- and Solvent-Localized States.[6] The identity, thermodynamics and kinetics of transient charged and radical species arising from ionizing radiation in non-aqueous solvents is critical to their application in radiolytic mechanistic studies. CH_3CN is an important solvent but it exhibits unique behavior, with the solvated electron, e^-_{solv}, existing as an equilibrium mixture of a conventional cavity-localized electron (e^-_{cav}; λ_{max} = 1450 nm) and a dimeric molecular anion ($(CH_3CN)_2^{\bullet-}$; λ_{max} = 500 nm), with equilibrium being established on an 80 ps timescale. This work used variable-temperature pulse radiolysis at 233-353K (Fig. 3, red data) to directly obtain, for the first time, thermodynamic parameters of the equilibrium between the two solvated electron states, with the enthalpy and entropy for the e^-_{cav} to $(CH_3CN)_2^{\bullet-}$ conversion corresponding to a 0.44 ± 0.35 equilibrium constant at 25 °C. An efficient Co(II) macrocyclic electron scavenger was used to establish the highest reported value for the radiation yield, $G(e^-_{solv})$, of solvated electrons in CH_3CN (>2.8/100 eV). An apparent molar absorption coefficient of (20.8 ± 1.5) × 10^3 M^{-1} cm^{-1} at 1450 nm and 20 °C for e^-_{solv}, and individual quantitative Vis-NIR absorption spectra of e^-_{cav} and $(CH_3CN)_2^{\bullet-}$ were derived from the data. Collectively, these results resolved several controversies in the literature concerning the solvated electron properties in CH_3CN and furnished requisite data for quantitative pulse radiolysis investigations in this solvent.

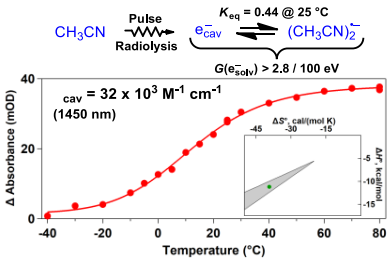

Figure 3. Variable temperature pulse radiolysis in CH_3CN.[6]

Reactivity of Radiolytically- and Photochemically-Generated Tertiary Amine Radicals Towards a CO_2 Reduction Catalyst.[S3] Homogeneous solar fuels photocatalytic systems often require several additives in solution with the catalyst to operate, such as a photosensitizer (PS), Brønsted acid/base, and sacrificial electron donor (SED). Tertiary amines, in particular triethylamine (TEA) and triethanolamine (TEOA), are ubiquitously deployed in photocatalysis applications as SEDs, and capable of reductively quenching the PS's excited state. Upon oxidation, TEA and TEOA form $TEA^{\bullet+}$ and $TEOA^{\bullet+}$ radical cations, respectively, which decay by proton transfer to generate redox non-innocent transient radicals, $TEA^{\bullet}$ and $TEOA^{\bullet}$, respectively, with redox potentials that allow them to participate in an additional electron transfer step, thus resulting in net one-photon / two-electron donation. However, the properties of the $TEA^{\bullet}$ and $TEOA^{\bullet}$ radicals are not well understood, including their reducing powers and kinetics of electron transfer to catalysts. We have used both pulse radiolysis and laser flash photolysis to generate $TEA^{\bullet}$ and $TEOA^{\bullet}$ radicals in CH_3CN, and combined with UV/Vis transient absorption and time-resolved mid-infrared (TRIR) spectroscopies, we have probed the kinetics of reduction of the well-established CO_2 reduction photocatalyst, *fac*-ReCl(bpy)$(CO)_3$ (bpy = 2,2'-bipyridine), by these radicals ($k_{TEA\bullet} = 4.4 \times 10^9$ M^{-1} s^{-1} and $k_{TEOA\bullet} = 9.3 \times 10^7$ M^{-1} s^{-1}). The ~50× smaller rate constant for $TEOA^{\bullet}$ indicates that in contrast to a previous assumption, $TEA^{\bullet}$ is a more potent reductant than $TEOA^{\bullet}$ (by ~0.2 V, as estimated using the Marcus cross relation). This knowledge will aid the design of photocatalytic systems involving SEDs. This work also demonstrates that TEA can be a useful radiolytic solvent radical scavenger for pulse radiolysis experiments in CH_3CN, effectively converting unwanted oxidizing radicals into useful reducing equivalents in the form of $TEA^{\bullet}$ radicals.

Other Progress:

- We synthesized a family of eight Re complexes with a wide range of reduction potentials, which will now allow us to bracket the oxidation potentials (reducing powers) of tertiary amine radicals in CH_3CN.
- We have developed a new strategy for performing reductive PR in CH_3CN in the presence of Brønsted acids. Such experiments are typically difficult to perform since the acids rapidly scavenge the solvated electrons.
- Characterized the physical and radiation chemistry of ionic liquids (ILs) with boronium centers in the cations (collab. w/J. Davis, U. So. Ala.). The boronium substitution provides paths to new cation structures, *without* adding susceptibility to excess electron capture in saturated systems. It also provides new insights into the radical chemistry of irradiated imidazolium ILs.
- Prepared and characterized the physical chemistry of thioether pyrrolidinium and imidazolium ILs and compared their transport properties to ether and alkyl congeners. Convincingly found that the thioethers are *more* viscous than the corresponding ethers, contradicting the literature.

Future Plans

- Electron transfer equilibria will be measured between tertiary amine radicals and suitable substrates, to determine amine radical oxidation potentials in CH_3CN. This will have far-reaching consequences for various types of photoredox catalysis, including CO_2 reduction.

- We will examine the reduction-first mechanism of CO_2 reduction by Re- and Mn-based catalysts, probing, for the first time, the reduction & protonation of key metallocarboxylate intermediates, using a new strategy for PR in CH_3CN in the presence of acids.
- We will attempt to identify the radiolytic oxidant(s) generated upon radiolysis of CH_3CN, permitting oxidative processes to be more easily probed in CH_3CN.
- PR-TRIR of alkyl carbonates will be performed, allowing degradation pathways of these important media from Li-ion batteries to be more fully understood.
- We will quantify the properties of super-oxidants and reductants by better determining the energy of solvated electrons in various solvents and the ability to make long-lived strong oxidants with pulse radiolysis.
- Determine impact of other molecules in extractants, like alcohols, on presolvated hole capture, and determine if damaging oxidation can be steered away from extractants.
- Expand investigation of ultrafast hole capture by extractants for UNF to other molecules; do all capture holes in < 10 ps and do all experience rapid damage like TODGA?
- We will use near-IR OFSS to measure the solvation dynamics of excess electrons in ionic liquids selected for diverse dynamical properties and correlate the dynamics to pre-solvated electron scavenging kinetics using scavengers with a wide array of electronic structures and functionalities.

Thrust 2: Charges and Excitons in Molecular Systems

Thrust 2 applies pulse radiolysis to better understand fundamental electron- and energy-transfer and transport processes in molecular systems relevant to solar energy conversion. An important motivation is to further improve the efficiency of organic solar cells (OSCs), which are characterized by delocalized charges on conjugated molecules in nonpolar films. We seek a better fundamental understanding of electron and energy transfer processes in this unique environment by investigating topics including redox potentials in nonpolar media, charge transport, recombination and escape, and electronic coupling. These findings also have implications for related topics including photocatalysis, artificial photosynthesis and energy storage.

Highly conjugated molecules, such as conjugated polymers, enable large oscillator strength for visible light absorption/emission as well as facilitating fast charge and energy transport. They can exploit almost limitless customizability through organic synthesis. Design principles can control HOMO/LUMO levels, absorption spectra, and molecular ordering, which have seen OSCs power conversion efficiency (PCE) increase. Most recently, non-fullerene electron acceptors (NFAs) have taken the record PCEs from 12% to almost 20%. Remaining efficiency losses are thought to be related to *non-radiative bimolecular charge recombination*, however, design principles for this are not well-established as theory is still catching up with synthetic progress. Rates are also notoriously hard to measure and vary depending on technique.

The *thermodynamics* and *kinetics* of electron transfer reactions involving highly delocalized charges in nonpolar film-like environments is poorly understood and challenging to measure. For

example, redox potentials are measured in polar solvents with 0.1 M electrolyte and are poorly defined for conjugated polymers. The free energy required for charges to escape is also not well understood in delocalized systems, although in films, estimates have ranged from tens to hundreds of meV. Furthermore, electronic coupling, that controls electron transfer rates in highly delocalized systems may be affected by donor and acceptor size, size mismatch, or symmetry mismatch, but these effects need to be quantified.

Specific questions we seek to address include: How are redox potentials ($E°$) changed in low polarity media? How do you define $E°$ for conjugated polymers? How does delocalization quantitatively affect coulomb binding energy and charge escape? How does dielectric environment affect charge transport along conjugated "molecular wires"? Can we exploit the Marcus inverted region to suppress highly exoergic back electron transfer? Can we establish design principles to reduce electronic coupling? What is the role of spin and local triplet states in charge recombination? Are there materials with different electronic structures that might do better?

Pulse radiolysis (PR) has a strong history of contributions to the understanding of electron transfer and transport, and it offers a unique way to probe many of these questions. It enables the rapid generation of *free* charges in nonpolar media, which is not possible with electrochemistry or flash photolysis. It also enables the facile generation of triplets in the solvent, which allows triplet radical ion pairs to be generated. Equally, radical ion pairs can be generated by recombination of scavenged holes and electrons on acceptor and donor molecules respectively. PR with IR detection of nitrile or carbonyl stretches can also assist in probing the nature of charges and even spin in conjugated systems.

Recent Progress

IR linewidth and intensity amplifications of nitrile vibrations report nuclear-electronic couplings and associated structural heterogeneity in radical anions.[4] We have previously shown that ν(C≡N) IR bands of nitrile-substituted conjugated molecules can act as IR probes for excess charges, based on IR frequency shifts, because of their exquisite sensitivity to the degree of electron delocalization and induced electric field. In more recent work[4], we showed that the IR intensity and linewidth can also provide unique and complementary information on the nature of charges. Quantifications of IR intensity and linewidth in a series of nitrile-functionalized oligophenylenes revealed that the ν(C≡N) vibration is coupled to the nuclear and electronic structural changes, which become more prominent when an excess charge is present. Using a new series of ladder-type oligophenylenes that possess planar aromatic structures, we demonstrated that ν (C≡N) vibrations can report charge fluctuations associated with nuclear movements, namely those driven by motions of flexible dihedral angles. This happens only when a charge has room to fluctuate in space.

The effect of molecular size on electronic coupling.[13] The Marcus inverted-region has the potential to slow down energy-wasting back electron transfer reactions in solar energy conversion. While small reorganization energy can enhance the inverted region effect, electronic coupling could also be used to obtain the optimal balance of forward and reverse rate constants. Many factors can influence electronic coupling, but here we used pulse radiolysis to investigate the effect of molecular size. By measuring the kinetics and thermodynamics of hole transfer, we compared the properties of ethene and naphthalene dimer cations in dichloromethane. The naphthalene radical cation was found to have a dimerization free energy of -218 meV. Very slow rates of hole

transfer from these dimers point to a new kind of reorganization energy for dimers. Measurements suggest that the smaller ethene dimer is 2-4 times more strongly bound than the larger naphthalene dimer, suggesting that molecular size can control the overall electronic coupling.

Triplet ion pairs.[S2] Energy loss from charge recombination in photovoltaics would be minimized if the only decay channel was to form the initial photo-generated excited state, S_1. Local triplet excited states, below S_1, are common to almost all donor/acceptor molecules and constitute an unwanted additional loss pathway upon charge recombination. We investigated the recombination of radical ion pairs (fluorene$^{+\bullet}$ and tetracyanoethene$^{-\bullet}$) created with pulse radiolysis, whose energy is insufficient to make the lowest triplet excited state of either donor or acceptor. By comparing this recombination with the pair (fluorene$^{+\bullet}$ and benzoquinone$^{-\bullet}$), which recombine with transport-limited kinetics, we investigated the possibility of using triplet radical ion pairs to block charge recombination. With computational and experimental data we estimated singlet-triplet splitting in the ion pair states and found lifetimes of microseconds. Kinetic data was suggestive of some degree of spin-sorting with most, if not all, recombining ions becoming long-lived triplet pairs. Predicting and measuring the lifetime of such triplet radical ion pairs is a relatively unexplored area, but pulse radiolysis provides a novel way of creating them between arbitrary molecules without the need for a triplet sensitizer.

Effects of Electrolyte on Redox Potentials.[7] Determining redox potentials in low polarity media with electrochemistry presents challenges, as ion pairing with the supporting electrolyte can significantly affect measurements. The recent methods developed in our group for determining the effects of electrolyte on redox potentials are summarized in this book chapter.[7] We highlight how, in tetrahydrofuran, electrolytes can shift redox potentials by as little as 20 mV (analyte: oligofluorene, electrolyte: $TBAPF_6$) to nearly half a volt (analyte: benzophenone, electrolyte: $NaBPh_4$). We also include new estimates of how the redox potential of the common internal standard, ferrocene, is shifted by the electrolyte. These results are important and suggest that there may be better candidates than ferrocene for internal standards that would be less affected by the choice of electrolyte.

Redox potentials of conjugated polymers in nonpolar media. Determining accurate, reproducible, one-electron redox potentials for conjugated polymers has been a frustrating unsolved problem since the inception of the field of organic electronics. These values are important for understanding and predicting the driving forces for electron transfer. Estimates of HOMO levels obtained from the leading approaches (cyclic voltammetry and UPS/IPES) have reported energy offsets in donor/acceptor films ranging from almost 0 eV to nearly 1 eV for the same two molecules. Using pulse radiolysis, we have developed a consistent and accurate way to determine referenced one-electron redox potentials of conjugated polymers with ~mV precision. To do this we built up a 'redox ladder' using many measurements of hole transfer equilibria between pairs of molecules, starting with ferrocene. This ladder acts as a measuring stick to measure new polymers/molecules against. These measurements are performed in o-xylene without added electrolyte and therefore reflect the dielectric environment of most molecular films. This new approach should enable a better understanding of charge transfer in these conjugated materials and lead to more efficient devices.

Characterizing triplet and charged states in carbene-metal-amide thermally-activated delayed fluorescence (TADF) photosensitizers.[S1] Carbene-metal-amide (cMa) complexes are strong candidates for photosensitizers in photocatalysis due to strong, tunable absorptions, large excited state redox potentials, long lifetimes, and robust electrochemical stability. These properties

are obtained due to their TADF properties, enabling long-lifetimes without heavy atoms. We performed pulse radiolysis experiments on a series of cMa's to characterize the triplet, radical anion and radical cation states. Identifying the spectroscopic signatures of these states enables the full interpretation of transient absorptions following flash photolysis where bimolecular electron and hole transfer reactions from the excited states could be verified, paving the way for their use in photocatalysis.

Cibalackrots for singlet fission. Cibalackrots are an indigoid dye that has properties that enable singlet fission which is a promising approach to go beyond the Shockley-Quiesser limit for photovoltaic efficiency. We characterized a series of these molecules with pulse radiolysis to determine their radical anion and cation spectra to enable the interpretation of transient absorption following flash photolysis. By using short path lengths and electron and hole mediators we were able to obtain the full spectrum, including ground state bleach, in terms of extinction coefficient. This approach goes beyond what can be achieved with spectro-electrochemistry, which can be limited by instability of reduced/oxidized states, multiple electron transfers and inability to get molar extinction coefficients.

Future Plans

Future work seeks to better understand the thermodynamics and kinetics of electron transfer processes in nonpolar, highly conjugated systems to improve solar energy conversion efficiency in molecular films. It is divided into three themes covering redox potentials, charge transport and escape, and electronic coupling and charge recombination.

- Investigate excess charge delocalization in carbonyl-substituted conjugated molecules and oligomers for organic solar cells.
- Complete a redox ladder for reductions to use to measure LUMO levels in nonpolar solvents and further develop methods to link to our ladder for measuring HOMO levels to complete the referenced redox potentials in nonpolar media project.
- Further develop our fundamental understanding of the lifetimes of triplet radical ion pairs to seek to find strategies to combine spin, delocalization and the inverted region to enhance solar energy conversion.
- Investigate additional fundamental molecular properties that affect electronic coupling.

Thrust 3: Accelerator Center for Energy Research

The BNL Accelerator Center for Energy Research (ACER) provides sophisticated tools for the application of radiation chemistry to problems relevant to energy production, storage and utilization, as well as the development of new, advanced materials and devices, improving the nuclear fuel cycle and mitigating its environmental consequences, developing principles for the design of massive particle detectors, and understanding the chemical mechanisms of biological systems. ACER stands as a separate third thrust of this FWP because the operation and continuing improvement of a sophisticated set of radiolysis facilities requires dedicated personnel, equipment, and administrative effort. ACER thus serves as an experimental resource not only for Thrusts 1 and 2, but also for other DOE projects and external users. ACER capabilities contribute significantly to efforts of the Artificial Photosynthesis (AP) group in our department (which studies transition metal catalyst systems for generating chemical fuels from water and CO_2, utilizing renewable solar energy), and the Molten Salts in Extreme Environments (MSEE) and Bioinspired

Light-Escalated Chemistry (BioLEC) Energy Frontier Research Centers. ACER supports DOE Nuclear Energy Fuel Cycle R&D researchers investigating the radiation chemistry of extractant systems and both stable and radioactive lanthanides and actinides.[5,11]

The principal elements of ACER are the Laser-Electron Accelerator Facility (LEAF), the Van de Graaff accelerator and two ^{60}Co sources. LEAF was the world's first pulse radiolysis facility based on an RF photocathode electron gun, which uses a laser and the photoelectric effect to generate picosecond electron pulses inside a high-field microwave cavity that accelerates them to ~8.7 MeV. Both accelerators include capabilities for UV-VIS-NIR transient absorption measurements using lamps and transient digitizers. The LEAF design provides synchronized laser probe beams to stroboscopically measure kinetics on the 5-10 picosecond time scale, faster than can be measured with detectors and digitizers. LEAF's unique and innovative Optical Fiber Single-Shot (OFSS) detection system multiplexes the laser stroboscopic method to simultaneously measure absorbances at 142 time delays after a single electron shot at selected wavelengths between 500-1600 nm. OFSS is of critical importance to Thrust 1 projects on *ultrafast* charge capture in organic and ionic liquids and for charge transport studied in Thrust 2. LEAF also features a unique, mid-IR-laser based time-resolved infrared (TRIR) detection system that provides a powerful, general purpose time-resolved and structurally-sensitive probe for pulse radiolysis (PR-TRIR). It is highly valued for both Thrust 1 and 2 projects examining radical chemistry, mechanisms of photoredox catalysis, charge distribution and ion pairing, and for selectively probing transition metal catalysts for artificial photosynthesis in the AP Group.

The 2 MeV electron Van de Graaff is a versatile instrument for kinetics on microsecond and longer timescales and can deliver larger radiolytic doses than LEAF. Its optical detection system is very sensitive and it is equipped with a pre-mixing system for studying the radical chemistry of species under conditions (such as pH) where they are not stable. Two complementary transient IR detection capabilities at the Van de Graaff take advantage of the larger available doses: (i) a TRIR detection method identical to that used at LEAF, and (ii) a unique, broadband, nanosecond time-resolved step-scan FTIR spectroscopic method[9] that allows TRIR spectra to be rapidly recorded over wide regions of the mid-IR to locate radiolytically-induced transient IR bands. A 2000-atm high-pressure sample vessel is used to measure pressure-dependent kinetics at the Van de Graaff, LEAF, and by laser flash photolysis. Activation volumes are very useful for the interpretation of reaction mechanisms. An OLIS rapid scanning monochromator system is available at the Van de Graaff to enable broadband UV-vis detection on millisecond and longer timescales, and is valuable for samples available in limited quantities. A microwave conductivity system supports research examining charge transport in Thrust 2.

We have two ^{60}Co sources (4800 and 410 Gy/hr) that are important resources for radiolysis product studies examining the effects of radiation on materials[8,10] and for competition kinetics.

Our accelerators and ^{60}Co sources are easy for experimenters to use with a modest amount of training that, in the case of LEAF, is truly remarkable for a picosecond accelerator. In addition, we have technical assistance at LEAF to support end users who just wish to collect data and do not need to be trained on the machine. *We prioritize our development projects to expand experimental capabilities by their potential to enable new science for our chemistry programs.* At the same time, we work constantly to make the more sophisticated parts of our experimental systems increasingly user friendly.

Through our User Support Program, we make ACER facilities and expertise available to outside researchers to study a broad spectrum of topics from environmentally-related chemistry, bacterial and yeast oxy radical scavenging systems, and electron transfer processes. We irradiate materials for research on advanced optoelectronic devices and solid-state NMR spectroscopy. ACER provides rare capabilities to the US and international research community, and we are constantly advertising the value of radiation chemistry to a broad range of science as we participate in national and international meetings and exchange information with our fellow researchers and sister laboratories.

Recent Progress

Radiation Chemistry of Actinides[5,11]

Our collaborators from INL (G. Holmbeck) and CSULB (S. Mezyk) have been investigating the transient redox chemistry of radioactive actinides. There is little understanding of the fundamental radiation chemistry of these materials, of critical importance to reprocessing and development of multi-scale models for reaction conditions in extraction systems. We measured the reactivity of higher actinide ions (Am, Cm, Bk, Cf) in acidic water with aqueous radiation-induced transients, $^{\bullet}OH$, $^{\bullet}NO_3$, e_{aq}^-, and $H^{\bullet}$. This work identified the important role of metal ion-ligand chemistry in reprocessing systems and established new redox chemistry/rate constants for these higher actinide ions. Knowledge of the unusual and short-lived redox states of these species is important to understanding their interactions in extraction systems, as well as their ability to cause extraction performance degradation.

Dynamic Nuclear Polarization Using Radicals Created by γ-Irradiation[10]

High-field magic angle spinning dynamic nuclear polarization (MAS DNP) can enhance the sensitivity of solid-state nuclear magnetic resonance (ssNMR) spectroscopy experiments by orders of magnitude. In a DNP experiment, the high spin polarization of unpaired electrons is transferred to nuclear spins. The unpaired electron spins for DNP are usually provided by exogenous organic radicals (e.g., TEMPO, trityl, etc.) but for many materials, there is no way to introduce exogenous radicals to allow NMR signals from the bulk to be amplified. A collaboration with Arron Rossini (Iowa State) showed that γ-irradiation induces the formation of stable radicals in silica-based glasses and organic solids like sugars and polymers. The radicals were then used to polarize ^{29}Si or ^{1}H spins uniformly throughout these non-porous materials. Significant MAS DNP enhancements greater than 400 and 30 were obtained for fused quartz and glucose respectively. These results demonstrate that ionizing radiation is a promising method to generate stable radicals for DNP in previously inaccessible bulk materials such as non-porous inorganic solids and insoluble polymers.

Future Plans

ACER development projects are prioritized by their potential to enable new science for our chemistry programs. Parallel to this focused capability development, we strive constantly to increase the performance, reliability and user-friendliness of our accelerator and experimental systems by adopting new technologies.

- Mid-IR fiber optics will be implemented for PR-TRIR experiments at our Van de Graaff (VdG) facility, opening up new avenues of PR-TRIR research previously thwarted by noise.

- OFSS will be improved by incorporation of new visible CCD cameras to address end-of-life issues with the existing cameras and provide increased performance. Changes to the optical system will address image and data quality from NIR OFSS, and a new fiber bundle will be implemented to both increase point density as well as extend to longer times.

References

S1. Kellogg, M.; Mencke, A.; Muniz, C.; Ahammad, R.; Cardoso-Delgado, F.; Baluyot-Reyes, N.; Sewell, M.; Bird, M.; Bradforth, S.; Thompson, M. "Intra- and Inter-Molecular Charge Transfer Dynamics of Carbene-Metal-Amide Photosensitizers" **2023** *submitted*.

S2. Bird, M. J.; Wu, Q.; Asaoka, S..; Miller, J. R. "Long Lived Triplet Radical Ion Pairs Halt Fast Langevin Recombination" **2023** *submitted*.

S3. Carr, C. R.; Vrionides, M. A.; Grills, D. C. "Reactivity of Radiolytically- and Photochemically-Generated Tertiary Amine Radicals Towards a CO_2 Reduction Catalyst" **2023** *submitted to J. Chem. Phys.*

Peer-Reviewed Publications Resulting from this Project (2021-2023)

1. Cook, A. R. "Sub-picosecond Production of Solute Radical Cations in Tetrahydrofuran after Radiolysis" *J. Phys. Chem. A* **2021**, *125*, 10189-10197. DOI: 10.1021/acs.jpca.1c08568
2. Toigawa, T.; Peterman, D. R.; Meeker, D. S.; Grimes, T. S.; Zalupski, P. R.; Mezyk, S. P.; Cook, A. R.; Yamashita, S.; Kumagai, Y.; Matsumura, T.; Horne, G. P. "Radiation-Induced Effects on the Extraction Properties of Hexa-*n*-octylnitrilo-triacetamide (HONTA) Complexes of Americium and Europium" *Phys. Chem. Chem. Phys.* **2021**, *23*, 1343-1351. DOI:10.1039/D0CP05720G
3. Celis Barros, C.; Pilgrim, C. D.; Cook, A. R.; Mezyk, S. P.; Grimes, T. S.; Horne, G. P. "Influence of Uranyl Complexation on the Reaction Kinetics of the Dodecane Radical Cation with Used Nuclear Fuel Extraction Ligands (TBP, DEHBA, and DEHiBA)" *Phys. Chem. Chem. Phys.* **2021**, *23*, 24589-24597. DOI:10.1039/D1CP03797H
4. Yan, J.; Wilson, R. W.; Buck, J. T.; Grills, D. C.; Reinheimer, E.; Mani, T. "IR linewidth and intensity amplifications of nitrile vibrations report nuclear-electronic couplings and associated structural heterogeneity in radical anions" *Chem. Sci.*, **2021**, *12*, 12107-12117 DOI: 10.1039/D1SC03455C
5. Horne, G. P.; Grimes, T. S.; Zalupski, P. R.; Meeker, D. S.; Albrecht-Schönzart, T. E.; Cook, A. R.; Mezyk, S. P. "Curium(III) radiation-induced reaction kinetics in aqueous media" *Dalton Trans.* **2021**, *50*, 10853-10859. DOI:10.1039/D1DT01268A.
6. Grills, D. C.; Lymar, S. V. "Solvated Electron in Acetonitrile: Radiation Yield, Absorption Spectrum, and Equilibrium between Cavity- and Solvent-Localized States" *J. Phys. Chem. B* **2022**, *126*, 262-269. DOI:10.1021/acs.jpcb.1c08946

7. Bird, M. J., Miller, J. R. “Effects of Electrolyte on Redox Potentials” *Redox Chemistry - From Molecules to Energy Storage*, *IntechOpen* **2022,** Ch. 4. ISBN: 978-1-80355-537-9. DOI: 10.5772/intechopen.103003

8. González-López, L.; Kearney, L.; Janke, C. J.; Wishart, J.; Kanbargi, N.; Al-Sheikhly, M., On the Mechanism of the Steady-State Gamma Radiolysis-Induced Scissions of the Phenyl-Vinyl Polyester-Based Resins. *Front. Chem.* **2022,** *9*, 803347. DOI: 10.3389/fchem.2021.803347

9. Grills, D. C.; Layne, B. H.; Wishart, J. F., Coupling Pulse Radiolysis with Nanosecond Time-Resolved Step-Scan Fourier Transform Infrared Spectroscopy: Broadband Mid-Infrared Detection of Radiolytically Generated Transients. *Appl. Spectrosc*. **2022**, *76*, 1142-1153. DOI: 10.1177/00037028221097429

10. Carnahan, S. L.; Chen, Y.; Wishart, J. F.; Lubach, J. W.; Rossini, A. J., Magic angle spinning dynamic nuclear polarization solid-state NMR spectroscopy of γ-irradiated molecular organic solids. *Solid State Nuclear Magnetic Resonance* **2022,** *119*, 101785. DOI: 10.1016/j.ssnmr.2022.101785

11. Horne, G. P.; Rotermund, B. M.; Grimes, T. S.; Sperling, J. M.; Meeker, D. S.; Zalupski, P. R.; Beck, N.; Huffman, Z. K.; Martinez, D. G.; Beshay, A.; Peterman, D. R.; Layne, B. H.; Johnson, J.; Cook, A. R.; Albrecht-Schonzart, T. E.; Mezyk, S. P., Transient Radiation-Induced Berkelium(III) and Californium(III) Redox Chemistry in Aqueous Solution. *Inorg. Chem.* **2022,** *61*, 10822-10832. DOI: 10.1021/acs.inorgchem.2c01106

12. Basak, P.; Zambelli, B.; Cabelli, D. E.; Ciurli, S.; Maroney, M. J., Pro5 is not essential for the formation of 'Ni-hook' in nickel superoxide dismutase. *J. Inorg. Biochem*. **2022**, *234*, 111858. DOI: 10.1016/j.jinorgbio.2022.111858

13. Myong, M. S.; Bird, M. J.; Miller, J. R. “Kinetics and Energetics of Electron Transfer to Dimer Radical Cations” *J. Phys. Chem. B* **2023**, 127, *13*, 2881–2886 DOI: 10.1021/acs.jpcb.2c07302

14. González-López, L.; Kearney, L. T.; Janke, C.; Wishart, J. F.; Naskar, A. K.; Kanbargi, N.; Bateman, F. B.; Al-Sheikhly, M., On the electron beam-induced degradation of vinyl ester thermosets. *Polymer Degradation and Stability* **2023,** *211*, 110307. DOI: 10.1016/j.polymdegradstab.2023.110307

15. Conrad, J. K.; Iwamatsu, K.; Woods, M. E.; Gakhar, R.; Layne, B.; Cook, A. R.; Horne, G. P. "Impact of iodide ions on the speciation of radiolytic transients in molten LiCl–KCl eutectic salt mixtures" *Phys. Chem. Chem. Phys.* **2023**, *25,* 16009-16017. DOI:10.1039/D3CP01477K

16. Horne, G. P.; Celis-Barros, C.; Conrad, J. K.; Grimes, T. S.; McLachlan, J. R.; Rotermund, B. M.; Cook, A. R.; Mezyk, S. P. "Impact of lanthanide ion complexation and temperature on the chemical reactivity of N,N,N′,N′-tetraoctyl diglycolamide (TODGA) with the dodecane radical cation" *Phys. Chem. Chem. Phys.* **2023**, *25*, 16404-16413. DOI:10.1039/D3CP01119D

17. Wang, Y.; Mezyk, S. P.; McLachlan, J. R.; Grimes, T. S.; Zalupski, P. R.; O’Bryan, H. M. T.; Cook, A. R.; Abergel, R. J.; Horne, G. P. "Radiolytic Evaluation of 3,4,3-LI(1,2-

HOPO) in Aqueous Solutions" *J. Phys. Chem. B* **2023**, *127*, 3931-3938. DOI:10.1021/acs.jpcb.3c01469

18. Ogbodo, R.; Karunaratne, W. V.; Acharya, G. R.; Emerson, M. S.; Mughal, M.; Yuen, H. M.; Zmich, N.; Nembhard, S.; Wang, F.; Shirota, H.; Lall-Ramnarine, S. I.; Castner, Jr., E. W.; Wishart, J. F.; Nieuwkoop, A. J.; Margulis, C. J., Structural Origins of Viscosity in Imidazolium and Pyrrolidinium Ionic Liquids Coupled with the NTf_2^- Anion. *J. Phys. Chem. B* **2023**, *127*, 6342-6353. DOI: 10.1021/acs.jpcb.3c02604
19. Horne, G. P.; Morco, R. P.; Cook, A. R.; Mezyk, S. P., Dioctyl ether radiolysis under used nuclear fuel reprocessing conditions: Foundational knowledge for the development of sacrificial ligand grafts. *Radiat. Phys. Chem.* **2023,** *313,* 11217. DOI: 10.1016/j.radphyschem.2023.111217

The emergent photophysics and photochemistry of molecular polaritons:

a theoretical and computational investigation

DE-SC0019188

Joel Yuen-Zhou

Department of Chemistry and Biochemistry,

University of California San Diego,

9500 Gilman Dr MC 0340, La Jolla, 92093-0314, USA

joelyuen@ucsd.edu

Program scope. This project started in September 2018 and aims to develop a comprehensive theoretical and computational framework to address a new class of emergent room-temperature photophysical and photochemical processes afforded by molecular polaritons (MPs), namely, hybrid states arising from the strong coupling of organic dye electronic/vibronic excitations and confined electromagnetic modes. Recent experimental progress on MPs prompts the development of robust theoretical tools that can describe the novel phenomenology afforded by these systems under realistic dissipative conditions. Our project aims to fill this gap. The molecular or photonic components of MPs can be tuned to rationally modify the physicochemical properties of molecular matter. In this work, we have pioneered formalisms based on open-quantum systems theory to address the low-energy dynamics of MPs in the presence of room-temperature realistic conditions such as in the presence of static and dynamic molecular disorder as well as absorptive losses in the electromagnetic environment. This framework allows us to harness MPs to design control strategies of great interest to the missions of DOE-BES such harvesting of dark molecular populations or even exotic paradigms for the remote control of chemical reactions in condensed phases. Given the emergent many-body flavor of the problems of interest where many electrons, vibrations, and photons interact with one another, we have constructed effective Hamiltonian theories that can capture the essential dynamical features of the problems in question. To ensure relevance to experiments, we routinely supplement our models with parameters obtained from computational quantum chemistry and from spectroscopic data in the literature or from our experimental collaborators.

Recent progress. One of the projects this award has enabled corresponds to a collaboration with the Friend group at the University of Cambridge, where we helped to theoretically rationalize the existence of polariton modes in a wide range of organic semiconductor thin films in the absence of optical cavities, owing solely to large dielectric contrast between the film and the surroundings [1]. These polariton modes manifest themselves in exciton transport measurements at ultrafast timescales exhibiting ballistic behavior that manifests into long-range (~270 nm) transport that seems to be absent in less packed dye ensembles.

Another work that we carried out during this project period is reflected in [2]. Polaritons that emerge within the collective strong coupling regime exhibit modes spread across a macroscopic number of molecules denoted as N≈ $10^6 - 10^{12}$. This implies that the involvement of polaritons in chemical reactions decreases proportionally as 1/N, rendering them seemingly inconsequential in scenarios with a large N. This issue is referred to as "the large N problem." A potential solution involves inducing a substantial occupation of these polaritons with N_{exc} excitations. Consequently, the reaction rates now scale as N_{exc}/N rather than 1/N. This widespread occupation is termed polariton condensation and has been experimentally demonstrated at room temperature using organic microcavities over the past decade. Although polariton condensates offer a fascinating study in many-body quantum mechanics, they have remained largely unexplored in the realm of chemical reactions. Our study proposes the concept that vibrational polariton condensation can address the large N problem in polariton chemistry and lead to innovative photochemical processes absent in laser-induced chemistry. In laser-induced chemistry, a reactant molecule absorbs a photon to acquire sufficient energy for a nuclear rearrangement. In contrast, with a polariton condensate, it is the condensate itself, acting as a reservoir of energy, that undergoes autonomous reactions. The calculations presented in this work serve as a proof-of-concept, illustrating how a polariton condensate can alter the nonequilibrium steady-states of an electron transfer reaction.

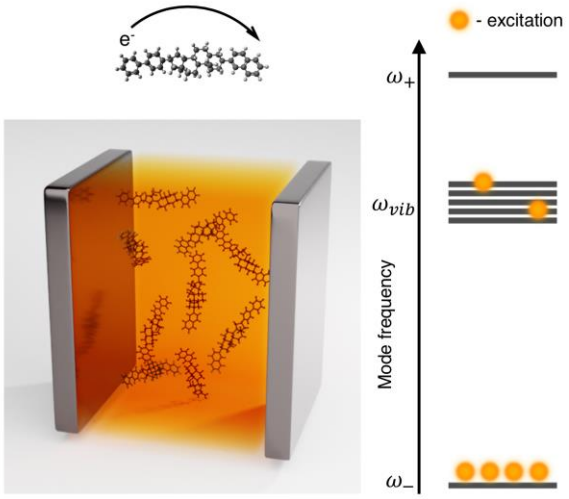

Fig. 1. This figure, adapted from Ref. 2, illustrates that beyond a specific threshold, the lower polariton (characterized by the frequency ω_-) can achieve a macroscopic occupation, even in the presence of numerous dark modes at the frequency ω_{vib}. This phenomenon, known as polariton condensation, opens up the potential to modify photochemical processes by leveraging polaritons.

In another work carried out in collaboration with the Xiong group at UCSD (co-corresponding authorship, [3]), we aimed to understand the mechanisms whereby vibrational strong coupling (VSC) alters reactions under IR pumping. To achieve this objective, we observed the rapid dynamics of a straightforward unimolecular vibrational energy exchange in iron pentacarbonyl [$Fe(CO)_5$] under VSC. Our investigation revealed two competing pathways: pseudorotation and intramolecular vibrational-energy redistribution (IVR). When subjected to polariton excitation, the energy exchange process was accelerated overall, with IVR occurring at a faster rate and pseudorotation slowing down. In contrast, dark-mode excitation exhibited dynamics similar to those outside the cavity, with pseudorotation prevailing. Despite debates regarding thermally activated VSC-altered chemistry, our findings demonstrate that VSC can indeed influence chemistry by non-equilibrium preparation of polaritons.

Finally, in [4], we theoretically examined a recent theoretical hypothesis put forward in the literature on how chemical reactivity can change via VSC under thermally-activated conditions.

This hypothesis relies on the Pollak–Grabert–Hänggi (PGH) theory, which extends beyond transition state theory (TST) and which accounts for cavity-induced frictions. However, this explanation, which focuses on a single reacting molecule coupled to light, overlook ensemble effects observed in experiments. Additionally, the relevant light–matter coupling should have been $\sqrt{N}$ times smaller than in previous works. Our study elucidates the significance of this distinction and its potential to negate the effects of cavity-induced frictions. Through an analytical extension of the cavity PGH model to realistic values of N, the research demonstrates how this model succumbs to the polariton large N problem explained above. This problem arises when the single reacting molecule experiences only a minute 1/N fraction of the collective light–matter interaction intensity, particularly when N is substantial.

Future plans. We are currently in our sixth year of the project as per a No-Cost Extension granted in June 2023. We have made significant progress in all our aims, including the comprehensive understanding of the MP dynamics in the linear excitation regime, the remote control of chemical processes and novel photophysics afforded by MPs. We have decided to concentrate our final efforts on polariton condensates and the types of reactions afforded by them; in particular, we plan to extend our work [] to the UV-visible regime.

References = Peer-reviewed publications resulting from this project (2021-2023)

[1] R. Pandya, R. Y. S. Chen, Q. Gu, J. Sung, C. Schnedermann, O. S. Ojambati, R. Chikkaraddy, J. Gorman, G. Jacucci, O. Onelli, T. Willhammar, D. N. Johnstone, S. M. Collins, P. A. Midgley F. Auras, T. Baikie, R. Jayaprakash, F. Mathevet, R. Soucek, M. Du, S. Vignolini, D. G Lidzey, J. J. Baumberg, R. H. Friend, T. Barrisien, L. Legrand, A. W. Chin, A. J. Musser, J. Yuen-Zhou, S. K. Saikin, P. Kukura, and A. Rao, Microcavity-like exciton-polaritons can be the primary photoexcitation in bare organic semiconductors, Nat. Commun. 12, 6519 (2021).

[2] S. Pannir-sivajothi, J. A. Campos-Gonzalez-Angulo, L. A. Martínez-Martínez, S. Sinha, and J. Yuen-Zhou, Driving chemical reactions with polariton condensates, Nat. Commun. 13, 1645 (2022).

[3] T.T. Chen, M. Du, Z. Yang, J. Yuen-Zhou, and W. Xiong, Cavity-Enabled Enhancement of Ultrafast Intramolecular Vibrational Redistribution over Pseudorotation, Science 378, 6621, 790-794 (2022).

[4] M. Du, Y. R. Poh, and J. Yuen-Zhou, Vibropolaritonic Reaction Rates in the Collective Strong Coupling Regime: Pollak–Grabert–Hänggi Theory, J. Phys. Chem. C. 127, 11 (2023).

LIST OF PARTICIPANTS

Anastassia Alexandrova

Heather Allen

Chibueze Amanchukwu

Scott Anderson

Polly Arnold

Veronica Augustyn

Abraham Badu-Tawiah

Carlos Baiz

L. Robert Baker

David Bartels

D. Kwabena Bediako

Elisa Biasin

Matthew Bird

David Blank

Monika Blum

Katherine Brown

Ian Carmichael

Andrew Cook

Ethan Crumlin

Tanja Cuk

Scott Cushing

Ismaila Dabo

James Dorman

Walter Drisdell

Michel Dupuis

Patrick El-Khoury

Chris Fecko

Yiping Feng

Gregory Fiechtner

Miriam Freedman

John Fulton

Mirza Galib

Etienne Garand

Sean Garrett-Roe

Franz Geiger

John Gordon

David Grills

Teresa Head-Gordon

Gregory Holmbeck

Christine Isborn

Ireneusz Janik

Britta Johnson

Mark Johnson

Kenneth Jordan

Shawn Kathmann

Bruce Kay

Munira Khalil

Greg Kimmel

Sarah King

Loni Kringle

Amber Krummel

Daniel Kuroda

Jay LaVerne

Keith Lawler

Eliane Lessner

David Limmer

Stephan Link

Aliaksandra Lisouskaya

Chong Liu

Kranthi Mandadapu

Claudio Margulis

Anne McCoy

Gail McLean

Raul Miranda

Valeria Molinero

Andres Montoya-Castillo

Karl Mueller

Christopher Mundy

Andrew Musser

Tod Pascal

Amish Patel

Jim Pfaendtner

Neeraj Rai

Jeffrey Rimer

Joaquín Rodríguez-López

Jennifer Roizen

Subramanian Sankaranarayanan

Richard Saykally

George Schatz

Gregory Schenter

Benjamin Schwartz

Craig Schwartz

Viviane Schwartz

Annabella Selloni

Thomas Settersten

Mary Jane Shultz

Susan Sinnott

Charles Sykes

Tibor Szilvasi

Ward Thompson

William Tisdale

Pratyush Tiwary

Andrei Tokmakoff

Marat Valiev

Omar Valsson

Bin Wang

Xue-Bin Wang

Marissa Weichman

Adam Willard

Kevin Wilson

James Wishart

Bryan Wong

Sotiris Xantheas

Joel Yuen-Zhou